Philipps Universität Marburg

The olfactory pathway of the red flour beetle *Tribolium castaneum* and its comparison to other Coleoptera

---

Die Riechbahn des Rotbraunen Reismehlkäfers *Tribolium castaneum* und ein Vergleich zu anderen Käfern

---

Dissertation
zur Erlangung des Doktorgrades
der Naturwissenschaften
(Dr. rer. nat.)

dem
Fachbereich Biologie
der Philipps-Universität Marburg
vorgelegt von
Martin Kollmann
aus Witten

Marburg/Lahn 2016

Vom Fachbereich Biologie der Philipps-Universität Marburg als Dissertation
angenommen am 22.06.2016

Erstgutachter: Prof. Dr. Joachim Schachtner

Zweitgutachter: Prof. Dr. Monika Hassel

Tag der mündlichen Prüfung am 29.08.2016

The biologist JBS Haldane was supposedly asked once if he could say anything about God from his study of nature. Haldane replied "He must have an inordinate fondness for beetles".

A famous statement about J.B.S. Haldane, one of the founder of modern genetics.

Inhaltsverzeichnis

Erklärung:

Eigene Beiträge und veröffentlichte Teile der vorliegenden Arbeit

Gemäß §8, Absatz 3 der Promotionsordnung der Philipps-Universität Marburg (Fassung vom 1989.04.12), ist es erforderlich, dass für alle Teilen der Dissertation die aus gemeinsamen Forschungsprojekten hervorgegangen sind, eine Aufschlüsselung der jeweiligen Leistungen beigefügt werden muss.

Kapitel 1:

Das 3D-Standardgehirn des Rotbraunen Reismehlkäfers *Tribolium castaneum*: Ein Werkzeug zur Untersuchung der Entwicklung während der Metamorphose und der Adultplastizität

Originaltitel: 3D Standard Brain of the Red Flour Beetle *Tribolium castaneum*: A Tool to Study Metamorphic Development and Adult Plasticity

- Anfertigung aller initialen Textabschnitte des Material- und Methodenteils sowie Teile der Ergebnisse, welcher weiterhin in einem iterativen Prozess (inklusive dem Rest des Manuskriptes) zusammen mit Dr. W. Huetteroth und Prof. Dr. J. Schachtner überarbeitet wurden, was von D. Dreyer, H. Vitt, B. Goetz und B. el Jundi unterstützt wurde.
- Anfertigung von ca. 50 % der Abbildungen.
- Überprüfung und teilweise Überarbeitung der ursprünglichen Rohdaten. 3D-Rekonstruktion von zwei neuen, individuellen, männlichen Gehirnen. Erstellen des neuen männlichen Standardgehirns basierend auf 18 3D-Rekonstruktionen von D. Dreyer und den 2 neu angefertigten 3D-Rekonstruktionen zusammen mit B. El Jundi, sowie errechnen das dazu nötigen neuen Template Gehirns zusammen mit Stefan Dippel.
- Erstellen der Volumenstatistiken des neuen männlichen Standardgehirns basierend auf 18 3D-Rekonstruktionen von D. Dreyer und den 2 neu angefertigten 3D-Rekonstruktionen.
- Anfertigung von ca. 15 % der 3D-Rekonstruktionen der individuellen Glomeruli.
- Dieses Kapitel wurde in der vorliegenden Form im Journal "Frontiers in Systems Neuroscience“ veröffentlicht:
  Dreyer D., Vitt H.*, Dippel S., Goetz B., El Jundi B., **Kollmann M.**, Huetteroth W., Schachtner J. (2010) 3D Standard Brain of the Red Flour Beetle *Tribolium castaneum*: A Tool to Study Metamorphic Development and Adult Plasticity. Frontiers in Systems Neuroscience. 04:03
- Die 3D-Rekonstruktuion von 18 Gehirnen männlicher und von 20 weiblicher Tiere und die damit verbundene Volumetrie, sowie der größere Teil der Untersuchung der individuellen Glomeruli waren Bestandteil der Diplomarbeit von D. Dreyer (Dreyer D. [2008] Erstellung eines standardisierten 3D Neuropilatlas und die Plastizität des Gehirns von *Tribolium castaneum*), sowie von der Examensarbeit von H. Vitt (Vitt H. [2008] Neuroarchitektur und Neurochemie des Gehirns des roten Reismehlkäfers *Tribolium castaneum*), welche in der Arbeitsgruppe Schachtner / Tierphysiologie / Biologie / Philipps Universität Marburg angefertigt wurden.

Kapitel 2:

Der Zentralkomplex der Insekten als Modell für Heterochronie in der Gehirnevolution - Hintergrund, Konzepte und Werkzeuge

Originaltitel: The insect central complex as model for heterochronic brain development - background, concepts, and tools

- Anfertigung der Textteile für Anatomie und Immunhistochemie des Manuskriptes, welcher weiterhin in einem iterativen Prozess zusammen mit Prof. Dr G. Bucher, Prof. Dr. J. Schachtner und mit Unterstützung von Dr. W. Hütteroth überarbeitet wurde.
- Anfertigung von ca. 50 % der Abbildungen.
- Anfertigung von ca. 90 % aller immunhistochemischen Präparate der Larven Inklusive der konfokalmikroskopischen Scans und 100 % der 3D-Rekonstruktionen sowie Identifikationen der Neuropile und Vergleich mit den korrespondierenden Färbungen der adulten Tiere.
- Dieses Kapitel wurde in der vorliegenden Form im Journal "Development Genes and Evolution“ veröffentlicht:
  Koniszewski N.D.B.*, **Kollmann M.***, Bigham M., Farnworth M., He B., Büscher M., Hütteroth W., Binzer M., Schachtner J., Bucher G. (2016) The insect central complex as model for heterochronic brain development - background, concepts, and tools. Development Genes and Evolution. 1-11.
- Die Charakterisierung von zwei der in dieser Arbeit vorgestellten transgenen Linien (G11410 und Glie-Blau"-Linie) war Bestandteil der Promotion von N.D.B. Koniszewski (Koniszewski N.D.B. [2011] Functional analysis of embryonic brain development in *Tribolium castaneum*), welche in der Arbeitsgruppe Bucher / Entwicklungbiologie / Biologie / Georg-August- Universität Göttingen angefertigt wurde.

Kapitel 3:

Morphologische und transcriptomische Analysen des chemosensitiven Systems eines Käfers zeigen ein olfaktorisches Zentrum im Unterschlundganglion

Originaltitel: Morphological and Transcriptomic Analysis of a Beetle Chemosensory System Reveals a Gnathal Olfactory Center

- Anfertigung von ca. 40% des initialen Textes des Manuskriptes, welcher weiterhin in einem iterativen Prozess (inklusive der restlichen 60 % des Manuskriptes) zusammen mit Prof. Dr. E.A. Wimmer, Prof. Dr. J. Schachtner und S. Dippel überarbeitet wurde.
- Anfertigung von ca. 95 % Abbildung des morphologischen Teils.
- Konzipierung der Versuche für die elektronenmikroskopische Untersuchung der Antenne, sowie die Betreuung der dazugehörigen Präparationen und deren Scans. Durchführung der Präparationen und Scans erfolgten von S. Frank.
- Charakterisierung und Beschreibung der Sensillen und ihre statistische Auswertung.
- Anfertigung aller konfokalmikroskopischen Scans der immunhistochemischen Färbungen der Schnitte der Antennen und Mundwerkzeuge. Ca. 90 % der Charakterisierung und Beschreibung der dadurch erhobenen Daten.
- Anfertigung von ca. 75 % der Backfills der Antennen und Mundwerkzeuge. Betreuung und Projektkonzipierung von den restlichen ca. 25 % der Backfills im Rahmen von Lehrveranstaltungen oder in Zusammenarbeit mit S. Dippel. Anfertigung von ca. 85 % der konfokalmikroskopischen Scans der Backfills. Ca. 90 % der Charakterisierung und Beschreibung der durch die Backfills erhobenen Daten.
- Anfertigung von ca. 50 % der Farbstoffinjektionen in die Antennalloben. Anfertigung von 100 % der konfokalmikroskopischen Scans dieser Farbstoffinjektionen. Ca. 80 % der Charakterisierung und

Beschreibung der dadurch erhobenen Daten.
- 100 % der Identifikation, der auf Volumendaten basierenden Zählung und statistische Auswertung der Kenyonzellen der Pilzkörper.
- Anfertigung von 40% der 3D-Reonstruktioennen der Antennalloben zur Bestimmung der Anzahl der Glomeruli und 100 % der dazugehörigen statistischen Auswertung.
- Dieses Kapitel wurde in der vorliegenden Form am 12 Mai 2016 im Journal "eLife“ *re-submitted*.

Kapitel 4:

Das Neuropeptidom des Antennallobus und Pilzkörpers von *Tribolium castaneum*

Originaltitel: The neuropeptidome of *Tribolium castaneum* antennal lobes and mushroom bodies

- Anfertigung des initialen Textes zu den Spezifikationstests und zu weiten Teilen der Neuropeptide Inotocin und ACP. Diese Textteile wurden weiterhin (inklusive des restlichen Teils des Manuskriptes) in einem iterativen Prozess zusammen mit M. Binzer, Dr. C.M. Heuer und Prof. Dr. J. Schachtner überarbeitet.
- Anfertigung von ca. 50 % der Spezifikationstests der Peptidantikörper. Betreuung und Projektkonzipierung der restlichen 50 % der Spezifikationstests im Rahmen von Lehrveranstaltungen.
- Erste Anwendung und Titrationen von 3 der 8 verwendeten Peptid-Antikörper, sowie "Optimierung" deren immunhistochemischer Färbeprotokolle.
- Anfertigung von immunhistochemischen Färbungen für die Neuropeptide Inotocin und ACP, sowie die Projektkonzipierung und Betreuung selbiger Färbungen im Rahmen von zwei Bachelorarbeiten von C. Knoll und von D. Lam (Im Fall von D. Lam in Zusammenarbeit mit M. Binzer).
- Dieses Kapitel wurde in der vorliegenden Form im Journal "Journal of Comparative Neurology“ veröffentlicht:
  Binzer M., Heuer C.M., **Kollmann M.**, Kahnt J., Hauser F., Grimmelikhuijzen C.J.P., Schachtner J. (2013) The neuropeptidome of *Tribolium castaneum* antennal lobes and mushroom bodies. Journal of Comparative Neurology. 522:337-357.
- Immunhistochemische Färbungen mit Antikörpern gegen die Neuropeptide Inotocin und ACP wurden von C. Knoll und von D. Lam im Rahmen ihrer Bachelorarbeiten (Knoll C. [2012] Immunohistochemical localization of insulin-like peptides, ACP and Inotocin in the nervous system of *Tribolium castaneum*; Lam D. [2014] Immunohistochemical localisation of insulin-like peptides, ACP and inotocin in the developing brain of the red flour beetle *Tribolium castaneum*) in der Arbeitsgruppe Schachtner / Tierphysiologie / Biologie / Philipps- Universität Marburg angefertigt.
  Teile ihrer Rohdaten wurden genutzt um die Interpretation der Färbemuster des Inotocin und ACP Antikörpers für die Veröffentlichung / diese Kapitel zu verbessern.

Kapitel 5:

Neuropeptide in den Pilzkörpern von Insekten

Originaltitel: Neuropeptides in insect mushroom bodies

- Anfertigung von ca. 33 % des initialen Textes des Manuskriptes, welcher weiterhin in einem iterativen Prozess (inklusive der restlichen 67 % des Manuskriptes) zusammen mit Dr. C.M. Heuer und Prof. Dr. J. Schachtner überarbeitet wurde.
- Ca. 80 % der Literaturrecherche bezüglich der zitierten Peptid-Antikörperfärbungen in anderen Spezies.

- Anfertigung von ca. 25 % der Präparate.
- Anfertigung von ca. 75 % konfokalmikroskopischen Scans.
- Anfertigung von ca. 75 % der Abbildungen, die in einem iterativen Prozess (inklusive der restlichen 25 % der Abbildungen) zusammen mit Dr. C.M. Heuer überarbeitet wurden.
- Auswertung und Interpretation von ca. 75 % der Daten (der konfokalmikroskopisch gescannten Daten und den Literaturdaten der anderen Spezies).
- Dieses Kapitel wurde in der vorliegenden Form im Journal "Arthropod Structure and Development“ veröffentlicht:
  Heuer C.M*., **Kollmann M*.**, Binzer M., Schachtner J. (2012) Neuropeptides in insect mushroom bodies. Arthropod Structure and Development. 41:199-226.

Kapitel 6:

Die Entdeckung eines neuen Insekten Neuropeptid-Signal-Systems, nahe verwandt zu dem Signal-System der Hormone Adipokin und Corazonin

Originaltitel: Discovery of a Novel Insect Neuropeptide Signaling System Closely Related to the Insect Adipokinetic Hormone and Corazonin Hormonal Systems

- Anfertigung aller initialen Textabschnitte über Immunhistochemie und Neuroanatomie (Material und Methoden sowie Ergebnisteil), welche von Prof. Dr. J. Schachtner überarbeitet wurden.
- Anfertigung aller Präparationen, immunhistochemischer Färbung sowie konfokalmikroskopischer Scans der Antikörperfärbungen.
- Dieses Kapitel wurde in der vorliegenden Form im Journal "The Journal of Biological Chemistry“ veröffentlicht:
  Hansen K.K., Stafflinger E., Schneider M., Hauser F., Cazzamali G., Williamson M., **Kollmann M.**, Schachtner J., Grimmelikhuijzen C.J. (2010) Discovery of a novel insect neuropeptide signaling system, closely related to the insect adipokinetic hormone and corazonin hormonal systems. The Journal of Biological Chemistry. 285:10736-10747.
- Die angefertigten immunhistochemischen Präparate / Scans, welche von mir im Rahmen dieses Projektes angefertigt wurden, sind auch Bestandteil der Dissertationen von K.K. Hansen und E. Stafflinger (K.K. Hansen [2011] Discovery of Novel Neuropeptide Signaling Systems in Arthropods; Angefertigt in der Arbeitsgruppe Grimmelikhuijzen / Bereich für Zellbiologie und Neurobiologie / Institut für Biologie / Universität von Copenhagen / Denmark) (E. Stafflinger [2009] The characterization of new hormonal systems in arthropods with focus on neuropeptide GPCRs; Angefertigt in der Arbeitsgruppe Grimmelikhuijzen / Bereich für Zellbiologie und Neurobiologie / Institut für Biologie / Universität von Copenhagen / Denmark).

Kapitel 7:

Eine neuartige Antennallobus-Struktur im kleinen Beutenkäfer *Aethina tumida*

Originaltitel: Novel antennal lobe substructures revealed in the small hive beetle *Aethina tumida*

- Anfertigung des initialen Textes des Manuskriptes, welcher weiterhin in einem iterativen Prozess zusammen mit Prof. Dr. J. Schachtner überarbeitet wurde. Unterstützung erfolgte durch Prof. Dr. P. Neumann und Dr. W. Huetteroth.
- Anfertigung von ca. 66 % der Abbildungen.

- Anfertigung von ca. 33 % der Präparationen, immunhistochemischen Färbungen und ca. 15 % der konfokalmikroskopischen Scans.
- Betreuung, Anleitung und teilweise praktische Unterstützung für die Auswertung der Daten im Rahmen der Diplomarbeit von A. Rupenthal.
- Anfertigung der 3D-Rekonstruktion des Gehirns.
- Dieses Kapitel wurde in der vorliegenden Form im Journal "Cell und Tissue Research“ veröffentlicht: **Kollmann M.**, Rupenthal A., Neumann P., Huetteroth W., Schachtner J. (2016) Novel antennal lobe substructures revealed in the small hive beetle *Aethina tumida.* Cell and tissue research. 363:679-692.
- Die Auszählung der Glomeruli und deren Untereinheiten, 3D-Rekonstruktion der Glomeruli und deren Untereinheiten, die Bestimmung deren Volumen und deren statistische Auswertung, wurden von A. Rupenthal im Rahmen ihrer Diplomarbeit erhoben (Rupenthal [2012] Anatomische und immuncytochemische Untersuchungen am olfaktorischen System des kleinen Beutenkäfers *Aethina tumida*), welche sie in der Arbeitsgruppe Schachtner / Tierphysiologie / Biologie / Philipps Universität Marburg anfertigte. Ihre Daten wurden für die Veröffentlichung / diese Kapitel überarbeitet.

Kapitel 8:

Variationen über ein Thema: Antennallobus Architektur der Coleoptera

Originaltitel: Variations on a theme: antennal lobe architecture across Coleoptera

- Anfertigung des initialen Textes des Manuskriptes, welcher weiterhin in einem iterativen Prozess zusammen mit Dr. M. Heuer und Prof. Dr. J. Schachtner überarbeitet wurde.
- Anfertigung aller Abbildungen.
- Anfertigung von ca. 85 % der Präparationen, ca. 50 % der immunhistochemischen Färbungen, ca. 90 % der 3D Rekonstruktionen und 100 % der konfokalmikroskopischen Scans von den Käfergehirnen. Vollständige Präparation, immunhistochemischen Färbung und Scanns der Gehirne der Wanzen und Grillen.
- Auszählung der Glomeruli von ca. 50 % aller ausgewerteten Spezies.
- Dieses Kapitel wurde in der vorliegenden Form am 19 Juni 2016 im Journal " POLS Biology“ *submitted*
- Immunhistochemische Färbungen und Untersuchungen an 21 Käferarten, 3D-Rekonstruktionen von Gehirnen von 7 Käferarten, sowie die Hälfte der Auszählung der Glomeruli wurden von R. Nothvogel im Rahmen ihrer Bachelor und Masterarbeit (Schmidt R. [*geborene Nothvogel*] [2013] Vergleichende Neuroanatomie der Coleoptera im ökologischen Kontext; Nothvogel R. [*geborene Nothvogel*] [2015] Neuroanatomie der Coleoptera im Ökologischen und Evolutionären Kontext II) in der Arbeitsgruppe Schachtner / Tierphysiologie / Biologie / Philipps- Universität Marburg durchgeführt.

[*Equal contribution]

In der angehangenen CD befinden sich die jeweiligen Kapitel als PDF, bzw. DOCX Datei. Im Fall von bereits veröffentlichten Publikationen (Kapitel 1, 2 und 4-7) sind die digitalen Anhänge der CD hinzugefügt. Im Fall von bisher noch nicht veröffentlichten Kapitel (Kapitel 3 und 8) befinden sich neben den digitalen Anhängen auch die jeweiligen Abbildungen in hochauflösender Qualität.

Ich versichere, dass ich meine Dissertation

"The olfactory pathway of the red flour beetle *Tribolium castaneum* and its comparison to other Coleoptera"

(Die Riechbahn des Rotbraunen Reismehlkäfers *Tribolium castaneum* und ein Vergleich zu anderen Käfern)

selbstständig, ohne unerlaubte Hilfe angefertigt und mich dabei keiner anderen als der von mir ausdrücklich bezeichneten Quellen und Hilfen bedient habe.

Die Dissertation wurde in der jetzigen oder einer ähnlichen Form noch bei keiner anderen Hochschule eingereicht und hat noch keinen sonstigen Prüfungszwecken gedient.

_____ _____

(Marburg, den) (Martin Kollmann)

Danksagung

Zunächst möchte ich meinen Dank all den Leuten aussprechen, die maßgeblich dafür verantwortlich sind, dass diese Dissertation in dieser Form vorliegt.

Als allererstes möchte ich Prof. Dr. Joachim Schachtner danken, der mir die Möglichkeit gab, an diesem interessanten Projekt zu arbeiten und es mir ermöglichte, das Projekt frei zu gestalten. Ferner möchte ich mich bei ihm dafür bedanken, dass er sich stets ausreichend Zeit für meine Anliegen nahm.

Zusätzlich will ich mich bei den weiteren (ehemaligen) Arbeitsgruppenleitern des Fachgebiets Tierphysiologie - Neurobiologie/Ethologie bedankenden. Prof. Dr. Uwe Homberg, Dr. Pfeiffer und Prof. Dr. Christian Wegener waren stets äußerst hilfsbereit und standen mir immer mit ihrem umfangreichen Wissen mit Rat und Tat zur Seite, wenn ich Fragen an sie hatte.

Bei Prof. Dr. Monika Hassel möchte ich mich wegen der Zweitkorrektur bedanken und dass sie während meines Grundstudiums und meines Diploms stets mein Interesse an der organismischen, zoologischen Biologie weckte.

Ich bedanke mich bei allen Kolleginnen und Kollegen die mich während meiner Promotion (und auch in der vorherigen Zeit) begleiteten und mir stets fachlich bzw. freundschaftlich zur Seite standen und mich unterstützen. Namentlich hervorheben will ich hier Anna Reifenrath, Basil el Jundi, Björn Trebels, Carsten Heuer, Daniela Schumacher, Fabian Schmeling, Joss von Hadeln, Marlene Binzer, Max Diesner, Peter Christ, Sergius Frank, Stefan Ries, Wencke Reiher und Wolf Hütteroth. Besonders hervorheben möchte ich an dieser Stelle Stefan Dippel, welcher mich bereits seit meinen Anfängen in der Arbeitsgruppe Schachtner begleitete und auch später an vielen Kooperationsprojekten beteiligt war. Er war mir stets ein guter Kollege und Freund, der mir sowohl fachlich als auch freundschaftlich immer beistand und ohne dessen Einsatz und Engagement die Erforschung des Geruchssystems von *Tribolium castaneum* undenkbar gewesen wäre.

Ich bedanke mich bei der technischen Assistentin Martina Kern, ohne die ein reibungsloses arbeiten im Labor nicht möglich gewesen wäre und dafür, dass sie bei meinen Proben so häufig Waschschritte übernahm und die Antikörper (oder Vergleichbares) wechselte und immer ein offenes Ohr für fachliche und andere Probleme hatte.

Ich bedanke mich bei all den vielen Personen, welche mir die jeweiligen Antikörper, Peptide und Versuchstiere zur Verfügung stellten und in den jeweiligen Kapiteln alle namentlich Erwähnung finden.

Ich bedanke mich weiterhin bei all meine Freunden innerhalb und außerhalb der Fachbereichs, bzw. außerhalb der Uni (insbesondere) in Marburg, Kassel und Gießen, welche den "nicht-akademischen Teil" meiner letzten Jahre bereicherten.

Schlussendlich will ich mich besonders bei meinen Eltern bedanken die mich stets unterstützen und ohne dessen Beistand ich nicht meine akademische Laufbahn hätte einschlagen können. Weiterhin entschuldige ich mich an dieser Stelle bei ihnen dafür, dass sie meine "sonderbaren Marotten" in den späteren Phasen meiner Promotion ertragen mussten.

Aim of the thesis

Insects are the most successful animals on earth. They have a great impact on almost all terrestrial ecosystems, affecting mankind by beneficial and harmful ways like facilitating vast amounts of human food production via pollination or by being a devastating pest to agricultural products and food stocks as well as spreading diseases. Among insects, Coleoptera are the most divers and species richest order, containing vast quantities of pest species.

The majority of insects depends heavily on their olfactory system to master most tasks they encounter during their lifespan, like finding food sources, hosts, native populations, and mates, or to avoid predators. Despite the diversity and species richness of beetles, as well as their impact as pest, not much is known about the olfactory system of these animals.

To investigate the olfactory system of Coleoptera, we analyzed 1) the olfactory pathway of one model organism in highly detail and 2) we examined particular brain regions of the olfactory system of many beetles and insects and compared them with each other.

1: For the highly detailed analysis of the olfactory pathway of one species we worked with the red flour beetle *Tribolium castaneum*, an already established model organism in some fields of biology like in development and evolution. Experiments requiring genetic methods had been performed in cooperation with the Georg-August-Universität Göttingen. Based on immunohistochemical stainings we created 3D-reconstructions of adult and larval brains, helping us to identifying the most prominent brain structures, as a starting point for following projects. On this basis, we decrypted the olfactory pathway of the adult *T. castaneum*. This includes A) morphological data of the antenna with its olfactory sensilla and neuroanatomical data of the brain structures involved in olfaction, as well as B) molecular data from antennal structures involved in olfaction (like olfactory respectively gustatory receptors or olfactory binding proteins). Furthermore, we identified neuropeptide families within the primary and one higher integration center for olfaction - namely the antennal lobe (AL) and mushroom body (MB) - of *T castaneum*. Additionally, we investigated one neuropeptide family and its respective receptor within the brain of *T. castaneum* in detail. We compared this neuropeptide family and its receptor with two structurally similar and closely related neuropeptide families and their receptors.

2: The second focus of this thesis was the investigation of single features of the olfactory pathway and their comparison between different coleopteran-, respectively insect species. In one project we studied the distribution of eight neuropeptide families within the MB of 24 different insect species and compared them with each other, looking for potential evolutionary correlations. Furthermore, we analyzed the AL of 63 different Coleoptera and found an unusual architecture of the AL in some species. In a related project we investigated such an unusual architectured AL of one species (the small hive beetle *Aethina tumida*) highly detailed.

In this thesis, the brain architecture and especially the olfactory system of Coleoptera had been investigated for the first time in high detail. We revealed new insights regarding the olfactory (respectively chemoreceptive) pathway of these animals. The findings will help to establish *T. castaneum* as the fist coleopteran model organism for insect neuroscience and in particular for insect olfaction.

The single projects of this thesis will be described in-depth in the following eight chapters.

General introduction

The Impact of insects

Insects exist for at least 400 million years. Since then they invaded and adapted to all terrestrial ecological niches. Thereby they had become the species richest and most diverse class on earth, reflected by most different morphologies, lifestyles, and behaviors. Rendering them as the most successful and dominating class in the animal kingdom (Grimaldi and Engel, 2005). From the about 1.4 million described recent animal species, approximately 70% are insects (Chapman, 2009). By performing tasks like pollination, maintaining soil structure and fertility, dispersing seeds, decomposition of detritus, and providing vast amounts of animal protein in the early stages of most terrestrial food webs they are an essential, biological basis for all terrestrial ecosystems and thereby have dramatic effects on world's ecological systems (Carpenter, 1928; Majer, 1987; Shurin et al., 2005).

I**nsect's impact on humans**: For us humans, insects have particular effects on the economy, food supply, agriculture, and health care system. Insects pollinate crops and other food items, they help to maintain the quality of grazing land, controlling pests, and they are providing merchandise like honey, shellac, cochineal, silk, or wax (Glover, 1867; Konishi and Ito, 1973; Waterhouse, 1974; Sheppard, 1989; Shimanuki, 1992; Metcalf and Metcalf, 1993; New, 1994; Hoebeke and Beucke, 1997; Morse and Calderone, 2000; Losey and Vaughan, 2006). On the other hand they cause serious threats for mankind by being a major pest for agricultural and stored food products and by spreading disease for humans and life stock.

Insects and agriculture: Insects damage huge amounts of agricultural products before harvesting as well as stored agricultural and processed food products (Altieri and Nicholls, 2004). More than 400,000 of the 1.4 million described insect species are herbivores (New, 1988), of which most are Coleoptera and Lepidoptera, making insects to our most important competitors for plant derived foods. Insects destroy annually agricultural products worth hundreds of billions of dollars, while invasive species threaten to cause economic losses worth trillions of dollars, making pest control a multibillion dollar market (Perlak et al., 1993; Metcalf and Luckmann, 1994; Cox, 1999; Nowak et al., 2001; Myers and Hosking, 2002; Simberloff, 2003; Altieri and Nicholls, 2004; Hood, 2004; Muirhead et al., 2006; Müller et al., 2008; Foottit and Adler, 2009; Safranyik et al., 2010; Priceet al., 2011; Fera, 2012; Stadelmann et al., 2013; Seidl et al., 2014).

Uprising global civilization (Gerland et al., 2014), increasing demands of meat consumption in BRIC states (containing almost half of the world's population) (Henderson, 2011; Ciochetto, 2013; Vlad et al., 2011), and the uprising market for biofuels (Mitchell, 2008; Rosegrant, 2008), caused by dwindling oil reserves (British Petroleum, 2014) will elevate our needs for more suitable agricultural products. Therefore effective pest management will be of huge significance in the near future and one key for such a pest management is the insect olfactory system (Howse et al., 1998; Witzgall et al., 2010; Zhou et al., 2010).

Disease-carrying insects: Insects are also the vectors for plenty diseases for humans like malaria, typhus, chagas, and yellow and dengue fever, (http://www.who.int/mediacentre/factsheets/fs387/en/; accessed 2015.11.11) as well as for livestocks like swamp fever, bluetongue disease, African horse sickness, Venezuelan equine encephalitis, or cattle grubs heel flies (Steelman, 1976; Hungerford, 1990). Comparable to the agricultural pest management, the olfactory system of insects is considered to be a keystone in management of disease-carrying insects (Justice et al., 2003; Carey and Carlson, 2011).

Orientation mechanisms in insects

Animals have to orientate for plenty reasons, to find food/pray, mating partners, oviposition or nesting sides, shelter, and to avoid predators, or

dangerous environments (Lehrer, 1997). Therefore animals have to have sense organs, allowing them to get a proper neuronal representation of its surrounding to orientate towards or against an object, target, or obstacle.

The orientation senses can be divided into two basic types, senses primarily for near and for wide field orientation. Prominent senses for near field orientation in insects are the tactile sense and gustation (Singh, 1997; Krause and Dürr, 2001). The visual system can be used effectively for orientation over long distances / migration via sky compass orientation, via chromatic and intensity gradients at the horizon, or via celestial landmarks like the milkyway or the moon (Sotthibandhu and Baker, 1979; Wehner et al., 1996; Gould, 1998; Homberg, 2004; Dackeet al., 2013; El Jundi et al., 2014). However, biased on low special / angular resolution and the missing ability of focusing, it is rather difficult to use the visual system for orientation toward an object in far distance (Wehner and Gehring, 1995; Dettner and Peters, 2011). Prominent senses for wide field orientation are e.g. the acoustic sense primarily used for acoustic communication (chiefly to attract mating partners) or for acoustic recognition of predators (most prominently against echolocating bats) (Hedwig, 2013; Göpfert and Hennig, 2015). The most imported senses for wide field orientation (towards an object) in most insects is considered to be the olfactory senses, allowing insects to detect objects in long-range distance, even if direct side is blocked (Lehrer, 1997; Schütz et al., 1999; Angioy et al., 2003). This makes the understanding of the insect olfaction to an important key for an effective management of disease-carrying and pest insects (Howse et al., 1998; Justice et al., 2003; Witzgall et al., 2010; Zhou et al., 2010; Carey and Carlson, 2011).

The olfactory system of insects

For the majority of insects, olfactory cues are vital for most tasks they encounter during their life history. Airborne volatiles can guide insects over a long distance to food sources, hosts, native populations, and mating partner, or to avoid predators (Borden, 1985; Visser, 1986; Scrimgeour et al., 1994; Abjörnsson et al., 1997; Tegoni et al., 2004; Dahanuka et al., 2005; Whiteman and Pierce, 2008; de Bruyne et al., 2010; Herbst et al., 2011; Leal, 2013). Over much shorter distances olfactory (as well as gustatory) cues can be used to distinguish between different food qualities, to avoid toxins or harmful substances; to differentiate between more or less suitable mating partners, to communicate intra- or interspecifically, and to find the best spot at a proper ovipositon site (Laska et al., 1999; Johansson and Jones, 2007; Liu et al., 2008; Whiteman and Pierce, 2008; Yang et al., 2008; Dicke, 2009; Weiss et al., 2011; Stensmyr et al., 2012; Sun et al., 2012; Linz et al., 2013; Paczkowski et al., 2014). The insect's olfactory sense can give the animals detailed information of odor identity, intensity and spatiotemporal distribution (Hansson et al., 1992; Hansson, 1995; Christensen et al., 1996, 2000; Hansson and Christensen, 1999; Vickers et al., 2001). For example, even less than six odor molecules, hitting the antennae of the moth *Spodoptera littoralis* triggered a behavior by altering the cardiac activity (Angioy et al., 2003).

The antenna and its morphology

The signal perception of the olfactory pathway starts at the surface of the antenna, the main odor perceiving organ in insects (von Frisch, 1921). There are two principal types of antenna found in Hexapoda (Schneider, 1964). The fist type is the segmented antenna which possesses several segments, with comparable design and muscles in all segments save the most distal segment. In Hexapoda this type can be found in Collembola and Diplura. The second type, found in the rest of the Hexapoda, is the flagellar antenna (annulated antennae) which can be separated in substructures: the scape, pedicel, and a flagellum (from proximal to distal), while the flagellum can be further subdivided in different segments. This antenna type has only muscles in the scape (Imms, 1938; Dettner and Peters, 2003).

The shape of the flagellum, which can vary tremendously between different species (Fig. 1), is adapted to the lifestyle of the animal (such as scavenging or soil-dwelling) (Seifert, 1995; Hansson

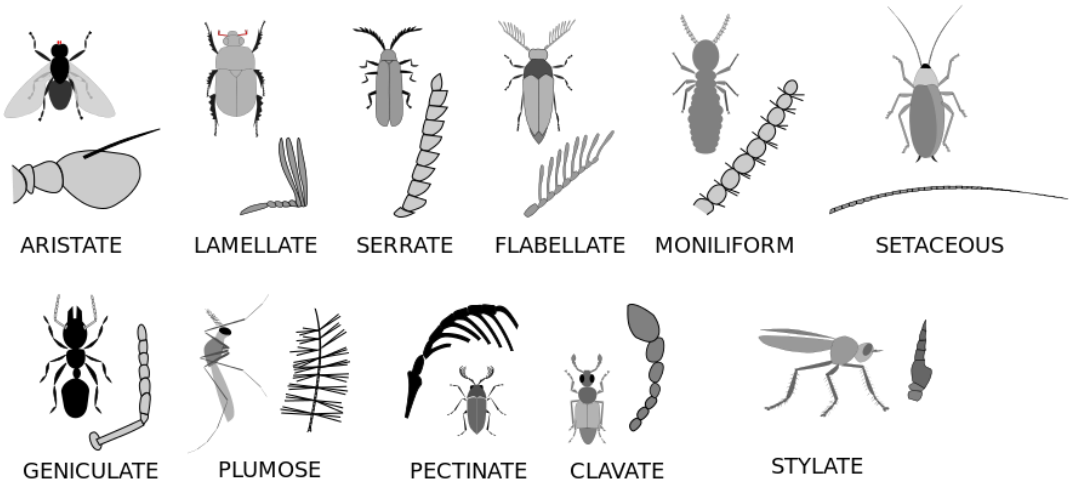

Fig. 1: Shapes of different antenna types found in insects. The varieties of shapes range from less segmented types (aristate and stylate), to types with many segmentations (like clavate or geniculate), sometimes with additional arborization (like plumose or flabellate) increasing the surface of the antenna and thereby enable the antenna to bear more sensilla. From https://en.wikipedia.org/wiki/Antenna_(biology) [accessed 2015.08.29].

and Stensmyr, 2011). Typically, the surface of the antenna is enlarged by elongation, thickening, branching, faulting, feathering, or similar modifications to give more space for sensilla (Imms, 1938). Example given, the antenna of the male silk moth *Bombyx mori* is less than 10 mm long, but because of its multiple branching, its surface is about 24 - 29 mm² (Schneider and Kaissling, 1957; Steinbrecht, 1970). However, more ancestral Hexapoda have antennae with fewer olfactory sensilla (Misof et al., 2007; Rebora et al., 2008) and Collembola and Diplura have antenna with huge flexibility of movement (based on the musculature throughout their antennae) (Schneider, 1964), indicating that insect antennae might have evolved from structures that mainly mediated mechanosensory input (Hansson and Stensmyr, 2011).

The olfactory sensilla

Along with sensilla suitable for tasks like gustation, hygroscopy, mechanoreception, and thermoreception, the insect antenna houses the olfactory sensilla. All or just same parts of the antenna are covered - to various extents - with olfactory sensilla (Schneider and Kaissling, 1957; Stocker, 2001; Misof et al., 2007; Rebora et al., 2008). The olfactory sensilla have a wide range of shapes, structures, and thereby classification (Schneider, 1964; Schneider and Steinbrecht, 1968; Altner, 1977; Steinbrecht, 1997). Typically, they occur in the form of pegs, hairs, or plates (Altner and Prillinger, 1980). Despite their variations in shape and structure they have the same function, to enclose und shield the sensitive dendrites of the olfactory sensory neurons (OSN), which detect the odor molecules (Zacharuk, 1980).

Olfactory sensilla at the mouthparts: Beside the antenna, olfactory sensilla have been described also on the maxillary and/or the labial palps of some taxa like Diptera (Anton et al., 2003; Jones et al., 2007; Kwon et al., 2007, Lu et al., 2007; Syed and Leal, 2007; Vosshall and Stocker, 2007; Pitts et al., 2011; Maeda et al., 2014; Rinker et al., 2015) and Lepidoptera (Lee et al., 1985; Bogner et al., 1986; Kent et al., 1986, Lee and Altner, 1986; Zhao et al., 2013), presumably contribution to the proper perception of olfactory stimuli.

The ultrastructure of the sensilla: The external structure of olfactory sensilla consist of a sclerotized cuticle (Schneider, 1964). To overcome this barrier and to reach the OSN, air borne odor molecules have to pass the cuticle via pores, which can be found at various regions of the sensilla. Typically, such a pore consist of a deepening (the pore kettle), which branches into various pore tubules, extending into the lumen of the sensilla (Fig. 2 A and B) (Ernst, 1969; Keil, 1987; Steinbrecht, 1997). The interior of an olfactory sensillum is filled with aqueous sensilla lymph (liquor), preventing the dendrites of the OSN from

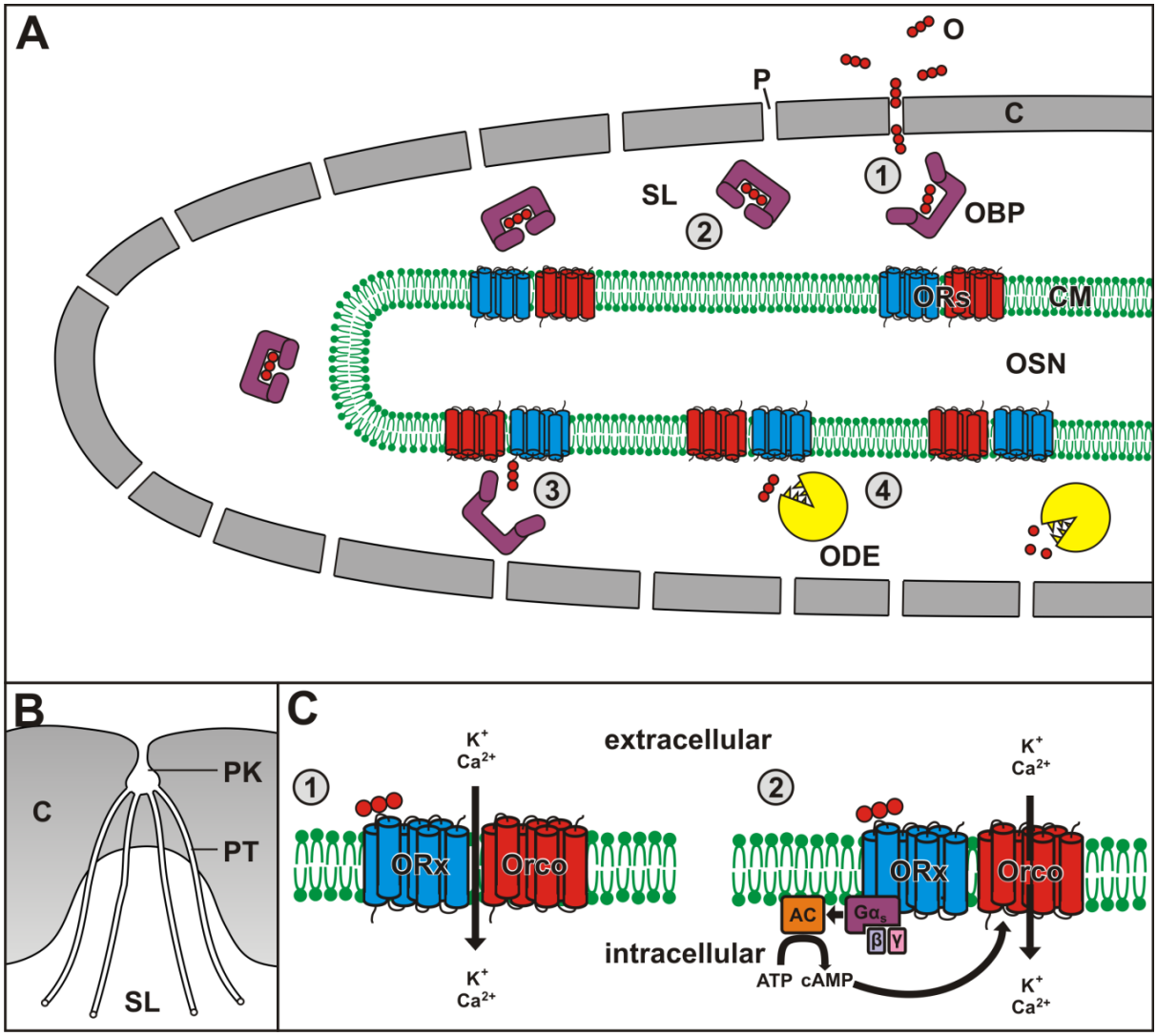

Fig. 2: A) Schematic drawing of the distal part of an insect olfactory sensillum. ① The odorants (O) can enter the sensillum via the pores (P) in the cuticle (C) and are bound by the odorant binding proteins (OBP) in the sensillar lymph (SL). ② The OBP carries the odorant to the odorant receptor (OR) embedded in the cell membrane (CM) of the olfactory sensory neuron (OSN). ③ In close proximity to the CM, the OBP release the odorant and it activates an OR. ④An odorant-degrading enzyme (ODE) degrades the odorant and thereby prevent the continuous excitation of the OSN. **B)** Schematic drawing of a pore in the cuticula (C) of the sensillum, consisting of the pore kettle (PK) separating into multiple pore tubes (PT), which terminating in the sensillum lymph (SL). **C)** There are two widespread models for odorant signalling pathways in insects: ① Ionotropic model: The ORx and the Orco functions together as an ion channel. ② Metabotropic model: The odorant activated specific odorant receptor (ORx) triggers via a G-protein ($G\alpha_s$ and the γ and β subunit) an adenylate cyclases (AC), which turns adenosintriphosphat (ATP) into cyclic adenosinmonophosphate (cAMP), which opens the general receptor (Orco), acting as an ion channel. A) Modified after Leal, 2013. B) Modified after Steinbrecht, 1997. C) Modified after Ha and Smith, 2009.

desiccation. Usually the OSN are associated with three different types of auxiliary cells, the trichogen, the tormogen, and the thecogen cells. During the development of an animal the hollow cuticular hair shaft and its inner sensillar lymph cavity is created by the trichogen and tormogen cells. This cells are capable to control the ion composition of the sensillum lymph and they produce vast amounts of odorant binding proteins (OBP) (Steinbrecht et al., 1992; Steinbrecht, 1998; Steinbrecht and Gnatzy, 1984; Keil, 1989). The thecogen cells envelope the soma and the basal part of the dendrites of the OSN, so that only the distal parts of the dendrite extends into the sensillum cavity (Schneider, 1964; Dettner and Peters, 2003; Stengl, 2010). The number of OSN per sensillum (and thereby also of the auxiliary cells) can vary among species (Starausfeld and Lee, 1990; Shanbhag et al., 1999).

The odorant binding proteins (OBP)

In rare cases, the pore tubules of the sensilla extend directly onto the surface of the OSN (Lopes, 2002), but typically the hydrophobic airborne odor molecules have to pass the aqueous sensillum lymph to reach the OSN. To effectively pass the aqueous sensillar lymph, it is supposed that the hydrophobic odors have to interact with OBP. OBP can be separated into two groups, the male specific pheromone binding proteins (PBP) and the general odorant binding proteins (GOBP). OBP are secreted in high concentration into the sensillar lymph mainly by trichogen and tormogen cells (Steinbrecht and Gnatzy, 1984; Keil, 1989; Steinbrecht et al., 1992; Steinbrecht, 1998). They are small, water soluble, globular proteins (generally 135–220 amino acids long) (Vogt, 2003; Sánchez-Gracia et al., 2009) and the numbers of genes coding for OBP vary dramatically among different species (from 4 in *Pediculus humanus* to 81 in *Anopheles gambiae*) (Wang et al., 2014). The gene family of the OBP is presumably as old as insects themselves, most likely evolved as an adaptation to the living on land, that made detection of airborne odors necessary (Forêt and Maleszka, 2006; Vieira and Rozas, 2011). But it is important to note that the vertebrates' OBP belong to the lipocalin family that are not homologues to the insects' OBP (Bianchet et al., 1996).

Function of the OPB: The exact function of the OPB is yet not fully understood (Laughlin et al., 2008; Hansson and Stensmyr, 2011; Leal, 2013). A widely accepted hypothesis is that OBP function as carriers that bind and transport the odor/pheromone molecules to the dendritic membrane of the OSN (Fig. 2 A ① and ②), where they can interact with the OR (Fig. 2 A ③). How the binding proteins release the odorants at the OSN membrane is still under debate. This release mechanism is presumably facilitated by a pH-dependent conformational change of the binding protein (Rützler und Zwiebel, 2005; Leal, 2013). However, in *Drosophila melanogaster* still a low response to the pheromone could be measured, when its sensilla lack PBP (Syed et al., 2006). This indicates that the OBP, respectively the PBP contribute enormous to the sensitivity of the insect olfactory system, but that it is not crucial for the perception of odor.

The odorant-degrading enzymes (ODE)

ODE belong to the biochemically diverse classes of detoxification enzymes. They are secreted into the sensilla lymph (Chertemps et al., 2012) or they might be embedded into the OSN membrane (Maïbèche-Coisne et al., 2004). They degrade (Vogt et al., 1985) or modify (Rybczynski et al., 1989) (Fig. 2 A ④) the odors/pheromones with a turnover number ranging from k_{cat} = 0.4 to about 1500 s^{-1} (Younus et al., 2014) and thereby removing the odors/pheromones from the sensilla lymph. This prevents continuous excitation and sensory adaptation of the OSN by already detected odor molecules and enable the OR to be activated more likely by odor molecules which entered the sensilla more recently. This mechanism is an improvement of the temporal resolution of odor/pheromone detection and discrimination and allows the animal to swiftly respond to changes in the odor environment (Jacquin-Joly and Merlin, 2004; Durand et al., 2011; Younus et al., 2014).

Chemosensory neurons of the antenna

In the Insect antenna usually three receptor families are involved in chemoreception, namely the odorant receptors (OR), the ionotropic receptors (IR), and the gustatory receptors (GR) (Vosshall and Stocker, 2007; Gu et al., 2014; Leal, 2013; Missbach et al., 2014). The three types are usually not coexpressesed in the same neuron (Benton et al., 2009).

However, most insects investigated so far have more genes coding for OR, than for IR or GR. Also, the number of genes expressed within the antenna, coding for OR, is typically higher than the number of expressed genes for IR or OR (Dippel et al., submitted [chapter 3]; Vosshall and Stocker, 2007; Pitts et al., 2011).

The Odorant receptors (OR): The OR are embedded into the dendritic membrane of the OSN. OR are seven transmembrane-domain receptors. Compared to the G protein-coupled odorant receptors known from vertebrates, they have an inverted transmembrane topology (Benton et al., 2006; Lundin et al., 2007). An additional difference between the OR of vertebrates an

insects is that insect OR form functional heteromers, typically consisting of a ligand-binding OR (also called tuning receptor or specific receptor and often abbreviated as ORx) and a general odorant receptor, the so-called odorant receptor co-receptor (Orco). (Vosshall et al., 2000; Larsson et al., 2004; Sato et al., 2008; Wicher et al., 2008; Smart et al., 2008; German et al., 2013; Mukunda et al., 2014). In all Insecta investigated so far, one Orco could be identified (with exception of the ancestral hexapoda *Thermobia domestica*, which posess three Orco candidates [Missbach et al., 2014]).

Originally, Orco had been termed different in different species (e.g. OR83b in *D. melanogaster* or OR1 in *Tribolium castaneum*), but due to their similarity, they all had been recently renamed as Orco (Vosshall and Hansson, 2011). Beside their function as part of the heteromeric receptor complex, Orco plays a role as chaperone, necessary for the integration of the ligand-binding OR into the dendritic membrane of the OSN (Larsson et al., 2004).

The OR genes, coding for the ligand-binding OR (ORx) are highly divergent within insects, while the genes, coding for Orco are highly conserved among insect species. Both - ORx and Orco - couldn't be found outside the Insecta (Nakagawa et al., 2012; Missbach et al., 2014). They are not homolog to the OR described in vertebrates and nematodes (Clyne et al., 1999, Vosshall et al., 1999). The number of genes can vary within the insecta, reaching from just 10 (in *P. humanus*: Kirkness et al., 2010) to several hundreds (as observed in *T. castaneum*: Dippel et al., submitted [chapter 3]). Beside Orco, each OSN expresses usually only one type of ORx. The molecular transduction mechanism of the Orco-ORx heteromers is still under debate, an ionotropic and a metabotropic mechanism is postulated (Sato et al., 2008; Wicher et al., 2008; Smart et al., 2008; Ha and Smith, 2009; Martin and Alcorta, 2011; Getahun et al., 2013; Nolte et al., 2013; Stengl and Funk, 2013) (Fig. 2 C ① and ②).

Both models have advantages and downsides. In the ionotropic model, the molecular transduction mechanism works very fast, due to non additional signal transduction, allowing a high temporal resolution (Fig. 2 C ①). This would be beneficial for insects that fly through odor plumes in the air, trying to localize odorant sources. The metabotropic model on the other hand would lack such a high temporal resolution (Fig. 2 C ②), but based on the amplifier cascade of the effector enzymes that produces second messengers and the second messenger themselves, this model would possess a high sensitivity. Important for insects that have to detect (small/week) odorant sources over a far distance. These two models are not mutually exclusive and it is likely, that even in one species both models could be realized in different sensilla, different OSN, or maybe even within the same OSN (Sato et al., 2008; Smart et al., 2008; Wicher et al., 2008; Martin and Alcorta, 2011; Getahun et al., 2013; Nolte et al., 2013; Stengl and Funk, 2013; Guidobaldi et al., 2014).

Ionotropic receptors (IR): IR are much older than OR, they belong to the family of the ionotropic glutamate receptors (iGluRs), and they are a highly conserved family of ligand-gated ion channels embedded into the dendritic membrane of the OSN (Benton et al., 2009; Peñalva-Arana et al., 2009; Croset et al., 2010), where they supposedly form tetrameric complexes (Gu et al., 2014). IR can be found in the olfactory organs across all Protostomia (Croset et al., 2010), and seems to be conserved within insects (Gu et al., 2014; Rytz et al., 2013). IR are discussed to be the ancestral type of receptors important for chemical perception over a long distance. The number of genes coding for IR can vary within insects, ranging from 10 (in *Apis mellifera*) to 95 (in *Aedes aegypti*) (Croset et al., 2010).

Detailed data of this receptor type is mostly limited to *D. melanogaster*. In *D. melanogaster*, 16 of the 66 genes for IR are expressed in the dendrites of OSN in the antenna (Benton et al., 2009; Croset et al., 2010). OSN expressing IR can be found in high number in coeloconic sensilla, as well as in the arista and sacculus. The arista and sacculus are structures of the *Drosophila* antenna, beside olfaction, this structures are also involved in hygrosensory and thermosensory, but weather the IR are also involved in this functions remains unknown (Foelix et al., 1989; Shanbhag et al., 1995; Benton et al., 2009; Abuin et al., 2011; Gallio et al., 2011). The IR25a had also be indentified in

basiconic and trichoid sensilla in low concentration, however there function in this sensilla is unclear (Benton et al., 2009).

In comparison to OR, IR are normally not co-expressed with Orco. Only the IR76b is in one coeloconic sensilla subtype (ac3) co-expressed with OR35a and Orco. Apart from IR76b and in analogy to ORx and Orco, the IR are typically co-expressed with IR8a or IR25a, rendering this two IR as IR co-receptors. This two co-receptors could also be identified in the moth *Agrotis ipsilon* (Gu et al., 2014). The non co-receptor IR will be termed IRx in this introduction.

Usually, OSN expressing IR are less sensitive and less broadly tuned than OSN expressing OR and they detect other classes of odors than OSN expressing OR. Typically, OSN expressing the co-receptors IR8a mainly respond to carboxylic acids/aldehydes, while OSN expressing the co-receptors IR25a mainly respond to amines. Additionally IR in general responds usually little or not to esters, alcohols, and ketones (de Bruyne et al., 2001; Yao et al., 2005; Hallem and Carlson, 2006; Silbering et al., 2011, Getahun et al., 2012). However, in *A. ipsilon* one IR could only be identified exclusively in the male antenna (IR12), rendering this IR as an IR involved in detection of female sex pheromones (Gu et al., 2014).

Gustatory receptors (GR): Comparable to OSN express OR respectively IR, gustatory receptor neurons (GRN) express GR. But while OSN are typically more restricted to the antenna and partly to mouthparts, GRN could be identified at the antenna, mouthparts, legs, wings, and at the female ovipositor. They can be found in specific taste/gustatory sensilla like taste bristles or taste pegs. Apart from this external structures, GRN have also been observed within the pharynx (Dahanukar et al., 2005; Vosshall and Stocker, 2007).

The number of genes coding for GR can vary within insects, ranging from 53 in *A. mellifera* (Wang et al., 2014) to 220 in *T. castaneum* (Dippel et al., submitted [chapter 3]). GR are a divergent group of receptors, distantly related to OR (Robertson et al., 2003). GR are mainly important for perception of sweet (Dahanukar et al. 2001, Dunipace et al. 2001, Wang et al. 2004) and bitter (Dunipace et al. 2001, Wang et al. 2004) taste, but they also supposed to be involved in thermotaxis (Montell, 2013).

Beside GR, GRN express additional receptors for taste perception like degenerin/epithelial sodium channel (DEG/ENaC) for the taste of salt (Vosshall and Stocker, 2007).

Of particular interest for olfaction are the CO_2 receptive GR, indentified in several insect species (Robertson and Kent, 2009). Neurons expressing such GR are often classified as OSN. However, in *D. melanogaster* OSN detecting CO_2 express two GR (Gr21a and Gr63a) (with paraloges identified in other species [Robertson and Kent, 2009]). In *D. melanogaster*, Gr21a and Gr63a forming a heterodimer, important for proper CO_2 perception (Jones et al., 2007). In *D. melanogaster*, the CO_2 receptive OSN are located in antennal sensilla (Suh et al., 2004; Benton et al., 2006; Faucher et al., 2006) and projecting in a single glomerulus of the AL, not innervated by OSN expressing other OR and/or GR (Vosshall and Stocker, 2007).

Similar observations of AL innervation of CO_2 receptive OSN had been made in Lepidoptera, there the CO_2 percepting OSN are located in the palps und projecting into a single AL glomerulus (Kent et al., 1986), comparable to the mosquito *Ae. aegypti* (Distler and Boeckh, 1997) and *An. gambiae* (Anton et al., 2003).

The antennal lobes (AL) and their glomeruli

The OSN axons of the antenna form the antennal nerve (AN), that projects towards the brain and enters typically the ipsilateral of the paired AL. The AL are the fist olfactory integration centers of the insect brain (Fig. 3). Typically, they consists of small, spherical substructures, the so-called olfactory glomeruli, the functional units of the AL. These glomeruli are dense synaptic neuropils, more or less enwrapped by glia (Schachtner et al., 2005; Hansson and Stensmyr, 2011). Within most Insecta, usually about 40 to 80 glomeruli can be found, e.g., in the ensiferan Orthoptera, and Diptera, but much more - up to 500 - had been described in several species like in ants (Ignell et al., 2005, Schachtner et al., 2005; Ghaninia et al.,

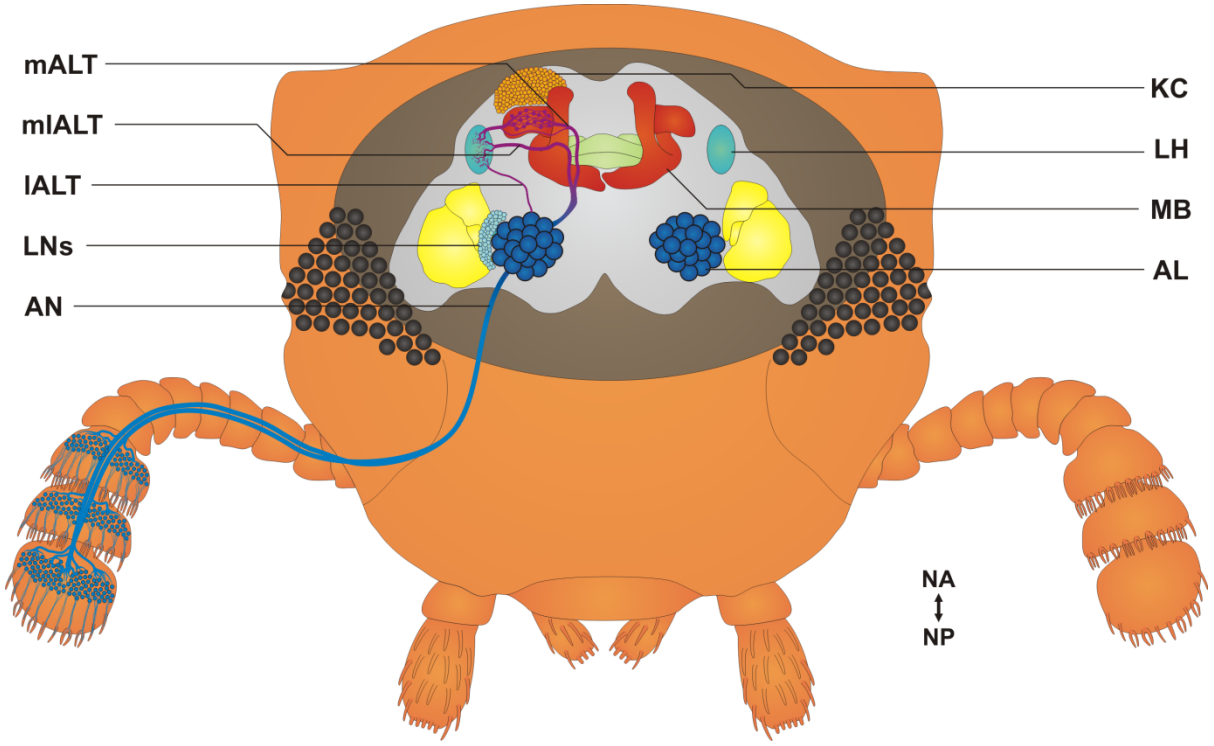

Fig. 3: Schematic drawing of the head capsule from the red flour beetle *Tribolium castaneum*, highlighting the most important compartments of the olfactory pathway. AN, OSN (blue part shown in the left antenna), the three ALT, LN, and KC are only illustrated at the left side. AL = antennal lobe, AN = antennal nerve, KC = Kenyon cells, lALT = lateral antennal lobe tract, LH = Lateral horn, LN = local interneurons, mALT = medial antennal lobe tract, MB = mushroom body, mlALT = mediolateral antennal lobe tract. Orientation bar: NA = anterior (neuraxis), NP = posterior (neuraxis).

2007; Mysore et al., 2009). The number of glomeruli, their size, shape, and position in the AL is genetically determined and typically in different individuals of the same species similar (with exception of sexual dimorphisms) (Laissue et al., 1999; Berg et al., 2002), but it is known, hat the olfactory input / environment can have an effect on the glomeruli size (Sachse et al., 2007).

Sexual dimorphism at the level of the AL: In the olfactory system of male insects, OR responsible for detection of the female sex pheromones project in specific glomeruli (like observed in beetles, cockroaches, bees, ants, wasps, moths, flies, and mosquitoes). In many of these species, sex glomeruli are noticeable larger than the remaining glomeruli. Their number per AL ranges typically from one to five. In many species they are forming the so-called “macroglomerular complex”. Also in females of some of these species such enlarged glomeruli can be found. There they termed “female sex specific glomeruli” and they are important to detect host plants for oviposition or in ants to detect trail pheromones (Jawlovski, 1948; Schachtner et al., 2005; van der Goes van Naters and Carlson, 2007; Vosshall und Stocker, 2007; Hu et al., 2011).

Sex glomeruli are typically arranged in the area of the AL where the AN enters the AL (Hansson, 1997; Anton and Homberg, 1999; Schachtner et al., 2005; Kleineidam et al., 2005). It is under debate, weather the glomeruli of the “macroglomerular complex” and the “female sex specific glomeruli” are homologue or not (Rospars and Hildebrand, 2000).

Beside the differences in size of some glomeruli, also the number of glomeruli can differ between sexes like in the honey bee or in ant species (Arnold et al., 1985; Nishikawa et al., 2008; Kuebler et al., 2010).

The AL circuit: Usually, all OSN expressing the same type of ORx project their axons into the same glomerulus, creating thereby a chemotropic map-like representation of chemical coding in the AL (Vosshall, 2000; Stocker 2001; Keller and Vosshall, 2003). This results in the central dogma of olfaction: One OSN expressing only one type of ORx and all OSN, expressing the same type of ORx,

converge into the same glomerulus (1 ORx/1 OSN/1 glomerulus) (Jefferis, 2005; Smith, 2008).

Comparable to ORx, also OSN expressing IRx, respectively CO_2 receptive GR (Gr21a and Gr63a in *D. melanogaster*), project their axons into the same glomerulus (Vosshall and Stocker, 2007; Rytz et al., 2013). Furthermore, with some exceptions (like Gr21a together with Gr63a, or IR76b together with OR35a and Orco), usually no glomerulus is innervated by OSN expressing different specific chemoreceptive receptor (ORx, IRx, and/or CO_2 receptive GR) (Kent et al., 1986; Distler and Boeckh, 1997; Anton et al. 2003; Vosshall and Stocker, 2007; Rytz et al., 2013). Indicating that the central dogma of olfaction does not solely apply to ORx, but likewise to IRx, and CO_2 receptive GR. Resulting in the speculative, expanded central dogma of olfaction: 1 specific chemoreceptive receptor/1 OSN/1 glomerulus.

A particular odor is encoded via a unique spatial and temporal activation pattern of glomeruli within the AL. By a constant odor concentration, this pattern is reproducible for a given odor in different individuals of the same species (Galizia et al., 1999; Sachse et al., 1999), indicating that these activation patterns are genetically determined. However, this spatial and temporal activation pattern can change with different odor concentrations (Sachse and Galizia, 2003; Strauch et al., 2012; Daly et al., 2015) or by adaptation or learning (Sachse et al., 2007; Galizia, 2014).

But how does the circuit in the AL looks like? Beside the axons of OSN, the glomeruli also contain the dendrites of local interneurons (LN) (Fig. 3), the dendrites of projection neurons (PN), and the axons of centrifugal neurons (CN) (Schachtner et al., 2005; Hansson and Stensmyr, 2011, Tanaka et al., 2012).

Local interneurons (LN) of the AL: The axons of the cholinergic OSN enter typically the ipsilateral AL and their information is processed by a complex network of LN and is forwarded by PN (Schachtner et al., 2005; Tanaka et al., 2012; Galizia, 2014).

Sometimes this dendrites branche in just one (uniglomerular) or few glomeruli, but typically they branch in many, if not all glomeruli (multiglomerular) of the AL. LN lack any arborizations outside the AL while their somata are arranged in one or several clusters near the AL. By interconnecting the glomeruli with each other. The LN help to structure olfactory representation of the odor via inhibiting, sometimes exiting, or modulating the OSN, respectively thePN. This brings several advantages like enhanced contrast across odors, enhanced sensitivity, or some olfactory generalisation across odor concentrations (Stopfer et al., 1997; Sachse and Galizia, 2002; Schachtner et al., 2005; Masse et al., 2009; Wilson, 2013; Galizia, 2014).

For inhibition and excitation, the LN contain the inhibitory transmitter gamma amino-butyric acid (GABA), histamine, or glutamate, or they can contain the excitatory transmitter acetylcholine (Stopfer et al., 1997; Sachse and Galizia, 2002; Wilson and Laurent, 2005; Olsen et al., 2007; Shang et al., 2007; Silbering and Galizia, 2007; Olsen and Wilson, 2008; Okada et al., 2009; Tanaka et al., 2009; Chou et al., 2010; Dacks et al., 2010; Olsen et al., 2010; Root, 2010; Wilson, 2013; Galizia, 2014; Fusca et al., 2015; Nagel et al., 2015). They also contain a vast set of neuropeptides (Homberg, 2002; Nässel, 2002; Schachtner et al., 2005; Carlsson et al., 2010; Neupert et al., 2012; Binzer et al., 2014; Siju et al., 2014, Fusca et al., 2015).

Projection neurons (PN) of the AL: PN have their dendrites located in the AL, while there axons project to other brain areas, particularly the ipsilateral MB and LH, typically their somata are placed near the AL (Schachtner et al., 2005; Wilson, 2013; Galizia, 2014). While the LN are usually multiglomerular, PN can be either uniglomerular or multiglomerular. Each glomerulus, which is targeted by dendrites of a uniglomerular PN, is typically targeted by dendrites of several similar architectured uniglomerular PN, termed sister PN. PN which releas neuromediators at their dendrites had been observed in *D. melanogaster*, allowing them to excite/modulate further PN or LN of the glomerulus. Typically, the majority of uniglomerular PN projecting to the MB and LH are excitatory/cholinergic, while most multiglomerular PN projecting to the LH are inhibitory/GABAergic. (Stopfer et al., 1997; Sachse and Galizia, 2002; Schachtner et al., 2005; Masse et al., 2009; Wilson, 2013; Galizia, 2014).

Depending on the species, the axons of the PN are typically arranged as one, two, or three distinct antennal lobe tracts (ALT) (Fig. 3) (Galizia and Rössler, 2010).

Centrifugal neurons (CN) of the AL: In addition to the axons of OSN, the AL is also targeted by axons from other neurons, the so-called CN. The dendrites and somata of the CN lie in other regions of the central nerves system. Typically, the axons of the CN branch into many or all glomeruli of the AL, but also innervations of a single glomerulus has been observed (Kollmann et al., 2011). This neurons occur in rather small numbers (Schachtner et al., 2005; Galizia, 2014).

In some species, neurons that might give feedback information from the LH, respectively MB to the AL had been described (Rybak and Menzel, 1993; Kirschner et al., 2006; Hu et al., 2010). Thereby this neurons, originating from higher olfactory processing centers, could shape the processing of the olfactory input of the AL, the primary integration center for olfaction.

An additional type of PN, which could shape the function of the AL had been observed in many species across the insects, characterized by its serotonin immunoreactivity and by its shape (which can by varying in detail among certain groups). There somata are arranged in close proximity to the AL while there dendrites typically located in the protocerebrum, as well as in the AL (Dacks et al., 2006). From flies and moth it is known, that serotonin can modulate the sensitivity of odors as well as of sex pheromones (Linn and Roelofs, 1986; Kloppenburg and Hildebrand, 1995; Hill et al., 2003; Gatellier et al., 2004; Dacks et al., 2009).

A further type of PN, which is supposed to be homolog within the insects, has its somata at the midline of the gnathal ganglia, it is octopaminergic and projects its axons in many, if not all glomeruli of the AL of both hemispheres (Schachtner et al., 2005; Schröter et al., 2007).

Also peptidergic PN had been described in several species. For example, the pars intercerebralis of several insects contains typically four prominent SIFamidergic somata, innervating typically vast regions of the entire brain including the AL (Carlsson et al., 2010; Heuer et al., 2012a; Binzer et al., 2014; Siju et al., 2014; Gellerer et al., 2015).

The mushroom bodies (MB)

The paired MB are higher, multimodal sensory integrative centers. They are primary known for their role in insect olfactory discrimination, learning, and memory storage and retrieval, but they are also important for processing and learning of visual, gustatory, acoustic, and mechanoreceptiv input, as well as for sleep regulation, place memory, and temperature preference (Mcguire et al., 2001; Menzel, 2001; Heisenberg, 2003; Davis, 2004; Heuer et al., 2012b).

The MB are easy identifiable due to their characteristic shape (Heisenberg, 1998) (Fig. 3). They consist of many, conspicuous small cells, the so-called Kenyon cells (KC). The number of the KC vary among insects (about 2,500 in *D. melanogaster* [Hinke, 1961; Mobbs] to about 180,000 in *A. mellifera* [1982; Strausfeld, 2002]), with their somata are arranged at the n-anterior side of the brain (Fig. 3). Typically, the dendritic arborizations of the KC (together with the PN of the AL and other brain areas) form the calyces (CA), in most cases a cap shaped structures, which are often embedded n-posterior to the cluster of KC somata (Fig. 3). Typically, the CA receive innervation from the PN of the ipsilateral AL via the ALT (Schachtner et al., 2005; Galizia and Rössler, 2010). The axons of the KC converge to thick bundles, the peduncle (PE), which run n-posterior. In most insects the PE split (at the level of the central complex) into two lobes, the medial and vertical lobes. The medial lobes (mL) extend towards the mid-sagittal plane, while the vertical lobes (vL) extend n-antero-dorsally (Fig. 3) (Heisenberg, 1998; Strausfeld et al., 2009; Aso et al., 2014). The CA as well as the PE and their lobes consist of further subcompartments, originating from the different classes/birthdates of the KC during development (Lee et al., 1999; Farris and Strausfeld, 2001; Strausfeld, 2002; Farris and Sinakevitch, 2003; Fukushima and Kanzaki, 2009; Aso et al., 2014), and which can contain different neuromediators (Schürmann and Erber, 1990; Crittenden et al., 1998; Sinakevitch et al., 2001; Sjöholm et al., 2006).

Extrinsic neurons of the MB project to different brain areas like the AL or the LH, capable of modulating the perception or evaluation function of this neuropils and thereby shaping the behavior of the animal (Rybak and Menzel, 1998; Kirschner et al., 2006; Hu et al. 2010; Okada et al., 2007).

The lateral horns (LH)

The LH are paired neuropil areas which had been identified in the lateral protocerebrum of several insects. While in some species a characterization of a distinct neuropil - due to its morphology - isn't possible, several authors prefer to use the term "lateral protocerebrum" instead of LH. However, typically the LH receive olfactory input from the AL via the PN organized into one to three ALT per brain hemisphere (Schachtner et al., 2005; Galizia and Rössler, 2010) (Fig. 3).

The LH are believed to be involved in the evaluation of quality and intensity of the odor information, and finally triggering immediate odor-driven behavior (both innate and learned), especially in response to food-related odors, sexual odors, or for appropriate oviposition sites (de Belle and Heisenberg, 1994; Connolly et al., 1996; Heimbeck et al., 2001; Wang et al., 2003; Yamagata et al., 2007; Jefferis et al., 2007; Galizia, 2014; Strutz et al., 2014). Beside input from the AL, the LH gets also input from the MB, therefore learned odors can directly influence odor valence readout in the LH (Rybak and Menzel, 1993).

However, odor evaluations of the LH are supposed to be dependent of the "inner state" of an animal. Example given, a hungry animal might evaluate the odor source of food as very important, while an thirsty animal might consider the odors related to water sources as more important. It is likely that the shift of odor evaluate of the LH is depended of factors like hunger, thirst, stress, attention, sexual arousal arousal, or need to oviposit (Galizia, 2014).

Neuromediators of the AL

The communication between the neurons of the olfactory pathway is facilitated by a vast set of different neuromediators as shown in several insect species, including signaling molecules like the classical neurotransmitters (like γ-amino butyric acid [GABA] and acetylcholine [ACh]), biogenic amines, and especially a wide range of neuropeptides. (Müller, 1997; Bicker, 1999a,b; Homberg and Müller, 1999; Hansson and Anton, 2000; Nässel, 2002; Homberg, 2002, Dacks et al., 2006; Carlsson et al., 2010; Neupert et al., 2012; Binzer et al., 2014; Siju et al., 2014, Fusca et al., 2015).

Classical neurotransmitters: The excitatory ACh is supposed to be the main transmitter of the OSN. But ACh has in the AL also been identified in LN (Shang et al., 2007), as well as in uniglomerular PN, targeting the MB and LH (Schachtner et al., 2005; Masse et al., 2009; Wilson, 2013; Fusca et al., 2015).

GABA is believed to be the insect nervous system main inhibitory transmitter. Within the AL it is prominently in the LN across al taxa. Typically, most multiglomerular PN projecting to the LH are GABAergic (Schachtner et al., 2005; Masse et al., 2009; Wilson, 2013).

Biogenic amines: In the insect nervous system biogenic amines have different functions like neuromodulators, neurohormones, and neurotransmitters (Bicker, 1999b; Homberg and Müller, 1999; Monastirioti, 1999; Nässel, 1999a; Hansson and Anton, 2000; Homberg, 2002; Roeder, 2005; Schachtner et al., 2005; Dacks et al., 2006; Schröter et al., 2007; Rein et al., 2013). Biogenic amines, identified frequently in the olfactory pathway of insects are serotonin, histamin, dopamin, and octopamin. Typically, this molecules are present in CN and LN (Schachtner et al., 2005; Dacks et al., 2006).

Neuropeptides: Neuropeptides are highly conserved across animals. Even ancestral taxa like coelenterates and nematodes possess several different neuropeptides (Grimmelikhuijzen et al., 1996; Bargmann, 1998; Brownlee and Fairweather, 1999). They have evolved to the largest and most diverse group of neuromediators within the insect nervous system, functioning as neuromodulators (Nässel, 2002). In the insect's life history, basically all physiological processes are regulated by neuropeptides, including reproduction,

developmental processes, behavioral functions, metabolic events, and signal processing (Nässel, 2002; Caers et al., 2012).

Numbers of neuropeptide precursor genes, respectively expressed neuropeptides are known from several species like *T. castaneum* (41 neuropeptide precursor genes, 80 functional neuropeptides [Li et al., 2008]), *D. melanogaster* (19 precursor genes, 46 neuropeptides [Clynen et al., 2010]), *Locusta migratoria* (23 identified precursor genes, about 60 neuropeptides [Burrows, 1996; Schoofs et al., 1997; How et al., 2015]), the cockroaches *Periplaneta americana* and *Rhyparobia maderae* (formally known as *Leucophaea maderae*) (more than 80 neuropeptides [Predel, 2001; Predel et al., 2004]), and *Ae. aegypti* (43 Neuropeptides [Predel et al., 2010]). The diversity of the neuropeptides can be partly explained by different posttranslational processing of the larger precursor proteins originating from neuropeptide precursor genes (Nässel, 2002; Predel et al., 2004; Altstein and Nässel, 2010).

Compared to classical neurotransmitters, little is known about the exact functions and mechanisms of neuropeptides within the insect's olfactory pathway (Nässel, 2002; Winther et al., 2006; Caers et al., 2012; Vecsey et al., 2014). The only neuropeptide, which function in the insect's olfactory pathway had been investigated in higher detail is the tachykinin-related peptide (TKRP) in *D. melanogaster*. Tachykinin is one of the oldest and most wide-spread neuropeptide families in the animal kingdom (Nässel, 1999b; Severini et al., 2002). The first TKRP that had been identified in invertebrates was the TKRP from *L. migratoria* (Schoofs et al., 1990a,b). The characteristic amino acid sequence of TKRP from all invertebrates having the conserved C-terminal Fx_1Gx_2Ramid (Schoofs et al., 1990a,b). In the brain of *D. melanogaster*, TKRP affects behavior. Knockdown of TKRP results in a reduction of odor perception and sensitivity, and an increase of locomotor activity, indicating a modulatory role in the AL and the central complex (CBX) (Winther et al., 2006). Additionally, knockdown of the TKRP receptors in OSN also alters olfactory behaviors, while over expression of the TKRP receptors showed an opposite behavioral phenotypes, demonstrating that tachykinergic LN modulate incoming signals of the OSN (Ignell et al., 2009; Winther and Ignell, 2010).

The significance of Coleoptera

Today, Coleoptera are supposed to be the species richest, most diverse, and most successful order in the animal kingdom. Of the about 1.4 million described animal species (of which about 70% are insects [Chapman, 2009]), approximately 400,000 are Coleoptera. That means that about 30% of all known animal species are beetles (Grimaldi and Engel, 2005; Hunt et al., 2007; Hauser et al., 2008). This successes can be explained by their long evolutionary history and multiple adaptations to their environments. Coleoptera exist since the late Permian (around 285 million years ago) (Crowson, 1981; Grimaldi and Engel, 2005). But only since the Cretaceous they started their evolutionary success due to 1) their co-evolution with angiosperms (Farrell, 1998) and mammals (Davis et al., 2002), and 2) their effective adaptation to geological and climatic changes during this time period (Erwin, 1985), allowing them to occupy multiple ecological niches.

Coleoptera are a major threat for the agricultural and timber industriy, endangering products worth billions of US $ annually (Perlak et al., 1993; Cox, 1999; Nowak et al., 2001; Myers and Hosking, 2002; Simberloff, 2003; Altieri and Nicholls, 2004; Muirhead et al., 2006; Müller et al., 2008; Foottit and Adler, 2009; Safranyik et al., 2010; Fera, 2012; Stadelmann et al., 2013; Seidl et al., 2014). This makes this order to an important research field.

Despite their ecological and economic impact (Grimaldi and Engel, 2005; Hunt et al., 2007) and the fact, that Coleoptera (like almost all other insects) strongly relay on their olfactory system (Borden, 1985; Leal, 2013; Visser, 1986; Scrimgeour et al., 1994; Abjörnsson et al., 1997; Tegoni et al., 2004; Dahanuka et al., 2005; Whiteman and Pierce, 2008; de Bruyne et al., 2010; Herbst et al., 2011), little is known about their olfactory system.

Only limited data of the Coleoptera olfactory pathway are available, including studies on the animals behavior (e.g. Dormont et al., 2010;

Weissteiner et al., 2012), antennal ultra-structure (e.g. Sen and Mitchell, 2001; Ritcey and Mclver et al., 1990), biochemistry of the olfactory system (e.g. Breidbach and Wegerhoff, 1994), neuroanatomy (Hu et al., 2011; Weissteiner et al., 2012), or genetics (Andersson et al., 2013). Today, no beetle reaches the level of a model organism for insect olfaction comparable to species like *D. melanogaster, A. mellifera, Manduca sexta, B. mori, Ae. aegypti, or An. gambiae* (Dippel et al., submitted [chapter 3]).

Tribolium castaneum, as a model organism

The genus *Tribolium* belongs to the Tenebrionidae family. They include 36 species with eight major pests for stored food product. They have spread worldwide by international shipments of infested grain and flour (Nakakita, 1982; Angelini and Jockusch, 2008; Angelini et al., 2009).

Within the last years, the red flour beetle *T. castaneum* Herbst, 1797 (Bonneton, 2008) has become an important model organism in some field like developmental (Brown et al., 2009). *T. castaneum* has after *D. melanogaster* the second fully annotated insect genome (Wang et al., 2007; Richards et al., 2008; Kim et al., 2010), and it is accessible to multiple powerful genetic tools such as systemic RNA interference (Bucher et al., 2002; Tomoyasu and Denell, 2004), forward genetics based on insertional mutagenesis (Trauner et al., 2009) and transgene-based misexpression systems (Schinko et al., 2010; Schinko et al., 2012).

Beside the multiple possibilities to manipulate *T castaneums* genome, this animal shows several additional advantages to be qualified as model organism. *T. castaneum* is very easy to culture, with low demands on space (per animal) and low maintenance costs, the animal is easy to handle and has a relative short generation time of approximate 55 days and a high reproduction rate. Compared to many other insect model organisms, *T. castaneum* has a remarkable longevity of about 200 days in average (and in maximum up to 3 years) (Bucher, 2009), making this species suitable for the investigation of long time effects.

Furthermore, *T. castaneum* has (compared to *D. melanogaster*) a short germband embryo development, which reflects the ancestral and most common form of arthropod embryogenesis (Sommer and Tautz, 1994; Schröder et al., 2008). Rendering *T. castaneum* for several questions as a better insect representative than *D. melanogaster.* Taking into account, that *T. castaneum* is 1) a major pest and that it represents an insect order containing many pest species, 2) that it represents the largest and most divers insect order, 3) that it is accessible to many genetic tools, and 4) that it is easy to culture, *T.* castaneum presents itself as a suitable "coleopteran model organism", especially for insect olfaction.

References

Åbjörnsson K., Wagner B.M.A., Axelson A., Bjerselius R., Olsén KH. (1997) Responses of *Acilius sulcatus* (Coleoptera: Dytiscidae) to Chemical Cues from Perch (Perca fluviatilis). Oecologia 111, 166–171.

Abuin L., Bargeton B., Ulbrich M.H., Isacoff E.Y., Kellenberger S., Benton R. (2011) Functional architecture of olfactory ionotropic glutamate receptors. Neuron. 69:44-60.

Altieri M.A., Nicholls C.I. (2004) Biodiversity and Pest Management in Agroecosystems, 2nd edition. Haworth Press Inc., Binghamton.

Altner H. (1977) Insektensensillen: Bau und Funktionsprinzipien. Verhandlungen der Deutschen Zoologischen Gesellschaft. 1977:139–53.

Altner H., Prillinger L. (1980) Ultrastructure of invertebrate chemo-, thermo-, and hygroreceptors and its functional significance. International Review of Cytology. 67:69–139.

Altstein M., Nässel D.R. (2010) Neuropeptide signaling in insects. Advances in Experimental Medicine and Biology. 692:155–165.

Andersson M.N., Grosse-Wilde E., Keeling C.I., Bengtsson J.M., Yuen M.M.S., Li M., Hillbur Y., Bohlmann J., Hansson B.S., Schlyter F. (2013) Antennal transcriptome analysis of the chemosensory gene families in the tree killing bark beetles, *Ips typographus* and *Dendroctonus*

ponderosae (Coleoptera: Curculionidae: Scolytinae). BMC Genomics. 14:198.

Angelini D.R., Jockusch E.L. (2008) Relationships among pest flour beetles of the genus *Tribolium* (Tenebrionidae) inferred from multiple molecular markers. Molecular Phylogenetics and Evolution. 46:127–141.

Angelini D.R., Kikuchi M., Jockusch E.L. (2009) Genetic patterning in the adult capitate antenna of the beetle *Tribolium castaneum*. Developmental Biology. 327:240–251.

Angioy A.M., Desogus A., Barbarossa I.T., Anderson P., Hansson B.S. (2003) Extreme sensitivity in an olfactory system. Chemical Senses. 28:279–284.

Anton S., van Loon J.J.A., Meijerink J., Smid H.M., Takken W., Rospars J.P. (2003) Central projections of olfactory receptor neurons from single antennal and palpal sensilla in mosquitoes. Arthropod Structure and Development. 32:319–329.

Arnold G., Masson C., Budharugsa S. (1985) Comparative study of the antennal lobes and their afferent pathway in the worker bee and the drone (*Apis mellifera*). Cell and Tissue Research. 242:593-605.

Aso Y., Hattori D., Yu Y., Johnston R.M., Iyer N.A., Ngo T.T., Dionne H., Abbott LF., Axel R., Tanimoto H., RubinG.M. (2014). The neuronal architecture of the mushroom body provides a logic for associative learning. Elife. 3:04577.

Bargmann C.I. (1998) Neurobiology of the Caenorhabditis elegans genome. Science. 282:2028–2033.

Benton R., Sachse S., Michnick S.W., Vosshall L.B. (2006) Atypical membrane topology and heteromeric function of *Drosophila* odorant receptors in vivo. PLoS Biolegy. 4:240.

Benton R., Vannice K.S., Gomez-Diaz C., Vosshall L.B. (2009) Variant ionotropic glutamate receptors as chemosensory receptors in *Drosophila*. Cell. 136:149–162.

Berg B.G., Galizia C.G., Brandt R., Mustaparta H. (2002) Digital Atlases of the Antennal Lobe in Two Species of Tobacco Budworm Moths, the Oriental *Helicoverpa assulta* (Male) and the American *Heliothis virescens* (Male and Female). Journal of Comparative Neurology. 446:123-134.

Bianchet M.A., Bains G., Pelosi P., Pevsner J., Snyder S.H., Monaco H.L., Amzel L.M. (1996) The three-dimensional structure of bovine odorant binding protein and its mechanism of odor recognition. Nature Structural and Molecular Biology. 3:934–939.

Bicker G. (1999a) Biogenic amines in the brain of the honeybee: cellular distribution, development, and behavioral functions. Microscopy Research and Technique. 44:166–178.

Bicker G. (1999b) Histochemistry of classical neurotransmitters in antennal lobes and mushroom bodies of the honeybee. Microscopy Research and Technique. 45:174–183.

Binzer M., Heuer C.M., Kollmann M., Kahnt J., Hauser F., Grimmelikhuijzen C.J., Schachtner J. (2014) Neuropeptidome of *Tribolium castaneum* antennal lobes and mushroom bodies. Journal of Comparative Neurology. 522:337–357.

Bogner F., Boppré M., Ernst K-D., Boeckh J. (1986) CO_2 sensitive receptors on labial palps of *Rhodogastria* moths (Lepidoptera: Artiidae): physiology, fine structure and central projection. Journal of Comparative Physiology A. 158:741–749.

Bonneton F. (2008). The beetle by the name of *Tribolium*: typology and etymology of *Tribolium castaneum* Herbst, 1797. Insect Biochemistry and Molecular Biology. 38:377–37910.

Borden J.H. (1985) Aggregation pheromones. In: Kerkut G.A., Gilbert L.I. (Ed). Comprehensive insect physiology, biochemistry and pharmacology. Vol. 9: Behavior. Pergamon Press, Oxford.

Breidbach O., Wegerhoff R. (1994) FMRFamide-like immunoreactive neurons in the brain of the beetle, *Tenebrio molitor* L. (Coleoptera: Tenebrionidae): constancies and variations in development from the embryo to the adult. International. Journal of Insect Morphology and Embryology. 23:383-404.

British Petroleum, BP (2014): BP Statistical Review of World Energy, June 20141. Available online at http://www.bp.com/content/dam/bp/pdf/Energy-

economics/statistical-review-2014/BP-statistical-review-of-world-energy-2014-full-report.pdf [accessed 2015.08.28].

Brown S.J., Shippy T.D., Miller S., Bolognesi R., Beeman R.W., Lorenzen M.D., Bucher G., Wimmer E.A., Klingler M. (2009) The red flour beetle, *Tribolium castaneum* (Coleoptera): a model for studies of development and pest biology. Cold Spring Harbor Protocols.

Brownlee D.J.A., Fairweather I. (1999) Exploring the neurotransmitter labyrinth in nematodes. Trends in Neurosciences. 220:16–24.

Bucher G. (2009) The beetle book. Available online at http://wwwuser.gwdg.de/~gbucher1/tribolium-castaneum-beetle-book1.pdf [accessed 2015.09.15].

Bucher G., Scholten J., Klingler M. (2002) Parental RNAi in *Tribolium* (Coleoptera). Current Biology. 12:85–86.

Caers J., Verlinden H., Zels S., Vandersmissen H.P., Vuerinckx K., Schoofs L. (2012) More than two decades of research on insect neuropeptide GPCRs: an overview. Frontiers in Endocrinology (Lausanne). 3:151.

Carey A.F., Carlson J.R. (2011) Insect olfaction from model systems to disease control. Proceedings of the National Academy of Sciences of USA . 108:12987–12995.

Carlsson M.A., Diesner M., Schachtner J. Nässel D.R. (2010) Multiple neuropeptides in the Drosophila antennal lobe suggest complex modulatory circuits. Journal of Comparative Neurology. 518:3359-3380.

Carpenter G.H. (1928) The Biology of Insects. Sidgwick and Jackson, London.

Chapman A.D. (2009) Numbers of living species in Australia and the world. Toowoomba, Australia: 2nd edition. Australian Biodiversity Information Services.

Chertemps T., François A., Durand N., Rosell G., Dekker T., Lucas P., Maïbèche-Coisne M. (2012) A carboxylesterase, Esterase-6, modulates sensory physiological and behavioral response dynamics to pheromone in Drosophila. BMC Biol 10:56.

Christensen T.A., Heinbockel T., Hildebrand J.G. (1996) Olfactory information processing in the brain: encoding chemical and temporal features of odors. Journal of Neurobiolog. 30:82–91.

Christensen T.A., Pawlowski V.M., Lei H., Hildebrand J.G. (2000) Multi-unit recordings reveal context-dependent modulation of synchrony in odor-specific neural ensembles. Nature Neurosci. 3:927–931.

Ciochetto L. (2013) Profit People Planet: The Environmental Implications of Development in Brazil, Russia, India and China (The BRIC Economies). International and Multidisciplinary Journal of Social Sciences. 2:145–65.

Clyne P.J., Warr C.G., Freeman MR., Lessing D., Kim J., Carlson J.R. (1999) A novel family of divergent seven-transmembrane proteins: candidate odorant receptors in *Drosophila*. Neuron. 22:327–338.

Clynen E., Reumer A., Baggerman G., Mertens I., Schoofs L. (2010) Neuropeptide biology in Drosophila. Advances in Experimental Medicine and Biology. 692: 192–210.

Connolly J.B., Roberts I.J., Armstrong J.D., Kaiser K., Forte M., Tully T., O'Kane C.J. (1996) Associative learning disrupted by impaired Gs signaling in Drosophila mushroom bodies. Science. 274:2104–2107.

Cox G.W. (1999). Alien Species in North America and Hawaii: Impacts on Natural Ecosystems. Island Press, Washington.

Crittenden J.R., Skoulakis E.M.C., Han K.A., Kalderon D., Davis R.L. (1998) Tripartite mushroom body architecture revealed by antigenic markers. Learning and Memory. 5:38-51.

Croset V., Rytz R., Cummins S.F., Budd A., Brawand D., Kaessmann H., Gibson T.J. Benton, R. (2010) Ancient protostome origin of chemosensory ionotropic glutamate receptors and the evolution of insect taste and olfaction. PLoS Genet. 6:1001064.

Crowson R.A. (1981), The Biology of Coleoptera. Academic Press, London.

Dacke M., Baird E., Byrne M., Scholtz C.H., Warrant E.J. (2013) Dung beetles use the milky way for orientation. Current Biology. 23:298-300.

Dacks A.M., Christensen T.A., Hildebrand J.G. (2006) Phylogeny of a SerotoninImmunoreactive Neuron in the Primary Olfactory Center of the Insect Brain. Journal of Comparative Neurology. 498:727–774.

Dacks A.M., Green D.S., Root C.M., Nighorn A.J., Wang J.W. (2009) Serotonin modulates olfactory processing in the antennal lobe of *Drosophila*. Journal of neurogenetics. 23:366-377.

Dacks A.M., Reisenman C.E., Paulk A.C., Nighorn A.J. (2010). Histamine-immunoreactive local neurons in the antennal lobes of the hymenoptera. Journal of Comparative Neurology. 518:2917-2933.

Dahanukar A., Foster K., van der Goes van Naters W.M., Carlson J.R. (2001) A Gr receptor is required for response to the sugar trehalose in taste neurons of Drosophila. Nature Neuroscience. 4:1182–1186.

Dahanukar A., Hallem E.A., Carlson J.R. (2005) Insect chemoreception. Current Opinion in Neurobiology. 15:423-430.

Daly K.C., Bradley S.P., Chapman P.D., Staudacher E.M., Tiede R., Schachtner J. (2015). Space Takes Time: Concentration Dependent Output Codes from Primary Olfactory Networks Rapidly Provide Additional Information at Defined Discrimination Thresholds. Frontiers in Cellular Neuroscience. 9:515.

Davis A.L.V., Scholtz C.H., Philips T.K. (2002) Historical biogeography of scarabaeine dung beetles. Journal of Biogeography. 29:1217-1256.

Davis R.L. (2004) Olfactory learning. Neuron. 44:31–48.

de Belle J.S., Heisenberg M. (1994) Associative odor learning in *Drosophila* abolished by chemical ablation of mushroom bodies. Science. 263:692–695.

de Bruyne M., Foster K., Carlson J.R. (2001) Odor coding in the *Drosophila* antenna. Neuron. 30:537-552.

de Bruyne M., Smart R., Zammit E., Warr C.G. (2010) Functional and molecular evolution of olfactory neurons and receptors for aliphatic esters across the *Drosophila* genus. Journal of Comparative Physiology A. 196:97–109.

Dettner K., Peters W. (2003) Lehrbuch der Entomolgie, 2nd edition. Spektrum Akademischer Verlag, München.

Dettner K., Peters W. (2011). Lehrbuch der Entomologie. Springer-Verlag, Berlin.

Dicke M. (2009) Behavioural and community ecology of plants that cry for help. Plant, Cell and Environmen. 32:654–665.

Dippel S., Kollmann M., Oberhofer G., Montino A., Knoll C., Krala M., Rexer K-R., Frank S., Kumpf R., Schachtner J., Wimmer EA. (submittet in eLife, 2016.05.12) Morphological and Transcriptomic Analysis of a Beetle Chemosensory System Reveals a Gnathal Olfactory Center.

Distler P., Boeckh J. (1997) Central projections of the maxillary and antennal nerves in the mosquito *Aedes aegypti*. Journal of experimental Biology. 200:1873-1879.

Dormont L., Jay-Robert P., Bessiere J.M., Rapior S., Lumaret J.P. (2010) Innate olfactory preferences in dung beetles. Journal of Experimental Biology. 213:3177–3186.

Dreyer D., Vitt H., Dippel S., Goetz B., El Jundi B., Kollmann M., Huetteroth W., Schachtner J. (2010) 3D Standard Brain of the Red Flour Beetle *Tribolium castaneum*: A Tool to Study Metamorphic Development and Adult Plasticity. Frontiers in Systems Neuroscience. 4,3.

Dunipace L., Meister S., McNealy C., Amrein H. (2001) Spatially restricted expression of candidate taste receptors in the *Drosophila* gustatory system. Current Biology. 11:822–835.

Durand N., Carot-Sans G., Bozzolan F., Rosell G., Siaussat D., Debernard S., Chertemps T., Maïbèche-Coisne M. (2011) Degradation of Pheromone and

Plant Volatile Components by a Same Odorant-Degrading Enzyme in the Cotton Leafworm, Spodoptera littoralis. PLoS One. 6:29147.

Dürr V., Krause A.F. (2014) Tactile Sensing in Insects. Encyclopedia of Computational Neuroscience.

El Jundi B., Pfeiffer K., Heinze S., Homberg U. (2014) Integration of polarization and chromatic cues in the insect sky compass. Journal of Comparative Physiology A. 200:575-589.

Ernst K.D. (1969) Die Feinstruktur von Riechsensillen auf der Antenne des Aaskäfers *Necrophorus* (Coleoptera). Zeitschrift für Zellforschung und Mikroskopische Anatomie. 94:72–102.

Erwin T.L. (1985) The taxon pulse: a general pattern of lineage radiation and extinction among carabid beetles. In: Ball G.E. (Ed.), Taxonomy, Phylogeny and Zoogeography of Beetles and Ants. W. Junk, Dordrecht, Netherlands.

Farhan A., Grabe V., Rybak J., Knaden M., Schmuker M., Hansson BS., Sachse S. (2014) Decoding odor quality and intensity in the *Drosophila* brain. eLife 3:04147

Farrell BD. (1998) "Inordinate Fondness"Explained: Why Are There So Many Beetles? Science 281:555–557

Farris S.M., Sinakevitch I. (2003) Development and evolution of the insect mushroom bodies: towards the understanding of conserved developmental mechanisms in a higher brain center. Arthropod Structure and Development. 32:79–101.

Farris S.M., Strausfeld N.J. (2001) Development of laminar organization in the mushroom bodies of the cockroach: Kenyon cell proliferation, outgrowth, and maturation. Journal of Comparative Neurology. 439:331–351.

Faucher C., Forstreuter M., Hilker M., de Bruyne M. (2006) Behavioral responses of *Drosophila* to biogenic levels of carbon dioxide depend on life-stage, sex and olfactory context. Journal of Experimental Biology. 209:2739-2748.

Fera (2012) Exploring the economic consequences of *Epitrix spp*. establishing across main crop potato production in England and options to reduce the likelihood of their introduction. Available online at http://s3.amazonaws.com/zanran_storage/ewda.csl.gov.uk/ContentPages/2522759539.pdf [accessed 2015.08.28]

Foelix R.F., Stocker R.F., Steinbrecht R.A. (1989) Fine structure of a sensory organ in the arista of *Drosophila melanogaster* and some other dipterans. Cell and Tissue Research. 258:277-287.

Foottit R.G., Adler P.H. (2009). Insect biodiversity: science and society. Oxford (UK): Wiley-Blackwell.

Forêt S., Maleszka R. (2006) Function and evolution of a gene family encoding odorant binding-like proteins in a social insect, the honey bee (*Apis mellifera*). Genome Research. 16:1404–1413.

Fukushima R., Kanzaki R., (2009) Modular subdivision of mushroom bodies by Kenyon cells in the silkmoth. Journal of Comparative Neurology. 513:315–330.

Fusca D., Schachtner J., Kloppenburg P. (2015) Colocalization of allatotropin and tachykinin-related peptides with classical transmitters in physiologically distinct subtypes of olfactory local interneurons in the cockroach (*Periplaneta americana*). Journal of Comparative Neurology. 523:1569–1586.

Galizia C.G. (2014). Olfactory coding in the insect brain: data and conjectures. European Journal of Neuroscience. 39:1784-1795.

Galizia C.G., Rössler W. (2010) Parallel Olfactory Systems in Insects: Anatomy and Function. Annual Review of Entomology. 55:399–420.

Galizia C.G., Sachse S., Rappert A., Menzel R. (1999) The glomerular code for odor representation is species specific in the honeybee *Apis mellifera*. Nature Neuroscience. 2:473–478.

Gallio M., Ofstad T.A., Macpherson L.J., Wang J.W., Zuker C.S. (2011) The coding of temperature in the *Drosophila* brain. Cell. 144:614-624.

Gatellier L., Nagao T., Kanzaki R. (2004) Serotonin modifies the sensitivity of the male silkmoth to

pheromone. Journal of Experimental Biology. 207:2487-2496.

Gellerer A., Franke A., Neupert S., Predel R., Zhou X., Liu S., Reiher W., Wegener C., Homberg U. (2015) Identification and distribution of SIFamide in the nervous system of the desert locust *Schistocerca gregaria*. Journal of Comparative Neurology 523:108-125.

Gerland P., Raftery A.E., Ševčíková H., Li N., Gu D., Spoorenberg T., Alkema L., Fosdick B.K., Chunn J., Lalic N., Bay G., Buettner T., Heilig G.K., Wilmoth J. (2014) World population stabilization unlikely this century. Science. 346:234–237.

German P.F., van der Poel S., Carraher C., Kralicek A.V., Newcomb R.D. (2013) Insights into subunit interactions within the insect olfactory receptor complex using FRET. Insect Biochemistry and Molecular Biology. 43:138–145.

Getahun M.N., Olsson S.B., Lavista-Llanos S., Hansson B.S., Wicher D. (2013) Insect Odorant Response Sensitivity Is Tuned by Metabotropically Autoregulated Olfactory Receptors. PLoS ONE. 8:58889.

Getahun M.N., Wicher D., Hansson B., Olsson S.B. (2012) Temporal response dynamics of *Drosophila* olfactory sensory neurons depends on receptor type and response polarity. Frontiers in Cellular Neuroscience. 6:54.

Ghaninia M., Hansson B.S., Ignell R. (2007) The antennal lobe of the African malaria mosquito, *Anopheles gambiae* – innervation and three-dimensional reconstruction. Arthropod Structure and Development. 36:23–39.

Glover T. (1867) Report of the Entomologist. Pp. 27–45. In Report of the Commissioner of Agriculture for the year 1866. Government Printing Office, Washington, DC.

Göpfert M., Hennig M. (2015). Hearing in Insects. Annual Review of Entomology. 61:257–276.

Gould J.L. (1998). Sensory bases of navigation. Current Biology. 8:731-738.

Grimaldi D., Engel M.S. (2005) Evolution of the Insects. Cambridge University Press, Cambridge.

Grimmelikhuijzen C., Leviev I.K., Carstensen K. (1996) Peptides in the nervous systems of cnidarians: structure, function, and biosynthesis. International Review of Cytology. 167:37–89.

Gu S.H., Sun L., Yang R.N., Wu K.M., Guo Y.Y., Li X.C., Zhang Y.J. (2014) Molecular characterization and differential expression of olfactory genes in the antennae of the black cutworm moth *Agrotis ipsilon*. PloS one. 9:103420.

Guidobaldia F., May-Conchaa I.J., Guerensteina P.G. (2014) Morphology and physiology of the olfactory system of blood-feeding insects. Journal of Physiology-Paris. 108: 96–111.

Ha T.S., Smith D.P. (2009) Odorant and pheromone receptors in insects. Frontiers in Cellular Neuroscience. 3:10.

Hallem E.A., Carlson J.R. (2006). Coding of odors by a receptor repertoire. Cell. 125:143-160.

Hansson B.S. (1995) Olfaction in Lepidoptera. Experientia. 51:1003–1027.

Hansson B.S., Anton S. (2000) Function and morphology of the antennal lobe: new developments. Annual Review of Entomology. 45:203–231.

Hansson B.S., Christensen T.A. (1999) Functional characteristics of the antennal lobe. In Hansson B.S. (ed.), Insect Olfaction. Springer Berlin, Heidelberg.

Hansson B.S., Ljungber H., Hallberg E., Löfstedt C. (1992) Functional specialization of olfactory glomeruli in a moth. Science. 256:1313–1315.

Hansson B.S., Stensmyr M.C. (2011) Evolution of Insect Olfaction. Neuron. 72:698–711.

Hauser F., Cazzamali G., Williamson M., Park Y., Li B., Tanaka Y., Predel R., Neupert S., Schachtner J., Verleyen P., Grimmelikhuijzen C. (2008). A genome-wide inventory of neurohormone GPCRs in the red flour beetle *Tribolium castaneum*. Frontiers in Neuroendocrinology. 29:142–165.

Hedwig B. (2013) Insect Hearing and Acoustic Communication. Springer Berlin, Heidelberg.

Heimbeck G., Bugnon V., Gendre N., Keller A., Stocker R.F. (2001) A central neural circuit for experience-independent olfactory and courtship behavior in *Drosophila melanogaster*. Proceedings of the National Academy of Sciences of USA. 98:15336–15341.

Heisenberg M. (1998) What do the mushroom bodies do for the insect brain? An introduction. Learning and Memory. 5:1–10.

Heisenberg M., (2003) Mushroom body memoir: from maps to models. Nature Reviews Neuroscience. 4:266–275.

Henderson J. (2015) Building US Agricultural Exports - one BRIC at a Time. Available online at https://www.kansascityfed.org/Publicat/EconRev/PDF/11q1Henderson.pdf [accessed 2015.08.28]

Herbst C., Baier B., Tolasch T., Steidle J.L.M. (2011) Demonstration of Sex Pheromones in the Predaceous Diving Beetle, *Rhantus suturalis* (MacLeay, 1825) (Dytiscidae). Chemoecology. 21:19–23

Heuer C., Binzer, M., Schachtner J. (2012a) SIFamide in the brain of the sphinx moth, *Manduca sexta*. Acta Biologica Hungarica. 63:48-57.

Heuer C., Kollmann M., Binzer M., Schachtner J. (2012b). Neuropeptides in insect mushroom bodies. Arthropod Structure and Development, 41:199-226.

Hill E.S., Okada K., Kanzaki R. (2003) Visualization of modulatory effects of serotonin in the silkmoth antennal lobe. Journal of experimental biology. 206:345-352.

Hinke W. (1961) Das relative postembryonale Wachstum der Hirnteile von *Culex pipiens, Drosophila melanogaster* und *Drosophila*-Mutanten. Zeitschrift für Morphologie und Ökologie der Tiere. 50:81–118.

Hoebeke E.R., Beucke K. (1997) *Adventive Onthophagus* (Coleoptera: Scarabaeidae) in North America: geographic ranges, diagnoses, and new distributional records. Entomological News. 108:345–362.

Homberg U. (2002) Neurotransmitters and neuropeptides in the brain of the locust. Microscopy Research and Technique. 56:189–209.

Homberg U. (2004) In search of the sky compass in the insect brain. Naturwissenschaften. 91:199-208.

Homberg U., Müller U. (1999) Neuroactive substances in the antennal lobe. In: Hansson B.S. (Ed.), Insect Olfaction. Springer Berlin, Heidelberg.

Hood W.M. (2004) The small hive beetle, *Aethina tumida*: a review. Bee World. 85:51–59.

Hou L., Jiang F., Yang P., Wang X., Kang L. (2015) Molecular characterization and expression profiles of neuropeptide precursors in the migratory locust. Insect biochemistry and molecular biology. 63:63-71.

Howse P.E., Stevens I.D.R., Jones O.T. (1998) Insect pheromones and their use in pest management. Chapman and Hall, London.

Hu A., Zhang W., Wang Z. (2010) Functional feedback from mushroom bodies to antennal lobes in the *Drosophila* olfactory pathway. Proceedings of the National Academy of Sciences of USA. 107:10262-10267.

Hu J.H., Wang Z.Y. Sun F. (2011) Anatomicalorganization of antennal-lobeglomeruli in males and females of the scarabbeetle *Holotrichia diomphalia* (Coleoptera: Melolonthidae). Arthropod Structure and Development. 40:420–428.

Hungerford T.G. (1990) Diseases of Livestock. McGraw-Hill, Sydney.

Hunt T., Bergsten J., Levkanicova Z., Papadopoulou A., John O.S., Wild R., Hammond P.M., Ahrens D., Balke M., Caterino M.S., Gómez-Zurita J., Ribera I., Barraclough T.G., Bocakova M., Bocak L., Vogler, A.P. (2007) A comprehensive phylogeny of beetles reveals the evolutionary origins of a superradiation. Science. 318:1913–1916.

Ignell R., Dekker T., Ghaninia M., Hansson B.S. (2005) Neuronal architecture of the mosquito deutocerebrum. Journal of Comparative Neurology. 493:207–240.

Imms A.D. (1938) On the antennal musculature in insects and other arthropods. Quarterly Journal of Microscopical Science. 81:273–320.

Jacquin-Joly E., Merlin C. (2004) Insect olfactory receptors: contributions of molecular biology to chemical ecology. Journal of Chemical Ecology. 30:2359–2397.

Jawlovski H. (1948) Studies on the insect's brain. Ann. Univ. M. Curie Sklodowska (C)3:1-30.

Jefferis G.S.X.E. (2005) Insect Olfaction: A Map of Smell in the Brain. Current Biology. 15:668–670

Jefferis G.S.X.E., Potter C.J., Chan A.M., Marin E.C., Marin E.C., Rohlfing T., Maurer Jr C.R., Luo L. (2007) Comprehensive maps of *Drosophila* higher olfactory centers: spatially segregated fruit and pheromone representation. Cell. 128:1187–1203.

Johansson B.G., Jones T.M. (2007) The role of chemical communication in mate choice. Biological Reviews Volume. 82:265–289.

Jones W.D, Cayirlioglu P, Kadow I.G, Vosshall L.B (2007) Two chemosensory receptors together mediate carbon dioxide detection in *Drosophila*. Nature 454:86–90.

Justice R.W., Biessmann H., Walter M.F., Dimitratos S.D., Woods D.F. (2003) Genomics spawns novel approaches to mosquito control. Bioessays. 25:1011–1020.

Keil T.A. (1987) Lectin-Binding Sites in Olfactory Sensilla of the Silkmoth, *Antheraea polyphemus*. Annals of the New York Academy of Sciences. 510:403–405.

Keil T.A. (1989) Fine structure of the pheromone-sensitive sensilla on the antenna of the hawkmoth, *Manduca sexta*. Tissue Cell. 21:139–151.

Keller A., Vosshall L.B. (2003) Decoding olfaction in Drosophila. Current Opinion in Neurobiology. 13:103–110.

Kent K.S., Harrow I.D., Quartararo P., Hildebrand J.G. (1986) An accessory olfactory pathway in Lepidoptera: the labial pit organ and its central projections in *Manduca sexta* and certain other sphinx moths and silk moths. Cell and Tissue Research. 245:237–245.

Kim H.S., Murphy T., Xia J., Caragea D., Park Y., Beeman R.W., Lorenzen M.D., Butcher S., Manak J.R., Brown S.J. (2010) BeetleBase in 2010: revisions to provide comprehensive genomic information for *Tribolium castaneum*. Nucleic Acids Research. 38:437–442.

Kirkness E.F., et al. (the human body louse genome consortium) (2010) Genome sequences of the human body louse and its primary endosymbiont provide insights into the permanent parasitic lifestyle. Proceedings of the National Academy of Sciences of USA. 107:12168-12173.

Kirschner S., Kleineidam C.J., Zube C., Rybak J., Grünewald B., Rössler W. (2006) Dual olfactory pathway in the honeybee, *Apis mellifera*. Journal of Comparative Neurology. 499:933-952.

Kloppenburg P., Hildebrand J.G. (1995) Neuromodulation by 5-hydroxytryptamine in the antennal lobe of the sphinx moth *Manduca sexta*. Journal of Experimental Biology. 198:603-611.

Kollmann, M., Huetteroth, W., Schachtner, J. (2011). Brain organization in Collembola (springtails). Arthropod structure and development. 40:304-316.

Konishi M., Ito Y. (1973) Early entomology in East Asia. In: Smith R.F., Mittler T.E., Smith C.N. (Ed). History of Entomology. Annual Reviews, Palo Alto, California.

Krause A.F., Dürr V. (2004). Tactile efficiency of insect antennae with two hinge joints. Biological cybernetics. 91:168-181.

Kuebler L.S., Kelber C., Kleineidam C.J. (2010). Distinct antennal lobe phenotypes in the leaf-cutting ant (Atta vollenweideri). Journal of Comparative Neurology. 518:352-365.

Kwon J.Y, Dahanukar A., Weiss L.A., Carlson J.R. (2007) The molecular basis of CO2 reception in *Drosophila*. Proceedings of the National Academy of Sciences of USA. 104:3574–3578.

L. Safranyik, A.L. Carroll, J. Regniere, D.W. Langor, W.G. Riel, T.L. Shore, B. Peter, B.J. Cooke, V.G. Nealis, S.W. Taylor (2010) Potential for range expansion of mountain pine beetle into the boreal

forest of North America. The Canadian Entomologist. 142:415-442.

Laissue P.P., Reiter C., Hiesinger P.R., Halter S., Fischbach K.F., Stocker R.F. (1999): Three-dimensional reconstruction of the antennal lobe in *Drosophila melanogaster*. Journal of Comparative Neurology. 405:543-552.

Larsson M.C., Domingos A.I., Jones W.D., Chiappe M.E., Amrein H., Vosshall L.B. (2004) Or83b encodes a broadly expressed odorant receptor essential for *Drosophila* olfaction. Neuron. 43:703-714.

Laska M., Galizia C.G., Giurfa M., Menzel R. (1999) Olfactory discrimination ability and odor structure-activity relationships in honeybees. Chemical Senses. 24:429–438.

Laughlin J.D., Ha T.S., Jones D.N., Smith D.P. (2008) Activation of pheromone-sensitive neurons is mediated by conformational activation of pheromone-binding protein. Cell. 133:1255–1265.

Leal W.S. (2013) Odorant Reception in Insects: Roles of Receptors, Binding Proteins, and Degrading Enzymes. Annual Review of Entomology. 58:373-391.

Lee J-K., Altner H. (1986) Primary sensory projections of the labial palp-pit organ of *Pieris rapae* L. (Lepidoptera: Pieridae). International Journal of Insect Morphology and Embryology. 15:439–448

Lee J-K., Selzer R., Altner H. (1985) Lamellated outer dendritic segments of a chemoreceptor within wall-pore sensilla in the labial palp-pit organ of the butterfly, *Pieris rapae* L. (Insecta, Lepidoptera). Cell and Tissue Research. 240:333–342.

Lee T., Lee A., Luo L. (1999) Development of the *Drosophila* mushroom bodies: sequential generation of three distinct types of neurons from a neuroblast. Development. 126:4065-4076.

Lehrer M. (1997) Orientation and Communication in Arthropods. Birkhäuser Verlag, Basel.

Li B., Predel R., Neupert S., Hauser F., Tanaka Y., Cazzamali G., Williamson M., Arakane Y., Verleyen P., Schoofs L., Schachtner J., Grimmelikhuijzen C.J.P., Park Y. (2008) Genomics, transcriptomics, and peptidomics of neuropeptides and protein hormones in the red flour beetle *Tribolium castaneum*. Genome Research. 18:113–122.

Linn C.E., Roelofs W.L. (1986) Modulatory effects of octopamine and serotonin on male sensitivity and periodicity of response to sexpheromone in the cabbage looper moth, *Trichoplusia ni*. Archives of insect biochemistry and physiology. 3:161–171.

Linz J., Baschwitz A., Strutz A., Dweck H.K.M., Sachse S., Hansson B.S., Stensmyr M.C. (2013) Host plant-driven sensory specialization in *Drosophila erecta*. Proceedings of the Royal Society of London B: Biological Sciences. 280:1760.

Liu M., Yu H., Li G. (2008) Oviposition deterrents from eggs of the cotton bollworm, *Helicoverpa armigera* (Lepidoptera: Noctuidae): chemical identification and analysis by electroantennogram. J Insect Physiol. 54:656–662.

Lopes O., Barata E.M., Mustaparta H., Araújo J. (2002) Fine structure of antennal sensilla basiconica and their detection of plant volatiles in the eucalyptus woodborer, *Phoracantha semipunctata* Fabricius (Coleoptera: Cerambycidae). Arthropod Structure and Development. 31:1–13.

Losey J.E., Vaughan M. (2006) The economic value of ecological services provided by insects. Bioscience. 56:311–323.

Lu T., Qiu Y.T., Wang G., Kwon J.Y., Rutzler M., Kwon H.W., Pitts R.J., van Loon J.J.A., Takken W., Carlson J.R., Zwiebel L.J. (2007) Odor Coding in the Maxillary Palp of the Malaria Vector Mosquito *Anopheles gambiae*. Current Biology. 17:1533–1544.

Lundin C., Kall L., Kreher SA., Kapp K., Sonnhammer E.L., Carlson J.R., Heijne G., Nilsson I. (2007) Membrane topology of the *Drosophila* OR83b odorant receptor. FEBS Lett. 581:5601–5604.

Maeda T., Tamotsu S., Iwasaki M., Nisimura T., Shimohigashi M., Hojo M.K., Ozaki M. (2014) Neuronal Projections and Putative Interaction of Multimodal Inputs in the Subesophageal Ganglion

in the Blowfly, *Phormia regina*. Chemical Senses. 39:391–401.

Maïbèche-Coisne M., Nikonov A.A., Ishida Y., Jacquin-Joly E., Leal W.S. (2004) Pheromone anosmia in a scarab beetle induced by in vivo inhibition of a pheromone-degrading enzyme. Proceedings of the National Academy of Sciences of USA. 101:11459–11464.

Majer J.D. (1987) The conservation and study of invertebrates in remnants of native vegetation. In: Saunders D.A., Arnold G.W., Burbridge A.A., Hopkins A.J.M. (Ed). Nature Conservation: The Role of Remnants of Native Vegetation. Surrey Beatty and Sons, Sydney.

Martin F., Alcorta E. (2011) Regulation of olfactory transduction in the orco channel. Frontiers in cellular neuroscience. 5:21.

Masse N.Y., Turner G.C., Gregory S.X.E.J. (2009) Olfactory Information Processing in *Drosophila*. Current Biology. 19:700–713.

Mcguire S.E., Le P.T., Davis R.L. (2001) The role of *Drosophila* mushroom body signaling in olfactory memory. Science. 10:1126-1129.

Menzel R. (2001) Searching for the memory trace in a mini-brain, the honeybee. Learning and Memory. 8:53-62.

Metcalf R.L., Metcalf R.A. (1993) Destructive and Useful Insects: Their Habits and Control, 5th edition. McGraw-Hill, New York.

Metcalf RL., Luckmann WH. (1994) Introduction to Insect Pest Management, 3rd edn. John Wiley and Sons, Inc., New York.

Misof B., Niehuis O., Bischoff I., Rickert A., Erpenbeck D., Staniczek A. (2007) Towards an 18S phylogeny of hexapods: accounting for group-specific character covariance in optimized mixed nucleotide/doublet models. Zoology. 110:409–429

Missbach C., Dweck H.K., Vogel H., Vilcinskas A., Stensmyr M.C., Hansson B.S., Grosse-Wilde E. (2014) Evolution of insect olfactory receptors. eLife. 3:e02115.

Mitchell D. (2008) A note on rising food prices. Policy Research Working Paper WPS 4682, World Bank, Washington, DC.

Mobbs P.G. (1982) The brain of the honeybee *Apis mellifera* . 1. The connections and spatial organization of the mushroom bodies. Philosophical Transactions of the Royal Society B: Biological. 298:309–354.

Monastirioti M. (1999) Biogenic amine systems in the fruit fly *Drosophila melanogaster*. Microscopy Res Technique. 45:106-121.

Montell C. (2013) Gustatory receptors: not just for good taste. Current Biology. 23:929-932.

Morse R.A., Calderone N.W. (2000) The value of honey bees as pollinators of U.S. crops in 2000. Bee Culture. 128:24–25.

Muirhead J.R., Leung B., Overdijk C., Kelly D.W., Nandakumar K., Marchant K.R., MacIsaac H.J. (2006) Modelling local and long-distance dispersal of invasive emerald ash borer *Agrilus planipennis* (Coleoptera) in North America. Diversity and Distributions. 12:71–79.

Mukunda L., Lavista-Llanos S., Hansson B.S., Wicher D. (2014) Dimerisation of the *Drosophila* odorant coreceptor Orco. Frontiers in Cellular Neuroscience. 8:261.

Müller J., Bussler H., Gossner M., Rettelbach T., Duelli P. (2008) The European spruce bark beetle *Ips typographus* in a national park: from pest to keystone species. Biodiversity and Conservation. 17:2979–3001.

Müller U. (1997) The nitric oxide system in insects. Progress in Neurobiology. 51:363–381.

Myers J.H. Hosking G. (2002) Eradication. In: Hallman G.J., Schwalbe C.P. (Ed). Invasive Arthropods in Agriculture: Problems and Solutions. Oxford and IBH Publishing, New Delhi.

Mysore K., Subramanian K.A., Sarasij R.C., Suresh A., Shyamala B.V., VijayRaghavan K., Rodrigues V. (2009) Caste and sex specific olfactory glomerular organization and brain architecture in two sympatric ant species, Camponotus sericeus and

Camponotus compressus (Fabricius, 1798). Arthropod Structure and Development, 38:485-497

Nakagawa T., Pellegrino M., Sato K., Vosshall L.B., Touhara K. (2012) Amino acid residues contributing to function of the heteromeric insect olfactory receptor complex. PLoS ONE. 7:e32372

Nakakita H. (1982) Effect of larval density on pupation of *Tribolium freemani* Hinton (Coleoptera: Tenebrionidae). Applied Entomology and Zoology. 17: 269–276.

Nässel D.R. (1999a) Histamine in the brain of insects: a review. Microscopy Res Technique. 44:121-136.

Nässel D.R. (1999b) Tachykinin-related peptides in invertebrates: a review. Peptides. 20:141-158.

Nässel D.R. (2002) Neuropeptides in the nervous system of *Drosophila* and other insects: multiple roles as neuromodulators and neurohormones. Progress in Neurobiology 68:1–84.

Neupert S., Fusca D., Schachtner J., Kloppenburg P., Predel R. (2012) Towards a Single-cell-based analysis of neuropeptide expression in Periplaneta americana antennal lobe neurons. Journal of Comparative Neurology. 520:694-716.

New T.R. (1988) Associations between Insects and Plants. New South Wales University Press, Kensington.

New T.R. (1994) Exotic Insects in Australia. Gleneagles Publishing, Adelaide.

Nishikawa M., Nishino H., Misaka Y., Kubota M., Tsuji E., Satoji Y., Ozaki M.,Yokohari F. (2008). Sexual dimorphism in the antennal lobe of the ant Camponotus japonicus. Zoological science. 25:195-204.

Nolte A., Funk N.W., Mukunda L., Gawalek P., Werckenthin A., Hansson B.S., Wicher D., Stengl M. (2013) In situ Tip-Recordings Found No Evidence for an Orco-Based Ionotropic Mechanism of Pheromone-Transduction in *Manduca sexta*. PLoS ONE. 8:e62648.

Nowak D.J., Pasek J.E., Sequeira R.A., Crane D.E., Mastro V.C. (2001) Potential effect of *Anoplophora glabripennis* (Coleoptera: Cerambycidae) on urban trees in the United States. Journal of Economic Entomology. 94: 116–122.

Okada R., Rybak J., Manz G., Menzel R. (2007) Learning-related plasticity in PE1 and other mushroom body-extrinsic neurons in the honeybee brain. The Journal of Neuroscience. 27:11736-11747.

Paczkowski S., Paczkowska M., Dippel S., Flematti G., Schütz S. (2014) Volatile Combustion Products of Wood Attract *Acanthocnemus nigricans* (Coleoptera: Acanthocnemidae). Journal of Insect Behavior. 27:228–238.

Peñalva-Arana D.C., Lynch M., Robertson H.M. (2009) The chemoreceptor genes of the waterflea *Daphnia pulex*: many Grs but no Ors. BMC Evolutionary Biology. 9:1.

Perlak F.J., Stone T.B., Muskopf Y.M., Petersen L.J., Parker G.B., McPherson S.A., Wyman J., Love S., Reed G., Biever D., Fischhoff D.A. (1993) Genetically improved potatoes: protection from damage by Colorado potato beetles. Plant Molecular Biology. 22:313–321.

Pitts R.J., Rinker D.C., Jones P.L., Rokas A., Zwiebel L.J. (2011) Transcriptome profiling of chemosensory appendages in the malaria vector Anopheles gambiae reveals tissue- and sex-specific signatures of odor coding. BMC Genomics 12:271.

Predel R. (2001) Peptidergic neurohemal system of an insect: mass spectrometric morphology. Journal of Comparative Neurology. 436:36-3375.

Predel R., Neupert S., Garczynski S.F., Crim J.W., Brown M.R., Russell W.K., Kahnt J., Russell D.H., Nachman R.J. (2010) Neuropeptidomics of the mosquito *Aedes aegypti*. Journal of Proteome Research. 9:2006–2015.

Predel R., Neupert S., Roth S., Derst, C., Nässel D.R. (2005) Tachykinin related peptide precursors in two cockroach species. FEBS Journal. 272:3365-3375.

Predel R., Neupert S., Wicher D., Gundel M., Roth S., Derst C. (2004) Unique accumulation of neuropeptides in an insect: FMRFamide-related peptides in the cockroach, *Periplaneta americana*. European Journal of Neuroscience. 20:1499–1513.

Price P.W. (1997) Insect Ecology, 3rd edition. Wiley, New York.

Price P.W., Denno R.F., Eubanks M.D., Finke D.L., Kaplan I. (2011) Insect ecology: behavior, populations and communities. Cambridge University Press, Cambridge.

Rebora M., Piersanti S., Gaino E. (2008) The antennal sensilla of the adult of *Libellula depressa* (Odonata: Libellulidae). Arthropod Structure and Development. 37:504–510.

Rein J., Mustard J.A., Strauch M., Smith B.H. Galizia C.G. (2013) Octopamine modulates activity of neural networks in the honey bee antennal lobe. Journal of Comparative Physiology A. 199:947-962.

Richards et al. (the *Tribolium* Genome Sequencing Consortium) (2008) The genome of the model beetle and pest *Tribolium castaneum*. Nature. 452:949–955.

Rinker D.C., Zhou X., Pitts R.J., Jones P.L., Rokas A., Zwiebel L.J, (2015) RNAseq in the mosquito maxillary palp: a little antennal RNA goes a long way. bioRxiv. 016998.

Ritcey G.M., Mclver S.B. (1990) External morphology of antennal sensilla of four species of adult flea beetles (Coleoptera: *Chrysomelidae, Alticinae*). International Journal of Insect Morphology and Embryology. 19:141-153.

Robertson H.M., Kent L.B. (2009) Evolution of the gene lineage encoding the carbon dioxide receptor in insects. Journal of Insect Science. 9:19.

Robertson H.M., Warr C.G., Carlson J.R. (2003) Molecular evolution of the insect chemoreceptor gene superfamily in *Drosophila melanogaster*. Proceedings of the National Academy of Sciences of USA. 100: 14537-14542.

Roeder T. (2005) Tyramine and Octopamine: Ruling Behavior and Metabolism. Annual Review Entomology. 50:447-477.

Rosegrant M.W. (2008). Biofuels and grain prices: impacts and policy responses (p. 4). Washington, DC: International Food Policy Research Institute.

Rützler M., Zwiebel L.J. (2005) Molecular biology of insect olfaction:recent progress and conceptual models. Journal of Comparative Physiology A. 191:777-790.

Rybak J., Menzel R. (1993) Anatomy of the mushroom bodies in the honey bee brain: the neuronal connections of the alpha-lobe. Journal of Comparative Neurology. 334:444-465.

Rybak J., Menzel R. (1998) Integrative properties of the Pe1 neuron, a unique mushroom body output neuron. Learning and Memory. 5:133–145.

Rybczynski R,. Reagan J,. Lerner M.R. (1989) A pheromone-degrading aldehyde oxidase in the antennae of the moth *Manduca sexta*. The Journal of Neuroscience. 9:1341–1353.

Rytz R., Croset V., Benton R. (2013) Ionotropic receptors (IRs): chemosensory ionotropic glutamate receptors in *Drosophila* and beyond. Insect Biochemistry and Molecular Biology. 43:888-897.

Sachse S., Galizia C.G. (2002). Role of inhibition for temporal and spatial odor representation in olfactory output neurons: a calcium imaging study. Journal of Neurophysiology. 87:1106–1117.

Sachse S., Rappert A., Galizia C.G. (1999) The spatial representation of chemical structures in the antennal lobe of honeybees: steps towards the olfactory code. European Journal of Neuroscience. 11:3970–3982.

Sachse S., Rappert A., Galizia C.G. (1999). The spatial representation of chemical structures in the antennal lobe of honeybees: steps towards the olfactory code. European Journal of Neuroscience. 11:3970-3982.

Sachse S., Rueckert E., Keller A., Okada R., Tanaka N.K., Ito K., Vosshall L.B. (2007). Activity-dependent plasticity in an olfactory circuit. Neuron. 56:838-850.

Sánchez-Gracia A., Vieira F.G., Rozas J. (2009) Molecular evolution of the major chemosensory gene families in insects. Heredity. 103:208–216.

Sato K., Pellegrino M., Nakagawa T.,Nakagawa T., Vosshall L.B., Touhara K. (2008) Insect olfactory receptors are heteromeric ligand-gated ion channels. Nature. 452:1002–1006.

Schachtner J., Schmidt M., Homberg U. (2005) Organization and evolutionary trends of primary olfactory brain centers in Tetraconata (Crustacea+Hexapoda). Arthropod Structure and Development. 34:257–299.

Schinko J.B., Hillebrand K.., Bucher G. (2012) Heat shock-mediated misexpression of genes in the beetle *Tribolium castaneum*. Development Genes and Evolution. 222:287–298.

Schinko J.B., Weber M., Viktorinova I., Kiupakis A., Averof M., Klingler M., Wimmer E.A., Bucher G. (2010) Functionality of the GAL4/UAS system in *Tribolium* requires the use of endogenous core promoters. BMC Developmental Biology. 10:53.

Schneider D. (1964) Insect antennae. Annual Review of Entomology. 9:103–122.

Schneider D., Kaissling K.E. (1957) Der Bau der Antenne des Seidenspinners *Bombyx mori* L. II. Sensillen, cuticulare Bildungen und innerer Bau. Zoologische Jahrbücher. Abteilung für Anatomie und Ontogenie der Tiere. 76:224–250.

Schneider D., Steinbrecht RA. (1968) Checklist of insect olfactory sensilla. Symposia of the Zoological Society of London. 23:279–297.

Schoofs L., Holman G.M., Hayes .K., Nachman R.J., De Loof A. (1990a) Locustatachykinins I and II, two novel insect neuropeptides with homology to peptides of the vertebrate tachykinin family. FEBS Letters, 261:340-397.

Schoofs L., Holman G.M., Hayes T.K., Nachman R.J., Kochansky J.P., De Loof A. (1990b). Locustatachykinins III and IV: two additional insect neuropeptides with homology to peptides of the vertebrate tachykinin family. Regulatory Peptides. 31:199-212.

Schoofs L., Veelaert D., Vanden Broek J., De Loof A. (1997) Peptides in the locusts, *Locusta migratoria* and *Schistocerca gregaria*. Peptides. 18:145–156.

Schröder R., Beermann A., Wittkopp N., Lutz R. (2008). From development to biodiversity—*Tribolium castaneum*, an insect model organism for short germband development. Development genes and evolution: 218:119-126.

Schröter U., Malun D., Menzel R. (2007) Innervation pattern of suboesophageal ventral unpaired median neurones in the honeybee brain. Cell and Tissue Research. 327:647–667.

Schürmann F.W., Erber J. (1990) FMRFamide-like immunoreactivity in the brain of the honeybee (*Apis mellifera*). A light- and electron microscopical study. Neuroscience. 38:797-807.

Schütz C., Dürr V. (2011) Active tactile exploration for adaptive locomotion in the stick insect. Philosophical Transactions of the Royal Society B. 366:2996–3005.

Schütz S., Weissbecker B., Hummel H.E., Apel K.H., Schmitz H., Bleckmann H. (1999). Insect antenna as a smoke detector. Nature. 398:298–299.

Scrimgeour G.J., Culp J.M., Cash K.J. (1994) Antipredator responses of mayfly larvae to conspecific and predator stimuli. Journal of the North American Benthological Society. 13: 299-309

Seidl R., Schelhaas M.J., Rammer W., Verkerk P.J. (2014) Increasing forest disturbances in Europe and their impact on carbon storage. Nature Climate Change. 4:806–810.

Seifert G. (1995). Entomologisches Praktikum, 3nd edition. Thieme, Stuttgart.

Sen A., Mitchell B.K. (2001) Olfaction in the Colorado potato beetle: Ultrastructure of antennal sensilla in Leptinotarsa sp. Journal of biosciences 26:233–246.

Severini C., Improta G., Falconieri-Erspamer G., Salvadori S., Erspamer V. (2002) The tachykinin peptide family. Pharmacological Reviews. 54:285-322.

Shanbhag S.R., Müller B., Steinbrecht R.A. (1999) Atlas of olfactory organs of *Drosophila melanogaster*: 1. Types, external organization, innervation and distribution of olfactory sensilla. International Journal of Insect Morphology and Embryology. 28:377–397.

Shanbhag S.R., Singh K., Singh R.N. (1995) Fine structure and primary sensory projections of sensilla located in the sacculus of the antenna of

Drosophila melanogaster. Cell and Tissue Research. 282:237-249.

Shang Y., Claridge-Chang A., Sjulson L., Pypaert M., Miesenböck G. (2007) Excitatory local circuits and their implications for olfactory processing in the fly antennal lobe. Cell. 128:601-612.

Sheppard W.S. (1989) A history of the introduction of honey bee races into the United States. American Bee Journal. 129:617-619.

Shimanuki H. (1992) The honey bee deserves to be our national insect. In: Adams J. (ed). Insect Potpourri: Adventures in Entomology. Sandhill Crane Press, Gainesville, Florida.

Shurin J.B., Gruner D.S., Hillebrand H. (2005) All wet or dried up? Real differences between aquatic and terrestrial food webs. Proceedings of the Royal Society. B. Biological Sciences. 273: 1–9.

Siju K.P., Reifenrath A., Scheiblich H., Neupert S., Predel R., Hansson B.S., Schachtner J., Ignell, R. (2014) Neuropeptides in the antennal lobe of the yellow fever mosquito, *Aedes aegypti*. Journal of Comparative Neurology. 522:592-608.

Silbering A.F., Rytz R., Grosjean Y., Abuin L., Ramdya P., Jefferis G.S., Benton R. (2011). Complementary function and integrated wiring of the evolutionarily distinct *Drosophila* olfactory subsystems. The Journal of Neuroscience. 31:13357-13375.

Simberloff (2003). Introduced insects. In: Resh V.H., Card'e R.T. (Ed). Encyclopedia of Insects. Academic Press, Amsterdam.

Sinakevitch I., Farris S.M., Strausfeld N.J. (2001) Taurine-, aspartate-, and glutamate-like immunoreactivity identifies chemically distinct subdivisions of kenyon cells in the cockroach mushroom body. Journal of Comparative. Neurology. 439:352-367.

Singh R.N. (1997). Neurobiology of the gustatory systems of *Drosophila* and some terrestrial insects. Microscopy research and technique. 39.547-563.

Sjöholm M., Sinakevitch I., Strausfeld N.J., Ignell R., Hansson BS. (2006) Functional division of intrinsic neurons in the mushroom bodies of male *Spodoptera littoralis* revealed by antibodies against aspartate, taurine, FMRF-amide, Masallatotropin and DC0. Arthropod Structure and Development. 35:153-168.

Smart R., Kiely A., Beale M., Vargas E., Carraher C., Kralicek A.V., Christie D.L., Chen C., Newcomb R.D., Warr C.G. (2008) *Drosophila* odorant receptors are novel seven transmembrane domain proteins that can signal independently of heterotrimeric G proteins. Insect Biochemistry and Molecular Biology. 38:770–780

Smith C.U.M. (2008) Biology of Sensory Systems. John Wiley & Sons Ltd, Chichester.

Sommer R.J., Tautz D. (1994) Expression Patterns of twist and snail in *Tribolium* (Coleoptera) Suggest a Homologous Formation of Mesoderm in Long and Short Germ Band Insects. Developmental Genetics. 15:32–37

Sotthibandhu S., Baker R.R. (1979) Celestial orientation by the large yellow underwing moth, *Noctua pronuba* L. Animal Behaviour. 27:786-800.

Stadelmann G., Bugmann H., Meier F., Wermelinger B., Bigler C. (2013) Effects of salvage logging and sanitation felling on bark beetle (*Ips typographus* L.) infestations. Forest Ecology and Management. 305: 273-281.

Starausfeld N.J., Lee J.K. (1989) Structure, distribution and number of surface sensilla and their receptor cells on the olfactory appendage of the male moth *Manduca sexta*. Journal of Neurocytology. 19:519-538 .

Steelman C.D. (1976) Effects of external and internal arthropod parasites on domestic livestock production. Annual review of entomology. 21:155-178.

Steinbrech R.A. (1970) Zur Morphometrie der Antenne des Seidenspinners, *Bombyx mori* L.: Zahl und Verteilung der Riechsensillen (Insecta, Lepidoptera). Zeitschrift für Morphologie der Tiere. 68:93-126.

Steinbrech R.A. (1997) Pore structures in insect olfactory sensilla: A review of data and concepts. International Journal of Insect Morphology and Embryology. 26:229–245.

Steinbrecht R.A., Gnatzy W., (1984) Pheromone receptors in *Bombyx mori* and Antheraea pernyi. I. Reconstruction of the cellular organization of the sensilla trichodea. Cell and Tissue Research. 235:25–34.

Steinbrecht R.A., Ozaki M., Ziegelberger G. (1992) Immunocytochemical localization of pheromone binding protein in moth antennae. Cell and Tissue Research. 270:287-302.

Steinbrecht RA. (1998) Odorant-Binding Proteins: Expression and Function. Annals of the New York Academy of Sciences. 855:323–332.

Stengl M. (2010). Pheromone transduction in moths. Frontiers in cellular neuroscience. 4.

Stengl M., Funk N.W (2013) The role of the coreceptor Orco in insect olfactory transduction. Journal of Comparative Physiology A. 199:897–909.

Stensmyr M.C., Dweck H.K.M., Farhan A., Ibba I., Strutz A., Mukunda L., Linz J., Grabe V., Steck K., Lavista-Llanos S., Wicher D., Sachse S., Knaden M., Becher P.G., Seki Y., Hansson B.S. (2012) A Conserved Dedicated Olfactory Circuit for Detecting Harmful Microbes in *Drosophila*. Cell. 151:1345–1357.

Stocker R.F. (2001) *Drosophila* as a focus in olfactory research: mapping of olfactory sensilla by fine structure, odor specificity, odorant receptor expression, and central connectivity. Microscopy Research and Technique. 55:284–296.

Stopfer M., Bhagavan S., Smith B.H., Laurent G. (1997) Impaired odour discrimination on desynchronization of odour-encoding neural assemblies. Nature. 390:70–77.

Strauch M., Ditzen M., Galizia C.G. (2012). Keeping their distance? Odor response patterns along the concentration range. Frontiers in systems neuroscience. 6:71.

Strausfeld N.J. (2002) Organization of the honey bee mushroom body: Representation of the calyx within the vertical and gamma lobes. Journal of Comparative Neurology. 450:4–33.

Strausfeld N.J., Sinakevitch I., Brown S.M., Farris S.M. (2009) Ground plan of the insect mushroom body: functional and evolutionary implications. Journal of Comparative Neurology. 513:265-291.

Strutz A., Soelter J., Baschwitz A., Farhan A., Grabe V., Rybak J., Knaden M., Schmuker M., Hansson B.S., Sachse S. (2014). Decoding odor quality and intensity in the Drosophila brain. eLife. 3.

Suh G.S., Wong A.M., Hergarden A.C., Wang J.W., Simon A.F., Benzer S., Axel R., Anderson D.J. (2004) A single population of olfactory sensory neurons mediates an innate avoidance behavior in *Drosophila*. Nature. 431:854–59.

Sun Y-L., Huang L-Q., Pelosi P., Wang C-Z. (2012) Expression in Antennae and Reproductive Organs Suggests a Dual Role of an Odorant-Binding Protein in Two Sibling Helicoverpa Species. PLoS ONE. 7:30040.

Syed Z., Ishida Y., Taylor K., Kimbrell D.A., Leal W.S. (2006) Pheromone reception in fruit flies expressing a moth's odorant receptor. Proceedings of the National Academy of Sciences of USA. 103:16538–16543.

Syed Z., Leal W.S. (2007) Maxillary Palps Are Broad Spectrum Odorant Detectors in *Culex quinquefasciatus*. Chemical Senses. 32:727–738.

Tanaka N.K., Endo K., Ito, K. (2012) Organization of antennal lobe-associated neurons in adult Drosophila melanogaster brain. Journal of Comparative Neurology. 520:4067-4130.

Tegoni M., Campanacci V., Cambillau C. (2004) Structural aspects of sexual attraction and chemical communication in insects. Trends in Biochemical Sciences. 29:257–264.

Tomoyasu Y., Denell R.E. (2004) Larval RNAi in *Tribolium* (Coleoptera) for analyzing adult development. Development Genes and Evolution. 214:575–578.

Trauner J., Schinko J., Lorenzen M.D., Shippy T.D., Wimmer E.A., Beeman R.W., Klingler M., Bucher G., Brown S.J. (2009) Large-scale insertional mutagenesis of a coleopteran stored grain pest, the red flour beetle *Tribolium castaneum*, identifies embryonic lethal mutations and enhancer traps. BMC Biology. 7:73.

van der Goes van Naters W., Carlson J.R. (2007) Receptors and neurons for fly odors in *Drosophila*. Current Biology. 17:606–612.

Vecsey C.G., Pírez N.,. Griffith L.C. (2014) The *Drosophila* neuropeptides PDF and sNPF have opposing electrophysiological and molecular effects on central neurons. Journal of Neurophysiology. 111:1033-1045.

Vickers N.J., Christensen T.A., Baker T.C., Hildebrand J.G. (2001) Odor-plume dynamics influence the brain's olfactory code. Nature. 410:466-470.

Vieira F.G., Rozas J. (2011) Comparative genomics of the odorant-binding and chemosensory protein gene families across the Arthropoda: origin and evolutionary history of the chemosensory system. Genome Biology and Evolution. 3:476–490.

Visser J.H. (1986) Host Odor Perception in Phytophagous Insects. Annu Rev Entomol. Annual review of entomology. 31:121–144.

Vlad L.B., Hurduzeu G., Josan A., Vlasceanu G. (2011) The rise of BRIC, the 21st century geopolitics and the future of the consumer society. Revista Română de Geografie Politică. 13:48-62.

Vogt R.G. (2003): Biochemical diversity of odor detection: OBPs, ODEs and SNMPs .In: Blomquist G., Vogt R.G. (Ed). Insect pheromone biochemistry and molecular biology. Academic Press, San Diego.

Vogt R.G., Riddiford L.M., Prestwich G.D. (1985) Kinetic properties of a sex pheromone-degrading enzyme: the sensillar esterase of Antheraea polyphemus. Proceedings of the National Academy of Sciences of USA. 82:8827–8831

von Frisch, K. (1921) Über den Sitz des Geruchssinnes bei Insekten. Zoologische Jahrbücher. Abteilung für allegemeine Zoologie und Physiologie der Tiere. 38:1-68

Vosshall L.B. (2000) Olfaction in *Drosophila*. Current Opinion in Neurobiology. 10:498–503.

Vosshall L.B., Amrein H., Morozov P.S., Rzhetsky A., Axel R. (1999) A spatial map of olfactory receptor expression in the *Drosophila* antenna. Cell. 96:725-736.

Vosshall L.B., Hansson B.S. (2011) A Unified Nomenclature System for the Insect Olfactory Coreceptor. Chemical Senses. 36: 497–498.

Vosshall L.B., Stocker R.F. (2007) Molecular architecture of smell and taste in *Drosophila*. Annual Review of Neuroscience. 30:505–533.

Vosshall L.B., Wong A.M., Axel R. (2000) An olfactory sensory map in the fly brain. Cell. 102:147–159

Wang L., Wang S., Li Y., Paradesi M.S., Brown S.J. (2007) Beetle Base: the model organism database for *Tribolium castaneum*. Nucleic Acids Research. 35:0476–0479.

Wang X., Fang X., YangP., Jiang X., Jiang F., Zhao D., Li B., Cui F., Wei J., Ma C., Wang Y., He J., Luo Y., Wang Z., Guo X., Guo W., Wang X., Zhang Y., Yang M., Hao S., Chen B., Ma Z., Yu D., Xiong Z., Zhu Y., Fan D., Han L., Wang B., Chen Y., Wang J., Yang L., Zhao W., Feng Y., Chen G., Lian J., Li Q., Huang Z., Yao X., Lv N., Zhang G., Li Y., Wang J., Wang J., Zhu B., Kang L. (2014) The locust genome provides insight into swarm formation and long-distance flight. Nature communications. 5.

Wang Y., Chiang A-S., Xia S., Kitamoto T., Tully T., Zhong Y. (2003) Blockade of Neurotransmission in Drosophila Mushroom Bodies Impairs Odor Attraction, but Not Repulsion. Current Biology. 13:1900–1904.

Wang Z., Singhvi A., Kong P., Scott K. (2004) Taste representations in the *Drosophila* brain. Cell. 117:981-991.

Waterhouse D.F. (1974) The biological control of dung. Scientific American. 230:100–109.

Wehner R., Gehring W.J. (1995) Zoologie, 23nd edition. Georg Thieme Verlag, Stuttgart.

Wehner R., Michel B., Antonsen P. (1996) Visual navigation in insects: coupling of egocentric and geocentric information. Journal of Experimental Biology. *199*:129-140.

Weiss L.A., Dahanukar A., Kwon J.Y., Banerjee D., Carlson J.R. (2011) The Molecular and Cellular Basis of Bitter Taste in *Drosophila*. Neuron. 69:258–272.

Weissteiner S., Hütteroth W., Kollmann M., Weißbecker B., Romani R., Schachtner J., Schütz S. (2012) Cockhafer larvae smell host root scents in soil. PLoS One. 7:45827

Whiteman N.K., Pierce N.E. (2008) Delicious poison: genetics of *Drosophila* host plant preference. Trends in Ecology and Evolution. 23:473–478.

Wicher D., Schäfer R., Bauernfeind R., Stensmyr M.C., Heller R. Heinemann S.H., Hansson B.S. (2008) *Drosophila* odorant receptors are both ligand-gated and cyclic-nucleotide-activated cation channels. Nature. 452:1007–1011.

Wilson R.I. (2013). Early olfactory processing in *Drosophila*: mechanisms and principles. Annual Review of Neuroscience. 36:217.

Winther Å.M.E., Acebes A., Ferrús A. (2006) Tachykinin-related peptides modulate odor perception and locomotor activity in *Drosophila*. Molecular and Cellular Neurosciences. 31:399-406.

Witzgall P., Kirsch P., Cork A. (2010). Sex pheromones and their impact on pest management. Journal of chemical ecology. 36:80-100.

Xu P., Atkinson R., Jones D.N., Smith D.P. (2005) Drosophila OBP LUSH is required for activity of pheromone-sensitive neurons. Neuron. 45:193-200.

Yamagata N., Nishino H., Mizunami M. (2007) Neural pathways for the processing of alarm pheromone in the ant brain. Journal of Comparative Neurology. 505:424–442.

Yang C.H., Belawat P., Hafen E., Jan L.Y., Jan Y.N. (2008) *Drosophila* egg-laying site selection as a system to study simple decision-making processes. Science. 319:1679–1683.

Yao C.A., Ignell R., Carlson J.R. (2005) Chemosensory coding by neurons in the coeloconic sensilla of the *Drosophila* antenna. The Journal of Neuroscience. 25:8359-8367.

Younus F., Chertemps T., Pearce S.L., Pandey G., Bozzolan F., Coppin C.W., Russell R.J., Maïbèche-Coisne M., Oakeshott J.G. (2014) Identification of candidate odorant degrading gene/enzyme systems in the antennal transcriptome of *Drosophila melanogaster*. Insect Biochemistry and Molecular Biology. 53:30-43.

Zacharuk R.Y. (1980) Ultrastructure and Function of Insect Chemosensilla. Annual Review of Entomology. 25:27–47.

Zhao X.C., Tang Q.B., Berg B.G., Liu Y., Wang Y.R., Yan F.M., Wang G.R. (2013) Fine structure and primary sensory projections of sensilla located in the labial-palp pit organ of Helicoverpa armigera (Insecta). Cell and Tissue Research. 353:399-408.

Zhou J.J., Field L.M., He X.L. (2010) Insect odorant-binding proteins: do they offer an alternative pest control strategy? Outlooks on Pest Management. 21:31-34.

Chapter 1

3D Standard Brain of the Red Flour Beetle *Tribolium castaneum*: A Tool to Study Metamorphic Development and Adult Plasticity

frontiers in
SYSTEMS NEUROSCIENCE

ORIGINAL RESEARCH ARTICLE
published: 03 March 2010
doi: 10.3389/neuro.06.003.2010

3D standard brain of the red flour beetle *Tribolium castaneum*: a tool to study metamorphic development and adult plasticity

David Dreyer[1,2], Holger Vitt[1], Stefan Dippel[1,3], Brigitte Goetz[1], Basil el Jundi[1], Martin Kollmann[1], Wolf Huetteroth[1,4] and Joachim Schachtner[1]*

[1] *Department of Biology, Animal Physiology, Philipps-University Marburg, Marburg, Germany*
[2] *Department of Biology, Animal Navigation, University of Oldenburg, Oldenburg, Germany*
[3] *Department of Developmental Biology, Johann-Friedrich-Blumenbach-Institute for Zoology and Anthropol, Georg-August-University Göttingen, Göttingen, Germany*
[4] *Department of Neurobiology, University of Massachusetts Medical School, Worcester, MA, USA*

Edited by:
Randolf Menzel, Freie Universität Berlin, Germany

Reviewed by:
Monika Stengl, Universität Kassel, Germany

****Correspondence:***
Joachim Schachtner, Department of Biology, Animal Physiology, Philipps-University Marburg, Karl-von-Frisch-Str. 8, D-35032 Marburg, Germany.
e-mail: schachtj@staff.uni-marburg.de

The red flour beetle *Tribolium castaneum* is emerging as a further standard insect model beside *Drosophila*. Its genome is fully sequenced and it is susceptible for genetic manipulations including RNA-interference. We use this beetle to study adult brain development and plasticity primarily with respect to the olfactory system. In the current study, we provide 3D standard brain atlases of freshly eclosed adult female and male beetles (A0). The atlases include eight paired and three unpaired neuropils including antennal lobes (ALs), optic lobe neuropils, mushroom body calyces and pedunculi, and central complex. For each of the two standard brains, we averaged brain areas of 20 individual brains. Additionally, we characterized eight selected olfactory glomeruli from 10 A0 female and male beetles respectively, which we could unequivocally recognize from individual to individual owing to their size and typical position in the ALs. In summary, comparison of the averaged neuropil volumes revealed no sexual dimorphism in any of the reconstructed neuropils in A0 *Tribolium* brains. Both, the female and male 3D standard brain are also used for interspecies comparisons, and, importantly, will serve as future volumetric references after genetical manipulation especially regarding metamorphic development and adult plasticity.

Keywords: brain, olfactory system, antennal lobe, insect, neuropil, digital neuroanatomy, coleoptera

INTRODUCTION

The red flour beetle *Tribolium castaneum* Herbst, 1797 (Bonneton, 2008), which is a major pest of stored grains, grain products, and other dried food, is emerging as a further standard insect model beside *Drosophila*. It's powerful reverse genetics (systemic RNA-interference; Bucher et al., 2002; Tomoyasu and Denell, 2004; Tomoyasu et al., 2008), the recently published full genomic sequence (Richards et al., 2008) and the established transgenesis systems (Berghammer et al., 1999) transform *Tribolium* into a primary model system. Since recently, an insertional mutagenesis screen database provides mutants and enhancer trap lines for the growing *Tribolium* community (http://134.76.20.145/Default.aspx). Meanwhile, *Tribolium* has become one of the most important models in the field of evolution and development ("evo-devo") because its development is more "insect typical", compared to that of the classical system *Drosophila* (Klingler, 2004). Currently, only little information on the brain or its embryonic and metamorphic development is available. With our pioneering study we provide for the first time anatomical descriptions for most of the brain areas of adult *Tribolium* including 3D reconstructions and an average brain atlas for selected brain neuropils. With the latter, we present the first standardization of a coleopteran brain.

Brains are typically organized in defined neuropils, which can usually be characterized by their spatial location, gross anatomy, and often by a certain function. For example, the olfactory bulbs of vertebrates and the antennal lobes (ALs) of insects have been attributed to be the first processing centers for olfactory information (for a review see Hildebrand and Shepherd, 1997). Compared to most vertebrate brains, insect brains are miniature versions being typically comprised of a lower number of neurons and neuropils. Owing to the lower complexity and certain technical advantages, insects have been widely used as models to study principal mechanisms of information processing and integration, in the context of defined sensory inputs but also complex behaviors including learning and memory formation (e.g. Menzel, 2001; Heisenberg, 2003).

Brains of animals of the same or of evolutionary related species typically share the same principal organization. For example in neopteran insects, the central olfactory pathway seems to be well conserved (Strausfeld et al., 1998; Schachtner et al., 2005). However, even within the same species, no brain is identical with the next, differing in size and shape of certain brain neuropils. These individual differences can result from a variety of parameters which are influencing brain organization during development but also during adulthood. In insects, such factors include brood temperature, sex, age, and experience (Groh et al., 2004; Technau, 2007; Molina and O'Donnell, 2008).

To study sexual brain dimorphism or the influence of defined parameters (ranging from single molecules to social experience) on brain development or adult plasticity, average or standardized brains or brain areas are needed to relate individual variations to

each other. Advances in imaging techniques, 3D reconstruction software, and computer power led so far to 3D reconstructions and subsequent standardization of brain areas of four insect species including *Drosophila melanogaster* (Rein et al., 2002; Jenett et al., 2006), the honeybee *Apis mellifera* (Brandt et al., 2005), the desert locust *Schistocerca gregaria* (Kurylas et al., 2008), and the sphinx moth *Manduca sexta* (el Jundi et al., 2009). To obtain such a standard insect brain, two methods have so far been established: The virtual insect brain (VIB) protocol and the iterative shape averaging (ISA) method. While the VIB protocol was mainly developed to compare wild type and genetically manipulated *Drosophila* (Rein et al., 2002; Jenett et al., 2006), the ISA method, first used for the honeybee, was aimed to register single reconstructed neurons from various individuals into one standard brain (Rohlfing et al., 2004; Brandt et al., 2005). Although the ISA method provides a far better representation of relative locations of brain areas, this high registration quality comes with the tradeoff of missing volumetric consistency for the neuropils. This means, a neuropil label of the standardized ISA brain does not represent the mean volume of all corresponding individual neuropil labels (Kuß et al., 2007; Kurylas et al., 2008). Thus, the VIB script remains advantageous for fast inter– and intraspecific comparisons of neuropils including sex-specific differences, while preserving volumetric consistency.

In the current study, we reconstructed in three dimensions and subsequently standardized brain areas of both sexes of the red flour beetle *Tribolium castaneum* using the VIB protocol. The aims of our study were to (1) compare adult brain neuropil volumes regarding sexual dimorphism (2) provide an adult female and male standard brain at A0 (freshly eclosed adults) as volume references for future genetical and behavioral studies, and (3) to compare the standard volumes of brain areas with previously published standard volumes of homologous brain areas of other neopteran insects. To obtain the desired datasets we labeled whole brains with an antiserum against the synaptic vesicle protein synapsin to visualize neuropil areas, analyzed the staining using confocal laser scanning microscopy, 3D reconstructed the selected brain neuropils using the software AMIRA (Visage Imaging, Fürth, Germany), and subsequently registered and standardized the neuropils using the (VIB) protocol. A standardization using the ISA method can be computed on request. Comparing the standardized neuropil volumes between females and males revealed no obvious sexual dimorphism in A0 *Tribolium* brains.

MATERIALS AND METHODS

ANIMALS

Wild type *Tribolium castaneum* (San Bernardino; Sokoloff, 1966) stock for egg laying was kept in plastic boxes (20 × 18 × 18 cm) in walk-in environmental chambers at 26°C under constant darkness. The boxes were half filled with substrate containing organic whole wheat flour supplemented with 5% dried yeast powder. To prevent sporozoan infections we added 0.05% (w/w) Fumidil-B (J. Webster Laboratories Inc., Princeville, Kanada; Berghammer et al., 1999).

For egg collection, we used similar procedures as described in Berghammer et al. (1999). The beetles were kept for 2 days in substrate and then separated from the substrate with a stainless steel sieve (710-µm mesh size; Retsch, Haan, Germany) to be transferred into a box filled with instant flour (type 405; Aurora Mühlen GmbH, Hamburg, Germany) for egg laying. After 2 days in instant flour, the beetles were separated again with the 710-µm sieve and the eggs fetched with a fine sieve (300-µm mesh size, Retsch, Haan, Germany). Instant flour was used for collecting eggs, because it becomes less clotted und does thus not clog the sieves in contrast to the normal white flour (Berghammer, et al., 1999). Eggs were then transferred into a separate box filled with fresh substrate. To optimize egg-laying performance, separated beetles were transferred back to substrate (Sokoloff, 1974). This separation technique was used to avoid the contamination of the substrate with secretions of the parents e.g. benzoquinones, because they can heavily influence the development of the larvae (Chapman, 1926; Happ, 1968; Sokoloff, 1974, 1977). The collected eggs were kept in substrate in smaller boxes (20 × 12 × 4 cm) in an incubator at 30°C and constant darkness. After about 4 weeks, the first beetles finished metamorphosis and freshly eclosed beetles (A0) could be collected. A0 beetles can be easily distinguished from older beetles by their white cuticle and their slow movement.

IMMUNOHISTOCHEMISTRY

For wholemount staining we adapted and refined the protocols described by Huetteroth and Schachtner (2005) and el Jundi et al. (2009). Whole brains were dissected in a drop of cold PBS (phosphate-buffered saline, 0.01 M, pH 7.4) and fixed subsequently in 4% formaldehyde (Roth, Karlsruhe, Germany) in 0.01-M PBS for 1–2 h at room temperature. The brains were then rinsed five times for 10 min at room temperature in 0.01 M PBS followed by preincubation for 1–2 days at 4°C in 5% normal goat serum (NGS; Jackson ImmunoResearch, Westgrove, PA, USA) in 0.01 M PBS containing 0,3% Triton X-100 (PBST). The monoclonal primary antibody from mouse against a fusion protein consisting of a glutathione-S-transferase and the first amino acids of the presynaptic vesicle protein synapsin I coded by its 5′-end (SYNORF1, Klagges et al., 1996) was used to selectively label neuropilar areas in the brain (3C11, #151101 (13.12.06), kindly provided by Dr. E. Buchner, Würzburg). Its specificity in *T. castaneum* was shown with Western blot (Utz et al., 2008). The brains were incubated in a 1:100 dilution of the synapsin antibody in PBST containing 2% NGS for 2–3 days at 4°C. Subsequently the brains were rinsed three times for 15 min with PBST before they were incubated with the secondary goat anti-mouse antibody conjugated to Cy5 (1:300, catalog code 115-175-146, lot 71608, Jackson ImmunoResearch, Westgrove, PA, USA) in PBST and 1% NGS for 2 days at 4 °C. Afterwards the brains were rinsed again with PBST five times for 10 min and subsequently dehydrated in an ascending ethanol series (50%, 70%, 90%, 95%, and two times 100%, for 2.5 min each) and then cleared in methyl salicylate (Merck, Gernsheim, Germany), until the tissue was transparent. At last the brains were mounted in Permount (Fisher Scientific, Pittsbourgh, PA, USA) between two coverslips using two reinforcing rings as spacers (Zweckform, Oberlaindern, Germany) to prevent compression of brains.

CLSM IMAGE ACQUISITION AND PROCESSING

The wholemount preparations for the standard brains were scanned with a confocal laser scanning microscope (CLSM, Leica TCS SP2) at 512 × 512 pixel resolution by using a 40× oil immersion objective

(HCX PL APO 40×/1.25–0.75 Oil CS (working distance: 0.1 mm); Leica, Bensheim, Germany). All brains were scanned with a voxel size of 0.73 × 0.73 × 0.5 µm, a speed of 200 Hz, a pinhole of 1 Airy unit and a line average of 2–4.

ALs were scanned at 1024 × 1024 pixel resolution with a 63× oil immersion objective (HCX PL APO 63×/1.32–0.60, Oil Ph3 CS (working distance: 70 µm); Leica, Bensheim, Germany) or a 40× oil immersion objective (HCX PL APO 40×/1.25–0.75 Oil CS (working distance: 0.1 mm); Leica, Bensheim, Germany) using a Leica TCS SP2 CLSM or with a 63× glycerol objective (HCX PL APO 63×/1.30 Glyc 21°C CS (working distance: 0.26 mm); Leica, Bensheim, Germany) using a Leica TCS SP5 CLSM. Depending on the zoom factor (1–4), the different CLSM and different objectives we scanned with varying voxel sizes 0.07–0.16 × 0.07–0.16 × 0.5–1 µm. ALs were scanned with a speed of 200–400 Hz, a pinhole of 1 Airy unit and a line average of 2–4.

IMAGE SEGMENTATION, RECONSTRUCTION, STANDARDIZATION AND VISUALIZATION

The selected 19 neuropils of the male and female brains were labeled with the segmentation editor in AMIRA 4.1 (Visage Imaging, Fürth, Germany). For the eight individual glomeruli of the right ALs we used AMIRA 5.2.1. For the segmentation and reconstruction details we refer to Kurylas et al. (2008). In short, semi-automatically created voxel-based label fields of eight paired and three unpaired neuropilar structures in 20 female and 20 male *T. castaneum* brains provided the underlying matrix of all computation processes performed (i.e. polygonal surface models, morphometric analysis, and shape averaging). For orientation guidance, brain outlines were reconstructed separately. This label field however was not standardized. The color code for neuropils of the standard brains is consistent with Brandt et al. (2005), Kurylas et al. (2008), and el Jundi et al. (2009). We offer the AMIRA label fields with color codes as online download (Supplement 1). The orientation of the brain structures is given with respect to the body axis.

The VIB protocol used for registration and standardization was described in detail by Jenett et al. (2006) and is available at http://www.neurofly.de. The functions of the VIB protocol are integrated features of the AMIRA graphical environment. The application of the VIB protocol requires a template brain which defines the position of individual neuropils in the visualized standard brain. To overcome a subjective bias, we selected the template brains according to optimal position and symmetry of the reconstructed neuropils. The selection contained three steps. First, according to Kurylas et al. (2008) and el Jundi et al. (2009) we calculated the distances of the centers of each of the reconstructed neuropils to the center of the respective brain. All distances for each brain were summed up, and the differences to the mean distance were calculated for all 20 brains of each sex respectively. In a second step, we calculated the symmetry of the brain areas by calculating the difference of the angles between the vectors connecting the centers of the neuropils. To obtain the angles, we calculated the vectors between the centers of the paired neuropils using the scalar product. In this way, we calculated angles between three neuropil pairs (AL–Me, AL–Ca, Ca–Me). The sum of the three angles served as the symmetry criterion. Both, the results of the distance and the angle calculations were normalized, with the worst brain set to one for each criterion. In the resulting combined ranking, the normalized values of both criteria were added. The third criterion for the choice of the template brain was a visual inspection of the three best ranked brains for each sex respectively. For the male template, we choose the brain ranking at number one according to the first two criteria. For the female template we choose number two, because visual inspection of the three best ranked brains revealed that the left peduncle of female brain number one was somehow twisted towards the midline. In the female ranking, brains number one and two were very close together. The choice of the template brain does not influence the resulting standard volumes (Kurylas et al., 2008). For creation of standard brain neuropil labels, we chose an overlap threshold of 40% for all neuropils.

The statistical analysis of these data was obtained using Excel XP for Windows. The synapsin-immunoreactivity (syn-ir) in **Figures 1 and 5** was auto-contrasted in the OrthoSlice module of AMIRA. For visualization, neuropils segmented in AMIRA, were filled with transparent colored labels using Adobe Photoshop 8 (Adobe Systems, San Jose, CA, USA). Snapshots taken in AMIRA and Pictures edited in Photoshop (**Figures 1–3 and 5**), and diagrams generated with Excel XP (**Figures 4 and 6**) were imported to Corel Draw 13 (Corel Corporation, Ottawa, Ontario, CA, USA) without any further modification.

RESULTS

RECONSTRUCTED NEUROPILS

Of all major areas of the *Tribolium* brain we reconstructed those which we were able to unambiguously delimit in all three dimensions (8 paired and 3 unpaired neuropils). In the optic lobes, we reconstructed the medulla (Me), the lobula (Lo), the lobula plate (LoP), and the accessory medulla (aMe) (**Figures 1A-d, B-c′ and 2**). The LoP which lays posterior to the Lo is exclusively found in Ephemeroptera, Trichoptera, Coleoptera, Lepidoptera, Diptera (Strausfeld, 2005), and Heteroptera (Settembrini and Villar, 2005).

In the central brain we divided the mushroom body into two neuropils, the pedunculus (Pe), which contained the vertical lobe (vL) and medial lobe (mL), and the calyx (Ca) (**Figures 1A-b, B-a′,b′ and 2**). Although visible in the synapsin immunostaining, we refrained from including subunits of the pedunculus described for the moth *Spodoptera littoralis* (Sjöholm et al., 2005) or *Bombyx mori* (Fukushima and Kanzaki, 2009); the resulting complexity of the pedunculus would have greatly interfered with standardization procedures, and would have also interfered with interspecies comparison. Nevertheless, with the exception of the β'-, and γ-lobe, which lay very tight together and which typically are one protrusion after reconstruction, the other lobes of the pedunculus, the α-, α'-, and β- lobe (Zhao et al., 2008) are discernible protrusions in our reconstructions (**Figure 2**). Between the left and right mushroom body lies the central complex, which comprises the protocerebral bridge (PB), the upper and lower unit of the central body (CBU, CBL) and a small paired neuropil ventrally attached to the central body, the noduli (No) (**Figures 1A-c,e,f,B–b′ and 2**). The anteriormost labeled neuropils were the deutocerebral antennal lobes (AL, **Figures 1A-a and 2**).

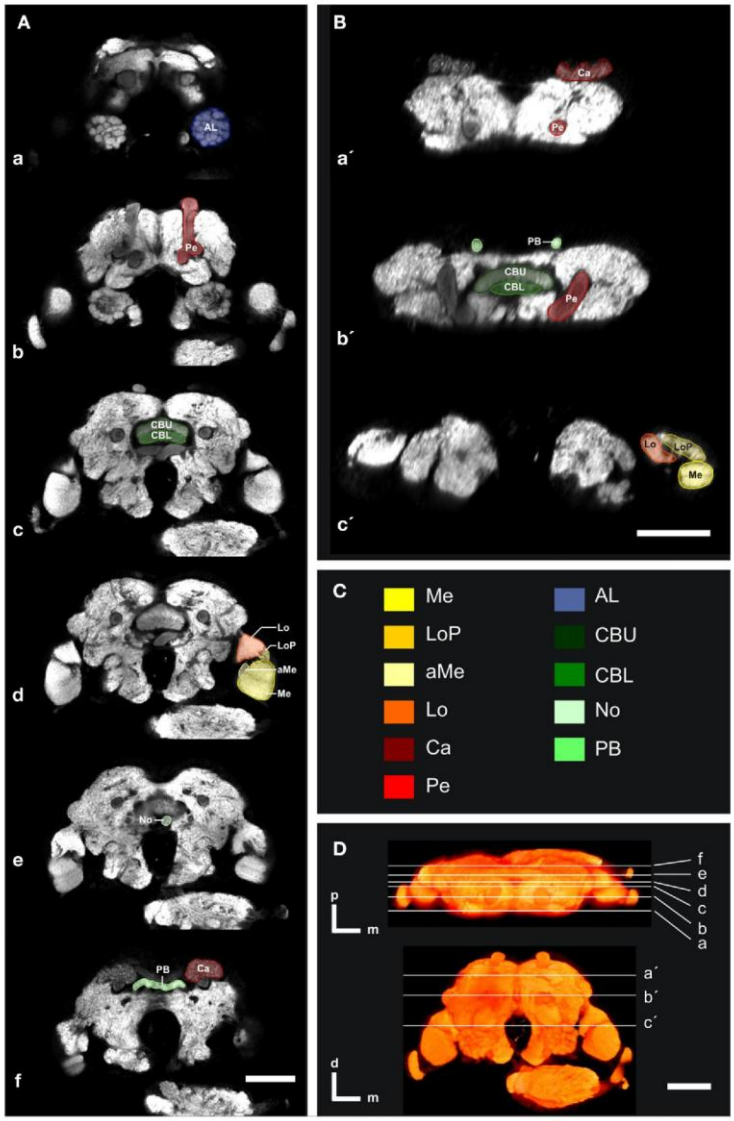

FIGURE 1 | Confocal images of the individual *T. castaneum* brain stained with an antibody against synapsin which was used as template for the VIB protocol. (A, B) Single optical sections through the brain in the frontal **(A)** and horizontal plane **(B)**. All manually labeled neuropil areas are shown as reconstructed in AMIRA. Labels of paired neuropils are only visualized in the left hemispheres, to provide a comparison to the unlabeled neuropils of the right hemispheres. **(A)** Frontal sections with the positions a–f from anterior to posterior and as described in **(D)**. **(B)** Horizontal sections with the positions a´–c´ from dorsal to ventral as described in **(D)**. **(C)** The color code of the labeled neuropils is consistent with Brandt et al. (2005), Kurylas et al. (2008), and el Jundi et al. (2009). AL, antennal lobe; Ca, Calyx; CBL, lower unit of the central body; CBU, upper unit of the central body; aMe, accessory medulla; Lo, lobula; LoP, lobula plate; Me, medulla; No, nodulus; PB, protocerebral bridge; and Pe, pedunculus with lobes. **(D)** Volume rendered (Voltex) view of the template brain from dorsal and frontal. The sections **(a–f)** and **(a′–c′)** represent the positions of the optical sections in **(A,B)**. Orientation bars, p, posterior; m, median; d, dorsal. All scale bars, 50 µm.

Representative outlines of all labels of these selected neuropils are shown in frontal and horizontal slices (**Figure 1**), an animation of all orthogonal sections of this brain can be found in the supplementary material (Supplement 2). Additionally, all reconstructed neuropils are displayed three-dimensionally to provide a 3D visualization of the whole brain (**Figure 2**).

THE STANDARD BRAINS

To apply the VIB protocol on the 3D brain reconstructions, one brain reconstruction had to be chosen as positional reference (Jenett et al., 2006). To reduce a subjective bias, we selected the template brains according to (1) position and (2) symmetry of the reconstructed neuropils, and (3) final visual inspection of the

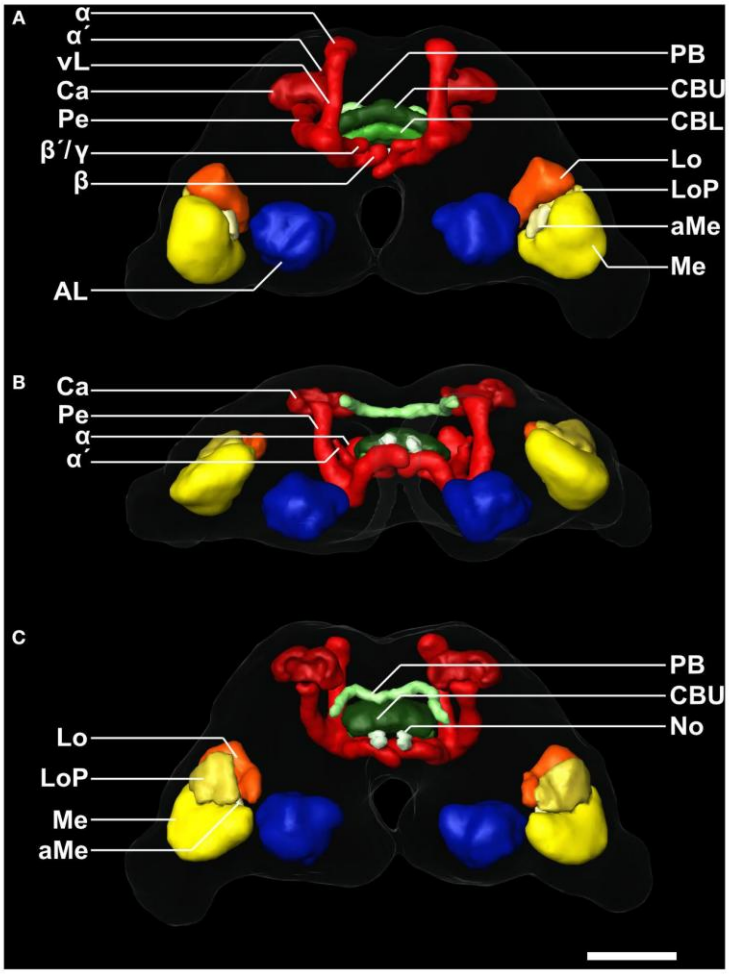

FIGURE 2 | 3D reconstruction of the male template brain of *T. castaneum* in (A) anterior (B) ventral, and (C) posterior view. The neuropils were visualized with the AMIRA tools SurfaceGen and Surfaceview. Note that the α and α´ lobes of the medial lobes can be clearly distinguished. In the medial lobes, the β-lobes are visible, while the second protrusion represents the β´- and the γ-lobes which were not discernable in the reconstruction. vL, vertical lobe. See **Figure 1** for color code and abbreviations. Scale bar, 50 μm.

three best brains resulting from criteria one and two (see Section "Materials and Methods"). The template brain used for generating the male standard brain is shown in **Figures 1 and 2**.

For the female and the male standard brain we reconstructed selected neuropils of 20 individual female and 20 individual male brains of freshly eclosed (A0) *T. castaneum*. With the VIB protocol we generated three-dimensional standard atlases of both sexes consisting of 19 neuropils (eight paired and three unpaired neuropils), including both hemispheres of the brain. The neuropil surface model and the corresponding average intensity map produced by direct volume rendering of the male standard brain are shown in **Figures 3A–C,A′–C′** from anterior, ventral and posterior. Volume rendering of all 20 label images after non-rigid registration reveal the high quality of registration (**Figures 3D,E**). Clear deviations are only visible in the vL of the MBs (**Figures 3D,E**). An animated view of the male standard brain can be seen in the online supplement (Supplement 3).

COMPARISON OF THE FEMALE AND MALE BRAINS

The VIB protocol also generates the standard volumes for each of the reconstructed brain areas of the 20 female and 20 male brains respectively. **Table 1** gives mean volumes, standard deviation and standard error of absolute and relative volumes of all 19 areas. Within each sex, a comparison of the volumes of the corresponding left and right brain neuropils using the two-tailed student t-test revealed no significant difference (not shown). Comparing the volumes of corresponding neuropils between females and males resulted also in no significant difference (**Figure 4**).

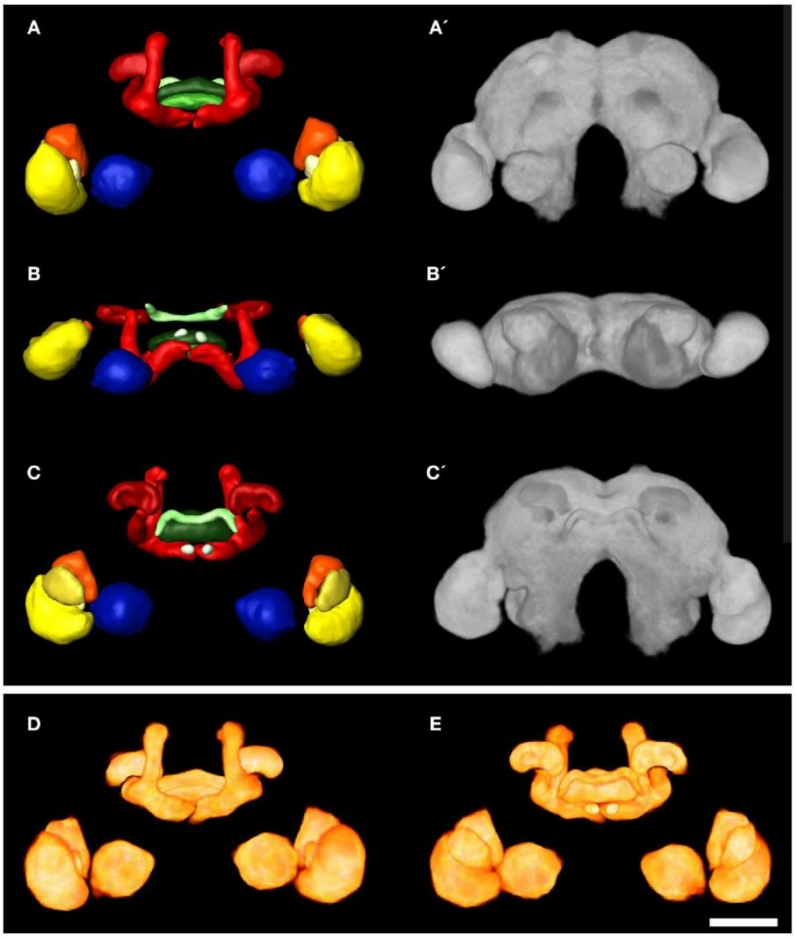

FIGURE 3 | 3D male standard brain of *T. castaneum* calculated from 20 individual brains by using the VIB protocol. (A–C) Surface reconstructions of all 18 averaged labels in **(A)** anterior **(B)** ventral, and **(C)** posterior view. The brain surface (as in **A´–C´**) is not labeled. See **Figure 1** for color code. **(A´–C´)** 3D visualization of the corresponding average intensity map by direct volume rendering with **(A´)** anterior **(B´)** ventral, and **(C´)** posterior view, using non-rigid transformation. **(D, E)** Direct volume rendered view of the resulting average label images from **(D)** anterior and **(E)** posterior, exhibiting deviations primarily in the lobes of the pedunculi of the MBs. Scale bar, 50 µm.

MALE – FEMALE GLOMERULUS COMPARISON

The glomerular array of ALs of adult female and male *T. castaneum* consists of about 70 glomeruli (Schachtner et al., 2007). The glomeruli are arranged in two layers around a central coarse neuropil. Anatomical sexual dimorphism in the ALs has been found in several species in which typically males have enlarged glomeruli at the entrance site of the antennal nerve (Schachtner et al., 2005). However, inspection of optical section series did not reveal an obvious morphological difference between A0 female and male ALs.

Searching for glomeruli which we could easily identify from animal to animal, we found an array of eight glomeruli at the lateral dorsal part of the AL, which we could unequivocally detect in 75% of our preparations. The set of dorso-lateral (dl) glomeruli consists of two larger glomeruli (dl-1, dl-2), three midsized (dl-3, dl-4, dl-7), and three smaller glomeruli (dl-5, dl-6, dl-8) with glomerulus dl-7 always being the most dorsal glomerulus of this set (**Figure 5**). We reconstructed these eight glomeruli from 10 female and 10 male right ALs with each AL stemming from a different specimen. Like the comparison between the AL volumes and all other reconstructed neuropils, comparison of the glomerular volumes between the two sexes revealed no significant difference in any one of the selected glomeruli (**Figure 6**).

DISCUSSION

Tribolium castaneum belongs to the most species-rich and most diverse order in the animal kingdom; Coleoptera comprise about 40% of all insect species and thus about 30% of all living animal species (Grimaldi and Engel, 2005; Hunt et al., 2007; Hauser et al., 2008). Worldwide, *Tribolium* is a major pest for stored grain and grain products and serves as a powerful model for the study of

Table 1 | Volume measures of neuropil structures in the male and female standard brain of *T. castaneum*. Mean volume (Mean vol.), relative volume (Rel. vol.), standard deviation (SD), relative standard deviation (Rel. SD), standard error (SE), and relative standard error (Rel. SE) of all segmented brain areas in the male (n = 20) and female (n = 20) standard brain of *T. castaneum*.

Structure	Sex	Mean vol. (µm³)	Rel. vol. (%)	SD (µm³)	Rel. SD (%)	SE (µm³)	Rel. SE (%)
Medulla (left)	♂	30339.91	14.85	7271.10	23.97	1625.87	5.36
	♀	34216.66	16.94	10668.84	31.18	2325.22	6.97
Medulla (right)	♂	31172.43	15.25	6053.76	19.42	1353.66	4.34
	♀	34157.33	16.91	9922.73	29.05	2162.61	6.50
Lobula plate (left)	♂	4824.63	2.36	1292.49	26.79	289.01	5.99
	♀	5251.18	2.60	850.56	16.20	185.37	3.62
Lobula plate (right)	♂	4599.73	2.25	1023.55	22.25	228.87	4.98
	♀	5073.72	2.51	681.34	13.43	148.50	3.00
Inner lobula (left)	♂	8685.43	4.25	1828.24	21.05	408.81	4.71
	♀	9554.28	4.73	1735.88	18.17	378.33	4.06
Inner lobula (right)	♂	9517.20	4.66	2256.13	23.71	504.49	5.30
	♀	9624.48	4.77	2820.86	29.31	614.79	6.55
Accessory medulla (left)	♂	1143.63	0.56	385.77	33.73	86.26	7.54
	♀	1173.94	0.58	350.44	29.85	76.38	6.67
Accessory medulla (right)	♂	1159.82	0.57	340.94	29.40	76.24	6.57
	♀	1230.22	0.61	406.31	33.03	88.55	7.39
Calyx (left)	♂	6003.60	2.94	1408.59	23.46	314.97	5.25
	♀	5515.65	2.73	1228.05	22.26	267.65	4.98
Calyx (right)	♂	6191.91	3.03	1084.28	17.51	242.45	3.92
	♀	5412.37	2.68	764.70	14.13	166.66	3.16
Pedunculus (left)	♂	17571.30	8.60	4577.99	26.05	1023.67	5.83
	♀	15796.60	7.82	3972.44	25.15	865.77	5.62
Pedunculus (right)	♂	17256.15	8.44	4794.07	27.78	1071.99	6.21
	♀	16057.83	7.95	3547.41	22.09	773.14	4.94
Central body upper unit	♂	10263.34	5.02	3179.91	30.98	711.05	6.93
	♀	8668.66	4.29	1842.36	21.25	401.53	4.75
Central body lower unit	♂	2838.02	1.39	1406.16	49.55	314.43	11.08
	♀	2364.33	1.17	713.66	30.18	155.54	6.75
Protocerebral bridge	♂	3551.02	1.74	863.97	24.33	193.19	5.44
	♀	3310.99	1.64	630.28	19.04	137.37	4.26
Nodulus (left)	♂	371.08	0.18	115.22	31.05	25.77	6.94
	♀	378.12	0.19	74.10	19.60	16.15	4.38
Nodulus (right)	♂	380.17	0.19	142.66	37.53	31.90	8.39
	♀	362.49	0.18	70.73	19.51	15.42	4.36
Antennal lobe (left)	♂	24373.09	11.93	5834.27	23.94	1304.58	5.35
	♀	22316.68	11.05	6733.24	30.17	1467.48	6.75
Antennal lobe (right)	♂	24105.27	11.80	6511.04	27.01	1455.91	6.04
	♀	21492.52	10.64	6132.60	28.53	1336.57	6.38

general insect development and evolution. Owing to the feasibility of transgenic approaches, such as powerful reverse genetics based on systemic RNA-interference, directed gene expression, the recently published full genome sequence, easy culturing, a short life cycle, high fecundity and longevity, *Tribolium* is emerging as a model system at many fronts. With the current study, we provide a reference for future anatomical studies of the brain in connection with genetical manipulation and external parameters as e.g. odor- or social environment and adaptive learning. The average brain atlas comes from freshly eclosed *Tribolium* of both sexes. Since we are especially interested in the development and plasticity of the olfactory system, we established an anatomical and volumetric reference of eight selected female and male olfactory glomeruli. Compared to existing insect standard brains, the *T. castaneum* standard poses - together with the *Drosophila* standard - the smallest brain.

STANDARD BRAIN GENERATION

Two methods have been established to obtain a standard insect brain: (1) the VIB protocol, as used for the fruit fly, the desert locust, and the sphinx moth (Rein et al., 2002; Jenett et al., 2006; Kurylas et al., 2008; el Jundi et al., 2009), and (2) the ISA method, as used for the honeybee and also the desert locust (Rohlfing et al., 2004; Brandt

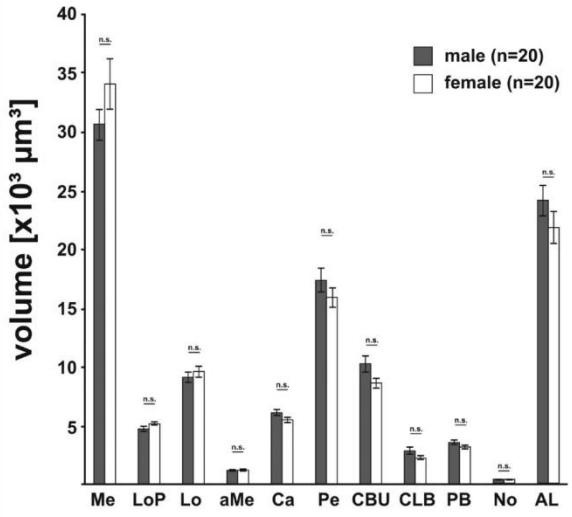

FIGURE 4 | Comparison of neuropil volumes between male (gray) and female (white) brains. The data revealed no significant difference (two-tailed Student's *t*-test) between the volumes of the corresponding neuropils of females and males. Bars, standard error; n.s., not significant.

et al., 2005; Kurylas et al., 2008). The VIB protocol was primarily developed to compare brain areas e.g. between wildtype and genetically manipulated *Drosophila*, while the ISA method aims to generate a synthetic but realistic standard brain, into which single reconstructed neurons from various individuals could be mapped. The VIB script keeps neuropil volumes rather unchanged, while the ISA method, in contrast, averages anatomical differences on the cost of volume accuracy (Kuß et al., 2007; Kurylas et al., 2008; el Jundi et al., 2009). Both methods require an initial reference or template brain for alignment. While the visualization of the standardized brain areas using the VIB protocol is clearly biased towards this template, the ISA method is thought to be independent of the choice of the template (Guimond et al., 2000; Brandt et al., 2005), with the notable exceptions of orientation and scale. During affine registration in the ISA method, all brains are resized using anisotropic scaling to match the size of the template brain. Thus, the resulting standard volumes of the brain areas generated by the ISA method depend on the choice of the template brain (Rohlfing et al., 2001; el Jundi et al., 2009). Therefore we decided to use the VIB protocol for standardization, since we primarily wanted to compare volumes of neuropils and did not aim for registration of reconstructed neurons (Rø et al., 2007; Kurylas et al., 2008). Given that both methods are established in our lab, a female and a male standard brain calculated by the ISA method could be computed on request.

It has to be noted that our whole mount specimens, like all immunohistochemical preparations, are subjected to considerable tissue shrinking (Bucher et al., 2000; Ott, 2008). Therefore absolute sizes are probably underestimated and make most sense in relative comparisons, i.e. comparisons might only be useful between brains after similar histological treatment. In a previous work, we already showed the usability of 3D reconstructions to quantify adult plasticity in the male antennal lobe of the sphinx moth (Huetteroth and Schachtner, 2005). Since we carefully checked for animal age, the female and male standard brain will serve as a reference in future quantitative studies using genetical or behavioral approaches.

BRAIN NEUROPIL COMPARISON BETWEEN SEXES

We found no volumetric differences between females and males in any one of the standardized brain neuropils, including the eight olfactory glomeruli. Anatomical sexual dimorphism in brain structures has been described in a variety of insects primarily with respect to the ALs (for a review see Schachtner et al., 2005). Enlarged glomeruli at the entrance site of the antennal nerve are described for males, as example for cockroaches (Jawlowski, 1948; Neder, 1959; Boeckh et al., 1987), bees (Arnold et al., 1984; Brockmann and Brückner, 2001), ants (Kleineidam et al., 2005; Nishikawa et al., 2008), flies (Kondoh et al., 2003), and moths (reviewed in Anton and Homberg, 1999; Hansson and Anton, 2000). These glomeruli are usually called macroglomeruli or macroglomerular complex (MGC). These glomeruli appear to be involved in pheromone signal processing (reviewed e.g. in Hansson and Christensen, 1999).

Why did we see no sexual dimorphism in the examined brain areas? In principal we expect sexual dimorphism on the level of the brain areas due to sexual specific input (e.g. in the case of the olfactory system a higher number of receptor neurons responsible for the detection of the female pheromone) and/or due to sexual specific behaviors which have to be coordinated from female or male brains in the context of sexual reproduction. The question is whether this dimorphism can be seen on the level of gross brain anatomy like in the case of the sexual specific glomeruli or whether it is due to a few special neurons or and/or different neurochemistry with only little or no effect on gross morphology. As individual variations in neuropil volumes range in the mean at around 20%, we cannot detect anatomical sexual dimorphism smaller than that. Furthermore, we looked at freshly eclosed animals. Thus, the animals are not sexually mature at that time and the brain has just started to get acquainted to the environmental cues including odor information like e.g. pheromones. Currently, we produce a female and male standard brain atlas for 7-day-old animals to examine how brain anatomy is changing in females and males. In *M. sexta* for example, the sexual dimorphic male glomeruli increase about 40% in volume during the first 4 days of adulthood (Huetteroth and Schachtner, 2005).

INTERSPECIES BRAIN COMPARISON

The relative size of a defined brain area is closely related to its apparent importance for the respective animal (e.g. Barton et al., 1995; Gronenberg and Hölldobler, 1999; Schoenemann, 2006). For example in insects larger optic lobes primarily correlate with larger complex eyes containing more photoreceptor cells, while the volume of ALs correlates with the amount of olfactory sensory axons entering this structure. Likewise, the volumes and the organization of higher order integration centers like the mushroom bodies correlate with the complexity of multimodal sensory integration (e.g. Technau, 2007; Molina and O'Donnell, 2008). Additionally, studies in several insect species demonstrated a correlation of volumes of brain areas with age, caste, sex and experience, including primary sensory integration centers like OL and AL, and higher integration centers like the mushroom bodies (Heisenberg et al., 1995; Barth

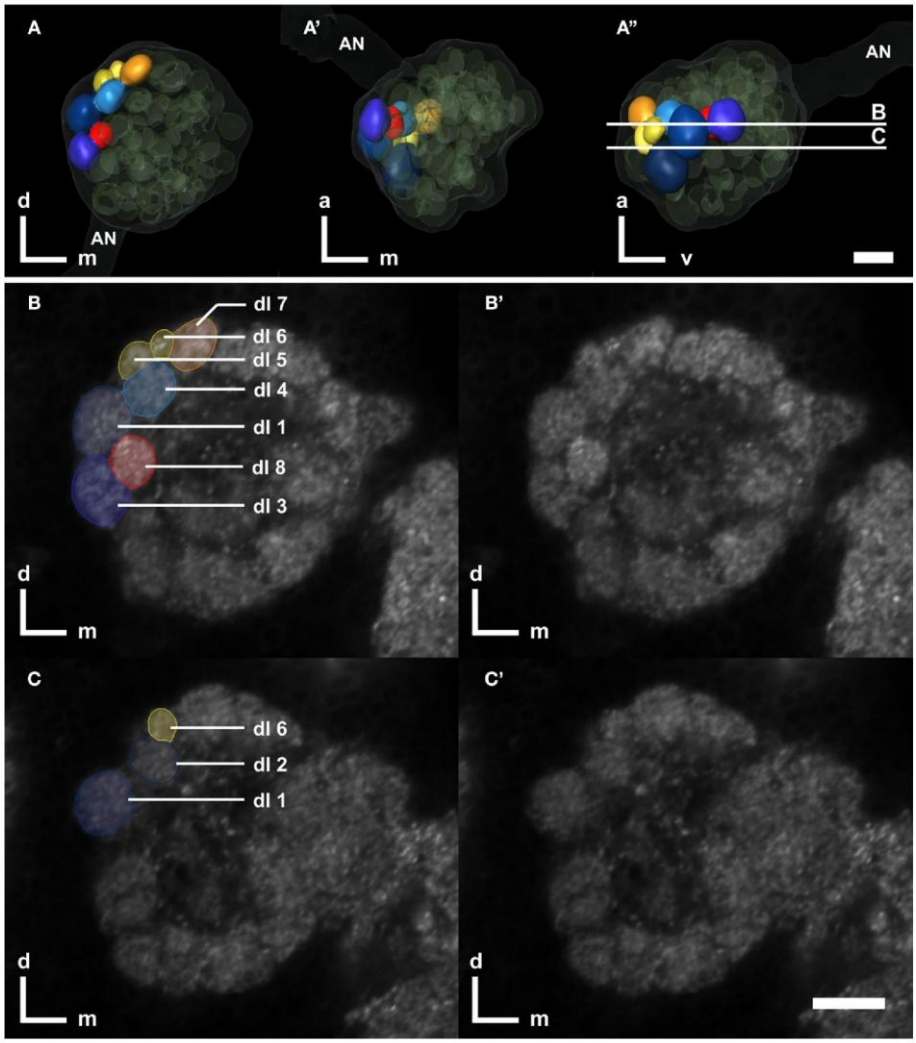

FIGURE 5 | Right antennal lobe of a male *T. castaneum* brain. (A–A′) Anterior **(A)**, ventral **(A′)**, and lateral view **(A″)** of 3D-reconstructed glomeruli including the antennal nerve (AN, transparent). The eight color coded dorso-lateral glomeruli (dl-1 to 8, compare with **B,C**) can be unequivocally identified in 75% of all preparations. Other glomeruli are depicted in transparent green; the displayed outline of the AL is shown in transparent gray. The transparent encasement around the AL represents the shape of the whole AL. The vertical bars in **(A″)** display section levels of **(B,C)** and **(B′,C′)**, respectively. Orientation bars: a, anterior; d, dorsal; m, medial; v, ventral. **(B,C)** Frontal confocal sections through the antennal lobe according to **(A″)**. The eight dorso-lateral glomeruli are manually labeled as reconstructed in AMIRA. **(B′,C′)** Confocal sections through the antennal lobe corresponding to **(B,C)**. All scale bars: 10 μm.

and Heisenberg, 1997; Barth et al., 1997; Sigg et al., 1997; Julian and Gronenberg, 2002; Groh et al., 2006; Technau, 2007; Krofczik et al., 2008; Molina and O'Donnell, 2008; Maleszka et al., 2009; Snell-Rood et al., 2009). So far, the few published insect standard brains give only a limited view on the respective relative volumes of defined brain areas of these species because they provide (1) data for only one sex (with the exception of *M. sexta*) and (2) one age (*D. melanogaster*: 5-day-old adult females; Rein et al., 2002; *M. sexta*: freshly eclosed adult females and males; el Jundi et al., 2009), or (3) a mixture of different ages (*A. mellifera* foragers: Brandt et al., 2005; *S. gregaria* males: Kurylas et al., 2008). Caste or possible experience dependent differences have also not been taken into account. Thus, a comparison between the relative volumes of the available standardized brain areas has to be judged under these prerequisites (**Table 2**).

In *T. castaneum*, the optic lobes show the smallest relative volumes, which corresponds to the relative small compound eyes (with 80–83 ommatidia per eye; Friedrich et al., 1996) compared to the other insect species. The ALs in contrast display the largest relative volume, which suggests that *Tribolium* may primarily rely upon chemical cues, a fact which has been generally proposed for insects inhabiting grain storage areas (Levinson and Levinson,

1995). Behavioral assays showed that *T. castaneum* prefers damaged or deteriorated grains to full grains and it responds best to volatiles characteristic of damaged or fungus-infested grain (Trematerra et al., 2000). Tenebrionid beetles, including *T. castaneum*, produce a rich repertoire of volatiles in a variety of glands. Major volatile secretions, stored in specialized prothoracic and postabdominal glands are the quinones which may act as defensive secretions and antimicrobial substances (Prendeville and Stevens, 2002; Yezerski et al., 2004, 2007). Adult males of *T. castaneum* possess setiferous glands on the femora of their prothoracic legs (Faustini et al., 1981, 1982), which secrete the highly volatile pheromone, 4,8-dimethyldecanal (DMD), which is attractive to females and, to a less extent, to males and was therefore classified as an aggregation pheromone (Suzuki, 1980, 1981). However, the male setiferous glands may not be the major source of DMD (Bloch Qazi et al., 1998; Arnaud et al., 2002). Moreover, a recent electrophysiological investigation on *Tribolium* volatile compounds led to the conclusion that several beetle produced compounds, in addition to DMD, may be part of a complex aggregation pheromone system (Verheggen et al., 2007).

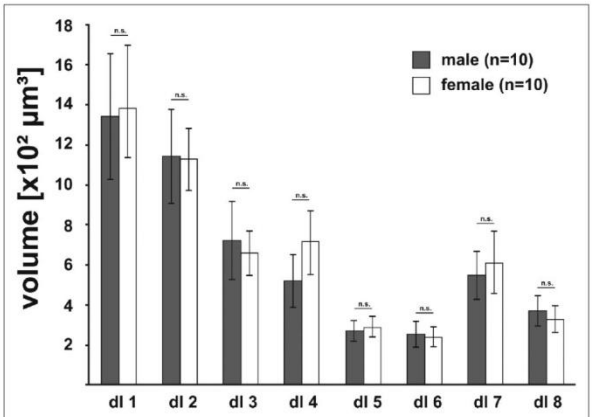

FIGURE 6 | Comparison of the volumes of the eight identified glomeruli between right male (gray; *n* = 10) and right female (white; *n* = 10) ALs, revealed no significant difference between the sexes (two-tailed student t-test). Bars, standard error; n.s., not significant.

Mushroom bodies (MBs) are generally associated with higher integration processes and learning (e.g. Menzel, 2001; Heisenberg, 2003), but might also serve a general function in the control of behavior (e.g. Huber, 1955a, b; Erber et al., 1987; Zars, 2000; Strausfeld et al., 2009). While the social honeybee by far exhibits the largest relative MB volumes, interestingly, *Tribolium* is second before *Drosophila* (**Table 2**). A recent study found similar development of MBs in *Tribolium* and *Drosophila*, with the remarkable difference, that adult neurogenesis occurs in *Tribolium* (Zhao et al., 2008). MBs vary in relative size in different nymphalid butterflies, without a correlation with optic or antennal lobe size. *Heliconius charitonius* for example has almost four times bigger mushroom bodies than other butterflies of that family (Sivinsky, 1989). This is attributed to its relative long life combined with its occurrence in forest habitats with only scattered food resources, and a shared resting place with conspecifics. As discussed by the author, remembering a common resting place and good food sites might be a higher evolutionary constraint for learning ability than finding proper egg-laying sites, which does not necessarily involve memory tasks (Sivinsky, 1989). For the ant *Cataglyphis*, Wehner et al. (2007) discussed social interaction rather than food gathering for being responsible of bigger mushroom bodies compared to other ant species, an idea originally brought up by von Alten (1910). The relative large size of the MBs in *Tribolium* suggests a high integrative capacity which may include olfactory components (see above). Additionally, a life expectation of months to years and a long reproductive period (Dawson, 1977) might also justify an investment into a brain structure dedicated to higher integration, memory, and behavioral control.

The function of the central complex still remains elusive, but is probably best described as a central coordinating function in sensory and motor integration (for reviews see Strauss, 2002; Wessnitzer and Webb, 2006; Homberg, 2008). Regarding the relative volume of the central complex, the sum of relative ellipsoid body volume and fan-shaped body volume in the fly and the relative volume of upper and lower units in locust, honeybee, moth, and beetle, *Tribolium* exceeds even that of the fly. This suggests a more complex function than in all other examined insects. In this context, it would be interesting to have comparable standardized central complex volumes of other coleopterans with different lifestyles e.g. water beetles or non-flying beetles.

Table 2 | Comparison of relative neuropilar volumes between different insect species obtained from five different insect orders, namely Diptera (*Drosophila melanogaster*: Rein et al., 2002), Hymenoptera (*Apis mellifera*: Brandt et al., 2005), Orthoptera (*Schistocerca gregaria*: Kurylas et al., 2008), Lepidoptera (*M. sexta*, el Jundi et al., 2009), and Coleoptera (*T. castaneum*, this work). We included the sex and the number of individuals which were used for respective standardization. Only neuropils which have complements in all examined animals were compared (optic lobes: medulla, lobula complex, and lobula plate; antennal lobes, mushroom bodies including calyces and pedunculi, upper and lower unit of the central body).

Order	**Diptera**	**Hymenoptera**	**Orthoptera**	**Lepidoptera**		**Coleoptera**	
Species	***D. melanogaster***	***A. mellifera***	***S. gregaria***	***M. sexta***		***T. castaneum***	
Sex	♀	♀	♂	♀	♂	♀	♂
Number of individuals	28	20	10	12	12	20	20
Optic lobes (%)	79.65	57.91	72.67	79.36	77.35	50,06	45,05
Antennal lobes (%)	9.36	8.53	9.68	12.86	15.09	22,41	24,50
Central body (%)	3.43	0.91	1.67	0.91	0.89	5,64	6,62
Mushroom bodies (%)	7.56	32.65	15.98	6.87	6.76	21,88	23,83

With the current study we provide a standard female and male brain of freshly eclosed *T. castaneum*. These standard brains will serve as a useful tool to study brain development and brain plasticity.

ACKNOWLEDGMENTS

The authors thank Dr. Erich Buchner (University of Würzburg, Germany) for kindly providing the anti-Synapsin antibody and Drs. Jochen Trauner and Gregor Bucher for supplying us with starter colonies of *Tribolium*. The authors are also grateful to Drs. Uwe Homberg, Ernst Wimmer and Stefan Schütz for many fruitful discussions and Martina Kern and Silke Redelfs for expert technical assistance. This work was supported by a DFG grant (SCHA 678/13-1) to Joachim Schachtner.

SUPPLEMENTARY MATERIAL

The Supplementary Material for this article can be found online at http://www.frontiersin.org/systemsneuroscience/paper/10.3389/neuro.06/003.2010/

REFERENCES

Anton, S., and Homberg, U. (1999). Antennal lobe structure. In Insect Olfaction, B. S. Hansson, ed. (Berlin, Springer), pp. 97–124.

Arnaud, L., Lognay, G., Verscheure, M., Leenaers, L., Gaspar, C., and Haubruge, E. (2002). Is dimethyldecanal a common aggregation pheromone of *Tribolium* flour beetles? *J. Chem. Ecol.* 28, 523–532.

Arnold, G., Masson, C., and Budharugsa, S. (1984). Demonstration of a sexual dimorphism in the olfactory pathways of the drones of *Apis mellifica L.* (Hymenoptera, Apidae). *Experientia* 40, 723–725.

Barth, M., and Heisenberg, M. (1997). Vision affects mushroom bodies and central complex in *Drosophila melanogaster*. *Learn. Mem.* 4, 219–229.

Barth, M., Hirsch, H. V., Meinertzhagen, I. A., and Heisenberg, M. (1997). Experience-dependent developmental plasticity in the optic lobe of *Drosophila melanogaster*. *J. Neurosci.* 17, 1493–1504.

Barton, R. A., Purvis, A., and Harvey, P. H. (1995). Evolutionary radiation of visual and olfactory brain systems in primates, bats and insectivores. *Philos. Trans. R. Soc. Lond., B, Biol. Sci.* 348, 381–392.

Berghammer, A., Bucher, G., Maderspacher, F., and Klingler, M. (1999). A system to efficiently maintain embryonic lethal mutations in the flour beetle *Tribolium castaneum*. *Dev. Genes Evol.* 209, 382–389.

Bloch Qazi, M. C., Boake, C. R. B., and Lewis, S. M. (1998). The femoral setiferous glands of *Tribolium castaneum* males and production of the pheromone 4,8-dimethyldecanal. *Entomol. Exp. Appl.* 89, 313–317.

Boeckh, J., Ernst, K. D., and Selsam, P. (1987). Neurophysiology and neuroanatomy of the olfactory pathway in the cockroach. *Ann. N. Y. Acad. Sci.* 510, 39–43.

Bonneton, F. (2008). The beetle by the name of *Tribolium*: typology and etymology of *Tribolium castaneum* Herbst, 1797. *Insect Biochem. Mol. Biol.* 38, 377–379.

Brandt, R., Rohlfing, T., Rybak, J., Krofczik, S., Maye, A., Westerhoff, M., Hege, H. C., and Menzel, R. (2005). Three-dimensional average-shape atlas of the honeybee brain and its applications. *J. Comp. Neurol.* 492, 1–19.

Brockmann, A., and Brückner, D. (2001). Structural differences in the drone olfactory system of two phylogenetically distant *Apis* species, *A. florea* and *A. mellifera*. *Naturwissenschaften* 88, 78–81.

Bucher, D., Scholz, M., Stetter, M., Obermayer, K., and Pflüger, H. J. (2000). Correction methods for three-dimensional reconstructions from confocal images: I. Tissue shrinking and axial scaling. *J. Neurosci. Methods* 100, 135–143.

Bucher, G., Scholten, J., and Klingler, M. (2002). Parental RNAi in *Tribolium* (Coleoptera). *Curr. Biol.* 12, R85–R86.

Chapman, R. N. (1926). Inhibiting the process of metamorphosis in the confused flour beetle (*Tribolium* confusum Duval). *J. Exp. Zool.* 45, 293–299.

Dawson, P. S. (1977). Life history strategy and evolutionary history of *Tribolium* flour beetles. *Evolution* 31, 226–229.

el Jundi, B., Huetteroth, W., Kurylas, A. E., and Schachtner, J. (2009). Anisometric brain dimorphism revisited: implementation of a volumetric 3D standard brain in *Manduca sexta*. *J. Comp. Neurol.* 517, 210–225.

Erber, J., Homberg, U. and Gronenberg, W. (1987). Functional roles of the mushroom bodies in insects. In Arthropod brain: Its evolution, Development, Structure, and Functions, A. P. Gupta, ed. (New York, NY, Wiley), pp. 485–511.

Faustini, D. L., Burkholder, W. E., and Laub, R. J. (1981). Sexually dimorphic setiferous sex patch in the male red flour beetles *Tribolium castaneum* (Herbst) (Coleoptera: Tenebrionidae): site of aggregation pheromone production. *J. Chem. Ecol.* 7, 465–480.

Faustini, D. L., Post, D. C., and Burkholder, W. E. (1982). Histology of aggregation pheromone gland in the red flour beetle. *Ann. Entomol. Soc. Am.* 75, 187–190.

Friedrich, M., Rambold, I., and Melzer, R. R. (1996). The early stages of ommatidial development in the flour beetle *Tribolium castaneum* (Coleoptera; Tenebrionidae). *Dev. Genes Evol.* 206, 136–146.

Fukushima, R., and Kanzaki, R. (2009). Modular subdivision of mushroom bodies by kenyon cells in the silkmoth. *J. Comp. Neurol.* 513, 315–330.

Grimaldi, D., and Engel, M. S. (2005). Evolution of the Insects. Cambridge, Cambridge University Press.

Groh, C., Ahrens, D., and Rössler, W. (2006). Environment- and age-dependent plasticity of synaptic complexes in the mushroom bodies of honeybee queens. *Brain Behav. Evol.* 68, 1–14.

Groh, C., Tautz, J., and Rössler, W. (2004). Synaptic organization in the adult honey bee brain is influenced by brood-temperature control during pupal development. *Proc. Natl. Acad. Sci. U.S.A.* 101, 4268–4273.

Gronenberg, W., and Hölldobler, B. (1999). Morphologic representation of visual and antennal information in the ant brain. *J. Comp. Neurol.* 412, 229–240.

Guimond, A., Meunier, J., and Thirion, J. P. (2000). Average brain models: a convergence study. *Comput. Vis. Image Underst.* 77, 192–210.

Hansson, B. S., and Anton, S. (2000). Function and Morphology of the Antennal Lobe: New Developments. *Annu. Rev. Entomol.* 45, 203–231.

Hansson, B. S. and Christensen, T. A. (1999). Functional characteristics of the antennal lobe. In Insect Olfaction. B. S. Hansson, ed. (Berlin, Springer). pp. 126–162.

Happ, G. M. (1968). Quinone and hydrocarbon production in the defensive glands of *Eleodes longicollis* and *Tribolium castaneum* (Coleoptera, Tenebrionidae). *J. Insect Physiol.* 14, 1821–1837.

Hauser, F., Cazzamali, G., Williamson, M., Park, Y., Li, B., Tanaka, Y., Predel, R., Neupert, S., Schachtner, J., Verleyen, P., and Grimmelikhuijzen, C. (2008). A genome-wide inventory of neurohormone GPCRs in the red flour beetle *Tribolium castaneum*. *Front. Neuroendocrinol.* 29, 142–165. doi:10.1016/j.yfrne.2007.10.003.

Heisenberg, M. (2003). Mushroom body memoir: from maps to models. *Nat. Rev. Neurosci.* 4, 266–275.

Heisenberg, M., Heusipp, M., and Wanke, C. (1995). Structural plasticity in the *Drosophila* brain. *J. Neurosci.* 15, 1951–1960.

Hildebrand, J. G., and Shepherd, G. M. (1997). Mechanisms of olfactory discrimination: convergent evidence for common principles across phyla. *Annu. Rev. Neurosci.* 20, 595–611.

Homberg, U. (2008). Evolution of the central complex in the arthropod brain with respect to the visual system. *Arthropod Struct. Dev.* 37, 347–362.

Huber, F. (1955a). Über die Funktion der Pilzkörper (*Corpora pedunculata*) beim Gesang der Keulenheuschrecke Gomphocerus rufus L. (Acrididae). *Naturwissenschaften* 20, 566–567.

Huber, F. (1955b). Sitz und Bedeutung nervöser Zentren für Instinkthandlungen beim Männchen von Gryllus campestris L. *Z. Tierpsychol.* 12, 12–48.

Huetteroth, W., and Schachtner, J. (2005). Standard three-dimensional glomeruli of the *Manduca sexta* antennal lobe: a tool to study both developmental and adult neuronal plasticity. *Cell Tissue Res.* 319, 513–524.

Hunt, T., Bergsten, J., Levkanicova, Z., Papadopoulou, A., St. John, O., Wild, R., Hammond, P. M., Ahrens, D., Balke, M., Caterino, M. S., Gómez-Zurita, J., Ribera, I., Barraclough, T. G., Bocakova, M., Bocak, L., and Vogler, A. P. (2007). A Comprehensive phylogeny of beetles reveals the evolutionary origins of a superradiation. *Science* 318, 1913–1916.

Jawlowski, H. (1948). Studies on the insect brain. *Ann. Univ. Mariae Curie Sklodowska C* 3, 1–30.

Jenett, A., Schindelin, J. E., and Heisenberg, M. (2006). The virtual insect brain protocol: creating and comparing standardized neuroanatomy. *BMC Bioinformatics* 7, 544.

Julian, G. E., and Gronenberg, W. (2002). Reduction of brain volume correlates with behavioral changes in queen ants. *Brain Behav. Evol.* 60, 152–164.

Klagges, B. R., Heimbeck, G., Godenschwege, T. A., Hofbauer, A., Pflugfelder, G. O., Reifegerste, R., Reisch, D., Schaupp, M., Buchner, S., and Buchner, E. (1996). Invertebrate synapsins: a single gene codes for

several isoforms in *Drosophila*. *J. Neurosci.* 16, 3154–3165.

Kleineidam, C. J., Obermayer, M., Halbich, W., and Rössler, W. (2005). A macroglomerulus in the antennal lobe of leaf-cutting ant workers and its possible functional significance. *Chem. Senses* 30, 383–392.

Klingler, M. (2004). *Tribolium*. *Curr. Biol.* 24, R639–R640.

Kondoh, Y., Kaneshiro, K. Y., Kimura, K., and Yamamoto, D. (2003). Evolution of sexual dimorphism in the olfactory brain of Hawaiian *Drosophila*. *Proc. Biol. Sci.* 270, 1005–1013.

Krofczik, S., Khojasteh, U., de Ibarra, N. H., and Menzel, R. (2008). Adaptation of microglomerular complexes in the honeybee mushroom body lip to manipulations of behavioral maturation and sensory experience. *Dev. Neurobiol.* 68, 1007–1017.

Kuß, A., Hege, H. C., Krofczik, S., and Borner, J. (2007). Pipeline for the creation of surface-based averaged brain atlases. In Proceedings of Winter School of Computer Graphics Vol. 1 pp. 17–24.

Kurylas, A. E., Rohlfing, T., Krofczik, S., Jenett, A., and Homberg, U. (2008). Standardized atlas of the brain of the desert locust, *Schistocerca gregaria*. *Cell Tissue Res.* 333, 125–145.

Levinson, A., and Levinson, H. (1995). Reflections on structure and function of pheromone glands in storage insect species. *Anz. Schädlingskd. Pfl. Umwelt.* 67, 99–118.

Maleszka, J., Barron, A. B., Helliwell, P. G., and Maleszka, R. (2009). Effect of age, behaviour and social environment on honey bee brain plasticity. *J. Comp. Physiol. A* 195, 733–740.

Menzel, R. (2001). Searching for the memory trace in a mini-brain, the honeybee. *Learn. Mem.* 8, 53–62.

Molina, Y., and O'Donnell, S. (2008). Age, sex, and dominance-related mushroom body plasticity in the paper-wasp *Mischocyttarus mastigophorus*. *Dev. Neurobiol.* 68, 950–959.

Neder, R. (1959). Allometrisches Wachstum von Hirnteilen bei drei verschieden großen Schabenarten. *Zool. Jahrb. Abt. Allg. Zool. Physiol.* 77, 411–467.

Nishikawa, M., Nishino, H., Misaka, Y., Kubota, M., Tsuji, E., Satoji, Y., Ozaki, M., and Yokohari, F. (2008). Sexual dimorphism in the antennal lobe of the ant *Camponotus japonicus*. *Zool. Sci.* 25, 195–204.

Ott, S. R. (2008). Confocal microscopy in large insect brains: zinc-formaldehyde fixation improves synapsin immunostaining and preservation of morphology in whole-mounts. *J. Neurosci. Methods* 172, 220–230.

Prendeville, H. R., and Stevens, L. (2002). Microbe inhibition by *Tribolium* flour beetles varies with beetle species, strain, sex, and microbe group. *J. Chem. Ecol.* 28, 1183–1190.

Rein, K., Zöckler, M., Mader, M. T., Grübel. C., and Heisenberg, M. (2002). The *Drosophila* standard brain. *Curr. Biol.* 12, 227–231.

Richards, S. Gibbs, R. A., Weinstock, G. M., Brown, S. J., Denell, R., Beeman, R. W., Gibbs, R., Beeman, R. W., Brown, S. J., Bucher, G., Friedrich, M., Grimmelikhuijzen, C. J., Klingler, M., Lorenzen, M., Richards, S., Roth, S., Schröder, R., Tautz, D., Zdobnov, E. M, Muzny, D., Gibbs, R. A., Weinstock, G. M., Attaway, T., Bell, S., Buhay, C. J., Chandrabose, M. N., Chavez, D., Clerk-Blankenburg, K. P., Cree, A., Dao, M., Davis, C., Chacko, J., Dinh, H., Dugan-Rocha, S., Fowler, G., Garner, T. T., Garnes, J., Gnirke, A., Hawes, A., Hernandez, J., Hines, S., Holder, M., Hume, J., Jhangiani, S. N., Joshi, V., Khan, Z. M., Jackson, L., Kovar, C., Kowis, A., Lee, S., Lewis, L. R., Margolis, J., Morgan, M., Nazareth, L. V., Nguyen, N., Okwuonu, G., Parker, D., Richards, S., Ruiz, S. J., Santibanez, J., Savard, J., Scherer, S. E., Schneider, B., Sodergren, E., Tautz, D., Vattahil, S., Villasana, D., White, C. S., Wright, R., Park, Y., Beeman, R. W., Lord, J., Oppert, B., Lorenzen, M., Brown, S., Wang, L., Savard, J., Tautz, D., Richards, S., Weinstock, G., Gibbs, R. A., Liu, Y., Worley, K., Weinstock, G., Elsik, C. G., Reese, J. T., Elhaik, E., Landan, G., Graur, D., Arensburger, P., Atkinson, P., Beeman, R. W., Beidler, J., Brown, S. J., Demuth, J. P., Drury, D. W., Du, Y. Z., Fujiwara, H., Lorenzen, M., Maselli, V., Osanai, M., Park, Y., Robertson, H. M., Tu, Z., Wang, J. J., Wang, S., Richards, S., Song, H., Zhang, L., Sodergren, E., Werner, D., Stanke, M., Morgenstern, B., Solovyev, V., Kosarev, P., Brown, G., Chen, H. C., Ermolaeva, O., Hlavina, W., Kapustin, Y., Kiryutin, B., Kitts, P., Maglott, D., Pruitt, K., Sapojnikov, V., Souvorov, A., Mackey, A. J., Waterhouse, R. M., Wyder, S., Zdobnov, E. M., Zdobnov, E. M., Wyder, S., Kriventseva, E. V., Kadowaki, T., Bork, P., Aranda, M., Bao, R., Beermann, A., Berns, N., Bolognesi, R., Bonneton, F., Bopp, D., Brown, S. J., Bucher, G., Butts, T., Chaumot, A., Denell, R. E., Ferrier, D. E., Friedrich, M., Gordon, C. M., Jindra, M., Klingler, M., Lan, Q., Lattorff, H. M., Laudet, V., von Levetsow, C., Liu, Z., Lutz, R., Lynch, J. A., da Fonseca, R.N., Posnien, N., Reuter, R., Roth, S., Savard, J., Schinko, J. B., Schmitt, C., Schoppmeier, M., Schröder, R., Shippy, T. D., Simonnet, F., Marques-Souza, H., Tautz, D., Tomoyasu, Y., Trauner, J., Van der Zee, M., Vervoort, M., Wittkopp, N., Wimmer, E.A., Yang, X., Jones, A. K., Sattelle, D. B., Ebert, P. R., Nelson, D., Scott, J. G., Beeman, R. W., Muthukrishnan, S., Kramer, K. J., Arakane, Y., Beeman, R. W., Zhu, Q., Hogenkamp, D., Dixit, R., Oppert, B., Jiang, H., Zou, Z., Marshall, J., Elpidina, E., Vinokurov, K., Oppert, C., Zou, Z., Evans, J., Lu, Z., Zhao, P., Sumathipala, N., Altincicek, B., Vilcinskas, A., Williams, M., Hultmark, D., Hetru, C., Jiang, H., Grimmelikhuijzen, C. J., Hauser, F., Cazzamali, G., Williamson, M., Park, Y., Li, B., Tanaka, Y., Predel, R., Neupert, S., Schachtner, J., Verleyen, P., Raible, F., Bork, P., Friedrich, M., Walden, K.K., Robertson, H. M., Angeli, S., Forêt, S., Bucher, G., Schuetz, S., Maleszka, R., Wimmer, E. A., Beeman, R. W., Lorenzen, M., Tomoyasu, Y., Miller, S. C., Grossmann, D., and Bucher, G. (The *Tribolium* Genome Sequencing Consortium) (2008). The genome of the model beetle and pest *Tribolium castaneum*. *Nature* 452, 949–955.

Rohlfing, T., Brandt, R., Maurer, C. R. Jr., and Menzel, R. (2001). Bee brains, B-splines and computational democracy: generating an average shape atlas. In IEEE Workshop on Mathematical Methods in Biomedical Image Analysis, Kauai, HI 2001, L. Staib, ed. (Los Alamitos, CA, IEEE Computer Society), pp. 187–194.

Rø, H., Müller, D., and Mustaparta, H. (2007). Anatomical organization of antennal lobe projection neurons in the moth Heliothis virescens. *J. Comp. Neurol.* 500, 658–675.

Rohlfing, T., Brandt, R., Menzel, R., and Maurer. C. R. Jr. (2004). Evaluation of atlas selection strategies for atlas-based image segmentation with application to confocal microscopy images of bee brains. *Neuroimage* 21, 1428–1442.

Schachtner, J., Goetz, B., Dippel, S., Dreyer, D. and Huetteroth, W. (2007). Metamorphic development of the antennal lobes of the red flour beetle *Tribolium castaneum*: 3D-reconstruction and neurochemistry. Program No. 135.2/F14. 2007 Neuroscience Meeting Planner. San Diego, CA: Society for Neuroscience (online).

Schachtner, J., Schmidt, M., and Homberg, U. (2005). Organization and evolutionary trends of primary olfactory brain centers in Tetraconata (Crustacea+Hexapoda). *Arthropod Struct. Dev.* 34, 257–299.

Schoenemann, P. T. (2006). Evolution of the size and functional areas of the human brain. *Annu. Rev. Anthropol.* 35, 379–406.

Settembrini, B. P, and Villar, M. J. (2005). FMRFamide-like immunocyrochemistry in the brain and subesophageal ganglion of *Triatoma infestans* (Insecta: Heteroptera). Coexpression with ß-pigment-dispersing hormone and small cardioactive peptide. *Cell Tissue Res.* 321, 299–310.

Sigg, D., Thompson, C. M., and Mercer, A. R. (1997). Activity-dependent changes to the brain and behavior of the honey bee, *Apis mellifera* (L.). *J. Neurosci.* 17, 7148–7156.

Sivinsky, J. (1989). Mushroom body development in nymphalid butterflies: a correlate of learning? *J. Insect Behav.* 2, 277–283.

Sjöholm, M., Sinakevitch, I., Ignell, R., Strausfeld, N. J., and Hansson, B. S. (2005). Organization of kenyon cells in subdivisions of the mushroom bodies of a lepidopteran insect. *J. Comp. Neurol.* 491, 290–304.

Snell-Rood, E. C., Papaj, D. R., and Gronenberg, W. (2009). Brain size: a global or induced cost of learning? *Brain Behav. Evol.* 73, 111–128.

Sokoloff, A. (1966). The Genetics of *Tribolium* and Related Species. Advances in Genetics, Suppl. 1. New York, Academic Press.

Sokoloff, A. (1974, 1977). The Biology of *Tribolium* with Special Emphasis on Genetic Aspects, Vol. II and III. Oxford, Clarendon Press/Oxford University Press.

Strausfeld, N. J. (2005). The evolution of crustacean and insect optic lobes and the origins of chiasmata. *Arthropod Struct. Dev.* 34, 235–256.

Strausfeld, N.J., Hansen, L., Li, Y., Gomez, R. S., and Ito, K. (1998). Evolution, discovery, and interpretations of arthropod mushroom bodies. *Learn. Mem.* 5, 11–37.

Strausfeld, N. J., Sinakevitch, I., Brown, S. M., and Farris, S. M. (2009). Ground plan of the insect mushroom body: functional and evolutionary implications. *J. Comp. Neurol.* 513, 265–291.

Strauss, R. (2002). The central complex and the genetic dissection of locomotor behaviour. *Curr. Opin. Neurobiol.* 12, 633–638.

Suzuki, T. (1980). 4,8-Dimethyldecanal: the aggregation pheromone of the flour beetles *Tribolium castaneum* and *T. confusum* (Coleoptera: Tenebrionidae). *Agric. Biol. Chem.* 44, 2519–2520.

Suzuki, T. (1981). A facile synthesis of 4,8-dimethyldecanal, aggregation pheromone of flour beetles, and its analogs. *Agric. Biol. Chem.* 45, 2641–2643.

Technau, G. M. (2007). Fiber number in the mushroom bodies of adult *Drosophila* melanogaster depends on age, sex and experience. *J. Neurogenet.* 21, 183–196.

Tomoyasu, Y., and Denell, R. E. (2004). Larval RNAi in *Tribolium* (Coleoptera) for analyzing adult development. *Dev. Genes. Evol.* 214, 575–578.

Tomoyasu, Y., Miller, S. C., Tomita, S., Schoppmeier, M., Grossmann, D., and Bucher, G. (2008). Exploring systemic RNA interference in insects: a genome-wide survey for RNAi genes in *Tribolium*. *Genome Biol.* 9, R10.

Trematerra, P., Sciarreta, A., and Tamasi, E. (2000). Behavioural responses of *Oryzaephilus surinamensis, Tribolium castaneum* and *Tribolium confusum* to naturally and artificially damaged durum wheat kernels. *Entomol. Exp. Appl.* 94, 195–200.

Utz, S., Huetteroth, W., Vömel, M., and Schachtner, J. (2008). Mas-allatotropin in the developing antennal lobe of the sphinx moth *Manduca sexta*: distribution, time course, developmental regulation, and colocalization with other neuropeptides. *Dev. Neurobiol.* 68, 123–142.

Verheggen, F., Ryne, C., Olsson, P. O., Arnaud, L., Lognay, G., Högberg, H. E., Persson, D., Haubruge, E., and Löfstedt, C. (2007). Electrophysiological and behavioral activity of secondary metabolites in the confused flour beetle, *Tribolium confusum*. *J. Chem. Ecol.* 33, 525–539.

von Alten, H. (1910). Zur Phylogenie des Hymenopterengehirns. *Jena. Z. Naturwiss.* 46, 511–590.

Wehner, R., Fukushi, T., and Isler, K. (2007). On being small: brain allometry in ants. *Brain Behav. Evol.* 69, 220–228.

Wessnitzer, J., and Webb, B. (2006). Multimodal sensory integration in insects – towards insect brain control architectures. *Bioinspir. Biomim.* 1, 63–75.

Yezerski, A., Ciccone, C., Rozitski, J., and Volingavage, B. (2007). The effects of a naturally produced benzoquinone on microbes common to flour. *J. Chem. Ecol.* 33, 1217–1225.

Yezerski, A., Gilmor, T. P., and Stevens, L. (2004). Genetic analysis of benzoquinone production in *Tribolium* confusum. *J. Chem. Ecol.* 30, 1034–1044.

Zars, T. (2000). Behavioral functions of the insect mushroom bodies. *Curr. Opin. Neurobiol.* 10, 790–795.

Zhao, X., Coptis, V., and Farris, S. M. (2008). Metamorphosis and adult development of the mushroom bodies of the red flour beetle, *Tribolium castaneum*. *Dev. Neurobiol.* 68, 1487–1502.

Conflict of Interest Statement: The authors declare that the research was conducted in the absence of any commercial or financial relationship that could be construed as a potential conflict of interest.

Received: 05 September 2009; paper pending published: 28 November 2009; accepted: 18 January 2010; published online: 03 March 2010.

Citation: Dreyer D, Vitt H, Dippel S, Goetz B, el Jundi B, Kollmann M, Huetteroth W and Schachtner J (2010) 3D standard brain of the red flour beetle Tribolium castaneum: a tool to study metamorphic development and adult plasticity. Front. Syst. Neurosci. ***4****:3. doi: 10.3389/neuro.06.003.2010*

Chapter 2:

The insect central complex as model for heterochronic brain development - background, concepts, and tools

Dev Genes Evol
DOI 10.1007/s00427-016-0542-7

REVIEW

The insect central complex as model for heterochronic brain development—background, concepts, and tools

Nikolaus Dieter Bernhard Koniszewski[1,2] · Martin Kollmann[3] · Mahdiyeh Bigham[1] · Max Farnworth[1] · Bicheng He[1] · Marita Büscher[1] · Wolf Hütteroth[3,4] · Marlene Binzer[3] · Joachim Schachtner[3] · Gregor Bucher[1]

Received: 8 February 2016 / Accepted: 17 March 2016

Abstract The adult insect brain is composed of neuropils present in most taxa. However, the relative size, shape, and developmental timing differ between species. This diversity of adult insect brain morphology has been extensively described while the genetic mechanisms of brain development are studied predominantly in *Drosophila melanogaster*. However, it has remained enigmatic what cellular and genetic mechanisms underlie the evolution of neuropil diversity or heterochronic development. In this perspective paper, we propose a novel approach to study these questions. We suggest using genome editing to mark homologous neural cells in the fly *D. melanogaster*, the beetle *Tribolium castaneum*, and the Mediterranean field cricket *Gryllus bimaculatus* to investigate developmental differences leading to brain diversification. One interesting aspect is the heterochrony observed in central complex development. Ancestrally, the central complex is formed during embryogenesis (as in *Gryllus*) but in *Drosophila*, it arises during late larval and metamorphic stages. In *Tribolium*, it forms partially during embryogenesis. Finally, we present tools for brain research in *Tribolium* including 3D reconstruction and immunohistochemistry data of first instar brains and the generation of transgenic brain imaging lines. Further, we characterize reporter lines labeling the mushroom bodies and reflecting the expression of the neuroblast marker gene *Tc-asense*, respectively.

Keywords Central complex · Brain · Heterochrony · Evolution · *Tribolium* · *Drosophila*

Communicated by Angelika Stollewerk

This article is part of the Special Issue "Size and Shape: Integration of morphometrics, mathematical modelling, developmental and evolutionary biology", Guest Editors: Nico Posnien—Nikola-Michael Prpic.

Nikolaus Dieter Bernhard Koniszewski and Martin Kollmann contributed equally to this work.

Electronic supplementary material The online version of this article (doi:10.1007/s00427-016-0542-7) contains supplementary material, which is available to authorized users.

✉ Gregor Bucher
gbucher1@uni-goettingen.de

[1] Department of Evolutionary Developmental Genetics, Johann-Friedrich-Blumenbach Institute, GZMB, CNMPB, Georg-August-University Göttingen, Göttingen Campus, Göttingen, Germany

[2] Institute of Medical Microbiology, Otto-von-Guericke-University, Magdeburg, Germany

[3] Department of Biology, Animal Physiology, Philipps-University, Marburg, Germany

[4] Department of Biology, Neurobiology, University of Konstanz, Constance, Germany

Diversity of adult brain morphology and developmental timing

The insect brain: morphological diversity based on a conserved architecture

The brain integrates sensory inputs, internal states, and other information to produce a specific behavioral pattern. Due to this essential role for survival, brain morphology and function are likely to be under high selective pressure. Indeed, the basic architecture of the insect brain is highly conserved and the different neuropils that serve particular functions are found in similar spatial arrangement in most adult insect species (Fig. 1) (Holmgren 1916; Hanström 1928; Snodgrass 1935; Weber 1966; Strausfeld 1976, 2005; Rein et al. 2002; Schachtner et al. 2005; Brandt et al. 2005; Kurylas et al. 2008; Homberg 2008;

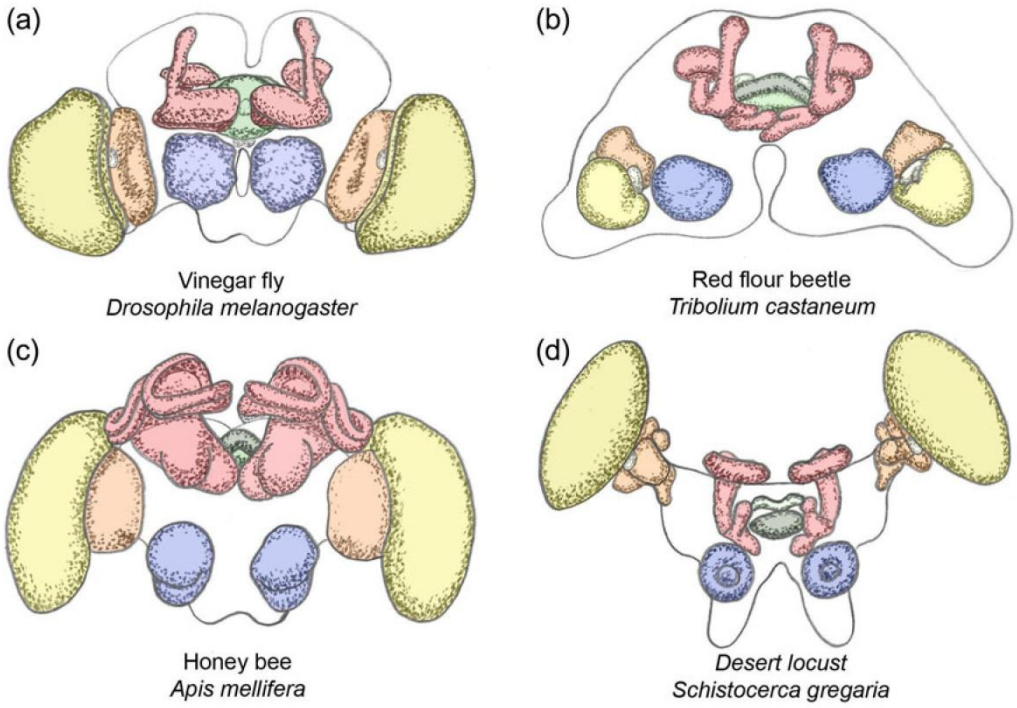

Fig. 1 Diversity of adult insect brains. Shown are illustrations of the brains of the vinegar fly *Drosophila melanogaster* (**a**), the red flour beetle *Tribolium castaneum* (**b**), the bee *Apis mellifera* (**c**), and the desert locust *Schistocerca gregaria* (**d**). Based on (Rein et al. 2002; Kurylas et al. 2008; Dreyer et al. 2010; Rybak et al. 2010). All brains were sized to the same width and the respective neuropils have the same color code: *blue* antennal lobes, *red* mushroom bodies, *yellow* lamina of optic lobes, *orange* lobula of optic lobes, *green* central complex

El Jundi et al. 2009a, b; Strausfeld et al. 2009; Dreyer et al. 2010). However, size and shape as well as timing of the development of the neuropils differ between insects. For example, 3D reconstructions of several insect brains revealed that the mushroom bodies of bees required for learning and memory have a large volume as compared to *Drosophila* and *Tribolium* (Brandt et al. 2005). Compared to the vinegar fly, the optic lobes (OLs) of the red flour beetle are small while its antennal lobes (ALs) are large (Dreyer et al. 2010). The combined relative volume of the central complex (CX) neuropils is larger in *Tribolium* as compared to *Drosophila* (for simplicity, we use the genus name of the model systems) (Rein et al. 2002; Brandt et al. 2005; Kurylas et al. 2008; El Jundi et al. 2009a; Dreyer et al. 2010). Interestingly, also, the timing of neuropil development varies. For instance, the CX is fully formed during embryogenesis in orthopteran insects while it develops postembryonically in flies. However, almost nothing is known about the genetic and cellular mechanisms that underlie the development of differences in morphology or developmental timing of neuropils between species. In this perspective paper, we present a novel developmental genetics approach to studying the development of homologous brain centers in different insect species. This approach has the power to reveal the cellular and genetic basis of insect brain diversification.

The conserved developmental basis: neural lineages and genetic control

The genetic mechanisms underlying insect neural development have been studied most extensively in the vinegar fly *Drosophila melanogaster* and appear to be similar in other insects (Campos-Ortega and Hartenstein 1985; Skeath and Thor 2003; Urbach and Technau 2004; Brody and Odenwald 2005; Technau et al. 2006; Hartenstein et al. 2008; Egger et al. 2008). The developmental units that build the brain are neural lineages, which consist of one neuroblast (neural stem cell) and all its daughter cells, which can be either neurons or glia. The cell bodies of a given lineage stay together and the projection patterns of all daughter neurons are usually similar (Technau et al. 2006; Spindler and Hartenstein 2010; Pereanu et al. 2011; Boyan and Reichert 2011). In type I neuroblasts, asymmetric divisions produce several ganglion mother cells (GMCs), each of which divides once more to form postmitotic cells. Type II neuroblasts generate transit amplifying progenitors (TA-GMC; also called intermediate neural progenitors INP), which themselves divide in a stem cell mode giving rise to GMCs (Bello et al. 2008;

Bowman et al. 2008; Boone and Doe 2008). Hence, many more daughter cells are produced per type II neuroblast. For instance, the *Drosophila* CX is formed from both types of neuroblasts (Bayraktar et al. 2010; Viktorin et al. 2011). Neural lineage development is not necessarily a continuous process. After an initial embryonic phase of division, many *Drosophila* neuroblasts enter quiescence for an extended period of time and resume proliferation at a later developmental stage (Egger et al. 2008).

Many aspects of cellular and genetic bases of neural development are conserved in animals (Denes et al. 2007; Hartenstein and Stollewerk 2015). In particular, the gene networks involved in specifying neural precursors and their spatial identity are highly conserved in insects and partly even in other arthropods (Wheeler et al. 2005; Stollewerk and Simpson 2005; Eriksson and Stollewerk 2010; Biffar and Stollewerk 2014; Stollewerk 2016). Homology of neural lineages has been suggested based on Crustacean neuroblasts, which show a comparable spatial arrangement, timing of delamination, transcription factor expression, and projection patterns as their insect counterparts (Ungerer and Scholtz 2008). Other examples are the similar location and the ongoing divisions of MB neuroblasts and the existence of type II neuroblasts at a comparable position and their contributions to the CX in a grasshopper (Boyan et al. 2010b; Boyan and Reichert 2011). In summary, at least the early development of the nervous system appears to be highly conserved.

The question

The diversity of neuropil morphology and instances of heterochrony in brain development are well documented in a plethora of species. These differences between species must have evolved by modifications of the embryonic and postembryonic developmental programs. However, the nature of the changes of cellular and genetic mechanisms remains unknown. In part, this may be due to the fact that for technical reasons, developmental genetic studies have been largely restricted to *Drosophila* for a long time. We propose that the emerging tools for functional genetics outside *Drosophila* will allow comparing developmental mechanism between species.

The concept: genome editing allows the genetic marking of homologous cells

In order to identify the differences in development between species, small groups of homologous cells need to be compared throughout development in both species, i.e., from the embryonic neuroblast to its progeny in the adult brain. There are several antibodies that allow marking for instance of serotonin-positive cells in different species. However, these markers do not mark neuroblasts or other neural progenitors during early phases of brain development. Furthermore, it has remained challenging even in *Drosophila* to mark a given lineage from the nascent neuroblast onwards and extensive enhancer trap collections marking subsets of neural cells are available only in *Drosophila*.

The recent development of genome editing tools changes the game because they have the potential to allow the genetic marking of groups of cells, which can be traced from neuroblast to the adult brain. By marking homologous cells in different taxa, the cellular basis of different developmental paths can be studied. We propose to establish such tools in a two-step process. First, groups of cells are genetically marked by their virtue of expressing a conserved transcription factor. Several transcription factors remain detectable in a certain lineage from the delaminating neuroblast to at least a subset of daughter cells of that neuroblast like engrailed (Kumar et al. 2009), and Ct, Dan, Dll, and Optix in type II neuroblasts (Bayraktar and Doe 2013). By genome editing, enhancer trap constructs encoding fluorescent protein can be integrated into the locus of such a neuroblast marker gene. The regulatory elements of that gene will drive expression of the fluorescent protein in all cells which express the gene. Transcription factors that are likely to be relevant should (1) be active in restricted regions in the neuroectoderm, (2) remain expressed in postmitotic neural cells of the brain, (3) be highly conserved in anterior brain development in bilaterians, and (4) their function should be required for the formation of the brain structure under study. Previous work identified good candidates: We and others showed that a set of conserved genes is required for patterning both vertebrate neural plate and invertebrate neuroectoderm (Lowe et al. 2003; Denes et al. 2007; Steinmetz et al. 2010; Posnien et al. 2011) and at least some of them were active in neural cells of the brain making them excellent candidates for marking homologous cells (Posnien et al. 2011).

In a second step, homology of marked cells needs to be corroborated by comparing location of marked cell bodies, projection patterns, neuromodulator content, and other features. A similar reasoning provided the basis of previous efforts to identify homologous neural cells based on molecular similarity (Urbach and Technau 2003; Arendt 2005; Tomer et al. 2010; Biffar and Stollewerk 2014). In addition, the assumed continuous expression from neuroblasts to the postmitotic cells will have to be shown for each reporter. The methods outlined here should be applicable to study the stage and the nature of developmental changes that lead to different morphologies or to differences in developmental timing. In the following, we describe an intriguing case of heterochronic development, which could be studied using this approach.

The central complex as a model for studying brain evolution

The central complex—a higher order integration center of the brain

We propose that the insect central complex (CX) is an excellent case to study heterochrony as one aspect of evolutionary adaptation of the brain. Before doing so, we briefly introduce to morphology and function of this neuropil—please refer to the recent review by Pfeiffer and Homberg for original work (2014). Apart from the paired noduli, the insect central complex (CX) typically consists of a set of unpaired neuropils spanning the midline (i.e., the protocerebral bridge (PB), central body (CB) with upper and lower unit, also called fan-shaped body (FB) and ellipsoid body (EB)) (Fig. 2a–c). The paired lateral accessory lobes (LAL) are not part of the CX but they are considered as strongly associated to the CX (Homberg 2008). The wiring scheme within and between these neuropils is highly ordered and reflects their organization in columns and layers. For instance, tangential neurons connect the columns within one neuropil while columnar neurons connect specific columns of different neuropils with each other while other neurons connect the CX to other brain parts (Power 1943; Williams 1975; Strausfeld 1976; Homberg 1985, 2008; Hanesch et al. 1989; Loesel et al. 2002; Boyan and Williams 2011; Pfeiffer and Homberg 2014). Among other higher order brain functions, the CX is involved in sky compass orientation, locomotor behavior, courtship, and memory among others (Strauss 2002; Homberg 2008; Pfeiffer and Homberg 2014; Heinze 2015). Similar midline neuropils have been found in many Arthropoda including Collembolans, Crustacea, Chelicerata, Myriapoda, and even Onychophora (Loesel et al. 2002; Strausfeld et al. 2006; Kollmann et al. 2011), and homology of the CX with the vertebrate basal ganglia has been suggested (Strausfeld and Hirth 2013). The function of the CX has become a major focus of neurobiology research and extensive imaging and misexpression resources are being generated (Hanesch et al. 1989; Loesel et al. 2002; Pfeiffer et al. 2008; Cardona et al. 2010; Young and Armstrong 2010a, b; Jenett et al. 2012; Takemura et al. 2013; Ito et al. 2014). Several neural lineages contributing to the CX were found but the embryonic part of their development remains poorly studied (Renn et al. 1999; Young and Armstrong 2010a, b; Pereanu et al. 2011; Riebli et al. 2013; Yang et al. 2013).

Heterochronic development of the central body

An intriguing divergence was observed regarding the timing of CX development, which was comprehensively described for the CB (Hanström 1925; Panov 1959; Wegerhoff and Breidbach 1992; Boyan and Williams 1997, 2011; Loesel et al. 2002; Boyan and Reichert 2011). In most hemimetabolous insects, the CB develops fully during embryogenesis. During postembryonic development, the CB just grows in size

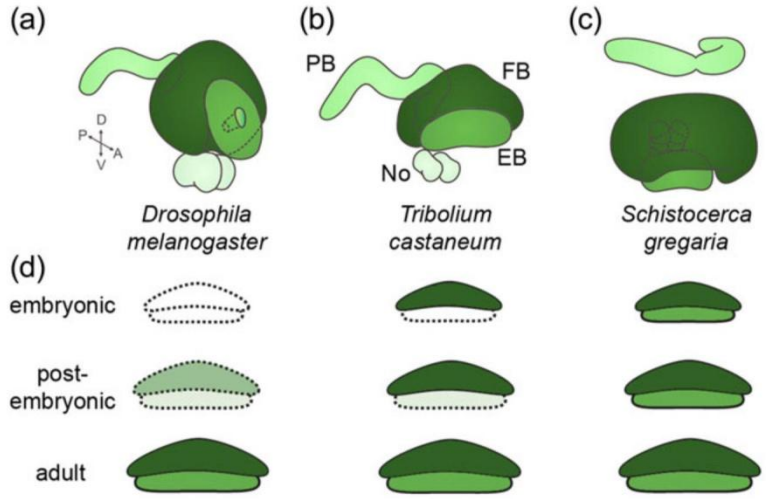

Fig. 2 Heterochronic development of the central complex. **a**–**d** The central complex of adult specimen of the vinegar fly *Drosophila melanogaster* (**a**), the red flour beetle *Tribolium castaneum* (**b**), and the desert locust *Schistocerca gregaria* (**c**) are shown sized to the same width. Note that the overall architecture of the CX components is similar as is their basic connectivity (not depicted). Central body with fan-shaped body (*FB*) and ellipsoid body (*EB*). *No* noduli; *PB* protocerebral bridge. **d** Heterochronic development of the CB is depicted schematically for the species (**a**–**c**). This neuropil is fully developed in desert locust hatchlings, representing the ancestral condition. In the beetle, only the FB (*dark green*) is present while the EB (*light green*) is added postembryonically. In the vinegar fly, the neuropil becomes apparent only at late larval and metamorphic stages. *Light colors* and *hatched outlines* mark neuropils that are developing but not yet functional while *white* indicates lack of detectable neuropil structure. Note that neuropil shapes are unified and other CX neuropils have been omitted for simplicity. **a**–**d** Redrawn from (Hanesch et al. 1989; Dreyer et al. 2010; Kaiser 2014)

with minor morphological changes. This has been shown for several orthopteran taxa including crickets (*Gryllus*, *Metrioptera*), grasshoppers (*Calliptamus*, *Schistocerca*), mantids (*Ameles*), and stick insects (*Dixippus*—now *Carausius*). Likewise, this has been found in hemipteran bugs (*Palomena*). By contrast, a CB neuropil is morphologically not detectable in hatchlings of some butterflies and moths (*Pieris*, *Ephestia*), mayflies (*Ephemera*), hymenoptera (*Apis*), and flies (*Musca*, *Drosophila*) (Panov 1959). However, in *Drosophila* first instar larva, some commissural tracts prefigure the location of the later CB (Hinke 1961; Riebli et al. 2013). A partial CB, namely the FB, was found in hatchlings of some Neuroptera (*Chrysopa*, *Ascalaphus*), Lepidoptera (*Antheraea*, *Manduca*), and a Diptera (*Culex*) (Panov 1959; Homberg and Hildebrand 1994). Within beetles, there are species where hatchlings do not yet display a CB like the curculionid *Anthonomus* or *Oryctes* (Jawlowski 1936) while a partial CB was detected in tenebrionid beetles (*Tenebrio molitor*, *Tribolium castaneum*) (Wegerhoff and Breidbach 1992; Wegerhoff et al. 1996; this work). The partial CB present in hatchlings usually represents the fan-shaped body. In summary, the timing of CB development has repeatedly been shifted relative to overall development of the animal during insect evolution with the full embryonic development probably being ancestral. Such evolutionary shifts of developmental timing have been termed "heterochrony" (Gould 1977). The different times of CB emergence within insect families like flies and beetles indicates that heterochrony has evolved several times. The functional relevance remains speculative: Most species where hatchlings lack a CB show no or only a poorly developed visual system (Panov 1959) and the embryonic development of the CX coincides with the emergence of walking legs—the legs are fully developed in hatchlings of hemimetabolous insects while tenebrionid larvae have reduced legs and *Drosophila* larvae do not have any legs (Pfeiffer and Homberg 2014).

Cricket, beetle, and fly as model systems to study the genetic basis of brain evolution

What insect model systems are likely to be most useful for research on the functional genetics of brain evolution? Of course, these model systems need to represent clear evolutionary changes of neuropil size, shape, or timing of development but they need to be amenable to functional genetics as well. Given these demands, the cricket *Gryllus bimaculatus*, the vinegar fly *D. melanogaster*, and the red flour beetle *T. castaneum* form an excellent group of model organisms. Functional genetic tools within orthopterans are best developed in the cricket *Gryllus* with RNAi and transgenesis established and it represents the ancestral state of CX development (Fig. 2d) (Panov 1959; Miyawaki et al. 2004; Nakamura et al. 2010; Zeng et al. 2013; Watanabe et al. 2014). Cellular development of the ancestral state of the CX has been described best in the orthopteran *Schistocerca gregaria* (Boyan et al. 2003, Boyan et al. 2010a, b; Williams et al. 2005; Boyan and Reichert 2011; Boyan and Williams 2011; Boyan and Liu 2014). However, due to their close phylogenetic relationship, it is likely that most knowledge gained in *S. gregaria* will be transferrable to *G. bimaculatus*.

Tenebrionid beetles represent the intermediate state where the FB forms during embryogenesis. It is only during the pupal stage that the ellipsoid body is eventually completed (Wegerhoff and Breidbach 1992; Wegerhoff et al. 1996) (Fig. 2d). Importantly, with respect to functional genetics, the red flour beetle *Tribolium* is second only to *Drosophila* including transgenesis, large-scale enhancer trap screen, misexpression tools, and in vivo imaging lines (Berghammer et al. 1999; Lorenzen et al. 2003; Trauner et al. 2009; Schinko et al. 2010; Posnien et al. 2011; Schinko et al. 2012; Sarrazin et al. 2012). RNAi-mediated gene knockdown is strong and is either environmental or systemic. Hence, when dsRNA is injected into the hemolymph, the knockdown spreads to reach all cells of the injected animal and is even transmitted to the offspring of injected females (Brown et al. 1999; Curtis et al. 2001; Bucher et al. 2002; Tomoyasu and Denell 2004; Miller et al. 2012; Peel et al. 2013). Mutant phenotypes were described for *Tc-knirps*, *Tc-Distal-less*, and *Tc-sex combs reduced* and in all these cases, RNAi phenocopied the null phenotype. Resources for large-scale RNAi screening are being established with currently half of the genome being covered by dsRNA templates (Dönitz et al. 2015; Schmitt-Engel et al. 2015). Finally, the CRISPR/Cas9 system has been established (Gilles et al. 2015).

Drosophila represents the most derived state of CX morphology, with the CX anlagen of the hatchling consisting of commissural tracts lacking neuropil morphology and synapses indicating non-functionality (Fig. 2d). Only during late larval stages and metamorphosis, the CX neuropils develop and mature (Renn et al. 1999; Young and Armstrong 2010a; Pereanu et al. 2011; Riebli et al. 2013; Pfeiffer and Homberg 2014). *Drosophila* is the prime model system for insect functional genetics with an excellent toolkit. Due to the delayed development in the fly, research on CX formation is focusing on the postembryonic phase (Viktorin et al. 2011; Jiang and Reichert 2012; Carney et al. 2012; Bayraktar and Doe 2013; Yang et al. 2013).

Studying brain development in the red flour beetle

Immunohistochemistry confirms presence of one central body neuropil in the L1 larval brain

Tribolium is a useful model for CX development for two reasons: first, it allows studying the embryonic aspects of CX

development. Second, comparison to *Drosophila* will reveal the cellular and genetic basis of the heterochronic shift between these species. In order to establish *Tribolium* as a model system for CX development, we first studied the L1 brain morphology by immunohistochemistry targeting synapsin followed by 3D reconstruction (Fig. 3; see Online Resource S1 for methods). We found the upper division of the central body (FB; dark green in Fig. 3a–g) with a flattened bar-like shape. An EB was not found at that stage. These data are in line with findings in *T. molitor* where the larval CB was described to consist of the FB only. The PB (Fig. 3b, e–g; light green) was present but medially split, probably

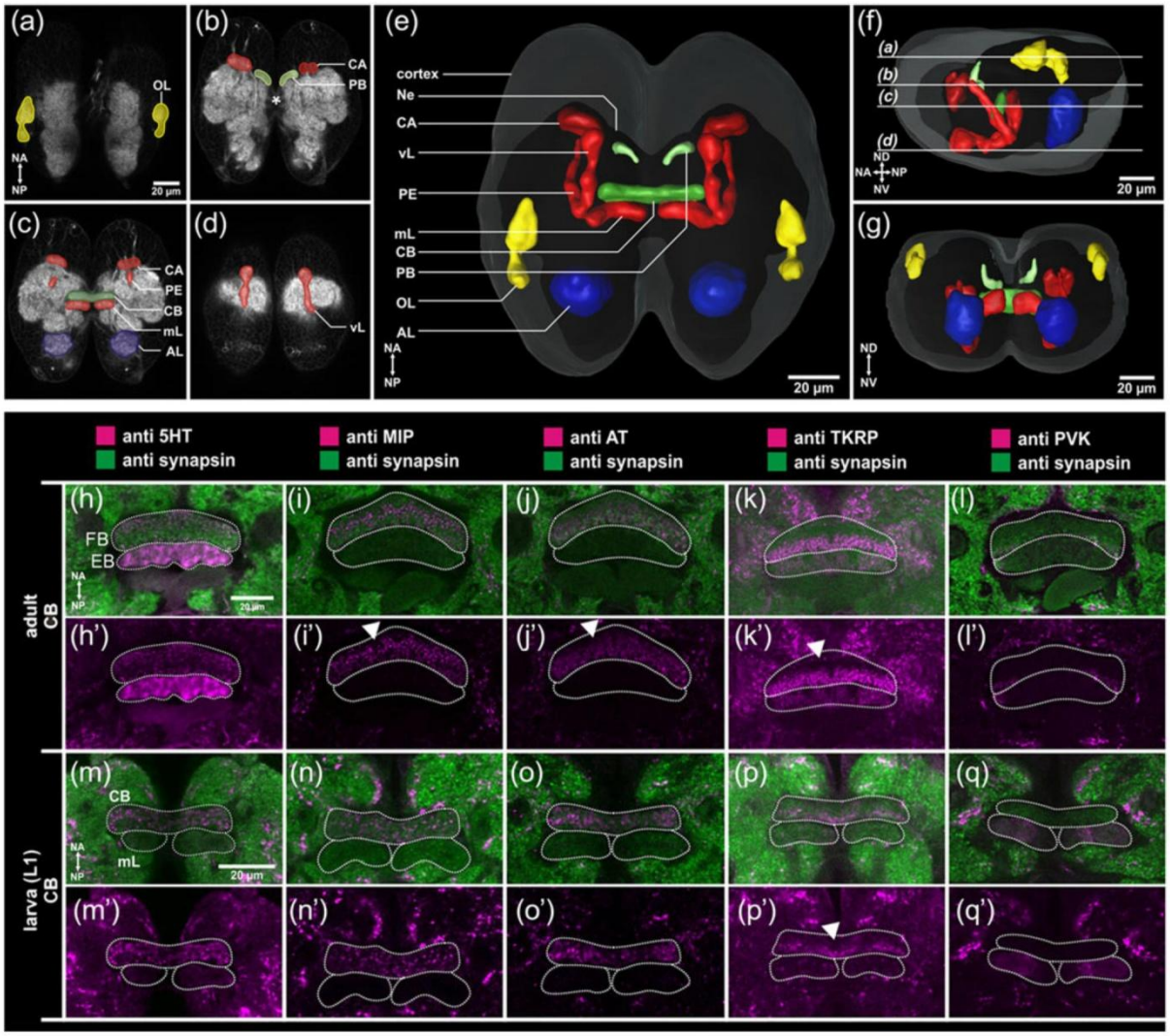

Fig. 3 The first instar larval brain of *Tribolium castaneum* and expression of neuromodulators in the CB. **a**–**d** Dorsal view of a first instar larval brain stained with an antibody detecting synapsin. The level of the sections is displayed in the reconstruction (**f**). **e**–**g** 3D reconstruction of neuropils based on the synapsin staining (**a**–**d**). Color code: *blue* antennal lobes (*AL*), *yellow* (anlagen of the) optic lobes (*OL*), and *red* mushroom bodies (*MB*) with calyx (*CA*); *PE* pedunculus, *vL* vertical lobe, and *mL* medial lobe. The cortex layer containing most cell bodies is shown in *light gray*, while the entire neuropilar mass of the brain is shown in *dark gray* (*Ne*). **h**–**q** Optical sections through the CB in adults (**h**, **l**) and first instar larvae (**m**, **q**) stained against serotonin (*5HT*), myoinhibitory protein (*MIP*), allatotropin (*AT*), tachykinin-related peptide (*TKRP*), and periviscerokinin (*PVK*). Neural anterior (n-anterior; *NA*) is up in all panels. *FB* fan-shaped body, *EB* ellipsoid body. The staining in the larval CB resembles staining of the FB in adult brains, corroborating the previous assumption that only the FB develops during embryogenesis. The anterior rim of the adult FB lacks MIP and AT expression (*white arrowheads* in *i* and *j*), which is not the case in larval CB. An n-anterior lack of TKRP reactivity, in contrast, is found in both larval and adult brains (white arrowhead in *k* and *p*). *Scale-* and *orientation bars* (**a**) account for (**b**–**d**), *bars* (**h**, **m**) account for *i*–*l*, *n*–*q*, *h* –*l* , and *m* –*q*

with some fibers connecting both parts (Fig. 3b; asterisk). Only during later larval development these two parts fuse (not shown). Interestingly, a PB was not detected in hatchlings of *T. molitor* but a split PB emerged at later larval stages before it fuses during metamorphosis (Wegerhoff and Breidbach 1992; Wegerhoff et al. 1996). Whether this reflects a heterochronic shift within Tenebrionidae or is due to different sensitivity of the methods used remains to be tested. We did detect no noduli in L1 larval brains.

Using immunohistochemistry, we found the biogenic amine serotonin (5HT) as well as the neuropeptides myoinhibitory peptide (MIP), allatotropin (AT), and tachykinin-related peptide (TKRP) in both the adult FB and the L1 CB. The neuropeptide periviscerokinin (PVK) was absent in the adult and larval CBs (compare Fig. 3h–k with h –k ; see Online Resource 1 for more detailed description and Fig. S1 in Online Resource 2 for comparison of other neuropils and Online Resources 3–14 for confocal stacks of adult and embryonic brains) (Wegerhoff and Breidbach 1992). Curiously, the n-anterior rim of the adult FB lacks MIP and AT immunoreactivity (white arrowheads in Fig. 3i and j) while in the larval CB, a correspondingly unstained rim was not found. In case of TKRP, n-anterior immunoreactivity lacked in both adult and larval CB (white arrowheads in Fig. 3k and p). The expression of synapsin and neuromodulators in the CB strongly indicates that the neuropil is functional in the hatchling already. As proof of principle, we tested several stainings in *Tc-six3* RNAi-knockdown animals, where CB deletion had previously been described (Posnien et al. 2011). The brains of L1 larvae were dissected and the previously published MB phenotype was confirmed by immunohistochemistry using the DC0 antibody (see Fig. S3 in Online Resource 2). Immunohistochemistry in *Tc-six3* RNAi-knockdown animals against DC0, 5HT, and MIP showed a specific signal in the brain as in wild type but the signal corresponding to the CB was not found confirming our previous data (see Fig. S3 in Online Resource 2).

To increase the repertoire of neural markers in *Tribolium*, we tested a number antibodies used in *Drosophila* research but most of them showed no or inconsistent signal (see Online Resource 16 for complete list). However, only the antibodies targeting reversed polarity (a marker for glia), aPKC, Bazooka (both asymmetrically loalized in neuroblasts), even skipped, engrailed (markers for subsets of neuroblasts and neurons), fasciclin 2 (marker for subsets of axons), death caspase 1 (marker for apoptosis), and phosphohistone-3 (marker for dividing cells) were confirmed to cross-react.

Transgenic lines marking the mushroom bodies and reporting *asense* expression

For the analysis of cell body location and projection patterns in wild-type and knockdown phenotypes, it is advantageous to have transgenic lines that mark specific subsets of neural cells or certain neuropils. From a previous enhancer trap screen (Trauner et al. 2009), we identified the line G11410 which marked the mushroom bodies with enhanced green fluorescent protein (EGFP) ("MB-green") (Fig. S2 in Online Resource 2) (Posnien et al. 2011; Binzer et al. 2014). Colocalization of EGFP with DC0 in the neuropil confirmed that MB was marked (Skoulakis et al. 1993; Farris and Strausfeld 2003) (Fig. S2 in Online Resource 2). In order to mark neuroblasts (NBs), we used an intronic fragment of the NB marker *Tc-asense* (see Online Resource 1 for sequence) to drive Gal4delta ("ase-Gal4") (Wheeler et al. 2003). Indeed, when crossed with the UAS-tGFP line, fluorescence was detected in the ventral nerve cord and the brain of late embryos (not shown). Double in situ hybridization confirmed co-expression of *Gal4delta* and *Tc-asense* (Fig. 4a, b).

Reporter lines for neural and glial cells allow in vivo imaging of brain development

We wanted to generate imaging lines marking neural cell types. An artificial promoter containing three eyless/Pax6 binding sites (3XP3) and the *Drosophila* heat-shock core promoter drove EGFP in the eyes in a wide range of animals (Sheng et al. 1997; Berghammer et al. 1999). However, recent work indicated that 3XP3 reports the expression of the homeobox gene *Pph13* rather than the *eyeless*/*Pax6* (Mishra et al. 2010). In *Tribolium*, we noted additional fluorescent signal in the brain with variable intensity. To render this signal more robust, we generated transgenic lines where six copies of the P3 elements (6XP3) drove either enhanced cyan fluorescent protein (ECFP) or dsRed-Express from the *Tribolium hsp68* core promoter. Both constructs led to a specific signal in glial cells (Posnien et al. 2011). The respective lines were called "glia-blue" and "glia-red." To determine the portion of marked glia, we tested for colocalization with the glia marker reverse polarity (4α3, Repo) (Fig. S2 in Online Resource 2) (Xiong et al. 1994). We found a large degree of co-expression in the nuclei of glia cells while the reporter additionally visualized the cell bodies. Quantification (excluding the OL) revealed that about 608 glial cells were marked by the Repo antibody ($n=5$; SD = 64; SE = 32) with about 524 (86 %) of them being positive for the ECFP signal as well ($n=5$; SD = 47.5; SE = 23.8). About eight ECFP-

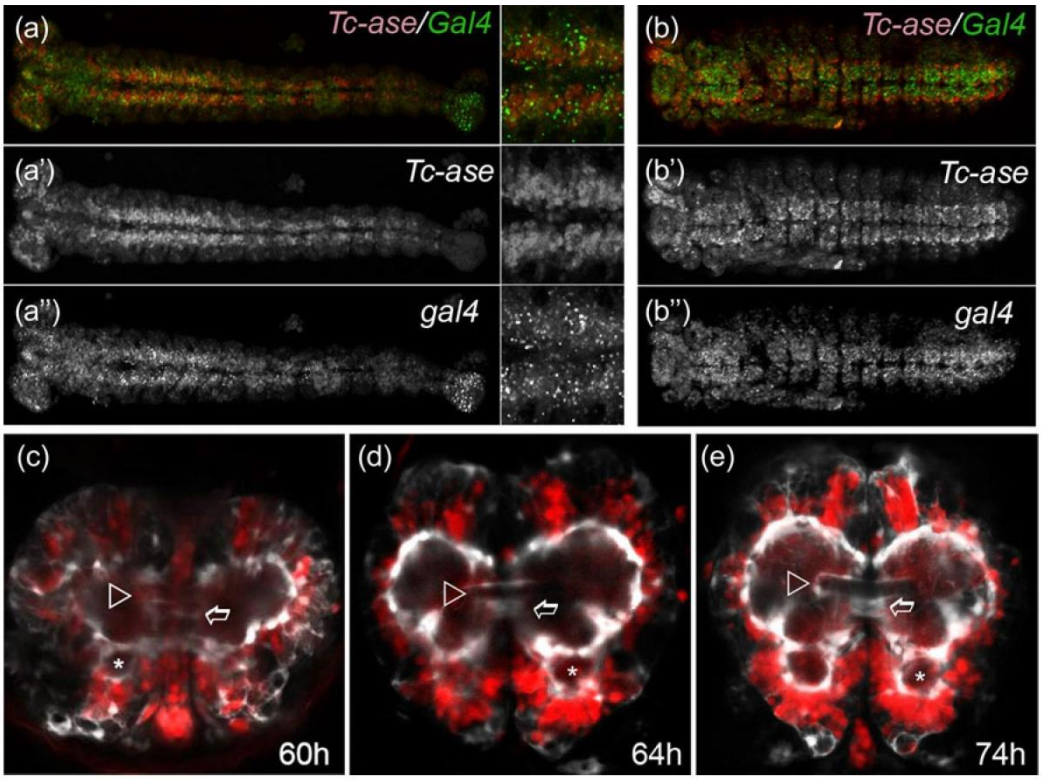

Fig. 4 Transgenic in vivo imaging reporters for brain research in *Tribolium castaneum*. **a**, **b** The regulatory region of *Tc-asense* drives expression of Gal4 in neuroblasts. The overlap of expression was confirmed with double in situ hybridization detecting *Tc-ase* (*red*) and *gal4* (*green*). **a**–**a**″ mid-embryogenesis; **b**–**b**″ late embryogenesis. **c**–**e** Developmental series of the fluorescence signal of the brainy line. The ECFP signal marking glia is shown in *white* while the DsRed-Express signal in neurons is depicted in *red*. Embryos are oriented n-anterior to the top. *White arrowhead* marks the developing central body; *stars* indicate the antennal lobes while *open arrows* mark the median lobes of the mushroom bodies. **d**, **e** The glial sheath of the central body is first detected in 60–64-h-old embryos and is clearly visible in brains of hatchlings (**e**). See Online Fig. S2 in Resource 2 for earlier stages

positive cells (1.5 %) did not show Repo staining ($n=5$; SD = 2.9; SE = 14). These could be glia of mesectodermal origin, which are Repo negative, at least in *Drosophila* (Parker and Auld 2006).

"Neuron-red" is a transgenic line where the upstream region of one of the *Tc-EF1-alphaB* paralogs unexpectedly drove DsRed-Express in neurons (Averof, personal communication; see Online Resource 1 for sequence) (Posnien et al. 2011). To monitor both glia and neurons in the same animal, we crossed the glia-blue and neuron-red lines establishing the "brainy" line (Fig. 4 and Fig. S2 in Online Resource 2; glia in white, neurons in red) (Posnien et al. 2011). To test the suitability for in vivo imaging, we monitored both signals in living embryos. Expression of ECFP was first detected in 17-h-old embryos (32 °C) while first expression of DsRedEx became detectable at 24 h (Fig. S2 in Online Resource 2). Strong branching of glia was observed in 40-h-old embryos. First signs of the CB were detected from 55 h onwards (open arrowhead in Fig. 4c–e). Antennal lobes (AL) and the median lobes of the mushroom bodies (mL) were detected from 60 h onwards (asterisks and open arrow in Fig. 4c–e, respectively).

Conclusion

The cellular and genetic mechanisms of the evolution of the tremendous diversity of neuropil morphology remain enigmatic. Using the models, concepts, and tools presented in this work, it will be possible to study this fascinating question. Further, we believe that the central complex is an excellent model system to study heterochrony as one aspect of brain evolution and we present tools that will turn out to be useful for the study of this and additional questions regarding the brain development of *Tribolium*.

Acknowledgments We thank Michalis Averof for the transgenic "neuron-red" line and Uwe Homberg for providing the 3D data stacks for the generation of the schematic of the CX of *S. gregaria*. NDBK was funded by the DFG Research Center "Molecular Physiology of the Brain" (CMPB).

Author contributions NDBK, MBig, and MBü generated and analyzed transgenic lines. MK established and analyzed stainings of the wild-type larval brain. WH and MBin contributed stainings of the adult brain. NDBK analyzed the RNAi knockdown. NDBK, MK, JS, MF, BH, and MBü contributed to the concept and the writing of the manuscript. GB designed the study and wrote the manuscript. All authors read and approved of the manuscript.

References

Arendt D (2005) Genes and homology in nervous system evolution: comparing gene functions, expression patterns, and cell type molecular fingerprints. Theory Biosci 124:185–197

Bayraktar OA, Doe CQ (2013) Combinatorial temporal patterning in progenitors expands neural diversity. Nature 498:449–455. doi:10.1038/nature12266

Bayraktar O, Boone JQ, Drummond ML, Doe CQ (2010) Drosophila type II neuroblast lineages keep Prospero levels low to generate large clones that contribute to the adult brain central complex. Neural Dev 5:26. doi:10.1186/1749-8104-5-26

Bello BC, Izergina N, Caussinus E, Reichert H (2008) Amplification of neural stem cell proliferation by intermediate progenitor cells in Drosophila brain development. Neural Dev 3:5. doi:10.1186/1749-8104-3-5

Berghammer AJ, Klingler M, Wimmer EA (1999) A universal marker for transgenic insects. Nature 402:370–371

Biffar L, Stollewerk A (2014) Conservation and evolutionary modifications of neuroblast expression patterns in insects. Dev Biol 388:103–116. doi:10.1016/j.ydbio.2014.01.028

Binzer M, Heuer CM, Kollmann M et al (2014) Neuropeptidome of Tribolium castaneum antennal lobes and mushroom bodies. J Comp Neurol 522:337–357. doi:10.1002/cne.23399

Boone JQ, Doe CQ (2008) Identification of Drosophila type II neuroblast lineages containing transit amplifying ganglion mother cells. Dev Neurobiol 68:1185–1195. doi:10.1002/dneu.20648

Bowman SK, Rolland V, Betschinger J et al (2008) The tumor suppressors brat and numb regulate transit-amplifying neuroblast lineages in Drosophila. Dev Cell 14:535–546. doi:10.1016/j.devcel.2008.03.004

Boyan G, Liu Y (2014) Timelines in the insect brain: fates of identified neural stem cells generating the central complex in the grasshopper Schistocerca gregaria. Dev Genes Evol 224:37–51. doi:10.1007/s00427-013-0462-8

Boyan GS, Reichert H (2011) Mechanisms for complexity in the brain: generating the insect central complex. Trends Neurosci 34:247–257. doi:10.1016/j.tins.2011.02.002

Boyan GS, Williams JLD (1997) Embryonic development of the pars intercerebralis/central complex of the grasshopper. Dev Genes Evol 207:317–329. doi:10.1007/s004270050119

Boyan G, Williams L (2011) Embryonic development of the insect central complex: insights from lineages in the grasshopper and Drosophila. Arthropod Struct Dev 40:334–348. doi:10.1016/j.asd.2011.02.005

Boyan GS, Bräunig P, Posser S, Williams JLD (2003) Embryonic development of the sensory innervation of the clypeo-labral complex: further support for serially homologous appendages in the locust. Arthropod Struct Dev 32:289–302

Boyan G, Herbert Z, Williams L (2010a) Cell death shapes embryonic lineages of the central complex in the grasshopper Schistocerca gregaria. J Morphol 271:949–959. doi:10.1002/jmor.10847

Boyan G, Williams L, Legl A, Herbert Z (2010b) Proliferative cell types in embryonic lineages of the central complex of the grasshopper Schistocerca gregaria. Cell Tissue Res 341:259–277. doi:10.1007/s00441-010-0992-6

Brandt R, Rohlfing T, Rybak J et al (2005) Three-dimensional average-shape atlas of the honeybee brain and its applications. J Comp Neurol 492:1–19. doi:10.1002/cne.20644

Brody T, Odenwald WF (2005) Regulation of temporal identities during Drosophila neuroblast lineage development. Curr Opin Cell Biol 17:672–675. doi:10.1016/j.ceb.2005.09.013

Brown SJ, Mahaffey JP, Lorenzen MD et al (1999) Using RNAi to investigate orthologous homeotic gene function during development of distantly related insects. Evol Dev 1:11–15

Bucher G, Scholten J, Klingler M (2002) Parental RNAi in Tribolium (Coleoptera). Curr Biol 12:R85–R86

Campos-Ortega JA, Hartenstein V (1985) The embryonic development of Drosophila melanogaster. Springer, New York

Cardona A, Saalfeld S, Preibisch S et al (2010) An integrated micro- and macroarchitectural analysis of the Drosophila brain by computer-assisted serial section electron microscopy. PLoS Biol. doi:10.1371/journal.pbio.1000502

Carney TD, Miller MR, Robinson KJ et al (2012) Functional genomics identifies neural stem cell sub-type expression profiles and genes regulating neuroblast homeostasis. Dev Biol 361:137–146. doi:10.1016/j.ydbio.2011.10.020

Curtis CD, Brisson JA, DeCamillis MA et al (2001) Molecular characterization of Cephalothorax, the Tribolium ortholog of sex combs reduced. Genesis 30:12–20

Denes AS, Jekely G, Steinmetz PR et al (2007) Molecular architecture of annelid nerve cord supports common origin of nervous system centralization in bilateria. Cell 129:277–288

Dönitz J, Schmitt-Engel C, Grossmann D et al (2015) iBeetle-Base: a database for RNAi phenotypes in the red flour beetle Tribolium castaneum. Nucleic Acids Res 43:D720–D725. doi:10.1093/nar/gku1054

Dreyer D, Vitt H, Dippel S et al (2010) 3D standard brain of the red flour beetle Tribolium castaneum: a tool to study metamorphic development and adult plasticity. Front Syst Neurosci 4:3. doi:10.3389/neuro.06.003.2010

Egger B, Chell JM, Brand AH (2008) Insights into neural stem cell biology from flies. Philos Trans R Soc Lond B Biol Sci 363:39–56. doi:10.1098/rstb.2006.2011

El Jundi B, Heinze S, Lenschow C et al (2009a) The locust standard brain: a 3D standard of the central complex as a platform for neural network analysis. Front Syst Neurosci 3:21. doi:10.3389/neuro.06.021.2009

El Jundi B, Huetteroth W, Kurylas AE, Schachtner J (2009b) Anisometric brain dimorphism revisited: implementation of a volumetric 3D standard brain in Manduca sexta. J Comp Neurol 517:210–225. doi:10.1002/cne.22150

Eriksson BJ, Stollewerk A (2010) Expression patterns of neural genes in Euperipatoides kanangrensis suggest divergent evolution of onychophoran and euarthropod neurogenesis. Proc Natl Acad Sci U S A 107:22576–22581. doi:10.1073/pnas.1008822108

Farris SM, Strausfeld NJ (2003) A unique mushroom body substructure common to basal cockroaches and to termites. J Comp Neurol 456: 305–320. doi:10.1002/cne.10517

Gilles AF, Schinko JB, Averof M (2015) Efficient CRISPR-mediated gene targeting and transgene replacement in the beetle Tribolium castaneum. Dev Camb Engl 142:2832–2839. doi:10.1242/dev.125054

Gould SJ (1977) Ontogeny and phylogeny. Harvard University Press, Harvard

Hanesch U, Fischbach K-F, Heisenberg M (1989) Neuronal architecture of the central complex in drosophila melanogaster. Cell Tissue Res 257:343–366. doi:10.1007/BF00261838

Hanström B (1925) Comparison between the brains of the newly hatched larva and the imago of Pieris brassicae. EntTidskr 46:43–52

Hanström B (1928) Vergleichende Anatomie des Nervensystems der Wirbellosen Tiere unter Berücksichtigung seiner Funktion. Springer, Berlin

Hartenstein V, Stollewerk A (2015) The evolution of early neurogenesis. Dev Cell 32:390–407. doi:10.1016/j.devcel.2015.02.004

Hartenstein V, Spindler S, Pereanu W, Fung S (2008) The development of the Drosophila larval brain. Adv Exp Med Biol 628:1–31. doi:10.1007/978-0-387-78261-4_1

Heinze S (2015) Neuroethology: unweaving the senses of direction. Curr Biol CB 25:R1034–R1037. doi:10.1016/j.cub.2015.09.003

Hinke W (1961) Das relative postembryonale Wachstum der Hirnteile von Culex pipiens, Drosophila melanogaster und Drosophila-mutanten. Z Für Morphol Ökol Tiere 50:81–118

Holmgren NF (1916) Zur vergleichenden Anatomie des Gehirns von Polychaeten, Onychophoren, Xiphosuren, Arachniden, Crustaceen, Myriapoden, und Insekten. Vorstudien zu einer Phylogenie der Arthropoden. K Sven Vetenskapsakad Handl 56:1–303

Homberg U (1985) Interneurons of the central complex in the bee brain Apis mellifera. J Insect Physiol 31:251–264

Homberg U (2008) Evolution of the central complex in the arthropod brain with respect to the visual system. Arthropod Struct Dev 37: 347–362. doi:10.1016/j.asd.2008.01.008

Homberg U, Hildebrand JG (1994) Postembryonic development of gamma-aminobutyric acid-like immunoreactivity in the brain of the sphinx moth manduca sexta. J Comp Neurol 339:132–149. doi:10.1002/cne.903390112

Ito K, Shinomiya K, Ito M et al (2014) A systematic nomenclature for the insect brain. Neuron 81:755–765. doi:10.1016/j.neuron.2013.12.017

Jawlowski H (1936) Über den Gehirnbau der Käfer. Z Morph Ökol Tiere 32:67–91

Jenett A, Rubin GM, Ngo T-TB et al (2012) A GAL4-driver line resource for Drosophila neurobiology. Cell Rep 2:991–1001. doi:10.1016/j.celrep.2012.09.011

Jiang Y, Reichert H (2012) Programmed cell death in type II neuroblast lineages is required for central complex development in the Drosophila brain. Neural Dev 7:3. doi:10.1186/1749-8104-7-3

Kaiser A (2014) Immuncytochemische Färbungen und 3D-Rekonstruktionen am Zentralkomplex der Westlichen Honigbiene Apis mellifera

Kollmann M, Huetteroth W, Schachtner J (2011) Brain organization in Collembola (springtails). Arthropod Struct Dev 40:304–316. doi:10.1016/j.asd.2011.02.003

Kumar A, Fung S, Lichtneckert R et al (2009) Arborization pattern of engrailed-positive neural lineages reveal neuromere boundaries in the Drosophila brain neuropil. J Comp Neurol 517:87–104. doi:10.1002/cne.22112

Kurylas AE, Rohlfing T, Krofczik S et al (2008) Standardized atlas of the brain of the desert locust, Schistocerca gregaria. Cell Tissue Res 333:125–145. doi:10.1007/s00441-008-0620-x

Loesel R, Nässel DR, Strausfeld NJ (2002) Common design in a unique midline neuropil in the brains of arthropods. Arthropod Struct Dev 31:77–91

Lorenzen MD, Berghammer AJ, Brown SJ et al (2003) piggyBac-mediated germline transformation in the beetle Tribolium castaneum. Insect Mol Biol 12:433–440

Lowe CJ, Wu M, Salic A et al (2003) Anteroposterior patterning in hemichordates and the origins of the chordate nervous system. Cell 113:853–865

Miller SC, Miyata K, Brown SJ, Tomoyasu Y (2012) Dissecting systemic RNA interference in the red flour beetle Tribolium castaneum: parameters affecting the efficiency of RNAi. PLoS One 7, e47431. doi:10.1371/journal.pone.0047431

Mishra M, Oke A, Lebel C et al (2010) Pph13 and orthodenticle define a dual regulatory pathway for photoreceptor cell morphogenesis and function. Dev Camb Engl 137:2895–2904. doi:10.1242/dev.051722

Miyawaki K, Mito T, Sarashina I et al (2004) Involvement of wingless/armadillo signaling in the posterior sequential segmentation in the cricket, Gryllus bimaculatus (Orthoptera), as revealed by RNAi analysis. Mech Dev 121:119–130

Nakamura T, Yoshizaki M, Ogawa S et al (2010) Imaging of transgenic cricket embryos reveals cell movements consistent with a syncytial patterning mechanism. Curr Biol CB 20:1641–1647. doi:10.1016/j.cub.2010.07.044

Panov AA (1959) Structure of the insect brain at successive stages of postembryonic development. II. The central body. Entomol Rev 38:276–283

Parker RJ, Auld VJ (2006) Roles of glia in the Drosophila nervous system. Semin Cell Dev Biol 17:66–77. doi:10.1016/j.semcdb.2005.11.012

Peel AD, Schanda J, Grossmann D et al (2013) Tc-knirps plays different roles in the specification of antennal and mandibular parasegment boundaries and is regulated by a pair-rule gene in the beetle Tribolium castaneum. BMC Dev Biol 13:25. doi:10.1186/1471-213X-13-25

Pereanu W, Younossi-Hartenstein A, Lovick J et al (2011) Lineage-based analysis of the development of the central complex of the Drosophila brain. J Comp Neurol 519:661–689

Pfeiffer K, Homberg U (2014) Organization and functional roles of the central complex in the insect brain. Annu Rev Entomol 59:165–184. doi:10.1146/annurev-ento-011613-162031

Pfeiffer BD, Jenett A, Hammonds AS et al (2008) Tools for neuroanatomy and neurogenetics in Drosophila. Proc Natl Acad Sci U S A 105: 9715–9720. doi:10.1073/pnas.0803697105

Posnien N, Koniszewski NDB, Hein HJ, Bucher G (2011) Candidate gene screen in the red flour beetle Tribolium reveals Six3 as ancient regulator of anterior median head and central complex development. PLoS Genet 7, e1002418. doi:10.1371/journal.pgen.1002416

Power ME (1943) The brain of Drosophila melanogaster. J Morphol 72: 517–559

Rein K, Zöckler M, Mader MT et al (2002) The Drosophila standard brain. Curr Biol CB 12:227–231

Renn SC, Armstrong JD, Yang M et al (1999) Genetic analysis of the Drosophila ellipsoid body neuropil: organization and development of the central complex. J Neurobiol 41:189–207

Riebli N, Viktorin G, Reichert H (2013) Early-born neurons in type II neuroblast lineages establish a larval primordium and integrate into adult circuitry during central complex development in Drosophila. Neural Dev 8:6. doi:10.1186/1749-8104-8-6

Rybak J, Kuß A, Lamecker H et al (2010) The digital bee brain: integrating and managing neurons in a common 3D reference system. Front Syst Neurosci. doi:10.3389/fnsys.2010.00030

Sarrazin AF, Peel AD, Averof M (2012) A segmentation clock with two-segment periodicity in insects.

Schachtner J, Schmidt M, Homberg U (2005) Organization and evolutionary trends of primary olfactory brain centers in Tetraconata

(Crustacea + Hexapoda). Arthropod Struct Dev 34:257–299. doi:10.1016/j.asd.2005.04.003

Schinko JB, Weber M, Viktorinova I et al (2010) Functionality of the GAL4/UAS system in Tribolium requires the use of endogenous core promoters. BMC Dev Biol 10:53

Schinko J, Hillebrand K, Bucher G (2012) Heat shock-mediated misexpression of genes in the beetle Tribolium castaneum. Dev Genes Evol Dev Genes Evol: 287–98

Schmitt-Engel C, Schultheis D, Schwirz J et al (2015) The iBeetle large-scale RNAi screen reveals gene functions for insect development and physiology. Nat Commun. doi:10.1038/ncomms8822

Sheng G, Thouvenot E, Schmucker D et al (1997) Direct regulation of rhodopsin 1 by Pax-6/eyeless in Drosophila: evidence for a conserved function in photoreceptors. Genes Dev 11:1122–1131

Skeath JB, Thor S (2003) Genetic control of Drosophila nerve cord development. Curr Opin Neurobiol 13:8–15. doi:10.1016/S0959-4388(03)00007-2

Skoulakis EM, Kalderon D, Davis RL (1993) Preferential expression in mushroom bodies of the catalytic subunit of protein kinase A and its role in learning and memory. Neuron 11:197–208

Snodgrass RE (1935) Principles of insect morphology. McGRaw Hill, New York

Spindler SR, Hartenstein V (2010) The Drosophila neural lineages: a model system to study brain development and circuitry. Dev Genes Evol 220:1–10. doi:10.1007/s00427-010-0323-7

Steinmetz PR, Urbach R, Posnien N et al (2010) Six3 demarcates the anterior-most developing brain region in bilaterian animals. Evodevo 1:14

Stollewerk A (2016) A flexible genetic toolkit for arthropod neurogenesis. Philos Trans R Soc Lond B Biol Sci. doi:10.1098/rstb.2015.0044

Stollewerk A, Simpson P (2005) Evolution of early development of the nervous system: a comparison between arthropods. Bioessays 27:874–883. doi:10.1002/bies.20276

Strausfeld NJ (1976) Atlas of an insect brain. Springer, Berlin Heidelberg

Strausfeld NJ (2005) The evolution of crustacean and insect optic lobes and the origins of chiasmata. Arthropod Struct Dev 34:235–256. doi:10.1016/j.asd.2005.04.001

Strausfeld NJ, Hirth F (2013) Deep homology of arthropod central complex and vertebrate basal ganglia. Science 340:157–161. doi:10.1126/science.1231828

Strausfeld NJ, Strausfeld CM, Loesel R et al (2006) Arthropod phylogeny: onychophoran brain organization suggests an archaic relationship with a chelicerate stem lineage. Proc Biol Sci 273:1857–1866. doi:10.1098/rspb.2006.3536

Strausfeld NJ, Sinakevitch I, Brown SM, Farris SM (2009) Ground plan of the insect mushroom body: functional and evolutionary implications. J Comp Neurol 513:265–291. doi:10.1002/cne.21948

Strauss R (2002) The central complex and the genetic dissection of locomotor behaviour. Curr Opin Neurobiol 12:633–638

Takemura S, Bharioke A, Lu Z et al (2013) A visual motion detection circuit suggested by Drosophila connectomics. Nature 500:175–181. doi:10.1038/nature12450

Technau GM, Berger C, Urbach R (2006) Generation of cell diversity and segmental pattern in the embryonic central nervous system of Drosophila. Dev Dyn 235:861–869

Tomer R, Denes AS, Tessmar-Raible K, Arendt D (2010) Profiling by image registration reveals common origin of annelid mushroom bodies and vertebrate pallium. Cell 142:800–809

Tomoyasu Y, Denell RE (2004) Larval RNAi in Tribolium (Coleoptera) for analyzing adult development. Dev Genes Evol 214:575–578

Trauner J, Schinko J, Lorenzen MD et al (2009) Large-scale insertional mutagenesis of a coleopteran stored grain pest, the red flour beetle Tribolium castaneum, identifies embryonic lethal mutations and enhancer traps. BMC Biol 7:73

Ungerer P, Scholtz G (2008) Filling the gap between identified neuroblasts and neurons in crustaceans adds new support for Tetraconata. Proc Biol Sci 275:369–376. doi:10.1098/rspb.2007.1391

Urbach R, Technau GM (2003) Molecular markers for identified neuroblasts in the developing brain of Drosophila. Development 130:3621–3637

Urbach R, Technau GM (2004) Neuroblast formation and patterning during early brain development in Drosophila. Bioessays 26:739–751

Viktorin G, Riebli N, Popkova A et al (2011) Multipotent neural stem cells generate glial cells of the central complex through transit amplifying intermediate progenitors in Drosophila brain development. Dev Biol 356:553–565. doi:10.1016/j.ydbio.2011.06.013

Watanabe T, Noji S, Mito T (2014) Gene knockout by targeted mutagenesis in a hemimetabolous insect, the two-spotted cricket Gryllus bimaculatus, using TALENs. Methods San Diego Calif 69:17–21. doi:10.1016/j.ymeth.2014.05.006

Weber H (1966) Grundriss der Insektenkunde, 4th edn. Gustav Fischer Verlag, Stuttgart

Wegerhoff R, Breidbach O (1992) Structure and development of the larval central complex in a holometabolous insect, the beetle Tenebrio molitor. Cell Tissue Res 268:341–358

Wegerhoff R, Breidbach O, Lobemeier M (1996) Development of locustatachykinin immunopositive neurons in the central complex of the beetle Tenebrio molitor. J Comp Neurol 375:157–166. doi:10.1002/(SICI)1096-9861(19961104)375:1<157::AID-CNE10>3.0.CO;2-S

Wheeler SR, Carrico ML, Wilson BA et al (2003) The expression and function of the achaete-scute genes in Tribolium castaneum reveals conservation and variation in neural pattern formation and cell fate specification. Development 130:4373–4381

Wheeler SR, Carrico ML, Wilson BA, Skeath JB (2005) The Tribolium columnar genes reveal conservation and plasticity in neural precursor patterning along the embryonic dorsal-ventral axis. Dev Biol 279:491–500

Williams JLD (1975) Anatomical studies of the insect central nervous system: a ground plan of the midbrain and an introduction to the central complex in the locust Schistocerca gregaria (Orthoptera). J Zool 204:1269–1280

Williams JL, Güntner M, Boyan G (2005) Building the central complex of the grasshopper Schistocerca gregaria: temporal topology organizes the neuroarchitecture of the w, x, y, z tracts. Arthropod Struct Dev 34:97–110

Xiong WC, Okano H, Patel NH et al (1994) repo encodes a glial-specific homeo domain protein required in the Drosophila nervous system. Genes Dev 8:981–994

Yang JS, Awasaki T, Yu H-H et al (2013) Diverse neuronal lineages make stereotyped contributions to the *Drosophila* locomotor control center, the central complex: lineage analysis of central complex neurons. J Comp Neurol 521:2645–2662. doi:10.1002/cne.23339

Young JM, Armstrong JD (2010a) Building the central complex in Drosophila: the generation and development of distinct neural subsets. J Comp Neurol 518:1525–1541

Young JM, Armstrong JD (2010b) Structure of the adult central complex in Drosophila: organization of distinct neuronal subsets. J Comp Neurol 518:1500–1524. doi:10.1002/cne.22284

Zeng V, Ewen-Campen B, Horch HW et al (2013) Developmental gene discovery in a hemimetabolous insect: de novo assembly and annotation of a transcriptome for the cricket Gryllus bimaculatus. PLoS One 8, e61479. doi:10.1371/journal.pone.0061479

Supplementary material

The insect central complex as model for heterochronic brain development – background, concepts and tools

Nikolaus Dieter Bernhard Koniszewski[1/2]*, Martin Kollmann[3]*, Mahdiyeh Bigham[1], Max Farnworth[1], Bicheng He[1], Marita Büscher[1], Wolf Hütteroth[3/4], Marlene Binzer[3], Joachim Schachtner[3], Gregor Bucher[1#]

[#]Corresponding author: Gregor Bucher

Details on L1 brain morphology

Anatomy of the brain of the first instar larva

Four pronounced neuropils could be identified in the first instar larva: We characterized the unpaired larval central complex (CX) and the paired mushroom bodies (MBs), antennal lobes (ALs), and optic lobes (OLs) (Fig. 3 a-g). The L1 CX consists of a central body (CB) with the upper unit (CBU), and the protocerebral bridge (PB), which is split into two parts connected by fibers. The lower unit of the CB (CBL) and the paired noduli (NOs) are missing. The MBs consist of the calyces (CAs) and the pedunculi (PEs) consisting of the median and vertical lobes (mL and vL), similar to adult animals. The larval ALs contain about 40 - 50 glomeruli, while the adults ALs have about 70-90 glomeruli per AL (Dreyer et al. 2010). The OLs exist only as anlagen and are differentiated in a distal and a proximal part.

Neuromediators in neuropils of larval and adult brains

Antibodies against neuromediators are known to stain distinct areas of adult insect brains. Here we discuss the similarities and differences of observed stainings in larval (L1) and adult brains of *T. castaneum* based on Fig. 3 h/h'-q/q' and supplementary Fig. 1 (this work) and previously published stainings of the adult ALs and MBs [1,2].

Central body

The antibodies against 5HT, MIP, and AT produced homogeneous scattered staining in both the adult and larval CBU (Fig. 3 h-j, h'-j' and m-o, m'-o'). Different from the CB in L1 larvae, the adult CBL is intensely labeled by the 5HT antibody. This supports the hypothesis that the CBL is absent in first instar larva, as described for *Tenebrio molitor* [3,4]. The antibody against TKRP predominantly stained the n-posterior part of the CBU in both adults and larvae (Fig. 3 k, p and k', p'). Hence, the staining patterns appear to be maintained from larval to the adult form. We also observed some differences: The distinction between MIP and AT positive and negative labeled regions in the adult CBU (Fig. 3 i' and j'; arrowhead) was not reflected in the larval pattern. Further, the staining with the PVK antibody revealed staining in a small part of the n-posterior-lateral CBU, while the larval CBU is devoid of any PVK staining.

Mushroom bodies

Adult and larval MBs show a high degree of overall similarity in the neuromediator staining patterns but differences are found as well. The 5HT antibody labels a scattered network of extrinsic fibers in the CAs of both stages. However, the other parts of the MBs do not show any staining in larvae while in the adult diffuse and homogeneous staining is found (Fig. 3 m, m', supplementary Fig. S1 p, p' and u-

x). The MBs were devoid of MIP and AT stainings in both adults and larvae except for a very small area near the junction of the PE, vL and mL in adult animals [1] (supplementary Fig. S1 q, q', r, r').

In adult animals the TKRP antibody labels mainly the inner core of the MB but also scattered areas of the PE, mL, and vL [1]. In the larva, the scattered patterns are found as well but a TKRP immunoreactive core was not found (supplementary Fig. S1 s, s'). This indicates that the neurons homologous to ab core neurons in Drosophila differentiate later during development [5,6].

The antibody against PVK showed no immunostaining in the MBs of adults [1]. By contrast, the larva showed immunoreactivity in a restricted area, resembling a belt around the middle of the mL, as well as at the distal tip of the vL (Fig. 3 q, q' and supplementary Fig. S1 t, t').

Optic lobes

The anlagen of the larval OLs of *T. castaneum* can be differentiated into a distal and a proximal part (Fig. 3e), while the adult OLs are composed of the lamina (LA), medulla (ME), lobula (LO), lobula plate (LOP), and accessory medulla (AME). Because the LA is often damaged during preparation, data of the LA are not included in this work. The differences of the larval and adult OLs make a comparison difficult. In the larva, staining with the 5HT and MIP antibody labeled the entire proximal part of the OL anlagen (supplementary Fig. S1 f, f', g, g'). Adult OLs showed immunoreactive areas in all parts (supplementary Fig. S1 a, a', b, b'). The antibody against AT did not label the OLs in neither larva nor adult (supplementary Fig. S1 c, c', h, h'). The antibodies against TKRP and PVK clearly stained distinct areas of the proximal part of the larval OL anlagen (supplementary Fig. S1 i, i', j, j'). In the adults however, the antibody against TKRP labeled the ME, LO, and LOP as well as faintly the AME (supplementary Fig. S1 d, d'), while the antibody against PVK labeled only the AME faintly (supplementary Fig. S1 e, e').

Antennal lobes

The overall anatomy of the larval and adult ALs are similar. Both are ball-shaped and composed of spherical glomeruli. However, in L1 there are about 40-50 glomeruli while in adults there are about 70 glomeruli (Dreyer et al. 2010). Immunostainings with the antibodies against 5HT and MIP stain the entire AL in the larva and in the adult (supplementary Fig. S1 k, k', l, l', y, and [1]). It seems that in both stages, the 5HT antibody labeled branches throughout the ALs, innervating only the surface of the glomeruli, while the MIP antibody labeled the entire volume of the glomeruli. The AT antibody produced a scattered staining across all glomeruli of the ALs in both stages (supplementary Fig. S1 m, m'; [1]). The labelling by the antibody against TKRP differed drastically between larva and adult. In adults, all glomeruli of the ALs were clearly labeled, while in the larva only a faint, scattered staining of the ALs was observed (supplementary Fig. 1 n, n' and [1]). The antibody against PVK labeled scattered spots between the glomeruli in the posterior portion of adult AL [1]. In contrast, the larval ALs seem to be devoid of any PVK immunoreactivity (supplementary Fig. 1 o, o').

Tc-asense regulatory region

The following regulatory sequence of the 1st intron of the *Tc-asense* gene drives expression in the pattern described in Fig. 4a,b.

Primer with overhang and restriction site (5´-3´)

GTGACTGGATCCACAAATAAACCGCTTTTGAAATGC

GTCAGTGGTACCGTCACTACTGTCTGTGTCAG

ACAAATAAACCGCTTTTGAAATGCTTTCCTGCTCGTTCCCGCACCTAGACCAGGAGCCAATTGAAAATAAACAA
TCAGAAGATAAAAAGACTAGAAATCGCTCAAAAGATTGCAAAACCCCTCTAAAAATTATCCCCAAATTCAATTA
CAACTACGTAGTTTTAGAAAAAATACAGGAGTTTCCTTGAAATTTTAGTGGTGATGCGGTATGTTTTCTCAGTCT
CTGATATAATTAGTTTTTAAAAAAAGGTCAATGCTAGTTTTTGTAATGTAAGGAAGAGATAATCTTAGACACTT
GTAGCAACATCCCTCTCTCTAACAATGATATTTATCCTAATGTTCCAATTTTTCTTGTTGTCTTAAATTTTTAAATA
GTCGCTGAGGAAGTGCTGATGTTGAAGCCCGAAACACAAGCATTCCAAAACATTTAAACCAGTAAGCCTTGAT
TGGTTATACTTTTCAAAAATGTCTCTACAAGAATCTGGTTTCCAATTGGATATTAATCTGATGGCTCTTTTTTATT
AAAATTAAGAAAAACACAATTAAATTAACTTTATTAAAATTAAGAAAAATCTCTTCAAAAAATAATACGTACCAT
ATTCTCTCACACATTGGAAGATAAGCGTAATCTATTTTTTTATTCTTTTCACACATTCAGTGTTGAGTTTTCGTGT
TATAACTCTTTCTATATTAGATATTCATGTAAAGTAATTCCTCGAGATATTAGTATTCGATAAAACAGTAAAATT
ATTATTATTCTAGGGTTGATTTCAATCGATGGAATGTATTAGAAATTCGCTTTCTCAGAGAGACTTTTTTGAAGA
AAATGCAACTGTTAGAAAAATTTTAATTACAGAACACTTTGCTAGATTATATAAAAACTAACATTTGTTCTTTAA
TTTTTGTTCCCAATTCCAAAAGCTTCATTTTTTTGGTATTCTCAATTACCGCAATTATTTTTCTGTAATAAGAAGTC
ACTGCTCTTATTTTTAATTTTTAAACTAATTTAGGAATGTCGTCATAAACTAATTCTTCTATTATGTCTGGTTTTAT
ACCTCAAATTGGAGCATATATTAAGATGTTAAGTAAATTCCCACCCAATTTAAAATTTTTATTTAGATCAAAATG
CCTATCGGCCTGACGGCCTTCACCAGTTCTTCGTCAAAACACTTCACATATAATTATTGTAATTAAAATCAAACA
TTATTACATTAAACACTTAAAATCAAGATTAAACTTTAAAATTTGTTTGCCCTTTCTTTTCTTTGACAGCCATTTGT
GCCGAAACCGGTATTCTGATCTAAATAAAAATTTAAAATTGGGAGGAATTTTACTTCAGACATGTACTTATAGC
GATTAAAACTACTTGTCTACTACTCAAGTATAGTGATTAAAACTAGTATTTTCTTTTACCAGAATTTTTTATTCTC
CAAAAGTAATTCAACATTATAATAAAATAACTACTTAGATTATCAGCTTACATCCCTATTGCATTTAAAAGAGTT
TTCTAAATCCATGACTTCTCGTAATTATGCTGAGGACAGCCTTAAAAGCCCATGGATTTTATTTTTGAAATAGTC
GAATTTGAATGACATGTAGAGACTGAGCCAAAGTTAGTCACTTTTCCAAAAAATTCTCGAACAGGTCGTTTTTA
TTTTTTCGAATGTTACATTTTGACGTCATAGTGATATTTATGATGTAAGAAAGATCTTTGTGTAATACTCTCAAT
GAGTTTTACAACTTTTTTATTTTGATTTCTTTGTTTTACAGTTTTTCTTGCTAGAATTTTTTGAATTTTTTATACTCA
TTTTATACTTATTCAAAACTATAAAAACGCCATCGTCGCATTGTCTCTCAAAATTAGCTGTTATAAATTATTCATG
CACTTCAAAAAATAATAGGTATAGTTATTTATTTAACAAGTTTGAGTGTAAATCGGACGTTTTATGTCACGAGT
GGATTATCAAACCACTATTTTACAATTTTTTATCAGTCTTATTTAAAAAAATAATTCGGTAAAATGCGAACTTGG
CGTTTTGAACAACTAATAGAACTCCATTTAAAATTAGTGATCCAGACTTCGTTCCTATATAACATAATTTCAAAA
TTTTTGACATTGATAATTGATTTAAAATGTAAAACAATAATCAAAAACCTGAGTTGTCATTAAAAAATTTAATAT
GATGTTATTACTCAAAAACGAATGACGTCAGGTCAAGTCAGGTCAGGTGATGACTTTATAGTGTCAAATTATAT
ATTTAAAAAAATAAAATCGACCTGTGCAAAAATTTTGACTCATTAGGAAGATACGATTTTGTGCGTTACTTTTA
GTTCAGTCTGTATTTTTTTAATTAATTAGGTCGAGTATTTTTTATCCATTCTCACTGTGAAAAATGTATTGGTAAA
AAAAATTTATTTAGAAATTTTTATCTTATGTTCGATAAATTTTTATTAGTTTATTTCCCCAAGCAATAAAAAAATT
GCTTCTACGATTCCTGCTTTTCTGCTTTTACTACATGATATCCAAGCATGCATTTACATTACGCTAAACTGACTCT
TTGCATTTTTTTTTATTTTAACGGTCGGTTTTAATGAGTCGGTTAGTAATTTAAAGTTTATTTAATTTTATGGATT
AGGGCCAATTTTCCGAGAAAAAGCCCATTTCCGCCGACTTCCGAATTTGTGTGAAAATCTTGCGATAGGTTCCG
TTTCCTGTATCGAATCCCCGTTCGTCCCCGTCGTTGTTTACCGTCCGATTCCCCTATGGGCAACAGCTGTGATCT
AAAAACCCACCCCTGGAACAGGGAGGGGTCGATTTATGTTACTGGTCTCGTGCCATGTGCGAAACAACGTTGA
GAATTTTTAGTTGCGTTCGATCTTTAGAAATACGCGCACGCGACACAATTCAACCCATCACCAATTACCCAACAT
CCGGTCCGGCATTGAAGTCATCCACTTAACAGATCTGAACTCTGACACAGACAGTAGTGAC

Tc-EF1-α-B regulatory region

The following upstream regulatory sequence of the *Tc-EF1-α-B* gene drives neural expression in the pattern shown in red in Fig. 4c-e and supplementary figure S2 p-x.

CDS of upstream gene (NCBI)
5´start of ORF

Primers used for amplification:

name	Tm	length	restriction	sequence (5´-3´)
TcEFb-F3	61C	2246	EcoRI	ggaattcCCATCACCGTCGAAACCATA
TcEFb-R2	59C		BamHI	cgggatccGATTACGAGTTTTGCCTGGAA

>ref|NW_001094328.1|TcaLGUn_WGA243_1:19....-194948 (gene LOC658093 = hmm350)
GACCCAGAAACTTAATCTGGTGGCTCGGGGCGACCCGGGCATTCGGGGGTGGACCAACTACCTTCCTTTG
TGGCCATCACCGTCGAAACCATAATTATTAATTGTTATGTAAATATTGCTAAATAAATTATTTCTTATTC
GCGTTTTAATTGCGTTTTTGAATTGAATCTCCCGCGCCGATTGCAACCCCGGCGACGTCACATCCCTTGA
TTTTTTTCGCGATCTCATTGGTTCAGTAATTTTAGACACTTCCCCTATTTCCCCAAAATTTGCATTTCCT
GTGAAAATTAATTGCGACTTTTGGCCCAAACTGCGTAAATCCCACTATTTTAGCACCGTTATTGGGCCAA
AAATGCAAAACGGTTTAAAAATGCCCTATTTCGCGTTGATCGTAAATCAATATCCTATCCCCACCATCCA
GATTCTCCTTCTATTTCCGTTTGCTCGCGGCTAGGAGAGGATTGTCGTTTTTCCCGTTCTCTTGCTGCAG
TTTCAGAGGTAAGTGGAGCTTTCCCGATTTTTTACAAATTTTATCAGTTATCAGTCTTTAAAATATTCAT
CCGGTGTGTGTGACAATCGCATAAATTCCCTCAAATCACGGAAAACTGCACTAGGGAGGTATTTTCTTTG
ATTATTCGAAATTTTGGCAGATTTTCTCGCCGGCACTTTGCATCGCCTACTTTTCGACTTTTCGCCCAAA
AGGCACTTTTTGCAATGTGTCAAATTCTGACAATCGATGATTTGTAAAAAAAAAACAATATTTTTTGCAAA
AAATAAACAAAATTCCTCGTGTCAGTTGAAAATTGTGCGAGCCGGTATGTATTTTCCATTGAATTATTTT
GTTGCATCAGATTTGCAAATGAATGAGTCAGTTTAAATCCCAGAATTGCGGTTTTTCGACCTACCTCAAT
AACGATTTTGCTCCTCGAGTCAATAACCAAAACCGGATTGCCAGTGGGGGAGTTAATCGATCGGCCAAAT
TTATTTGGGATTTTTTGATAATATTGATTTAAATGGATTGCAACACAAAATGGCCGCCCTATTGTTCAAA
GCTGCATTTCTTAGCCGGCCGGCGGCCCGGAGGCACTTAATTTTTTAACAATAAGTCAATTTCGGAATGG
CAATAACACGGGTTCAACGACCTCACAGTTTCACTATTAGATTTTTACCTGTTTGATAAAAAACCAACTG
CATTGTTTTGCAGCGGTTTATTTTCCTGTTTGGCTAATTGAGTCAAGGTCGTGGAACACCGTTAGTTCCA
GTGCTTGTAAACACATGATTTTCGAGTCAGGGACTCGGCATTAGGCCCCAGATACGATTTCAAATCTATC
TAGTATTTGGCTGGCCTTATTGATCACCTGAACAGAACCTGTGAAGGTTTTACCTAATCTAAGGTTCAAG
GGCTGTATAGCCAGAACATTCATCCGTTTTAAAATTGTAAAAATACCTTTCTATATCACCCAATTTTAAT
ATCTTTACTAATAATAAATAATTCAAATTCTAGGTACTAAAGAATCATAATTCCGCATGATTCACTCACT
GCATACCTAAGTTTTTATTCACTTTGATATATCAAAATTAATCGCTTTTAATTCTGGTTTAAGTTCATAG
CCAGTGGCGTATTTAGGTTCATTGCTTCTCAGGGATACTTAATTTTGCCGTCCCTGCATATATTTCTTTA
AAAAATTGTCGTGCTTTGGAAATTTGTAGCACCATTCGTATTTTCAAAATTTTAAATGGTACCACCCTTC
TTGTGCCAAATGAACTACTCGAAAAATGCAAAATTAACTTTAAATACCTGAAAAAATTGAAAAAAAACTG
AAAAAATGCACTAGATTTTTAAATCTTCCCTTTATTTCTATTAAAAAATACCCTGTATTTATTTAAGAAA
GTTTTTGTTTCTGAAAAACCATAGCCATTTTTACACTTTTTTTATGTTATCGCTGACTTTTTTCAAAGAT
GTGTACTGTTCAGGCTTTCTCTCATCACTCGAGGTTTAAGTCCACTCGTGGAATAAAGAGTCCGATGTTA
TTCACTCAGGCTCGTTAAATAAATAACTATATTAACAAACTAGCAATATTCGACAGTAAATTAAATTCAA
TAACGTGGCAAACAAAAGAGCAACAATTAGGGCGGTTCCTACCGAAAAAATTAAAAAAGTTGCTTGGAAA
GAAATTTTGAATCATTTAAAAAACACTGCGTTATTTGAGTTGTAATGCAAAAGTTTTTAGAGCCAATTTT
TGGTGGGGGTTCACACCACCCTCACAGAGTGTGTGGGCGCCGCTGACGTTTGCTCTTTTTCCAGGCAAAA
CTCGTAATCCGCCATGGGTAAGGAAAAGATCCATATTAACATCGTCGTG

Material and Methods:

Beetle strains:

The "mushroom body green" line is an enhancer trap found in the GEKU screen [7]. The "glia blue" line was generated by driving ECFP with 6 copies of the artificial P3 Promoter using the *Tc-hsp68* core promoter. The "neuron red" line was generated by Michalis Averof by driving dsRedExpress using the regulatory sequence of the *elongation factor 1 alpha-B (Tc-EFB)* gene, which has two copies in *Tribolium*. While Tc-EFA drives ubiquitously as expected [8] the *Tc-EFB* enhancer unexpectedly drove in neural cells. The "brainy" line was generated by crossing these two lines. By sibling crossings, these lines were made homozygous.

Immunohistochemistry:

The fluorescence signal of the brainy line enabled us to dissect the brain of the first instar larvae (L1) by using a fluorescence binocular (SteREO Lumar. V12; Zeiss, Jena, Germany) equipped with a NeoLumar S 1.5x FWD 30 mm ocular (Zeiss). Brains were dissected in a concavity slide in cold PBS (phosphate-buffered saline, 0.01 M, pH 7.4) and fixed in 4% formaldehyde (FA, Roth, Karlsruhe, Germany) in PBS (for up to 60 min on ice or up to 3 h at room temperature (RT)). Brains were rinsed in PBS 3 x 10 min at RT. Transfer into different solutions was performed by a pipette (0.1 – 2.5 µl; Eppendorf, Hamburg, Germany). Preincubation was done for about 1 h on ice in 5% normal goat serum (NGS; Jackson ImmunoResearch, Westgrove, PA, USA) in PBS containing 0,3% Triton X-100 (PBST; Sigma-Aldrich, Steinheim, Germany). We incubated the brains over night at 4°C in a 1:50 dilution of the synapsin antibody in PBST containing 2% NGS in combination with one of the rabbit antisera (anti 5HT, 1:10000; anti MIP: 1:5000, anti AT: 1:5000, anti TKRP, 1:50000 in L1 or 1:20000 in adult; anti PVK, 1:4000; anti DC0: 1:200; or Repo: 1:500). For the anatomical studies we also used Alexa Fluor 488-coupled phalloidin (phalloidin; Molecular Probes, Eugene, OR, USA). The brains were rinsed 3 x 10 min with PBST, afterwards they were incubated with the secondary goat anti-mouse conjugated to Cy5 (GAM Cy5) and goat anti-rabbit antibody conjugated to Cy3 (GAR Cy5), or GAM Cy3 and GAR Cy5 (each 1:300, Jackson ImmunoResearch, Westgrove, PA, USA) in PBST and 1% NGS for 4 – 6 h at RT or over night at 4°C. Subsequently the brains were rinsed again with PBST 3 x 10 min and were finally mounted in 80 % glycerol (Sigma-Aldrich) and 20 % PBS. To prevent the brains from compression, we mounted them between two coverslips using one reinforcing ring as spacer (Zweckform, Oberlaindern, Germany).

Adult brains were treated according to the protocol published in Binzer et al. (2013). In short, adult brains were dissected in cold PBS, fixed in 4% FA in PBS over night at 4°C. Subsequently washed 5 x 10 min with PBS at RT and were preincubated with PBST containing 5 % NGS for 1-2 days. Afterwards brains were incubated with primary antibody (see above) for 2-3 days, washed 5 x 10 min with PBST at RT and incubated in secondary antibody (see above) for 2 days at 4°C. Subsequently we washed the brains 5 x 10 min with PBS at RT followed by dehydrated in an ascending ethanol series (50%, 70%, 90%, 95%, and two times 100%, for 2.5 min each) and then cleared in methyl salicylate (Merck, Gernsheim, Germany), until the tissue was transparent. Finally brains were mounted in Permount (Fisher Scientific, Pittsburgh, PA, USA) using two reinforcing rings as spacers between two coverslips.

Primary and secondary Antibodies and tissue markers:

All used antisera are highly conserved among insects (neuropeptides: [9–11]; serotonin: [12]; DC0: [13]; Repo: [14]. The antibodies against neuropeptides and synapsin were tested in *Tribolium castaneum* by [1,15]. The monoclonal primary antibody from mouse against a fusion protein consisting

of a glutathione-S-transferase and the first amino acids of the presynaptic vesicle protein synapsin I coded by its 5′-end (SYNORF1; 3C11, #151101), was used to selectively label neuropilar areas, especially for 3D reconstructions of the brain. It was kindly provided by Dr. Erich Buchner (University of Würzburg, Germany) and was first described by Klagges et al. (1996). The antibody was used at a dilution of 1:50. The polyclonal antiserum against the biogenic amine serotonin (5HT) was raised in rabbit (DiaSorin, Kansas City, MO, USA).). It was used at a dilution of 1:10000. The antiserum against the neuropeptide *Manduca sexta* allatotropin (Mas-AT, pGFKNVEMMTARGFamide) was raised in rabbit. It was kindly provided by Dr. J. Veenstra (University of Bordeaux, Talence, France) and first described by [16]. The antibody was used at a dilution of 1:5000. The antiserum against the neuropeptide *Periplaneta americana* myoinhibitory 1 (Pea-MIP1, GWQDLQGGWamide) was raised in rabbit. The antiserum was kindly provided by Dr. H. Agricola (University of Jena, Germany) and has been described by [17]. It was used at a dilution of 1:5000.

The antiserum against the neuropeptide *Locusta migratoria* Tachykinin 2 (Lom-TK2, APLSGFYGVRamide) was raised in rabbit. It was kindly provided by Dr. H. Agricola (University of Jena, Germany) and first described by [18]. The antibody was used at a dilution of 1:20000 in adults or 50000 in larva.

The antiserum against the neuropeptide *Periplaneta-americana* Periviscerokinin 2 (Pea-PVK2, GSSSGLISMPRVamide) was raised in rabbit, The Antiserum was kindly donated by Dr. M. Eckert (University of Jena, Germany) and first described by [19].

The DC0 antiserum recognizes the catalytic subunit of the protein kinase A (PKAc) of the vinegar fly *D. melanogaster*. Anti-DC0 was raised in rabbit and was kindly provided by Dr. D. Kalderon (Columbia University, NY, USA). It was first described by [20]. We used this antiserum in a concentration of 1:200).

The Reversed-Polarity (4α3) (Repo) antiserum is directed against the transcription factor Reversed-Polarity of *D. melanogaster* and was used to visualize somata of glia cells (Halter et al., 1995). It was raised in rabbit and kindly provided by Dr. B. Altenhein (University of Mainz, Germany) and had been described by Halter et al. (1995). It was used in a dilution of 1:500.

As secondary antibody we used goat anti-mouse conjugated to Cy5 (GAM Cy5) and goat anti-rabbit antibody conjugated to Cy3 (GAR Cy5), or GAM Cy3 and GAR Cy5 (all Jackson ImmunoResearch, Westgrove, PA, USA). Each secondary antiserum was used in a dilution of 1:300. Alexa Fluor 488-coupled phalloidin (phalloidin; Molecular Probes, Eugene, OR, USA) was used to visualize F-actin of axons, to label the whole brain structure. It was used at a dilution of 1:200.

Data analysis and three-dimensional reconstruction:

Fluorescence signals were scanned with a confocal laser scanning microscope (Leica TCS SP5 CLSM; Leica, Bensheim, Germany) equipped with a 63× glycerol objective (HCX PL APO 63x/1.30 Glyc 21°C CS (working distance: 0.26 mm); Leica, Bensheim, Germany) or 40x oil objective (HCX PL APO 40x/1.25-0.75 Oil Lbd. bl. (working distance: 0.1 mm); Leica) at a resolution of 1024x1024 or 512x512 pixel, a pinhole of 1 Airy unit, a scanning speed of 400 or 200 Hz, a step size of 0.5–1.0 µm, a line average of 2–4, and a digital zoom of 1.0–2.5.

Images taken from AMIRA 5.1 or 5.2 (FEI, Hillsboro, OR, USA) were arranged and cropped by using CorelDRAW X3 (Corel, Ottawa, Ontario, CA). 3D reconstructions of brains were performed by using the

segmentation editor and the polygonal surface model in AMIRA, based on stainings with the synapsin antibody or alexa Fluor 488-coupled phalloidin, according to Kurylas et al. 2008 [7].

Signal colocalization and cell counting:

Larval brains were scanned with a step size of 0.5 µm (see above) resulting in a stack of appr. 80 – 90 optical sections. Using the model "ProjectionView" in AMIRA 5.1 or 5.2, we merged 10 successive sections to one maximum intensity projection, respectively, in which we counted the cell numbers and colocalization of the signals.

Orientation of the adult and larval brain

To compare adult and larval brains, we used the neuraxis instead of the body axis for orientation [21].

References:

1. Binzer, M., Heuer, C. M., Kollmann, M., Kahnt, J., Hauser, F., Grimmelikhuijzen, C. J. P. & Schachtner, J. 2014 Neuropeptidome of Tribolium castaneum antennal lobes and mushroom bodies. *J. Comp. Neurol.* **522**, 337–357. (doi:10.1002/cne.23399)
2. Heuer, C. M., Kollmann, M., Binzer, M. & Schachtner, J. 2012 Neuropeptides in insect mushroom bodies. *Arthropod Struct. Dev.* **41**, 199–226. (doi:10.1016/j.asd.2012.02.005)
3. Wegerhoff, R., Breidbach, O. & Lobemeier, M. 1996 Development of locustatachykinin immunopositive neurons in the central complex of the beetle Tenebrio molitor. *J. Comp. Neurol.* **375**, 157–166. (doi:10.1002/(SICI)1096-9861(19961104)375:1<157::AID-CNE10>3.0.CO;2-S)
4. Wegerhoff, R. & Breidbach, O. 1992 Structure and development of the larval central complex in a holometabolous insect, the beetle Tenebrio molitor. *Cell Tissue Res* **268**, 341–358.
5. Zhao, X., Coptis, V. & Farris, S. M. 2008 Metamorphosis and adult development of the mushroom bodies of the red flour beetle, Tribolium castaneum. *Dev. Neurobiol.* **68**, 1487–1502. (doi:10.1002/dneu.20669)
6. Lin, H.-H., Lai, J. S.-Y., Chin, A.-L., Chen, Y.-C. & Chiang, A.-S. 2007 A Map of Olfactory Representation in the Drosophila Mushroom Body. *Cell* **128**, 1205–1217. (doi:10.1016/j.cell.2007.03.006)
7. Trauner, J., Schinko, J., Lorenzen, M. D., Shippy, T. D., Wimmer, E. A., Beeman, R. W., Klingler, M., Bucher, G. & Brown, S. J. 2009 Large-scale insertional mutagenesis of a coleopteran stored grain pest, the red flour beetle Tribolium castaneum, identifies embryonic lethal mutations and enhancer traps. *BMC Biol* **7**, 73.
8. Sarrazin, A. F., Peel, A. D. & Averof, M. 2012 A Segmentation Clock with Two-Segment Periodicity in Insects. *Science*
9. Nässel, D. R. 2002 Neuropeptides in the nervous system of Drosophila and other insects: multiple roles as neuromodulators and neurohormones. *Prog. Neurobiol.* **68**, 1–84.
10. Homberg, U. 2002 Neurotransmitters and neuropeptides in the brain of the locust. *Microsc. Res. Tech.* **56**, 189–209. (doi:10.1002/jemt.10024)
11. Nässel, D. R. & Homberg, U. 2006 Neuropeptides in interneurons of the insect brain. *Cell Tissue Res.* **326**, 1–24. (doi:10.1007/s00441-006-0210-8)
12. Dacks, A. M., Christensen, T. A. & Hildebrand, J. G. 2006 Phylogeny of a serotonin-immunoreactive neuron in the primary olfactory center of the insect brain. *J. Comp. Neurol.* **498**, 727–746. (doi:10.1002/cne.21076)
13. Farris, S. M. & Strausfeld, N. J. 2003 A unique mushroom body substructure common to basal cockroaches and to termites. *J. Comp. Neurol.* **456**, 305–320. (doi:10.1002/cne.10517)
14. Halter, D. A., Urban, J., Rickert, C., Ner, S. S., Ito, K., Travers, A. A. & Technau, G. M. 1995 The homeobox gene repo is required for the differentiation and maintenance of glia function in the embryonic nervous system of Drosophila melanogaster. *Dev. Camb. Engl.* **121**, 317–332.
15. Utz, S., Huetteroth, W., Vömel, M. & Schachtner, J. 2008 Mas-allatotropin in the developing antennal lobe of the sphinx moth Manduca sexta: Distribution, time course, developmental regulation, and colocalization with other neuropeptides. *Dev. Neurobiol.* **68**, 123–142. (doi:10.1002/dneu.20579)
16. Veenstra, J. A. & Hagedorn, H. H. 1993 Sensitive enzyme immunoassay for Manduca allatotropin and the existence of an allatotropin-immunoreactive peptide in Periplaneta americana. *Arch. Insect Biochem. Physiol.* **23**, 99–109. (doi:10.1002/arch.940230302)
17. Predel, R., Rapus, J. & Eckert, M. 2001 Myoinhibitory neuropeptides in the American cockroach. *Peptides* **22**, 199–208.
18. Veenstra, J. A., Lau, G. W., Agricola, H. J. & Petzel, D. H. 1995 Immunohistological localization of regulatory peptides in the midgut of the female mosquito Aedes aegypti. *Histochem. Cell Biol.* **104**, 337–347.

19. Eckert, M., Herbert, Z., Pollák, E., Molnár, L. & Predel, R. 2002 Identical cellular distribution of all abundant neuropeptides in the major abdominal neurohemal system of an insect (Periplaneta americana). *J. Comp. Neurol.* **452**, 264–275. (doi:10.1002/cne.10382)
20. Lane, M. E. & Kalderon, D. 1993 Genetic investigation of cAMP-dependent protein kinase function in Drosophila development. *Genes Dev.* **7**, 1229–1243.
21. Ito, K. et al. 2014 A systematic nomenclature for the insect brain. *Neuron* **81**, 755–765. (doi:10.1016/j.neuron.2013.12.017)

Supplementary Figures:

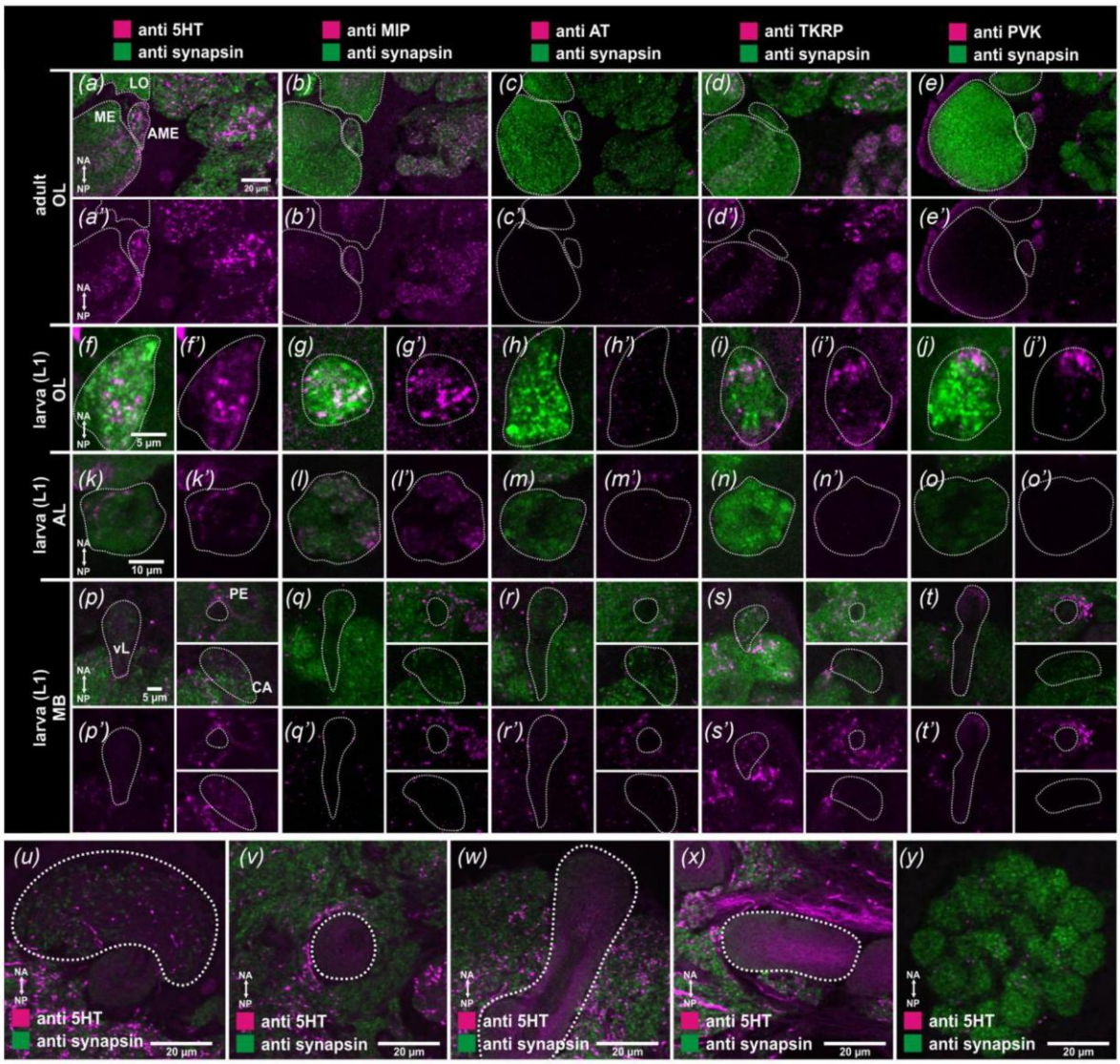

Supplementary figure S1 Comparison of brain areas between adults and first instar larvae of *Tribolium*
Immunostainings of adult and first instar larval (L1) brains of *Tribolium* of three of the four main neuropils: (a-j and a'-j') optic lobes (OL); (k-o and k'-o') antennal lobes (AL) and (p-t and p'-t') mushroom body (MB). An antibody against synapsin (green) was used in combination with one additional antibody against a neuromediator (5HT: serotonin, MIP: Myoinhibitory Peptide , AT: Allatotropin, TKRP: Tachykinin related peptide, PVK: Periviscerokinin) (magenta). AME: accessory medulla, CA: calyx, LO: lobula, ME: medulla, mL: median lobe, PE: pedunculus, and vL: ventral lobe. Scale bars, orientation bars (NA: neuraxis anterior and NP: neuraxis posterior), labeling of the neuropils and scale bars in the left column of the line applies for all pictures of the line. *(u-y)* Immunostainings of neuropils from the adult animal against 5HT and synapsin of the Ca *(u)*, the PE *(v)*, the vL *(w)*, the median lobe *(x)*, and the AL *(y)*.

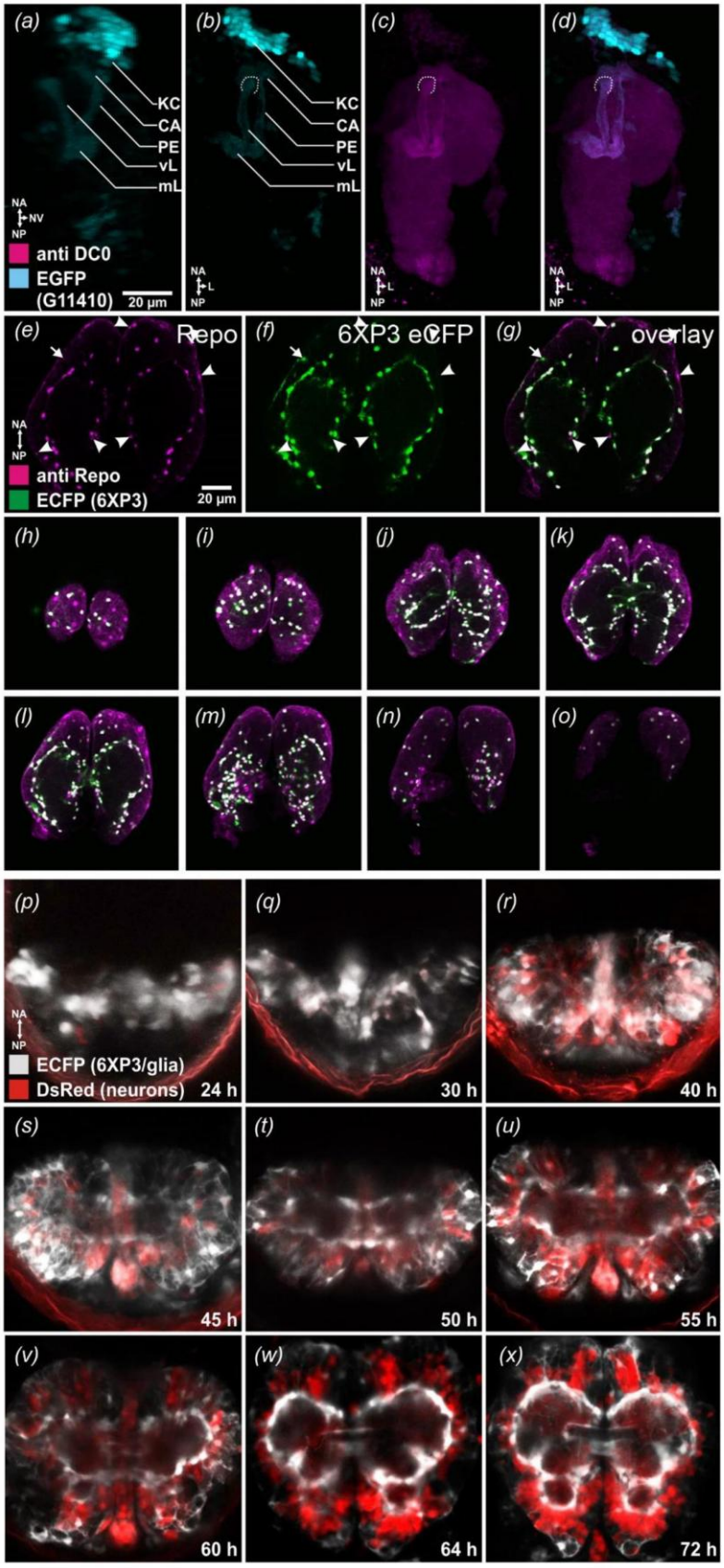

Supplementary figure S2

Characterization of the MB-green and the brainy line

(a-d) Characterization of the enhancer trap line G11410 (MB-green), which marks the MB. *(a,b)* One MB shown from two different angles to display all details. Labelling as in figure 3, KC: Kenyon cells. *(c,d)* Colocalization of the EGFP signal of G11410 with the DC0 antibody confirms labelling of the MB. Note that the KC are marked in G11410 but not by the DC0 antibody. *(e-o)* Characterization of the glia-blue line (6XP3), which marks glia with ECFP (green) in combination with an antibody against *Drosophila* Repo (magenta). Overlay of both signals *(g-o)*. Most cell bodies marked with ECFP are Repo positive confirming glia-specific staining. Note that some glia cells are not marked by glia-blue (white arrowheads in *e-g*) and some ECFP marked cells are not Tc-Repo positive (arrows in e-g). *(p-x)* Embryonic developmental series of fluorescence signal in the brainy-line. Orientation bars in *(e)* and *(p)* apply for *f-o* and *q-x*, respectively).

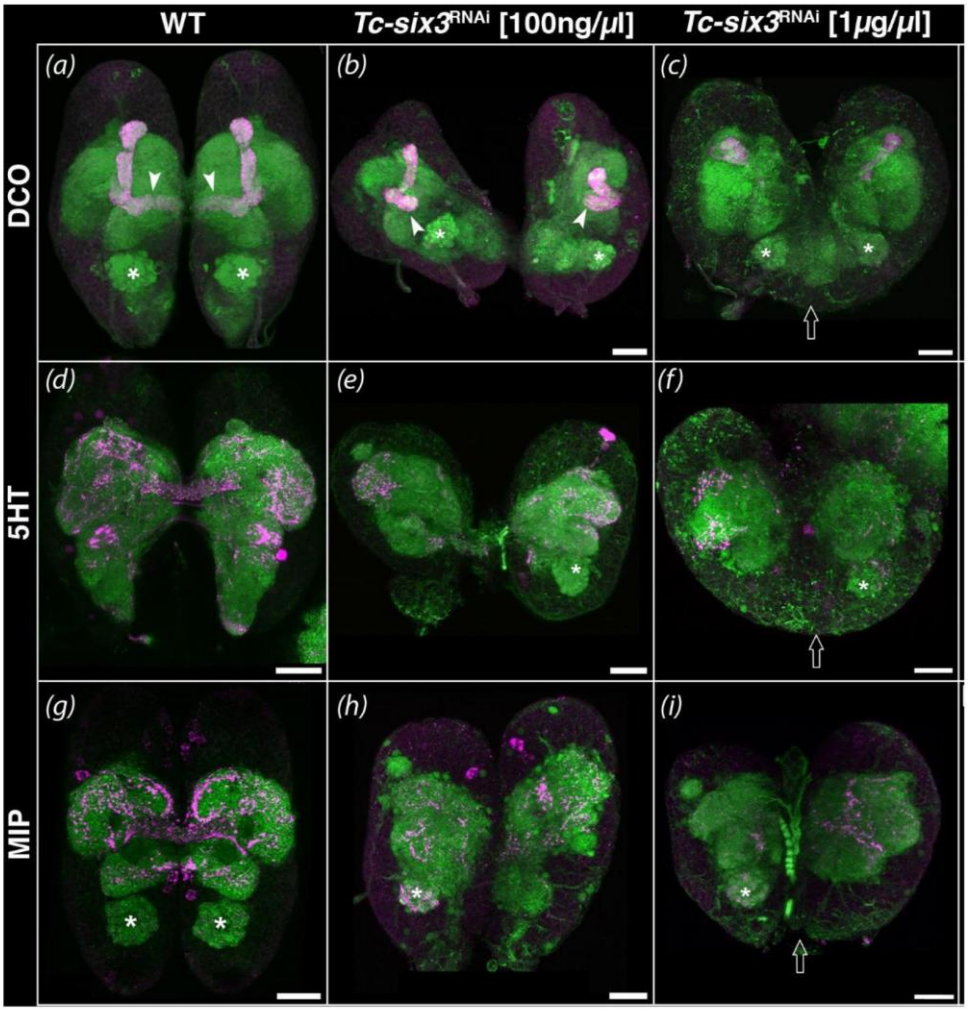

Supplementary Figure S3 Analysis of the *Tc-six3* phenotype by immunohistochemistry

(a,d,g) L1 wildtype brains stained for DC0 *(a)*, serotonin (5HT) *(d)*, and myoinhibitory protein (MIP) *(g)*. *(b,c,e,f,h,i)* Brains of late *Tc-six3* RNAi knock-down embryos. Anterior is up and phalloidin staining is shown in green in all panels. In mild RNAi treatments (100 ng/µl), the mushroom bodies are still present but the median lobes do not touch at the midline (compare location of arrowheads in *(a,b)*). The CBU is marked by serotonin and MIP, but is absent in RNAi embryos *(e,h)*. With higher RNAi concentrations (1 µg/µl), the phenotype gets stronger and the midline of the brain becomes more severely affected (open arrow in *(c,f,i)*). Scale bars depict 20 µm.

The insect central complex as model for heterochronic brain development
– background, concepts and tools

Nikolaus Dieter Bernhard Koniszewski[1/2]*, Martin Kollmann[3]*, Mahdiyeh Bigham[1], Max Farnworth[1],
Bicheng He1, Marita Büscher1, Wolf Hütteroth3/4, Marlene Binzer3, Joachim Schachtner3, Gregor Bucher1#
[#]Corresponding author: Gregor Bucher

***Drosophila* gene**	**Symbol**	**Antibody**	**Immunoreactivity in *Tribolium***	
Achaete	Ac	m monoclonal	-	
atypical Protein Kinase	aPKC	r polyclonal[1]	++	
Armadillo	Arm	m monoclonal	-	
Asense	Ase	r polyclonal	-	
Bazooka	Baz	r polyclonal	+	*
Bazooka N-terminal	Baz	rat polyclonal	-	
BP102		m monoclonal	-	
BP106		m monoclonal	-	
Brain Tumor	Brat	m polyclonal	-	
Drosophila Death Caspase-1	D-Ccp-1	r polyclonal[2]	+++	
DE-Cadherin	DE-Cad	m monoclonal	-	
Deadpan	Dpn	gp polyclonal	-	
Derailed	Drl	r polyclonal	-	
Diaphanous	Dia	m monoclonal	-	
Dichaete	D	r polyclonal	-	
Discs large	Dlg	m monoclonal	-	
Discs large	Dlg	gp polyclonal	-	
Dorsocross2	Doc	r polyclonal	-	
Eagle	Eg	r polyclonal	-	
Embryonic lethal abnormal vision	ELAV	rat monoclonal	-	
Empty spiracles	EMS	r polyclonal	-	
Engrailed/Invected	En/Inv	m monoclonal[3]	++	
Even-skipped (2B10)	Eve	m monoclonal[4]	+	
Even-skipped	Eve	r polyclonal	-	
Fasciclin 2 (1D4)	Fas 2	m monoclonal[5]	+	
Fasciclin 3	Fas 3	m monoclonal	-	
Flamingo	Fmi	m monoclonal	-	
Futsch (22C10)	Futsch	m monoclonal	-	
G protein α-i subunit	Gαi	r polyclonal	-	
Hepatocyte-nuclear-factor 4	HNF4	m polyclonal	-	
Hunchback	Hb	gp polyclonal	-	
Hunchback	Hb	rat polyclonal	-	
Extra-extra (Hb9)	exex	r polyclonal	-	
Inscuteable	Insc	r polyclonal	-	
Klumpfuss	Klu	r polyclonal	-	
Krueppel	Kr	gp polyclonal	-	
Lim3	Lim3	gp polyclonal	-	
Miranda	Mira	m monoclonal	-	
Miranda	Mira	r polyclonal	-	
Miranda C-terminus	Mira	r polyclonal	-	

Miranda N-terminus	Mira	r polyclonal	-	
Mirror	Mirr	r polyclonal	-	
Drop (Muscle-specific homeobox)	Dr	r polyclonal	-	
Neuromancer 1 (H15)	Nmr1	r polyclonal	-	
Neuromancer 2 (Midline)	Nmr2	gp polyclonal	-	
Nubbin	Nub	r polyclonal	-	
Numb	Numb	r polyclonal	-	
Numb	Numb	gp polyclonal	-	
Par6	Par6	r polyclonal	+	*
Partner of Inscutable	Pins	r polyclonal	-	
Partner of Inscutable C-terminus	Pins	rat polyclonal	-	
Partner of Numb	Pon	r polyclonal	-	
Phospho-histone-3	PH3	r polclonal[6]	+++	
Prospero	Pros	m monoclonal	-	
Reversed polarity	Repo	m monoclonal[7]	+++	
Reversed polarity	Repo	r polyclonal[8]	+++	
Reversed polarity	Repo	gp polyclonal[9]	+	
Retinal Homeobox	Rx	r polyclonal	-	
Runt	Run	r polyclonal	-	
Runt	Run	gp polyclonal	-	
Singleminded	Sim	m monoclonal	-	
Snail	Sna	m monoclonal	-	
SoxNeuro	SoxN	m polyclonal	-	
Ventral-nerve-cord defective	Vnd	r polyclonal	-	
Visual homeobox protein1 N-terminus	Vsx1	gp polyclonal	-	
Visual homeobox protein1 C-terminus	Vsx1	gp polyclonal	-	
Wingless	Wg	m monoclonal	-	
Worniu	Wor	m polyclonal	-	
Wrapper	Wrapper	m monoclonal	-	
Zinc finger homeodomain 1	Zfh-1	r polyclonal	-	

1: Santa Cruz Biotechnology, product number sc-216
2: Cell Signaling Technology, product number 9578
3, 4, 5, 7: Developmental Studies Hybridoma Bank, University of Iowa
6: Upstate, product number 06-570
8, 9: von Hilchen et al. (2013), Development 140(17), 3657-68
r: rabbit; m: mouse; gp: guinea pig; r: rat

Chapter 3:

Morphological and Transcriptomic Analysis of a Beetle Chemosensory System Reveals a Gnathal Olfactory Center

Morphological and Transcriptomic Analysis of a Beetle Chemosensory System Reveals a Gnathal Olfactory Center

Stefan Dippel[1*], Martin Kollmann[2*], Georg Oberhofer[3], Alice Montino[1], Carolin Knoll[2], Milosz Krala[2], Karl-Heinz Rexer[4], Sergius Frank[2], Robert Kumpf[5], Joachim Schachtner[2#], Ernst A Wimmer[1#]

sdippel@gwdg.de, martin.kollmann@biologie.uni-marburg.de, goberho@gwdg.de, amontino@gwdg.de, carok406@gmail.com, milosz.krala@physik.uni-marburg.de, rexer@biologie.uni-marburg.de, sergiusfrank84@gmail.com, robert.kumpf@psb.vib-ugent.be, joachim.schachtner@biologie.uni-marburg.de, ewimmer@gwdg.de

[1]Georg-August-University Goettingen, Johann-Friedrich-Blumenbach-Institute of Zoology and Anthropology, Dept. of Developmental Biology, Göttingen Center for Molecular Biosciences (GZMB), Ernst-Caspari-Haus, Justus-von-Liebig-Weg 11, 37077 Göttingen, Germany

[2]Philipps-University Marburg, Dept. of Biology - Neurobiology/Ethology, Karl-von-Frisch-Str. 8, 35032 Marburg, Germany

[3]Georg-August-University Goettingen, Johann-Friedrich-Blumenbach-Institute of Zoology and Anthropology, Dept. of Evolutionary Developmental Genetics, GZMB, Ernst-Caspari-Haus, Justus-von-Liebig-Weg 11, 37077 Göttingen, Germany

[4]Philipps-University Marburg, Dept. of Biology - Mycology, Karl-von-Frisch-Str. 8, 35032 Marburg, Germany

[5]Flanders Institute for Biotechnology, Dept. of Plant Systems Biology, Technologiepark 927, 9052 Gent, Belgium

*Equal contribution.

#Corresponding authors.

Table 1. Abbreviations

AL	antennal lobe
ALT	antennal lobe tract
CA	calyx of the MB
CSN	chemosensory neuron
cSTri	chemosensilla trichoidea
GNG	gnathal ganglia
GOC	gnathal olfactory center
GR	gustatory receptor
GSN	gustatory sensory neuron
IHC	Immunohistochemistry
IR	Ionotropic glutamate-like receptor
-ir	immunoreactive
KC	Kenyon cells
LG	lobus glomerulatus
MB	mushroom body
mSTri	mechanosensilla trichoidea
OBP	odorant binding protein
ODE	odorant degrading enzyme
OR	odorant receptor
Orco	odorant receptor co-receptor
ORF	open reading frame
OSN	olfactory sensory neurons
PN	projection neuron
RPKM	reads per kilobase per million
SBas	sensilla basiconica
Scam	sensilla campaniformes
SCha	sensilla chaetica
SCoe	sensilla coeloconica
SEM	scanning electron microscope
SNMP	sensory neuron membrane protein
SpaB	spaculate bristle
TKRP	tachykinin related peptide

Abstract

In *Tribolium castaneum*, our detailed morphological description of the olfactory pathway in combination with genome-wide expression analysis of the relevant gene families involved in chemoreception revealed that besides the antennae also the mouthparts are highly involved in olfaction and that their respective contribution is processed separately. This is in contrast to the current picture that in holometabolous insects all olfactory input allegedly converge in the antennal lobe. In this beetle, olfactory sensory input from the mouthparts is processed in the lobus glomerulatus, a structure so far only being characterized in hemimetabolous insects, as well as in a so far non-described unpaired glomerularly organized olfactory neuropil in the gnathal ganglion, we term gnathal olfactory center. The importance of the maxillary and labial palps in olfaction of the red flour beetle is also supported by the high number of functional odorant receptor genes expressed in the mouthparts.

Introduction

Insects use chemical cues for most tasks they encounter during their life history. Over long distances airborne chemical stimuli guide insects to food sources, mates, and places for oviposition (Visser 1986; Tegoni et al. 2004; Dahanukar et al. 2005; Whiteman and Pierce 2008; de Bruyne et al. 2010; Leal 2013). Within close range, olfaction as well as gustation are used to discriminate between different food qualities, to avoid toxins or harmful microbes, to communicate intra- or interspecifically, to identify suitable mating partners, and to find appropriate egg-laying sites (Laska et al. 1999; Yang et al. 2008; Liu et al. 2008; Whiteman and Pierce 2008; Dicke 2009; Weiss et al. 2011; Sun et al. 2012; Stensmyr et al. 2012; Linz et al. 2013; Paczkowski et al. 2014). Because of insects' devastating impact on agriculture and stored food products, as well as their ability to serve as vectors for detrimental diseases, insect olfaction has become an important research field in biology (Leal 2013).

Chemical signals are typically perceived within specialized antennal and palpal cuticular structures, the olfactory or gustatory sensilla. These chemosensory sensilla form a hollow structure filled with aqueous lymph and harbor the dendritic branches of the chemosensory neurons (CSNs), namely the olfactory (OSNs) or gustatory sensory neurons (GSNs) (Steinbrecht 1996; de Bruyne and Warr 2006). They are divided into several sub-types according to their different morphology (Steinbrecht 1996). The volatile molecules enter the cavity through wall pores to finally reach and activate the chemoreceptors on the dendrites of the OSNs. To enhance olfactory sensitivity and specificity, odorant binding proteins (OBPs) or potentially chemosensory proteins (CSPs) facilitate the translocation of many, mostly hydrophobic chemicals through the aqueous lymph (Pelosi et al. 2014). In insects typically three different receptor families are involved in chemoreception (Leal 2013): the ionotropic

glutamate-like receptors (IRs) (Benton et al. 2009; Rytz et al. 2013), the gustatory receptors (GRs) (Montell 2009; Weiss et al. 2011), and the odorant receptors (ORs) (Sato et al. 2008; Wicher et al. 2008; Missbach et al. 2014). The IRs are evolutionary highly conserved chemoreceptors involved in protostome olfaction (Benton et al. 2009),), they contain three transmembrane domains, and form functional heteromers between an odor specific IR and a co-receptor (IR8a and IR25a) The GRs are seven transmembrane receptors found across arthropods (Sánchez-Gracia et al. 2001; Chyb 2004; Cao 2014; Chipman et al. 2014) whose quaternary structure (Jiao et al. 2008; Lee et al. 2009; Weiss et al. 2011; Freeman et al. 2014), as well as the signal transduction mechanism (Ishimoto et al. 2005; Sato et al. 2011) are still under debate. The typical ORs are seven transmembrane receptors found in pterygote insects (Missbach et al. 2014) that form functional heteromers with the atypical (general) odorant receptor co-receptor (Orco) (Sato et al. 2008; Wicher et al. 2008; Smart et al. 2008; German et al. 2013; Mukunda et al. 2014). Their signal transduction mechanism is currently discussed and they might either from an ionotropic receptor complex that is regulated by second messengers or are functional metabotropic receptors (Sato et al. 2008; Wicher et al. 2008; Smart et al. 2008; Martin and Alcorta 2011; Getahun et al. 2013; Nolte et al. 2013; Stengl and Funk 2013). The described influence of G-proteins and affiliated second messengers on insect olfaction supports both mechanisms (Riesgo-Escovar et al. 1995; Miura et al. 2005; Chatterjee et al. 2009; Deng et al. 2011; Sargsyan et al. 2011; Martin et al. 2013; Ignatious Raja et al. 2014). Moreover, sensitive pheromone detection requires the OR/Orco complex to interact with a sensory neuron membrane protein (SNMP) related to the scavenger receptor CD36 (Benton et al. 2007; Jin et al. 2008; Li et al. 2014). Besides the perireceptor events involved in effective activation, the high temporal resolution of olfactory reception probably also requires signal termination, which is supposedly mediated by secreted or membrane-bound odorant-degrading enzymes (ODEs) (Maïbèche-Coisne et al. 2004; Ishida and Leal 2005; Durand et al. 2011; Chertemps et al. 2012; Younus et al. 2014).

Activation of the described chemoreceptors elicits action-potentials in the CSNs that are further transmitted via the antennal nerve to the AL, the first integration center of the olfactory pathway in the brain, or in case of GSNs to the primary gustatory center of the gnathal ganglion (GNG) (Scott et al. 2001). The AL of insects consists typically of spherical sub compartments, the olfactory glomeruli (Schachtner et al. 2005). Usually OSNs express only one typical (specific) OR gene and all antennal OSNs expressing the same typical OR converge into the same olfactory glomerulus, creating a chemotropic map-like representation of chemical coding in the AL (Vosshall 2000; Stocker 2001; Keller and Vosshall 2003), known as the central dogma of olfaction (Jefferis 2005; Smith 2008). In *Drosophila melanogaster*, the OR/Orco and IR derived sensory information from the antennae and the maxillary palps is processed in the AL (Couto et al. 2005), whereas in several hemimetabolous insects CSNs from the palps converge typically in the lobus glomerulatus (LG), next to but outside of the AL (Ernst et al. 1977; Ignell et al. 2000; Schachtner et al. 2005; Hofer et al. 2005). In the AL, olfactory information from the OSNs, is processed by a complex network of local interneurons (Christensen et al. 1993; Schachtner et al. 2005; Chou et al. 2010; Seki et al. 2010). The processed odor information is further relayed by distinct antennal lobe tracts (ALTs) formed by the projection neurons (PNs) to the mushroom body (MB) and the lateral horn (LH) (Schachtner et al. 2005; Galizia and Rössler 2010). The MBs are higher order integration centers for multiple processed sensory information and are responsible for odor discrimination, associative learning, as well as memory storage and retrieval. The LHs receive odor input directly from the ALs or indirectly from the MBs, decode the quality and intensity of the information, and finally trigger immediate odor-driven behavior (Belle and Heisenberg 1994; Connolly et al. 1996; Heimbeck et al. 2001; Wang et al. 2003; Yamagata et al. 2007; Jefferis et al. 2007; Strutz et al. 2014).

Despite the evolutionary success and ecological as well as economic importance of beetles (Morris 2007; Hunt et al. 2007), little is known on the neuroanatomy, genetics, or biochemistry of their olfactory pathway. Within the Coleoptera, the red

flour beetle *T. castaneum* has become the prime model organism for developmental biology and pest management (Brown et al. 2009). With its fully annotated genome (Wang et al. 2007; Richards et al. 2008; Kim et al. 2010) and the multiple powerful genetic tools – such as systemic RNA interference (Bucher et al. 2002; Tomoyasu and Denell 2004), insertional mutagenesis (Lorenzen et al. 2003) and transgene-based misexpression systems (Schinko et al. 2010; Schinko et al. 2012) – *T. castaneum* represents an eligible "beetle model organism" for olfaction. In the current study, we present a substantial overview of the olfactory pathway in *T. castaneum*, covering the morphology of the sensilla and the antenna, all major neuropils including AL, MB, LH, LG and the gnathal olfactory center (GOC), a previously undescribed glomerularly organized neuropil in the GNG. Additional support for the importance of the gnathal input into olfaction is provided by genome-wide expression analysis of gene families involved in chemoreception (e.g. ORs, GRs, IRs, SMNPs, and ODEs) and CSPs and OBPs, which have recently been published (Dippel et al. 2014).

Results

The Antenna of *Tribolium castaneum*

In order to determine the distribution and number of CSNs, we used immunohistochemistry (IHC) with a cross-reactive antibody against Orco, fluorescent *in situ* hybridization with an *Orco*-specific probe, and a transgenic line, *EF1-B-DsRed*, that labels almost all and only CSNs in the adult antenna (see Material and Methods for detailed characterization). Moreover, we generated an *Orco-Gal4* line that partially covers the Orco pattern, which we refer to as "partial Orco-Gal4 line" (see Material and Methods for detailed characterization). These different approaches unequivocally confirm that CSNs are restricted to the distal three segments (9-11) that form the enlarged club of the antenna (Roth and Willis 1951) (Figure 1A, Figure 1 – figure supplement 1, 2). To improve on previous data in respect to the characterization, location, and exact number of antennal sensilla (Roth and Willis 1951), we used in addition to the confocal laser-scanning microscopy (CLSM) approaches also scanning electron microscopy (SEM) (Figure 1B-H, Figure 2A-G). This morphologically verified the presence of chemosensory sensilla exclusively on the three club segments (Roth and Willis 1951), with the highest number and diversity on the apical part of the terminal segment 11 (Figure 1B-B'', Figure 1 – figure supplement 3).

Four mechanoreceptive and three chemoreceptive sensilla types could be confirmed by the combination of these techniques (Figure 1B-B'') and the respective number of contained CSNs was identified. The mechanoreceptive sensilla include the spatulate bristles (SpaB; Figure 1D-D''''), the mechanosensilla trichoidea (mSTri; Figure 1E-E''''), the sensilla campaniformes (SCam; Figure 1B''), and the sensilla chaetica (SCha; Figure 1C-C'''), which are the most dominant sensilla type present on the lateral sites of all eleven segments (Figure 1A). The chemoreceptive sensilla subdivide into chemo-sensilla trichoidea (cSTri, Figure 1F-F'''), sensilla basiconica (SBas; Figure 1G-G''''), and sensilla coeloconica (SCoe, Figure 1H-H'''). In respect to chemoreceptive sensilla, segments 9 and 10 carry mostly SBas (about 15) arranged in an axial ring at the apical edge of each segment (Figure 2F, G) and two SCoe (Figure 2F', G'), whereas the terminal segment 11 harbors SBas (about 25), some SCoe (about 7), and many cSTri (about 87) (Figure 1B-B''). Detailed analysis of number and distribution of the different sensilla types in males and females revealed no sexual dimorphism (Figure 1 – figure supplement 3).

The number of CSNs per antenna was estimated based on the number of CSNs per sensillum or prong and the number of the respective sensilla per antenna. cSTri contain typically one Orco-ir OSN (Figure 1 – figure supplement 3I, 4A). This type of sensilla is known for its pheromone receiving abilities in Lepidoptera (Vogt and Riddiford 1981; Keil 1989; Almaas and Mustaparta 1990) and had been described as olfactory sensilla in *D. melanogaster* (Stocker 2001) and *Culex quinquefasciatus* (Hill et al. 2009). SBas of *T. castaneum* consist of up to five prongs (Figure 2A-E) similar to other Tenebrionidae (Roth and Willis 1951; Alabi et al. 2013). Each prong harbors about six CSNs (Figure 1 – figure supplement 3I) – the

same number as in *Tenebrio molitor* (Harbach and Larsen 1977). Of them four to five can be considered olfactory based on Orco-ir (Figure 1 – figure supplement 4B). Findings in *Tribolium brevicornis* (Alabi et al. 2013) suggest an additional gustatory function of SBas, leading to the conclusion that the SBas are bimodal chemosensilla. Because of this constant number of CSNs per prong and the shared lymphatic space (Figure 1G-G''), we propose that multiple pronged SBas are derived from a fusion of single sensilla. Nonetheless, we refer to and count multiple pronged SBas as a single sensillum independent of the number of prongs. SCoe contain three CSNs (Figure 1 – figure supplement 3I) without Orco-ir (Figure 1 – figure supplement 4C). The SCoe in *T. castaneum* might therefore harbor IRs as shown in *D. melanogaster* (Shanbhag et al. 1999; Benton et al. 2009). Altogether, we found on each antenna about 100 prongs of SBas with six CSNs each, 87 cSTri with one CSN), and eleven SCoe with about three CSNs (Figure 1 – figure supplement 3). This leads to a total number of about 720 CSNs per antenna of *T. castaneum*.

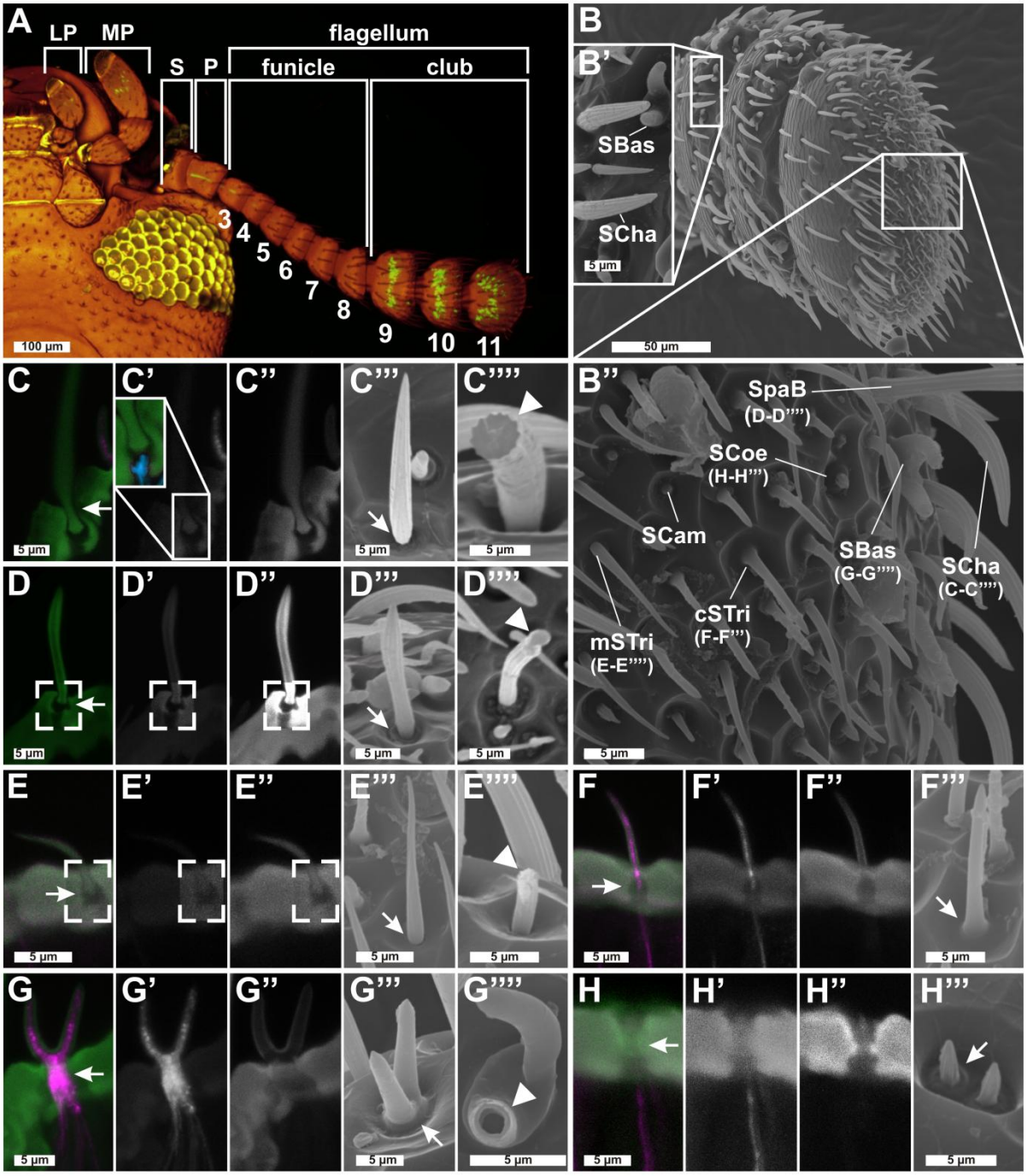

Figure 1. Sensilla types and their distribution on the antennae of *T. castaneum* I. (A) In *T. castaneum*, chemosensory sensilla are restricted to the distal three segments 9-11 (club) of the antenna and the last segment of the labial (LP) and maxillary palp (MP). Voltex projection of a confocal laser-scanning microscopic (CSLM) image stack of the ventral side of the head of the partial *Orco-Gal4/UAS*-tGFP line (tGFP reporter signal, green; auto-fluorescence of the cuticle, brownish). The antenna is composed of scape (S), pedicel (P), and flagellum that is subdivided into funicle and club. Reporter expression labeled about half of the olfactory sensory neurons (see material and methods; signal in the compound eye is due to auto-fluorescence). **(B-B'')** Scanning electron microscopic (SEM) image of the club segments of the antenna with close up of segment 9 **(B')** and segment 11 **(B'')**, showing all sensilla types: mechanoreceptive: sensilla chaetica (SCha; **C-C''''**), sensilla campaniformes (SCam), spatulate bristle (SpaB; **D-D''''**), and mechanosensilla trichoidea (mSTri; **E-E''''**); chemoreceptive: chemo sensilla trichoidea (cSTri; **F-F'''**), sensilla basiconica (SBas; **G-G''''**), and sensilla coeloconica (SCoe; **H-H'''**). SCam are small, smooth, and dome shaped sensilla and restricted to segment 11 (Figure 1 – figure supplement 3A). **(C-C'''')** SCha – previously described as spines (Roth and Willis 1951) – are longitudinally corrugated, connected to a neuron at the socket (**C'**; blue), jointed (**C'''**; arrow), and solid (**C''''**; arrowhead). **(D-D'''')** SpaB – in *Tribolium brevicornis* also called sensilla squamiformium (Alabi et al. 2013) – resemble modified SCha (Harbach and Larsen 1977) with a slightly thicker tip that are restricted to segment 11 (Figure 1 – figure supplement 3B). **(E-E'''')** mSTri are structurally similar to SCha but have a smaller more hair like appearance. Non-olfactory STri have already been described in other species (Altner 1977; Missbach et al. 2014). We identified about 37 mSTri on the apical site of segment 11 and four in the lateral corners of segments 9 and 10 (Figures 2F, F', 2G, G', and Figure 1 – figure supplement 3C, H). **(F-F'''')** cSTri are hair like structures with a rounded tip and a smooth transition of the base and restricted to segment 11 (Figure 1 – figure supplement 3D). **(G-G'''')** SBas are smooth-surfaced pegs with rounded tips and a smooth transition at the base (**G'''**; arrow), arranged in an axial ring (**B-B''**, Figures 2F, G) at the distal margins of all three club segments. **(H-H'''')** SCoe are short, corrugated, and their transition into the antennal cuticle shows a typical elevation **(B'', H''')**. Previously they were described as "minute spicule-like sensilla trichoidea" (Roth and Willis 1951). They are relatively rare (Figure 1 – figure supplement 3E) and located at the apical side of segment 11 and in the lateral corner of segments 9 and 10 (Figure 2F', G'). **(C-H, C'-H', C''-H'')** CLSM, maximum intensity projections of different sensilla, **(C-H)** overlays of antibody enhanced DsRed reporter signal (*EF1-B*-DsRed) in magenta **(C'-H')** and cuticle (green, auto-fluorescence at about 560 nm, **C''-H''**). All chemoreceptive sensilla **(F-G, F'-H')** house dendritic branches of chemosensory neurons (CSNs) labeled by DsRed. Close up in **C'** shows a non-CSN fiber entering only the base of a SCha labeled with phalloidin (blue). CLSM analysis revealed joint like structures at the base of mechanoreceptive sensilla **(C-E, C''-E'')**. **(C'''-H''')** SEM analysis of different sensilla revealed that only the mechanoreceptive sensilla **(C'''-E''')** show a small gap at their base (arrow). Chemoreceptive sensilla **(F'''-H''')** show a more smooth transition into the cuticle of the segment (arrow). **(C''''-G'''')** SEM scans of fractured sensilla. All mechanoreceptive sensilla **(C''''-E'''')** are solid cuticular structures; in contrast, chemoreceptive SBas **(G'''')** appear hollow.

Anatomy of the olfactory pathway in the red flour beetle brain

Antennal projections. To get an impression about the innervation pattern of chemosensory neuropils we performed antennal and palpal backfills. Backfills via the antennal nerve labeled the ipsilateral AL (Figure 3A, Figure 3 – figure supplement 1, 2), the antennal mechanosensory and motor center (AMMC) (Figure 3B), as well as a distinct area in the GNG (Figure 3C While this ipsilateral resctriction is common in many insects (Schachtner et al. 2005), it is in contrast to *D. melanogaster* and *Ceratitis capitata,* where the majority of OSNs innervate the ipsi- and contralateral side (Stocker 2001; Solari et al. 2016). The antennal backfills labeled all AL glomeruli except one, which is the only glomerulus labeled by backfills of the maxillary palp via the GNG (Figure 3A, Figure 3 – figure supplement 1). This resembles the situation in Lepidoptera, where CO_2 responsive CSNs from the palp project into a single AL glomerulus devoid of antennal innervation (Kent et al. 1986). The descending antennal projections into the GNG (Figure 3C) are not labeled in the partial *Orco*-Gal4/*UAS*-DsRed line and might therefore be from gustatory or mechanosensory neurons, as described in *P. americana* and *L. migratoria* (Bräunig et al. 1983; Nishino et al. 2005).

Antennal lobe. For the AL of freshly eclosed adults about 70 distinguishable olfactory glomeruli have been previously described using a synapsin antibody (Dreyer et al. 2010). To evaluate the glomeruli number in ALs of beetles, seven days after adult eclosion, we improved the analysis by deconvolution as well as using an additional antiserum against tachykinin related peptides (TKRP), which distinctly labels also densely-packed

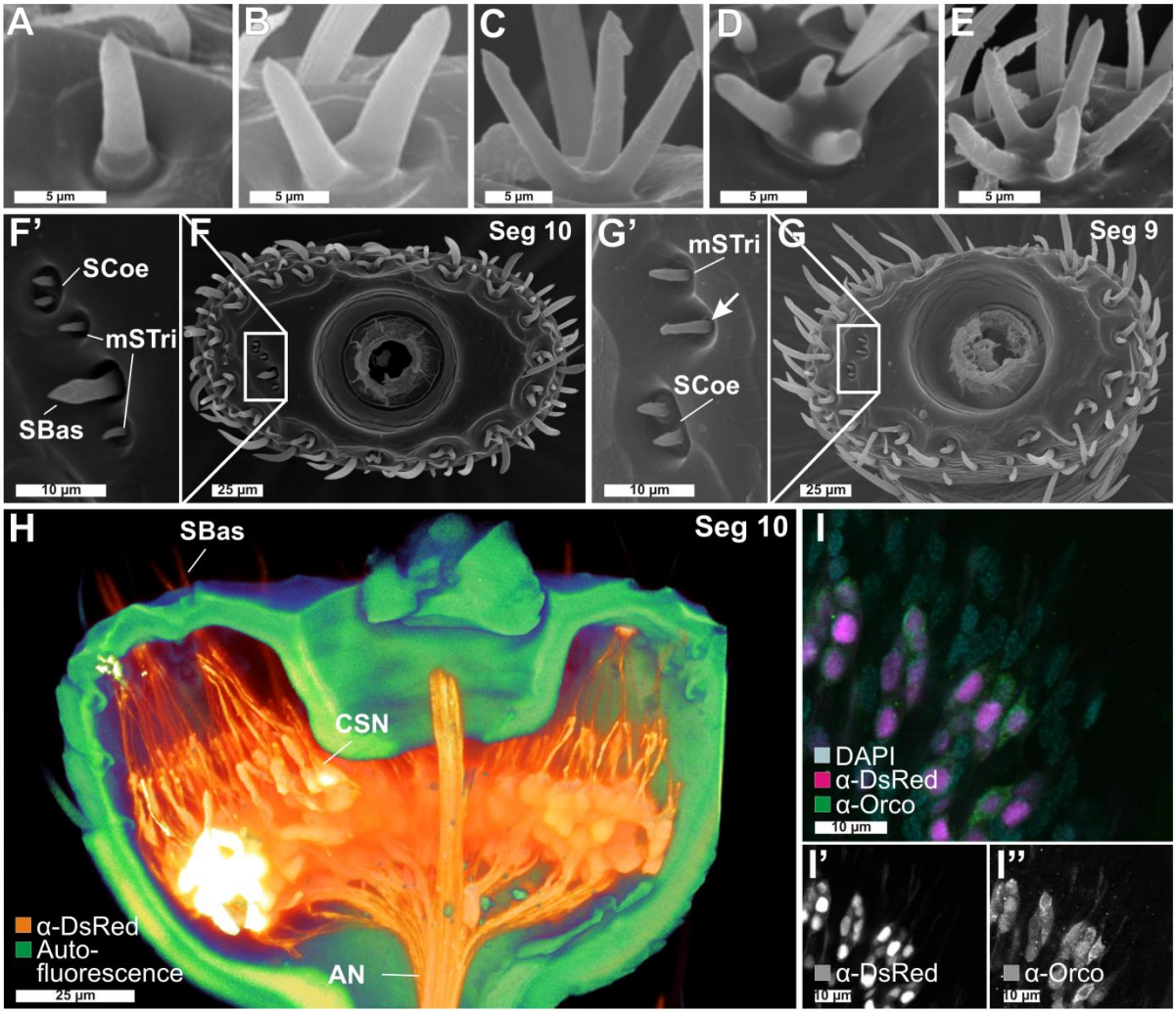

Figure 2. Sensilla types and their distribution on the antennae of *T. castaneum* II. (A-E) Scanning electron microscopic (SEM) images of sensilla basiconica (SBas) with one to five prongs. **(F and F')** SEM image of the 10th segment of the antenna with close up of the lateral corner (F') containing sensilla coeloconica (SCoe), sensilla basiconica (SBas), and mechano sensilla trichoidea (mSTri). **(G and G')** SEM image of the 9th segment with close up of the lateral corner (G') showing SCoe and mSTri. **(H)** Voltex projection based on a confocal laser-scanning microscopic (CLSM) image stack of the 10th segment from the *EF1-B*-DsRed line displaying chemosensory neurons (CSNs, orange) and auto-fluorescence of the cuticle (green). The dendrites of the CSNs converge into the SBas (in average six per prong), while the axons unite at the center of the segment and join the antennal nerve (AN). **(I-I'')** Overlay of the signals of the DsRed reporter (magenta, I') and the Orco antibody (green, I'') together with DAPI staining (light blue) in the *EF1-B*-DsRed line demonstrate a high level of colocalization between DsRed and Orco in segment 9 and 10, but not in 11, were some DsRed-ir CSNs are spared (compare with Figure 1 – figure supplement 2).

glomeruli (Binzer et al. 2014). This more advanced analysis resulted in the 3D-reconstruction of about 90 glomeruli per AL with no obvious sexual dimorphism (females: mean 89.2, SD = 4.9, n = 5; males: mean 89.4, SD, 7.6, n = 5).

Palpal projections into accessory olfactory centers. Whole mouthparts or maxillary palp backfills (Figure 3D, E) revealed – besides the already mentioned single AL glomerulus – innervation of three distinct neuropil areas: an unpaired glomerular organized neuropil in the GNG, the primary gustatory center also in the GNG (Miyazaki and Ito 2010), as well as an area nearby the AL, resembling the LG of hemimetabolous insects (Schachtner et al. 2005; Farris 2008). The unpaired neuropil located n-anterodorsal in the GNG consists of 30 to 40 glomeruli (Figure 3D, inset), which are all innervated from both sides of the mouthparts. This neuropil is also labeled by the partial *Orco*-Gal4/*UAS*-DsRed line (Figure 3F, Figure 3 – figure supplement 3), which indicates innervation by OSNs originating in the maxillary or labial palps (Figures 1A, 3F, 4A'', 4B'', Figure 1 –

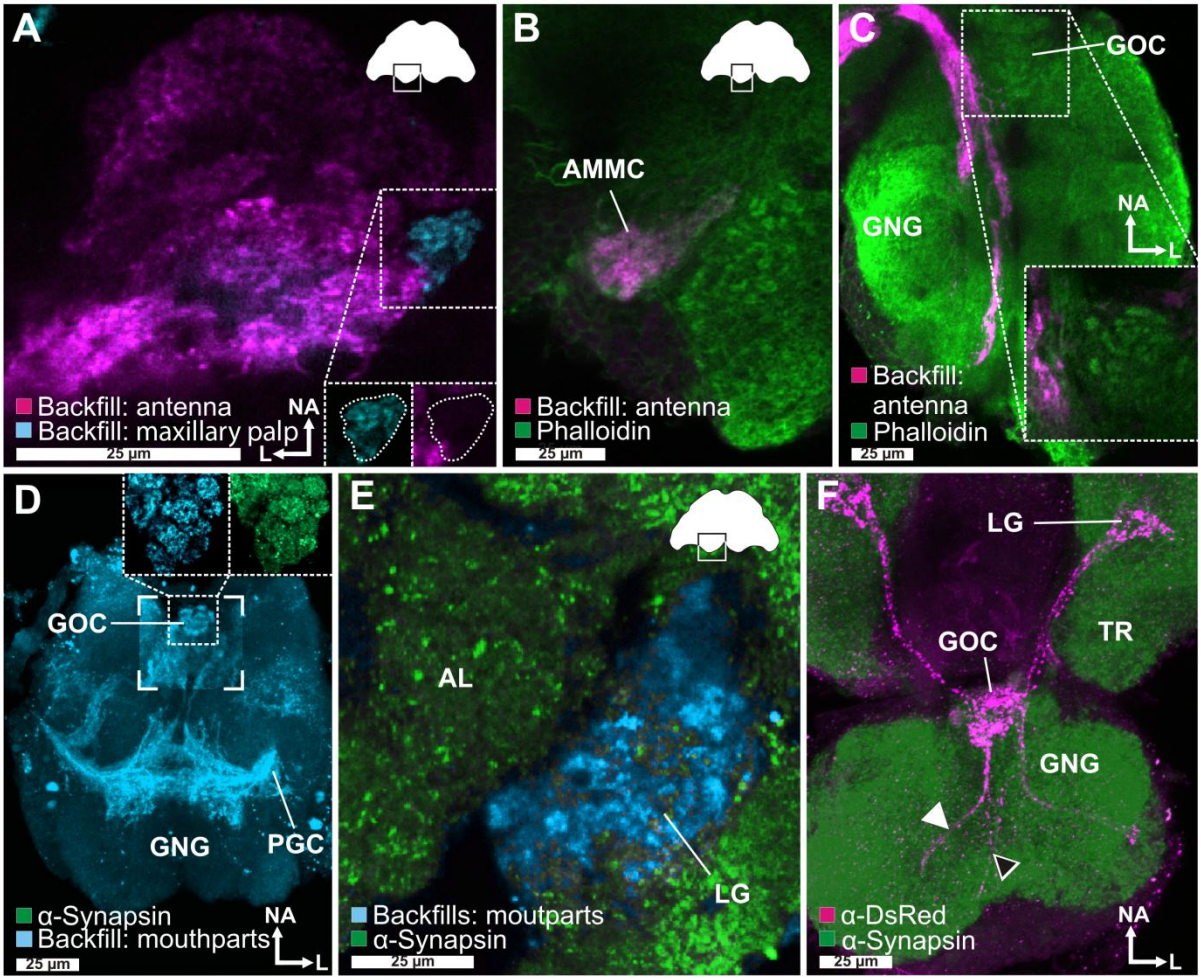

Figure 3. The central olfactory pathway of *T. castaneum*. (A) Backfill of one antenna (magenta) stains all glomeruli in the ipsilateral antenal lobe (AL) except one; this glomerulus is exclusively labeled by a backfill of a maxillary palp (cyan). **(B)** In addition to the AL glomeruli, backfilling (magenta) of one antenna labeled the ipsilateral antennal mechanosensory and motor center (AMMC), located n-dorsally to the AL, **(C)** as well as descending fibers to the gnathal ganglion (GNG). **(D)** Maximum intensity projection of the backfills of mouthparts (cyan) shows massive innervation of the GNG including the gnathal olfactory center (GOC) (magnifications in the inset) and the primary gustatory center (PGC). **(E)** Backfill of the mouthparts (cyan) revealed in the cerebral ganglion beside innervation of a single ipsilateral AL glomerulus also projections in the ipsilateral LG. **(F)** Reporter expression of the partial *Orco*-Gal4/*UAS*-DsRed line (magenta) revealed two paired input tracts (black and white arrowheads) from the maxillary (white arrowhead) and labial palps (black arrowhead), that converge in a medial and n-anterodorsally located glomerular area, the GOC and ascend to a microglomerularly organized area, the lobus glomerulatus (LG) see also Figure 3 - figure supplement 3). Orientation bars in (A) also apply for B and E. N refers to the neuroaxis; A, anterior; L, lateral.

figure supplement 5) that project via two tracts into the GNG. This neuropil therefore represents an olfactory processing center in the GNG that has to our knowledge never been described before and we term “gnathal olfactory center” (GOC). Some of the fibers labeled by the palpal backfills, as well as the partial *Orco*-Gal4/*UAS*-DsRed line pass through the GOC, ascend via the neck connectives and terminate ipsilaterally in an area medioventral to the AL (Figure 3D), resembling the LG, which to date had only been described in hemimetabolous insects (Schachtner et al. 2005; Farris 2008). Since the position, innervation, and glomerularly organized structure of this paired neuropil in *T. castaneum* is similar to the LG in cockroach, locust, and silverfish, (Ernst et al. 1977; Ignell et al. 2000; Schachtner et al. 2005; Hofer et al. 2005) we refer to it as LG. In summary, our data suggest that in *T. castaneum* odor information from the antennae and the mouthparts are processed separately. It appears that OSNs from the mouthparts do not project into the AL but into the GOC and the LG.

Projection neurons. Dye injections into the AL of adult *T. castaneum* revealed three ALTs formed by the PNs (Figure 5), exclusively in the ipsilateral hemisphere. The most prominent tract, the medial antennal lobe tract (mALT) connects the AL with the CA of the MB and the LH. The mediolateral antennal lobe tract (mlALT) runs towards the spur of the MB (Figure 5) and further projects to the LH. The lateral antennal lobe tract (lALT) projects directly to the most posterior part of the LH. We could not observe any obvious direct projections of the mlALT and the lALT to the CA, as described for other holometabolous insects (Galizia and Rössler 2010). Previously only the mALT had been clearly identified in Coleoptera and the existence of a mlALT had only been presumed (Galizia and Rössler 2010). Our results indicate that three ALTs are a common feature among most holometabolous insects, including beetles.

Mushroom body. The detailed architecture of the MB of *T. castaneum* is described in (Binzer et al. 2014). The CA is innervated by the mALT (Figure 5) and microglomerularly organized as indicated by phalloidin or synapsin antibody stainings (Figure 5, inset). This is similar to several insects including *Apis mellifera* (Frambach and Schürmann 2004; Groh et al. 2012) and *D. melanogaster* (Leiss et al. 2009; Caron et al. 2013) and suggests a comparable wiring with the PNs. The KCs were identified in DAPI (4',6-diamidino-2-phenylindole) stainings based on their smaller and brighter stained nuclei (Binzer et al. 2014). The number of about 2700 KCs was determined by interpolation of volumetric data as well as by counting of the stained nuclei using MorphoGraphX (Reuille et al. 2015). Both procedures resulted in comparable numbers with the interpolation of 13 CAs from seven animals estimating about 2800 KCs (2795; SD: 214) and the counting of nine CAs from five specimen indicating approximately 2600 KCs (2613; SD 204) per MB.

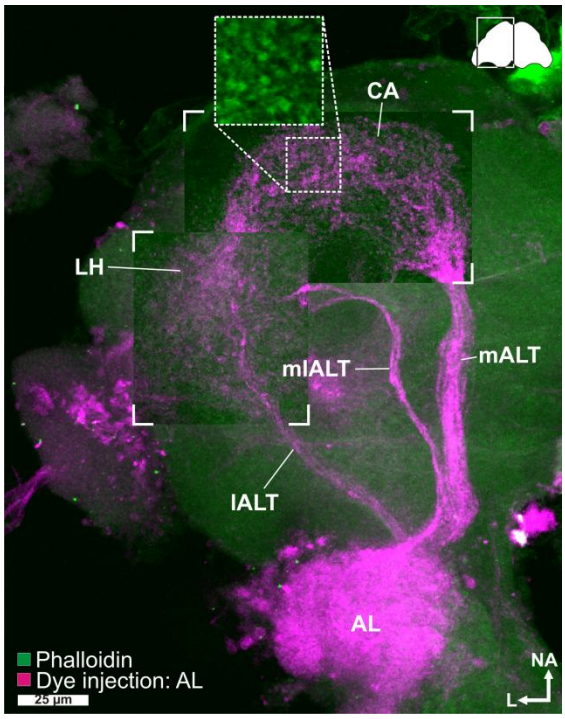

Figure 5. Antennal lobe tracts. Maximum intensity projection of a confocal laser-scanning microscopic image stack after dye injection into the antennal lobe (AL, magenta) revealed three antennal lobe tracts (ALT), the medial (mALT), mediolateral (mlALT), and the lateral antennal lobe tract (lALT), as well as the calyx (CA) and the lateral Horn (LH). In the CA, most fibers from the mALT forming microglomeruli (inset obtained from another preparation). The staining in the optical lobe is an artifact caused by diffusion of the dye during application. Phalloidin counterstaining in green.

Genome-wide expression analysis of genes involved in chemoreception in *T. castaneum*

The fully sequenced genome of *T. castaneum* (Wang et al. 2007; Richards et al. 2008; Kim et al. 2010) led to the annotation of the major gene families involved in chemoreception. Based on genome data and computational gene predictions, the OBPs (Foret and Maleszka 2006), CSPs (Forêt et al. 2007), IRs (Croset et al. 2010), GRs (Richards et al. 2008), ORs (Engsontia et al. 2008), and SNMPs (Nichols and Vogt 2008; Vogt et al. 2009) were annotated, but only for the ORs a RT-PCR-based expression analysis was performed (Engsontia et al. 2008). To validate or correct the predicted gene models of these gene family members and to determine their tissue-specific expression, we performed transcriptome analyses of adult male and female antennae, heads (without antennae, but including mouthparts), mouthparts (the part of the head capsule, anterior to the antennal bases), legs, and bodies (without legs and head. In addition, we identified potential ODEs, as well as orthologs from further genes described to be involved in *D. melanogaster* olfaction. The detailed analysis of the OBPs and CSPs has already been published (Dippel et al. 2014) and revealed that

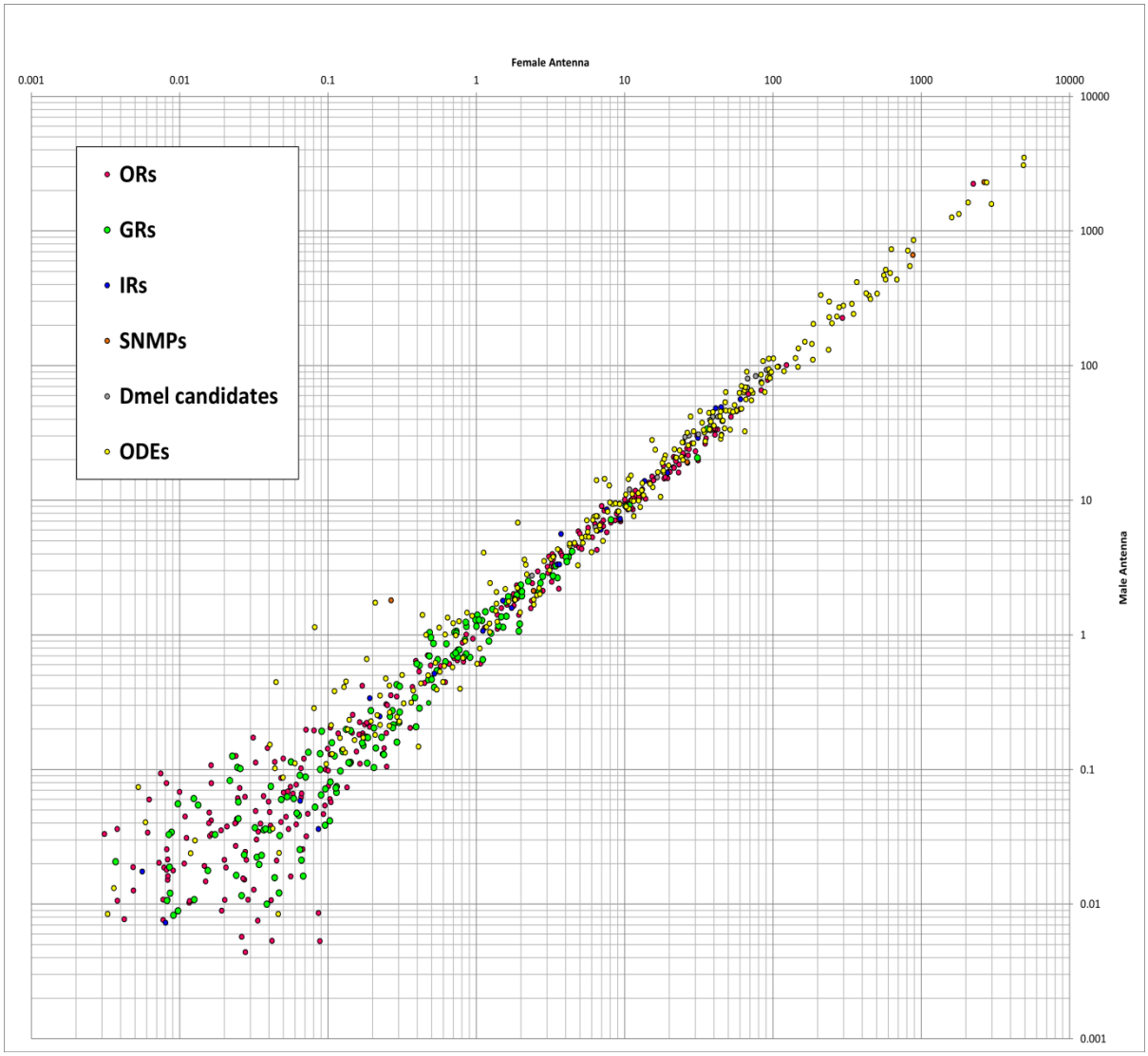

Figure 6. Comparison of expression levels in male and female antenna. Comparison of expression levels of odorant receptors (ORs, magenta), gustatory receptors (GRs, green), IRs (ionotropic glutamate-like receptors, blue), SNMPs (sensory neuron membrane proteins, orange), orthologous of candidates obtained from *D. melanogaster* (*Dmel* candidates, grey) and potential ODEs (odorant degrading enzymes, yellow) in male and female antennae, average values based on two male and three female antennal samples. Scatter plot of the RPKM values.

the majority of the classic OBPs and antenna binding proteins II (ABPII) seem to be involved in chemoreception while only a few of the C-OBPs and CSPs are enriched in antenna or mouthparts. The following results are based on this same set of transcriptome data (GEO accession number: GSE63162; http://www.ncbi.nlm.nih.gov/geo/query/acc.cgi?acc=GSE63162). Similar to OBPs and CSPs (Dippel et al. 2014), also for the genes presented here, no significant differences on the expression level between male and female antenna samples were identified (Figure 6). Therefore, the female and male antenna samples can serve as biological replicates and indicate that reads above 0.1 RPKM are reproducible (Figure 6). However, in order to minimize the rate of potential false positives in our description, we only considered genes with RPKM≥0.5 as expressed. We are aware that this might lead to an underestimation of the expressed gene numbers for each class of genes. Since it is impossible to determine the exact amount of genes that are functionally involved in chemoreception only based on transcriptomic expression analyses, we always present two values for expressed genes, one based on RPKM≥0.5 and the other defined by statistical analysis as significantly enriched over body. All raw values and the re-annotated gene models are summarized in Supplemental Table 1.

Tissue-specific expression of ionotropic glutamate-like receptors. The RNAseq based revision of the 23 previously annotated IRs (Croset et al. 2010) confirmed the sequences of three ORFs, 17 had to be modified, two were incompletely covered by reads, and for a single one no expression was detected (color coded in Supplemental Table 1, column B). In antennae, 16 IRs them being significantly enriched compared to body (Figure 7, Figure 7 – figure supplement 1). In the mouthparts, five IRs are expressed, two are significantly enriched.

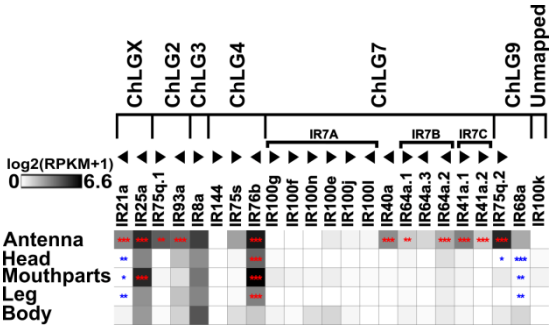

Figure 7. Expression of *T. castaneum*s IRs. Heatmap showing the expression level of the 23 ionotropic glutamate-like receptors (IRs) as log2[RPKM+1] value in different tissues (adult antennae, head (missing antennae but including mouthparts), mouthparts, legs, body). The candidates are ordered according to their chromosomal localization (figure supplement 2), horizontal brackets above indicate clustering in the genome, the arrowheads represent the orientation of the open reading frame. The expression levels are represented by a greyscale with highest shown expression levels labeled black. The asterisks mark statistically significantly differentially expressed genes compared to body. The red asterisks represent up- and the blue down-regulation (p-values adjusted are * < 0.05; ** < 0.01; *** < 0.001).

Comparing expression profiles of the IRs from *T. castaneum*, *D. melanogaster*, and *Anopheles gambiae* confirmed the antennal specific expression, as well as the high degree of phylogenetic conservation of the "antennal IRs" (Figure 8, Figure 8 – figure supplement 1; highlighted in yellow) as proposed (Croset et al. 2010). In contrast, the "divergent IRs" are non-antennal specifically expressed and are highly radiated within species clades as previously shown or predicted (Croset et al. 2010). *T. castaneum* has a lower number of IRs compared to *D. melanogaster* and *An. gambiae*, due to lesser expansions of "divergent IRs", but maintains the basic repertoire of "antennal IRs" (Figure 8; highlighted in yellow). The homologs of IR25a, IR93a, and IR40a which are necessary for humidity perception in *D. melanogasters* (Enjin et al. 2016) are significantly enriched in antennae. IR40a is exclusively expressed in antennae, which correlates with the essential role of antennae in *T. castaneum* hygro-perception (Roth and Willis 1951). The homolog of the high sensitive salt receptor IR76b (Zhang et al. 2013) is significantly enriched in antennae, mouthparts, and legs, while the co-receptors IR8a and IR25a (Rytz et al. 2013) are highly expressed in all tissues of *T. castaneum* (Figure 7).

Tissue-specific expression of gustatory receptors. Of the 220 previously annotated GRs (Richards et al. 2008), only 207 genes had available gene models (Wang et al. 2007; Kim et al. 2010). Our transcriptome analysis verified the ORFs of 58 GRs, showed slight differences for 20 GRs, but did not or only incompletely cover 129 GRs (Supplemental Table 1; column B). In the antennae 62 GRs are expressed, with 34 being significantly enriched and 10 being antennal-specific. Of the 69 mouthpart-expressed GRs, 36 are significantly enriched and 19 exclusive. 17 GRs are significantly enriched in both antenna and mouthparts. In legs, 18 GRs are expressed with three being significantly enriched (Figure 9, Figure 9 – figure supplement 1).

The phylogenetic comparison of the GRs in *T. castaneum*, *D. melanogaster*, and *An. gambiae* (Figure 10, Figure 10 – figure supplement 1) confirmed that only the CO_2 receptors (highlighted in orange) are highly conserved (Robertson and Kent 2009). The other GRs seem to have undergone independent radiations during the transition to *T. castaneum*: E.g. the sugar receptor-related branch (highlighted in light yellow) contains 16 genes (Kent and Robertson 2009), twice the number compared to the two chosen dipterans. In addition, the single fructose receptor (highlighted in grey) found in *D. melanogaster* and *An. gambiae* is represented by eight homologs in *T. castaneum*. The remaining 180 GRs belong to several *T. castaneum*-specific expansion groups. Specific orthologs to the known bitter receptors of *D. melanogaster* (Weiss et al. 2011) as well as to the thermo-sensitive *Dmel*GR28bD (Ni et al. 2013) cannot be predicted based on our phylogenetic analysis.

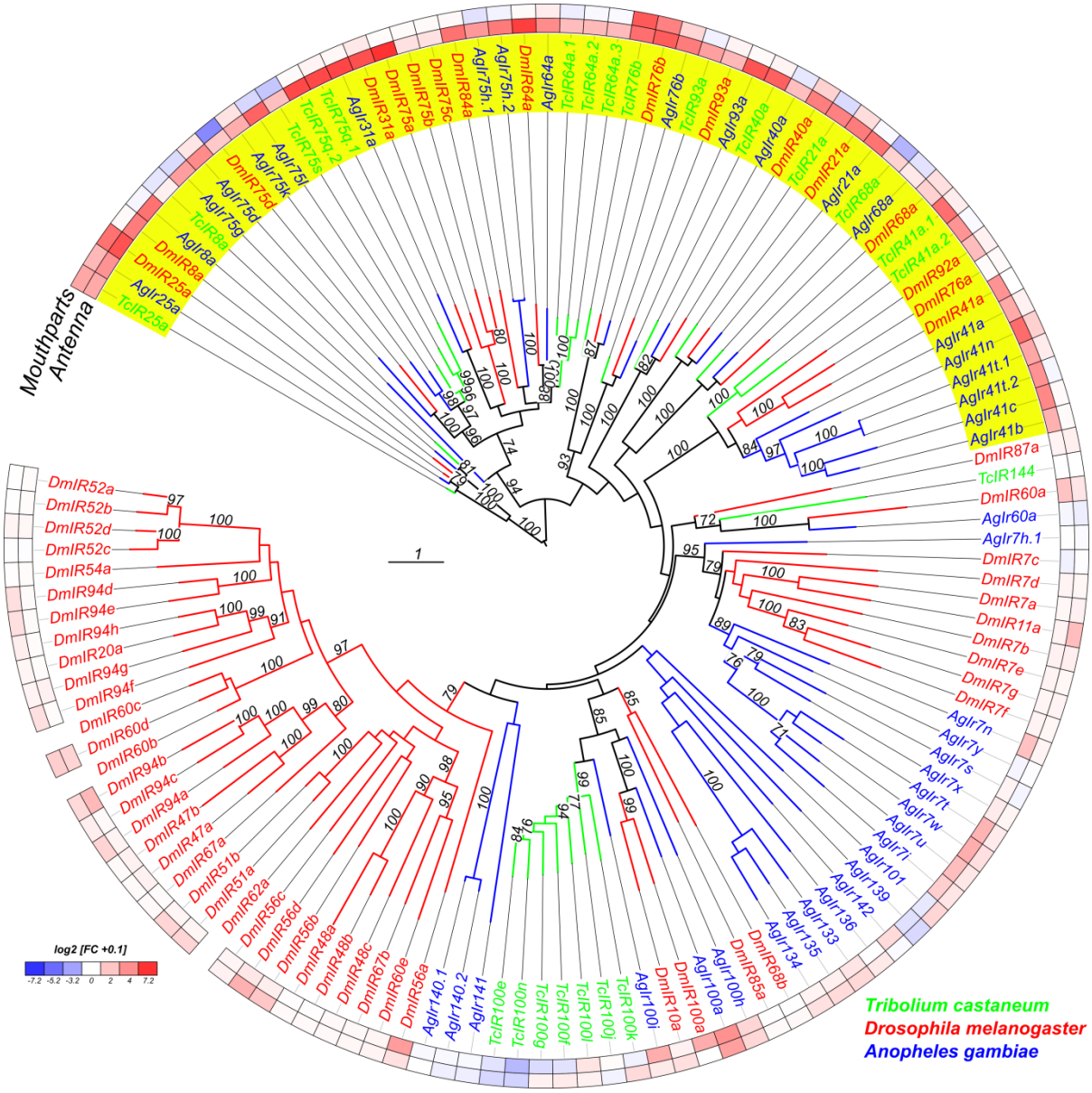

Figure 8. Phylogenetic tree of IRs. Based on protein sequences from *T. castaneum* (green branches), *D. melanogaster* (red branches), and *An. gambiae* (blue branches). The tree was rooted using the IR8/IR25 clade, according to (Croset et al. 2010). Robustness of the tree topology was evaluated by 100 rapid bootstrap replications. Outer rings represent the expression in antennae and "mouthparts" (*T. castaneum*: palps, mandible, labrum and labium; *D. melanogaster*: palp and proboscis; *An. gambiae*: maxillary palp) as log2 fold change compared to body corresponding to the scale in the left lower corner. The scale bars within the trees represent one amino acid substitution per site. Antennal IRs are highlighted in yellow. Basically the same figure is available with absolute values instead of fold changes to get an impression of the tissue-specific abundance of the transcripts as figure supplement 1.

Similar to other insects (Robertson and Wanner 2006; Wanner and Robertson 2008; Robertson and Kent 2009), *T. castaneum* has three CO_2 receptors (*Tcas*GR1, *Tcas*GR2 and *Tcas*GR3), while *D. melanogaster* has only two that form functional heteromers (Jones et al. 2007; Kwon et al. 2007). In *T. castaneum*, the expression of the CO_2 receptors is not restricted to one of the chemosensory organs with *Tcas*GR2 and *Tcas*GR3 being significantly enriched in antennae but also being expressed together with *Tcas*GR1 in the mouthparts (Figure 9; highlighted in orange). This dual input is in contrast to but combines both, the expression of the three *An. gambiae* CO_2 receptors that are restricted to the maxillary palps (Lu et al. 2007; Pitts et al. 2011), as well as the two *D. melanogaster* CO_2 receptors that are mainly expressed in the antennae (Jones et al. 2007; Kwon et al. 2007; Hartl et al. 2011).

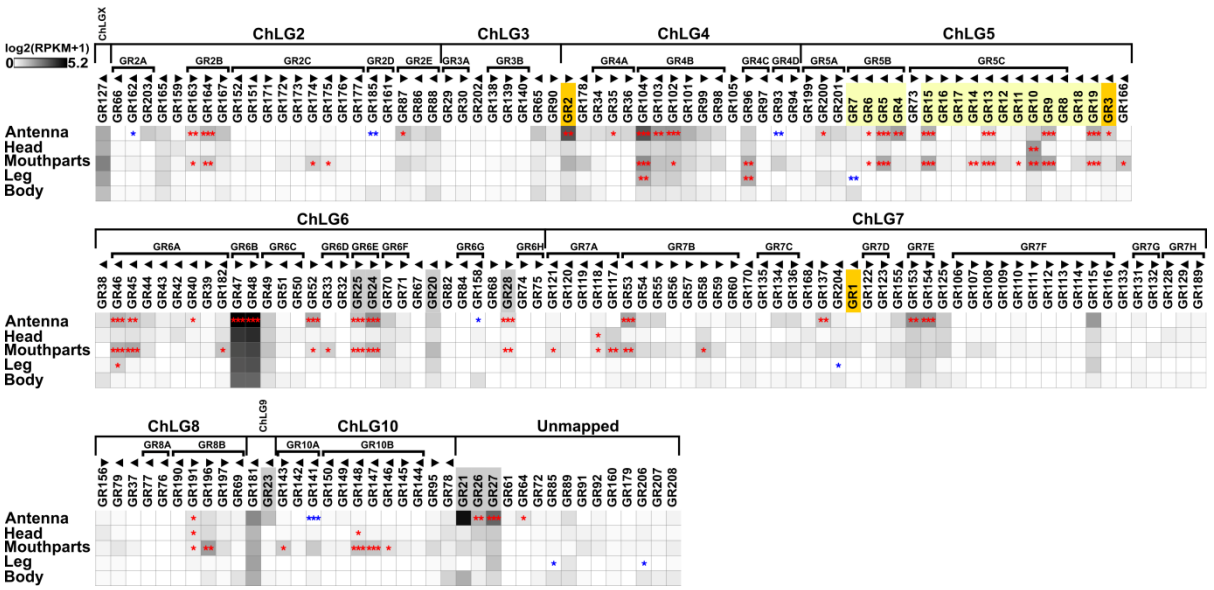

Figure 9. Expression of *T. castaneum*s GRs. Heatmap showing the expression level of the 207 analyzed gustatory receptors (GRs) as log2[RPKM+1] value in different tissues (adult antennae, head (missing antennae but including mouthparts), mouthparts, legs, body). The candidates are ordered according to their chromosomal localization (figure supplement 2), horizontal brackets above indicate clustering in the genome, the arrowheads represent the orientation of the open reading frame. The expression levels are represented by a greyscale with highest shown expression levels labeled black. The asterisks mark statistically significantly differentially expressed genes compared to body. The red asterisks represent up- and the blue down-regulation (p-values adjusted are * < 0.05; ** < 0.01; *** < 0.001). CO_2 receptors are highlighted in orange, fructose receptor related genes in grey and sugar receptors in yellow.

The presence of GRs on insect antenna had previously been postulated based on physiological response to sugars (Ramaswamy 1987; de Brito Sanchez et al. 2005; Alabi et al. 2013; Popescu et al. 2013) and was identified by antennal expression analysis (Dunipace et al. 2001; Robertson and Wanner 2006; Kwon et al. 2007; Pitts et al. 2011; Jacquin-Joly et al. 2012; Andersson et al. 2013). Our interspecies comparison (Figure 10) confirms the antennal enrichment of several GRs in the two analyzed dipterans. However, the high number of 34 significantly enriched GRs in the antenna of *T. castaneum* is unusual, but reflects the increased total number of GRs in this species. Interestingly, the GRs of *T. castaneum* are present in both, antenna and mouthparts at similar numbers and expression levels (Figure, Figure 9 – figure supplement 1).

Tissue-specific expression of odorant receptors. Of the 341 previously annotated OR sequences (Engsontia et al. 2008), we could re-analyze 337 based on our RNAseq data. This revision confirmed 97, 22 were re-annotated reviving eight previously indicated pseudogenes (Engsontia et al. 2008), namely *Tcas*OR2, *Tcas*OR18, *Tcas*OR19, *Tcas*OR22, *Tcas*OR85, *Tcas*OR99, *Tcas*OR104, and *Tcas*OR122. 219 genes were not or only partially covered by our transcriptome data (color coded in Supplemental Table1; column B). Over all samples, 170 ORs are expressed (Figure 11, Figure 11 - figure supplement 2). In antennae, 129 ORs are expressed, with 92 being significantly enriched and 99 exclusive. In the mouthparts, 49 ORs are expressed, with 28 being significantly enriched and 27 exclusive. In addition, 16 of the significantly mouthpart-enriched ORs are not enriched in the antenna (Figure 11). The expression of typical ORs in the mouthparts is consistent with the high expression of Orco in this tissue (Figure 1A, Figure 4) and with observations in other insect species (Vosshall and Stocker 2007; Lu et al. 2007; Pitts et al. 2011; Sparks et al. 2014). In legs, 10 ORs are expressed but only one, namely *Tcas*OR127, is statistically enriched (Figure 11– figure supplement 2).

The phylogenetic comparison of OR expression patterns in *T. castaneum, D. melanogaster* and *An. gambiae* (Figure 12, Figure 12 – figure supplement 1) revealed that the atypical odorant co-receptor Orco (in *T. castaneum* previously called *Tc*OR1 (Engsontia et al. 2008)) is the highest expressed OR in all tissues of all three species. In *T. castaneum*,

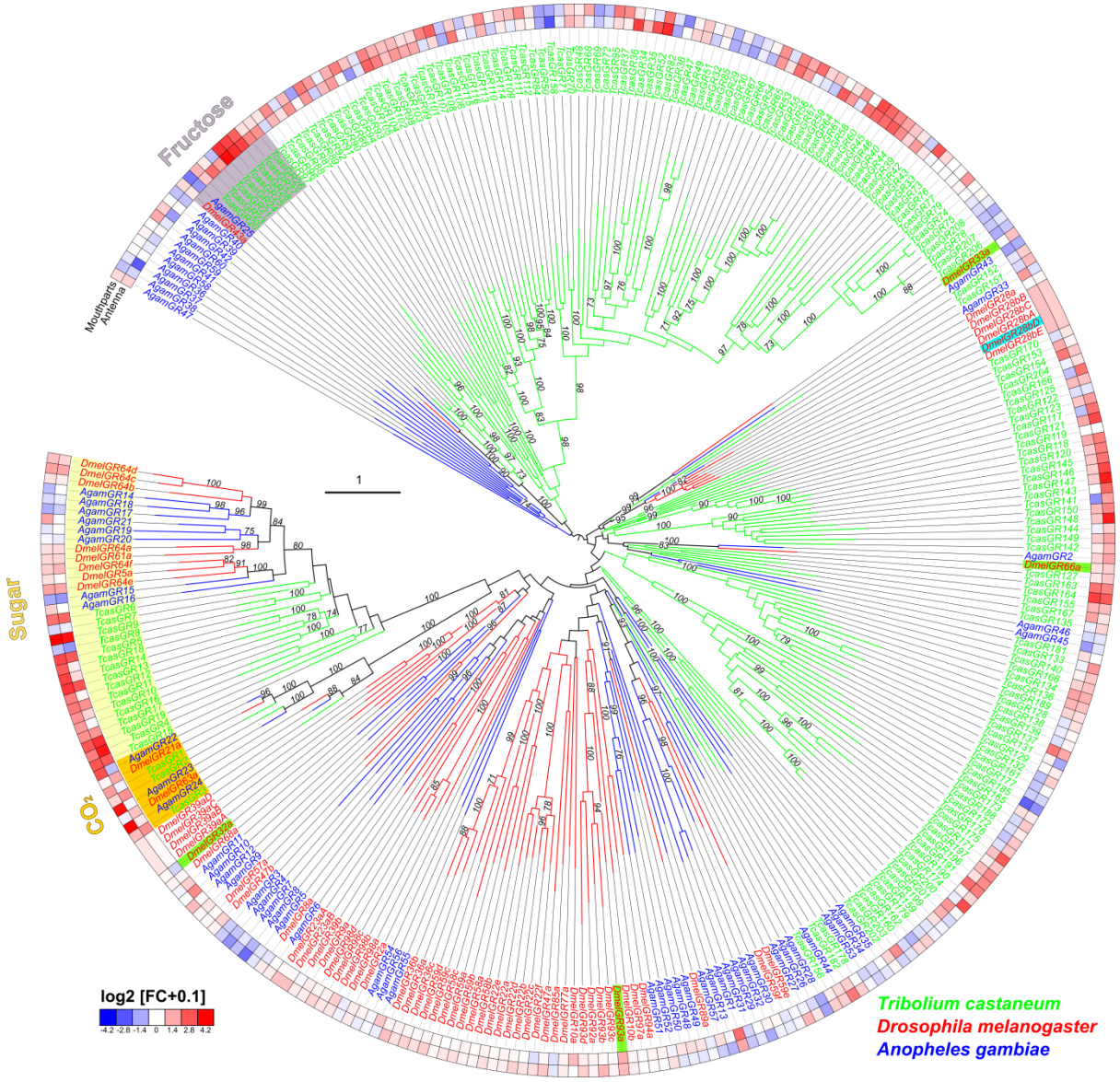

Figure 10. Phylogenetic tree of GRs. Mid-point rooted tree based on protein sequences from *T. castaneum* (green branches), *D. melanogaster* (red branches), and *An. gambiae* (blue branches). Robustness of the tree topology was evaluated by 100 rapid bootstrap replications. Outer rings represent the expression in antennae and "mouthparts" (*T. castaneum*: palps, mandible, labrum and labium; *D. melanogaster*: palp and proboscis; *An. gambiae*: maxillary palp) as log2 fold change compared to body corresponding to the scale in the left lower corner. The scale bars within the trees represent one amino acid substitution per site. Potential sugar receptors (highlighted in yellow), fructose receptors (highlighted in grey), and CO_2 receptors (highlighted in orange) are labeled. Known bitter receptors from *D. melanogaster* are highlighted in green, the thermos-sensitive GR28bD in light blue. Basically the same figure is available with absolute values instead of fold changes to get an impression of the tissue-specific abundance of the transcripts as figure supplement 1.

Orco is highest expressed in antenna, followed by mouthparts. Orco is the only OR of *T. castaneum* with clear orthologs in dipterans (Krieger 2003; Engsontia et al. 2008). The high expression levels, the distribution, and the evolutionary conservation of Orco are consistent with its ancestral origin (Missbach et al. 2014) and its outstanding role as chaperone and co-receptor, forming functional heteromers with all typical ORs (Jones et al. 2005; Vosshall and Hansson 2011).

The exceptional high number of typical ORs (Figure 12) in *T. castaneum* is the result of large gene radiations within the coleopteran and tenebrionid lineages (Andersson et al. 2013), which were previously subdivided into six expansion groups (Figure 12) (Engsontia et al. 2008). Expansion group 1, 2 and 3 are conserved in other coleopterans (Andersson et al. 2013) and are mainly expressed in antennae. The ORs of the expansion groups 4, 5, and 6 are highly derived, have no described

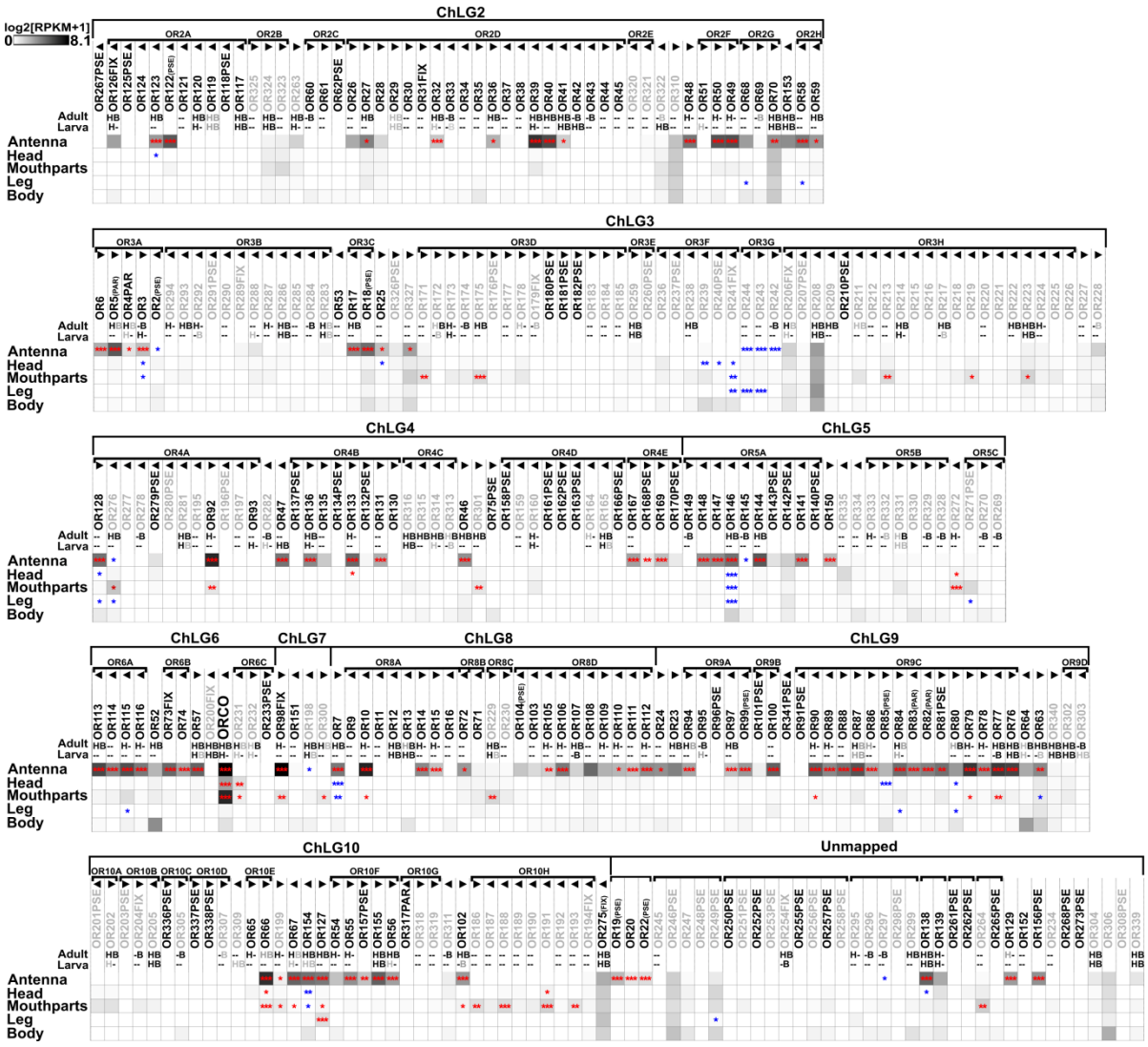

Figure 11. Expression of *T. castaneum*s ORs. Heatmap showing the expression levels of the 337 analyzed odorant receptors (OR) as log2[RPKM+1] with an maximum of 8.1, (*Orco* has a value of 11.1 in antenna) in different tissues (adult antennae, head (missing antennae but including mouthparts), mouthparts, legs, body). The candidates are ordered according to their chromosomal localization (figure supplement 3), horizontal brackets above indicate clustering in the genome, the arrowheads represent the orientation of the open reading frame. ORs that are member of the clades four, five and six (Engsontia et al. 2008) are written in grey letters. The line labeled with "Adult" and "Larva" referring to data from (Engsontia et al. 2008). The character H respectivly B indicates that the corresponding OR was detected in head or body cDNA samples by reverse PCR of the labeled developmental stage, a black letter indicates that a amplicon was detected in the majority of replicates, a grey letter means only in few replicates, - indicating no PCR product and no character means no data available. A comparison of the number of expressed genes is summarized in as figure supplement 3. The expression levels are represented by a greyscale with highest shown expression levels (3 RPKM or higher) labeled black to make sure that also low level expression is indentifyably presented. The asterisks mark statistically significantly differentially expressed genes compared to body. The red asterisks represent up- and the blue down-regulation (p-values adjusted are * < 0.05; ** < 0.01; *** < 0.001).

homologs in other insects, and their expression is unusually often mouthpart-enriched (Figure 11; grey lettering). This is consistent with the elaborated role of the mouthparts in *T. castaneum* olfaction. Specific orthologs to deorphanized ORs of *D. melanogaster* (Münch and Galizia 2016) cannot be predicted based on our phylogenetic analysis.

Identification and expression of potential odorant degrading enzymes. The genome of *T. castaneum* contains 15 aldehyde dehydrogenases (ALDHs) (Figure 13) with two of them being significantly enriched, but not exclusively expressed in antenna. We found four predicted genes encoding aldehyde oxidases (ALOXs) with one being highly enriched in antennae and mouthparts, which in contrast to

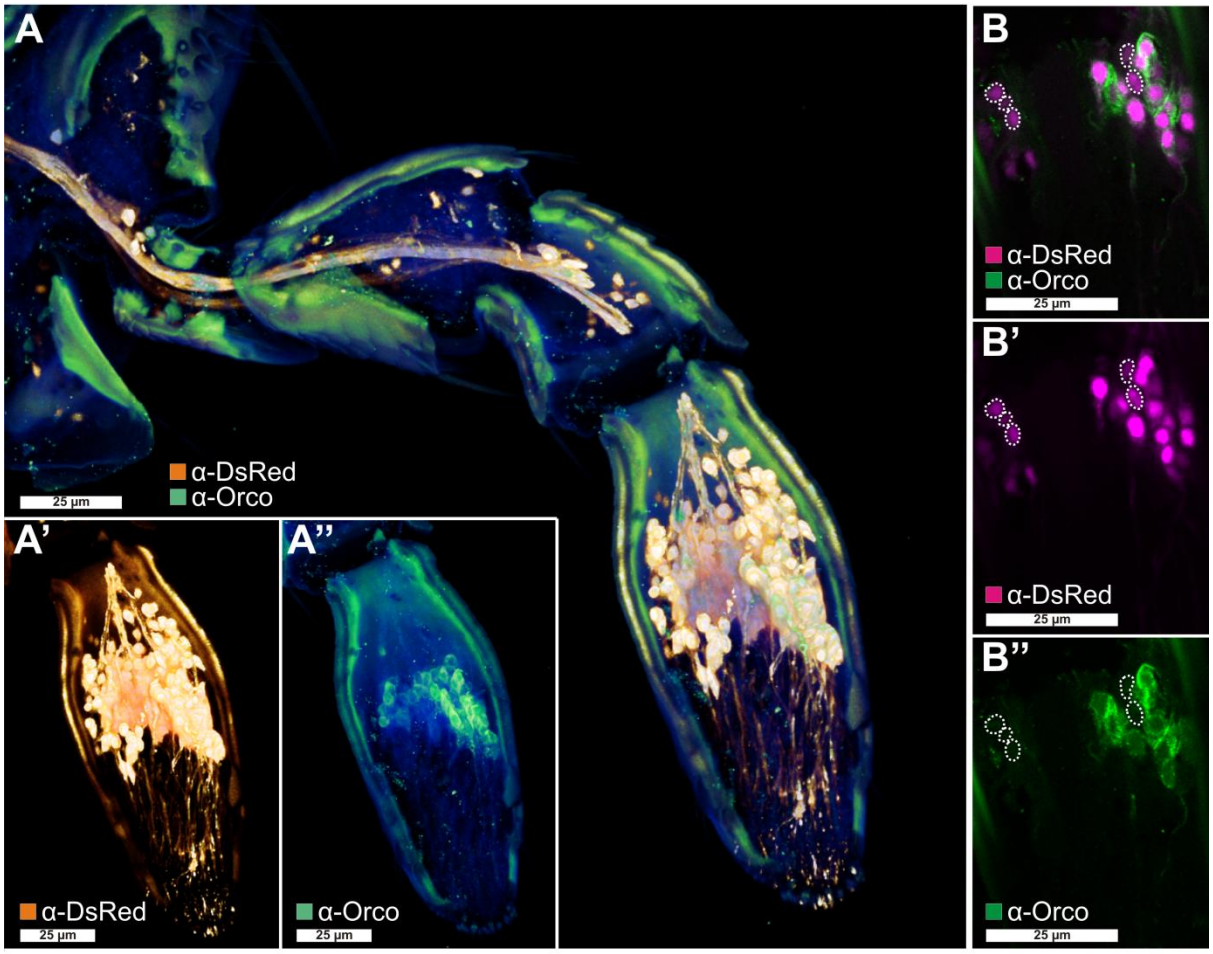

Figure 4. Orco-ir sensory neurons in the maxillary palp. (A) Voltex projection of a confocal image stack showing antibody enhanced reporter expression of the *EF1-B*-DsRed line (**A'**, orange) and Orco-ir cells (A'', green) in a halved maxillary palp. **(B-B'')** Single optical section of **(A)** showing partial colocalization of Orco immunoreactivity and the reporter expression of the *EF1-B*-DsRed line (magenta). Dotted lines in **B** highlight reporter-expressing cells that are not Orco-ir.

ALOX ODEs from Lepidopterans (Rybczynski et al. 1990; Pelletier et al. 2007; Choo et al. 2013) does not encode a signal peptide (Figure 13). Five of the 54 identified carboxylesterases (CESs) are significantly enriched in antenna, with two of them also in the mouthparts. Two other CESs are significantly enriched exclusively in the mouthparts. Five of these seven candidates show a predicted signal peptide for secretion (Figure 13). The *Tcas*CESXA shares sequence similarities with *D. melanogaster* Est6 and the *Tcas*CES7J with *Dmel*JHEdup, with both *D. melanogaster* homologs having previously been identified as ODE candidates (Chertemps et al. 2012; Younus et al. 2014). *TcasCES10C* is highest expressed in antennae and related to a pheromone degrading enzyme from the Japanese beetle, *Popillia japonica* (Ishida and Leal 2008). We identified six epoxide hydrolases (EHs), which are supposed to be membrane bound ODEs (Vogt 2005), with one being significantly enriched in antennae and having a predicted signal peptide (Figure 13). The glutathione S-transferases (GSTs) of *T. castaneum* had already been annotated (Shi et al. 2012). The revision confirmed most gene models, only *TcasGSTd2* and *TcasMGST2* had to be modified (available in Supplemental Table 1). Eight of the 41 GSTs are significantly enriched in antennae, with three also in the mouthparts (Figure 13). One of these three, *TcasGSTd2,* represents a member of the GST delta subfamily such as GST-msolf1 from *Manduca sexta*, which is an olfactory-specific GST expressed specifically in the sex pheromone detecting sensilla (Rogers et al. 1999). Analysis of the 141 previously described cytochrome P450s (CYP) (Zhu et al. 2013) revealed that two predicted gene models (*CYP347A4*, *CYP351B1*) were fusions of two separate genes (now termed *CYP347A4A* and *CYP347A4B*, as well as *CYP351B1A* and *CYP351B1B*, respectively). Seven other predictions

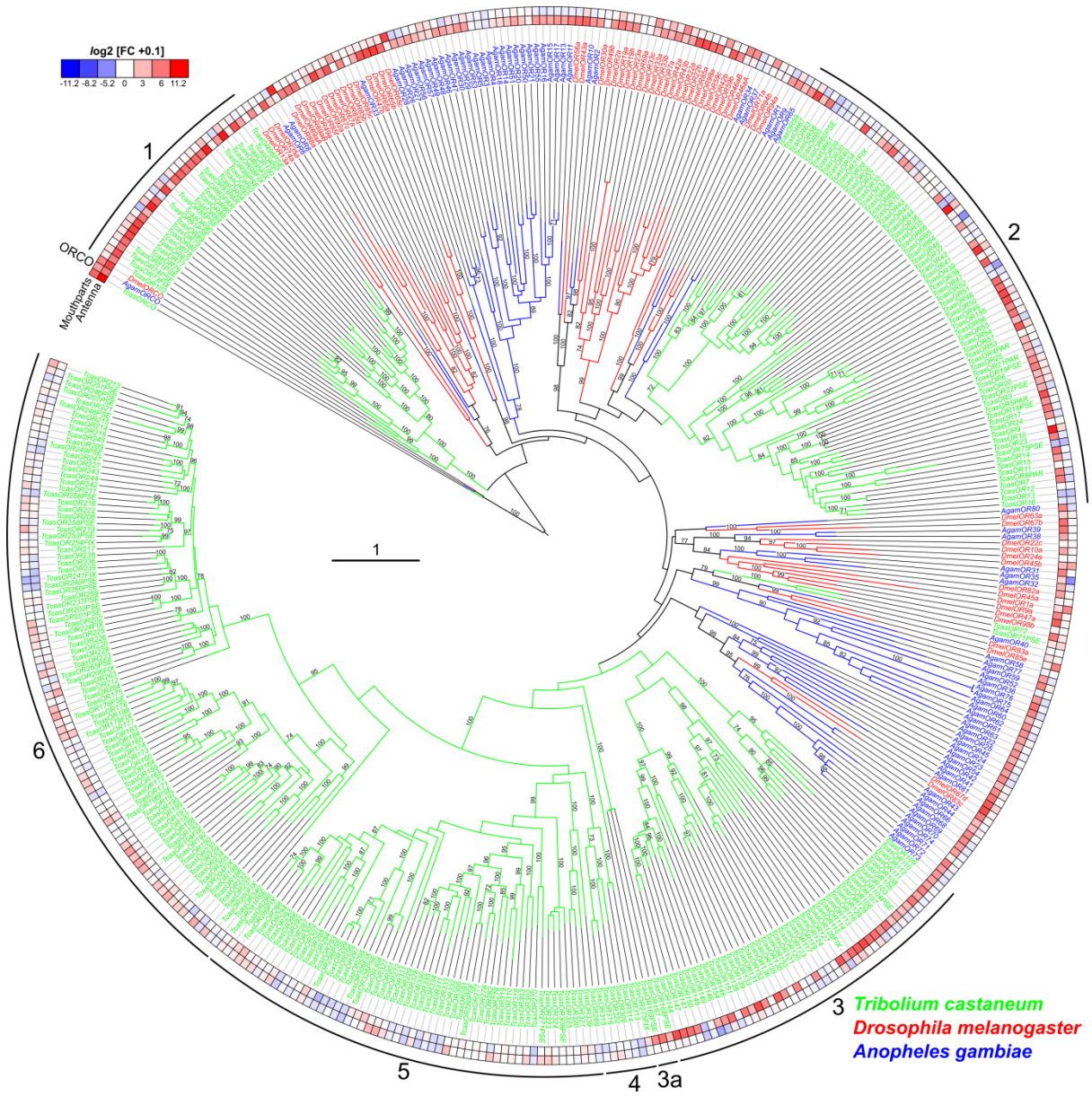

Figure 12. Phylogenetic tree of ORs. Protein sequences (>300 AA) from *T. castaneum* (green branches), *D. melanogaster* (red branches), and *An. gambiae* (blue branches). The tree was rooted using the Orco clade, according to (Missbach et al. 2014). Robustness of the tree topology was evaluated by 100 rapid bootstrap replications. Outer rings represent the expression in antennae and "mouthparts" (*T. castaneum*: palps, mandible, labrum and labium; *D. melanogaster*: palp and proboscis; *An. gambiae*: maxillary palp) as log2 fold change compared to body corresponding to the scale in the left upper corner. The surrounding numbers on outer thin line indicate the expansion groups 1 to 6 (Engsontia et al. 2008), *TcasOR71* and *TcasOR72PSE* were previously assigned to expansion group 1. The scale bar within the tree represents one amino acid substitution per site. Basically the same figure is available with absolute values instead of fold changes to get an impression of the tissue-specific abundance of the transcripts as figure supplement 1.

had to be adjusted based on RNAseq data (sequences available in Supplemental Table 1). The expression analysis of these 141 genes showed that 26 are significantly enriched in the antenna, with eleven also in the mouthparts (Figure 13). In addition, six CYPs are significantly enriched in mouthparts, but not in antennae. For the coleopteran *Phyllopertha diversa*, CYPs have been shown to be involved in pheromone degradation in a membrane bound manner (Maïbèche-Coisne et al. 2004.

Expression of potential olfaction signal transduction pathway components. The orthologs of genes encoding signal transduction pathway components known to be involved in olfaction of

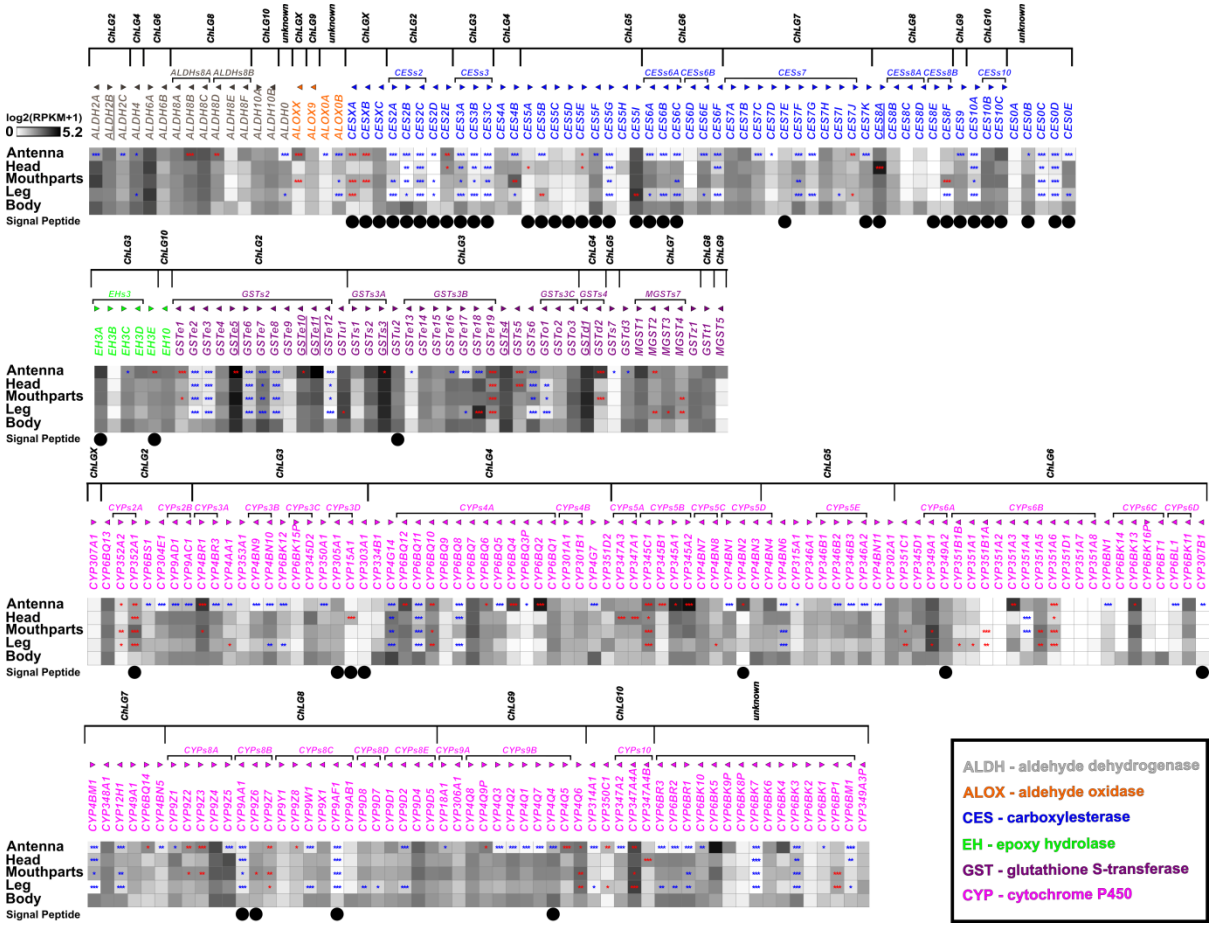

Figure 13. Expression of *T. castaneums* potential ODEs. Heatmap showing the expression level of the 263 potential odorant degrading enzymes as log2[RPKM+1] value in different tissues (adult antennae, head (missing antennae but including mouthparts), mouthparts, legs, body). The candidates are ordered according to their protein family and chromosomal localization, horizontal brackets above indicate clustering in the genome (figure supplement 1), the arrowheads represent the orientation of the open reading frame, underlined genes were previously found on protein level in antennae by(Dippel et al. 2014). The expression levels are represented by a greyscale with highest shown expression levels labeled black. The asterisks mark statistically significantly differentially expressed genes compared to body. The red asterisks represent up- and the blue down-regulation (p-values adjusted are * < 0.05; ** < 0.01; *** < 0.001). A black dot in the lowest line indicates a predicted signal peptide according to SignalP 4.0 (Petersen et al. 2011) prediction.

D. melanogaster (Martin et al. 2013) were identified by BLAST and manually curated. The expression analysis revealed that four of them (*rdgB*, *itpr*, *dgkd*, and *dgkt*) are significantly enriched in the antennae (Figure 14). However, there is no chemosensory-specific candidate being exclusively expressed in antennae or mouthparts. Our data therefore do not indicate a chemosensory-specific metabotropic signal transduction pathway.

Expression and distribution of sensory neuron membrane proteins. The transcriptome analysis revealed that one of the seven previously identified *Tcas*SNMPs (Nichols and Vogt 2008; Vogt et al. 2009), namely XP_969729 (Nichols and Vogt 2008), was incorrectly annotated and does not encode for a CD36 related protein. Moreover, the gene model previously named SNMP1c (XM_001816389) was a fusion of two SNMPs and was overlapping with SNMP1d (XM_001816391) (Vogt et al. 2009). In our re-annotation, we removed XP_969729 and separated *Tcas*SNMP1c and *Tcas*SNMP1d. In addition, the gene models of *Tcas*SNMP2, *Tcas*SNMP1a, and XP_975606 (Nichols and Vogt 2008) had to be modified based on transcriptome and RACE-PCR data. For XP_975606, we propose the name *Tcas*SNMP3, to reflect its unclear phylogenic relationship. Despite the more SNMP1 like expression pattern (Figure 15) and chromosomal localization (Figure 7 – figure supplement 2) of *Tcas*SNMP3, the comparison of

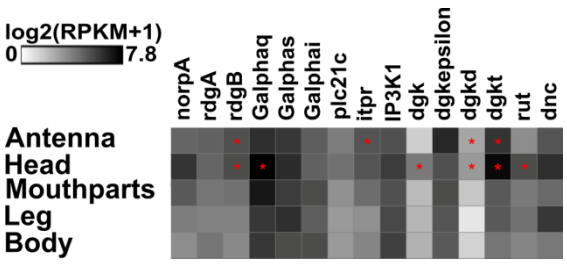

Figure 14. Expression of *T. castaneum*s homologs of genes described to be involved in olfaction of *D. melanogaster*. Heatmap showing the expression level of the several genes supposed to be involved in *D. melanogasters* olfaction, as log2[RPKM+1] value in different tissues (adult antennae, head (missing antennae but including mouthparts), mouthparts, legs, body). The expression levels are represented by a greyscale with highest shown expression levels labeled black. The asterisks mark statistically significantly differentially expressed genes compared to body. The red asterisks represent up- and the blue down-regulation (p-values adjusted are * < 0.05; ** < 0.01; *** < 0.001).

the amino acid composition revealed no clear affiliation to either the SNMP1 or the SNMP2 subgroup (Forstner et al. 2008). Interspecies comparison revealed no clear orthology of *Tcas*SNMP3 to SNMPs from other species, including the so called "SNMP3" of *Calliphora stygia* (Leitch et al. 2015) which based on phylogeny clearly represents an SNMP1 homolog. All six *Tcas*SNMPs are expressed in antennae (Figure 15), which was also confirmed by RACE-PCR based on an antennae cDNA pool but only *Tcas*SNMP1a-d and *Tcas*SNMP3 are significantly enriched in antennal tissue. Moreover, three of the *Tcas*SNMP1, as well as *Tcas*SNMP3 are also enriched in mouthparts (Figure 15), further supporting the importance of the mouthparts for olfaction in *T. castaneum*. In contrast, *Tcas*SNMP2 is highest expressed in body and significantly underrepresented in antennae and mouthparts (Figure 15), which is similar to its ortholog in *D. melanogaster* (Benton et al. 2007). Despite the observation that in most insects with a fully sequenced genome only two SNMPs were found (Nichols and Vogt 2008; Vogt et al. 2009), the relative high amount of six *Tcas*SNMPs of *T. castaneum* is not unique, since transcriptome analysis e.g. of other beetles revealed four SNMPs in *Dendroctonus valens* (Gu et al. 2015) and *Dastarcus helophoroides* (Wang et al. 2014a), as well as three in *Ips typographus* and *Dendroctonus ponderosae* (Andersson et al. 2013). However, *T. castaneum* is currently only exceeded by the Hessian fly (*Mayetiola destructor*) with seven expressed SNMPs (Andersson et al. 2014).

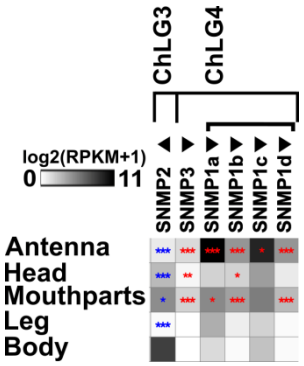

Figure 15. Expression of *T. castaneum*s SNMPs. Heatmap showing the expression level of the six sensory neuron membrane proteins of *T. castaneum*, as log2[RPKM+1] value in different tissues (adult antennae, head (missing antennae but including mouthparts), mouthparts, legs, body, as well as larval head and body). The candidates are ordered according to their chromosomal localization (Figure 7 – figure supplement 1), horizontal brackets above indicate clustering in the genome, the arrowheads represent the orientation of the open reading frame. The expression levels are represented by a greyscale with highest shown expression levels labeled black. The asterisks mark statistically significantly differentially expressed genes compared to body. The red asterisks represent up- and the blue down-regulation (p-values adjusted are * < 0.05; ** < 0.01; *** < 0.001).

Discussion

Independent integration centers for antennal and palpal olfactory perception. In *T. castaneum*, odorants are mainly perceived with the last three segments of the antenna carrying three types of chemoreceptive sensilla (SBas, cSTri, and SCoe), as well as with the maxillary and labial palps (Figure 16). Accordingly, expression analysis revealed that ORs are mostly expressed in antennae, but also in the mouthparts (Figure 11, Figure 12, Figure 11 – figure supplement 2) as previously shown for several dipteran species (Vosshall and Stocker 2007; Lu et al. 2007; Syed and Leal 2007; Pitts et al. 2011; Rinker et al. 2015). In contrast to the Diptera, where the palps are chemosensory

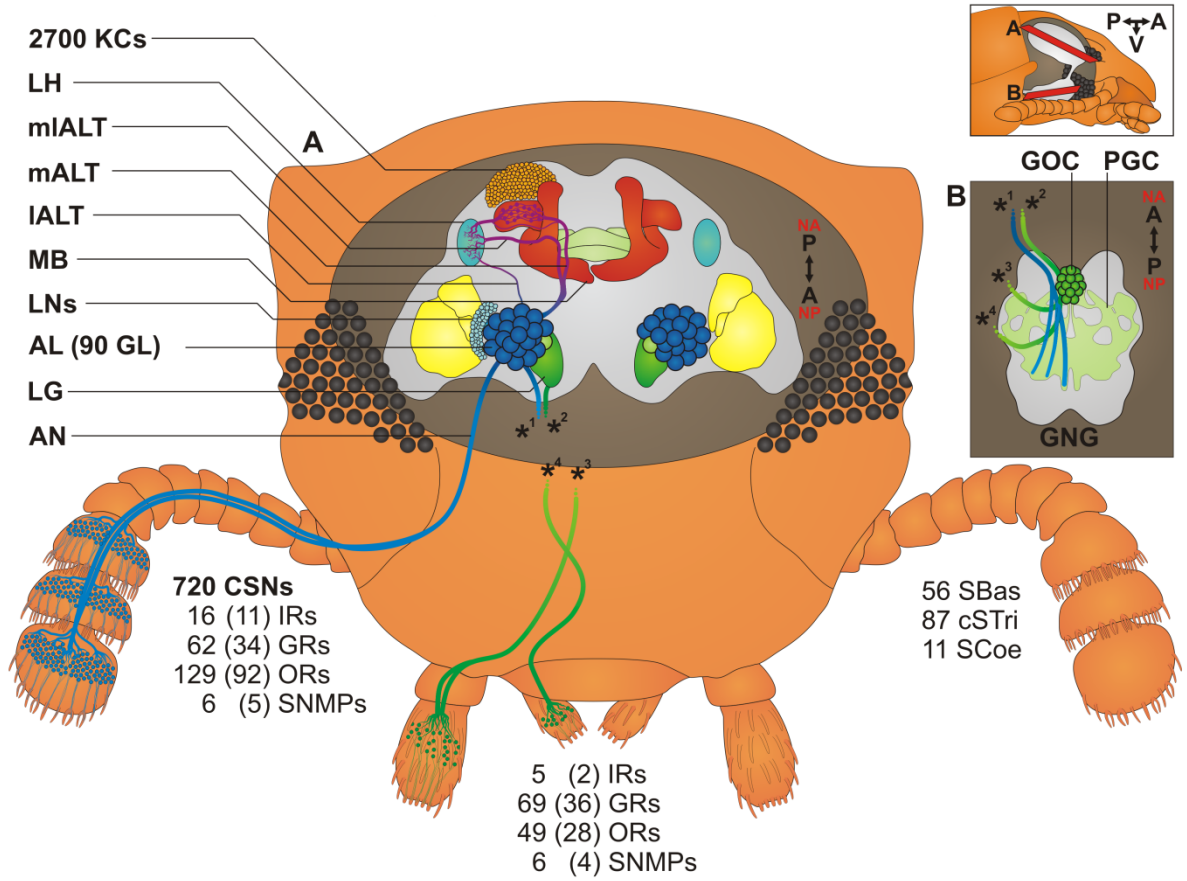

Figure 16. Scheme of the *T. castaneum* head including the major components of the olfactory pathway. (A) Dorsal view of a head section depicting the brain and the chemosensory neurons from the antenna (blue) and the mouthparts (green). **(B)** Ventral view of a head section depicting the gnathal ganglion (GNG). Orientation of the sections is indicated in the scheme at the right upper corner presenting a lateral view of the head. Chemical signals are sensed by about 720 chemosensory neurons (CSNs) located in 56 sensilla basiconica (SBas), 87 chemoreceptive sensilla trichoidea (cSTri), and eleven sensilla coeloconica (SCoe) at the last three antennal segments. These CSNs are expressing 16 ionotropic glutamate-like receptors (IRs), 62 gustatory (GRs), 129 odorant receptors (ORs), and six sensory neuron membrane proteins (SNMPs). In addition, chemosensory information is perceived in the palps by five IRs, 69 GRs, 49 ORs, and six SMNPs. The number in brackets indicates significantly enriched members compared to body. The antennal nerve (AN) projects into the ipsilateral antennal lobe (AL), where all of the about 90 glomeruli (GL, dark blue) are innervated except for one (light green). A separate antennal tract ($*^1$) descends into the GNG (**B**, blue), where most likely gustatory- and mechanosensory information is processed. In the AL, a complex network of local interneurons (LNs) is involved in processing the incoming sensory information, which is further relayed by projection neurons forming three antennal lobe tracts (ALTs). The medial ALT (mALT) projects to and arborizes in the calyx of the mushroom body (MB) that is formed by about 2700 Kenyon cells (KCs, orange) to eventually reach and innervate the lateral horn (LH, light blue). The mediolateral ALT (mlALT) and lateral ALT (lALT) directly innervate the LH. From the mouthparts, chemosensory neurons project via the maxillary ($*^3$) and labial palp nerves ($*^4$) into the GNG. Within the GNG the gustatory information is processed in the primary gustatory center (PGC). The olfactory sensory input from the palps is processed in an unpaired glomerularly organized structure in the GNG, the “gnathal olfactory center” (GOC), as well as in the lobus glomerulatus (LG) that receives input from some of the palpal OSNs via ascending neurons ($*^2$) passing through the GOC. Some of the palp derived chemosensory information is also processed in the single AL glomerulus that lacks antennal innervation and is therefore exclusively innervated by projections from the mouthparts (light green). The double headed arrows indicate the body (A, anterior ↔ P, posterior; black) and neuro-axis (NA, n-anterior ↔ NP, n-posterior; red), respectively.

appendages with limited odor coding complexity, the relative high amount of Orco-ir CSNs (Figure 4) as well as the high number of expressed ORs, SNMPs, potential ODEs and OBPs (Dippel et al. 2014) in *T. castaneum* mouthparts (Figure 11 – figure supplement 2) imply a more prominent role of the palps in olfaction.

Moreover, in addition to the differences on the perception level, major dissimilarities to the Diptera occur on the level of odor processing. The data from the partial *Orco*-Gal4 line as well as the backfills from the antenna and the mouthparts indicate that processing olfactory information at least at the level of the first central relay station occurs independently from each other (Figure 16). This is surprising, as many of the ORs expressed on the mouthparts are also expressed on the antennae. In contrast, typical OR expression is mutually exclusively between antenna and palps in *D. melanogaster* and *An. gambiae* (Vosshall and Stocker 2007; Pitts et al. 2011), where in addition projections from the palps innervate several AL glomeruli (Anton et al. 2003; Couto et al. 2005; Ghaninia et al. 2007). In *T. castaneum*, the olfactory input stemming from the antenna seems to be processed exclusively in the AL (Figure 3A, Figure 3 – figure supplement 1, 2), whereas the palpal derived olfactory information is essentially processed outside the AL, in the LG (Figure 3E, F; Figure 3 – figure supplement 1) and the GOC, an unpaired and glomerularly organized first olfactory center in the GNG (Figure 3D, F, Figure 3 – figure supplement 3). The LG had, as far as we know, previously been described only in hemimetabolous insects (Ernst et al. 1977; Ignell et al. 2000; Schachtner et al. 2005; Hofer et al. 2005; Farris 2008). A glomerularly organized olfactory center in the GNG such as the GOC has, to our knowledge, not been described in any insect so far. The number of 49 ORs (with 28 being significantly enriched compared to body) that are expressed in the mouthparts is roughly consistent with the estimated 30 to 40 glomeruli in the GOC. This suggests that the wiring in the GOC may resemble the situation in the ALs with the difference of convergence into an unpaired medial structure. The only palpal projection into the AL is a mutually exclusive innervation of a single ipsilateral glomerulus (Figure 3A and Figure 3 – figure supplement 1), which may be involved in CO_2 perception, similar to the situation described in several moth species (Kent et al. 1986) and proposed for some mosquitoes (Anton et al. 2003; Ignell et al. 2005).

Antennae serve also as key organs for gustatory perception. In *T. castaneum*, antennae and mouthparts express similar high numbers and levels of GRs, which indicates the antenna as key gustatory organ besides the mouthparts (Figure 9 and Figure 9 – figure supplement 1). This finding may reflect the beetles' ground-dwelling life style and indicates that the scanning behavior with the antennae, not only gathers tactile, but also chemical stimuli. This is in contrast to higher dipterans, where the labellum is the main gustatory organ (Dahanukar et al. 2001; Bohbot et al. 2007; Vermehren-Schmaedick et al. 2011).

Postulation of exceptions to the central dogma. The amount of 129 ORs that we found to be expressed in *T. castaneum* antennae (Figure 11 and Figure 11 – figure supplement 1) exceed the amount of about 90 glomeruli in the AL. Moreover, some glomeruli are likely to get exclusive innervation by OSN that express IRs, as described in *D. melanogaster* (Rytz et al. 2013). These observations do not conciliate with the central dogma postulating that OSNs express only one typical OR and all OSNs carrying this same OR converge into one and the same glomerulus, which was hypothesized to be the typical situation for insects (Jefferis 2005; Vosshall and Stocker 2007; Kaupp 2010). However, for *D. melanogaster*, both co-expression of more than one typical OR per OSN as well as co-convergence due to innervation of one AL glomerulus by more than one OSN sub-type have been already described as exceptions (Goldman et al. 2005; Vosshall and Stocker 2007). For *T. castaneum*, we propose that such exceptions are much more frequent.

Large repertoire of potentially functional odorant receptor genes and possible environmental regulation. The genome of *T. castaneum* harbors 341 OR genes (Engsontia et al. 2008; Richards et al. 2008), of which 270 seem to encode for functional ORs. Of the 337 ORs with available full sequence information (Engsontia et al. 2008), we find in our RNAseq data 161 ORs to be expressed in adult antennae, mouthparts, and head by a threshold of 0.5 RPKM (Figure 11 – figure supplement 1). In comparison to the RT-PCR based data from (Engsontia et al. 2008), who found 112 ORs to be clearly expressed in adult heads, we only confirmed 82 ORs. In addition, we identified 41 ORs previously declared as not expressed and 37 ORs previously not tested (Engsontia et al. 2008) as expressed (Figure 11 – figure supplement 2). This

Table 2. Comparison of main components of the olfactory system of different insect model organisms.

species	chemo-receptive Sensilla (per antenna)	CSNs (per antenna)	IRs (genes)	GRs (genes)	ORs (genes)	AL glomeruli (per AL)	KCs (per MB)
T. castaneum	154	720	23[1]	220[2]	341[3]	70[4] – 90	2 700
D. melanogaster	530[5]	1 200[5,6]	66[1]	73[7]	62[8]	43[6] – 54[9]	2 500[10]
An. gambiae	714 f[11]* 738 f[12]	1 500 – 1 600 f[11]*	46[1]	60[7]	79[8] 76[13]	60 f[14] 61 m[14]	
Ae. aegypti	928 f[15]	1946 f[15]	95[1]		131[16]	50 f[17] 49 m[17]	
B. mori	>24 500 m[18]* >21 000 f[18]*	50 000 m[18]* 30 000 f[18]*	18[1]	56[7]	48[7]	55–60[18]	
M. sexta	190 000 m[19]	255 000 – 450 000 m[20]*,[19] 169 000 f[20]*				63[21]	
A. mellifera (worker)	5 000 – 5 100[22]	60 000[23]* 63 700[22]	10[1]	53[7]	163[8]	156–166[24]	170 000[25] – 184 000[26]
P. americana	65 500 m[27]	241 000 m[27]				125 f[27] 126 m[27]	175 000[28]
Locusts	*Lmig* 4 700[29]	50 000[30]*	*Lmig* 11[7]	*Lmig* 75[7]	*Lmig* 95[7]	*Sgre* 1 000[30] *Sgre* 2 500 - 3 000[31]	*Sgre* 50 000[30]

*, Olfactory sensory neurons/sensilla (otherwise chemosensory neurons/sensilla); f, female; m, male; *Sgre, Schistocerca gregaria; Lmig, Locusta migratoria* [1](Croset et al. 2010), [2](Richards et al. 2008), [3](Engsontia et al. 2008), [4] (Dreyer 2010), [5] (Stocker 2001), [6](Vosshall and Stocker 2007), [7] (Wang et al. 2014b), [8](Sánchez-Gracia et al. 2001), [9](Grabe et al. 2015), [10](Hinke 1961), [11](Qiu et al. 2006), [12](Pitts and Zwiebel 2006), [13](Pitts et al. 2011), [14](Ghaninia et al. 2007), [15](McIver 1978), [16](Bohbot et al. 2007), [17](Ignell et al. 2005), [18](Koontz and Schneider 1987), [19](Lee and Strausfeld 1990), [20](Homberg et al. 1989), [21](Rospars and Hildebrand 2000), [22](Esslen and Kaissling 1976), [23](Frasnelli et al. 2010), [24](Galizia et al. 1999), [25](Mobbs 1982), [26](Strausfeld 2002), [27](Boeckh and Ernst 1987), [28](Neder 1957), [29](Greenwood and Chapman 1984), [30](Laurent and Naraghi 1994), [31](Schachtner et al. 2005)

discrepancy might be partially due to the different type of methodology used to identify expression. However, culturing conditions and used strain specific genetic variations might also be responsible for the differences.

Taking both studies together, there is clear experimental evidence for 191 ORs that are expressed in the adult head. By including adult leg and all adult body data, 223 ORs seem to be expressed in total, of which 17 actually do not encode an intact OR. However, for 64 OR functional gene models no expression could be detected so far. This might be due to low expression in a single OSN or conditional expression under exceptional circumstances. The red flour beetle can live up to two years (Good 1936). During this long period in their natural environment, the beetles can encounter a variety of challenges such as food shortage, which possibly triggers flight migrations over tens of kilometers (Ridley et al. 2011). Under such exceptional circumstances the not or low-expressed receptor genes may become active (Engsontia et al. 2008), as shown in studies in *D. melanogaster* (Hodges et al. 2014) and *An. gambiae* (Rinker et al. 2013) were up to fivefold upregulation of several ORs was triggered by temperature or feeding state.

Inter-species comparison of olfactory components. The comparison of the number of main components of the chemosensory pathway of different insect species reveals the high diversity of evolutionary strategies to enable proper chemoreception and thus reflects the diversity of insects and the manifold adaptations to their specialized lifestyles (Table 2). In particular, *T. castaneum* has by far the lowest amount of chemoreceptive sensilla (154) and consequently also of CSNs (725). In contrast to this low number,

the amount of GRs (220) and ORs (341), but not of the IRs (23) encoded in the genome is exceptionally high. The number of olfactory glomeruli in the AL is within the range of most other species (Table 2) (Schachtner et al. 2005; Hu et al. 2011)). Comparing the relation of OR genes and number of glomeruli, the highest discrepancy occurs with about four fold higher numbers of OR genes in *T. castaneum*. However, also in *Ae. aegypti*, OR gene numbers more than double the amount of glomeruli (Bohbot et al. 2007). In most other analyzed insects, except ensiferan orthopterans that have hundreds of microglomeruli (Flook et al. 1999; Ignell et al. 2001), the number of OR genes is typically similar to the number of glomeruli (Table 2). Despite the relative low number of IRs encoded in the genome of *T. castaneum*, the repertoire of IRs involved in olfaction is highly conserved (Figure 8). The amount of KCs is roughly the same as in *D. melanogaster* and seems to be independent of the OR or AL glomeruli number (Table 2) (Farris and Roberts 2005).

No apparent sexual dimorphism. In many insect species, a sexual dimorphism of the olfactory system is described (Kondoh et al. 2003; Kleineidam et al. 2005; Schachtner et al. 2005; Hu et al. 2011). However, in contrast to other coleopterans (Ågren 1985; Allsopp 1990; Okada et al. 1992; Jourdan et al. 1995; Ruther et al. 2000) our analysis revealed no apparent sexual dimorphism on antenna morphology or number and distribution of sensilla (Figure 1 – figure supplement 4). Expression analysis of male and female antenna samples revealed only a small but not significant dimorphism in the OBP expression levels described earlier (Dippel et al. 2014). Also for IRs, GRs, ORs, and SNMPs, we could not find any significant differences (Figure 6) in contrast to described situations in Diptera and Lepidoptera (Couto et al. 2005; Fishilevich and Vosshall 2005; Grosse-Wilde et al. 2010; Pitts et al. 2011). Different numbers of glomeruli or different sized glomeruli were observed in several insect species (Kondoh et al. 2003; Schachtner et al. 2005; Galizia and Rössler 2010) including the beetle *Holotrichia diomphalia* (Hu et al. 2011). However, the comparison of the ALs of *T. castaneum* males and females disclosed no obvious dimorphism as previously described also for the small hive beetle (*Aethina tumida*) (Kollmann et al. 2015). In summary, our study did not reveal any sexual dimorphism of the olfactory system in *T. castaneum.* This finding is consistent with behavioral studies that showed an attraction of both sexes to the aggregation pheromone 4,8-Dimethyldecanal (Suzuki 1980) and no sex preference in mating choice of males (Serrano et al. 1991).

Conclusion

Detailed analysis of the olfactory system in *T. castaneum*, a holometabolous insect of special importance for the study of coleopteran and pest biology, reveals that olfactory sensory input from the antennae is processed mostly in the antennal lobes of the brain, as observed in other insect species. However, tracing of olfactory projections from the mouthparts enabled the identification of two additional neuropils: a lobus glomerulatus described previously only in a hemimetabolous insect and an unpaired glomerularly organized olfactory neuropil in the gnathal ganglion (the "gnathal olfactory center"), which has never before been described. In addition, the high number of gustatory receptors on both the antennae and mouthparts indicates no organotopic separation of olfaction and gustation in this beetle. These findings are a reminder of the wide variety of solutions to chemoreception that have evolved in the holometabolous insects. This should remind us that we have much still to learn about olfactory systems in general.

Materials and Methods

Tribolium castaneum rearing and transgenic lines

Tribolium castaneum (Herbst, 1797; Insecta, Coleoptera, Tenebrionidae) wild type strain San Bernardino, as well as the transgenic lines partial *Orco*-Gal4, *UAS*-DsRed, *UAS*-tGFP (Schinko et al. 2010), and *EF1-B*-DsRed (Posnien et al. 2011) were breed at about 30°C and 40% relative humidity on organic whole wheat flour supplemented with 5% yeast powder (Berghammer et al. 1999a). The *Orco*-Gal4 and *UAS*-DsRed lines were generated by

piggyBac-based insertional mutagenesis (Berghammer et al. 1999b). The used donor plasmids were assembled by a versatile two-step cloning procedure (Horn et al. 2003).

For the partial *Orco*-Gal4 line, a donor plasmid was generated by cloning a blunted and BamHI (Fermentas, Vilnius, Lithuania) digested PCR product containing *Gal4delta-SV40pA* (amplified with primers Gal4deltafor and SV40rev from plasmid CH#757, see supplemental sequences) into the BamHI and EcoRV (Fermentas) digested pSLfa1180 vector (Horn and Wimmer 2000). After propagation a BamHI and BfuAI digested PCR product containing 2.5 kb upstream of the *TcasOrco* (amplified with TcOR1upfor and TcOR1uprev from San Bernardino gDNA) was cloned into the corresponding restriction sites to generate pSLfa1180[2.5kbOrcoUp_GAL4delta]. The whole cassette was shuttled with AscI and FseI (New England Biolabs, Ipswich; MA, USA) into the pBac[*3XP3-Tcv*] (Siebert et al. 2008) donor plasmid. The tissue specific expression of Gal4 in the *Orco*-Gal4 line was determined by crossing it with an *UAS*-tGFP (Schinko et al. 2010) line and performing immunohistochemistry on the antennae with α-tGFP and α-Orco antibody or by staining of the whole brain with α-tGFP and an α-synapsin counterstaining. These stainings revealed that only Orco-ir neurons are labeled in antennae (Figure 1 – figure supplement 6A), which indicates the specificity of the Orco-Gal4 driver line. However, only half of the Orco-ir neurons in the antenna are expressing tGFP (Figure 1 – figure supplement 1A), which implies that the *Orco*-Gal4 line only partially covers the Orco pattern resulting in labelling of only half of the AL glomeruli (Figure 1 – figure supplement 6B). The same approach with an *UAS*-dsRed line and an α-RFP antibody was used to characterize the palps, in which the reporter is also exclusively expressed in *Orco*-ir neurons, but in only 10 – 20 % of the cells (Figure 1 – figure supplement 5). We therefore refer to it as "partial *Orco*-Gal4 line".

For *UAS*-DsRed, the donor plasmid pBac[*3XP3*-eYFP_*UAS-Tchsp68bP*-DsRedex-*SV40*] was generated by cloning the DsRed express ORF (Clontech laboratories Inc., Mountain view, CA, USA; catalog no. 632412) into the pSLfa[*UAS-Tc'Hsp-p*-tGFP-*SV40*]fa shuttle vector (Schinko et al. 2010) by using KpnI and NotI. Followed by transferring the *UAS-hsp*-DsRed-SV40 cassette into the pBac[*3XP3*-eYFP] (Horn and Wimmer 2000) by using AscI and FseI. The *UAS*-DsRed line as well as the *UAS*-tGFP line were analyzed by confocal microscopy to ensure that no reporter expression is present in the relevant tissues in the absence of a Gal4 driver line (Figure 1 – figure supplement 7).

The *EF1-B*-DsRed line (elongation factor1-alpha regulatory region-DsRedExpress; kindly provided by Michalis Averof, Institut de Génomique Fonctionnelle de Lyon, France) has been described to label most neurons in the central nervous system of first instar larvae (Posnien et al. 2011) and also shows high expression in the adult central nervous system. However, in the peripheral nervous system clearly not all neurons are labeled. We therefore re-analyzed adult antennae of this line using confocal microscopy in combination with antibody stainings. The labeled neurons in the antenna resemble the typical morphology of CSNs with the dendrites being embedded in the sensilla cavities (Figure 2H, Figure 1F, G and H) and the axons converging to the antennal nerve (Figure 2H and Figure 1 – figure supplement 2). No labelling was detected at mechanosensory sensilla (Figure 1C, D, E,) except the scolopidia cells of the Johnston's organ (Figure 1 – figure supplement 2). In addition to almost all Orco-ir ORNs (Figure 2I), this line labels also non Orco-ir neurons that are affiliated with sensilla coeloconica (Figure 1H) and sensilla basiconica (Figure 1G). Whereas in the palps only about 30 to 50% of the DsRed-ir cells are also Orco-ir (Figure 4), in antennal segment 11 a higher percentage of CSNs is double labeled, and in segments 9 and 10 the vast majority of CSNs are double labeled (Figure 2I-I'', Figure 1 – figure supplement 2). This suggests that almost all and only CSNs are labeled by this line in the adult antenna.

Tissue preparation for SEM

Antennae of sex separated adults were dissected and immediately fixed for at least 2 h in 5% glutaraldehyde in 0.1 M PBS, pH 7.1, washed and post-fixed in osmium-tetroxide (1% in 0.1 M Sörensen buffer, pH 7.2). Fixed samples were washed in water, dehydrated overnight in

ethyleneglycolmonoethylether and then transferred into acetone via at least three 10-min changes with 100% acetone as described in (Santos et al. 2006). The samples were critical-point-dried by using a Polaron E 3000 (Balzers Union, Quorum Technologies Ltd, Darmstadt, Germany). After being sputtered with gold (Balzers Union Sputter Coater, Balzers, Liechtenstein; Quorum Technologies Ltd, Ringmer, UK), the material was examined by using a Hitachi S-530 SEM (Hitachi High-Technologies Europe GmbH, Krefeld, Germany). Micrographs (Figure 1B-B'', C'''-C'''', D'''-D'''', E'''-E'''', F''', G'''-G'''' H'', 2A-G) were taken by digital image acquisition (DISS 5, point electronic, Halle, Germany).

Immunohistochemistry

Whole mount brain immunohistochemistry (IHC) was performed as described in (Dreyer et al. 2010). The animals were cold anesthetized, their brains were dissected in cold PBS (phosphate-buffered saline, 0.01M, pH 7.4), and fixed subsequently over night at 4°C or for 1-2 h at room temperature in PBS containing 4% paraformaldehyde (PFA; Roth, Karlsruhe, Germany). The tissue was rinsed 4 times for 10 minutes with PBS. and pre-incubated with 5% normal goat serum (NGS, Jackson ImmunoResearch, Westgrove, PA, USA) in PBT (PBS containing 0.3% Triton X-100; Sigma-Aldrich, Steinheim, Germany) for 1-3 days at 4°C. After preincubation, nervous tissue was transferred to the primary antibody solution containing 2% NGS in PBT and incubated for 2-4 days at 4°C. To selectively label neuropil regions, a monoclonal primary antibody from mouse against synapsin was used in combination with specific additional antibodies and various dyes (for an overview of the employed antibodies and dyes see Supplemental Table 2). After rinsing 5 times for 10 minutes with PBT, the brains were incubated with appropriate secondary antibodies and various dyes (Supplemental Table 2) diluted in PBT containing 2% NGS for 1-3 days at 4°C, followed by 3 to 5 washing steps for 10 minutes each with PBT. Brains and ganglia were dehydrated in an ascending ethanol series (50%, 70%, 90%, 95%, 100%, 100%; 2.5 minutes each) and cleared with methyl salicylate (Merck, Gernsheim, Germany). Finally, they were mounted on coverslips using Permount mounting medium (Fisher Scientific, Pittsburgh, PA, USA) and a stack of two reinforcement rings (Zweckform, Oberlaindern, Germany) as spacers to prevent compression. Brains and ganglia of some of the backfills were not dehydrated and directly mounted in Aqua-Poly/Mount (Polysciences Europe Inc., Eppelheim, Germany).

Antennae and palps of the *EF1-B*-DsRed, the *Orco*-Gal4/*UAS*-tGFP, or *Orco*-Gal4/*UAS*-dsRed lines were dissected and fixed over night at 4°C in 4% PFA and 10% methanol in PBT. Afterwards they were transferred into silicone molds, embedded in tissue freezing media (Leica, Wetzlar, Germany), and frozen for at least 1 hour at -80°C, followed by cutting into 50 µm sections at -23°C on a Cryotome (Cryotome CM 1959, Leica Microsystems, Wetzlar, Germany) resulting in longitudinally halved antennae. The half mounts were collected in a tube and rinsed 4 times 20 min each at room temperature in PBT. The samples were pre-incubated with 5% NGS in PBT over night at 4°C followed by incubation with primary antibodies and dyes together with 5% NGS in PBT overnight. After washing 4 times 20 min with PBT the samples were incubated with appropriate secondary antibodies (Supplemental Table 2) over night at 4°C. Finally the antennae were rinsed four times with PBT for 20 minutes and embedded on a coverslips in Aqua-Poly/Mount with one layer of reinforcement rings as spacers.

The specificity of the Orco-antiserum (Moth-R2, kindly provide by Jürgen Krieger) in *T. castaneum* could be demonstrated by IHC on antennae of animals with RNA interference-mediated knock-down of *Orco* (Engsontia et al. 2008). To circumvent problems during dsRNA synthesis previously observed with the full length CDS of *TcasOrco,* we cloned a 476 bp fragment from San Bernadino cDNA containing only a part of CDS and the majority of the *3´UTR* amplified by Advantage2 Taq Polymerase and primers *TcasOrco3UTRrev* and *Tcas*Orco3for (see supplemental sequences) into PCRII vector (Invitrogen). By PCR a bidirectional template was generated followed by dsRNA synthesis with the MEGAscript T7 transcription kit (Ambion, Austin, USA) (Schmitt-Engel et al. 2015). The *Orco dsRNA* was injected into pupa of the strain San Bernardino. About seven days after

adult eclosion, the antennae of the treated animals were collected together with antennae of untreated beetles of the *black* strain, which can be easily discriminated based on the cuticle color and thus serve as internal staining control. A maximal projection of a confocal stack of the Orco-antiserum (Moth-R2) treated antennae shows no detectable antibody staining in RNAi-treated animals (Figure 1 – figure supplement 8A) in contrast to the *black* beetle internal control (Figure 1 – figure supplement 8B).

***In vivo* backfills of the antenna, single maxillary palps, and whole mouthparts**

Cold anesthetized animals were mounted with dental wax (S-U-wax wire, 2.0 mm, hard; Schuler Dental, Ulm, Germany) and modelling clay (Das große Dino-Knet-Set; moses. Verlag GMBH, Kempen, Germany) by using a low temperature solering iron (Solder-Unit ST 081; Star Tec Products, Bremen, Germany) or with rubber cement (Fixogum, Marabu, Tamm, Germany) with their dorsal side on a microscope slide. The last three segments of the antenna and the most distal segment of the maxillary palp were removed and 4% neurobiotin in 1 M KCl (Vector Laboratories, Burlingame, UK) for the antenna and Texas Red coupled dextran 50 mg/ml in PBS (3000 MW; Molecular Probes, Invitrogen) for the maxillary palps were used as neuronal tracers. Glass micropipettes were drawn (Model P-97, Sutter Instrument, Novato, USA) from borosilicate glass (inner diameter, 0.75 mm; outer diameter, 1.5 mm; Hilgenberg, Malsfeld, Germany) and broken to a tip diameter matching to the antenna/maxillary palp stump. The dye filled glass micropipette was put on the antenna/maxillary palp stump for about 4-6 hours in a moist chamber at 4°C. For the backfills of the whole mouthparts, the maxillary and labial palps were cut and the antennae were protected from unintentional dye filling by covering them with dental wax (S-U-wax wire, 2.0 mm, hard). A crystal of biotin-conjugated dextran (3000 MW; Molecular Probes, Invitrogen) was placed onto the prepared mouthparts, covered with a drop of distilled water, and stored for about 4 h in a moist chamber at 4°C. Brains and ganglia were dissected, fixed, washed, and stained as described above. Neurobiotin was visualized with Cy3 conjugated streptavidin (Dianova, Hamburg, Germany) diluted 1/200 in PBT (0.3% TrX). The Staining solution contained in addition Alexa Fluor 488-coupled phalloidin (1/200), DAPI (1/20.000) and 2% NGS. Incubation time was 2-3 day at 4°C. Biotin-coupled dextran was visualized with Alexa Fluor 488 coupled streptavidin (Molecular Probes, Invitrogen) diluted 1/200 in PBT (0.3% TrX and 2% NGS) and applied together with synapsin (1/300) for 2-3 days at 4°C

***In vivo* dye injection into the antennal lobes**

Cold anesthetized animals with fluorescent labeled ALs (partial *Orco*-Gal4/*UAS*-DsRed) were mounted with their ventral side pointing upside down with dental wax on a microscope slide. The pronotum and the head-capsule were opened using a piece of a razor blade held by a blade breaker, with two parallel, longitudinal cuts along the compound eyes. The cuticle, fat tissue and tracheae were removed. Afterwards, head capsule and pronotum had been covered with ringer solution (Galizia et al. 1997). The tungsten needle was sharpened in 2M KOH with 5-8 volts similar as described in (Pellegrino et al. 2010) followed by coating with Texas Red conjugated dextran (3000 MW; Molecular Probes, Invitrogen) solved in NGS and had been air-dried. The dye injection in the DsRed-labeled AL was performed manually under a fluorescence stereomicroscope (SteREO Lumar.V12, Carl Zeiss MicroImaging, Jena, Germany) by careful perforation. The treated animals were kept in a moist chamber for about 1 h at room temperature to let the dye diffuse. Afterwards the brains were dissected, fixed, washed, and preincubated with NGS as described previously and afterwards incubated with Alexa Fluor 488-coupled phalloidin (1/200), DAPI (1/20.000) und 2% NGS for 2 day at 4°C. Subsequently brains were washed, dehydrated, cleared and mounted in Permount as described above.

Microscopic image acquisition, processing and analysis

The fluorescent labeled microscopic samples were scanned with a confocal laser-scanning microscope (TCS SP5, Leica Microsystems) at 1024×1024 or 2048x2048 pixel resolution, a scanning speed between 100 and 200 Hz, a pinhole of 1 Airy, a line average of 2-4 and a step size between 0,5 and 2,5µm. Confocal images and image stacks were analyzed with the Amira 5.3.3 graphics software (FEI, Hillsboro, OR, USA). The final image processing and figure arrangements were processed by using Corel Draw X3 (Corel, Ottawa, Ontario, Canada), Adobe Photoshop CS3 (Adobe Systems, San Jose, CA, USA), or Inkscape (http://www.inkscape.org/).

The number of CSNs per sensillum was determined based on high resolution CLSM stacks taken from antennae of the *EF1-B*-DsRed line after antibody enhancement of the DsRed reporter signal in combination with Orco antibody staining. In order to determine the number of CSNs and Orco-ir OSNs we traced the stained dendrites of the CSNs to their associated soma of several sensilla and calculated their average number (Figure 1 – figure supplement 3I, Figure 2H).

AL glomeruli were separately labeled in the AMIRA "Segmentation Editor" and 3D reconstructed (Dreyer 2010) based on CLSM stacks of brains labeled with synapsin and TKRP antibodies of five male and five female A7 beetles (one AL from a random hemisphere for each brain). To optimize the data quality the CLSM stacks were previously deconvoluted in AMIRA using the blind method with initial estimation set to input data, with a border width of 10, 10, 10 and an iteration of 10 cycles.

Kenyon cells were identified based on their position, size, and density in DAPI stainings (Binzer et al. 2014). The total volumes of the whole CAs (13 CAs of 7 A7 males), as well as the volumes of three randomly assigned clusters of 20 Kenyon cell per CA, were measured using 3D-reconstruction. For the segmentation and reconstruction details we refer to (Kurylas et al. 2008). Briefly, different layers of a structure were labeled in the "Segmentation Editor" and wrapped. Volumes of reconstructed structures were taken from "Material Statistics". Based on the ratios between whole CA volume and volumes of the three clusters of 20 KCs, the total number of KCs per CA was interpolated. In addition, we counted the KCs by an independent method using MorphoGraphX (www.MorphoGraphX.org). The CLSM stacks were processed with the arithmetic tool of AMIRA to mask the CAs and consequently to remove the remaining materials. The resulting stacks, were converted to TIFF files with FIJI (Schindelin et al. 2012) by preserving the image properties. These files were analyzed with the "Local Maxima" tool of MorphoGraphX (Reuille et al. 2015) with the following parameter X-/Y-/Z-radius = 1µm, Start Label -1, Min Color 1.

RNA isolation and sequencing

Total RNA of body parts namely antennae, mouthparts (piece of the head capsule anterior of the antennae), legs, head (without antennae but including mouthparts) and remaining body of sex separated adult was isolated using the ZR Tissue & Insect RNA Micro Prep Kit (Zymo Research, Irvine, CA, USA) following manufacturer´s protocol. The Library preparations for RNA-Seq were performed using the TruSeq RNA Sample Preparation Kit (Illumina, San Diego, CA, USA) and cDNA libraries were amplified and sequenced by using the cBot and HiSeq2000 from Illumina (paired end; 2x100 bp). For details see (Dippel et al. 2014).

Reannotation of olfactory genes

For manual inspection, the obtained reads were mapped against the *T. castaneum* 4.0 genome using BLAT (Kent 2002) and a genome browser was set up (http://bioinf.uni-greifswald.de/gb2/gbrowse/tcas). In a genome independent approach a *de novo* assembly was built with Trinity (release 2013_08_14) (Grabherr et al. 2011) as described in (Dippel et al. 2014). The previously published OR (Engsontia et al. 2008), GR (Richards et al. 2008), IR (Croset et al. 2010), and SNMP (Nichols and Vogt 2008; Vogt et al. 2009) sequences were used for further analysis. To identify the potential odorant degrading enzymes the official (OGS3) (Wang et al. 2007; Richards et al. 2008; Kim et al. 2010), the preliminary AU2 and AU3, and the NCBI (Maglott

et al. 2007; Pruitt et al. 2007) gene sets were used and a protein functional analysis was conducted using InterProScan (Zdobnov and Apweiler 2001). All genes belonging to a protein family containing known ODEs in other insect species were collected (namely aldehyde dehydrogenase (ALDH), aldehyde oxidase (ALOX), carboxylesterase (CES), epoxide hydrolase (EH), glutathione S-transferase (GST), and cytochrome P450 (CYP) (Leal 2013)). The redundant genes were removed and the sequences were reviewed. The identified GSTs and CYPs were collated to already published (Shi et al. 2012; Zhu et al. 2013) sequences and the names were adapted. For all other candidates a genome based name was built reflecting the protein family and the chromosomal localization (e.g. CES2D is the fourth carboxylesterase on the second chromosome).

The genes supposed to be involved in olfactory transduction of *D. melanogaster* were taken from (Martin et al. 2013), the corresponding gene sequences were downloaded from the FlyBase (Attrill et al. 2016) and the *T. castaneum* orthologs were identified by pBLAST embedded in the genome browser (http://bioinf.uni-greifswald.de/tcas/).

The revision of the olfactory genes was performed in an iterative process based on sequence comparison with the de-novo assembly and the RNA-seq based gene annotations (AU3), conserved domain search (Marchler-Bauer et al. 2011), and manual inspection of the aligned reads in the genome browser. In case of discrepancies the gene models were manually curated. Finally the chromosomal localization of the olfactory genes was determined by pBLAST against the genome assembly Tcas4.0. The ODE candidates were searched for signal peptides using the SignalP4.1 server (Petersen et al. 2011). The sequences and read numbers are summarized in Supplemental Table 1, the complete dataset including all relevant parameters has been deposited to the National Center for Biotechnology Information (NCBI) database repository 'Gene Expression Omnibus' (GEO accession number: GSE63162).

***Tribolium castaneum* expression profiling**

The olfactory genes were identified in the AU3 gene set by pBLAST and the corresponding gene models were replaced with the reannotated candidate sequences. The resulting enhanced AU3 gene set was used to map the RNAseq data with bowtie2 (Langmead and Salzberg 2012) using the very-sensitive presetting.

The mapped reads were counted with samtools (Li et al. 2009) and normalized as RPKM values. The RPKMs were visualized (matrix2png interface, version 1.2.1; (Pavlidis and Noble 2003)) and the figures were arranged in inkscape (http://www.inkscape.org/). Male and female reads from the sequenced tissues were pooled and considered as biological replicates. Statistical analysis was performed in R (R Core Team 2013) with the DESeq package (version1.12.0) (Anders and Huber 2010) from bioconductor (Gentleman et al. 2004). All tissues were compared to body as reference. Significant differentially expressed genes (false discovery rate < 0.05) are marked with asterisks in the heatmaps. Genes with an RPKM≥0.5 were considered as tissue specifically expressed the tissue comparison was visualized as Venn diagrams (e.g. Figure 7 – figure supplement 1) (http://bioinformatics.psb.ugent.be/webtools/Venn/).

Phylogenetic analysis and interspecies comparison

We compared the *T. castaneum* IR, GR, and OR sequences independent from each other on protein level with data from *D. melanogaster* (Martin et al. 2013; Attrill et al. 2016) and *An. gambiae* (Lawson et al. 2009; Pitts et al. 2011). The sequences were aligned using MAFFT (v7.040b (Katoh et al. 2005)) (--genafpair --maxiterate 1000 --bl 62 --op 1.53 --ep 0.123) and the phylogeny was calculated using RAxML (version 7.8.6 (Stamatakis 2006)), with the LG substitution model and GAMMA correction. Robustness of the tree topology was evaluated by 100 rapid bootstrap replications. The relative expression levels were calculated as log2 fold changes of antenna/body and palp (mouthpart)/body as described in (Dippel et al. 2014). The *D. melanogaster* data set was

downloaded from EMBL gene expression atlas (Kapushesky et al. 2011), originally published in (Farhadian et al. 2012) and the *An. gambiae* data were obtained from (Pitts et al. 2011). The phylogenetic tree was visualized by iTOL (Letunic and Bork 2007) and descriptions were added using inkscape (http://www.inkscape.org/).

Acknowledgments

We thank the transcriptome analysis laboratory (TAL) of the University Medical Center Göttingen, Germany, especially Gabriela Salinas-Riester for sequencing and technical support; Jürgen Krieger for providing a cross-reactive Orco antibody; Gregor Bucher and Michalis Averof for sharing transgenic beetle lines and plasmids; Hugh M. Robertson and Kimberly K. O. Walden for providing unpublished sequence information; Mario Stanke und Lizzy Gerischer for the iBeetle Genome Browser; Richard Smith for support on MorphoGraphiX; Martina Kern, Marlene Binzer, and Peter Christ for technical assistance; Montserrat Torres Oliva and Jan Kropf for technical advice; as well as Uwe Homberg and the members of the DFG Priority Program SPP 1392 "Integrative Analysis of Olfaction" for fruitful discussion.

Competing Interests

The authors have declared that no competing interests exist.

References

Ågren L (1985) Architecture of a lamellicorn flagellum (*Phyllopertha horticola*, scarabaeidae, coleoptera, insecta). J Morphol 186:85–94. doi: 10.1002/jmor.1051860108

Alabi T, Marion-Poll F, Danho M, et al (2013) Identification of taste receptors and proteomic characterization of the antenna and legs of *Tribolium brevicornis*, a stored food product pest. Insect Mol Biol n/a–n/a. doi: 10.1111/imb.12056

Allsopp PG (1990) Sexual Dimorphism in the Adult Antennae of *Antitrogus Parvulus* Britton and *Lepidiota Negatoria* Blackburn (coleoptera: Scarabaeidae: Melolonthinae). Aust J Entomol 29:261–266. doi: 10.1111/j.1440-6055.1990.tb00360.x

Almaas TJ, Mustaparta H (1990) Pheromone reception in tobacco budworm moth, *Heliothis virescens.* J Chem Ecol 16:1331–1347. doi: 10.1007/BF01021030

Altner H (1977) Insektensensillen: Bau und Funktionsprinzipien. Verhandlungen Dtsch Zool Ges 139–153.

Anders S, Huber W (2010) Differential expression analysis for sequence count data. Genome Biol 11:R106. doi: 10.1186/gb-2010-11-10-r106

Andersson MN, Grosse-Wilde E, Keeling CI, et al (2013) Antennal transcriptome analysis of the chemosensory gene families in the tree killing bark beetles, *Ips typographus* and *Dendroctonus ponderosae* (Coleoptera: Curculionidae: Scolytinae). BMC Genomics 14:198. doi: 10.1186/1471-2164-14-198

Andersson MN, Videvall E, Walden KK, et al (2014) Sex- and tissue-specific profiles of chemosensory gene expression in a herbivorous gall-inducing fly (Diptera: Cecidomyiidae). BMC Genomics 15:501. doi: 10.1186/1471-2164-15-501

Anton S, van Loon JJA, Meijerink J, et al (2003) Central projections of olfactory receptor neurons from single antennal and palpal sensilla in mosquitoes. Arthropod Struct Dev 32:319–327. doi: 10.1016/j.asd.2003.09.002

Attrill H, Falls K, Goodman JL, et al (2016) FlyBase: establishing a Gene Group resource for *Drosophila melanogaster*. Nucleic Acids Res 44:D786–D792. doi: 10.1093/nar/gkv1046

Belle J de, Heisenberg M (1994) Associative odor learning in *Drosophila* abolished by chemical ablation of mushroom bodies. Science 263:692–695. doi: 10.1126/science.8303280

Benton R, Vannice KS, Gomez-Diaz C, Vosshall LB (2009) Variant Ionotropic Glutamate Receptors as

Chemosensory Receptors in *Drosophila*. Cell 136:149–162. doi: 10.1016/j.cell.2008.12.001

Benton R, Vannice KS, Vosshall LB (2007) An essential role for a CD36-related receptor in pheromone detection in *Drosophila*. Nature 450:289–293. doi: 10.1038/nature06328

Berghammer A, Bucher G, Maderspacher F, Klingler M (1999a) A system to efficiently maintain embryonic lethal mutations in the flour beetle *Tribolium castaneum*. Dev Genes Evol 209:382–389.

Berghammer AJ, Klingler M, Wimmer EA (1999b) A universal marker for transgenic insects. Nature 402:370–371. doi: 10.1038/46463

Binzer M, Heuer CM, Kollmann M, et al (2014) Neuropeptidome of *Tribolium castaneum* antennal lobes and mushroom bodies. J Comp Neurol 522:337–357. doi: 10.1002/cne.23399

Boeckh J, Ernst K-D (1987) Contribution of single unit analysis in insects to an understanding of olfactory function. J Comp Physiol A 161:549–565. doi: 10.1007/BF00603661

Bohbot J, Pitts RJ, Kwon H-W, et al (2007) Molecular characterization of the *Aedes aegypti* odorant receptor gene family. Insect Mol Biol 16:525–537. doi: 10.1111/j.1365-2583.2007.00748.x

Bräunig P, Pflüger H-J, Hustert R (1983) The specificity of central nervous projections of locust mechanoreceptors. J Comp Neurol 218:197–207. doi: 10.1002/cne.902180207

Brown SJ, Shippy TD, Miller S, et al (2009) The red flour beetle, *Tribolium castaneum* (Coleoptera): a model for studies of development and pest biology. Cold Spring Harb Protoc 2009:pdb.emo126. doi: 10.1101/pdb.emo126

Bucher G, Scholten J, Klingler M (2002) Parental RNAi in *Tribolium* (Coleoptera). Curr Biol CB 12:R85-86.

Cao TNP (2014) Genome annotation and evolution of chemosensory receptors in spider mites. Dissertation, Ghent University

Caron SJC, Ruta V, Abbott LF, Axel R (2013) Random convergence of olfactory inputs in the *Drosophila* mushroom body. Nature 497:113–117. doi: 10.1038/nature12063

Chatterjee A, Roman G, Hardin PE (2009) Go contributes to olfactory reception *in Drosophila melanogaster*. BMC Physiol 9:22. doi: 10.1186/1472-6793-9-22

Chertemps T, François A, Durand N, et al (2012) A carboxylesterase, Esterase-6, modulates sensory physiological and behavioral response dynamics to pheromone in *Drosophila*. BMC Biol 10:56. doi: 10.1186/1741-7007-10-56

Chipman AD, Ferrier DEK, Brena C, et al (2014) The First Myriapod Genome Sequence Reveals Conservative Arthropod Gene Content and Genome Organisation in the Centipede *Strigamia maritima*. PLoS Biol 12:e1002005. doi: 10.1371/journal.pbio.1002005

Choo Y-M, Pelletier J, Atungulu E, Leal WS (2013) Identification and Characterization of an Antennae-Specific Aldehyde Oxidase from the Navel Orangeworm. PLoS ONE 8:e67794. doi: 10.1371/journal.pone.0067794

Chou Y-H, Spletter ML, Yaksi E, et al (2010) Diversity and wiring variability of olfactory local interneurons in the *Drosophila* antennal lobe. Nat Neurosci 13:439–449. doi: 10.1038/nn.2489

Christensen TA, Waldrop BR, Harrow ID, Hildebrand JG (1993) Local interneurons and information processing in the olfactory glomeruli of the moth *Manduca sexta*. J Comp Physiol A Neuroethol Sens Neural Behav Physiol 173:385–399. doi: 10.1007/BF00193512

Chyb S (2004) *Drosophila* gustatory receptors: from gene identification to functional expression. J Insect Physiol 50:469–477. doi: 10.1016/j.jinsphys.2004.03.012

Connolly JB, Roberts IJ, Armstrong JD, et al (1996) Associative learning disrupted by impaired Gs signaling in *Drosophila* mushroom bodies. Science 274:2104–2107.

Couto A, Alenius M, Dickson BJ (2005) Molecular, Anatomical, and Functional Organization of the

Drosophila Olfactory System. Curr Biol 15:1535–1547. doi: 10.1016/j.cub.2005.07.034

Croset V, Rytz R, Cummins SF, et al (2010) Ancient Protostome Origin of Chemosensory Ionotropic Glutamate Receptors and the Evolution of Insect Taste and Olfaction. PLoS Genet 6:e1001064. doi: 10.1371/journal.pgen.1001064

Dahanukar A, Foster K, van der Goes van Naters WM, Carlson JR (2001) A Gr receptor is required for response to the sugar trehalose in taste neurons of *Drosophila*. Nat Neurosci 4:1182–1186. doi: 10.1038/nn765

Dahanukar A, Hallem EA, Carlson JR (2005) Insect chemoreception. Curr Opin Neurobiol 15:423–430. doi: 10.1016/j.conb.2005.06.001

de Brito Sanchez MG, Giurfa M, de Paula Mota TR, Gauthier M (2005) Electrophysiological and behavioural characterization of gustatory responses to antennal "bitter" taste in honeybees. Eur J Neurosci 22:3161–3170. doi: 10.1111/j.1460-9568.2005.04516.x

de Bruyne M, Smart R, Zammit E, Warr CG (2010) Functional and molecular evolution of olfactory neurons and receptors for aliphatic esters across the *Drosophila* genus. J Comp Physiol A Neuroethol Sens Neural Behav Physiol 196:97–109.

de Bruyne M, Warr CG (2006) Molecular and cellular organization of insect chemosensory neurons. BioEssays 28:23–34. doi: 10.1002/bies.20338

Deng Y, Zhang W, Farhat K, et al (2011) The Stimulatory Gαs Protein Is Involved in Olfactory Signal Transduction in *Drosophila*. PLoS ONE 6:e18605. doi: 10.1371/journal.pone.0018605

Dicke M (2009) Behavioural and community ecology of plants that cry for help. Plant Cell Environ 32:654–665. doi: 10.1111/j.1365-3040.2008.01913.x

Dippel S, Oberhofer G, Kahnt J, et al (2014) Tissue-specific transcriptomics, chromosomal localization, and phylogeny of chemosensory and odorant binding proteins from the red flour beetle *Tribolium castaneum* reveal subgroup specificities for olfaction or more general functions. BMC Genomics 15:1141. doi: 10.1186/1471-2164-15-1141

Dreyer (2010) 3D standard brain of the red flour beetle *Tribolium castaneum*: a tool to study metamorphic development and adult plasticity. Front Syst Neurosci. doi: 10.3389/neuro.06.003.2010

Dreyer D, Vitt H, Dippel S, et al (2010) 3D Standard Brain of the Red Flour Beetle *Tribolium castaneum*: A Tool to Study Metamorphic Development and Adult Plasticity. Front Syst Neurosci 4:3. doi: 10.3389/neuro.06.003.2010

Dunipace L, Meister S, McNealy C, Amrein H (2001) Spatially restricted expression of candidate taste receptors in the *Drosophila* gustatory system. Curr Biol 11:822–835. doi: 10.1016/S0960-9822(01)00258-5

Durand N, Carot-Sans G, Bozzolan F, et al (2011) Degradation of Pheromone and Plant Volatile Components by a Same Odorant-Degrading Enzyme in the Cotton Leafworm, Spodoptera littoralis. PLoS ONE 6:e29147. doi: 10.1371/journal.pone.0029147

Engsontia P, Sanderson AP, Cobb M, et al (2008) The red flour beetle's large nose: an expanded odorant receptor gene family in *Tribolium castaneum*. Insect Biochem Mol Biol 38:387–397. doi: 10.1016/j.ibmb.2007.10.005

Enjin A, Zaharieva EE, Frank DD, et al (2016) Humidity Sensing in *Drosophila*. Curr Biol. doi: 10.1016/j.cub.2016.03.049

Ernst DKD, Boeckh J, Boeckh V (1977) A neuroanatomical study on the organization of the central antennal pathways in insects. Cell Tissue Res 176:285–308. doi: 10.1007/BF00221789

Esslen J, Kaissling K-E (1976) Zahl und Verteilung antennaler Sensillen bei der Honigbiene (*Apis mellifera* L.). Zoomorphologie 83:227–251. doi: 10.1007/BF00993511

Farhadian SF, Suárez-Fariñas M, Cho CE, et al (2012) Post-fasting olfactory, transcriptional, and feeding responses in *Drosophila*. Physiol Behav 105:544–553. doi: 10.1016/j.physbeh.2011.09.007

Farris SM (2008) Tritocerebral tract input to the insect mushroom bodies. Arthropod Struct Dev 37:492–503. doi: 10.1016/j.asd.2008.05.005

Farris SM, Roberts NS (2005) Coevolution of generalist feeding ecologies and gyrencephalic mushroom bodies in insects. Proc Natl Acad Sci U S A 102:17394–17399. doi: 10.1073/pnas.0508430102

Fishilevich E, Vosshall LB (2005) Genetic and Functional Subdivision of the *Drosophila* Antennal Lobe. Curr Biol 15:1548–1553. doi: 10.1016/j.cub.2005.07.066

Flook PK, Klee S, Rowell CHF (1999) Combined Molecular Phylogenetic Analysis of the Orthoptera (Arthropoda, Insecta) and Implications for Their Higher Systematics. Syst Biol 48:233–253. doi: 10.1080/106351599260274

Foret S, Maleszka R (2006) Function and evolution of a gene family encoding odorant binding-like proteins in a social insect, the honey bee (*Apis mellifera*). Genome Res 16:1404–1413. doi: 10.1101/gr.5075706

Forêt S, Wanner KW, Maleszka R (2007) Chemosensory proteins in the honey bee: Insights from the annotated genome, comparative analyses and expressional profiling. Insect Biochem Mol Biol 37:19–28. doi: 10.1016/j.ibmb.2006.09.009

Forstner M, Gohl T, Gondesen I, et al (2008) Differential expression of SNMP-1 and SNMP-2 proteins in pheromone-sensitive hairs of moths. Chem Senses 33:291–299. doi: 10.1093/chemse/bjm087

Frambach I, Schürmann FW (2004) Separate distribution of deutocerebral projection neurons in the mushroom bodies of the cricket brain. Acta Biol Hung 55:21–29. doi: 10.1556/ABiol.55.2004.1-4.4

Frasnelli E, Anfora G, Trona F, et al (2010) Morpho-functional asymmetry of the olfactory receptors of the honeybee (*Apis mellifera*). Behav Brain Res 209:221–225. doi: 10.1016/j.bbr.2010.01.046

Freeman EG, Wisotsky Z, Dahanukar A (2014) Detection of sweet tastants by a conserved group of insect gustatory receptors. Proc Natl Acad Sci 201311724. doi: 10.1073/pnas.1311724111

Galizia CG, Joerges J, Küttner A, et al (1997) A semi-in-vivo preparation for optical recording of the insect brain. J Neurosci Methods 76:61–69.

Galizia CG, Rössler W (2010) Parallel Olfactory Systems in Insects: Anatomy and Function. Annu Rev Entomol 55:399–420. doi: 10.1146/annurev-ento-112408-085442

Galizia CG, Sachse S, Rappert A, Menzel R (1999) The glomerular code for odor representation is species specific in the honeybee *Apis mellifera*. Nat Neurosci 2:473–478. doi: 10.1038/8144

Gentleman RC, Carey VJ, Bates DM, et al (2004) Bioconductor: open software development for computational biology and bioinformatics. Genome Biol 5:R80. doi: 10.1186/gb-2004-5-10-r80

German PF, van der Poel S, Carraher C, et al (2013) Insights into subunit interactions within the insect olfactory receptor complex using FRET. Insect Biochem Mol Biol 43:138–145. doi: 10.1016/j.ibmb.2012.11.002

Getahun MN, Olsson SB, Lavista-Llanos S, et al (2013) Insect Odorant Response Sensitivity Is Tuned by Metabotropically Autoregulated Olfactory Receptors. PLoS ONE 8:e58889. doi: 10.1371/journal.pone.0058889

Ghaninia M, Hansson BS, Ignell R (2007) The antennal lobe of the African malaria mosquito, *Anopheles gambiae* - innervation and three-dimensional reconstruction. Arthropod Struct Dev 36:23–39. doi: 10.1016/j.asd.2006.06.004

Goldman AL, Van der Goes van Naters W, Lessing D, et al (2005) Coexpression of Two Functional Odor Receptors in One Neuron. Neuron 45:661–666. doi: 10.1016/j.neuron.2005.01.025

Good NE (1936) The Flour Beetles of the Genus *Tribolium*. United States Department of Agriculture

Grabe V, Strutz A, Baschwitz A, et al (2015) Digital in vivo 3D atlas of the antennal lobe of *Drosophila melanogaster*. J Comp Neurol 523:530–544. doi: 10.1002/cne.23697

Grabherr MG, Haas BJ, Yassour M, et al (2011) Full-length transcriptome assembly from RNA-Seq data without a reference genome. Nat Biotechnol 29:644–652. doi: 10.1038/nbt.1883

Greenwood M, Chapman RF (1984) Differences in numbers of sensilla on the antennae of solitarious and gregarious *Locusta migratoria* L. (Orthoptera: Acrididae). Int J Insect Morphol Embryol 13:295–301. doi: 10.1016/0020-7322(84)90004-7

Groh C, Lu Z, Meinertzhagen IA, Rössler W (2012) Age-related plasticity in the synaptic ultrastructure of neurons in the mushroom body calyx of the adult honeybee *Apis mellifera*. J Comp Neurol 520:3509–3527. doi: 10.1002/cne.23102

Grosse-Wilde E, Stieber R, Forstner M, et al (2010) Sex-specific odorant receptors of the tobacco hornworm *Manduca sexta*. Front Cell Neurosci 4:22. doi: 10.3389/fncel.2010.00022

Gu X-C, Zhang Y-N, Kang K, et al (2015) Antennal Transcriptome Analysis of Odorant Reception Genes in the Red Turpentine Beetle (RTB), *Dendroctonus valens*. PloS One 10:e0125159. doi: 10.1371/journal.pone.0125159

Harbach RE, Larsen JR (1977) Fine structure of antennal sensilla of the adult mealworm beetle, *Tenebrio molitor* L. (Coleoptera : Tenebrionidae). Int J Insect Morphol Embryol 6:41–60. doi: 10.1016/0020-7322(77)90029-0

Hartl M, Loschek LF, Stephan D, et al (2011) A new Prospero and microRNA-279 pathway restricts CO_2 receptor neuron formation. J Neurosci Off J Soc Neurosci 31:15660–15673. doi: 10.1523/JNEUROSCI.2592-11.2011

Heimbeck G, Bugnon V, Gendre N, et al (2001) A central neural circuit for experience-independent olfactory and courtship behavior in *Drosophila melanogaster*. Proc Natl Acad Sci 98:15336–15341. doi: 10.1073/pnas.011314898

Hill SR, Hansson BS, Ignell R (2009) Characterization of antennal trichoid sensilla from female southern house mosquito, *Culex quinquefasciatus* Say. Chem Senses 34:231–252. doi: 10.1093/chemse/bjn080

Hinke DW (1961) Das relative postembryonale Wachstum der Hirnteile von *Culex pipiens*, *Drosophila melanogaster* und *Drosophila-mutanten*. Z Für Morphol Ökol Tiere 50:81–118. doi: 10.1007/BF00407351

Hodges TK, Cosme LV, Athrey G, et al (2014) Species-specific chemosensory gene expression in the olfactory organs of the malaria vector *Anopheles gambiae*. BMC Genomics 15:1089. doi: 10.1186/1471-2164-15-1089

Hofer S, Dircksen H, Tollbäck P, Homberg U (2005) Novel insect orcokinins: Characterization and neuronal distribution in the brains of selected dicondylian insects. J Comp Neurol 490:57–71. doi: 10.1002/cne.20650

Homberg U, Christensen TA, Hildebrand JG (1989) Structure and function of the deutocerebrum in insects. Annu Rev Entomol 34:477–501.

Horn C, Offen N, Nystedt S, et al (2003) piggyBac-Based Insertional Mutagenesis and Enhancer Detection as a Tool for Functional Insect Genomics. Genetics 163:647–661.

Horn C, Wimmer EA (2000) A versatile vector set for animal transgenesis. Dev Genes Evol 210:630–637.

http://www.inkscape.org/ Inkscape.

Hu J-H, Wang Z-Y, Sun F (2011) Anatomical organization of antennal-lobe glomeruli in males and females of the scarab beetle *Holotrichia diomphalia* (Coleoptera: Melolonthidae). Arthropod Struct Dev 40:420–428. doi: 10.1016/j.asd.2011.03.003

Hunt T, Bergsten J, Levkanicova Z, et al (2007) A comprehensive phylogeny of beetles reveals the evolutionary origins of a superradiation. Science 318:1913–1916. doi: 10.1126/science.1146954

Ignatious Raja JS, Katanayeva N, Katanaev VL, Galizia CG (2014) Role of Go/i subgroup of G proteins in olfactory signaling of *Drosophila melanogaster*. Eur J Neurosci 39:1245–1255. doi: 10.1111/ejn.12481

Ignell R, Anton S, Hansson BS (2001) The antennal lobe of orthoptera - anatomy and evolution. Brain Behav Evol 57:1–17. doi: 47222

Ignell R, Anton S, Hansson BS (2000) The maxillary palp sensory pathway of Orthoptera. Arthropod Struct Dev 29:295–305. doi: 10.1016/S1467-8039(01)00016-0

Ignell R, Dekker T, Ghaninia M, Hansson BS (2005) Neuronal architecture of the mosquito deutocerebrum. J Comp Neurol 493:207–240. doi: 10.1002/cne.20800

Ishida Y, Leal WS (2005) Rapid inactivation of a moth pheromone. Proc Natl Acad Sci U S A 102:14075–14079. doi: 10.1073/pnas.0505340102

Ishida Y, Leal WS (2008) Chiral discrimination of the Japanese beetle sex pheromone and a behavioral antagonist by a pheromone-degrading enzyme. Proc Natl Acad Sci 105:9076–9080. doi: 10.1073/pnas.0802610105

Ishimoto H, Takahashi K, Ueda R, Tanimura T (2005) G-protein gamma subunit 1 is required for sugar reception in *Drosophila*. EMBO J 24:3259–3265. doi: 10.1038/sj.emboj.7600796

Jacquin-Joly E, Legeai F, Montagné N, et al (2012) Candidate chemosensory genes in female antennae of the noctuid moth *Spodoptera littoralis*. Int J Biol Sci 8:1036–1050. doi: 10.7150/ijbs.4469

Jefferis GSXE (2005) Insect Olfaction: A Map of Smell in the Brain. Curr Biol 15:R668–R670. doi: 10.1016/j.cub.2005.08.033

Jefferis GSXE, Potter CJ, Chan AM, et al (2007) Comprehensive Maps of *Drosophila* Higher Olfactory Centers: Spatially Segregated Fruit and Pheromone Representation. Cell 128:1187–1203. doi: 10.1016/j.cell.2007.01.040

Jiao Y, Moon SJ, Wang X, et al (2008) Gr64f is required in combination with other gustatory receptors for sugar detection in *Drosophila*. Curr Biol CB 18:1797–1801. doi: 10.1016/j.cub.2008.10.009

Jin X, Ha TS, Smith DP (2008) SNMP is a signaling component required for pheromone sensitivity in *Drosophila*. Proc Natl Acad Sci U S A 105:10996–11001. doi: 10.1073/pnas.0803309105

Jones WD, Cayirlioglu P, Kadow IG, Vosshall LB (2007) Two chemosensory receptors together mediate carbon dioxide detection in *Drosophila*. Nature 445:86–90. doi: 10.1038/nature05466

Jones WD, Nguyen T-AT, Kloss B, et al (2005) Functional conservation of an insect odorant receptor gene across 250 million years of evolution. Curr Biol 15:R119–R121. doi: 10.1016/j.cub.2005.02.007

Jourdan H, Barbier R, Bernard J, Ferran A (1995) Antennal sensilla and sexual dimorphism of the adult ladybird beetle *Semiadalia undecimnotata* Schn. (Coleoptera: Coccinellidae). Int J Insect Morphol Embryol 24:307–322. doi: 10.1016/0020-7322(95)98584-Z

Kapushesky M, Adamusiak T, Burdett T, et al (2011) Gene Expression Atlas update-a value-added database of microarray and sequencing-based functional genomics experiments. Nucleic Acids Res 40:D1077–D1081. doi: 10.1093/nar/gkr913

Katoh K, Kuma K, Toh H, Miyata T (2005) MAFFT version 5: improvement in accuracy of multiple sequence alignment. Nucleic Acids Res 33:511–518. doi: 10.1093/nar/gki198

Kaupp UB (2010) Olfactory signalling in vertebrates and insects: differences and commonalities. Nat Rev Neurosci. doi: 10.1038/nrn2789

Keil TA (1989) Fine structure of the pheromone-sensitive sensilla on the antenna of the hawkmoth, *Manduca sexta*. Tissue Cell 21:139–151. doi: 10.1016/0040-8166(89)90028-1

Keller A, Vosshall LB (2003) Decoding olfaction in *Drosophila*. Curr Opin Neurobiol 13:103–110. doi: 10.1016/S0959-4388(03)00011-4

Kent KS, Harrow ID, Quartararo P, Hildebrand DJG (1986) An accessory olfactory pathway in Lepidoptera: the labial pit organ and its central projections in *Manduca sexta* and certain other sphinx moths and silk moths. Cell Tissue Res 245:237–245. doi: 10.1007/BF00213927

Kent LB, Robertson HM (2009) Evolution of the sugar receptors in insects. BMC Evol Biol 9:41. doi: 10.1186/1471-2148-9-41

Kent WJ (2002) BLAT—The BLAST-Like Alignment Tool. Genome Res 12:656–664. doi: 10.1101/gr.229202

Kim HS, Murphy T, Xia J, et al (2010) BeetleBase in 2010: revisions to provide comprehensive genomic information for *Tribolium castaneum*. Nucleic Acids Res 38:D437-442. doi: 10.1093/nar/gkp807

Klagges BRE, Heimbeck G, Godenschwege TA, et al (1996) Invertebrate Synapsins: A Single Gene Codes for Several Isoforms in *Drosophila*. J Neurosci 16:3154–3165.

Kleineidam CJ, Obermayer M, Halbich W, Rössler W (2005) A macroglomerulus in the antennal lobe of leaf-cutting ant workers and its possible functional significance. Chem Senses 30:383–392. doi: 10.1093/chemse/bji033

Kollmann M, Rupenthal AL, Neumann P, et al (2015) Novel antennal lobe substructures revealed in the small hive beetle *Aethina tumida*. Cell Tissue Res 363:679–692. doi: 10.1007/s00441-015-2282-9

Kondoh Y, Kaneshiro KY, Kimura K, Yamamoto D (2003) Evolution of sexual dimorphism in the olfactory brain of Hawaiian *Drosophila*. Proc Biol Sci 270:1005–1013. doi: 10.1098/rspb.2003.2331

Koontz MA, Schneider D (1987) Sexual dimorphism in neuronal projections from the antennae of silk moths (*Bombyx mori, Antheraea polyphemus*) and the gypsy moth (*Lymantria dispar*). Cell Tissue Res 249:39–50. doi: 10.1007/BF00215416

Krieger J (2003) A candidate olfactory receptor subtype highly conserved across different insect orders. J Comp Physiol A Neuroethol Sens Neural Behav Physiol 189:519–26. doi: 10.1007/s00359-003-0427-x

Kurylas AE, Rohlfing T, Krofczik S, et al (2008) Standardized atlas of the brain of the desert locust, *Schistocerca gregaria*. Cell Tissue Res 333:125–145. doi: 10.1007/s00441-008-0620-x

Kwon JY, Dahanukar A, Weiss LA, Carlson JR (2007) The molecular basis of CO_2 reception in *Drosophila*. Proc Natl Acad Sci U S A 104:3574–3578. doi: 10.1073/pnas.0700079104

Langmead B, Salzberg SL (2012) Fast gapped-read alignment with Bowtie 2. Nat Methods 9:357–359. doi: 10.1038/nmeth.1923

Laska M, Galizia CG, Giurfa M, Menzel R (1999) Olfactory discrimination ability and odor structure-activity relationships in honeybees. Chem Senses 24:429–438.

Laurent G, Naraghi M (1994) Odorant-induced oscillations in the mushroom bodies of the locust. J Neurosci Off J Soc Neurosci 14:2993–3004.

Lawson D, Arensburger P, Atkinson P, et al (2009) VectorBase: a data resource for invertebrate vector genomics. Nucleic Acids Res 37:D583–D587. doi: 10.1093/nar/gkn857

Leal WS (2013) Odorant Reception in Insects: Roles of Receptors, Binding Proteins, and Degrading Enzymes. Annu Rev Entomol 58:373–391. doi: 10.1146/annurev-ento-120811-153635

Lee JK, Strausfeld NJ (1990) Structure, distribution and number of surface sensilla and their receptor cells on the olfactory appendage of the male mothManduca sexta. J Neurocytol 19:519–538. doi: 10.1007/BF01257241

Lee Y, Moon SJ, Montell C (2009) Multiple gustatory receptors required for the caffeine response in *Drosophila*. Proc Natl Acad Sci 106:4495–4500. doi: 10.1073/pnas.0811744106

Leiss F, Groh C, Butcher NJ, et al (2009) Synaptic organization in the adult *Drosophila* mushroom body calyx. J Comp Neurol 517:808–824. doi: 10.1002/cne.22184

Leitch O, Papanicolaou A, Lennard C, et al (2015) Chemosensory genes identified in the antennal transcriptome of the blowfly *Calliphora stygia*. BMC Genomics 16:255. doi: 10.1186/s12864-015-1466-8

Letunic I, Bork P (2007) Interactive Tree Of Life (iTOL): an online tool for phylogenetic tree display and annotation. Bioinformatics 23:127–128. doi: 10.1093/bioinformatics/btl529

Li H, Handsaker B, Wysoker A, et al (2009) The Sequence Alignment/Map format and SAMtools. Bioinformatics 25:2078–2079. doi: 10.1093/bioinformatics/btp352

Li Z, Ni JD, Huang J, Montell C (2014) Requirement for *Drosophila* SNMP1 for rapid activation and termination of pheromone-induced activity. PLoS Genet 10:e1004600. doi: 10.1371/journal.pgen.1004600

Linz J, Baschwitz A, Strutz A, et al (2013) Host plant-driven sensory specialization in *Drosophila erecta*. Proc R Soc Lond B Biol Sci 280:20130626. doi: 10.1098/rspb.2013.0626

Liu M, Yu H, Li G (2008) Oviposition deterrents from eggs of the cotton bollworm, *Helicoverpa armigera* (Lepidoptera: Noctuidae): chemical identification and analysis by electroantennogram. J Insect Physiol 54:656–662. doi: 10.1016/j.jinsphys.2008.01.002

Lorenzen MD, Berghammer AJ, Brown SJ, et al (2003) piggyBac-mediated germline transformation in the beetle *Tribolium castaneum*. Insect Mol Biol 12:433–440.

Lu T, Qiu YT, Wang G, et al (2007) Odor Coding in the Maxillary Palp of the Malaria Vector Mosquito *Anopheles gambiae*. Curr Biol CB 17:1533–1544. doi: 10.1016/j.cub.2007.07.062

Maglott D, Ostell J, Pruitt KD, Tatusova T (2007) Entrez Gene: gene-centered information at NCBI. Nucleic Acids Res 35:D26-31. doi: 10.1093/nar/gkl993

Maïbèche-Coisne M, Nikonov AA, Ishida Y, et al (2004) Pheromone anosmia in a scarab beetle induced by in vivo inhibition of a pheromone-degrading enzyme. Proc Natl Acad Sci U S A 101:11459–11464. doi: 10.1073/pnas.0403537101

Marchler-Bauer A, Lu S, Anderson JB, et al (2011) CDD: a Conserved Domain Database for the functional annotation of proteins. Nucleic Acids Res 39:D225-229. doi: 10.1093/nar/gkq1189

Martin F, Alcorta E (2011) Regulation of olfactory transduction in the orco channel. Front Cell Neurosci 5:21. doi: 10.3389/fncel.2011.00021

Martin F, Boto T, Gomez-Diaz C, Alcorta E (2013) Elements of Olfactory Reception in Adult *Drosophila melanogaster*. Anat Rec 296:1477–1488. doi: 10.1002/ar.22747

McIver S (1978) Structure of sensilla trichodea of female *Aedes aegypti* with comments on innervation of antennal sensilla. J Insect Physiol 24:383–390. doi: 10.1016/0022-1910(78)90079-3

Missbach C, Dweck HK, Vogel H, et al (2014) Evolution of insect olfactory receptors. eLife. doi: 10.7554/eLife.02115

Miura N, Atsumi S, Tabunoki H, Sato R (2005) Expression and localization of three G protein α subunits, Go, Gq, and Gs, in adult antennae of the silkmoth (*Bombyx mori*). J Comp Neurol 485:143–152. doi: 10.1002/cne.20488

Miyazaki T, Ito K (2010) Neural architecture of the primary gustatory center of *Drosophila melanogaster* visualized with GAL4 and LexA enhancer-trap systems. J Comp Neurol 518:4147–4181. doi: 10.1002/cne.22433

Mobbs PG (1982) The Brain of the Honeybee *Apis Mellifera*. I. The Connections and Spatial Organization of the Mushroom Bodies. Philos Trans R Soc Lond B Biol Sci 298:309–354. doi: 10.1098/rstb.1982.0086

Montell C (2009) A Taste of the *Drosophila* Gustatory Receptors. Curr Opin Neurobiol 19:345–353. doi: 10.1016/j.conb.2009.07.001

Morris SC (2007) Grimaldi, D. & Engel, M. S. 2005. Evolution of the Insects. xv + 755 pp. Cambridge, New York, Melbourne: Cambridge University Press. ISBN 0 521 82149 5. Geol Mag 144:1035–1036. doi: 10.1017/S001675680700372X

Mukunda L, Lavista-Llanos S, Hansson BS, Wicher D (2014) Dimerisation of the *Drosophila* odorant coreceptor Orco. Front Cell Neurosci 8:261. doi: 10.3389/fncel.2014.00261

Münch D, Galizia CG (2016) DoOR 2.0 - Comprehensive Mapping of *Drosophila melanogaster* Odorant Responses. Sci Rep 6:21841. doi: 10.1038/srep21841

Neder R (1957) Allometrisches Wachstum von Hirnteilen bei drei verschieden grossen Schabenarten (Doctoral dissertation).

Ni L, Bronk P, Chang EC, et al (2013) A gustatory receptor paralogue controls rapid warmth avoidance in *Drosophila*. Nature 500:580–584. doi: 10.1038/nature12390

Nichols Z, Vogt RG (2008) The SNMP/CD36 gene family in Diptera, Hymenoptera and Coleoptera: *Drosophila melanogaster*, *D. pseudoobscura*, *Anopheles gambiae*, *Aedes aegypti*, *Apis mellifera*, and *Tribolium castaneum*. Insect Biochem Mol Biol 38:398–415. doi: 10.1016/j.ibmb.2007.11.003

Nishino H, Nishikawa M, Yokohari F, Mizunami M (2005) Dual, multilayered somatosensory maps formed by antennal tactile and contact chemosensory afferents in an insect brain. J Comp Neurol 493:291–308. doi: 10.1002/cne.20757

Nolte A, Funk NW, Mukunda L, et al (2013) In situ Tip-Recordings Found No Evidence for an Orco-Based Ionotropic Mechanism of Pheromone-Transduction in *Manduca sexta*. PLoS ONE 8:e62648. doi: 10.1371/journal.pone.0062648

Okada K, Mori M, Shimazaki K, Chuman T (1992) Morphological Studies on the Antennal Sensilla of the Cigarette Beetle, *Lasioderma serricorne* (F.) (Coleoptera: Anobiidae). Appl Entomol Zool 27:269–276. doi: 10.1303/aez.27.269

Paczkowski S, Paczkowska M, Dippel S, et al (2014) Volatile Combustion Products of Wood Attract *Acanthocnemus nigricans* (Coleoptera: Acanthocnemidae). J Insect Behav 27:228–238. doi: 10.1007/s10905-013-9430-4

Pavlidis P, Noble WS (2003) Matrix2png: a utility for visualizing matrix data. Bioinformatics 19:295–296. doi: 10.1093/bioinformatics/19.2.295

Pellegrino M, Nakagawa T, Vosshall LB (2010) Single Sensillum Recordings in the Insects *Drosophila melanogaster* and *Anopheles gambiae*. J Vis Exp. doi: 10.3791/1725

Pelletier J, Bozzolan F, Solvar M, et al (2007) Identification of candidate aldehyde oxidases from the silkworm *Bombyx mori* potentially involved in antennal pheromone degradation. Gene 404:31–40. doi: 10.1016/j.gene.2007.08.022

Pelosi P, Iovinella I, Felicioli A, Dani FR (2014) Soluble proteins of chemical communication: an overview across arthropods. Integr Physiol 5:320. doi: 10.3389/fphys.2014.00320

Petersen TN, Brunak S, von Heijne G, Nielsen H (2011) SignalP 4.0: discriminating signal peptides from transmembrane regions. Nat Methods 8:785–786. doi: 10.1038/nmeth.1701

Pitts RJ, Rinker DC, Jones PL, et al (2011) Transcriptome profiling of chemosensory appendages in the malaria vector *Anopheles gambiae* reveals tissue- and sex-specific signatures of odor coding. BMC Genomics 12:271. doi: 10.1186/1471-2164-12-271

Pitts RJ, Zwiebel LJ (2006) Antennal sensilla of two female anopheline sibling species with differing host ranges. Malar J 5:26. doi: 10.1186/1475-2875-5-26

Popescu A, Couton L, Almaas T-J, et al (2013) Function and central projections of gustatory receptor neurons on the antenna of the noctuid moth *Spodoptera littoralis*. J Comp Physiol A 199:403–416. doi: 10.1007/s00359-013-0803-0

Posnien N, Koniszewski NDB, Hein HJ, Bucher G (2011) Candidate Gene Screen in the Red Flour Beetle *Tribolium* Reveals Six3 as Ancient Regulator of Anterior Median Head and Central Complex Development. PLoS Genet. doi: 10.1371/journal.pgen.1002416

Pruitt KD, Tatusova T, Maglott DR (2007) NCBI reference sequences (RefSeq): a curated non-redundant sequence database of genomes, transcripts and proteins. Nucleic Acids Res 35:D61-65. doi: 10.1093/nar/gkl842

Qiu YT, Loon JJA van, Takken W, et al (2006) Olfactory Coding in Antennal Neurons of the Malaria Mosquito, *Anopheles gambiae*. Chem Senses 31:845–863. doi: 10.1093/chemse/bjl027

R Core Team (2013) R: A Language and Environment for Statistical Computing. http://www.R-project.org. Accessed 11 Nov 2013

Ramaswamy SB (1987) Behavioural responses of *Heliothis virescens* (Lepidoptera: Noctuidae) to stimulation with sugars. J Insect Physiol 33:755–760. doi: 10.1016/0022-1910(87)90062-X

Reuille PB de, Routier-Kierzkowska A-L, Kierzkowski D, et al (2015) MorphoGraphX: A platform for quantifying morphogenesis in 4D. eLife 4:e05864. doi: 10.7554/eLife.05864

Richards S, Gibbs RA, Weinstock GM, et al (2008) The genome of the model beetle and pest *Tribolium castaneum*. Nature 452:949–955. doi: 10.1038/nature06784

Ridley AW, Hereward JP, Daglish GJ, et al (2011) The spatiotemporal dynamics of *Tribolium castaneum* (Herbst): adult flight and gene flow. Mol Ecol 20:1635–1646. doi: 10.1111/j.1365-294X.2011.05049.x

Riesgo-Escovar J, Raha D, Carlson JR (1995) Requirement for a phospholipase C in odor response: overlap between olfaction and vision in *Drosophila*. Proc Natl Acad Sci 92:2864–2868. doi: 10.1073/pnas.92.7.2864

Rinker DC, Pitts RJ, Zhou X, et al (2013) Blood meal-induced changes to antennal transcriptome profiles reveal shifts in odor sensitivities in *Anopheles gambiae*. Proc Natl Acad Sci U S A 110:8260–8265. doi: 10.1073/pnas.1302562110

Rinker DC, Zhou X, Pitts RJ, et al (2015) RNAseq in the mosquito maxillary palp: a little antennal RNA goes a long way. bioRxiv 16998. doi: 10.1101/016998

Robertson HM, Kent LB (2009) Evolution of the gene lineage encoding the carbon dioxide receptor in insects. J Insect Sci Online 9:19. doi: 10.1673/031.009.1901

Robertson HM, Wanner KW (2006) The chemoreceptor superfamily in the honey bee, *Apis mellifera*: Expansion of the odorant, but not gustatory, receptor family. Genome Res 16:1395–1403. doi: 10.1101/gr.5057506

Rogers ME, Jani MK, Vogt RG (1999) An olfactory-specific glutathione-S-transferase in the sphinx moth *Manduca sexta*. J Exp Biol 202:1625–1637.

Rospars JP, Hildebrand JG (2000) Sexually Dimorphic and Isomorphic Glomeruli in the Antennal Lobes of the Sphinx *Moth Manduca* sexta. Chem Senses 25:119–129. doi: 10.1093/chemse/25.2.119

Roth LM, Willis ER (1951) Hygroreceptors in adults of *Tribolium* (coleoptera, tenebrionidae). J Exp Zool 116:527–570. doi: 10.1002/jez.1401160309

Ruther J, Reinecke A, Thiemann K, et al (2000) Mate finding in the forest cockchafer, *Melolontha hippocastani*, mediated by volatiles from plants and females. Physiol Entomol 25:172–179. doi: 10.1046/j.1365-3032.2000.00183.x

Rybczynski R, Vogt RG, Lerner MR (1990) Antennal-specific pheromone-degrading aldehyde oxidases from the moths *Antheraea polyphemus* and *Bombyx mori*. J Biol Chem 265:19712–19715.

Rytz R, Croset V, Benton R (2013) Ionotropic receptors (IRs): chemosensory ionotropic glutamate receptors in *Drosophila* and beyond. Insect Biochem Mol Biol 43:888–897. doi: 10.1016/j.ibmb.2013.02.007

Sánchez-Gracia A, Vieira FG, Almeida FC, Rozas J (2001) Comparative Genomics of the Major Chemosensory Gene Families in Arthropods. In: eLS. John Wiley & Sons, Ltd,

Santos JG, Pollák E, Rexer K-H, et al (2006) Morphology and metamorphosis of the peptidergic Va neurons and the median nerve system of the fruit fly, *Drosophila melanogaster*. Cell Tissue Res 326:187–199. doi: 10.1007/s00441-006-0211-7

Sargsyan V, Getahun MN, Llanos SL, et al (2011) Phosphorylation via PKC Regulates the Function of the *Drosophila* Odorant Co-Receptor. Front Cell Neurosci. doi: 10.3389/fncel.2011.00005

Sato K, Pellegrino M, Nakagawa T, et al (2008) Insect olfactory receptors are heteromeric ligand-gated ion channels. Nature 452:1002–1006. doi: 10.1038/nature06850

Sato K, Tanaka K, Touhara K (2011) Sugar-regulated cation channel formed by an insect gustatory receptor. Proc Natl Acad Sci 108:11680–11685. doi: 10.1073/pnas.1019622108

Schachtner J, Schmidt M, Homberg U (2005) Organization and evolutionary trends of primary olfactory brain centers in Tetraconata (Crustacea+Hexapoda). Arthropod Struct Dev 34:257–299. doi: 10.1016/j.asd.2005.04.003

Schindelin J, Arganda-Carreras I, Frise E, et al (2012) Fiji: an open-source platform for biological-image analysis. Nat Methods 9:676–682. doi: 10.1038/nmeth.2019

Schinko JB, Hillebrand K, Bucher G (2012) Heat shock-mediated misexpression of genes in the beetle *Tribolium castaneum*. Dev Genes Evol 222:287–298. doi: 10.1007/s00427-012-0412-x

Schinko JB, Weber M, Viktorinova I, et al (2010) Functionality of the GAL4/UAS system in *Tribolium* requires the use of endogenous core promoters. BMC Dev Biol 10:53. doi: 10.1186/1471-213X-10-53

Schmitt-Engel C, Schultheis D, Schwirz J, et al (2015) The iBeetle large-scale RNAi screen reveals gene functions for insect development and physiology. Nat Commun 6:7822. doi: 10.1038/ncomms8822

Scott K, Brady R Jr, Cravchik A, et al (2001) A chemosensory gene family encoding candidate gustatory and olfactory receptors in *Drosophila*. Cell 104:661–673.

Seki Y, Rybak J, Wicher D, et al (2010) Physiological and Morphological Characterization of Local Interneurons in the *Drosophila* Antennal Lobe. J Neurophysiol 104:1007–1019. doi: 10.1152/jn.00249.2010

Serrano JM, Castro L, Toro MA, López-Fanjul C (1991) The genetic properties of homosexual copulation behavior in *Tribolium castaneum*: diallel analysis. Behav Genet 21:547–558.

Shanbhag SR, Müller B, Steinbrecht RA (1999) Atlas of olfactory organs of *Drosophila melanogaster*: 1. Types, external organization, innervation and distribution of olfactory sensilla. Int J Insect Morphol Embryol 28:377–397. doi: 10.1016/S0020-7322(99)00039-2

Shi H, Pei L, Gu S, et al (2012) Glutathione S-transferase (GST) genes in the red flour beetle, *Tribolium castaneum*, and comparative analysis with five additional insects. Genomics 100:327–335. doi: 10.1016/j.ygeno.2012.07.010

Siebert KS, Lorenzen MD, Brown SJ, et al (2008) Tubulin superfamily genes in *Tribolium castaneum* and the use of a Tubulin promoter to drive transgene expression. Insect Biochem Mol Biol 38:749–755. doi: 10.1016/j.ibmb.2008.04.007

Smart R, Kiely A, Beale M, et al (2008) *Drosophila* odorant receptors are novel seven transmembrane domain proteins that can signal independently of heterotrimeric G proteins. Insect Biochem Mol Biol 38:770–780. doi: 10.1016/j.ibmb.2008.05.002

Smith C (2008) Biology of Sensory Systems. John Wiley & Sons

Solari P, Corda V, Sollai G, et al (2016) Morphological characterization of the antennal lobes in the Mediterranean fruit fly Ceratitis capitata. J Comp Physiol A Neuroethol Sens Neural Behav Physiol 202:131–146. doi: 10.1007/s00359-015-1059-7

Sparks JT, Bohbot JD, Dickens JC (2014) The genetics of chemoreception in the labella and tarsi of *Aedes aegypti*. Insect Biochem Mol Biol 48:8–16. doi: 10.1016/j.ibmb.2014.02.004

Stamatakis A (2006) RAxML-VI-HPC: maximum likelihood-based phylogenetic analyses with thousands of taxa and mixed models. Bioinforma Oxf Engl 22:2688–2690. doi: 10.1093/bioinformatics/btl446

Steinbrecht RA (1996) Structure and function of insect olfactory sensilla. Ciba Found Symp 200:158-174-177.

Stengl M, Funk NW (2013) The role of the coreceptor Orco in insect olfactory transduction. J Comp Physiol A 199:897–909. doi: 10.1007/s00359-013-0837-3

Stensmyr MC, Dweck HKM, Farhan A, et al (2012) A Conserved Dedicated Olfactory Circuit for Detecting Harmful Microbes in *Drosophila*. Cell 151:1345–1357. doi: 10.1016/j.cell.2012.09.046

Stocker RF (2001) *Drosophila* as a focus in olfactory research: mapping of olfactory sensilla by fine

structure, odor specificity, odorant receptor expression, and central connectivity. Microsc Res Tech 55:284–296. doi: 10.1002/jemt.1178

Strausfeld NJ (2002) Organization of the honey bee mushroom body: representation of the calyx within the vertical and gamma lobes. J Comp Neurol 450:4–33. doi: 10.1002/cne.10285

Strutz A, Soelter J, Baschwitz A, et al (2014) Decoding odor quality and intensity in the *Drosophila* brain. eLife 3:e04147. doi: 10.7554/eLife.04147

Sun Y-L, Huang L-Q, Pelosi P, Wang C-Z (2012) Expression in Antennae and Reproductive Organs Suggests a Dual Role of an Odorant-Binding Protein in Two Sibling *Helicoverpa* Species. PLoS ONE 7:e30040. doi: 10.1371/journal.pone.0030040

Suzuki T (1980) 4, 8-Dimethyldecanal: The aggregation pheromone of the flour beetles, *Tribolium castaneum* and *T. confusum* (Coleoptera: Tenebrionidae). Agric Biol Chem 44:2519–2520.

Syed Z, Leal WS (2007) Maxillary Palps Are Broad Spectrum Odorant Detectors in *Culex quinquefasciatus*. Chem Senses 32:727–738. doi: 10.1093/chemse/bjm040

Tegoni M, Campanacci V, Cambillau C (2004) Structural aspects of sexual attraction and chemical communication in insects. Trends Biochem Sci 29:257–264. doi: 10.1016/j.tibs.2004.03.003

Tomoyasu Y, Denell RE (2004) Larval RNAi in *Tribolium* (Coleoptera) for analyzing adult development. Dev Genes Evol 214:575–578. doi: 10.1007/s00427-004-0434-0

Utz S, Huetteroth W, Vömel M, Schachtner J (2008) Mas-allatotropin in the developing antennal lobe of the sphinx moth *Manduca sexta*: Distribution, time course, developmental regulation, and colocalization with other neuropeptides. Dev Neurobiol 68:123–142. doi: 10.1002/dneu.20579

Veenstra JA, Lau GW, Agricola HJ, Petzel DH (1995) Immunohistological localization of regulatory peptides in the midgut of the female mosquito *Aedes aegypti*. Histochem Cell Biol 104:337–347.

Vermehren-Schmaedick A, Scudder C, Timmermans W, Morton DB (2011) *Drosophila* gustatory preference behaviors require the atypical soluble guanylyl cyclases. J Comp Physiol A 197:717–727. doi: 10.1007/s00359-011-0634-9

Visser JH (1986) Host Odor Perception in Phytophagous Insects. Annu Rev Entomol 31:121–144. doi: 10.1146/annurev.en.31.010186.001005

Vogt RG (2005) Molecular Basis of Pheromone Detection in Insects. In: Comprehensive Insect Physiology, Biochemistry, Pharmacology and Molecular Biology. Elsevier, London,

Vogt RG, Miller NE, Litvack R, et al (2009) The insect SNMP gene family. Insect Biochem Mol Biol 39:448–456. doi: 10.1016/j.ibmb.2009.03.007

Vogt RG, Riddiford LM (1981) Pheromone binding and inactivation by moth antennae. Nature 293:161–163. doi: 10.1038/293161a0

Vosshall LB (2000) Olfaction in *Drosophila*. Curr Opin Neurobiol 10:498–503.

Vosshall LB, Hansson BS (2011) A Unified Nomenclature System for the Insect Olfactory Coreceptor. Chem Senses bjr022. doi: 10.1093/chemse/bjr022

Vosshall LB, Stocker RF (2007) Molecular architecture of smell and taste in *Drosophila*. Annu Rev Neurosci 30:505–533. doi: 10.1146/annurev.neuro.30.051606.094306

Wang J, Li D-Z, Min S-F, et al (2014a) Analysis of chemosensory gene families in the beetle *Monochamus alternatus* and its parasitoid *Dastarcus helophoroides*. Comp Biochem Physiol Part D Genomics Proteomics 11:1–8. doi: 10.1016/j.cbd.2014.05.001

Wang L, Wang S, Li Y, et al (2007) BeetleBase: the model organism database for *Tribolium castaneum*. Nucleic Acids Res 35:D476–D479. doi: 10.1093/nar/gkl776

Wang X, Fang X, Yang P, et al (2014b) The locust genome provides insight into swarm formation and long-distance flight. Nat Commun. doi: 10.1038/ncomms3957

Wang Y, Chiang A-S, Xia S, et al (2003) Blockade of Neurotransmission in *Drosophila* Mushroom Bodies Impairs Odor Attraction, but Not Repulsion. Curr Biol 13:1900–1904. doi: 10.1016/j.cub.2003.10.003

Wanner KW, Robertson HM (2008) The gustatory receptor family in the silkworm moth *Bombyx mori* is characterized by a large expansion of a single lineage of putative bitter receptors. Insect Mol Biol 17:621–629. doi: 10.1111/j.1365-2583.2008.00836.x

Weiss LA, Dahanukar A, Kwon JY, et al (2011) The Molecular and Cellular Basis of Bitter Taste in *Drosophila*. Neuron 69:258–272. doi: 10.1016/j.neuron.2011.01.001

Whiteman NK, Pierce NE (2008) Delicious poison: genetics of *Drosophila* host plant preference. Trends Ecol Evol 23:473–478. doi: 10.1016/j.tree.2008.05.010

Wicher D, Schäfer R, Bauernfeind R, et al (2008) *Drosophila* odorant receptors are both ligand-gated and cyclic-nucleotide-activated cation channels. Nature 452:1007–1011. doi: 10.1038/nature06861

Yamagata N, Nishino H, Mizunami M (2007) Neural pathways for the processing of alarm pheromone in the ant brain. J Comp Neurol 505:424–442. doi: 10.1002/cne.21500

Yang C-H, Belawat P, Hafen E, et al (2008) *Drosophila* egg-laying site selection as a system to study simple decision-making processes. Science 319:1679–1683. doi: 10.1126/science.1151842

Younus F, Chertemps T, Pearce SL, et al (2014) Identification of candidate odorant degrading gene/enzyme systems in the antennal transcriptome of *Drosophila melanogaster*. Insect Biochem Mol Biol 53:30–43. doi: 10.1016/j.ibmb.2014.07.003

Zdobnov EM, Apweiler R (2001) InterProScan - an integration platform for the signature-recognition methods in InterPro. Bioinforma Oxf Engl 17:847–848.

Zhang YV, Ni J, Montell C (2013) The Molecular Basis for Attractive Salt-Taste Coding in *Drosophila*. Science 340:1334–1338. doi: 10.1126/science.1234133

Zhu F, Moural TW, Shah K, Palli SR (2013) Integrated analysis of cytochrome P450 gene superfamily in the red flour beetle, *Tribolium castaneum.* BMC Genomics 14:174. doi: 10.1186/1471-2164-14-174

Supplement material

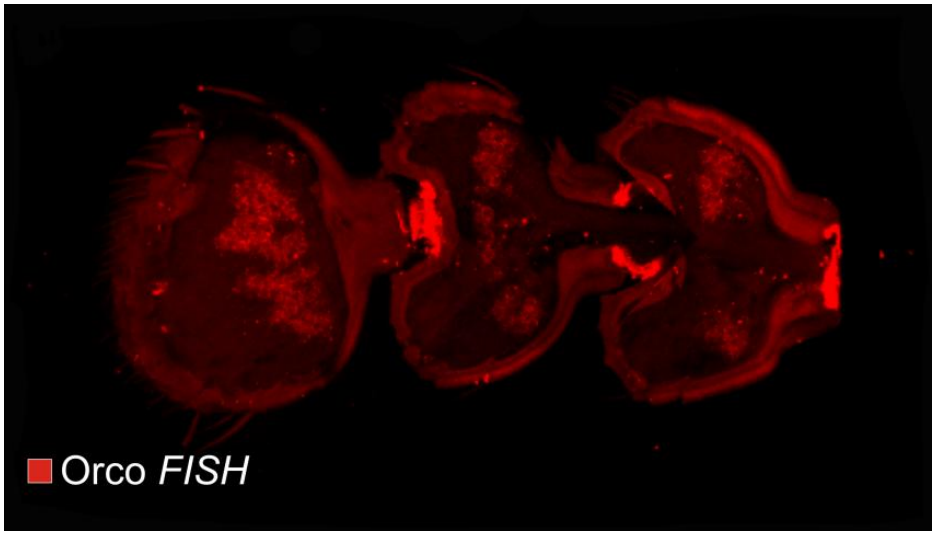

Figure 1 - figure supplement 1. Fluorescent *in situ* hybridization against *Orco* in the club segments in a maximum projection of a halved antenna.

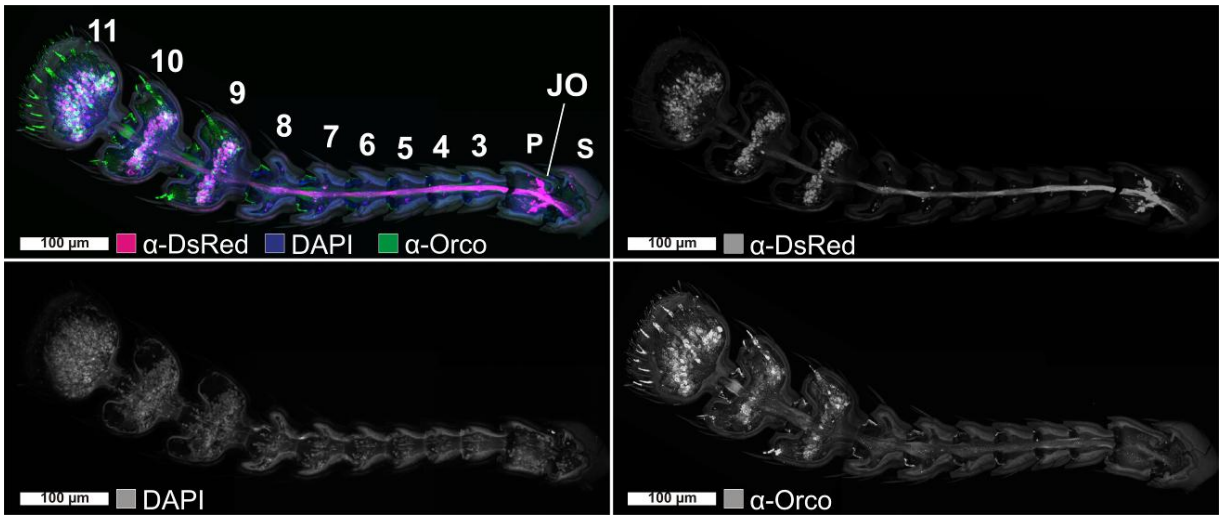

Figure 1 - figure supplement 2. Antibody staining against DsRed and Orco of the EF1-B-DsRed line. Maximum projection of a confocal image stack of a halved antenna of the *EF1-B*-DsRed line, with an antibody staining against DsRed and Orco and in addition DAPI. Showing Orco immunoreactivity in the last three segments and particularly in the SBas. The DsRed reporter line labels in addition the scolopidia cells of the Johnston's organ (JO) in the pedicellus (P). S, scapus

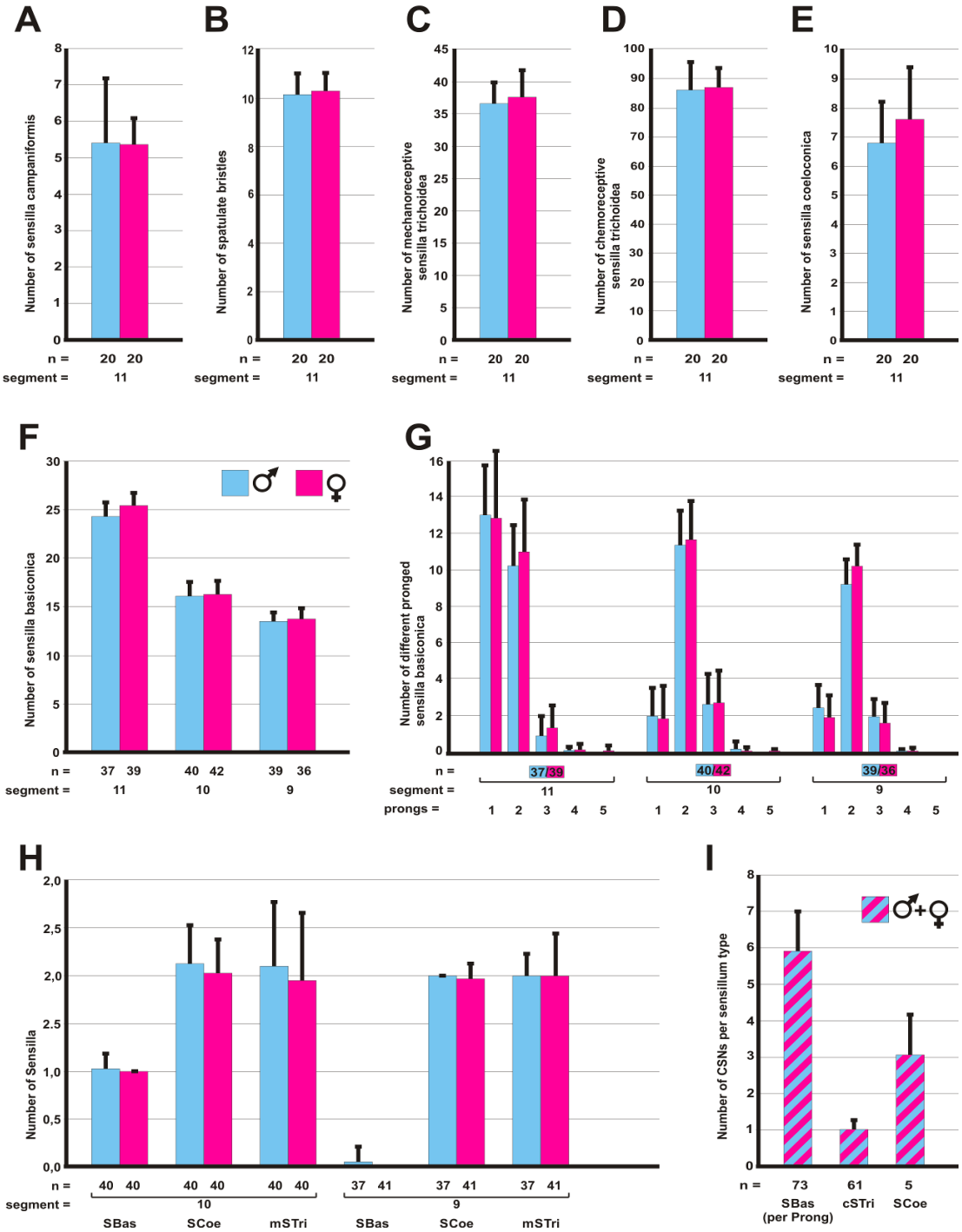

Figure 1 - figure supplement 3. Comparison of sensilla type numbers on the antenna of *Tribolium castaneum* and chemosensory neurons entering the sensilla types. (A-E) Number of different sensilla types on the eleventh segment of the antenna: (A) sensilla campaniformis (Scam: ♂ 5.4; SD 1.8; ♀ 5.4; SD 0.8), (B) spatulate bristles (SpaB: ♂ 10.2; SD 0.9; ♀ 10.3; SD 0.9), (C) mechanoreceptive sensilla trichoideum (mSTri: ♂ 36.9; SD 3; ♀ 37.6; SD 4.3), (D) chemoreceptive sensilla trichoideum (cSTri: ♂ 86.3; SD 9.3; ♀ 87.1; SD 6.9), (E) sensilla coeloconica (SCoe: ♂ 6.8; SD 1.4; ♀ 7.6; SD 1.1). (F) Amount of sensilla basiconica on the club segments (11th: ♂ 24.4; SD 1.5; ♀ 25.5; SD 1.3; 10th: ♂ 16.2; SD 1.5; ♀ 16.4; SD 1.4; 9th: ♂ 13.6; SD 0.9; ♀ 13.8; SD 1.1), regardless of the number of prongs. (G) Number of sensilla basiconica as in (F), but considering the prong number. (H) Number of different sensilla in the lateral corner of the 10th and 9th segment. (I) Number of chemosensory neurons (CSNs) entering the chemoreceptive sensilla: SBas 5.92 CSNs per prong (SD = 1.2; n = 73 prongs of total 48 SBas), cSTri 1.07 CSNs (SD = 0.25; n = 61), and SCoe 3.16 CSNs (SD = 1.10; n = 5). Error bars represent standard deviations; n = number of antennae.

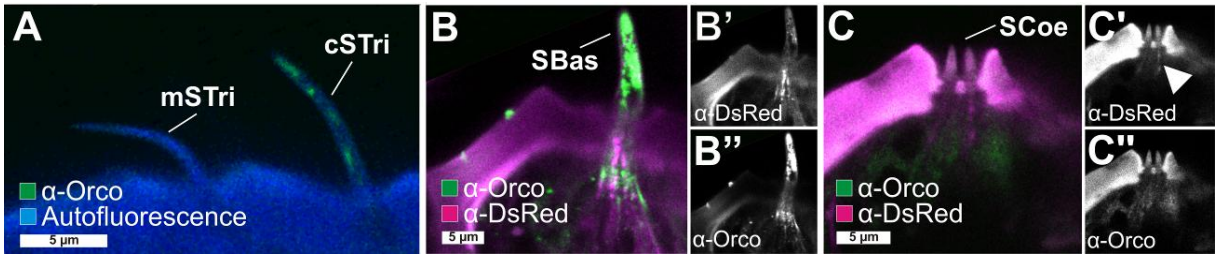

Figure 1 - figure supplement 4. Antibody staining against Orco in different sensilla. (A) Optical section of a mechano- and chemosensillum trichoideum (mSTri and cSTri) labeled with an Orco antibody (green) shows immunoreactivity only within the sensillum cavity of the cSTri; in blue autofluorescence of the cuticle at 560 nm. **(B-B'')** Single optical section of a sensilla basiconica (SBas) in the *EF1-B*-DsRed (magenta, B') line labeled with an Orco antibody (green, B'') reveals signals of both channels particularly within the cavity and at the base of the sensillum; both channels also show autofluorescence of the cuticle. **(C-C'')** Optical section of two sensilla coeloconica (SCoe) in the *EF1-B*-DsRed (magenta, C') line labeled with an Orco antibody (green, C'') reveals no specific immunoreactivity within the sensilla cavities; both channels also show autofluorescence of the cuticle.

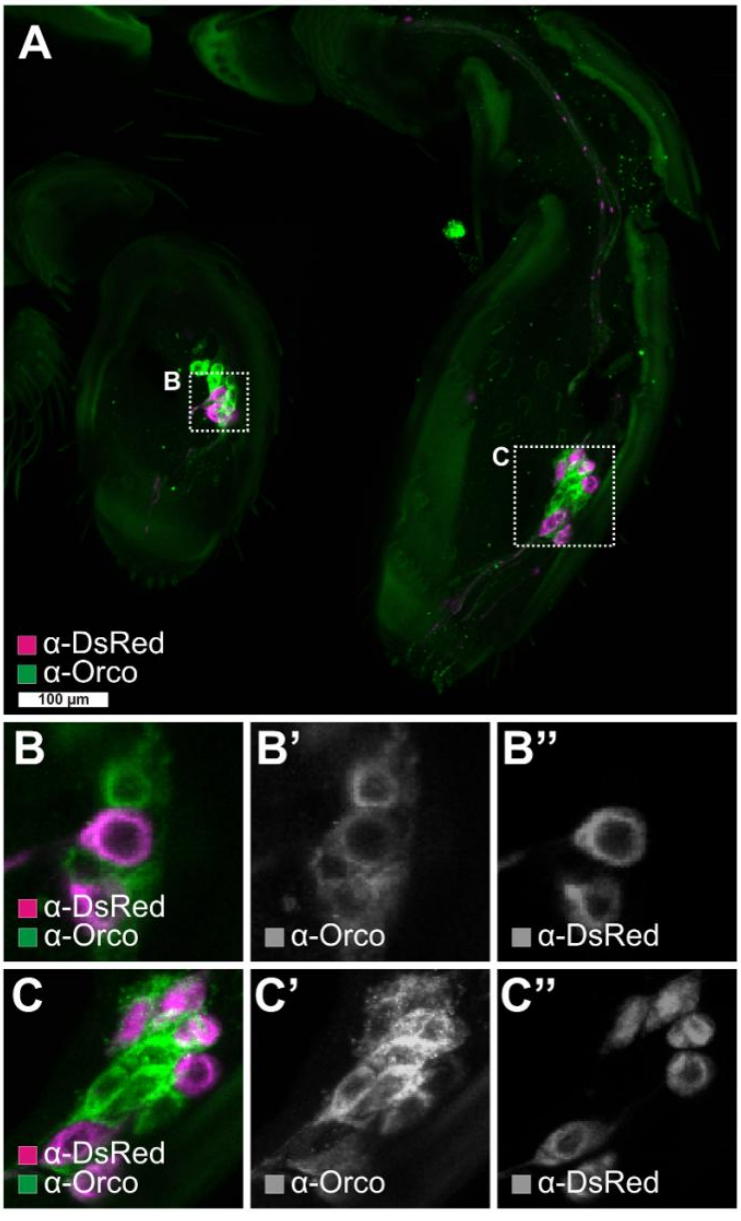

Figure 1 – figure supplement 5. Immunohistochemical characterization of the partial Orco-Gal4 line in the palps. (A). Double immuno-staining against Orco (green) and dsRed (magenta) in the palps of the *Orco-Gal4/UAS*-dsRed line reveals that all genetically labeled neurons are also Orco-ir. However, in contrast to the antennae, in which about half of the Orco-ir neurons are labeled in the partial *Orco-Gal*4 line, only a few of the the Orco-ir odorant receptor neurons express the reporter in the palps. The Cy2 (Orco) signal is quenched by dsRed.

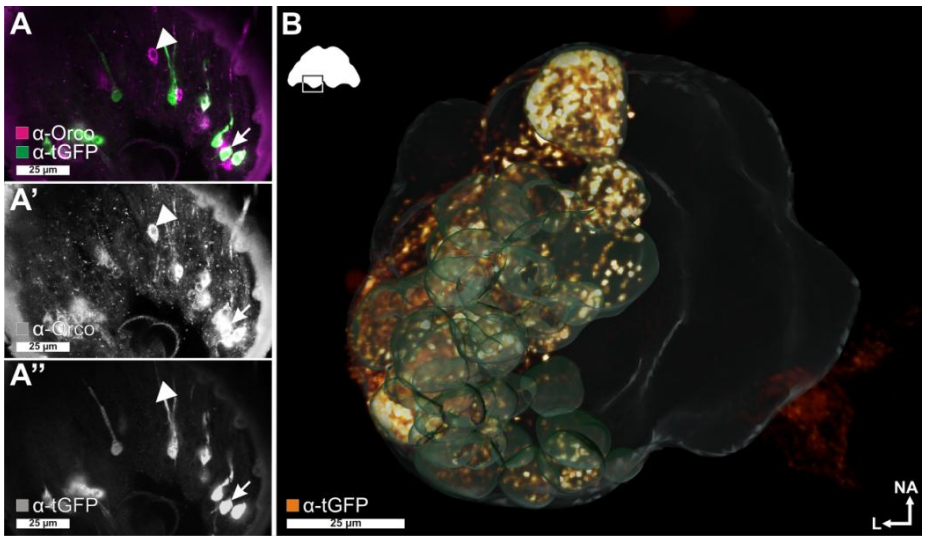

Figure 1 - figure supplement 6. Immunohistochemical characterization of the *Orco-Gal*4 line in the antenna and brain. (A-A'') Double immune-staining against Orco (magenta) and tGFP (green) in the antennae revealed that only half of the Orco-ir neurons expressing tGFP (arrow indicates colocalization, arrowhead as an example for no colocalization). **(B)** Antibody staining against tGFP in the *Orco-Gal4/UAS*-tGFP line (orange) labels only half of the AL glomeruli represented as 3D-reconstruction (light green, based on a phalloidin staining). AL glomeruli not labeled are not shown.

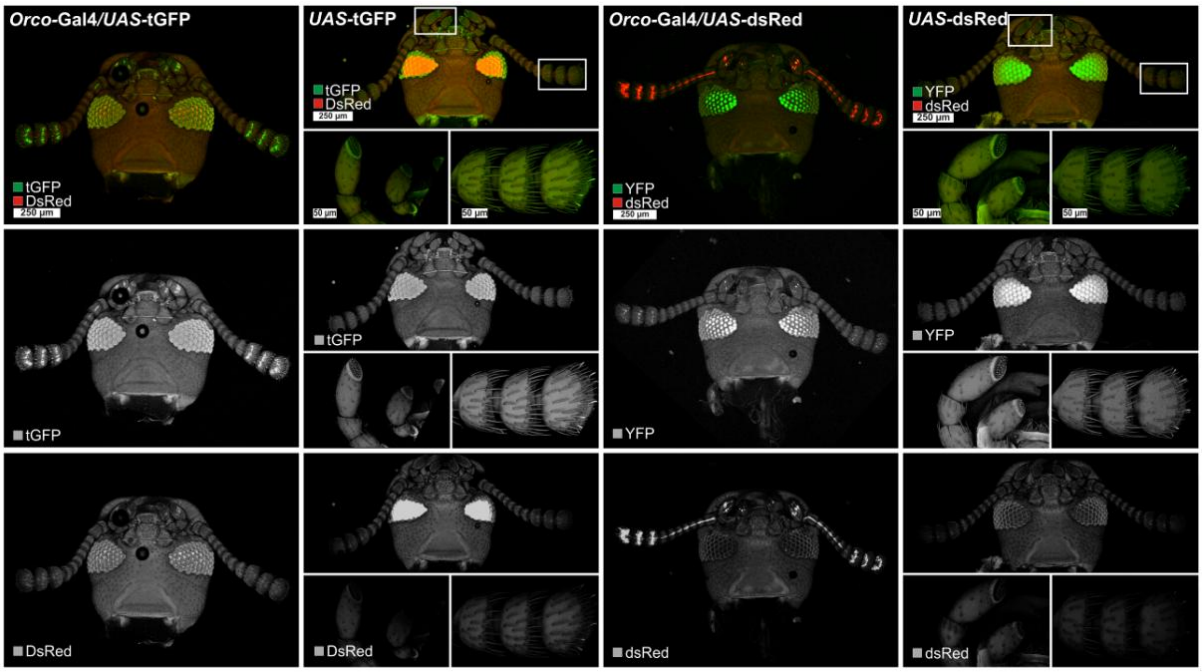

Figure 1 – figure supplement 7. UAS responder lines in the absence of Gal4 driver. In the four rows maximum projections of head capsules from different transgenic strains (*Orco*-Gal4/*UAS*-tGFP, *UAS*-tGFP, *Orco*-Gal4/*UAS*-dsRed, and *UAS*-dsRed) are depicted. The upper row represents the overlay of both channels (GFP/YFP in green and dsRed in red). In case of the UAS responders without the Gal4 driver, high resolution images of the palps and the antennal club are provided. In the second and third rows the separated channels are given as greyscale images. The UAS-tGFP and UAS-dsRed lines do not show leaky reporter expression in the absence of a Gal4 driver in the antennae and palps. The presence of the genetic constructs is indicated by the eye markers: pBac[3XP3-dsRed_UAS-Tchsp68bP-tGFP-SV40] and pBac[3XP3-eYFP_UAS-Tchsp68bP-DsRedex-SV40]. The marker signal is quenched in the crossed lines by the vermillion rescue marker of the Orco-Gal4 construct pBac[3XP3-gVerm_2.5kbOrcoUp_GAL4delta].

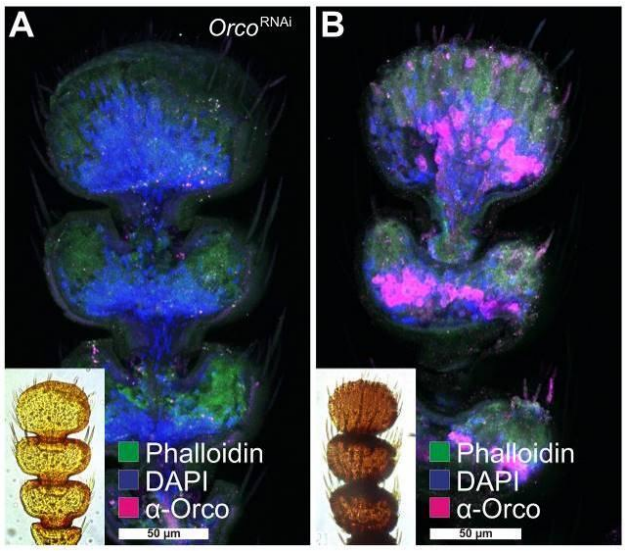

Figure 1 – figure supplement 8. Specificity of the Orco antibody. IHC against Orco in antennae of (A) a San Bernadino beetle after *Orco*^{RNAi} treatment (light cuticle, inset in the left lower corner) and (B) an untreated control included in the IHC (black strain identified by dark cuticle). The crossreactive Orco antiserum results in no detectable staining in the antenna after *Orco* knockdown, whereas in the antenna of the untreated beetles, the odorant receptor neurons (ORNs) are clearly labeled by the antiserum (magenta). This indicates the specificity of the Orco antiserum against *Tcas*Orco. Counterstaining with Phalloidin (green) and DAPI (blue). The Orco antibody staining was labeled with a goat anti rabbit Cy3 secondary antibody.

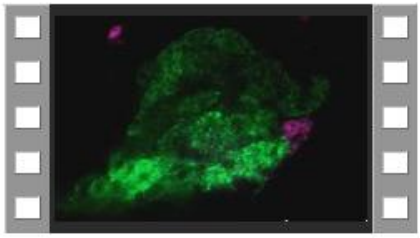

Figure 3 - figure supplement 1. Camera path through a confocal stack of the AL with backfills of the antenna and maxillary palp. ***(see CD for content)*** Obtained from the same confocal stack as Figure 3A. Antennal backfill in green and maxillary palp in magenta.

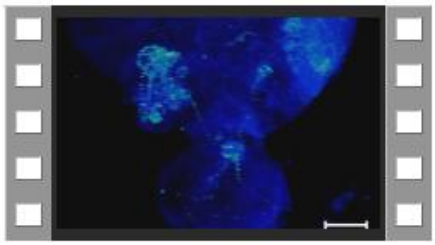

Figure 3 - figure supplement 3. Voltex projection of the gnathal ganglion and part of the brain of the *Orco*-Gal4/*UAS*-DsRed line. ***(see CD for content)*** The video was obtained from the same confocal stack as Figure 3F. And shows two paired input tracts from the maxillary and labial palps that converge in GOC and ascend to the LGs, as well as the partially labeled ALs.

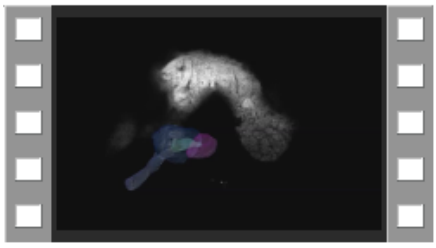

Figure 3 - figure supplement 4. 3D reconstructions of the antennal nerve, antennal lobe, antennal mechanosensory and motor center, and lobus glomerulatus. ***(see CD for content)*** Z-stack video of a phalloidin stained brainwith embedded 3D-Reconstruction of antennal lobe (dark blue), antennal nerve (light blue), antennal mechanosensory and motor center (turquoise), and the lobus glomerulatus (magenta). Later the neuropils are embedded in a voltex projection of the brain, also based on phalloidin staining (orange)

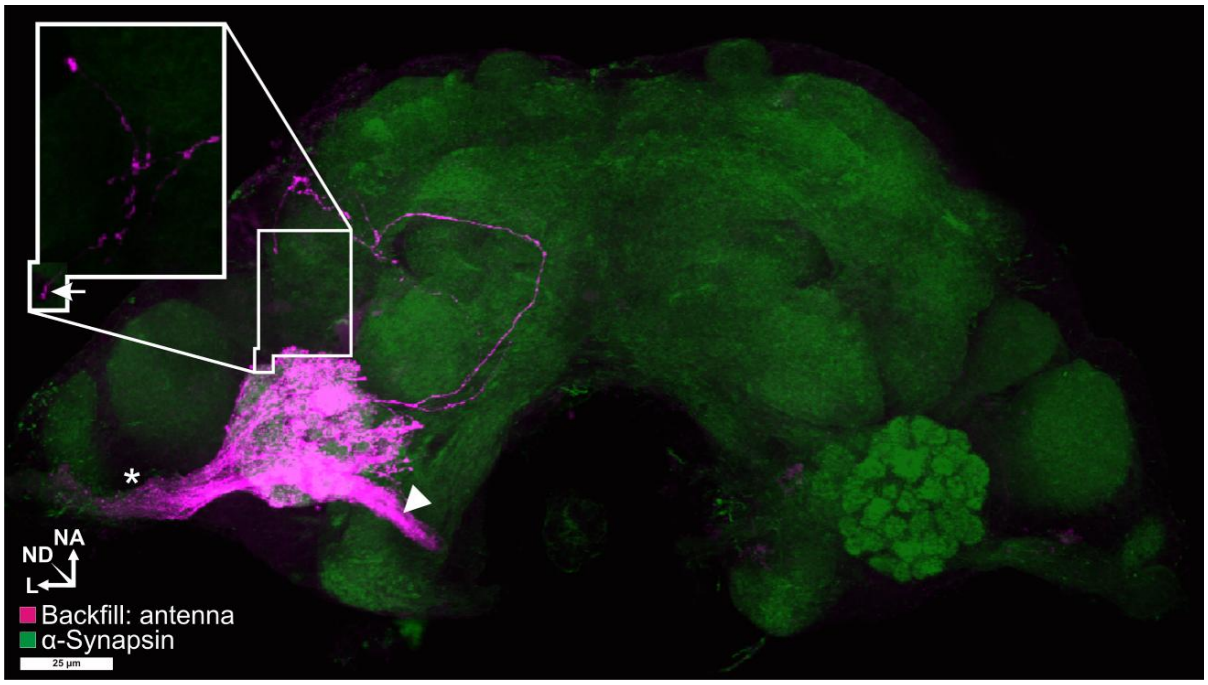

Figure 3 - figure supplement 2. Ipsilateral antennal projection. Maximum intensity projection of a brain labeled with an antibody against synapsin (green) and a neurotracer resulting from an antennal backfill (magenta). The antennal backfill labels exclusively structures in the ipsilateral hemisphere, mainly the AL via the antennal nerve (*), and a tract (arrowhead) descending to the gnathal ganglion. The inset depicts a projection of only a few optical sections showing fibers interconnecting the AL and the protocerebrum with some arborizations in the accessory medulla of the optical lobe (arrow) suggesting an integration of circadian information.

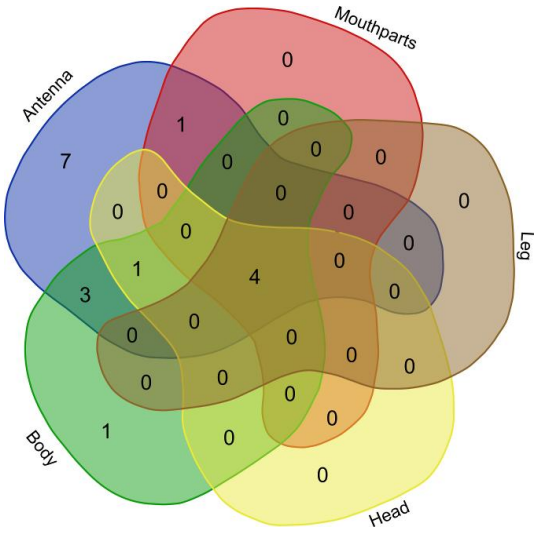

Figure 7 - figure supplement 1. Venn diagrams of numbers of IRs expressed in different tissues. Venn diagram showing the number of IRs expressed (RPKM≥0.5) in the different body parts: antennae, legs, mouthparts (as piece of the head capsule anterior of the antennae), heads (the whole head capsule including “mouthparts” but excluding the antennae), and bodies (excluding head and legs).

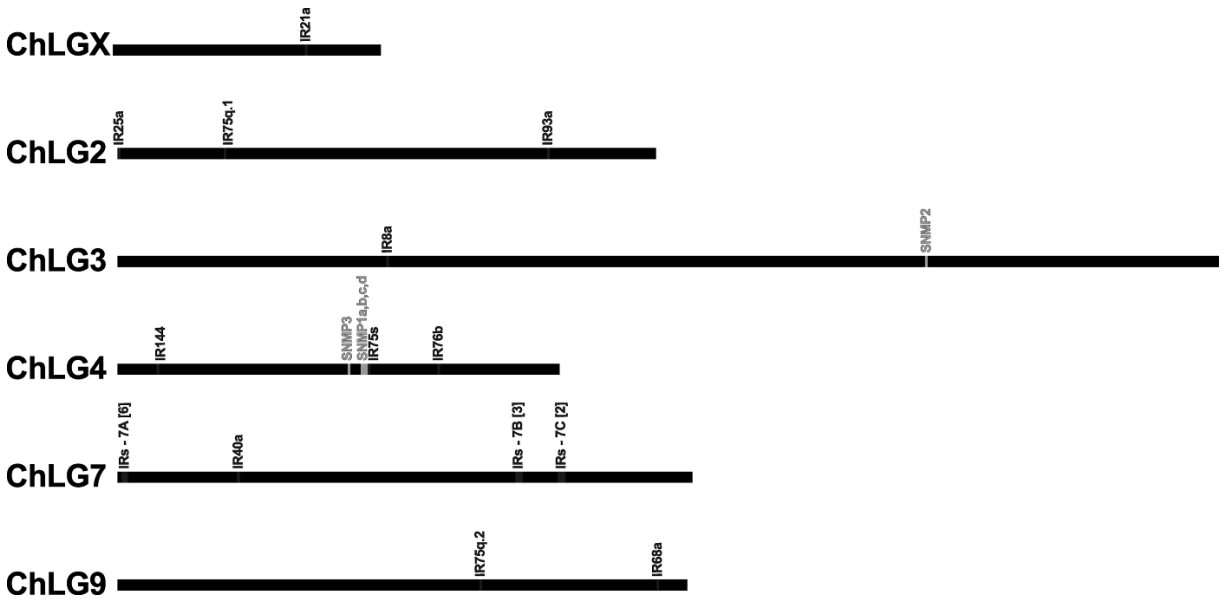

Figure 7 - figure supplement 2. Chromosomal localization of *T. castaneums* IRs and SNMPs. Based on Georgia GA-2 strain genome assembly 3 (Richards et al. 2008), only chromosomal linkage groups containing an IR or SNMP are depicted. Genecluster are indicated by a number referring to the chromosome and a letter conveys its relative position on the chromosome, the number of genes within this cluster is indicated in the square brackets.

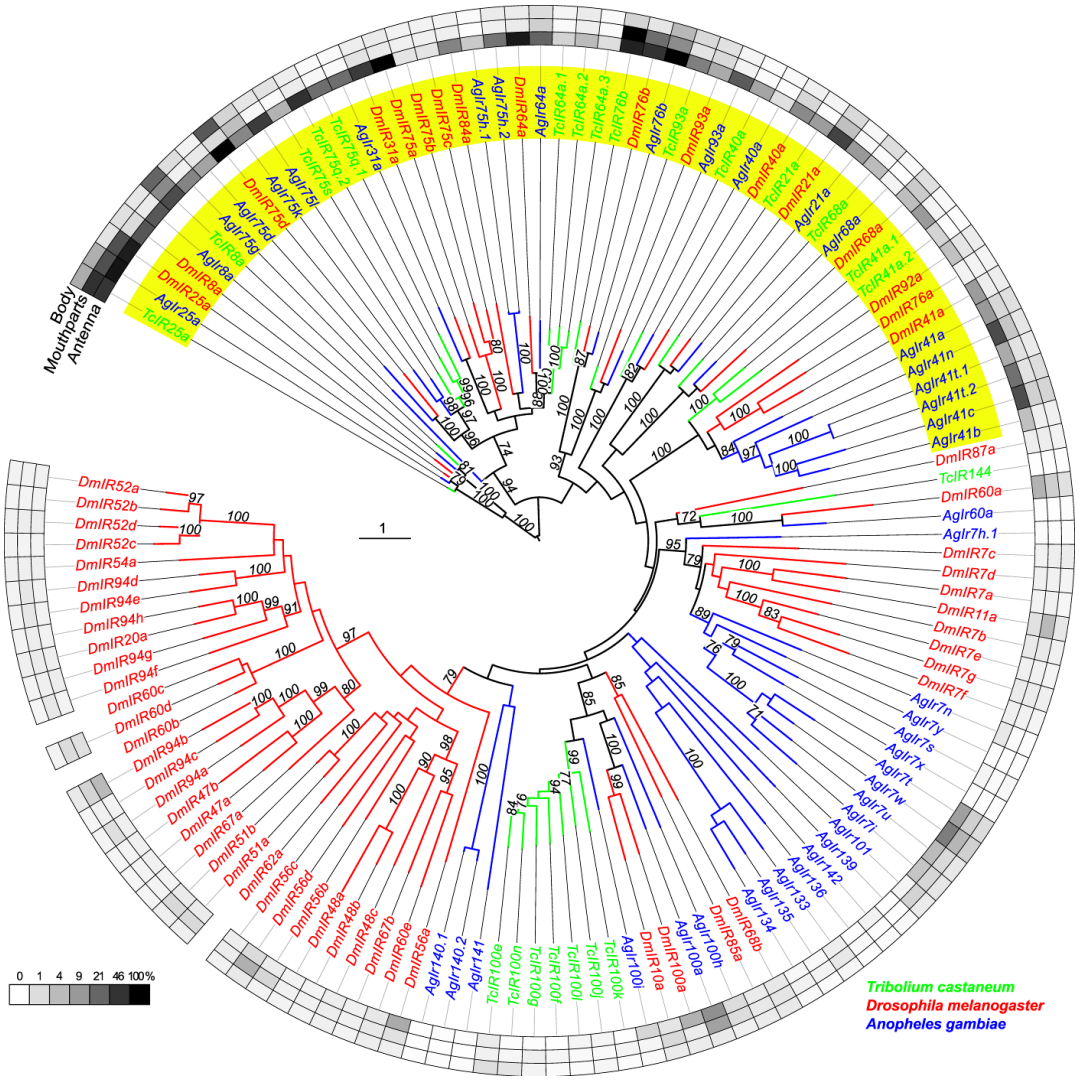

Figure 8 - figure supplement 1. Phylogenetic tree of IRs. Outer rings represent the expression in body, "mouthparts" (*T. castaneum*: palps, mandible, labrum and labium; *D. melanogaster*: palp and proboscis; *An. gambiae*: maxillary palp) and antenna as percentage compared to the highest expressed gene according to the scale in the left upper corner. Please note that the methods used to obtain the different expression data (RNAseq and microarray) are not directly comparable this figure can thus only give an impression of the tissue-specific abundance of the transcripts. The scale bars within the trees represent 1 amino acid substitution per site. Antennal IRs are highlighted in yellow.

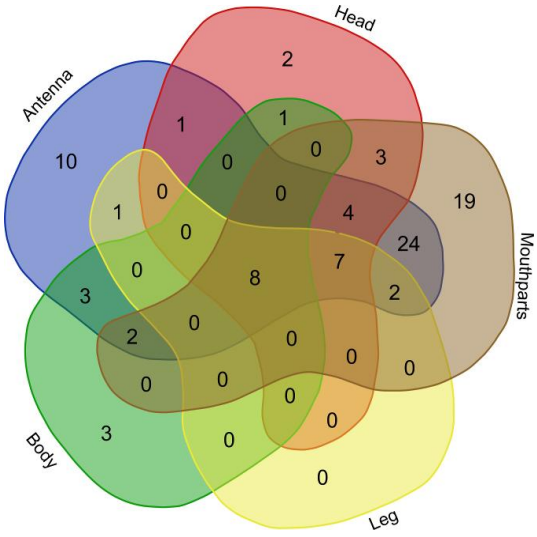

Figure 9 - figure supplement 1. Venn diagrams of numbers of GRs expressed in different tissues. Venn diagram showing the number of GRs expressed (RPKM≥0.5) in the different body parts: antennae, legs, mouthparts (as piece of the head capsule anterior of the antennae), heads (the whole head capsule including "mouthparts" but excluding the antennae), and bodies (excluding head and legs).

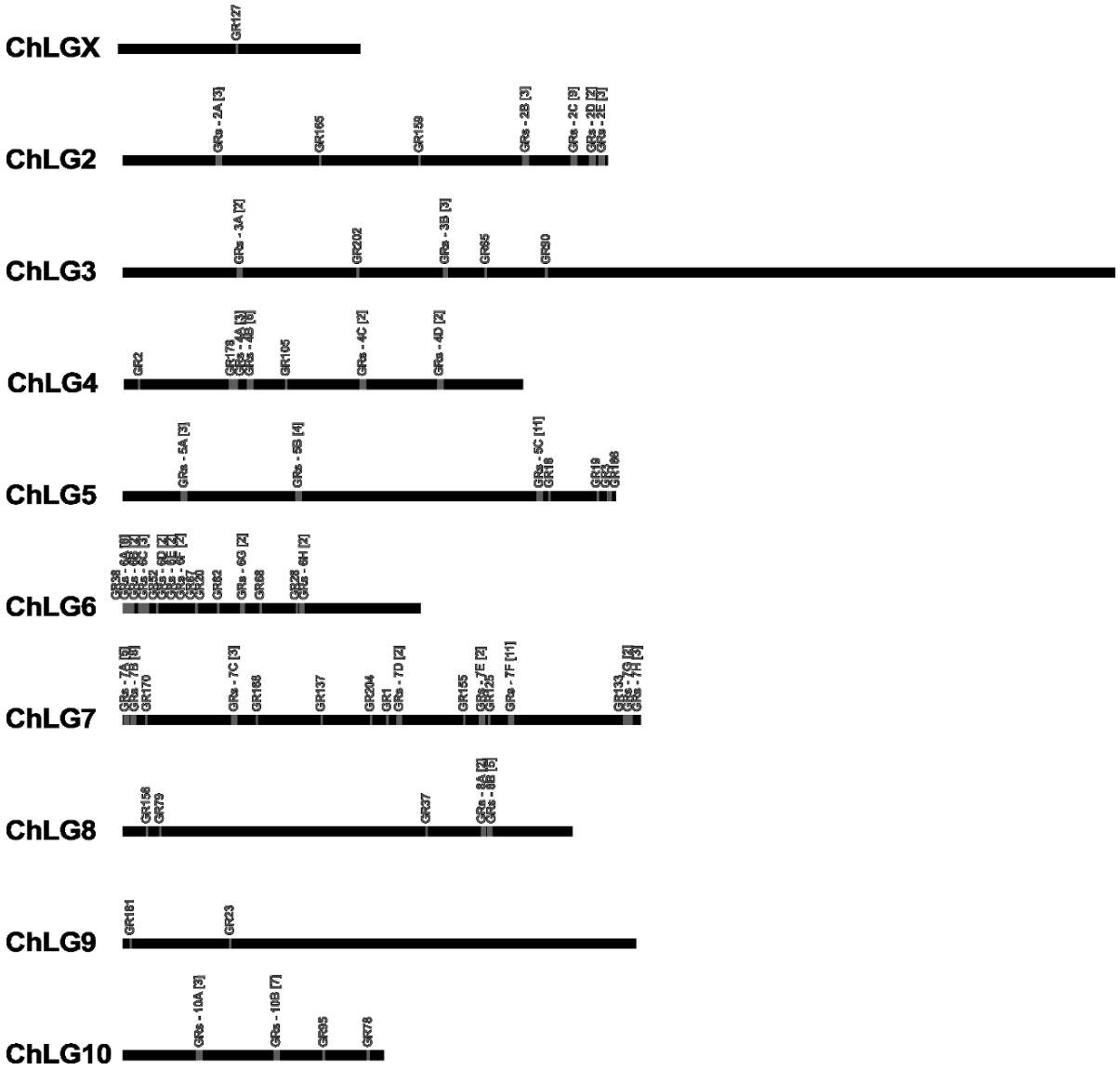

Figure 9 - figure supplement 2. Chromosomal localization of *T. castaneums* GRs. Based on Georgia GA-2 strain genome assembly 3.0 (Richards et al. 2008), only chromosomal linkage groups containing an IR or SNMP are depicted. Genecluster are indicated by a number referring to the chromosome and a letter conveys its relative position on the chromosome, the number of genes within this cluster is indicated in the square brackets.

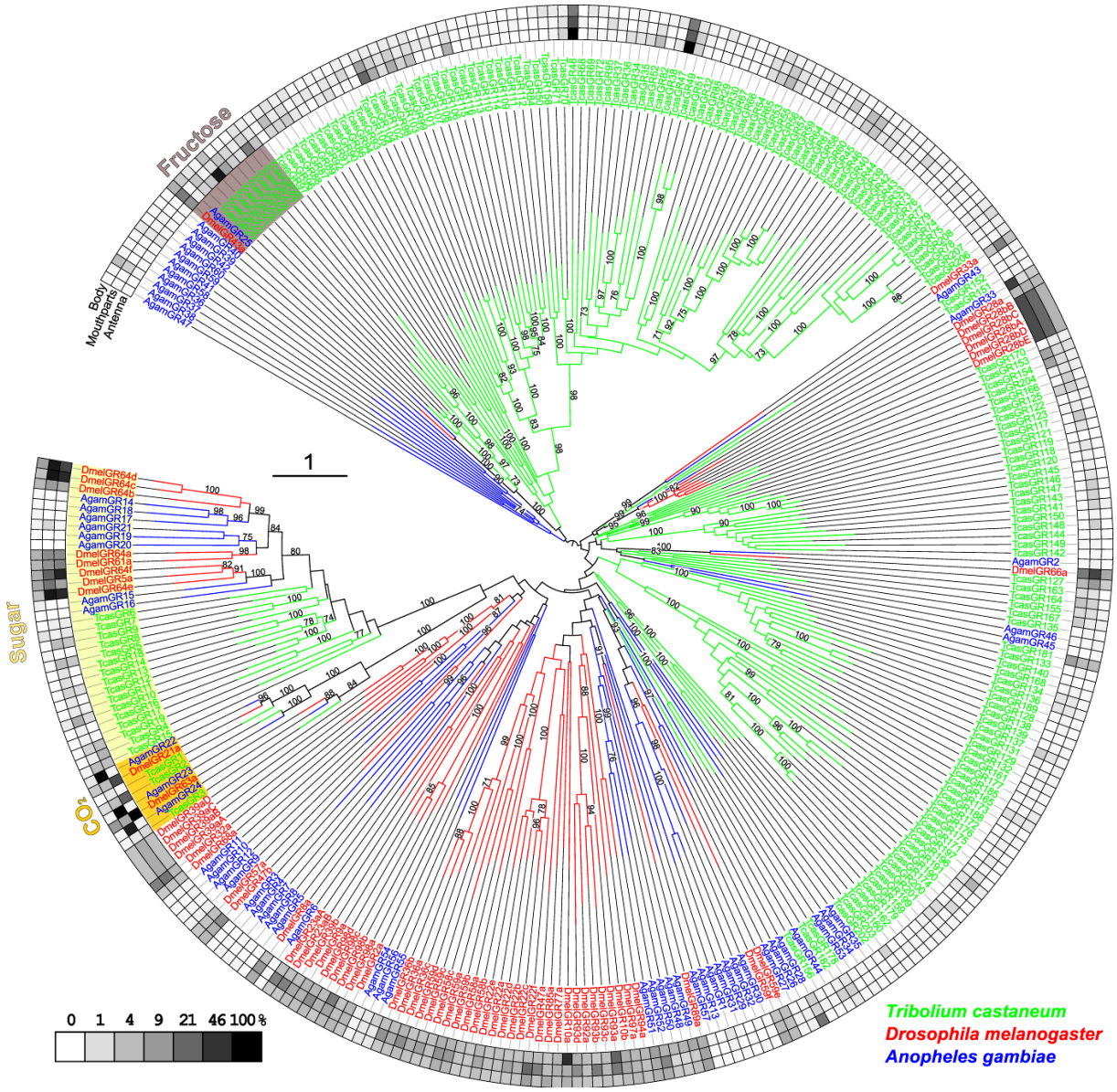

Figure 10 - figure supplement 1.Phylogenetic mid-point rooted tree of the GRs based on protein sequences. Outer rings represent the expression in body, "mouthparts" (*T. castaneum*: palps, mandible, labrum and labium; *D. melanogaster*: palp and proboscis; *An. gambiae*: maxillary palp) and antenna as percentage compared to the highest expressed gene according to the scale in the left upper corner. Please note that the methods used to obtain the different expression data (RNAseq and microarray) are not directly comparable this figure can thus only give an impression of the tissue-specific abundance of the transcripts. The scale bars within the trees represent 1 amino acid substitution per site. Potential sugar and fructose receptors are labeled and highlighted in yellow and in grey, CO_2 receptors are highlighted in orange.

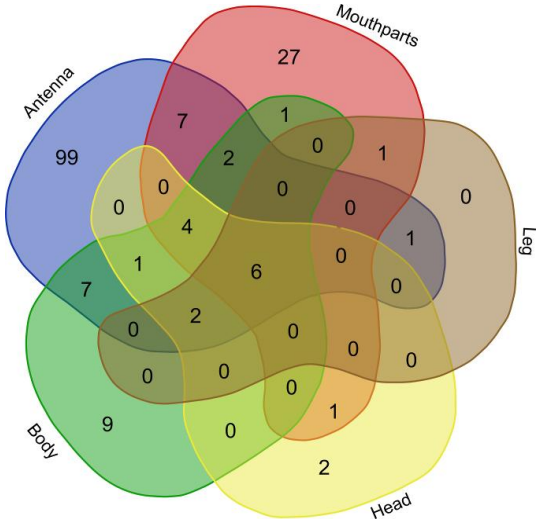

Figure 11 - figure supplement 1. Venn diagrams of numbers of ORs expressed in different tissues. Venn diagram showing the number of ORs expressed (RPKM≥0.5) in the different body parts: antennae, legs, mouthparts (as piece of the head capsule anterior of the antennae), heads (the whole head capsule including "mouthparts" but excluding the antennae), and bodies (excluding head and legs).

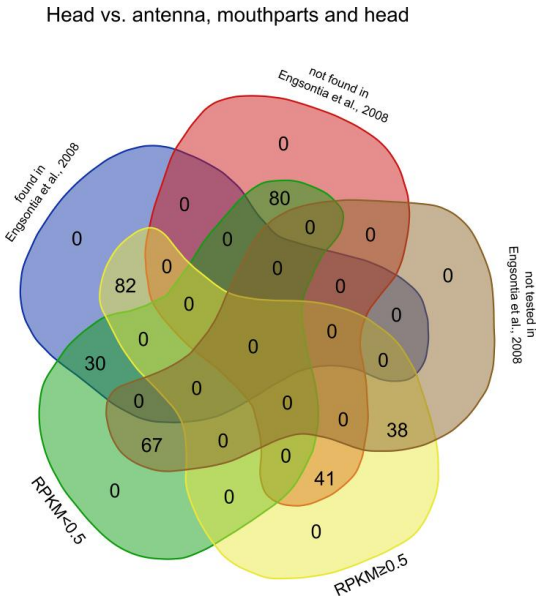

Figure 11 - figure supplement 2. Venn diagram comparing our results with data from Engsontia et al., 2008. Amount of expressed ORs, either defined by RPKM≥0.5 (yellow), or by RT-PCR (blue), or not expressed RPKM<0.5 (green) or no RT-PCR amplicon (red), ORs of the brown group were previously not tested.

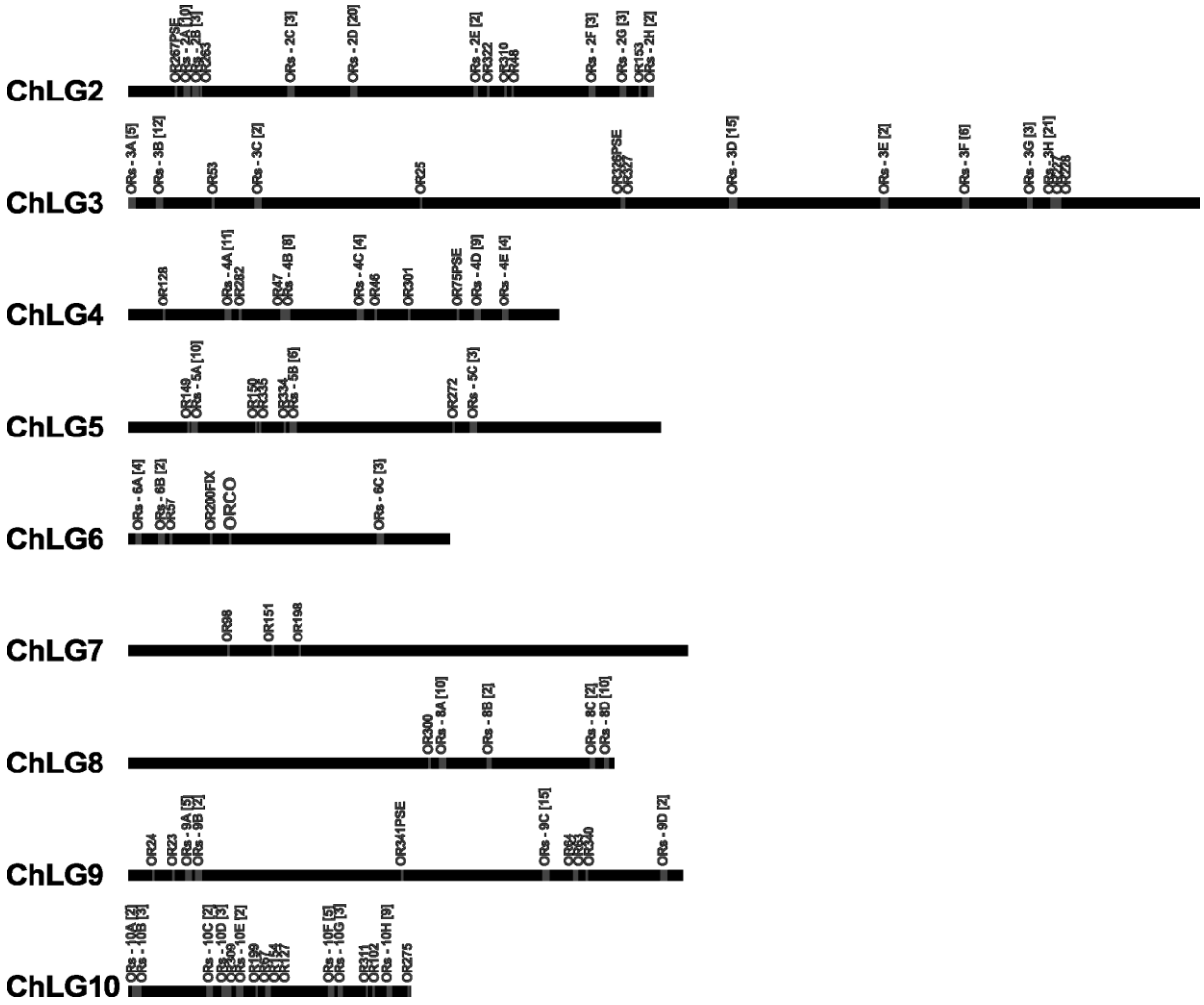

Figure 11 - figure supplement 3. Chromosomal localization of *T. castaneums* ORs. Based on Georgia GA-2 strain genome assembly 3.0 (Richards et al. 2008), only chromosomal linkage groups containing an IR or SNMP are depicted. Genecluster are indicated by a number referring to the chromosome and a letter conveys its relative position on the chromosome, the number of genes within this cluster is indicated in the square brackets

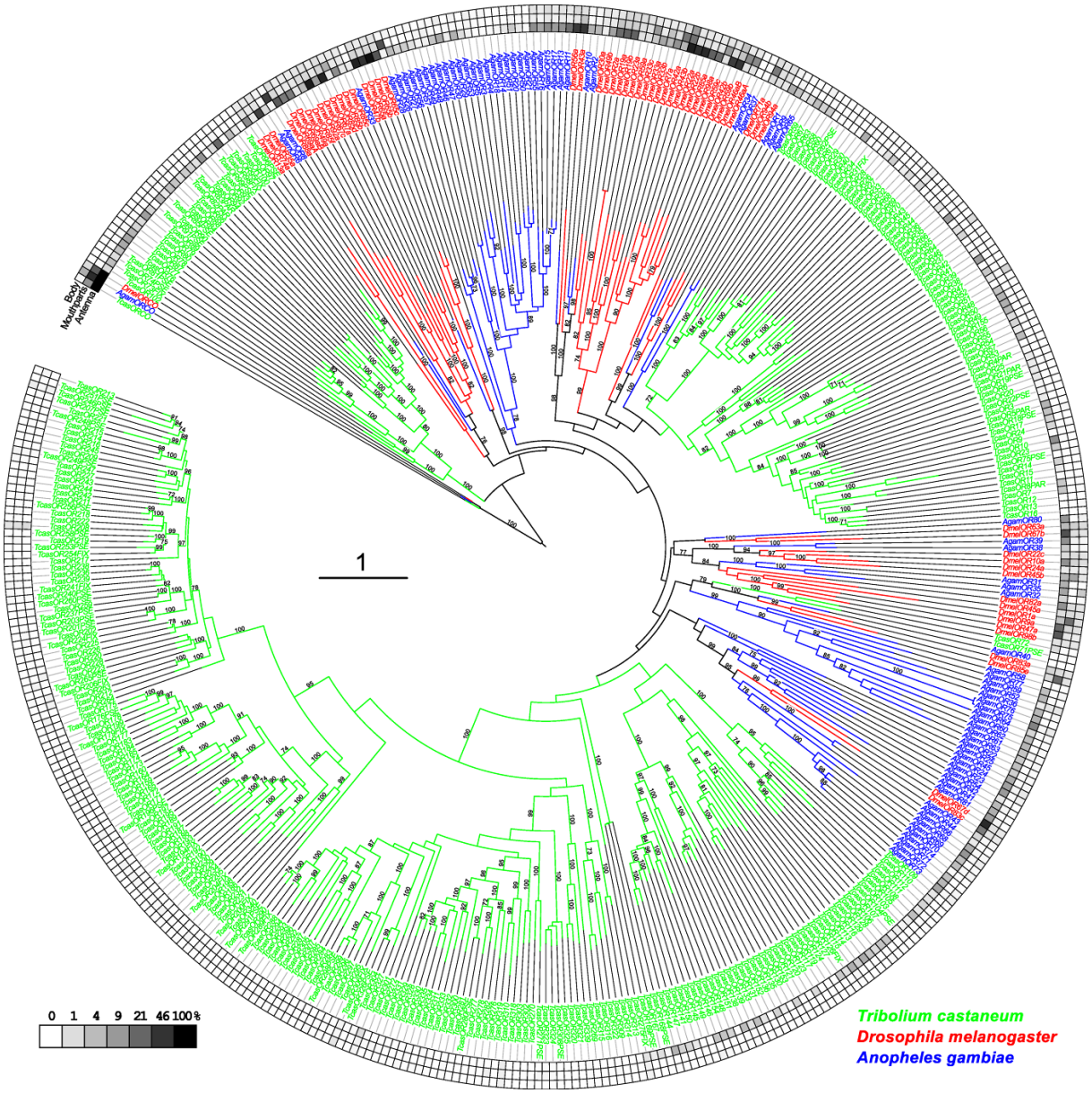

Figure 12 - figure supplement 1. Phylogenetic tree of the ORs based on protein sequences. Outer rings represent the expression in body, "mouthparts" (*T. castaneum*: palps, mandible, labrum and labium; *D. melanogaster*: palp and proboscis; *An. gambiae*: maxillary palp) and antenna as percentage compared to the highest expressed gene according to the scale in the left upper corner. Please note that the methods used to obtain the different expression data (RNAseq and microarray) are not directly comparable this figure can thus only give an impression of the tissue-specific abundance of the transcripts. The scale bars within the trees represent 1 amino acid substitution per site.

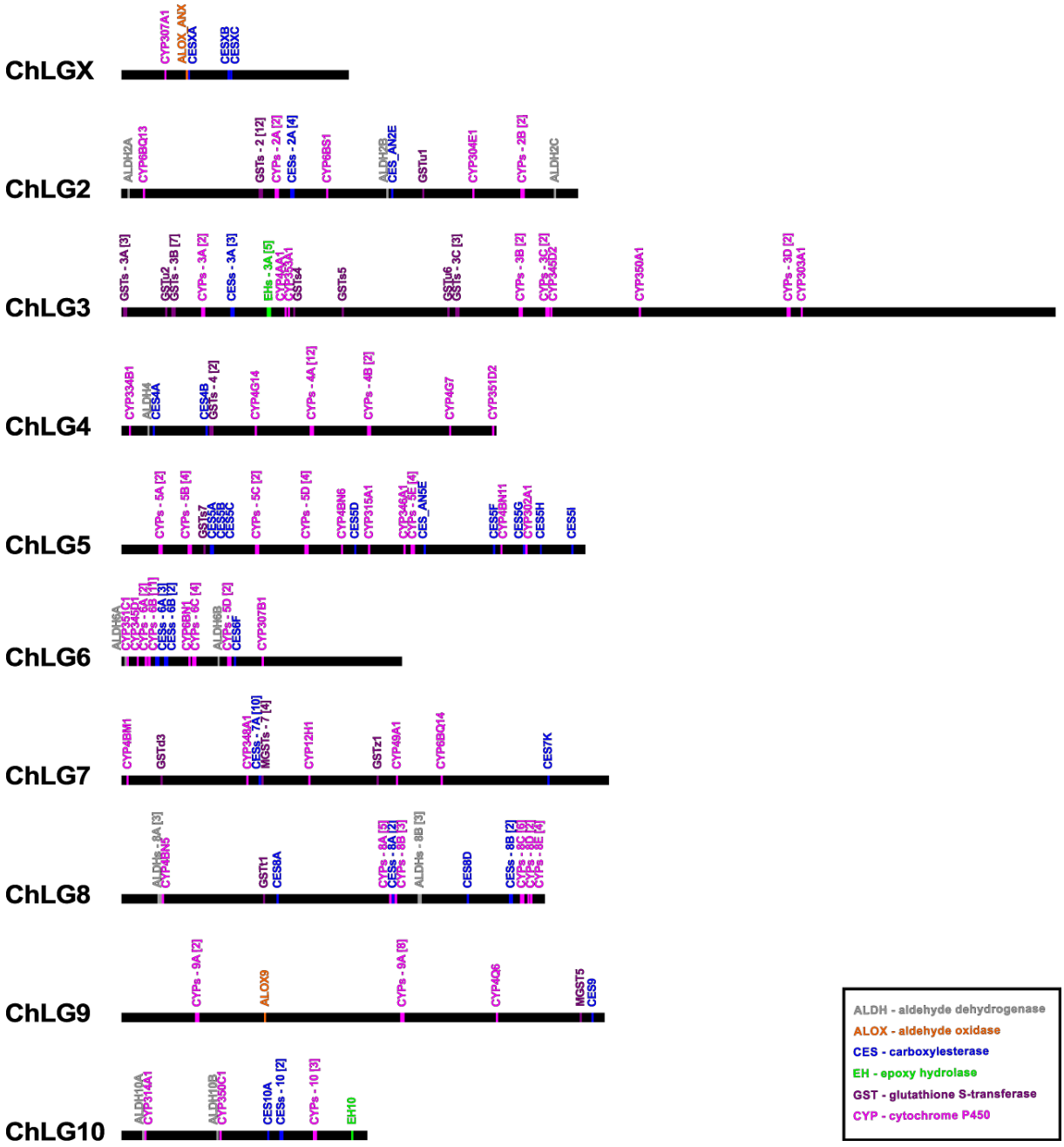

Figure 13 - figure supplement 1. Chromosomal localization of *T. castaneums* potential ODEs. Based on Georgia GA-2 strain genome assembly 3.0 (Richards et al. 2008), aldehyde dehydrogenase (ALDH, in grey), aldehyde oxidase (ALOX, in orange), carboxylesterase (CES, in blue), epoxide hydrolase (EH, in green), and glutathione S-transferase (GST, in purple), cytochrome P450 (CYP, in magenta),. Genecluster are indicated by a number referring to the chromosome and a letter conveys its relative position on the chromosome, the number of genes within this cluster is indicated in the square brackets.

Supplemental Table 1. Summary of the RNAseq data. ***(see CD for content)***

In column (A) the gene name of the GRs according to (Richards et al. 2008), the ORs from (Engsontia et al. 2008), the SNMPs modified after (Nichols and Vogt 2008; Vogt et al. 2009), the *T. castaneum* orthologous of *D. melanogaster* genes named after candidates obtained from (Martin et al. 2013), the GSTs named after (Shi et al. 2012), the CYPs named after (Zhu et al. 2013) and the remaining ODE candidates *de novo* named according to their chromosomal localization (Figure 13-figure supplement 1). In column (B) the sequences of the ORF based on published annotations or existing gene models, but modified if necessary. Confirmed gene models are highlighted in grey, modified ones are highlighted in yellow, only partially covered but expressed ones are highlighted in orange, genes with low and scattered coverage are highlighted in red, not highlighted sequences were not manually checked. In column (C-I) the average RPKM values of antennae, mouthparts (piece of the head capsule anterior of the antennae), legs, head (without antennae but including mouthparts) and remaining body of sex separated adult animals and from head and body of larvae. In column (J-Q) the results of the statistical analysis conducted in R (R Core Team 2013) with the DESeq package (version1.12.0) (Anders and Huber 2010)(from bioconductor (Gentleman et al. 2004), based on 5 antenna samples and 2 replicates for the other adult tissues in comparison to body.

Supplemental Table 2. Used primary/secondary antibodies and dyes with all important additional information such as source and specificity.

Primary antibodies					
Name	Abbreviation	Host Species	Used dilution	Donor/source, reference	Specificity
D. melanogaster Synapsin I	α-Synapsin	Mouse	1/50	Dr. E. Buchner, University of Würzburg, Germany; Klagges et al., 1996	Utz et al., 2008
Moth Odorant receptor coreceptor	α-Orco	Rabbit	1/500	Dr. J. Krieger, Martin-Luther-Universität Halle-Wittenberg, Germany	RNAi Figure 1 - figure supplement 8
Locusta migratoria Tachykinin II	α-TKRP	Rabbit	1/10000	Dr. H. Agricola University of Jena, Germany; Veenstra et al., 1995	Binzer et al., 2014
Red fluorescent protein	α-DsRed	Chicken	1/2000	Rockland Immunochemicals INC, Limerick, PA, USA	
Red fluorescent protein	α-DsRed	Rat	1/1000	ChromoTek GmbH, Planegg-Martinsried, Germany	
Turbo Green fluorescent protein	α-tGFP	Rabbit	1/8000	Evrogen, Moscow, Russia	
Secondary antibodies					
Name	Abbreviation	Coupled dye	Used dilution	Donor/source, reference	
goat anti-rabbit	GAR	Cy2	1/300	Jackson ImmunoResearch; Westgrove, PA, USA	
goat anti-rabbit	GAR	Cy5	1/300		
goat anti-mouse	GAM	Cy5	1/300		
goat anti-chicken	GAC	Alexa488	1/300		
goat anti-rat	GARat	Cy5	1/300		
Stain					
Name	Abbreviation	stains	Dilution	Donor / source / reference	
4',6-Diamidin-2-phenylindol	DAPI	nuclei	1/20000	Sigma-Aldrich, Taufkirchen, Germany	
Alexa Fluor 488 coupled phalloidin	Phalloidin	f-actin	1/200	Molecular Probes, Eugene, OR, USA	
Neurobiotin		neurotracer	4% solution	Vector Laboratories, Burlingame, UK	
Texas-Red coupled 3000 MW dextran		neurotracer	50 mg/ml or crystals	Molecular Probes, Invitrogen, Karlsruhe, Germany	
Biotin coupled 3000 MW dextran		neurotracer	crystals	Molecular Probes, Invitrogen, Karlsruhe, Germany	
Cy3 coupled Streptavidin		biotin	1/200	Dianova, Hamburg, Germany	

Supplemental Sequences. Sequences of primers and template plasmid used to generate pSLfa1180[2.5kbOrcoUp_GAL4delta]. ***(see CD for content)***

Chapter 4:

The neuropeptidome of *Tribolium castaneum* antennal lobes and mushroom bodies

RESEARCH ARTICLE

Neuropeptidome of *Tribolium castaneum* Antennal Lobes and Mushroom Bodies

Marlene Binzer,[1] Carsten M. Heuer,[1] Martin Kollmann,[1] Jorg Kahnt,[2] Frank Hauser,[3] Cornelis J.P. Grimmelikhuijzen,[3] and Joachim Schachtner[1]*

[1]Philipps-University Marburg, Department of Biology, Animal Physiology, 35043 Marburg, Germany
[2]Max Planck Institute for Terrestrial Microbiology, 35043 Marburg, Germany
[3]Center for Functional and Comparative Insect Genomics, Department of Biology, University of Copenhagen, 2100 Copenhagen, Denmark

ABSTRACT

Neuropeptides are a highly diverse group of signaling molecules that affect a broad range of biological processes in insects, including development, metabolism, behavior, and reproduction. In the central nervous system, neuropeptides are usually considered to act as neuromodulators and cotransmitters that modify the effect of "classical" transmitters at the synapse. The present study analyzes the neuropeptide repertoire of higher cerebral neuropils in the brain of the red flour beetle *Tribolium castaneum*. We focus on two integrative neuropils of the olfactory pathway, the antennal lobes and the mushroom bodies. Using the technique of direct peptide profiling by matrix-assisted laser desorption/ionization time-of-flight (MALDI-TOF) mass spectrometry, we demonstrate that these neuropils can be characterized by their specific neuropeptide expression profiles. Complementary immunohistological analyses of selected neuropeptides revealed neuropeptide distribution patterns within the antennal lobes and the mushroom bodies. Both approaches revealed consistent differences between the neuropils, underlining that direct peptide profiling by mass spectrometry is a fast and reliable method to identify neuropeptide content. J. Comp. Neurol. 522:337–357, 2014.

INDEXING TERMS: neuropeptides; mass spectrometry; immunohistochemistry; olfactory system; insect

Neuropeptides form the largest and most diverse group of signaling molecules in the insect nervous system. This diversity can in part be attributed to their biosynthesis, as the posttranslational processing of larger precursor proteins encoded by single genes often yields a variety of distinct functional neuropeptides (Nässel, 2002; Predel et al., 2004; Altstein and Nässel, 2010). Thus, analyses of the fully sequenced genome of the red flour beetle *Tribolium castaneum* Herbst 1797 (Coleoptera, Tenebrionidae) (Richards et al., 2008) have identified 41 neuropeptide precursor genes which, in theory, could give rise to about 80 functional neuropeptides (Li et al., 2008). Twenty-one of these genes encode a core set of neuropeptide precursors that appears to be highly conserved across insects (Hauser et al., 2010). Accordingly, these neuroactive substances, which include e.g., adipokinetic hormones, C-type allatostatins, SIFamide, sNPFs, and tachykinin-related peptides, have been speculated to play cardinal roles in common physiological processes such as development, metabolism, or reproduction (Hauser et al., 2010). However, a deeper understanding of the functional implications of neuropeptides in the insect central nervous system is just beginning to emerge, largely on the basis of mutant screens and targeted genetic interference in the model system *Drosophila melanogaster* (e.g., Renn et al., 1999; Winther et al., 2006; Terhzaz et al., 2007; Chen and Ganetzky, 2012; Hergarden et al., 2012). Considering the evolutionary highly derived position of drosophilid flies within the dipteran radiation (Meusemann et al., 2010; Wiegmann et al., 2011), the coleopteran *T. castaneum* - with its amenability to powerful

The first two authors contributed equally to this work.

Grant sponsor: Deutsche Forschungsgemeinschaft - priority program "Integrative analysis of olfaction" (SPP 1392); Grant number: SCHA 678/13-2.

*CORRESPONDENCE TO: Joachim Schachtner, Philipps-University Marburg, Department of Biology, Animal Physiology, Karl-von-Frisch-Straße 8, 35043 Marburg, Germany. E-mail: joachim.schachtner@biologie.uni-marburg.de

Received November 23, 2012; Revised May 27, 2013;
Accepted June 19, 2013.
DOI 10.1002/cne.23399
Published online July 1, 2013 in Wiley Online Library (wileyonlinelibrary.com)

genetic manipulations (Bucher et al., 2002; Brown et al., 2003; Tomoyasu and Denell, 2004; Peel, 2009; Trauner et al., 2009) - represents another excellent model for investigations into neuropeptide functions in a more basal holometabolous insect. As a notorious pest of stored cereal products (Levinson and Levinson, 1978; Levinson et al., 1983), olfactory information is likely to represent one of the most dominant sensory inputs in *T. castaneum* (Cox and Collins, 2002). This is reflected in its large number of odorant receptor genes (Engsontia et al., 2008) and the general neuroanatomical makeup of the *T. castaneum* brain (Dreyer et al., 2010). In the present account, we therefore focus on a detailed characterization of the neuropeptide repertoire of two prominent centers of the olfactory pathway: the antennal lobes and the mushroom bodies. We show that direct peptide profiling by mass spectrometry (Schachtner et al., 2010) offers a quick and reliable way to assess the neuropeptide content of the selected brain compartments. Thus, the information provided in this account forms a valuable basis for future studies on the role of neuropeptides in the context of nervous system development as well as adult nervous system function and plasticity in *T. castaneum*.

MATERIALS AND METHODS

Animals

Wildtype *Tribolium castaneum* (San Bernardino; Sokoloff, 1966) were reared under permanent dark conditions in plastic boxes kept at 30°C in walk-in environmental chambers. Boxes were half filled with organic whole wheat flour, supplemented with 5% dried yeast powder (Bierhefepulver, Heirler Cenovis, Radolfzell, Germany) and 0.05% Fumidil-B (J. Webster Laboratories, Princeville, Canada; Berghammer et al., 1999) to prevent sporozoan infections. For egg collection, we used similar procedures as described in Berghammer et al. (1999). Beetles were kept for 2 days in organic flour, then sifted (stainless steel sieve 710 μm mesh size; Retsch, Haan, Germany) and transferred into a box filled with instant flour (Rosenmehl Wiener Griessler, Ergoldig, Germany) for egg laying. After another 2 days, adult beetles were again transferred back to organic flour and the instant flour substrate was sifted for eggs (stainless steel sieve 300 μm mesh size, Retsch). Eggs were isolated in a separate box filled with fresh whole grain flour. Hatching took place after ~5–6 days, pupation after about 18 days. Freshly eclosed male animals (stage A0) were collected in plastic containers and were sacrificed after 7 days (stage A7).

Transgenic beetles of the enhancer trap line G11410 (http://www.geku-base.uni-goettingen.de) are a product of a large-scale insertional mutagenesis screen (Trauner et al., 2009) and exhibit mushroom body-specific expression of enhanced green fluorescent protein (EGFP, see Fig. 1D; Posnien et al., 2011). Animals were kept under constant darkness and at room temperature. Eggs were collected once a week and were transferred to plastic containers filled with substrate and kept at 28°C, the slightly lower temperature being necessary to preserve the GFP signal. Similar to the procedures described above, freshly hatched male *T. castaneum* were separated and were dissected at 7 days of age.

Matrix-assisted laser desorption/ionization time-of-flight (MALDI-TOF) mass spectrometry

Neuropeptide content of antennal lobes and mushroom bodies was analyzed using the method of direct peptide profiling by MALDI-TOF mass spectrometry. Sample preparation followed the protocol described in Schachtner et al. (2010). Beetles were anesthetized on ice and dissected in a drop of cold 0.01M NH_4Cl-phosphate-buffer. For further dissection, i.e. tissue excision, whole brains were transferred to fresh buffer. Antennal lobes were separated from the brain using a pair of extra-fine forceps (Fig. 1A,B). Excision of GFP-expressing mushroom body subcompartments (Fig. 1C–H) was carried out under a fluorescence imaging stereomicroscope (SteREO Lumar.V12, Carl Zeiss MicroImaging, Germany). Tissue samples were directly transferred to a 384 spot stainless steel target plate using a glass capillary connected to a mouthpiece. Excess buffer was removed and the tissue was given time to dry at room temperature before each tissue spot was covered with 0.1 μl matrix solution, consisting of a saturated solution of α-cyano-4-hydroxycinnamic acid (Sigma, St. Louis, MO) in ethanol, methanol, H_2O, and trifluoroacetic acid (30/30/39/1). Samples were again left to dry at room temperature and were then analyzed with a 4800 Proteomics Analyzer (MDS Sciex, Forster City, CA) operating in the positive reflectron mode. For mass calibration synthetic peptide calibration standard (Bruker Daltonics, Bremen, Germany; Angiotensin III: 931.515, Angiotensin II: 1046.542, Angiotensin I: 1296.685, ACTH (18-39): 2465.199) was used. Spectra were obtained for a mass range between 800 and 3000 Da and consisted of 500 to 1500 accumulated laser shots each. Mass spectra were analyzed with the Data Explorer software (v. 4.1, MDS Sciex); mass peaks were discarded if they fell below a signal-to-noise threshold of 25 (calculated within a window width [m/z] of 250) and did not match peptide typical

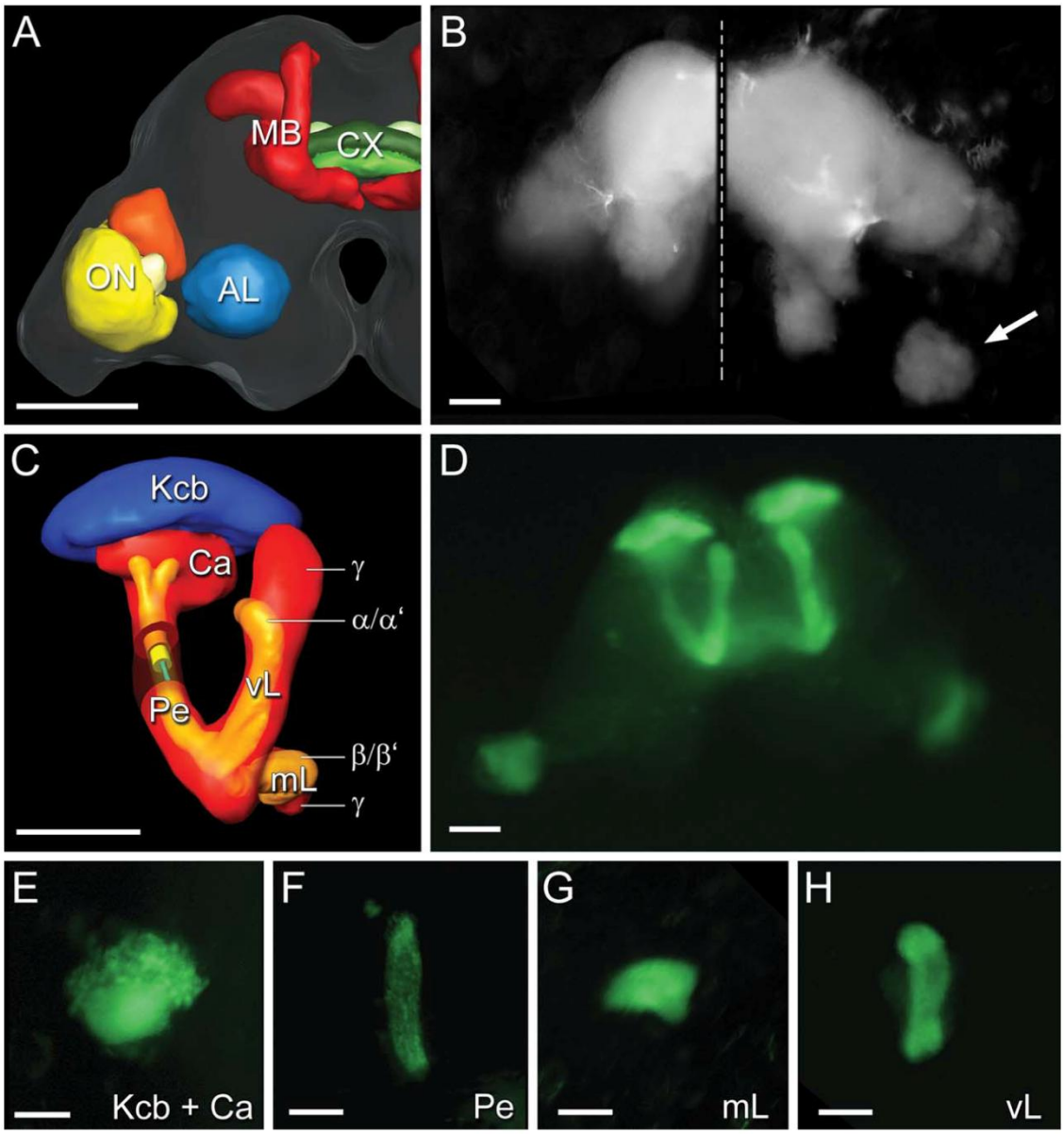

Figure 1. Antennal lobe and mushroom body tissue sampling for MALDI-TOF mass spectrometric analyses. **A:** Frontal view of the left hemisphere of the *T. castaneum* standard brain (adapted from Dreyer et al., 2010), showing the location of the central complex (CX), the mushroom body (MB), the optic neuropils (ON), and the antennal lobe (AL). **B:** The antennal lobes are located in the anterior part of the brain (left). Using extrafine forceps, the whole antennal lobe neuropil can selectively be separated from the brain (right, arrow). Note the visibility of the olfactory glomeruli in the antennal lobes. **C:** 3D reconstruction of the *T. castaneum* mushroom body as seen from a frontal angle. The neuropil comprises a knob-shaped calyx region (Ca) that is capped by densely packed Kenyon cell bodies (Kcb), a peduncle (Pe) that extends anterioventrad, and a medial (mL) and a vertical lobe (vL). Within the peduncle, distinct laminae are discernible (transparent section). They are formed by axon-like processes of successive Kenyon cell generations that are produced by neuroblasts situated on top of the calyx (Zhao et al., 2008). In the lobes, the laminae segregate to form the α/α', β/β', and γ subdivisions, respectively. **D:** Transgenic animals of the G11410 strain express EGFP in all parts of the mushroom bodies and in the distal parts of the optic lobes. **E–H:** EGFP-expression allows the selective micro-dissection of mushroom body subcompartments under a fluorescence imaging stereomicroscope. Scale bars = 50 μm.

TABLE 1.
Overview of the Antisera Employed in the Immunohistochemical Studies

Antiserum against	Abbreviation	Target sequence	Dilution	Donor	Reference
Tribolium castaneum adipokinetic hormone/ corazonin-related peptide	Trc-ACP	pQVTFSRDWNPa	1:10000	Dr. C. J. P. Grimmelikhuijzen	Hansen et al., 2010
Manduca sexta Allatotropin	Mas-AT	pGFKNVEMMTARGFa	1:4000 – 1:5000	Dr. J. Veenstra	Veenstra and Hagedorn, 1993
FMRFamide	FMRFa	FMRF-NH_2	1:2000 – 1:7000	Dr. E. Marder	Marder et al., 1987
Tribolium castaneum Insect oxytocin/ vasopressin-like hormone (Inotocin)	Trc-INO	CLITNCPRG a	1:10000	Dr. C. J. P. Grimmelikhuijzen	this study
Periplaneta americana Myoinhibitory peptide 1	Pea-MIP-1	GWQDLQGGW	1:4000 – 1:5000	Dr. M. Eckert	Predel et al., 2001
Periplaneta americana *Periviscerokinin* 2	Pea-PVK-2	GSSSGLISMPRVa	1:4000	Dr. M. Eckert	Eckert et al., 2002
Procambarus clarkii SIFamide	Prc-SIFa	GYRKPPFNGSIFa	1:20000	Dr. A. Yasuda	Yasuda et al., 2004
Locusta migratoria Tachykinin 2	Lom-TK -2	APLSGFYGVRa	1:10000 – 1:15000	Dr. H. Agricola	Veenstra et al., 1995b
Drosophila melanogaster Synapsin I	Syn		1:50	Dr. E. Buchner	Klagges et al., 1996

The list includes target sequences, applied dilutions, antibody sources, and references of the used antisera.

isotopic patterns (IsoPro 3.0). Tandem mass spectrometry was performed in gas-off mode. Fragmentation spectra of peptides were analyzed manually by comparing the fragment ion patterns of the masses corresponding to calculated masses of known *Tribolium* peptides with the theoretical fragment ions generated in Data Explorer.

Immunohistochemistry

Wholemount immunohistochemistry followed the protocol described in Dreyer et al. (2010). Briefly, animals were cold-anesthetized and then dissected in a drop of cold PBS (phosphate-buffered saline, 0.01M, pH 7.4). Whole brains were fixed for 1–2 hours at room temperature or overnight at 4°C in 0.01M PBS containing 4% formaldehyde (Roth, Karlsruhe, Germany). Fixation was stopped by rinsing 5 × 10 minutes in 0.01M PBS containing 0.3% Triton X-100 (PBS-TrX; Sigma-Aldrich, Steinheim, Germany). Brains were then transferred to a blocking solution containing 5% normal goat serum (NGS; Jackson ImmunoResearch, West Grove, PA) in PBS-TrX. After 1–2 days at 4°C, brains were transferred from the blocking solution to the primary antiserum. Detailed antibody characterizations are provided below; for an overview of the employed antibodies and dilutions see Table 1. To selectively label cerebral neuropil regions, a monoclonal primary antibody from mouse against synapsin was added to each batch. After 1–2 days at 4°C, incubation was stopped by rinsing 5 × 10 minutes in PBS-TrX. Subsequently, brains were incubated with secondary antiserum, comprising Cy3-conjugated goat anti-rabbit antibodies (Jackson ImmunoResearch, West Grove, PA) at a dilution of 1:300, Cy5-conjugated goat anti-mouse antibodies (Jackson ImmunoResearch) at a dilution of 1:300, and the nuclear marker DAPI (4',6-diamidinophenyindole; Sigma-Aldrich, Steinheim, Germany) at a dilution of 1:10000 in PBS-TrX with 1% NGS. Brains incubated for 1-2 days at 4°C; then, brains were rinsed again 5 × 10 minutes in PBS-TrX. Subsequently, brains were dehydrated in an ascending ethanol series (50%, 70%, 90%, 95%, 100%, 100%; 2.5 minutes each) and then cleared to transparency in methyl salicylate (Merck, Gernsheim, Germany). Lastly, brains were mounted on coverslips using Permount mounting medium (Fisher Scientific, Pittsburgh, PA) and a layer of two reinforcing rings (Zweckform, Oberlaindern, Germany) as spacers to prevent tissue compression.

Antibody characterization

ACP-antiserum

The polyclonal *T. castaneum* adipokinetic hormone/corazonin-related peptide (Trc-ACP) antiserum was obtained commercially from GeneMed Synthesis (San Antonio, TX). It was raised in rabbit against synthetic *Tribolium* ACP (pQVTFSRDWNPamide; Hansen et al., 2010) that was N-terminally elongated with a cysteine residue (CQVTFSRDWNPamide) and N-terminally

coupled via this residue to keyhole limpet hemocyanin. Specificity was tested in *Tribolium* with preimmune antiserum and preabsorption of the ACP antiserum with synthetic ACP (pQVTFSRDWNPamide; synthesized by GeneMed Synthesis), both of which showed no immunostaining (Hansen et al., 2010).

AT-antiserum

The polyclonal *Manduca sexta* allatotropin (Mas-AT) antiserum (No. 13.3.91) was kindly donated by Dr. J. Veenstra (Bordeaux, France). It was raised in rabbit against synthetic *M. sexta* AT (GFKNVEMMTARGFamide) glutaraldehyde-coupled to thyroglobulin (Veenstra and Hagedorn, 1993) and fully crossreacts with Lom-AG-MT-1, the locust member of the AT family (Veenstra and Hagedorn, 1993; Homberg et al., 2004). For the flour beetle, specificity was confirmed by preabsorption of the antiserum with synthetic Mas-AT (GFKNVEMMTARG-Famide, Bachem, Switzerland) at concentrations of 10 nM, 100 nM, 10 µM, and 100 µM. Preabsorption with synthetic Mas-AT completely abolished immunostaining at all tested concentrations.

FMRFamide-antiserum

The polyclonal FMRFamide (FMRFa) antiserum (No. 671N) was a gift from Dr. E. Marder (Brandeis University, Waltham, MA). It was raised in rabbit against synthetic FMRFa conjugated to thyroglobulin (Marder et al., 1987). Specificity tests by radio-immunoassay showed crossreactivity of the antiserum with various C-terminally extended RFamides (Marder et al., 1987). Specificity in *Tribolium* was verified by preabsorption of the antiserum with synthetic FMRFa (Sigma, Germany) at concentrations of 10 nM, 100 nM, 10 µM, and 100 µM. Preabsorption with 10 µM synthetic FMRFa led to very faint stainings, 100 µM synthetic FMRFa completely abolished immunostaining.

Inotocin-antiserum

The polyclonal *T. castaneum* insect oxytocin/vasopressin-like hormone (Inotocin; G5481 1st bleeding; Trc-INO) antiserum was commercially obtained from GeneMed Synthesis. It was raised against *Tribolium* inotocin (CLITNCPRGamide, where the two cysteine residues form a cysteine bridge; Stafflinger et al., 2008) N-terminally coupled with glutaraldehyde to keyhole limpet hemocyanin. Specificity in *Tribolium* was tested with preimmune antiserum and preabsorption of the Trc-INO antiserum with synthetic *Tribolium* inotocin (CLITNCPRGamide, GeneMed Synthesis) at concentrations of 100 nM, 1 µm, 10 µM, and 100 µM. Immunostainings with the preimmune serum at a concentration of 1:10000 showed in some samples a faint staining of the calyx of the mushroom body, at concentrations of 1:2000 additional faint staining of the vertical lobe, medial lobe, and peduncle could be detected. Preabsorption with 100 µM, 10 µm, and 1 µM of synthetic inotocin in combination with the Trc-INO antiserum abolished all immunostaining, except for unspecific mushroom body staining.

MIP-antiserum

The polyclonal *Periplaneta americana* Myoinhibitory peptide 1 (Pea-MIP-1) antiserum was kindly donated by Dr. M. Eckert (Jena, Germany). It was raised in rabbit against the full sequence of synthetic *P. americana* MIP-1 (GWQDLQGGWamide), coupled to thyroglobulin with glutaraldehyde. Specificity was confirmed by replacing the antiserum with preimmune rabbit serum, as well as by liquid-phase preabsorption using neuropeptide-conjugate of synthetic Pea-MIP-1 (Predel et al., 2001). Specificity in *T. castaneum* was verified by preabsorption of the antiserum with synthetic Pea-MIP-1 (GWQDLQGGWamide, kindly provided by Dr. M. Eckert) at concentrations of 10 nM, 100 nM, 10 µM, and 100 µM. Preabsorption with synthetic Pea-MIP-1 completely abolished the immunostaining at all concentrations.

PVK-antiserum

The unpurified and polyclonal *P. americana* Periviserokinin 2 (Pea-PVK-2) antiserum was a generous donation of Dr. M. Eckert (Jena, Germany). It was raised in rabbit against thyroglobulin-glutaraldehyde conjugates of *P. americana* PVK-2 (GSSSGLISMPRVamide; Eckert et al., 2002). The unpurified antiserum recognizes peptides with the C-terminal sequence PRXamide and is known to react with periviserokinins and with pyrokinins (Eckert et al., 2002). It has been used to specifically label these substances in a variety of insect species (*D. melanogaster*: Wegener et al., 2004; *Nezara viridula*: Predel et al., 2006; *Manduca sexta*: Neupert et al., 2009); *Schistocerca gregaria*: Herbert et al., 2010; *Acyrthosiphon pisum*: Kollmann et al., 2011a), in the chelicerate *Ixodes ricinus* (Neupert et al., 2005), and in the clitellate annelid *Eisenia fetida* (Herbert et al., 2009). Specificity in *T. castaneum* was verified by preabsorption of the antiserum with synthetic Lem-PVK 2 (GSSGLISMPRVamide, kindly provided by Dr. R. Predel, Cologne, Germany) at concentrations of 10 nM, 100 nM, 1 µM, 10 µM, and 100 µM. Preabsorption with 10 µM and 100 µM synthetic Lem-PVK 2 completely abolished the immunostaining.

SIFamide-antiserum

The polyclonal *Procambarus clarkii* SIF-amide (Prc-SIFa) antiserum was a gift from Dr. A. Yasuda (Osaka, Japan).

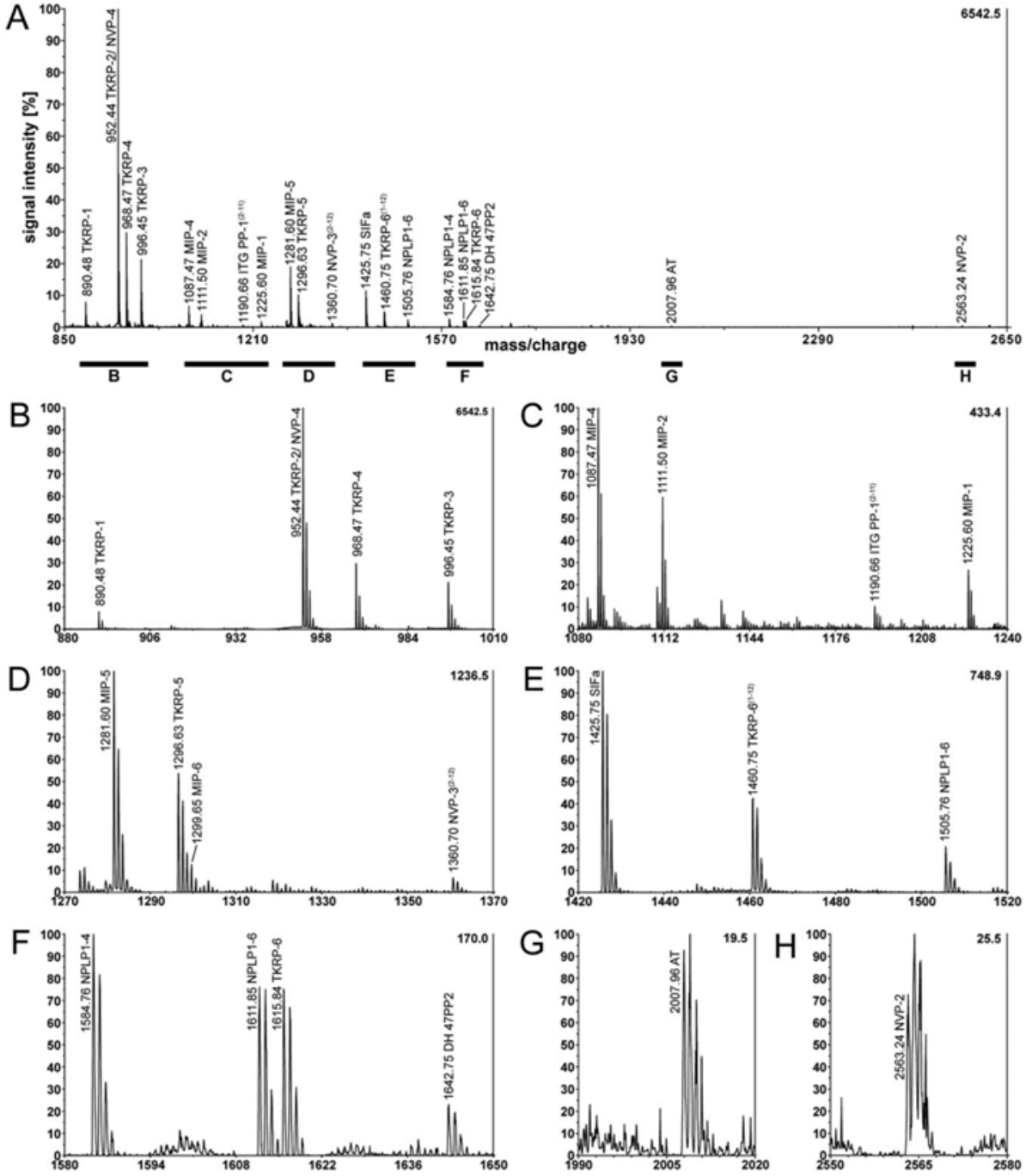

Figure 2. Representative MALDI-TOF mass spectrum of a single *T. castaneum* antennal lobe sample. **B–H:** Magnifications of the spectral sections marked in **A**. Left y-axes: relative signal intensity after autoscaling to the maximum peak intensity in the selected x-range (mass/charge values). Right y-axes: peak intensity in absolute census.

It was raised in rabbit against synthetic SIFa of the crayfish *Procambarus clarkii* (GYRKPPFNGSIFa), coupled to bovine serum albumin (Yasuda et al., 2004; Polanska et al., 2007). As the C-terminus of crustacean SIFa is identical to the predicted C-terminus of *Tribolium*-SIFa (TYRKPPFNGSIFa; Li et al., 2008), Prc-SIFa antiserum was used to label neurons containing SIFa in *T. castaneum*. Specificity was

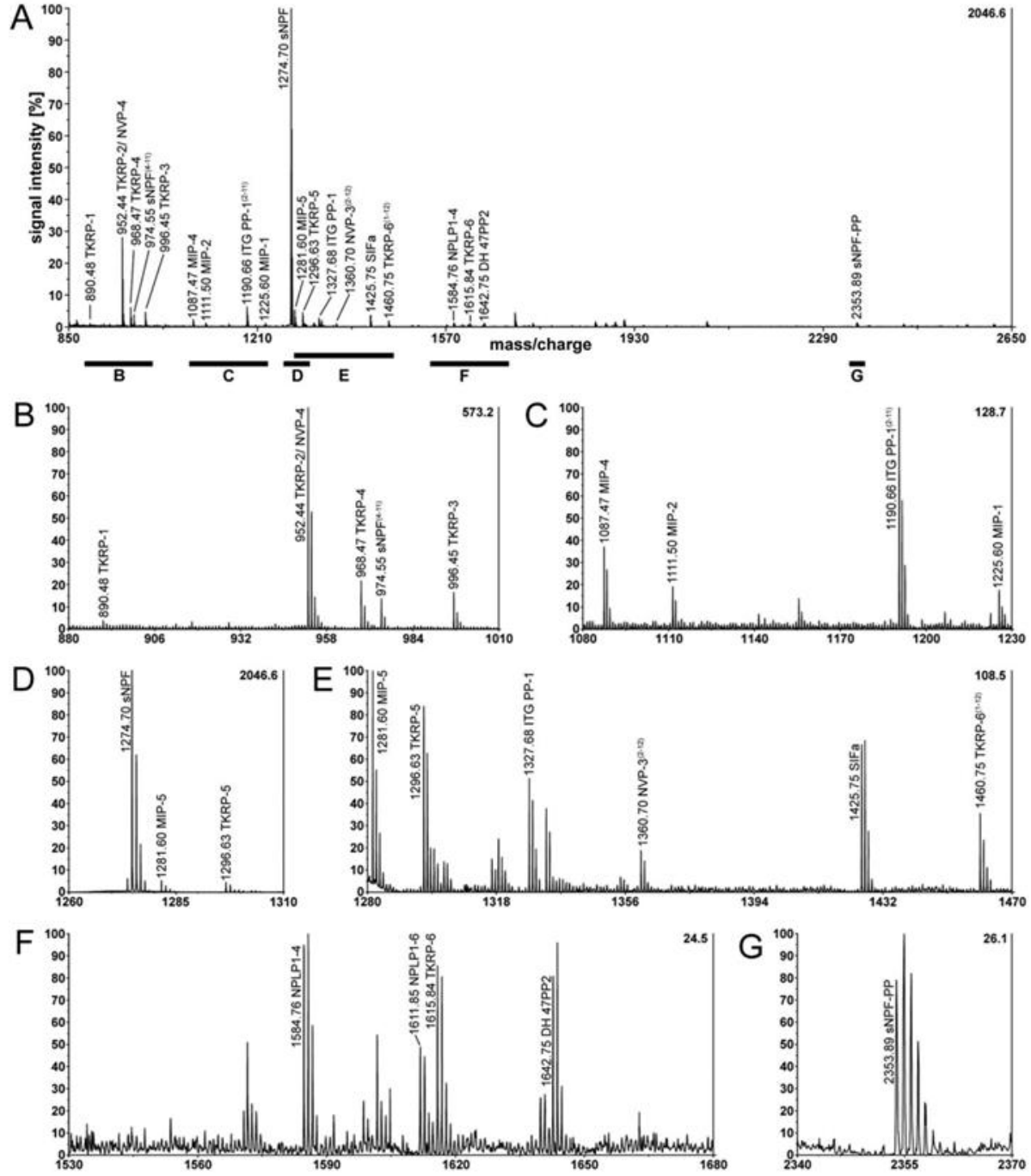

Figure 3. Representative MALDI-TOF mass spectrum of a single *T. castaneum* mushroom body sample. Mass spectra for the vertical lobe (shown here), the medial lobe, calyx, and peduncle showed no explicit differences. **B–G:** Magnifications of the spectral sections marked in **A**. Left y-axes: relative signal intensity after autoscaling to the maximum peak intensity in the selected x-range (mass/charge values). Right y-axes: peak intensity in absolute census.

confirmed by preabsorption of the antiserum with synthetic Prc-SIFa (GYRKPPFNGSIFa, Iris Biotech, Marktredwitz, Germany) at concentrations of 10 nM, 100 nM, 10 µM, and 100 µM. Preabsorption with 100 µM synthetic SIFa completely abolished the immunostaining.

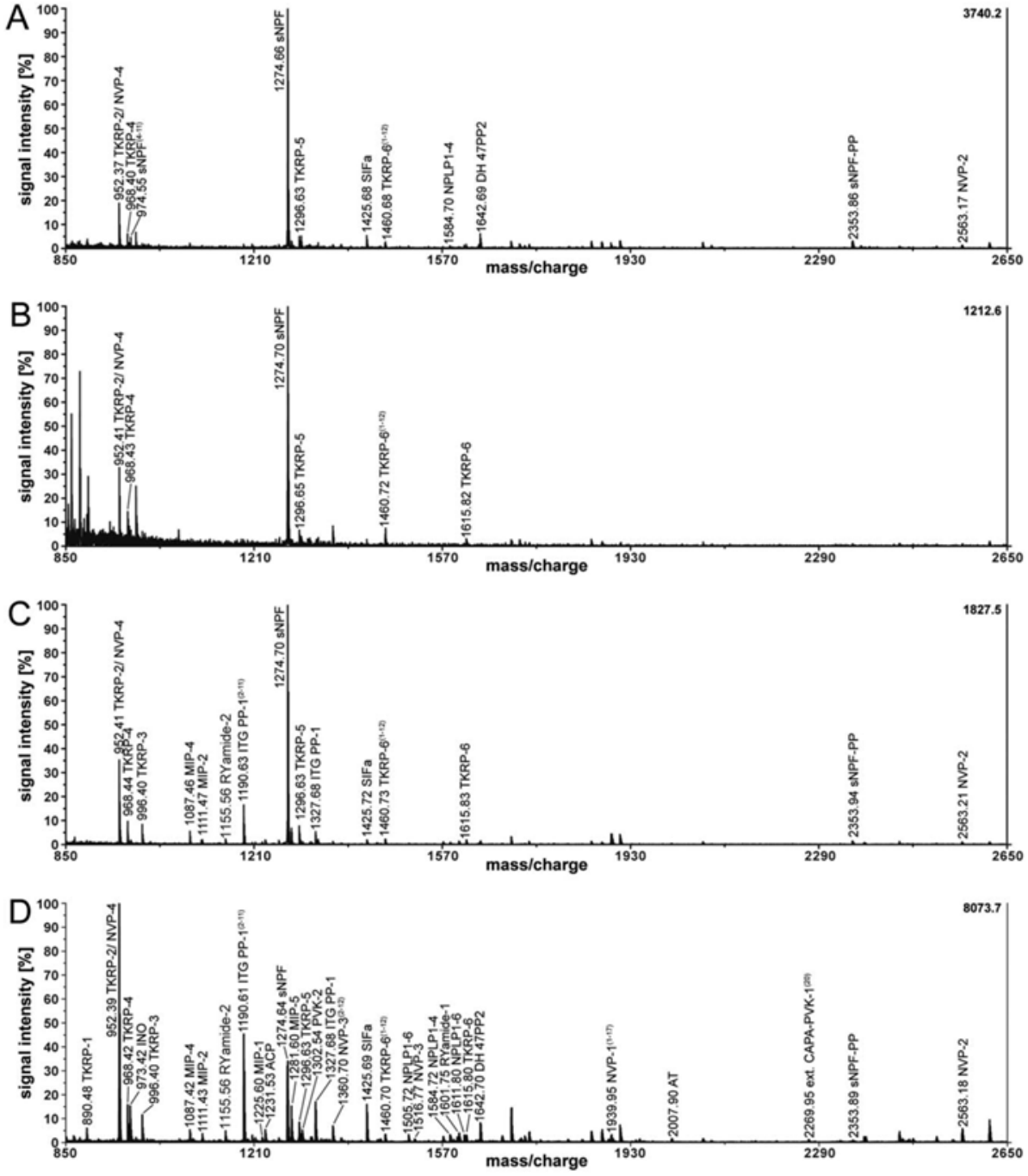

Figure 4. Representative MALDI-TOF mass spectra of *T. castaneum* brain tissue samples. Mass spectra of a single **(A)** medial lobe, **(B)** calyx, and **(C)** peduncle show typical profile of mushroom body mass spectra. **D:** A representative mass spectrum of tissue next to the mushroom body in the lateral protocerebrum displays a nonmushroom body profile. Left y-axes: relative signal intensity after autoscaling to the maximum peak intensity in the selected x-range (mass/charge values). Right y-axes: peak intensity in absolute census.

TKRP-antiserum

The polyclonal *Locusta migratoria* Tachykinin 2 (Lom-TK-2) antiserum (K1-50820091) was a kind donation of Dr. H. Agricola (Jena, Germany). It was raised in rabbits against locustatachykinin-2 (APLSGFYGVRamide), glutaraldehyde-conjugated to bovine thyroglobulin

TABLE 2.

Predicted *T. castaneum* Neuropeptide Sequences and Their Calculated Masses, Matched to Masses Detected by Direct Peptide Profiling MALDI-TOF Mass Spectrometry of Isolated Antennal Lobe Samples (n = 20)

					AL
Peptide	Sequence	Calculated mass	Detected mass	Mean deviation	Detection frequency [%]
Allatotropin					
AT	GIEALKYHNMDLGTARGYa	2008.01	2007.97	0.04	50
Apis *ITG-like peptide*					
ITG PP-1	LTGLAGFKRPMH-OH	1327.73	1327.67	0.02	20
ITG PP-1$^{(1-11)}$	LTGLAGFKRPM-OH	1190.67	1190.61	0.01	35
Apis *NVP-like peptide*					
NVP-2	AHPQLNVGEHGREVPYYSKPTAI-OH	2563.31	2563.25	0.02	35
NVP-3$^{(2-12)}$	DARKIRLDSRM-OH	1360.75	1360.68	0.04	85
*NVP-4	GRWGGFADS-OH	952.43	952.43	0.03	100
CRF-like diuretic hormone 31					
DH 31	GLDLGLGRGFSGSQAAKH LMGLAAANFAGGPa	2940.53	2940.54	0.06	30
CRF-like diuretic hormone 47					
DH 47PP2	AFLQSRASGTYDNNV-OH	1642.78	1642.73	0.05	80
Insulin-like peptide 1					
Inlp1-5	WSSPHMVHLMN-OH	1338.61	1338.57	0.02	10
Myoinhibitory peptide / allatostatin-B					
MIP-1	DWNKDLHIWa	1225.61	1225.57	0.01	90
MIP-2	GWNNLHEGWa	1111.51	1111.48	0.02	90
MIP-4	NWGQFHGGWa	1087.49	1087.46	0.02	100
MIP-5	SKWDNFRGSWa	1281.61	1281.58	0.04	100
MIP-6	EPAWSNLKGIWa	1299.68	1299.63	0.03	100
Neuropeptide-like protein 1					
NPLP1-2	NLEALARAGYIRTLPNPDEEDPNN-OH	2682.31	2682.32	0.06	25
NPLP1-3	SLSTLAKNDQLPTTFQNNES-OH	2208.08	2208.04	0.00	5
NPLP1-4	NVGSLARNFNFPSYa	1584.79	1584.74	0.05	100
NPLP1-5	YLASLVRNGELKYSa	1611.89	1611.82	0.05	100
NPLP1-6	NIASIKAQYPGTRS-OH	1505.81	1505.76	0.04	100
Periviscerokinin					
PVK-2	RIGKMVSFPRIa	1302.78	1302.61	0.02	55
SIFamide					
SIFa	TYRKPPFNGSIFa	1425.76	1425.73	0.04	100
Tachykinin-related peptide					
TKRP-1	APSGFTGVRa	890.48	890.47	0.03	85
*TKRP-2	APSGFMGMRa	952.45	952.43	0.03	100
TKRP-3	APMGFMGMRa	996.46	996.44	0.03	95
TKRP-4	APSGFFGMRa	968.48	968.45	0.03	100
TKRP-5	MPRQAGFFGMRa	1296.65	1296.61	0.04	100
TKRP-6	YPYQFRGKFVGVRa	1615.89	1615.83	0.04	100
TKRP-6$^{(1-12)}$	YPYQFRGKFVGV-OH	1460.77	1460.72	0.04	100

In total, 28 neuropeptides belonging to 11 neuropeptide families were identified. Samples were collected from 7-day-old adult male *T. castaneum* specimens (A7m).

*Since TKRP-2 and NVP-4 display the same calculated mass, these two neuropeptides could not be distinguished by mass matching. Fragmentation analysis by tandem mass spectrometry indicated the presence of both neuropeptides.

(Veenstra et al., 1995). The resulting antiserum is known to detect TKRPs (consensus sequence FXGXRamide) in other insects as well (Vitzthum and Homberg, 1998). Specificity in *T. castaneum* was confirmed by preabsorption of the antiserum with synthetic Lom-TK II (APLSGFYGVRamide, Peninsula Laboratories, San Carlos, CA) at concentrations of 10 nM, 100 nM, 1 µM, 10 µM, and 100 µM. Preabsorption with 10 µM and 100 µM of synthetic peptide completely abolished the immunostaining.

Synapsin

The monoclonal synapsin antibody (3C11, #151101 (13.12.06), kindly provided by Dr. E. Buchner, Würzburg, Germany) from mouse against a fusion protein consisting of a glutathione-S-transferase and the first amino acids of the presynaptic vesicle protein synapsin I coded by its 5′-end (SYNORF1; Klagges et al., 1996) was used to selectively label neuropilar areas in the brain. Its specificity in *T.*

TABLE 3.

Predicted *T. castaneum* Neuropeptide Sequences and Their Calculated Masses, Matched to Masses Detected by Direct Peptide Profiling MALDI-TOF Mass Spectrometry of Isolated Mushroom Body Samples (n = 20)

Peptide	Sequence	Calculated mass	Detected mean	Mean deviation	vL	mL	Ca	Pe
					Detection frequency [%]			
ACP								
ACP	pQVTFSRDWNPa	1231.59	1231.53	0.02	0	0	0	10
Apis *ITG-like peptide*								
ITG PP-1	LTGLAGFKRPMH-OH	1327.73	1327.66	0.02	45	20	0	25
ITG PP-1$^{(1-11)}$	LTGLAGFKRPM-OH	1190.67	1190.63	0.00	55	40	5	50
Apis *NVP-like peptide*								
NVP-2	AHPQLNVGEHGREVPYYSKPTAI-OH	2563.31	2563.12	0.05	40	30	0	20
NVP-3$^{(2-12)}$	DARKIRLDSRM-OH	1360.75	1360.71	0.08	45	25	20	35
*NVP-4	GRWGGFADS-OH	952.43	952.41	0.02	95	95	90	75
CRF-like diuretic hormone 31								
DH 31	GLDLGLGRGFSGSQAAKHLMGLAAANFAGGPa	2940.53	2940.41	0.01	35	5	0	10
CRF-like diuretic hormone 47								
DH 47PP2	AFLQSRASGTYDNNV-OH	1642.78	1642.71	0.03	80	70	0	45
Ecdysis-triggering hormone								
ETH-2	SNTNKNTNIDEMGKFFMKASKSVPRIa	2956.51	2956.29	0.01	0	0	0	5
FMRFamide								
FMRFa-4	NQPKATTNYLRFa	1451.78	1451.71	0.05	0	0	0	10
FMRFa-5	DTSNFLRFa	998.51	998.44	0.00	0	0	0	5
Insulin-like peptide 1								
Inlp1-5	WSSPHMVHLMN-OH	1338.61	1338.59	0.03	5	0	0	10
Myoinhibitory peptide / allatostatin-B								
MIP-1	DWNKDLHIWa	1225.61	1225.55	0.04	5	5	0	0
MIP-2	GWNNLHEGWa	1111.51	1111.47	0.00	5	5	0	5
MIP-4	NWGQFHGGWa	1087.49	1087.47	0.02	15	10	0	5
MIP-5	SKWDNFRGSWa	1281.61	1281.56	0.05	65	55	5	45
MIP-6	EPAWSNLKGIWa	1299.68	1299.64	0.01	0	10	0	5
Neuropeptide-like protein1								
NPLP1-2	NLEALARAGYIRTLPNPDEEDPNN-OH	2682.31	2682.10	0.02	10	0	0	0
NPLP1-4	NVGSLARNFNFPSYa	1584.79	1584.71	0.02	45	15	0	25
NPLP1-5	YLASLVRNGELKYSa	1611.89	1611.77	0.01	35	20	0	20
NPLP1-6	NIASIKAQYPGTRS-OH	1505.81	1505.73	0.02	10	0	0	10
Periviscerokinin								
PVK-2	RIGKMVSFPRIa	1302.78	1302.56	0.04	15	0	0	5
RYamide								
RYamide-1	VQNLATFKTMMRYa	1601.83	1601.74	0.02	0	5	0	10
RYamide-2	ADAFFLGPRYa	1155.60	1155.55	0.01	0	5	0	5
short neuropeptide F								
**sNPF	SGRSPSLRLRFa	1274.74	1274.71	0.02	100	100	100	100
sNPF$^{(4-11)}$	SPSLRLRFa	974.59	974.54	0.02	55	70	0	20
sNPF-PP	SDASMTPEAAFMMAQAVDHETN-OH	2353.97	2353.86	0.10	75	90	15	60
SIFamide								
SIFa	TYRKPPFNGSIFa	1425.76	1425.70	0.0	85	80	50	80
Sulfakinin								
SK-1	pQTSDDYGHLRFa	1320.60	1320.53	0.01	0	0	0	5
SK-2	GEEPFDDYGHMRFa	1598.67	1598.57	0.01	10	0	0	5
Tachykinin-related peptide								
TKRP-1	APSGFTGVRa	890.48	890.44	0.03	25	0	0	15
*TKRP-2	APSGFMGMRa	952.45	952.41	0.02	95	95	90	75
TKRP-3	APMGFMGMRa	996.46	996.42	0.01	40	15	5	25
TKRP-4	APSGFFGMRa	986.48	968.45	0.02	75	65	25	55
TKRP-5	MPRQAGFFGMRa	1296.65	1296.68	0.02	100	95	70	95
TKRP-6	YPYQFRGKFVGVRa	1615.89	1615.79	0.05	35	40	10	55
TKRP-6$^{(1-12)}$	YPYQFRGKFVGV-OH	1460.77	1460.68	0.03	55	65	35	55

In total, 37 neuropeptides belonging to 16 neuropeptide families were identified. Samples were collected from 7-day-old adult male *T. castaneum* specimens (A7m).

*Fragmentation analysis by tandem mass spectrometry indicated that both neuropeptides contribute to the mass peak at 952.41 Da.

**The calculated mass of sNPF equals that of the neuropeptide (QDVDHVFLRFa, 1274.66, Li et al., 2008). However, fragmentation by tandem mass spectrometry confirmed the identity of the detected mass as sNPF (Fig. 5).

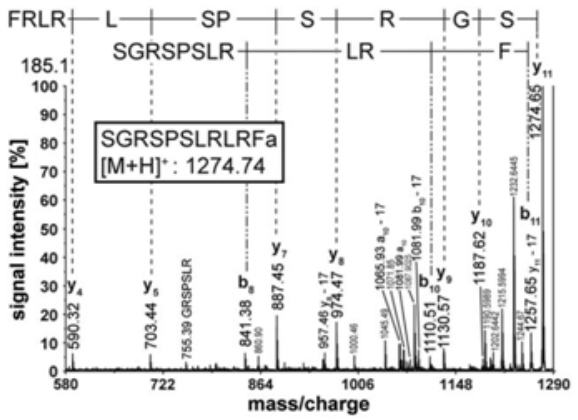

Figure 5. Representative MALDI-TOF/TOF fragmentation spectrum of *T. castaneum* sNPF at m/z 1274.7 from a single median lobe sample. Peaks of fragment ions which could be assigned to sNPF are labled. Additional ion signals were not assignable, neither to sNPF nor to myosuppressin (QDVDHVFLRFa, 1274.66, Li et al., 2008).

castaneum was shown by western blot analysis (Utz et al., 2008).

Image acquisition and processing

Images were taken with a confocal laser-scanning microscope (TCS SP5, Leica Microsystems, Wetzlar, Germany). Cy3 fluorescence was detected using a DPSS laser (excitation wavelength 561 nm), Cy5 fluorescence with an helium/neon laser (excitation wavelength 633 nm). DAPI fluorescence was visualized with a UV laser (excitation wavelength 405 nm). Images were acquired in sequential scan mode at resolutions of 2048 × 2048 or 1024 × 1024 pixels, a step size of 1 µm, and a scanning speed between 200 and 100 Hz. Confocal images and image stacks were analyzed with the Amira 5.3.3 graphics software (Visage Imaging, Berlin, Germany). For further processing (i.e., level adjustments, contrast, and brightness optimization) and final figure arrangements, snapshots of single sections or projection views taken in Amira were processed using Adobe Photoshop CS3 (Adobe Systems, San Jose, CA).

RESULTS

MALDI-TOF mass spectrometry

Mass spectrometric analyses of *T. castaneum* olfactory neuropils revealed numerous mass peaks between 800 and 3000 Da, corresponding to a broad range of neuropeptides (Figs. 2, 3; Tables 2, 3). Obtained spectra were nearly identical for each neuropil type, respectively, providing typical mass spectrometric fingerprints for antennal lobes and mushroom bodies (compare Figs. 2, 3, 4). Only in a few cases, analyses revealed additional neuropeptide mass peaks. The obtained mass spectra for the four mushroom body subcompartments (vertical lobe, medial lobe, calyx, and peduncle) were highly similar (Table 3, Fig. 4). In contrast, the comparison of mushroom body mass spectra and antennal lobe mass spectra showed considerable differences (Figs. 2, 3, 4). Spectra differed not only in their overall appearance but also in the detected masses - for example, a prominent peak at 1274.70 is present in all mushroom body spectra but is completely missing in the antennal lobe spectra - and in the detection frequency of individual masses. Moreover, mass spectrometric fingerprints of olfactory neuropils differed markedly from spectra of samples from the neighboring lateral protocerebrum (Fig. 4).

Antennal lobe

MALDI-TOF mass spectra of antennal lobes from 20 individual male *T. castaneum* revealed 28 mass peaks that could be assigned to neuropeptides encoded by 10 different genes (Table 2). Diuretic hormones 47 (DH 47), myoinhibitory peptides / allatostatin-B (MIPs), neuropeptide-like precursor 1 (Nplp1), NVP-motif containing peptides (NVPs), and SIFamide (SIFa) as well as tachykinin-related peptides (TKRPs) were identified in most spectra. Diuretic hormones 31 (DH 31), insulin-like peptides 1 (Inlp1), and ITG-motif containing peptides (ITGs) were only detected in few spectra and usually exhibited a low signal intensity. Mass peaks corresponding to allatotropin (AT) and periviscerokinin 2 (PVK-2) showed similarly low signal intensity, but occurred in about half of the recorded spectra. The dominant ion signal in each spectrum was located at 952.43 Da (Fig. 2), indicating the presence of either TKRP-2 or NVP-4, both of which display almost identical monoisotopic masses. Fragmentation of this signal by tandem mass spectrometry yielded characteristic masses for both peptides, suggesting that TKRP-2 and NVP-4 are both expressed in the antennal lobe (data not shown).

Mushroom body

Mass spectrometric analyses of the four mushroom body subcompartments (calyx, peduncle, vertical, and medial lobe; sampled from a total of 44 individual male *T. castaneum*) revealed the presence of 36 different neuropeptides (Table 3). With the exception of AT - which was only detected in antennal lobe tissue- all corresponding peptide masses detected in antennal lobe samples were also identified in spectra of the mushroom bodies. Moreover, detailed analyses revealed additional masses that occurred exclusively in the

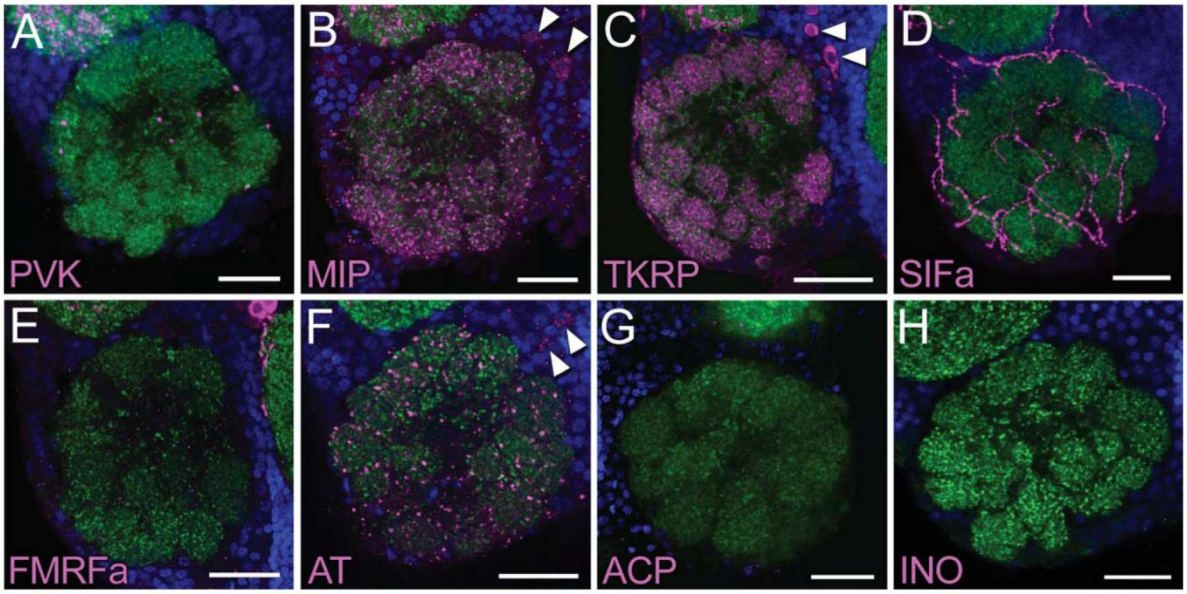

Figure 6. Neuropeptide immunoreactivity in the antennal lobes of *T. castaneum*. **A:** Periviscerokinin-like immunoreactivity is restricted to scattered spots between the olfactory glomeruli in the posterior portion of the antennal lobe **B:** Myoinhibitory peptide-like immunoreactivity can be observed in all glomeruli and in about 9 somata of local interneurons lateral to the antennal lobe (arrowheads). **C:** Tachykinin related peptide-like immunoreactivity in the antennal lobe looks highly similar to B, labeling a dense network of fibers innervating all glomeruli. These fibers originate from an average of 36 cell bodies (arrowheads) that form aggregations lateral and ventral to the antennal lobe neuropil. **D:** The SIFamide antiserum stains extrinsic fibers stemming from four cell bodies in the pars intercerebralis. These projections invade the antennal lobes and braid most of the glomeruli. **E:** Staining against FMRFamides produces no immunoreactivity in the antennal lobe neuropil. **F:** Allatotropin-like immunostaining in the antennal lobe is spotty but shows a homogeneous distribution across all glomeruli. Weak staining is observed in six antennal lobe-associated cell bodies (arrowheads). **G:** No immunoreactivity to the adipokinetic hormone/corazonin-related peptide antiserum could be detected in the antennal lobe. **H:** All glomeruli are devoid of inotocin-like immunoreactivity. Images show either single optical sections or maximum projection views of 2–10 optical sections; DAPI-labeled cell nuclei are depicted in blue, synapsin-immunoreactivity in green, and neuropeptide immunoreactivity in magenta. Scale bars = 20 μm.

mushroom bodies but not in the antennal lobes. These correspond to extended FMRFamides, ecdysis-triggering hormones (ETHs), sulfakinins (SKs), RYamides, adipokinetic hormone/corazonin-related peptide (ACP), periviscerokinin 2 (PVK 2), and short neuropeptide Fs (sNPFs). The calculated mass of sNPF (1274.74) equals that of the neuropeptide myosuppressin (QDVDHVFLRFa, 1274.66; Li et al., 2008). Fragmentation by tandem mass spectrometry confirmed the identity of the detected mass as sNPF (Fig. 5). sNPF was present in all mushroom body spectra and typically represented the mass with the highest signal intensity (Figs. 3A, 4A–C). The other mushroom body-exclusive peptides pertain to peaks with low signal intensities and were only detected in 5% to 15% of all spectra (Table 3). A comparison of the identified neuropeptides in the different mushroom body subcompartments shows that not all masses were detected with consistent frequency. Especially in spectra of calyx samples, detection frequency of some neuropeptides was rather low, and a few peptides that occurred in other samples (e.g., $sNPF^{(4-11)}$ and DH 47PP-2) were not detected at all (Table 3).

Immunohistochemistry

To verify the results obtained by MALDI-TOF mass spectrometry and to further elucidate neuropeptide distribution within the antennal lobes and the mushroom bodies, brains of 7-day-old male *T. castaneum* were stained against selected neuropeptides, including adipokinetic hormone/corazonin-related peptide (ACP), allatotropin (AT), FMRFamide related peptides (FaRPs), Inotocin (INO), myoinhibitory peptides (MIPs), periviscerokinins (PVKs), SIFamide (SIFa), and tachykinin-related peptides (TKRPs). All immunostainings complied with the mass spectrometric results.

Antennal lobe

The antennal lobe of adult *T. castaneum* beetles (Fig. 1A,B) comprises about 70 olfactory glomeruli (Dreyer

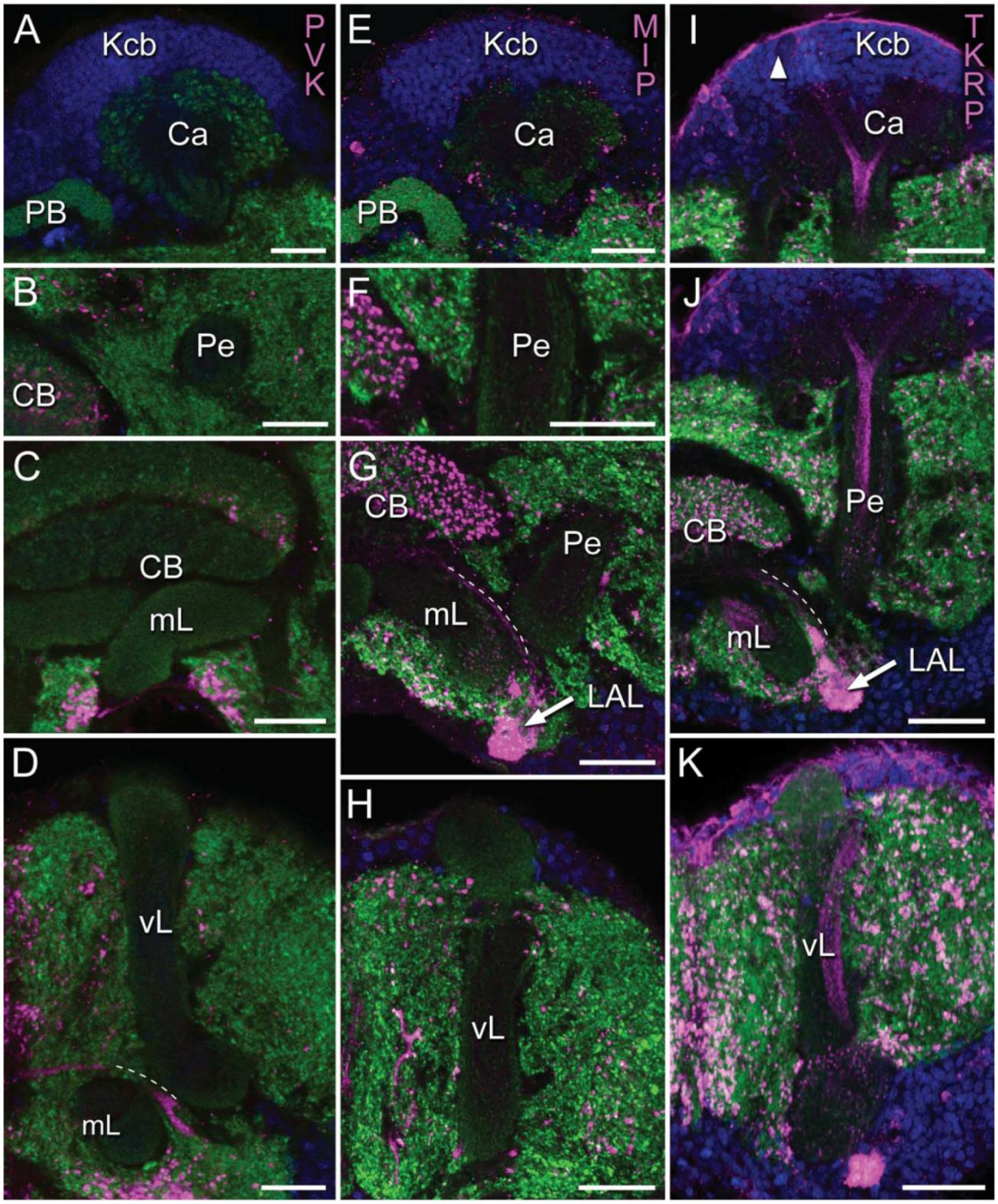

Figure 7. The mushroom body neuropil in *T. castaneum*. **A–D:** All mushroom body subcompartments are devoid of periviscerokinin-like immunoreactivity. **E–H:** Staining against myoinhibitory peptides reveals scant immunoreactivity in the calyx (Ca) region and a small immunoreactive zone at the junction between the peduncle (Pe) and the lobes (mL, vL). The immunoreactive zone is immediately adjacent to the isthmus tract (indicated by dashed line) that connects the central body (CB) with the lateral accessory lobes (LAL, arrow). **I–K:** Tachykinin related peptide-like immunoreactivity can be observed in Kenyon cell processes that extend throughout the neuropil and form the ingrowth core and the α/β division. Faint immunostaining is even discernible in the mushroom body neuroblasts (arrowhead) and in adjacent Kenyon cell bodies (Kcb). Images show either single optical sections or maximum projection views of 2–10 optical sections; DAPI-labeled cell nuclei are depicted in blue, synapsin-immunoreactivity in green, and neuropeptide immunoreactivity in magenta. mL, median lobe; vL, vertical lobe; PB, protocerebral bridge. Scale bars = 20 μm.

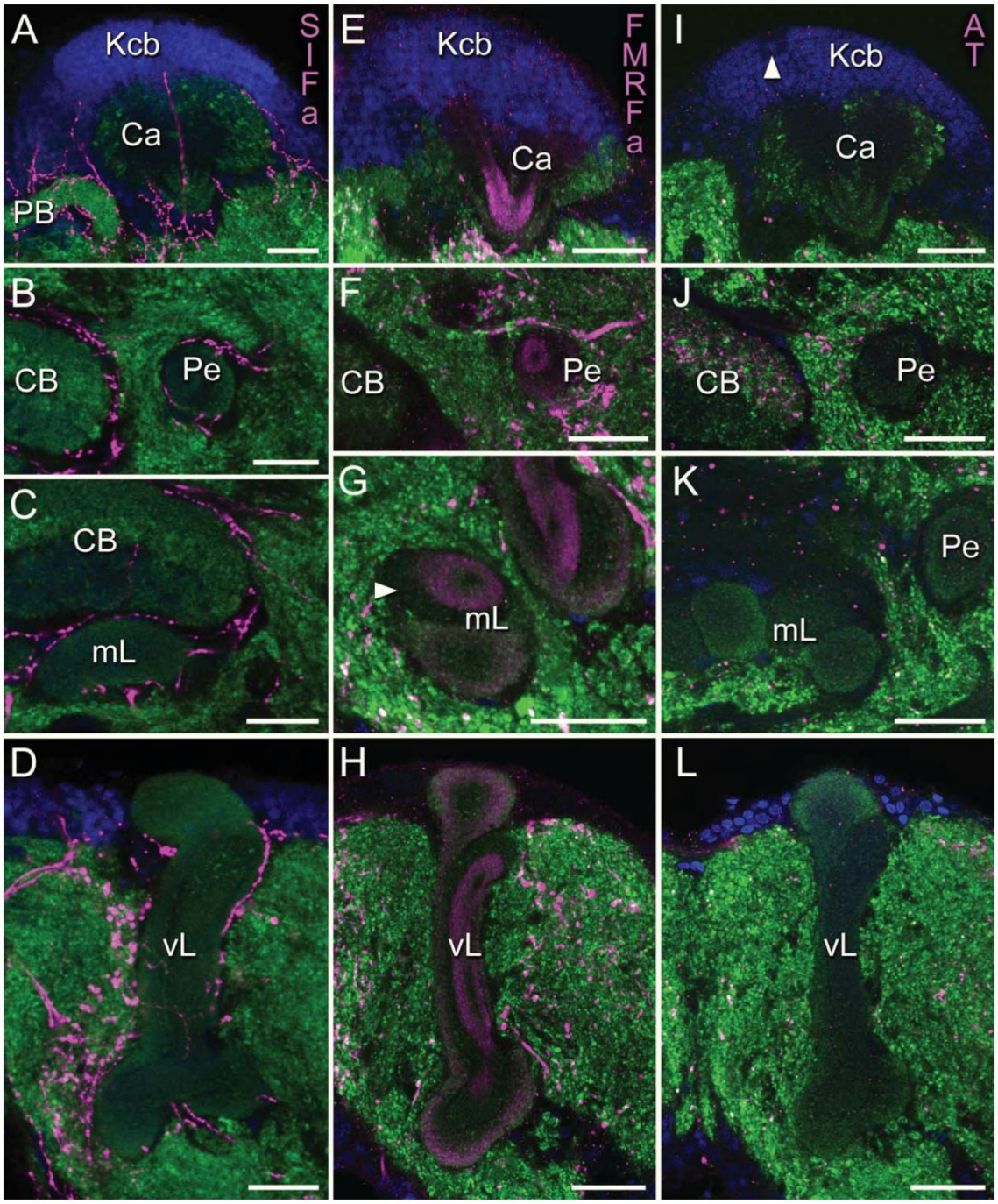

Figure 8. Neuropeptide immunoreactivity in the mushroom body neuropil of *T. castaneum*. **A–D:** SIFamide-like immunoreactivity reveals immunostained extrinsic fibers that closely envelop the neuropil. Single processes also innervate the mushroom body calyx (Ca), peduncle (Pe), and lobes (mL, vL). **E–H:** The antiserum against FMRFamides produces staining in subsets of intrinsic mushroom body neurons. Immunoreactivity can be observed in Kenyon cell bodies (Kcb) and in Kenyon cell processes that constitute the α/β and the γ divisions, but not in α'/β' Kenyon cells (arrowhead). **I–L:** The mushroom bodies exhibit no immunoreactivity towards allatotropin. Images show either single optical sections or maximum projection views of 2–5 optical sections of the left hemisphere; DAPI-labeled cell nuclei are depicted in blue, synapsin-immunoreactivity in green, and neuropeptide immunoreactivity in magenta. Arrowhead in (I) mushroom body neuroblast; CB, central body; mL, median lobe; vL, vertical lobe; PB, protocerebral bridge. Scale bars = 20 μm.

et al., 2010) that receive terminals of the olfactory sensory neurons. Pea-PVK-2 immunoreactivity (Fig. 6A) was detected as scattered spots outside the glomeruli and was restricted to the posterior portion of the antennal lobe. Staining patterns produced by antisera directed against Pea-MIP-1 and Lom-TK-2 differed only slightly (Fig. 6B,C). In both stainings, dense immunolabeling was observed in arborizations of local interneurons that have their cell bodies lateral and ventral to the neuropil and that innervate all glomeruli. In comparison to the olfactory glomeruli, staining of the coarse neuropil at the center of the antennal lobe was less pronounced. Prc-SIFa immunoreactivity revealed a reticular meshwork of extrinsic fibers braiding the olfactory glomeruli (Fig. 6D). The FMRFa antiserum produces no immunostaining in the antennal lobe (Fig. 6E). Staining against Mas-AT revealed granular immunoreactivity scattered throughout the antennal lobe and labeled few cell bodies in the vicinity of the neuropil (Fig. 6F). The antisera against Trc-ACP and Trc-INO produced no immunoreactivity in the *Tribolium* antennal lobe (Fig. 6G,H).

Mushroom body

The mushroom body neuropil of *T. castaneum* (compare Fig. 1C,D) is formed by the processes of Kenyon cells that are successively produced by two neuroblasts situated on top of the calyx (Zhao et al., 2008). In general, neuropeptide immunoreactivity in the mushroom bodies of *T. castaneum* revealed rather distinct distribution patterns (Figs. 7, 8). The antiserum against Pea-PVK-2 produced no immunostaining in the mushroom body neuropil (Fig. 7A–D) but revealed a strong immunoreactivity in the protocerebrum outside the mushroom bodies. Pea-MIP-1 immunoreactivity (Fig. 7E–H) was restricted to a small area at the junction of the peduncle and the vertical and medial lobes, in close proximity to immunostained fibers of the isthmus tract (Fig. 7G). The rest of the neuropil was devoid of immunostaining. Lom-TK-2 immunoreactivity could be observed in all mushroom body subcompartments (Fig. 7I–K), labeling intrinsic neurons of the core and the α/β subdivisions (compare Fig. 1C), as well as the Kenyon cell neuroblasts. The antiserum against Prc-SIFa revealed immunoreactive fibers that closely enveloped all parts of the mushroom bodies and partially also invaded the neuropil (Fig. 8A–D). FMRFa immunoreactivity revealed a peculiar staining pattern of intrinsic mushroom body neurons (Fig. 8E–H). Throughout the neuropil, prominent staining was evident in the peripheral layers of the α/β subdivisions, while the core region and α'/β' Kenyon cells were unlabeled. Somewhat weaker staining could be observed in the outer layer of the peduncle and in the periphery of the γ divisions in the vertical and medial lobe. The Mas-AT-antiserum produced no immunostaining in the mushroom bodies (Fig. 8I–L). The Trc-ACP antiserum produced no immunoreactivity in the mushroom bodies but labeled other parts of the *Tribolium* brain (Fig. 9A–D). In each hemisphere a single cell medial to the calyx was stained, as well as a single cell in the posterior and in the lateral protocerebrum, respectively. Scattered Trc-ACP immunoreactivity was found in the dorsal, medial, and lateral protocerebrum. Immunoreactive fibers follow the dorsal outlines of the central body neuropil and contralaterally intersect in the ventral protocerebrum. The Trc-INO antiserum produced no immunoreactivity in the mushroom body neuropil (Fig. 9E–H) but stained a fibrous meshwork in the lateral protocerebrum with arborizations projecting towards the tritocerebrum and the dorsomedial protocerebrum.

DISCUSSION

The combined mass spectrometric and immunohistological investigation of olfactory neuropils in the red flour beetle revealed characteristic sets of neuropeptide signaling molecules in the antennal lobes and the mushroom bodies, respectively (Tables 2, 3). Mass spectrometric neuropil "fingerprints" of the two neuropils could easily be differentiated due to distinctive mass distributions and typical relations between the detected mass peaks (Figs. 2–4).

MALDI-TOF mass spectrometry of *T. castaneum* antennal lobes suggests the constitutive expression of members of six neuropeptide families: TKRPs, MIPs, Nplp1, NVPs, DH 47, and SIFa. Furthermore, PVK-2 and AT were detected in half of the analyzed material. Complementary immunohistology confirmed the presence of five mass spectrometrically identified peptide families. Mas-AT immunoreactivity appeared granular and scattered, but was distributed homogeneously throughout the antennal lobe neuropil. Antisera against Lom-TK-2 and Pea-MIP-1 produced highly congruent staining patterns, revealing dense labeling in all glomeruli as well as individual immunostained somata. These observations indicate that Lom-TK-2 and Pea-MIP-1 are expressed in local interneurons and thus play a role in the early processing of olfactory information. Staining with Prc-SIFa antiserum showed an intricate innervation of the antennal lobes by extrinsic neurons that also supply ramifications to most other cerebral neuropils, suggesting a broad modulatory function of this neuropeptide. Mass spectrometrically identified FaRPs in *T. castaneum* include the extended FMRFamides, myosuppressins, sNPFs, and sulfakinins (Li et al., 2008). The FMRFa antiserum used in this study recognizes most

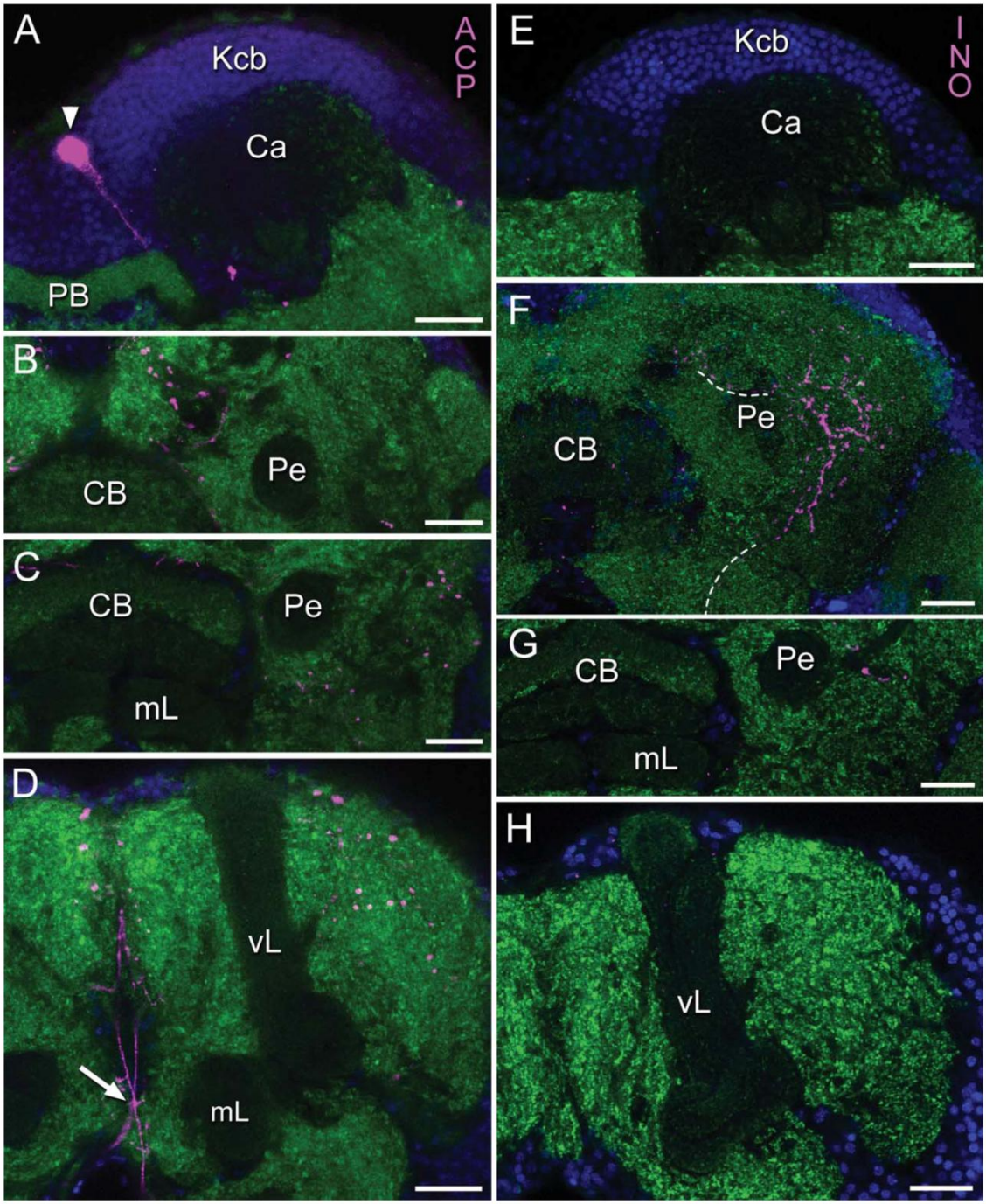

Figure 9. The mushroom body subcompartments of *T. castaneum*. **A–D:** The mushroom bodies showed no adipokinetic hormone/corazonin-related peptide immunoreactivity. In each hemisphere a single cell medial to the calyx (Ca) was stained (arrowhead), as well as a single cell in the posterior and one in the lateral protocerebrum. Fiber bundles contralaterally intersect in the ventral protocerebrum. **E–H:** The mushroom bodies exhibit no immunoreactivity towards the inotocin-antiserum. The inotocin antiserum stained a fiber meshwork in the lateral protocerebrum with arborizations towards the tritocerebrum and the dorsomedial protocerebrum (dashed lines). Images show single optical sections of the left hemisphere; DAPI-labeled cell nuclei are depicted in blue, synapsin-immunoreactivity in green, and neuropeptide immunoreactivity in magenta. CB, central body; Kcb, Kenyon cell bodies; mL, median lobe; vL, vertical lobe; PB, protocerebral bridge; Pe, peduncle. Scale bars = 20 μm.

members of the FaRPs, revealing in principle a combined staining pattern that reflects the peptide expression of all four neuropeptide genes of this superfamily. In terms of a negative control, the lack of FaRP-specific masses in the MALDI-TOF spectra was matched by a lack of FMRFa immunoreactivity in the antennal lobes of *T. castaneum*. The Pea-PVK-2 antiserum produced sparse and scattered immunoreactivity in the posterior part of the antennal lobe and the adjoining neuropil region. This area caused the mass spectrometric detection in 55% of the antennal lobe samples. The glomeruli are devoid of Pea-PVK-2 immunoreactivity.

However, the absence of mass peaks in the obtained MALDI-TOF spectra must not necessarily reflect the absence of the corresponding neuropeptide in the tissue sample. Peptides might also escape mass spectrometric detection due to adverse chemical/physical properties (Perkins et al., 1999; Krause et al., 1999) and competitive ionization (Cohen et al., 1996). Finally, very low detection frequencies can also pertain to contaminations from neighboring non-target tissue. Indeed, non-antennal lobe material clinging to the sample very likely seems to be the reason for the identification of ITG-motif containing peptides, and diuretic hormone 31 in the antennal lobe samples, considering the sporadic detection frequency, the low signal intensity of the corresponding mass peaks, and the detection frequency of 100% ($n = 20$) in neighboring lateral protocerebral tissue.

Direct profiling MALDI-TOF analyses and immunohistological stainings have also demonstrated the presence of TKRPs in the antennal lobes of the dipteran species *D. melanogaster* (Carlsson et al., 2010) and *Aedes aegypti* (Siju et al., 2013). In the fruit fly, nervous system-specific knockdown of TKRPs via RNA interference was demonstrated to reduce odor perception sensitivity and to increase locomotor activity (Winther et al., 2006). Further knockdown experiments targeting TK receptors of olfactory sensory neurons (OSNs) provided additional evidence for a signal modulation mediated by peptidergic interneurons of the antennal lobe connecting to OSNs (Ignell et al., 2009). The antennal lobes of *A. aegypti* and *D. melanogaster* also contain MIPs; members of this family were also identified in antennal lobe samples of the sphinx moth *M. sexta* (Utz et al., 2007). However, the functional role of MIPs in the antennal lobes is unclear so far. As for the other peptide families identified in the antennal lobes of *T. castaneum*, Nplp1 were also detected in *A. aegypti*, SIFa in *A. aegypti* and *D. melanogaster*, and AT in the lepidopterans *M. sexta* and *Heliothis virescens* and in *A. aegypti* (an orthologous sequence is lacking in *D. melanogaster*; Hewes and Taghert, 2001; Berg et al., 2007; Utz et al., 2007; Carlsson et al., 2010; Siju et al., 2013). Conversely, the antennal lobes of the two dipteran representatives were demonstrated to contain A-type allatostatins (AST-As) and short neuropeptide Fs (sNPFs). The former family and their corresponding receptors are not encoded in the *T. castaneum* genome (Li et al., 2008) and masses corresponding to sNPFs were not detected in our analyses of antennal lobe spectra. PVK-2 belongs to the CAPA-PVKs, which appear to act as diuretic or myotropic hormones (Predel and Wegener, 2006). Contrary to the findings in *Tribolium,* mass spectrometric and/or immunohistochemical data showed no evidence for the presence of CAPA-PVKs in the antennal lobes of *D. melanogaster*, *A. aegypti*, and the cockroach *P. americana* (Eckert et al., 1999; Carlsson et al., 2010; Neupert et al., 2012; Siju et al., 2013) or in immunohistochemical stainings of the antennal lobe in different collembolan species (Kollmann et al., 2011b).

Mass spectrometry of mushroom body subcompartments provided strong evidence for the presence of at least five different neuropeptide families: TKRPs, sNPFs, *Apis* NVP-like peptides (NVPs), DH 47, and SIFa. Evidence for some neuropeptide families (ACP, ETH, PVKs, RYamides, and SKs) was found in only 5% to 15% of the mushroom body subcompartment spectra. Given the low detection frequency and a low signal intensity of the corresponding mass peaks, they are likely to be caused by contamination from surrounding tissue. For example ACP, INO, and PVK-2 were detected in mass spectra of the lateral protocerebrum (in 90%, 75%, and 100% of 20 samples, respectively; data not shown) and the respective antisera revealed immunoreactive areas in the lateral protocerebrum in the vicinity of the mushroom bodies. Although mass spectra obtained from different subcompartments showed high similarity, neuropeptide detection frequencies tended to be lower in the calycal samples than in peduncle and lobe samples. This might reflect the fact that neuropeptide signaling molecules expressed by intrinsic mushroom body neurons are transported along the axon-like projections and accumulate at storage and release sites in the distal portions of the lobes (Nässel and Homberg, 2006; Johard et al., 2008; Heuer et al., 2012a). It also implies that extrinsic neurons targeting the calyces - often regarded as the primary input region of the mushroom bodies - do not employ exclusive or unique sets of neuropeptides in *T. castaneum*.

In accordance with the mass spectrometric analyses, immunohistochemical experiments revealed the mushroom bodies of *T. castaneum* to be devoid of Pea-PVK-2, Trc-ACP, Trc-INO, and Mas-AT immunoreactivity. The absence of an ion signal corresponding to the mass of

INO in the mushroom body neuropil proves the findings of the preabsorption tests. Prc-SIFa immunostaining was observed in extrinsic neuronal processes that closely wrap the mushroom bodies and sparsely innervate the neuropil. These ramifications apparently account for the SIFa peak in the obtained mass spectra, as Prc-SIFa immunopositive Kenyon cell bodies could not be identified. Instead, similar to other holometabolous insect species (Verleyen et al., 2004; Heuer et al., 2012b), Prc-SIFa-immunoreactive processes seem to arise from four large and prominently stained somata in the pars intercerebralis. Pea-MIP-1 immunoreactivity within the mushroom bodies is likewise suggestive of an extrinsic innervation, as immunostaining was limited to just a small region of the neuropil and no immunopositive Kenyon cell somata were observed. Moreover, the immunoreactive zone was located at the junction of the peduncle and the lobes, exactly where subcompartments were separated for individual spectrometric analysis, thus offering an explanation for the mass spectrometrical identification of MIPs in the lobes and the peduncle. Immunostainings against Lom-TK-2 clearly labeled intrinsic mushroom body neurons, confirming the results obtained by mass spectrometry. Mass spectrometry, in situ hybridizations, and immunohistology have shown that TKRPs are also prominently expressed in the Kenyon cells of the honey bee *Apis mellifera* (Takeuchi et al., 2003, 2004; Boerjan et al., 2010; Heuer et al., 2012a), where they have been tentatively linked to social behavior (Takeuchi et al., 2004; Boerjan et al., 2010) and foraging activities (Brockmann et al., 2009). However, TKRPs also appear to be present in the mushroom bodies of other insect species, including the basal zygentome *Thermobia domestica* (see Heuer et al., 2012a), pointing towards a more conserved and/or basic function of this neuropeptide in the mushroom body circuitry. Immunostainings in *T. castaneum* also revealed intrinsic mushroom body neurons to be strongly immunoreactive towards an FMRFa antiserum. The FMRFa antiserum used in this study recognizes various C-terminally extended -RFamides (FaRPs), including the extended FMRFamides and sNPFs that were identified by direct peptide profiling of *T. castaneum* mushroom bodies. The most dominant mass peak in all mushroom body spectra was located at 1274.74 Da (Figs. 3,4), a mass that could unambiguously be assigned to sNPF by tandem mass spectrometry (Fig. 5). Similar to the detected extended FMRFamides (FMRFa-4 and FMRFa-5), *T. castaneum* sNPFs display a C-terminal "LRF-NH_2" motif (Table 3). In *D. melanogaster*, most Kenyon cells that exhibit FMRFa immunoreactivity actually carry sNPF, as demonstrated by comparative immunohistochemistry and in situ hybridization (Johard et al., 2008; Nässel et al., 2008). It thus appears reasonable to attribute the prominent FMRFa immunostaining in the mushroom bodies of *T. castaneum* at least partly, if not as a whole, to the presence of sNPF. It is also noteworthy that the FMRFa antiserum as well as the antiserum directed against Lom-TK-2 both produced distinct staining patterns in the mushroom bodies. This suggests that in *T. castaneum*, Kenyon cell populations distinguishable by birthdate and morphology (Zhao et al., 2008) express different neuropeptides. "Older" cells of the γ-division contain FMRFamides (viz. sNPF in this case) while "younger" cells surrounding the ingrowth core utilize TKRPs. α/β Kenyon cells seem to be equipped with transmitter molecules from both neuropeptide families. Thus, like in other insects (Schürmann and Erber, 1990; Crittenden et al., 1998; Sinakevitch et al., 2001; Sjöholm et al., 2006; Heuer et al., 2012b), the Kenyon cells in *T. castaneum* are not only morphologically but also biochemically heterogeneous.

In summary, the current study not only demonstrates the reliability of the technique of direct peptide profiling to analyze the expression of neuropeptides in defined brain areas but also reveals neuropeptide variability and distribution in two central brain areas that are major neuropils for olfactory information processing in *T. castaneum*. Both large variety and distinct localization of neuropeptides to specific neuron types are in accordance with findings in other insect species (antennal lobes: e.g., Schachtner et al., 2005 [review]; Carlsson et al., 2010; Neupert et al., 2012; Siju et al., 2013; mushroom bodies: recently reviewed in Heuer et al., 2012a) and suggest a broad range of modulation and plasticity in the central olfactory systems of insects in general. Functional roles of neuropeptides in the insect central olfactory pathway are just beginning to emerge. So far a clear role for only one neuropeptide family, the TKRPs, has been suggested in the context of modulating olfactory signaling in the *Drosophila* antennal lobe (see above, Ignell et al., 2009; Winther and Ignell, 2010). Questions that will need to be addressed in the future include whether other neuropeptides can also be linked to defined functions, and how different neuropeptides may act together to affect olfactory signaling.

The present study will serve as an important prerequisite to further elucidate neuropeptide regulation and function in the olfactory system of *T. castaneum*. Direct peptide profiling by MALDI-TOF mass spectrometry of individual neuropils of the central olfactory pathway offers a means to better understand development and plasticity-related events in this system. In conjunction with an internal standard that allows for a semiquantitative analysis, direct peptide profiling can provide a fast

and reliable way to assess fluctuations in neuropeptide expression in specific regions of the brain. In addition to manipulation experiments, e.g., genetically via RNAi knockdown of, e.g., odorant receptors or neuropeptides and, e.g., odor deprivation experiments, we hope to gain insights in the regulation and role of neuropeptides for the central olfactory pathway.

ACKNOWLEDGMENTS

MALDI-TOF analyses build upon earlier feasibility studies conducted by Holger Vitt, whose work is gratefully acknowledged here. We thank Peter Christ for contributing TKRP stainings and Martina Kern for technical assistance. We also thank all colleagues who supplied us with peptides, antisera, and transgenic beetles (see Materials and Methods).

CONFLICT OF INTEREST

The authors declare no conflict of interest.

ROLE OF AUTHORS

All authors had full access to all the data in the study and take responsibility for the integrity of the data and the accuracy of the data analysis. Study concept and design: MB, CMH, JS; Acquisition of data: MB, CMH, MK, and JK; Analysis of data: MB, CMH, MK, JK, and JS; Interpretation of data: all authors; FH and CPJC provided the ACP antibody and the new inotocin antiserum; Drafting of the article: MB, CMH, JS; All authors were involved in discussing and editing the article and approved the final version; Obtained funding: JS.

LITERATURE CITED

Altstein M, Nässel DR. 2010. Neuropeptide signaling in insects. Adv Exp Med Biol 692:155–165.

Berg BG, Schachtner J, Utz S, Homberg U. 2007. Distribution of neuropeptides in the primary olfactory center of the heliothine moth *Heliothis virescens*. Cell Tissue Res 327: 385–398.

Boerjan B, Cardoen D, Bogaerts A, Landuyt B, Schoofs L, Verleyen P. 2010. Mass spectrometric profiling of (neuro)-peptides in the worker honeybee, *Apis mellifera*. Neuropharmacology 58:248–258.

Brockmann A, Annangudi SP, Richmond TA, Ament SA, Xie F, Southey BR, Rodriguez-Zas SR, Robinson GE, Sweedler JV. 2009. Quantitative peptidomics reveal brain peptide signatures of behavior. Proc Natl Acad Sci U S A 106: 2383–2388.

Brown SJ, Denell RE, Beeman RW. 2003. Beetling around the genome. Genet Res 82:155–161.

Bucher G, Scholten J, Klingler M. 2002. Parental RNAi in *Tribolium* (Coleoptera). Curr Biol 12:R85–86.

Carlsson MA, Diesner M, Schachtner J, Nässel DR. 2010. Multiple neuropeptides in the *Drosophila* antennal lobe suggest complex modulatory circuits. J Comp Neurol 518: 3359–3380.

Chen X, Ganetzky B. 2012. A neuropeptide signaling pathway regulates synaptic growth in *Drosophila*. J Cell Biol 196: 529–543.

Cohen SL, Chait BT. 1996. Influence of matrix solution conditions on the MALDI-MS analysis of peptides and proteins. Anal Chem 68:31–37.

Cox PD, Collins LE. 2002. Factors affecting the behaviour of beetle pests in stored grain, with particular reference to the development of lures. J Stored Prod Res 38:95–115.

Crittenden JR, Skoulakis EMC, Han K-A, Kalderon D, Davis RL. 1998. Tripartite mushroom body architecture revealed by antigenic markers. Learn Mem 5:38–51.

Dreyer D, Vitt H, Dippel S, Goetz B, el Jundi B, Kollmann M, Huetteroth W, Schachtner J. 2010. 3D standard brain of the red flour beetle *Tribolium castaneum*: a tool to study metamorphic development and adult plasticity. Front Sys Neurosci 4:3.

Eckert M, Predel R, Gundel M. 1999. Periviscerokinin-like immunoreactivity in the nervous system of the American cockroach. Cell Tissue Res 295:159–170.

Eckert M, Herbert Z, Pollák E, Molnár L, Predel R. 2002. Identical cellular distribution of all abundant neuropeptides in the major abdominal neurohemal system of an insect (*Periplaneta americana*). J Comp Neurol 452:264–275.

Engsontia P, Sanderson AP, Cobb M, Walden KKO, Robertson HM, Brown S. 2008. The red flour beetle's large nose: an expanded odorant receptor gene family in *Tribolium castaneum*. Insect Biochem Mol Biol 38:387–397.

Hansen KK, Stafflinger E, Schneider M, Hauser F, Cazzamali G, Williamson M, Kollmann M, Schachtner J, Grimmelikhuijzen CJP. 2010. Discovery of a novel insect neuropeptide/ GPCR signaling system closely related to the insect adipokinetic hormone and corazonin hormonal systems. J Biol Chem 285:10736–10747.

Hauser F, Neupert S, Williamson M, Predel R, Tanaka Y, Grimmelikhuijzen CJP. 2010. Genomics and peptidomics of neuropeptides and protein hormones present in the parasitic wasp *Nasonia vitripennis*. J Proteome Res 9: 5296–5310.

Herbert Z, Pollák E, Zougman A, Boros A, Kapan N, Molnár L. 2009. Identification of novel neuropeptides in the ventral nerve cord ganglia and their targets in an annelid worm, *Eisenia fetida*. J Comp Neurol 514:415–432.

Herbert Z, Rauser S, Williams L, Kapan N, Güntner M, Walch A, Boyan G. 2010. Developmental expression of neuromodulators in the central complex of the grasshopper *Schistocerca gregaria*. J Morphol 271:1509–1526.

Heuer CM, Kollmann M, Binzer M, Schachtner J. 2012a. Neuropeptides in insect mushroom bodies. Arthropod Struc Dev 41:199–226.

Heuer CM, Binzer M, Schachtner J. 2012b. SIFamide in the brain of the sphinx moth, *Manduca sexta*. Acta Biol Hung 63:48–57.

Hergarden AC, Tayler TD, Anderson DJ. 2012. Allatostatin-A neurons inhibit feeding behavior in adult *Drosophila*. Proc Natl Acad Sci U S A 109:3967–3972.

Hewes RS, Taghert PH. 2001. Neuropeptides and neuropeptide receptors in the *Drosophila melanogaster* genome. Genome Res 11:1126–1142.

Homberg U, Brandl C, Clynen E, Schoofs L, Veenstra JA. 2004. Mas-allatotropin/Lom-AG-myotropin I immunostaining in the brain of the locust, *Schistocerca gregaria*. Cell Tissue Res 318:439–457.

Ignell R, Root CM, Birse RT, Wang JW, Nässel DR, Winther AME. 2009. Presynaptic peptidergic modulation of olfactory receptor neurons in *Drosophila*. Proc Natl Acad Sci U S A 106:13070–13075.

Johard HAD, Enell LE, Gustafsson E, Trifilieff P, Veenstra JA, Nässel DR. 2008. Intrinsic neurons of *Drosophila*

mushroom bodies express short neuropeptide F: relations to extrinsic neurons expressing different neurotransmitters. J Comp Neurol 507:1479–1496.

Klagges BR, Heimbeck G, Godenschwege TA, Hofbauer A, Pflugfelder GO, Reifegerste R, Reisch D, Schaupp M, Buchner S, Buchner E. 1996. Invertebrate synapsins: a single gene codes for several isoforms in *Drosophila*. J Neurosci 16:3154–3165.

Kollmann M, Minoli S, Bonhomme J, Homberg U, Schachtner J, Tagu D, Anton S. 2011a. Revisiting the anatomy of the central nervous system of a hemimetabolous model insect species: the pea aphid *Acyrthosiphon pisum*. Cell Tissue Res 343:343–55.

Kollmann M, Huetteroth W, Schachtner J. 2011b. Brain organization in Collembola (springtails). Arthropod Struc Dev 40:304–316.

Krause E, Wenschuh H, Jungblut PR. 1999. The dominance of arginine-containing peptides in MALDI-derived tryptic mass fingerprints of proteins. Anal Chem 71:4160–4165.

Levinson HZ, Levinson AR. 1978. Dried seeds, plant and animal tissues as food favoured by storage insect species. Entomol Exp Appl 24:505–517.

Levinson HZ, Mori K. 1983. Chirality determines pheromone activity for flour beetles. Naturwissenschaften 70:190–192.

Li B, Predel R, Neupert S, Hauser F, Tanaka Y, Cazzamali G, Williamson M, Arakane Y, Verleyen P, Schoofs L, Schachtner J, Grimmelikhuijzen CJP, Park Y. 2008. Genomics, transcriptomics, and peptidomics of neuropeptides and protein hormones in the red flour beetle *Tribolium castaneum*. Genome Res 18:113–122.

Marder E, Calabrese RL, Nusbaum MP, Trimmer B. 1987. Distribution and partial characterization of FMRFamide-like peptides in the stomatogastric nervous system of the rock crab, *Cancer borealis*, and the spiny lobster *Panulirus interruptus*. J Comp Neurol 259:150–163.

Meusemann K, Reumont BM von, Simon S, Roeding F, Strauss S, Kück P, Ebersberger I, Walzl M, Pass G, Breuers S, Achter V, Haeseler A von, Burmester T, Hadrys H, Wägele JW, Misof B. 2010. A phylogenomic approach to resolve the arthropod tree of life. Mol Biol Evol 27:2451–2464.

Nässel DR. 2002. Neuropeptides in the nervous system of *Drosophila* and other insects: multiple roles as neuromodulators and neurohormones. Prog Neurobiol 68:1–84.

Nässel DR, Winther AME. 2010. *Drosophila* neuropeptides in regulation of physiology and behavior. Prog Neurobiol 92:42–104.

Nässel DR, Enell LE, Santos JG, Wegener C, Johard HAD. 2008. A large population of diverse neurons in the *Drosophila* central nervous system expresses short neuropeptide F, suggesting multiple distributed peptide functions. BMC Neurosci 9:90.

Neupert S, Predel R, Russell WK, Davies R, Pietrantonio PV, Nachman RJ. 2005. Identification of tick periviscerokinin, the first neurohormone of Ixodidae: single cell analysis by means of MALDI-TOF/TOF mass spectrometry. Biochem Biophys Res Commun 338:1860–1864.

Neupert S, Fusca D, Schachtner J, Kloppenburg P, Predel R. 2012. Toward a single-cell-based analysis of neuropeptide expression in *Periplaneta americana* antennal lobe neurons. J Comp Neurol 520:694–716.

Peel AD. 2009. Forward genetics in *Tribolium castaneum*: opening new avenues of research in arthropod biology. J Biol 8:106.

Perkins DN, Pappin DJC, Creasy DM, Cottrell JS. 1999. Probability-based protein identification by searching sequence databases using mass spectrometric data. Electrophoresis 20:3551–3567.

Polanska MA, Yasuda A, Harzsch S. 2007. Immunolocalisation of crustacean-SIFamide in the median brain and eyestalk neuropils of the marbled crayfish. Cell Tissue Res 330: 331–344.

Posnien N, Koniszewski NDB, Hein HJ, Bucher G. 2011. Candidate gene screen in the red flour beetle *Tribolium* reveals six3 as ancient regulator of anterior median head and central complex development. PLoS Genet 7:e1002416.

Predel R, Wegener C. 2006. Biology of the CAPA peptides in insects. Cell Moll Life Sci 63:2477–2490.

Predel R, Rapus J, Eckert M. 2001. Myoinhibitory neuropeptides in the American cockroach. Peptides 22:199–208.

Predel R, Neupert S, Wicher D, Gundel M, Roth S, Derst C. 2004. Unique accumulation of neuropeptides in an insect: FMRFamide-related peptides in the cockroach, *Periplaneta americana*. Eur J Neurosci 20:1499–1513.

Predel R, Russell WK, Neupert S, Russell DH, Esquivel JF, Nachman RJ. 2006. Identification of the first neuropeptides from the CNS of Hemiptera: CAPA peptides of the southern green stinkbug *Nezara viridula* (L.). Peptides 27: 2670–2677.

Renn SC, Park JH, Rosbash M, Hall JC, Taghert PH. 1999. A pdf neuropeptide gene mutation and ablation of PDF neurons each cause severe abnormalities of behavioral circadian rhythms in *Drosophila*. Cell 99:791–802.

Richards S, Gibbs RA, Weinstock GM, Brown SJ, Denell R. 2008. The genome of the model beetle and pest *Tribolium castaneum*. Nature 452:949–955.

Schachtner J, Schmidt M, Homberg U. 2005. Organization and evolutionary trends of primary olfactory brain centers in Tetraconata (Crustacea + Hexapoda). Arthropod Struct Dev 34:257–299.

Schachtner J, Wegener C, Neupert S, Predel R. 2010. Direct peptide profiling of brain tissue by MALDI-TOF mass spectrometry. Methods Mol Biol 615:129–135.

Schürmann FW, Erber J. 1990. FMRFamide-like immunoreactivity in the brain of the honeybee (*Apis mellifera*). A light- and electron microscopical study. Neuroscience 38:797–807.

Siju KP, Reifenrath A, Scheiblich H, Neupert S, Predel R, Hansson BS, Schachtner J, Ignell R. 2013. Neuropeptides in the antennal lobe of the yellow fever mosquito, *Aedes aegypti*. J Comp Neurol (in press).

Sinakevitch I, Farris SM, Strausfeld NJ. 2001. Taurine-, aspartate-, and glutamate-like immunoreactivity identifies chemically distinct subdivisions of Kenyon cells in the cockroach mushroom body. J Comp Neurol 439:352–367.

Sjöholm M, Sinakevitch I, Strausfeld NJ, Ignell R, Hansson BS. 2006. Functional division of intrinsic neurons in the mushroom bodies of male *Spodoptera littoralis* revealed by antibodies against aspartate, taurine, FMRF-amide, Mas-allatotropin and DC0. Arthropod Struct Dev 35:153–168.

Stafflinger E, Hansen K. K, Hauser F, Schneider M, Cazzamali G, Williamson M, Grimmelikhuijzen CJP. Cloning and identification of an oxytocin/vasopressin-like receptor and its ligand from insects. Proc Natl Acad Sci U S A 2008;105:3262–3267.

Takeuchi H, Yasuda A, Yasuda-Kamatani Y, Sawata M, Matsuo Y, Kato A, Tsujimoto A. 2004. Prepro-tachykinin gene expression in the brain of the honeybee *Apis mellifera*. Cell Tissue Res 316:281–293.

Terhzaz S, Rosay P, Goodwin SF, Veenstra JA. 2007. The neuropeptide SIFamide modulates sexual behavior in *Drosophila*. Biochem Biophys Res Commun 352:305–310.

Tomoyasu Y, Denell RE. 2004. Larval RNAi in *Tribolium* (Coleoptera) for analyzing adult development. Dev Genes Evol 214:575–578.

Trauner J, Schinko J, Lorenzen MD, Shippy TD, Wimmer EA, Beeman RW, Klingler M, Bucher G, Brown SJ. 2009. Large-scale insertional mutagenesis of a coleopteran stored grain pest, the red flour beetle *Tribolium castaneum*, identifies embryonic lethal mutations and enhancer traps. BMC Biol 7:73.

Utz S, Huetteroth W, Wegener C, Predel R, Schachtner J. 2007. Direct peptide profiling of lateral cell groups of the antennal lobes of *Manduca sexta* reveals specific composition and changes in neuropeptide expression during development. Dev Neurobiol 67:764–777.

Utz S, Huetteroth W, Vömel M, Schachtner J. 2008. Mas-allatotropin in the developing antennal lobe of the sphinx moth *Manduca sexta*: distribution, time course, developmental regulation, and colocalization with other neuropeptides. Dev Neurobiol 68:123–142.

Veenstra JA, Hagedorn HH. 1993. Sensitive enzyme immunoassay for *Manduca* allatotropin and the existence of an allatotropin-immunoreactive peptide in *Periplaneta americana*. Arch Insect Biochem Physiol 23:99–109.

Veenstra JA, Lau GW, Agricola HJ, Petzel DH. 1995. Immunohistological localization of regulatory peptides in the midgut of the female mosquito *Aedes aegypti*. Histochem Cell Biol 104:337–347.

Verleyen P, Huybrechts J, Baggerman G, Lommel A Van, Loof A De, Schoofs L. 2004. SIFamide is a highly conserved neuropeptide: a comparative study in different insect species. Biochem Biophys Res Commun 320:334–341.

Vitzthum H, Homberg U. 1998. Locustatachykinin I/II-immunoreactive neurons in the central complex of the locust brain. J Comp Neurol 390:455–469.

Wegener C, Hamasaka Y, Nässel DR. 2004. Acetylcholine increases intracellular Ca2+ via nicotinic receptors in cultured PDF-containing clock neurons of *Drosophila*. J Neurophysiol 91:912–923.

Wiegmann BM, Trautwein MD, Winkler IS, Barr NB, Kim JW, Lambkin C, Bertone MA, Cassel BK, Bayless KM, Heimberg AM, Wheeler BM, Peterson KJ, Pape T, Sinclair BJ, Skevington JH, Blagoderov V, Caravas J, Kutty SN, Schmidt-Ott U, Kampmeier GE, Thompson FC, Grimaldi DA, Beckenbach AT, Courtney GW, Friedrich M, Meier R, Yeates DK. 2011. Episodic radiations in the fly tree of life. Proc Natl Acad Sci U S A 208:5690–5695.

Winther AME, Acebes A, Ferrús A. 2006. Tachykinin-related peptides modulate odor perception and locomotor activity in *Drosophila*. Mol Cell Neurosci 31:399–406.

Yasuda A, Yasuda-Kamatani Y, Nozaki M, Nakajima T. 2004. Identification of GYRKPPFNGSIFamide (crustacean-SIFamide) in the crayfish *Procambarus clarkii* by topological mass spectrometry analysis. Gen Comp Endocrinol 135: 391–400.

Zhao X, Coptis V, Farris SM. 2008. Metamorphosis and adult development of the mushroom bodies of the red flour beetle, *Tribolium castaneum*. Dev Neurobiol 68:1487–1502.

Chapter 5:

Neuropeptides in insect mushroom bodies

Arthropod Structure & Development 41 (2012) 199–226

Contents lists available at SciVerse ScienceDirect

Arthropod Structure & Development

journal homepage: www.elsevier.com/locate/asd

Review

Neuropeptides in insect mushroom bodies

Carsten M. Heuer [1], Martin Kollmann [1], Marlene Binzer, Joachim Schachtner*

Philipps-University Marburg, Department of Biology, Animal Physiology, Karl-von-Frisch Str. 8, D-35032 Marburg, Germany

ARTICLE INFO

Article history:
Received 28 October 2011
Accepted 23 February 2012

Keywords:
Neuropeptides
Neuropil
Evolution
Network
Mushroom body

ABSTRACT

Owing to their experimental amenability, insect nervous systems continue to be in the foreground of investigations into information processing in – ostensibly – simple neuronal networks. Among the cerebral neuropil regions that hold a particular fascination for neurobiologists are the paired mushroom bodies, which, despite their function in other behavioral contexts, are most renowned for their role in learning and memory. The quest to understand the processes that underlie these capacities has been furthered by research focusing on unraveling neuroanatomical connections of the mushroom bodies and identifying key players that characterize the molecular machinery of mushroom body neurons. However, on a cellular level, communication between intrinsic and extrinsic mushroom body neurons still remains elusive. The present account aims to provide an overview on the repertoire of neuropeptides expressed in and utilized by mushroom body neurons. Existing data for a number of insect representatives is compiled and some open gaps in the record are filled by presenting additional original data.

1. Introduction

1.1. Mushroom body architecture in insects

Insect mushroom bodies – *corpora pedunculata* in the older literature – are paired protocerebral neuropils that are easily distinguished and identified by their characteristic architecture and their "bizarre shape" (Heisenberg, 1998, page 1) (Fig. 1). Each neuropil is formed by thousands of neurites that emanate from dense aggregations of small-diameter cell bodies in the dorsal part of the brain. Cell counts for these intrinsic neurons – in insects termed Kenyon cells – range from approximately 2.500 per mushroom body in *Drosophila melanogaster* (Hinke, 1961) to 175.000 in the cockroach *Periplaneta americana* (Neder, 1959). Proximally, Kenyon cell neurites give rise to dendritic arborizations that form the calyx, a neuropil substructure that is often embedded within the mass of Kenyon cell somata. Calyx morphology is known to show substantial variability in different insect species (Fig. 1A–C), a fact that is attributed to the kind and the amount of afferents targeting this region (Strausfeld et al., 2009). Ventral to the calyx region, axon-like Kenyon cell processes converge and arrange in parallel, thereby forming a stalk-like structure that is recognized as peduncle. Distally, the peduncle splits up and gives rise to an arrangement of lobes. In most insects, a medial lobe that extends towards the mid-sagittal plane and a vertical lobe that extends antero-dorsally can be differentiated (Fig. 1A–C). Like the calyx, the morphology of medial and vertical lobes varies in different taxa. Calyx and lobes are also typically further subcompartmentalized into distinct structural divisions (for a review see Farris, 2005b). This reflects the heterogeneity of the Kenyon cell assembly, which comprises subpopulations that can be discriminated by their birthdate and their morphology (Lee et al., 1999; Farris and Strausfeld, 2001; Strausfeld, 2002; Farris and Sinakevitch, 2003; Fukushima and Kanzaki, 2009), as well as by their biochemistry (Schürmann and Erber, 1990; Crittenden et al., 1998; Sinakevitch et al., 2001; Sjöholm et al., 2006).

1.2. Mushroom body function in insects

Insect mushroom bodies are higher integrative brain centers that are best-known for their role in olfactory discrimination learning and memory storage and retrieval (Mcguire et al., 2001; Menzel, 2001; Heisenberg, 2003; Davis, 2004). This concept is supported by a substantial body of physiological and behavioral studies in the dipteran *D. melanogaster* and the hymenopteran *Apis mellifera* (*D. melanogaster*: Heisenberg et al., 1985; de Belle and Heisenberg, 1994; Connolly et al., 1996; Dubnau et al., 2001; *A. mellifera*: Erber et al., 1980; Hammer, 1993; Hammer and Menzel, 1998; Fiala et al., 1999). However, olfactory information is a dominant input not only in Diptera and Hymenoptera, but indeed in most terrestrial insect species (Farris, 2005a). It is relayed to the dendritic terminals of the calycal neuropil via projection neurons of the inner antennocerebral tract that connect to first-order olfactory

* Corresponding author.
E-mail address: schachtj@staff.uni-marburg.de (J. Schachtner).
[1] These authors contributed equally to the work.

1467-8039/$ – see front matter © 2012 Elsevier Ltd. All rights reserved.
doi:10.1016/j.asd.2012.02.005

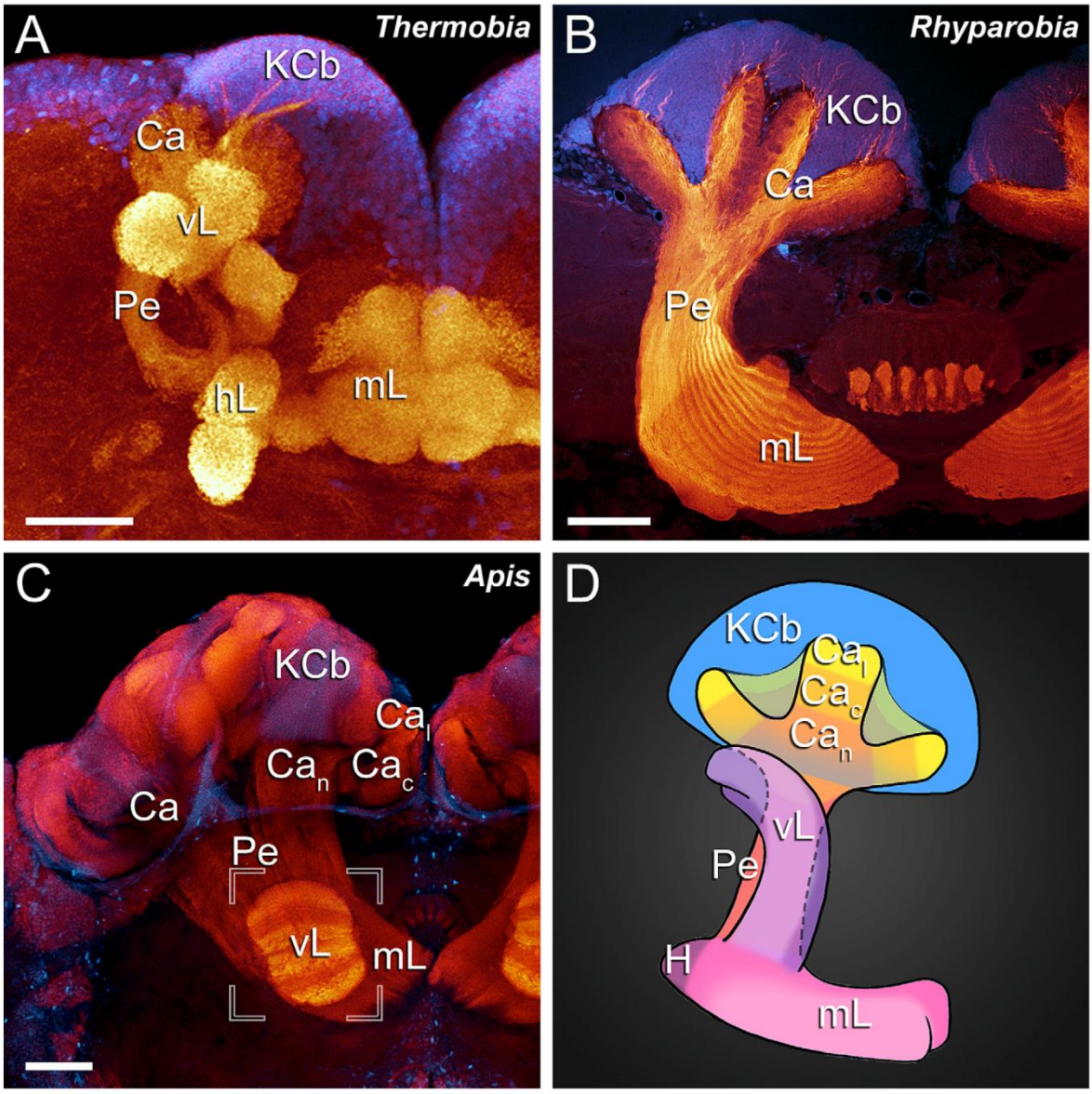

Fig. 1. Frontal views of mushroom body neuropils in representatives of different insect orders (A–C), along with a schematic image of an idealized insect mushroom body (D), illustrating the principal architecture and characteristic substructures. (A) Mushroom body in the firebrat *Thermobia domestica*, revealed by an antibody directed against the catalytic subunit of protein kinase A (anti-DC0, glow) in combination with a marker for cell nuclei (DAPI, blue). The calyx region (Ca) in this ancestral insect is roughly spheroid and the peduncle (Pe) gives rise to a medial lobe (mL), a vertical lobe (vL), and a horizontal lobe (hL), each of which forms globular subdivisions ('Trauben') in the distal part. (B) Mushroom body morphology in the brain of the hemimetabolous representative *Rhyparobia (Leucophaea) maderae*, visualized by anti-DC0 and DAPI. Two cup-shaped calyces are capped by a dense aggregation of Kenyon cell bodies (KCb). A stalk-like peduncle extends ventrally and splits into a medial lobe (mL) and a vertical lobe (not shown). Within the medial lobe, differential immunoreactivity generates a laminated pattern. (C) Similar presentation of the mushroom body neuropil in the honeybee *Apis mellifera*. The mushroom bodies in this holometabolous representative comprise two cup-shaped calyces with distinct sub-regions referred to as lip (Ca_l), collar (Ca_c), and neck (Ca_n). Axon-like processes of the Kenyon cells form a massive peduncle that bifurcates into a medial lobe and a vertical lobe (insert, superimposed from a different projection plane). Within the vertical lobe, varying immunostaining intensities mark distinct laminae corresponding to discrete Kenyon cell subpopulations. (D) Illustration of an idealized mushroom body, providing anatomical reference for neurotransmitter distribution in different species. Subdivisions of the medial and vertical lobe, as present e.g. in *Drosophila melanogaster* and *Tribolium castaneum*, are indicated by lighter shadings. H: heel (sometimes also referred to as spur). Scale bars: (A) 50 µm, (B, C) 100 µm.

centers in the deutocerebrum, the olfactory glomeruli. As olfactory sensory neurons that express the same olfactory receptors converge upon discrete glomeruli (Bhalerao et al., 2003), each glomerulus is assumed to supply a specific odor quality to subsequent neuropils – a view that is, however, simplified for convenience as it omits information processing in and between olfactory glomeruli by local interneurons (Keene and Waddell, 2007; Olsen et al., 2007; Carlsson et al., 2010). In the mushroom

bodies, intrinsic neurons – i.e. Kenyon cells – are thought to integrate information across different odor qualities by acting as coincidence detectors in such a way that a given odor is represented by the activity of a unique set of Kenyon cells (Perez-Orive et al., 2002; Jortner et al., 2007). Extrinsic neurons that form synapses on the axon-like projections of the Kenyon cells complement the circuitry and are involved in olfactory learning processes by modulating Kenyon cell output. Among these, dopaminergic and octopaminergic neurons are assumed to play a key role in the acquisition of aversive and appetitive behavioral responses, respectively (Schwaerzel et al., 2003; Unoki et al., 2005; Schroll et al., 2006).

It would be erroneous, however, to interpret insect mushroom bodies solely as higher centers of the olfactory pathway. Such a misconception is readily rejected by the presence of mushroom bodies in insects that lack glomerular antennal lobes, such as mayflies, dragonflies and cicadas (Strausfeld et al., 2009). Mushroom bodies in these species do not receive ascending fibers that provide olfactory input and are usually not equipped with a distinct calyx. However, as "calyxless mushroom bodies do not operate in an afferent vacuum" (Strausfeld, 2002; page 22), the peduncle and lobes in these insects are assumed to receive and process non-olfactory inputs. In the odonate *Aeschna grandis*, for example, the tip of the peduncle appears to be supplied by afferents from the optic neuropils (Sviderskiy and Plotnikova, 2004). However, even in insects with an unimpaired sense of smell, there is compelling evidence that the mushroom bodies are in fact involved in the integration and processing of a broad range of sensory modalities. In the honeybee, olfactory input is complemented by prominent visual, mechanosensory, and gustatory afferents that supply mutually exclusive zones of the elaborate calycal neuropil (Gronenberg, 1986; Gronenberg, 2001; Ehmer and Gronenberg, 2002; Schröter and Menzel, 2003). Direct visual input to a distinct subcompartment of the calyx has also been demonstrated in herbivorous scarab beetles (Farris, 2008a). While similar connections appear to be lacking in *Drosophila*, the mushroom bodies of the fruit fly have been shown to exhibit structural plasticity in response to visual stimulation (Barth and Heisenberg, 1997) and to play a role in visual information processing and visual learning (Liu et al., 1999). Gustatory and possibly also mechanosensory input to the mushroom body calyces is encountered in representatives of different insect orders (Weiss, 1981; Schröter and Menzel, 2003; Farris, 2008b), prompting speculations about an early evolutionary function of the mushroom bodies in taste perception (Farris, 2008b). Furthermore, studies in crickets and cockroaches suggest that the mushroom bodies are also involved in the processing of tactile and acoustic stimuli (Schildberger, 1984; Mizunami et al., 1998a,b). In addition to these direct multimodal inputs, the mushroom bodies are also supplied by secondary afferents from different parts of the protocerebrum (Ito et al., 1998; Strausfeld, 2002; Tanaka et al., 2008), by neuromodulatory innervations (Waddell et al., 2000; Mao and Davis, 2009), and by extrinsic neurons that provide recurrent feedback (e.g. Grünewald, 1999). Many of these projections do not target the calyx but the peduncle and the lobes, obliterating the conventional concept of the calyx as 'input region' of the mushroom bodies.

Matching the complexity of their neuronal connections, the mushroom bodies have been implicated in diverse functions beyond the context of olfaction (Table 1), including pattern recognition and the integration of sensory and motor signals (Wessnitzer and Webb, 2006). A role in feature extraction and sensory filtering is supported by investigations in the fruit fly (Zhang et al., 2007; Xi et al., 2008). Interestingly, these functions might – at least in part – account for volume changes of the mushroom bodies in different castes of polyethic insects (Withers et al., 1993; Gronenberg et al., 1996) and in different life phases of locusts (Ott and Rogers, 2010; Farris, 2011). Experimental evidence for a role in activity and locomotion control has been provided by investigations in cockroaches, crickets, and fruit flies (Huber, 1960; Martin et al., 1998; Mizunami et al., 1998a; Okada and Ikeda, 1999). In addition, the mushroom bodies in *D. melanogaster* are also involved in the regulation of sleep (Joiner et al., 2006). Investigations in the cockroach *P. americana* further indicate a role in place memory (Mizunami et al., 1998b), adding yet another facet to the plethora of functional implications. Thus, the familiar picture of mushroom bodies as brain centers dedicated solely to the processing of

Table 1
Overview summarizing functions in which the insect mushroom bodies have been implicated.

Function	Species (Reference)	Evidence from
Processing of olfactory information	olfactory information is probably relayed in all insects equipped with antennal lobes (reviewed in e.g. Schachtner et al., 2005; Fiala, 2007; Galizia and Rössler, 2010)	neuroanatomy, electrophysiology, calcium imaging
Olfactory learning	*Apis* (e.g. Menzel, 2001; Menzel et al., 2006; Fahrbach and Dobrin, 2009), *Drosophila* (reviewed in e.g. Davis, 2005; Fiala, 2007; Keene and Waddell, 2007), locust (e.g. Simões et al., 2011; Perez-Orive et al., 2002; Cassenaer and Laurent, 2007, 2012)	mutant screens, genetic studies, behavioral experiments, pharmacological studies, electrophysiology, calcium imaging
Processing of visual information	Hymenoptera (Gronenberg, 1986, 2001; Paulk and Gronenberg, 2008), scarab beetles (Farris, 2008a), *Spodoptera* (Sjöholm et al., 2005), *Periplaneta* (Strausfeld and Li, 1999; Nishino et al., 2012), crickets (Honegger and Schürmann, 1975; Schildberger, 1984), *Aeschna* (Sviderskiy and Plotnikova, 2004)	neuroanatomy, electrophysiology
Visual learning/ visual cognitive tasks	*Drosophila*: context generalization (Liu et al., 1999), choice behavior (Tang and Guo, 2001; Zhang et al., 2007), fixation behavior (Xi et al., 2008), feature extraction (Peng et al., 2007)	genetic studies, behavioral experiments, ablation experiments
Processing of gustatory information	*Thermobia*, hemi- and holometabolous representatives (Farris, 2008b), *Apis* (Schröter and Menzel, 2003)	neuroanatomy
Gustatory learning	*Drosophila* (Masek and Scott, 2010)	genetic studies
Processing of mechanosensory information	*Thermobia*, hemi- and holometabolous representatives (Farris, 2008b), *Apis* (Schröter and Menzel, 2003)	neuroanatomy
Processing of acoustic information	*Periplaneta* (Li and Strausfeld, 1997, 1999), *Acheta* (Schildberger, 1984)	neuroanatomy, electrophysiology
Activity and locomotion	crickets (Huber, 1960; Otto, 1971), grasshopper (Wadepuhl, 1983), *Drosophila* (Martin et al., 1998), *Periplaneta* (Mizunami et al., 1998a; Okada and Ikeda, 1999)	ablation experiments, electrophysiology, behavioral experiments
Sleep regulation	*Drosophila* (Joiner et al., 2006; Pitman et al., 2006; Guo et al., 2011)	genetic studies, ablation experiments
Place memory	*Periplaneta* (Mizunami et al., 1993, 1998b)	behavioral tests, ablation experiments
Temperature preference	*Drosophila* (Hong et al., 2008; Bang et al., 2011)	mutant screens, genetic studies

olfactory information is almost certainly missing other, perhaps even more vital aspects.

1.3. Mushroom bodies in other taxa

Anatomically, mushroom bodies are defined as cerebral neuropils with a lobed shape which are composed of dendritic and axon-like projections of numerous small-diameter cell bodies that form dense aggregations in the dorsal part of the brain (Flögel, 1876; Holmgren, 1916). While neopteran mushroom bodies are prime examples for this type of neuropil, brain centers matching the definition provided above have also been described in odonates, ephemeropterans (Strausfeld et al., 2009), and in basal hexapods (Kollmann et al., 2011a). Furthermore, mushroom bodies are also present in chelicerates (Hanström, 1928; Fahrenbach, 1977; Doeffinger et al., 2010), myriapods (Hanström, 1928; Strausfeld et al., 1995), onychophorans (Strausfeld et al., 2006), in 'errant' polychaetes (Heuer and Loesel, 2008; Heuer et al., 2010) and in polyclad platyhelminthes (Turner, 1946; Keenan et al., 1981). However, despite the anatomical commonalities of mushroom bodies in various taxa, the apparent lack of mushroom bodies in crustaceans and the phylogenetic distance between arthropods (Ecdysozoa) and annelids (Lophotrochozoa) have raised doubts about early homology assessments (Holmgren, 1916; Hanström, 1928). While arguments supporting an independent origin of mushroom bodies in different arthropod subphyla have been discussed (Strausfeld, 1998; Farris, 2008c), recent studies on gene expression patterns in mushroom body neurons suggest not only a homology between insect and polychaete mushroom bodies, but even propose the mushroom bodies to be homologous to the vertebrate pallium (Tomer et al., 2010), a telencephalic division that in mammals gives rise to the neocortex (Medina and Abellán, 2009). If true, this would push the evolutionary origin of mushroom bodies back to the last common ancestor of protostomes and deuterostomes ('Urbilateria'). In this light, a detailed understanding of *what* functions the mushroom bodies actually serve and *how* these functions are accomplished might be more desirable than ever before.

1.4. Neuropeptides in the insect mushroom bodies

Over the years, immunohistological studies on insect brains have employed a rich palette of antibodies to analyze and visualize central nervous structures, thereby contributing continuously to our knowledge about the presence and distribution of neuroactive substances in the mushroom body neuropils. In addition, the ongoing quest to unravel the basics of olfactory learning in fruit flies, honeybees, and a few other model organisms, has revealed genes and gene products that are preferentially expressed in either extrinsic or intrinsic mushroom body neurons (reviewed in e.g. Davis, 2005; Keene and Waddell, 2007). Immunohistological investigations, for example, have shown that individual Kenyon cell subsets can be characterized biochemically due to the expression of the putative neuroactive substances aspartate, glutamate, and taurine (Crittenden et al., 1998; Sinakevitch et al., 2001; Sjöholm et al., 2006). However, these studies have also demonstrated that neurotransmitter expression in intrinsic mushroom body neurons can vary over the life of an insect: while newborn Kenyon cells projecting into the so-called ingrowth lamina express comparatively high levels of glutamate, glutamate expression is down regulated in more mature cells and is superseded by the expression of aspartate. In addition, some of the mature Kenyon cells also express high levels of taurine. Recent studies suggest that glutamate functions as an autocrine or paracrine agent during mushroom body development (Sinakevitch et al., 2010), while the almost ubiquitous expression of aspartate in mature Kenyon cells has been interpreted as a hint that this amino acid might act as an independent transmitter or a cotransmitter. However, a neurotransmitter expressed exclusively but universally in Kenyon cells has not yet been identified (Johard et al., 2008).

Among the neuroactive substances that mediate neuronal communication, neuropeptides are by far the largest and most diverse group. This diversity is in part brought about by post-translational processing of precursor polypeptides encoded by single genes. Thus, enzymatic cleavage and modification of individual precursors may yield several distinct neuropeptides (Altstein and Nässel, 2010). In this regard, the most extensive processing described to date has been demonstrated in the cockroach *P. americana*, in which a single FMRFamide precursor has been shown to be cleaved into 23 neuropeptide forms (Predel et al., 2004). In species for which the entire genome has been sequenced, the number of encoded neuropeptides can be estimated by sequence comparison and analysis. A recent survey across the genomes of seven holometabolous insects revealed a core set of 19 highly conserved neuropeptide precursors that could be identified in all genomes, as well as a set of 26 variable precursors that are not present in all of these genomes (Hauser et al., 2010). The genome of *Drosophila*, for instance, contains approximately 42 genes that encode neuropeptide and protein hormone precursors (Nässel and Winther, 2010); in the lepidopteran *Bombyx mori* the number amounts to 37 neuropeptide genes (Roller et al., 2008), in the coleopteran *Tribolium castaneum* to 41 genes (Li et al., 2008), and in the hymenopteran *A. mellifera* to about 33 genes (Hummon et al., 2006; Predel and Neupert, 2007). Examining the precursor sequences for putative proteolytic cleavage sites, an approximation of the number of processed neuropeptides can be calculated. However, since not every conventional cleavage site is necessarily used and because neuropeptide expression can vary during development and in specific tissues, it is important to verify the presence of predicted neuropeptides by means of, e.g., immunohistochemistry or mass spectrometry. Thus, while genetic data indicate the presence of about 75 functional neuropeptides in *Drosophila* (Nässel and Winther, 2010), only 42 of these have been detected in extracts of adult fly brains (Yew et al., 2009) and only 38 in extracts of the larval nervous system (Baggerman et al., 2005). Similarly, not all of the approximately 80 predicted neuropeptide molecules in *T. castaneum* have yet been confirmed by chromatographic or mass spectrometric methods (Li et al., 2008). Mature neuropeptides mediate their effect by biochemically interacting with competent receptors – mostly G-protein coupled receptors – that have a high affinity for a specific section in the amino acid sequence of the neuropeptide. These biologically active regions are usually highly conserved, both within and across species, and neuropeptides are commonly grouped into families according to these characteristic sequence similarities (Table 2).

The present review article aims to provide a comprehensive overview on mushroom body-associated neuropeptides in insects. In order to cover a broad taxonomic range, we have in many instances decided to supplement information from the literature by original data from our own investigations. Findings from both sources are presented side by side in the 'Results' section, which is subdivided into chapters on eight major neuropeptide families: A-type allatostatins, myoinhibitory peptides, allatotropin, FMRFamide related peptides, orcokinin, SIFamide, short neuropeptide Fs, and tachykinins. Each chapter starts with a brief introduction that provides information on the discovery of the neuropeptides, their characteristic sequences, their identification in different insect species, and their known functions. The introductory part is followed by a segment that focuses on the presence and distribution of the neuropeptides in mushroom body-associated neurons as

Table 2
List of neuropeptides reviewed in the present article, including characteristic sequence motifs. Xaa denotes a variable amino acid residue in the sequence.

Neuropeptide family	Synonyms and Abbreviations	Characteristic sequence motif
A-type allatostatins	AST-A	Tyr/Phe-Xaa-Phe-Gly-Leu/Ile-amide
B-type allatostatins	AST-B MIPs, myoinhibitory peptides	Trp-$(Xaa)_6$-Trp-amide
Allatotropin	AT	Thr-Ala-Arg-Gly-Phe-amide
Extended FMRF-amids	FMRFa	Phe-Met-Arg-Phe-amide
Orcokinin	OK	Asn-Phe-Asp-Glu-Ile-Asp-Arg
Short Neuropeptide Fs	sNPF	Arg-Leu/Pro-Arg-Phe/Trp-amide
SIFamide	SIFa	Pro-Phe-Asn-Gly-Ser-Ile-Phe-amide
Tachykinin-related peptides	TRPs, TKRPs	Phe-Xaa-Gly-Xaa-Arg-amide

described in the literature. Unpublished data from own experiments are presented in a separate paragraph. Chapters end on a short synopsis in which the described data are analyzed from an evolutionary and/or functional point of view. A comparative analysis of the complete dataset for patterns that could indicate an evolutionary conservation of the peptide biochemistry of mushroom body neurons is provided in the 'Conclusions'.

2. Materials and Methods

To compliment the survey of the available literature, the present account aims to contribute new data for a broad range of insect species. Naturally, not all investigated insect species were reared at our own facilities, but many specimens were generously provided by fellow researchers. Similarly, we applied a wide spectrum of antisera in our immunohistological stainings, most of which were kindly donated by colleagues. Finally, brain preparations of different animals and stainings with different antisera frequently require adjustments of the staining protocol. The following paragraphs provide brief information on the animals, staining protocols, and antisera.

2.1. Animals

Firebrats (*Thermobia domestica*) were reared at our facilities and were kept in an incubator under warm (35 °C) and humid conditions. The largest animals in the colony were identified as adults and only such specimens were used for immunohistochemical investigations. Madeira cockroaches (*Rhyparobia maderae*, formerly *Leucophaea maderae*) were taken from breeding colonies in the lab; American cockroaches (*P. americana*) were kindly provided by Dr. R. Predel (University of Jena, Germany). Specimens of the Pink-winged stick insect (*Sipyloidea sipylus*) and the Indian stick insect (*Carausius morosus*) were a generous gift of Dr. S. Dietrich (University of Marburg, Germany); Annam stick insects (*Medauroidea extradentata*) were kindly provided by Dr. A. Büschges (University of Cologne, Germany). A breeding population of Yellow fever mosquitoes (*Aedes aegypti*) was established from eggs provided by Dr. R. Ignell (SLU, Alnarp, Sweden). Animals were kept under a 12:12 light:-dark cycle at 27 °C and a relative humidity of 70% in walk-in environmental chambers. Larvae hatched in tap water and were raised on fish food (TetraMin, Tetra GmbH, Melle, Germany). Adult animals were fed with 10% sugar solution in distilled water. Ten-day old females were allowed to blood-feed on young mice or hamster. Worker honeybees (*A. mellifera*) were collected from a hive established at the Institute from a nucleus colony provided by Dr. R. Büchler (Bieneninstitut Kirchhain, Germany). Bumblebees (*Bombus terrestris*) were kindly provided by Dr. A. Brockmann (University of Würzburg, Germany). Turnip moths (*Agrotis segetum*) were kindly provided by Dr. C. Gadenne (INRA, Centre de Recherches de Versailles, France); Silkmoths (*B. mori*) were a generous gift of Dr. R. Kanzaki (University of Tokyo, Japan). Hawk moths (*Manduca sexta*) were bred in the lab and were fed with an artificial diet. They were raised under a long-day photoperiod (L:D = 17:7) at 26 °C in walk-in environmental chambers (Bell and Joachim, 1978). Tobacco Budworms (*Heliothis virescens*) were a generous gift from Dr. Bente Berg (University of Trondheim, Norway). Small hive beetles (*Aethina tumida*) were collected from beehives at the University of Pretoria (South Africa) by Dr. P. Neumann and A. L. Rupenthal. Colorado potato beetles (*Leptinotarsa decemlineata*) were collected in the woodlands surrounding the University of Marburg, Germany. Wild type *T. castaneum* (San Bernardino; Sokoloff, 1966) were raised under constant darkness at 26 °C in walk-in environmental chambers in flour supplemented with 5% dried yeast powder with 0.05% (w/w) Fumidil-B (J. Webster Laboratories Inc., Princeville, Canada; Berghammer et al., 1999). *D. melanogaster* (w1118) were raised under a 12:12 light:dark cycle at 25 °C, reared on a standard cornmeal/soymeal/glucose/agar diet.

2.2. Wholemount immunohistochemistry

Insect brains were dissected in cold PBS (phosphate-buffered saline, 0.01M or 0.1M, pH 7.4) and fixed in 4% formaldehyde (FA, Roth, Karlsruhe, Germany) in PBS. Fixation times varied for brains of different sizes, ranging from 3 h of fixation at room temperature (e.g. mosquitoes) to overnight fixation at 4 °C (e.g. cockroaches). Subsequently, brains were rinsed in 0.01 or 0.1 PBS (PBS molarity in this and all following steps corresponded to the molarity initially used). Rinsing steps were again adapted to brain size (3–6 times 10–15 min). Brains were then pre-incubated in PBS containing 0.3% Triton X-100 (PBS-TrX; Sigma–Aldrich, Steinheim, Germany) and 3%–5% normal goat serum (NGS, Jackson ImmunoResearch, Westgrove, PA, USA) for 1–2 days. After pre-incubation, brains were transferred to PBS-TrX containing 2–5% NGS and primary antibodies. Usually, a monoclonal antibody directed against synapsin was used to label neuropil areas and thus provide morphological reference; this was combined with a second primary antibody directed against the neuropeptide of interest. Further details on primary antibodies are given in the next paragraph and in Table 3. Incubation times related to brain size, varying between 2 and 5 days at 4 °C. Brains were then rinsed again in PBS-TrX (3–6 times 10–15 min) and were afterwards incubated with secondary antibodies (goat-anti-mouse Cy5 and goat-anti-rabbit Cy3 or vice versa, Jackson ImmunoResearch, Westgrove, PA, USA) at a dilution of 1:300 in PBS-TrX containing 2–5% NGS. Incubation time varied from 2 to 5 days at 4 °C. In some instances, additional markers were added to this solution to produce triple labelings. These included Alexa Fluor 488-coupled phalloidin at a dilution of 1:200 (phalloidin; Molecular Probes, Eugene, OR, USA) to visualize axonal f-actin as well as the nuclear marker DAPI (4′,6-diamidinophenyindole; Sigma–Aldrich, Steinheim, Germany) at a dilution of 1:1000. After incubation, brains were washed in PBS (3–6 times 10–15 min) and then dehydrated in an ascending ethanol series (50%, 70%, 90%, 95%, and two times 100%, 2–4 min each). Tissue was then cleared to transparency in methyl salicylate (Merck, Gernsheim, Germany). Finally, brains were mounted in Permount (Fisher Scientific, Pittsbourgh, PA, USA) using several reinforcing rings (depending on size of the brains; Zweckform, Oberlaindern, Germany) as spacers between two coverslips.

Table 3
List of antisera used, including target sequences, applied dilutions, antibody sources and references.

Name, anti-	Abbreviation, anti-	Target sequence	Dilution	Donor	Antibody reference
Manduca sexta Allatotropin	Mas-AT	pGFKNVEMMTARGF-NH_2	1:4000–1:5000	Dr. J. Veenstra	Veenstra and Hagedorn, 1993
Diploptera punctata Allatostatin 7	Dip-AST 7	APSGAQRLYGFGL-NH_2	1: 5000–1:15000	Dr. H. Agricola	Vitzthum et al., 1996
Ortonectes limosus Asn13-Orcokinin (syn.)	Asn13-OK	NFDEIDRSGFGFN-OH	1: 1000	Dr. H. Dircksen	Bungart et al., 1994
Periplaneta americana Myoinhibitory Peptide	Pea-MIP	GWQDLQGGW-NH_2	1:4000–1:5000	Dr. M. Eckert	Predel et al., 2001
Locusta migratoria Tachykinin II	Lom-TK II	APLSGFYGVR-NH_2	1:10000–1:15000	Dr. H. Agricola	Veenstra and Lambrou, 1995
FMRFamide (syn.)	FMRFamide	FMRF-NH_2	1:2000–1:7000	Dr. E. Marder	Marder et al., 1987
Procambarus clarkii SIFamide (syn.)	SIFamide	GYRKPPFNGSIF-NH_2	1:20000	Dr. A. Yasuda	Yasuda et al., 2004
Drosophila melanogaster Short Neuropeptide F–3	Drm-sNPF–3	PQRLRW-NH_2	1:1000–1:4000	Dr. J. Veenstra	Johard et al., 2008
Drosophila melanogaster Synapsin I	Synapsin		1:50	Dr. E. Buchner	Klagges et al., 1996
Drosophila melanogaster Catalytic subunit of protein kinase A	DC0		1:1000	Dr. D. Kalderon	Lane and Kalderon, 1993

2.3. Vibratome section immunohistochemistry

In some cases, comparatively large brains – e.g. cockroach or honeybee brains – were cut into sections to facilitate antibody penetration. For this, fixed and rinsed brains (see above) were embedded in a gelatine/albumin medium which was hardened overnight in 4% or 8% FA in PBS at 8 °C. Blocks were then cut into 40–80 μm thick sections with a vibrating blade microtome (Leica VT 1200S, Wetzlar, Gemany). Subsequent treatment of free-floating vibratome sections basically followed the protocol for wholemount immunohistochemistry provided above. However, for rinsing SST (0.3 M NaCl, 0.1 M Tris/HCl, pH 7.4) containing 0.1% TrX was used, and incubations were done in SST containing 0.5% TrX. After final rinsing, sections were dehydrated in an ascending ethanol series (50%, 70%, 90%, 95%, 100%, for 2–4 min each), transferred to xylene (2 times 100%, 2–4 min), and finally mounted in Entellan (Merck, Darmstadt, Germany).

2.4. Primary antisera

A complete list of primary antibodies – including target sequences, dilutions, and references – is provided in Table 3. Mushroom body morphology in selected species was revealed by a polyclonal antibody directed against the catalytic subunit of *D. melanogaster* protein kinase A (anti-DC0, a generous gift of Dr. D. Kalderon). Anti-DC0 production was described by Lane and Kalderon (1993) and the antibody has been shown to reliably label Kenyon cells in a variety of insects, including apterygote representatives (Farris, 2005b). The antibody was used at a concentration of 1:1000. To visualize the basic neuropil layout, a monoclonal primary antibody raised in mouse and directed against a fusion protein consisting of a glutathione-S-transferase and the presynaptic vesicle protein synapsin I (SYNORF1; 3C11, #151101) was used. The antibody was kindly provided by Dr. E. Buchner (University of Würzburg, Germany) and was first described by Klagges et al. (1996). It was used at a dilution of 1:50.

Neuropeptide antibodies were all raised in rabbit and targeted characteristic neuropeptide sequences presumed to be highly conserved among insects (for reviews see Nässel, 2002; Homberg, 2002; Nässel and Homberg, 2006; Verleyen et al., 2009). The antiserum against *M. sexta* allatotropin (Mas-AT) was kindly provided by Dr. J. Veenstra (University of Bordeaux, France) and was first described in Veenstra and Hagedorn (1993). Antisera against *Diploptera punctata* allatostatin 7 (Dip-AST 7, as specified in Vitzthum et al., 1996), *Locusta migratoria* tachykinin II (Lom-TK II, specified in Veenstra and Lambrou, 1995), and *P. americana* myoinhibitory peptide (Pea-MIP, specified in Predel et al., 2001) were generously provided by Dr. M. Eckert (University of Jena, Germany). Anti-Asn13-orcokinin (Asn13-OK) was a gift from Dr. H. Dircksen (University of Stockholm, Sweden); the antibody was first characterized by Bungart et al. (1994). The antiserum against FMRFamide was kindly provided by Dr. E. Marder (Brandeis University, Waltham, USA), who was also the first to describe the antibody (Marder et al., 1987). The antiserum recognizes FMRFamide and FLRFamide peptides (Marder et al., 1987; Kingan et al., 1990), including the three FaRPs identified in *M. sexta* (Kingan et al., 1990, 1996; Miao et al., 1998). The sNPF antiserum is directed against *D. melanogaster* sNPF-3 (PQRLRWa), which is highly similar to the sNPF-3 in *A. aegypti* (Predel et al., 2010). It was kindly provided by Dr. J. Veenstra and is described in Johard et al. (2008). Antiserum against synthetic *Procambarus clarkii* SIFamide (GYRKPPFNGSIFamide) was raised in rabbit (Yasuda et al., 2004) and was kindly provided by Dr. A. Yasuda (Suntory Institute for Bioorganic Research, Osaka, Japan).

2.5. Image acquisition and processing

Images were taken with a confocal laser-scanning microscope (TCS SP5, Leica Microsystems, Wetzlar, Germany). Cy3 fluorescence was detected using a helium/neon laser (excitation wavelength 543 nm), Cy5 fluorescence with an argon/krypton laser (excitation wavelength 647 nm). DAPI fluorescence was visualized with a UV laser (excitation wavelength 405 nm). Images were acquired in sequential scan mode at resolutions of 1024 × 1024 or 512 × 512 pixels and a scanning speed between 400 and 100 Hz. Confocal images and image stacks were analyzed with the Amira 5.2 graphics software (Visage Imaging, Berlin, Germany). For further processing (i.e. level adjustments, contrast and brightness optimization) and final figure arrangements, snapshots of single sections or projection views taken in Amira were processed using Corel Draw X3 (Corel, Ottawa, Ontario, Canada) and Adobe Photoshop CS3 (Adobe Systems, San Jose, CA, USA). In some image stacks, the intensity of the synapsin-immunoreactivity obscured the immunostaining produced by neuropeptide antisera. In these instances, it was chosen to display only neuropeptide immunoreactivity but to demarcate neuropil boundaries by adding outlines based on synapsin channels.

3. Neuropeptides in insect mushroom bodies

3.1. A-type allatostatin (AST-A)

Allatostatins, named for their inhibitory effect on juvenile hormone synthesis in the *corpora allata*, form three distinct groups (A-type, B-type, C-type allatostatins) of structurally unrelated peptides encoded by different genes (see Nässel, 2002; Nässel and Winther, 2010). A-type allatostatins were first discovered in the cockroach *D. punctata* (Pratt et al., 1989; Woodhead et al., 1989) and have therefore also been referred to as cockroach or *Diploptera* type allatostatins (dipstatins). In *D. punctata*, 13 different AST-A isoforms

have been identified, all of which are processed from a 370 amino acid precursor protein encoded by a single gene (Donly et al., 1993). Common to all isoforms is a conserved C-terminal Tyr/Phe-Xaa-Phe-Gly-Leu/Ile-amide sequence (Table 2) that is also characteristic for AST-As in other insects. Members of the AST-A peptide family have, among others, been identified in different cockroach species (Bellés et al., 1999), in locusts (Veelaert et al., 1995) and moths (Davis et al., 1997; Davey et al., 1999; Secher et al., 2001), in the cricket *Gryllus bimaculatus* (Meyering-Vos, 2003), the termite *Reticulitermes flavipes* (Yagi et al., 2005; Elliott et al., 2009) and the pea aphid *Acyrthosiphon pisum* (Huybrechts et al., 2010), the mosquito *A. aegypti* (Veenstra et al., 1997), and in *Drosophila* (Lenz et al., 2000). Not only their wide-spread occurrence in insects, but also the presence of highly similar peptides in Crustaceans (Dircksen et al., 1999; Christie et al., 2008) is suggestive of an early evolutionary origin of the AST-A-like neuropeptide family. In this light, it is interesting to note that sequence mining for AST-A peptides and AST-A receptor genes in the fully sequenced genome of the red flour beetle *T. castaneum* did not yield any matches (Li et al., 2008), suggesting a secondary loss of this neuropeptide family in Coleoptera. However, more recent physiological, immunological, and biochemical investigations in the closely related mealworm beetle *Tenebrio molitor* provide contrasting evidence, indicating AST-A related peptides to be present in this species (Wasielewski et al., 2009; Elliott et al., 2010).

AST-As derive their name from their inhibitory effect on the biosynthesis of juvenile hormone, demonstrated e.g. in the dictyopteran *D. punctata* (Pratt et al., 1989; Woodhead et al., 1989), the orthopteran *G. bimaculatus* (Lorenz et al., 1995a), and the isopteran *R. flavipes* (Yagi et al., 2005). However, contrary to their terminology, members of the AST-A family do not affect juvenile hormone production in every insect species (e.g. *Calliphora vomitoria*: Duve et al., 1993; *A. aegypti*: Li et al., 2004). Moreover, while the allatostatic effect is mediated by neurons directly innervating the *corpora allata*, members of the AST-A family usually also occur in numerous other neurons, pointing towards pleiotropic functions beyond the regulation of juvenile hormone synthesis (Stay and Tobe, 2007). Thus, in *D. punctata*, AST-As have been shown to inhibit hindgut contractions (Lange et al., 1995) and to stimulate enzyme activity in the lumen contents of the midgut (Fusé et al., 1999); additional functions are likely to include roles as neuromodulators and endocrine agents, but have so far been poorly investigated (Nässel and Winther, 2010).

Detailed descriptions of AST-A-like immunoreactivity in the mushroom body neuropils are scarce. A thorough analysis of the distribution of AST-As in the brain of the honeybee was recently published by Kreissl et al. (2010), showing that in the mushroom bodies, AST-A immunolabeling produces distinct patterns in the lobes, the peduncle, and the calyces. Immunoreactive fibers originate from a group of cell bodies located beneath the optic tubercle of each hemisphere. Their neurites enter the mushroom body neuropil between the medial and lateral calyx, splitting into two fractions. One group of collaterals extends through the peduncle and directly supplies the medial and vertical lobes, forming a fibrous meshwork. The other group first diverts to the neck region of the calyces from where it provides side branches to other parts of the calyces as well. It then runs down through the peduncle and innervates the medial and vertical lobes, forming distinct strata in the latter. While the branching patterns of these extrinsic AST-A immunoreactive neurons are suggestive of a mushroom body feedback circuit, intrinsic Kenyon cells exhibit no AST-A-like immunoreactivity in *A. mellifera* (Kreissl et al., 2010). In contrast, in the desert locust *Schistocerca gregaria*, Kenyon cell somata, the lateral calyces, the peduncle and the lobes have been reported to show immunoreactivity towards an antiserum raised against *D. punctata* AST-5 (Veelaert et al., 1995). Remarkably, in the same species, an antiserum directed against *D. punctata* AST-1 produced no immunostaining in intrinsic mushroom body neurons, leaving the peduncle and lobes unlabeled. Weak immunoreactivity was only observed in arborizations of extrinsic neurons invading the calyx region (Vitzthum et al., 1996). In their discussion, Vitzthum and coworkers argued that the observed differences probably derive from a much higher specificity of the Dip-AST-1 antiserum in comparison to the Dip-AST-5 antiserum used by Veelaert et al. (1995).

Our own immunohistological studies employed the same antiserum as originally used by Vitzthum et al. (1996, see Table 3. Note that due to a change in nomenclature, the antiserum is now termed anti-Dip-AST-7). In the zygentome *T. domestica*, the antiserum reveals single immunoreactive fibers penetrating the calyx (Fig. 2A). However, these extrinsic projections appear to cross the calyx region without forming ramifications or varicosities within the neuropil. Other regions of the mushroom body neuropil are devoid of immunostaining. While AST-A-like immunoreactivity in *P. americana* is likewise restricted to the calyces, immunostained fibers are dispersed in a reticular fashion throughout the cup-shaped subcompartment (Fig. 2B). In the stick insect *Sypiloidea sypilus*, the calyx region also exhibits pronounced immunostaining (Fig. 2C). Immunoreactivity within the peduncle is difficult to assess but appears to be missing, although distinctive immunostaining is apparent in the core region of the vertical and medial lobe, indicating the presence of AST-A-like peptides in intrinsic fibers. Similar staining patterns can also be observed in the mushroom bodies of two other stick insect species, *C. morosus* and *Medauroidea extradentata* (data not shown). In the lepidopteran species *A. segetum* (Fig. 2D), *B. mori* (Fig. 2E), *H. virescens* and *M. sexta* (data not shown), AST-A-like immunostaining is again restricted to the calyces, with immunoreactive blebs being scattered throughout the neuropil. Mushroom body peduncles and lobes in these species display no immunoreactivity. As indicated by genomic data (see above), AST-A neuropeptides appear to be lacking in the coleopteran *T. castaneum*. Consequently, the AST-A antiserum produces no immunostaining in this species (data not shown). Mushroom body-associated immunoreactivity in *A. aegypti* (Fig. 2F) somewhat resembles the conditions described for *T. domestica*, in that a distinctly labeled fiber passes through the calyx region while the rest of the neuropil is devoid of immunostaining. In the mosquito, however, the invading fiber appears to form individual varicosities within the calyx neuropil. The mushroom body neuropils in the fruit fly *D. melanogaster* exhibit no AST-A-like immunoreactivity but the peduncle is encircled by immunolabeled fibers (data not shown).

Comparing AST-A-like immunoreactivity in mushroom body-associated neurons of the different species, an extrinsic innervation of the calyces can be observed in nearly all taxa examined so far (Figs. 10 and 11). Particularly strong commonalities are discernable in Lepidoptera, where scattered immunoreactivity was found in the calyces of each investigated species. These findings are also in accordance with observations in the cotton leafworm *Spodoptera littoralis*, for which a similar staining pattern was reported (Sinakevitch et al., 2008). Notable exceptions are found in *Drosophila*, in which AST-A immunopositive fibers only wrap the peduncle but do not enter the calyces or any other part of the neuropil, and in the bumblebee, in which an extrinsic innervation was not discernable (data not shown). The latter condition contrasts with reports on AST-A immunoreactivity in the honeybee brain, according to which all parts of the mushroom bodies are innervated by AST-A immunopositive extrinsic neurons (Kreissl et al., 2010). The disparity between the two hymenopteran species is even more pronounced as *B. terrestris* exhibits extensive

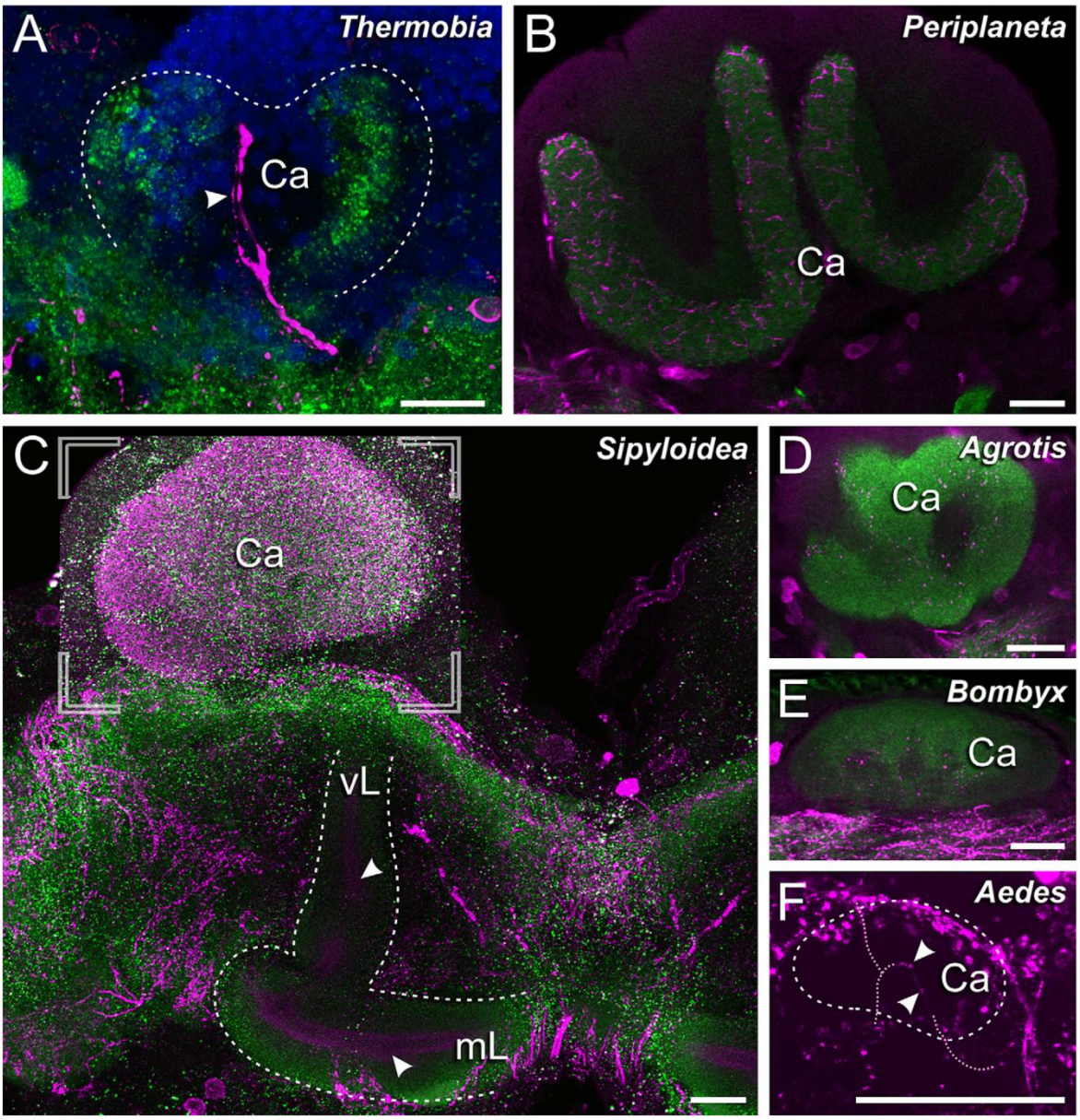

Fig. 2. Allatostatin-A-like immunoreactivity in insect mushroom bodies. (A) In the zygentome *Thermobia domestica*, immunostained fibers (arrowhead) penetrate the calyx region (Ca) but do not form extensive arborizations within the neuropil. (B) The calyces in the cockroach *Periplaneta americana*, in contrast, are riddled with immunopositive ramifications. However, similar to the conditions in *T. domestica*, the rest of the mushroom body neuropil is devoid of immunostaining. (C) Anti-AST-A immunostaining in the stick insect *Sypiloidea sypilus* reveals scattered immunoreactivity in the calyx region (insert, superimposed from a different projection plane). Ventrally, aggregated immunoreactive fibers (arrowheads) can be observed in the core of the medial (mL) and vertical lobe (vL). (D, E) AST-A-like immunoreactivity in the mushroom bodies of the lepidopteran representatives *Agrotis segetum* (D) and *Bombyx mori* (E) is restricted to scattered blebs in the calyx region. (F) In *Aedes aegypti*, a single immunoreactive fiber crosses the calyx region, reminiscent of the condition observed in *T. domestica*. While the fiber does not give rise to finer arborizations, sparse varicosities are discernable within the neuropil (arrowheads). All images show frontal aspects of the mushroom bodies, dorsal is towards the top and lateral to the left of each picture. blue: DAPI-labeled cell nuclei, green: synapsin-immunoreactivity, magenta: AST-A-like immunoreactivity. Scale bars: 50 µm.

staining of intrinsic mushroom body neurons (data not shown) that is not evident in *A. mellifera*. Outside Hymenoptera, labeling of intrinsic neurons has also been reported for the dictyopteran *R. maderae* (formerly *L. maderae*; Nässel and Homberg, 2006). In addition, our own data show particularly congruent AST-A-like staining patterns in intrinsic and extrinsic mushroom body neurons of three stick insects species. Comparing the staining patterns across all investigated taxa, AST-A neuropeptides seem to have a broader role in the mushroom body circuitry of Phasmatodea and Hymenoptera than in the other analysed taxa. In the

coleopteran *T. castaneum*, in contrast, genes for the AST-A peptide precursor and the receptor are missing.

3.2. B-Type Allatostatin (AST-B)/myoinhibitory peptide (MIP)

Four peptides discovered to inhibit juvenile hormone synthesis in the cricket *G. bimaculatus* but showing no structural resemblance to A-type allatostatins were, for their functional analogy, named B-type allatostatins (Lorenz et al., 1995b). The amino acid sequences of these peptides, however, share similarities with a neuropeptide originally isolated from *L. migratoria* that had been termed myoinhibitory peptide (Lom-MIP) due to its suppressive effect on contractions of the hindgut and oviduct (Schoofs et al., 1991). Although the AST-B terminology is still used, this neuropeptide family is now most commonly referred to as MIPs. Its members carry a C-terminal amide moiety and are characterized by two tryptophan (W) residues located at positions 2 and 9 in the sequence (Table 2). MIP isoforms have since been identified in various insect taxa, including *P. americana* (Predel et al., 2001), *C. morosus* (Lorenz et al., 2000), *M. sexta* (Blackburn et al., 1995, 2001), *A. aegypti* (Predel et al., 2010), *Drosophila melanogster* (Williamson et al., 2001) and *T. castaneum* (Li et al., 2008). In addition, sequence mining in the aphid *A. pisum* has recently led to the prediction of two unusual MIP isoforms, differing from the typical W(X_6)W-amide motif by the insertion of a seventh amino acid residue between the two tryptophans (Huybrechts et al., 2010). Interestingly, MIP encoding sequences appear to be lacking in the genome of the hymenopterans *A. mellifera* (Hummon et al., 2006) and *Nasonia vitripennis* (Hauser et al., 2010). Similar to AST-As, different MIP isoforms – usually nonapeptides – seem to be processed from a larger precursor protein by proteolytic cleavage and amidation (Williamson et al., 2001).

As their name(s) suggest, MIPs have been demonstrated to inhibit contractions of smooth musculature in the gut and other internal organs of insects (Schoofs et al., 1991; Blackburn et al., 1995, 2001) and to suppress juvenile hormone biosynthesis in the *corpora allata* of crickets (Lorenz et al., 1995b). Furthermore, MIPs have been postulated to influence molting and ecdysis in *M. sexta* and *B. mori* (Davis et al., 2003) and have recently been shown to act as potent ligands on sex peptide receptors in *Drosophila* and *A. aegypti* (Kim et al., 2010). MIP isoforms have also been localized in the lateral cell group of the antennal lobes in metamorphic stages and adults of *M. sexta* (Utz et al., 2007) and in a novel neuron type exhibiting extensive arborizations in the optic neuropils of *Drosophila* (Kolodziejczyk and Nässel, 2010), indicating that these peptides also play a role in information processing in the central nervous system.

So far, MIP-like immunoreactivity in neurons associated with the mushroom bodies has not been investigated in any depth. Investigations in *L. migratoria* showed that an antibody directed against locustamyoinhibiting peptide (Lom-MIP) does not produce immunostaining in the mushroom body neuropils (Schoofs et al., 1996). In their publication on the isolation of a myoinhibitory neuropeptide from the cockroach *P. americana* (Pea-MIP), Predel et al. (2001) show a picture demonstrating a band-like immunoreactive pattern in the vertical lobe of the mushroom bodies and state that immunostained fibers can be observed in the alpha lobe and the calyces. Evidence for an extrinsic innervation of the calycal neuropil by MIP immunopositive fibers has also been provided for *R. maderae* (Nässel and Homberg, 2006). Finally, the recent publication by Kolodziejczyk and Nässel (2010) includes one image in which MIP immunopositive processes appear to braid – and possibly also to invade – parts of the peduncle.

Immunohistochemical preparations of brains of the firebrat *T. domestica* reveal scattered MIP-like immunoreactivity in the calycal neuropil and microglomeruli (Fig. 3A). In addition, immunopositive varicosities can be observed in two 'Trauben' (grapes) of the medial lobes (Fig. 3A'). The rest of the mushroom body neuropil is devoid of MIP-like immunoreactivity and the Kenyon cell bodies exhibit no immunolabeling (Supplementary Fig. 1A). Analyses of anti-MIP immunostaining in *P. americana* confirm the presence of immunopositive fibers within the cup-shaped calyces but provide no evidence for immunoreactive bands in the vertical lobes (Fig. 3B). Mushroom body-associated immunoreactivity in *A. aegypti* is confined to a subdivision of the medial lobe while the rest of the neuropil is devoid of immunostaining (Fig. 3C). In the coleopteran representative *Leptinotarsa decemlineata*, the calyx region contains individual immunopositive fibers and varicosities (Fig. 3D). Interestingly, immunoreactivity in the red flour beetle *T. castaneum* reveals a different pattern, showing immunostaining at the transition between peduncle and medial lobe but not in the calycal neuropil (data not shown).

Analyses of MIP-like immunoreactivity in *Drosophila* confirm the presence of immunostained fibers tightly enveloping the peduncle (Kolodziejczyk and Nässel, 2010) but provide no evidence for fibers actually entering the neuropil (Figs. 10 and 11). The condition in *Drosophila*, therefore, differs markedly from that observed in the other dipteran, *A. aegypti*, in which immunostaining is only detectable in a subdivision of the medial lobe. Mushroom body-associated immunoreactivity in the two coleopteran representatives is likewise disparate, indicating that innervation patterns of MIP-immunoreactive neurons are highly variable in insects. However, one commonality in all investigated species is the apparent lack of MIP-like immunoreactivity in Kenyon cell bodies (compare Supplementary Fig. 1A) and their projections, indicating that myoinhibitory peptides are not expressed by intrinsic mushroom body neurons but rather act as neuromodulators released by extrinsic neurons that innervate the calyx and/or partitions of the lobes.

3.3. Allatotropin (AT)

The first member of this family to be described was a 13-residue peptide with the sequence GFKNVEMMTARGF-amide that was purified from adult specimens of the tobacco hornworm *M. sexta* (Kataoka et al., 1989). Due to its stimulating effect on the synthesis and secretion of juvenile hormone in the *corpora allata*, the peptide was named allatotropin. Identical forms of AT have since been predicted to occur in the lepidopteran species *Pseudaletia unipuncta* (Truesdell et al., 2000) and *B. mori* (Park et al., 2002), and AT-like peptides have also been identified in noctuid moths (e.g. *Helicoverpa armigera*: Duve et al., 1999; *Lacanobia oleracea*: Duve et al., 2000; *Spodoptera frugiperda*: Oeh et al., 2000). However, AT-like peptides are not specific to Lepidoptera, as they have been predicted and demonstrated to occur in coleopterans like *L. decemlineata* (Spittaels et al., 1996a) and *T. castaneum* (Li et al., 2008), in the orthopteran *L. migratoria* (here termed accessory gland myotropin I, Lom-AG-MTI; Paemen et al., 1991, 1992), as well as in the mosquitoes *A. aegypti* (Veenstra and Costes, 1999) and *Anopheles gambiae* (Riehle et al., 2002). Interestingly, so far no orthologous sequences or peptides have been identified in *Drosophila* and *A. mellifera* (Li et al., 2008).

AT-related neuropeptides share a high sequence similarity and a conserved C-terminal TARGF-amide motif (Table 2). While they are most renowned for their stimulating effect on juvenile hormone production and release in the *corpora allata* of adult insects, ATs have also been shown to have a myotropic effect on the heart (Veenstra et al., 1994; Rudwall et al., 2000; Koladich et al., 2002) and the gut (Duve et al., 1999, 2000; Rudwall et al., 2000; Oeh, 2003) and to influence midgut ion transport (Lee et al., 1998,

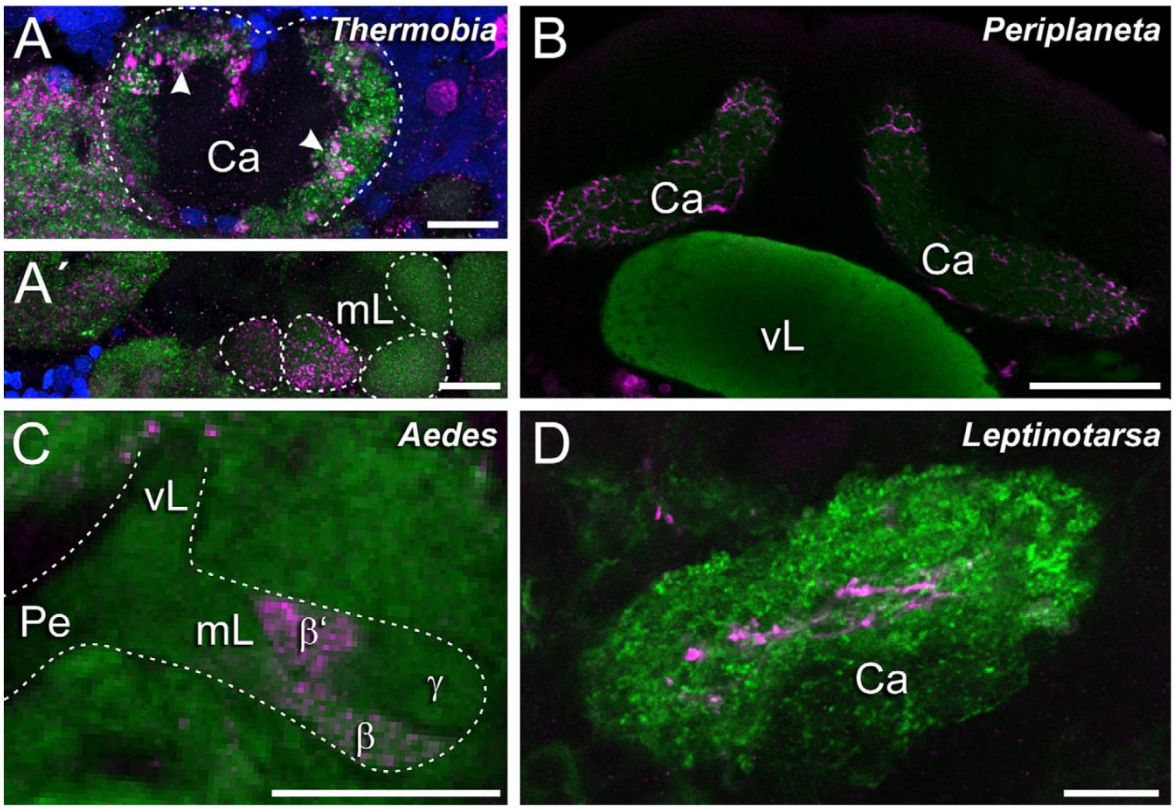

Fig. 3. Allatostatin B/Myoinhibitory peptide-like immunoreactivity in insect mushroom bodies. (A, A′) The center of the knob-shaped calyx (Ca) in *Thermobia domestica* contains sparse and scattered immunoreactivity and some of the peripherally arranged microglomeruli are labeled (arrowheads). Furthermore, immunostained varicosities are evident in specific 'Trauben' of the medial lobes (mL) of the firebrat's mushroom bodies. (B) In *Periplaneta americana*, immunopositive fibers form a loose meshwork in the calyces while the rest of the neuropil, including the vertical lobes (vL), is devoid of immunoreactivity. (C) In the mosquito *Aedes aegypti*, MIP-like immunoreactivity is restricted to parts of the β/β′ subdivisions of the medial lobe; the vertical lobe and the peduncle (Pe) contain no immunostaining. (D) In the Colorado potato beetle *Leptinotarsa decemlineata*, immunostained fiber elements and varicosities can be observed in the calyx; the rest of the neuropil contains no immunoreactivity. All images show frontal aspects of the mushroom bodies, dorsal is towards the top and lateral to the left of each picture. blue: DAPI-labeled cell nuclei, green: synapsin-immunoreactivity, magenta: MIP-like immunoreactivity. Scale bars: 20 µm, except B: 100 µm.

2002) and hemolymph circulation (Koladich et al., 2002). Furthermore, ATs are suspected to affect circadian rhythms (Petri et al., 2002) and migration behavior of insects (McNeil and Tobe, 2001).

Detailed descriptions of allatotropin-like immunoreactivity in the mushroom bodies are available for the locust *S. gregaria* (Homberg et al., 2004) and the moth *S. littoralis* (Sjöholm et al., 2006). In the locust, projections from a single extrinsic neuron, the cell body of which resides laterally to the lateral horn, form beaded ramifications throughout the primary calyx. In addition, the same neuron also supplies projections that enter the vertical lobe, the peduncle, and the lateral horn. The accessory calyx, a bulbous neuropil structure that arises posteriorly to the primary calyx, exhibits dense granular immunostaining. Immunolabeled processes can be traced back to a small group of projection neurons connecting the accessory calyx with the glomerular lobe, possibly providing a pathway for gustatory input into the mushroom bodies (Homberg et al., 2004). In *S. littoralis*, the AT-antiserum has been reported to produce immunostaining in a subset of Kenyon cells that have their cell bodies arranged in two centrally located caps above the calyces. Accordingly, immunoreactivity was observed in the calyx region, the peduncle and the vertical and medial lobes. However, a detailed analysis of the fiber bundles contributing to the immunostaining revealed that only the α/β and α'/β' divisions of the peduncle and the lobes are immunopositive, while the γ division and the so-called Y-tract – a separate peduncle-like structure bearing terminal lobelets and arising from a distinct cluster of Kenyon cells – are devoid of immunostaining (Sjöholm et al., 2006). A homogeneous immunostaining of the mushroom body neuropils, probably indicating immunoreactivity of intrinsic neurons, can also be observed in the tobacco budworm *H. virescens* (Berg et al., 2007). However, in this species, in contrast to *S. littoralis*, the γ divisions of the lobes appear to be immunopositive as well.

Own observations show that immunostaining in the mushroom bodies of the firebrat *T. domestica* is limited to individual microglomeruli in the knob-shaped calyx region (Fig. 4A), probably indicating an extrinsic innervation of the subcompartment. The peduncle and lobes are devoid of AT-like immunoreactivity. In the cockroach *P. americana*, anti-Mas-AT produces a staining pattern reminiscent of the conditions described for the locust (Homberg et al., 2004): the calyces exhibit a meshwork of immunoreactive arborizations (Fig. 4B) and discrete, albeit weakly stained, immunoreactive bands are discernable in the vertical and medial lobes (Fig. 4B′, B″). In addition, fine arborizations of an immunoreactive extrinsic neuron can be observed at the tip of the vertical lobe

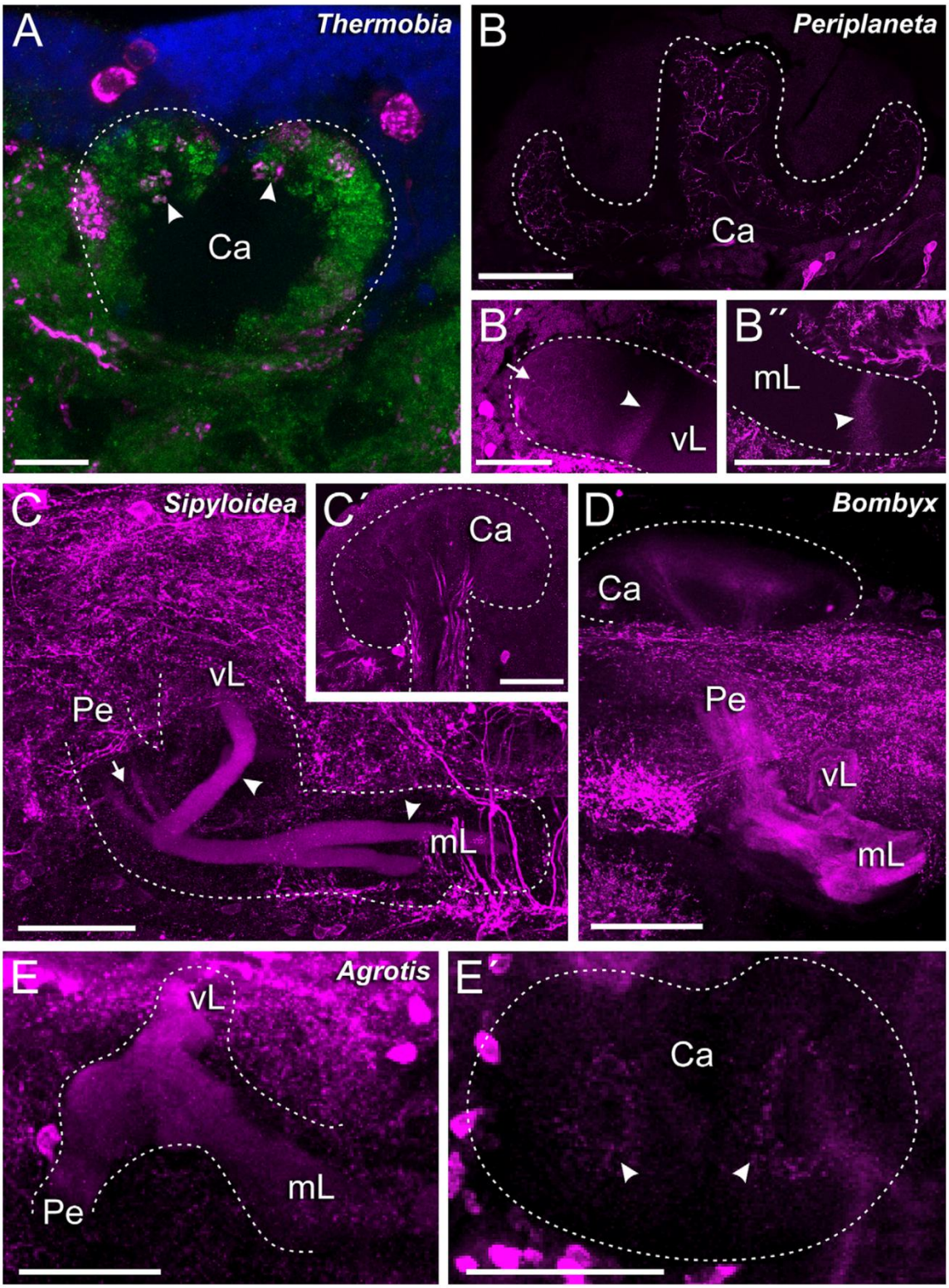
A
Thermobia
Ca
B
Periplaneta
Ca
B´
vL
B´´
mL
C
Sipyloidea
Pe
vL
mL
C´
Ca
D
Bombyx
Ca
Pe
vL
mL
E
Agrotis
vL
Pe
mL
E´
Ca

(Fig. 4B′). AT-like immunoreactivity is prominent in the mushroom bodies of the stick insect *S. sypilus* (Fig. 4C, C′). Immunostained Kenyon cell processes form loose aggregations as they emanate from the calyx and enter the peduncle (Fig. 4C′). At the transition between the peduncle and the lobes, these bundles congregate further, forming a densely stained core region that extends into the subdivisions of the vertical and medial lobes (Fig. 4C). However, in the closely related stick insects *C. morosus* and *M. extradentata*, staining of intrinsic neurons could not be confidently demonstrated (data not shown, compare Figs. 10 and 11). In *C. morosus*, an innervation of the calyx by immunoreactive fibers could be observed, but immunoreactivity in the peduncle and lobes remained inconclusive due to poor staining quality. In *M. extradentata*, the calyx was similarly supplied by immunopositive processes and scattered immunostaining could be discerned in and around the vertical lobe. The medial lobe contained no AT-like immunostaining. In the three moth species that were investigated, *B. mori* (Fig. 4D), *A. segetum* (Fig. 4E, E′), and *M. sexta* (data not shown), all parts of the mushroom bodies exhibit AT-like immunoreactivity, similar to the conditions described for the lepidopteran species *S. littoralis* and *H. virescens* (Sjöholm et al., 2006; Berg et al., 2007). Particularly intense immunostaining was observed in *B. mori*, where faint labeling is even discernable within Kenyon cell somata (see Supplementary Fig. 1B). In *A. segetum*, no staining can be detected in the Kenyon cell bodies and subdivisions of the lobes seem to be immunonegative. The Mas-AT antiserum produces no immunostaining in the mushroom bodies of the dipteran *A. aegypti* and the coleopteran *T. castaneum* (data not shown, compare Figs. 10 and 11).

In summary, the presented data indicate that AT-like immunoreactivity in the mushroom body neuropils may reside in extrinsic neurons as well as in Kenyon cells (Figs. 10 and 11). In the hemimetabolous taxa, extrinsic innervation seems to be highly divergent, with *T. domestica* showing only scattered immunoreactivity in parts of the calyx region and *S. gregaria* displaying scattered immunoreactivity in all compartments of the mushroom bodies. Intrinsic AT-like staining can be found in representatives of three hemimetabolous orders, but is lacking in *T. domestica* and two of the examined stick insect species. In the latter group, disparities become particularly evident. While staining of intrinsic neurons is prominent in the pink-winged stick insect *S. sypilus*, the mushroom bodies in the other two species appear to receive only extrinsic processes of AT-positive neurons. Within the holometabolous insects, the lepidopteran species exhibit extensive AT-like immunoreactivity in intrinsic mushroom body neurons. In contrast, neither *A. aegypti* nor *T. castaneum* show any immunoreactivity in the MBs; in *Drosphila* and *A. mellifera*, the AT precursor gene is missing. Thus, the available data suggests that AT plays a major role in the mushroom body circuitry of Lepidoptera but, in contrast, no role in that of non-lepidopteran holometabolous insects.

3.4. FMRFamide related peptides (FaRPs)

The large and diverse superfamily of FMRFamide related peptides (FaRPs) contains among the most wide-spread and conserved signaling molecules in metazoan animals. Although all FaRPs have a C-terminal RF-amide in common, members of the individual subfamilies – myosuppressins, sulfakinins, sNPFs, NPFs and extended FMRFamides – derive from different precursors encoded by different genes. For detailed information on the evolutionary relationships of FaRPs across different phyla and their physiological relevance in insects, the reader is kindly referred to papers by Espinoza et al. (2000), Orchard et al. (2001), Nässel (2002), and Walker et al. (2009). 'True' FMRFamide, a tetrapeptide with the sequence Phe-Met-Arg-Phe-amide, was originally isolated from the marine mollusc *Macrocallista nimbosa* (Price and Greenberg, 1977). In insects, only N-terminally extended forms of FMRFamide (extended FMRFamides) are known, the first of which were identified in *Drosophila* (Nambu et al., 1988; Schneider and Taghert, 1988). Variations in their N-terminal amino acid composition allowed the discrimination of five different FMRFamide peptides and a closely related FIRF-amide, all of which are produced by endoproteolytic cleavage of a large precursor protein encoded by a single gene (Schneider and Taghert, 1988). Subsequently, extended FMRFamides were also identified in the dipterans *Drosophila virilis* (Taghert and Schneider, 1990), *C. vomitoria* and *Lucilia cuprina* (Duve et al., 1992, 1994), but not in other insect orders. Investigations in the cockroach *P. americana* later showed that of the 23 neuropeptides encoded by the orthologous FMRF gene in this species, not a single one contains a canonical FMRFamide motif, but that ten peptides exhibit a C-terminal FIRF-amide sequence (Predel et al., 2004). Thus, it was speculated that two FIRF-amide peptides previously isolated from *L. migratoria* (Lange et al., 1994) actually represent products of the FMRF gene in this species. Likewise, two heptapeptides with a C-terminal FLRFamide that were identified in *M. sexta* (Kingan et al., 1996) have lately been classified as members of the extended FMRFamide family (Walker et al., 2009).

Immunohistological investigations into the distribution of FMRFamides in insect nervous systems should be regarded warily, as antibodies targeting FMRFamide are prone to recognize epitopes of other FaRPs as well. Such stainings provide no true evidence for the presence of FMRFamide neuropeptides and should thus be referred to as 'FMRFamide-like immunoreactivity' (Nässel and Winther, 2010). That being said, FMRFamide-like immunostaining in the mushroom body neuropils has been described for e.g. the honeybee *A. mellifera* (Schürmann and Erber, 1990; Strausfeld et al., 2000), the moths *M. sexta* (Homberg et al., 1990) and *S. littoralis* (Sjöholm et al., 2006), the meal beetle *T. molitor* (Breidbach and Wegerhoff, 1994), the kissing bug *Triatoma infestans* (Settembrini and Villar, 2005), the cockroach species *P. americana* (Strausfeld and Li, 1999) and *R. maderae* (Nässel and Homberg, 2006), and the desert locust *S. gregaria* (Homberg, 2002). In the honeybee, FMRFamide-like immunoreactivity reveals an intricate pattern of parallel layers (immunoreactive strata) that extend throughout the peduncle and into the mushroom body lobes (Schürmann and Erber, 1990; Strausfeld et al., 2000). These immunoreactive strata correspond to discrete bundles of axon-like Kenyon cell projections, indicating that different subpopulations of intrinsic mushroom body neurons can be distinguished by the signaling molecules they express. Similar evidence for the biochemical heterogeneity of Kenyon cells has also been procured in studies focusing on the expression of FMRFamide in the silkmoth *B. mori*

Fig. 4. Allatotropin-like immunoreactivity in insect mushroom bodies. (A) In the firebrat, individual microglomeruli of the calyx (Ca) are braided by immunostained varicosities (arrowheads). (B, B′, B″) In *Periplaneta americana*, AT-like immunoreactivity reveals a reticular pattern of immunostained fibers in the calycal neuropil. While the peduncle appears devoid of immunostaining, discrete immunolabeled bands (arrowheads) are discernable in the vertical (vL) and medial lobe (mL). Furthermore, the tip of the vertical lobe is also supplied by fine extrinsic arborizations (arrow). (C, C′) Immunostaining in the phasmatodean *Sypiloidea sypilus* reveals scattered immunoreactivity in the calyces as well as individual fibers that converge and arrange in parallel as they enter the peduncle (Pe). In the ventral part of the peduncle, the immunoreactive fibers aggregate (arrow) and form intensely stained core regions (arrowheads) that extend into the subdivisions of the median and vertical lobe. (D) In the silkmoth *Bombyx mori*, the AT-antiserum produces immunostaining in all parts of the mushroom bodies but staining intensity in the calyx region is comparatively weak. (E, E′) In another lepidopteran species, *Agrotis segetum*, immunostaining in the calyx region is scattered, but pronounced immunoreactivity can be observed in the vertical and medial lobe. In this species, the peduncle exhibits no immunoreactivity. blue: DAPI-labeled cell nuclei, green: synapsin-immunoreactivity, magenta: AT-like immunoreactivity. Scale bars: 100 µm.

(Fukushima and Kanzaki, 2009) and the cotton leafworm *S. littoralis* (Sjöholm et al., 2006). Comparatively weak immunostaining can be observed in the dendritic arborizations of the calyx, and only a few individual Kenyon cell somata exhibit FMRFamide-like immunoreactivity. Immunohistochemical investigations in *P. americana*, *M. sexta*, *S. gregaria* and *T. molitor* show similar immunoreactive strata in the mushroom bodies (Homberg, 2002; Homberg et al., 1990; Breidbach and Wegerhoff, 1994; Strausfeld and Li, 1999). Although immunostained Kenyon cell bodies are not always discernable – e.g. in the meal beetle, somata exhibit no immunoreactivity – these patterns indicate that FMRFamide-like neuropeptides are present in intrinsic mushroom body neurons of all these species. In the hemipteran species, however, the mushroom body lobes were reported to be devoid of FMRFamide-like immunoreactivity, and the peduncle and calyx showed only moderate immunostaining, even though individual Kenyon cell somata were immunolabeled (Settembrini and Villar, 2005).

In our own immunohistochemical studies we employed an antiserum produced and characterized by Marder et al. (1987; for details see Materials and Methods section). In the firebrat, this antiserum reveals scattered immunoreactive varicosities in the calyx (Fig. 5A) but produces no staining in the peduncle or the lobes, suggesting the neuropeptide to be located in extrinsic but not in intrinsic neurons of the mushroom bodies. In the mushroom bodies of the lepidopteran *H. virescens*, scattered immunoreactivity can be observed in the calycal neuropil, possibly indicating extrinsic cell processes (Fig. 5B). Furthermore, staining can also be detected in specific subdivisions of the peduncle (Fig. 5B′), but not in the vertical and medial lobe. In the honeybee, immunoreactivity is evident in all parts of the mushroom body neuropil (Fig. 5C). Immunoreactive fibers converge in the calyx and the neck region, thus forming immunopositive strata that extend through the peduncle and into the lobes. Immunopositive and immunonegative layers produce distinctive patterns – especially in the vertical lobes – which closely match the descriptions of immunoreactive Kenyon cell subpopulations provided by Strausfeld et al. (2000). Surprisingly, the same FMRFamide antiserum produces no immunostaining in the mushroom bodies of the bumblebee, *B. terrestris* (data not shown, compare Figs. 10 and 11). In contrast to this, but similar to the pattern in *A. mellifera*, the mushroom bodies in *T. castaneum* display FMRFamide-like immunostaining in all subcompartments (Fig. 5D), indicating the antigen to reside in axon-like processes of the Kenyon cells. Immunoreactivity appears to be especially intense in the α'/β' divisions of the lobes. These observations are in accordance with similar findings in the closely related tenebrionid *T. molitor* (Breidbach and Wegerhoff, 1994). Moreover, a comparable FMRFamide-like staining pattern is also revealed in the dipteran *A. aegypti*, in which all parts of the mushroom bodies are labeled (Fig. 5 E–E‴). Again, staining in single divisions of the vertical and medial lobes seems to be more pronounced than in others.

The FMRFamide antisera used over the years, including the one used in our laboratory, very likely recognize various neuropeptides with a C-terminal RFamide motif, thus labeling most members of the FaRP superfamily (Nässel and Winther, 2010). For instance, in *Drosophila*, most neurons labeled by the FMRFamide antibody actually carry sNPF; in particular, most of the 2.500 Kenyon cells of each mushroom body express sNPF, as demonstrated by immunohistochemistry and *in situ* hybridization (Johard et al., 2008; Nässel et al., 2008). Comparing FMRFamide and sNPF immunostaining in the analyzed insect species indeed revealed a close match within Diptera (Fig. 11, compare below). The FMRFamide antiserum also labels intrinsic and extrinsic axons in most of the examined moth species, in P. americana, R. maderae, and S. gregaria. In *T. infestans* and *T. domestica*, only extrinsic neurons show immunoreactivity towards the FMRFamide antiserum. In summary, the available data suggest a major function of sNPF in the mushroom body circuit in Diptera. Whether sNPF or other members of the FaRPs play a role in the neuronal network of the mushroom bodies in non-dipteran taxa has to remain unresolved at the moment for the lack of a specific sNPF antibody for these taxa.

3.5. Orcokinin

Orcokinins derive their name from the crayfish *Orconectes limosus* – the species from which the first of these neuropeptides was originally isolated – and from their stimulating effect on the musculature of the hindgut in this species (Stangier et al., 1992). Several isoforms of this non-amidated peptide have since been identified in the central nervous system of malacostracan crustaceans (Bungart et al., 1994; Yasuda-Kamatani and Yasuda, 2000; Skiebe et al., 2002; Huybrechts et al., 2003), differing from the original sequence only in punctual amino acid substitutions. Thus, orcokinins can be regarded as a highly conserved neuropeptide family. The first insect orcokinin was described in the cockroach *Blattella germanica* (Pascual et al., 2004), and further orcokinins have been shown to be present in the silverfish *Lepisma saccharina*, the Madera cockroach *R. maderae*, and the locusts *S. gregaria* and *L. migratoria* (Hofer et al., 2005). In addition, database sequence comparison has led to the prediction of two orcokinin-like neuropeptides in the mosquito *A. gambiae* (Pascual et al., 2004), comprising the typical N-terminal NFDEIDR motif (Table 2). Similarly, MALDI-TOF mass spectrometry has recently confirmed the presence of orcokinins in the CNS of *A. aegypti* (Predel et al., 2010). These findings conflict and partially rebut earlier speculations, based upon the lack of orthologous sequences in *Drosophila* and *T. castaneum* and the absence of orcokinin-like immunoreactivity in immunohistochemical preparations of *Drosophila*, *M. sexta*, and *A. mellifera*, that orcokinins have either been lost or are highly modified in holometabolous insects (Hofer et al., 2005).

Orcokinin-like immunoreactivity in the brain of *L. saccharina*, *R. maderae*, *S. gregaria*, and *L. migratoria* was described by Hofer et al. (2005). Immunolabeling was wide-spread in all four species and immunostaining could be observed in all major neuropils. In *L. saccharina* (compare to the zygentome *T. domestica*, Fig. 1A), the calyx region shows only weak immunoreactivity but signal intensity increases towards the distal parts of the lobes, where strong immunolabeling can be detected. In *R. maderae*, orcokinin-immunoreactive processes from extrinsic neurons innervate the basal parts of the calyces, the peduncle and the lobes. Within the neuropil, immunolabeling reveals laminated patterns in the peduncle and in the lobes (compare Nässel and Homberg, 2006), the latter showing comparatively strong immunoreactivity (Fig. 6). Immunolabeling in *S. gregaria* and *L. migratoria* reveals a similar picture, suggesting that in the cockroach and the locust species, orcokinin is expressed in extrinsic neurons as well as in subpopulations of intrinsic Kenyon cells. Information on the distribution of orcokinin-like immunoreactivity in a hemipteran insect was provided in a recent publication on the neuroanatomy of the pea aphid *A. pisum* (Kollmann et al., 2011b). Immunostaining within the mushroom body neuropils of this species was observed to be most intense in the distal parts of the vertical and medial lobes, resembling the condition described for the silverfish.

Though only a few hemimetabolous insects have been analyzed to date, all investigated species exhibit orcokinin-like immunoreactivity in intrinsic mushroom body neurons (Fig. 10). Extrinsic innervations of the calyx are clearly discernable in *R. maderae* and *S. gregaria*. For *A. pisum*, the question of a possible extrinsic innervation remains unresolved at the moment, and in *L. saccharina*,

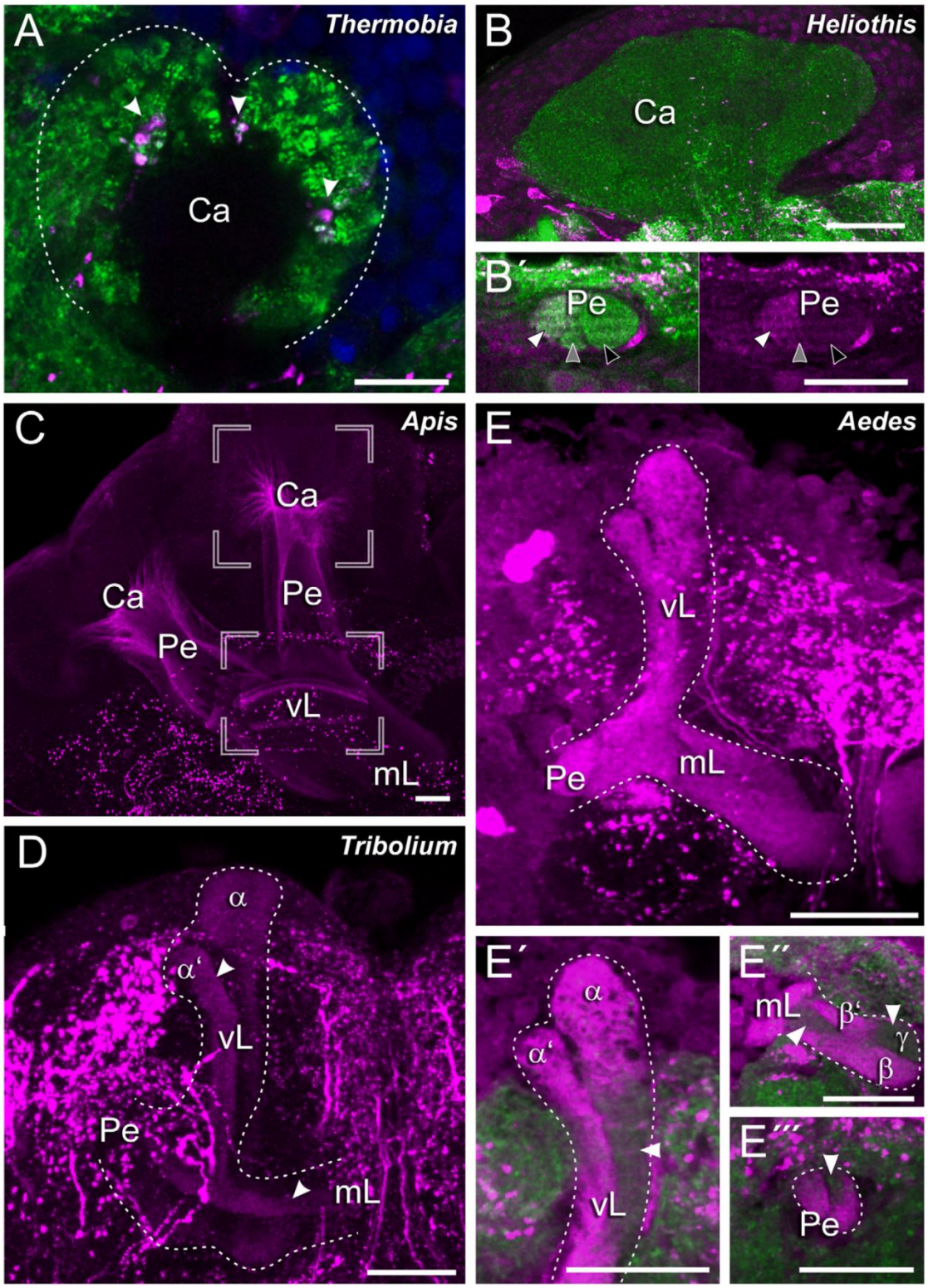
A
Thermobia
Ca
B
Heliothis
Ca
B´
Pe
Pe
C
Apis
Ca
Ca
Pe
Pe
vL
mL
D
Tribolium
α
α‘
vL
Pe
mL
E
Aedes
vL
Pe
mL
E´
α
α‘
vL
E´´
mL
β‘
γ
β
E´´´
Pe

extrinsic fibers in the calyx might be masked by strong intrinsic neuron immunoreactivity.

3.6. SIFamide

AYRKPPFNGSIFamide, isolated from the grey flesh fly *Neobellieria bullata*, was the first member of this family to be sequenced and described (Janssen et al., 1996). Since then, SIFamides have been identified in a variety of holometabolous insects, including dipteran (*D. melanogaster*, *A. gambiae*), hymenopteran (*A. mellifera*), coleopteran (*T. molitor*, *T. castaneum*), and lepidoteran (*B. mori*) representatives (Verleyen et al., 2009). Sequence comparisons in these groups indicate that SIFamides are extremely conserved, as the isoforms do not only share the eponymous C-terminal Ser-Ile-Phe-amide sequence but in fact differ only in the N-terminal amino acid residue, which can be Ala, Thr, or Gly (Table 2). Furthermore, highly similar SIFamides have also been reported to be present in crustaceans and in the chelicerate *Ixodes scapularis* (Verleyen et al., 2009). Interestingly, despite thorough examination by means of MALDI-TOF mass spectrometry, SIFamides have not been detected in *L. migratoria* (Clynen et al., 2001) and they have only recently been shown to occur in hemimetabolous insect species at all (Hemiptera: *A. pisum* Verleyen et al., 2009; *Rhodnius prolixus* Ons et al., 2010).

Despite a paucity of literature on the topic, available data indicate that SIFamide-like immunoreactivity in holometabolous insects shares a common pattern: SIFamide-antisera have consistently been found to exclusively stain four cell bodies in the *pars intercerebralis* that send projections across the midline of the brain and extend throughout the entire CNS (Verleyen et al., 2004; Roller et al., 2008; compare Supplementary Fig. 2A). This implies that any immunostaining observed within the mushroom body neuropil is likely to be due to an innervation by these extrinsic neurons. Likewise, the presence of SIFamide in MALDI-TOF mass spectra of calyx tissue isolated from the brain of worker honeybees, as reported by Boerjan et al. (2010), is probably indicative of extrinsic neurons arborizing in the calyx region (see below).

The notion that SIFamide-like immunoreactivity resides in extrinsic, but not in intrinsic mushroom body neurons is also supported by our own investigations. In the zygentome, immunopositive neurons of the *pars intercerebralis* are complemented by additional immunoreactive cells that have their somata located near the calyces and in the lateral and the ventral protocerebrum (compare Supplementary Fig. 1B). While there is no evidence for immunoreactivity in the Kenyon cells, immunostained extrinsic fibers closely braid and also enter individual 'Trauben' of the vertical lobes (Fig. 7A). In *P. americana*, the calyces are supplied by a fine meshwork of immunopositive fibers but the rest of the mushroom bodies is devoid of immunostaining (Fig. 7B). In the red flour beetle *T. castaneum* immunoreactive neurons of the pars intercerebralis give rise to fibers that envelop parts of the vertical lobes (Fig. 7C). Moreover, individual fibers also penetrate the calyx, forming varicosities within the neuropil (Fig. 7C′). In the honeybee, parts of the calycal collar are sparsely braided by immunopositive fibers (Fig. 7D), probably accounting for the SIFamide peaks in the MALDI-TOF spectra obtained by Boerjan et al. (2010, see above). Furthermore, varicosities are also evident around the vertical lobe and in one of the strata of the vertical lobe (Fig. 7D′). In *A. aegypti*, a few individual immunoreactive blebs are discernable in all subcompartments of the mushroom bodies (Fig. 7E–E‴).

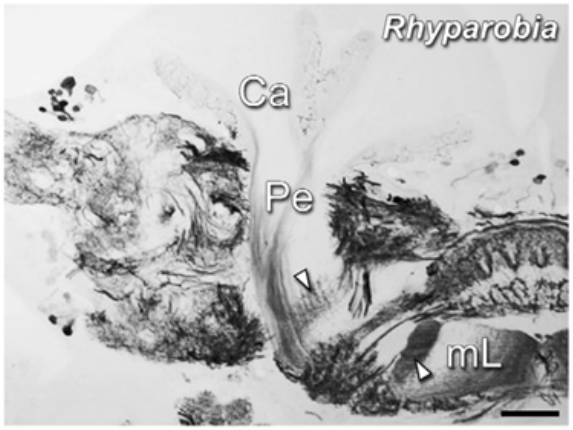

Fig. 6. Orcokinin-like immunoreactivity in a frontal section through the brain of *Rhyparobia (Leucophaea) maderae*. The mushroom bodies exhibit laminated immunostaining in the peduncle (Pe) and the median lobe (mL); additional band-like patterns (arrowheads) indicate an extrinsic innervation of both compartments. In the calyces (Ca), a fine meshwork of immunopositive fibers is discernable. Modified and reproduced from Hofer et al. (2005), with kind permission from John Wiley and Sons. Scale bar: 200 µm.

3.7. Short neuropeptide F (sNPF)

'Neuropeptide F', designated after its C-terminal phenylalanine-amide residue, was first isolated from the platyhelminth tapeworm *Moniezia expansa* (Maule et al., 1991). NPF-related proteins have since been discovered to form a family of invertebrate neuropeptides that comprises two groups: long NPFs composed of 36–40 amino acid residues, and short NPFs with 6–11 amino acid residues. While long NPFs are regarded as structural homologs of the vertebrate neuropeptide Y family (de Jong-Brink et al., 2001), it remains uncertain whether the affiliation between long and short NPFs really pertains to a common evolutionary root. The first sNPFs to be identified in insects were isolated from head extracts of *A. aegypti* and were therefore originally designated 'head peptides' (Matsumoto et al., 1989). Later, sNPFs were isolated from the Colorado potato beetle *L. decemlineata* (Spittaels et al., 1996b), the cockroach *P. americana* (Veenstra and Lambrou, 1995) and the locust *S. gregaria* (Schoofs et al., 2001). Genome analysis led to the prediction of sNPFs in *Drosophila* (Vanden Broeck, 2001) and *A. gambiae* (Riehle et al., 2002), and mass spectrometric analyses detected sNPFs in different hemipteran species (Predel et al., 2008). Common to all these peptides is a conserved C-terminal sequence

Fig. 5. FMRFamide-like immunoreactivity in insect mushroom bodies. (A) In the firebrat, single microglomeruli (arrowheads) of the calyx region (Ca) show immunoreactivity towards the FMRFamide antiserum while the rest of the neuropil is devoid of immunostaining. (B, B′) In the moth *Heliothis virescens*, scattered immunoreactive blebs are dispersed throughout the calycal neuropil. Immunostaining can be observed in the lateral (white arrowhead) and central (grey arrowhead) peduncle (Pe), but not in the medial subdivision (black arrowhead). (C) In the honeybee, FMRFamide-like immunoreactivity is restricted to distinct layers that project from the calyces to the vertical (vL) and median lobes (mL). (D) All subcompartments of the mushroom bodies in *Tribolium castaneum* exhibit immunoreactivity, but staining of the lobes is most intense at the tips and in the α'/β' subdivisions (arrowheads). (E) A projection view of the mushroom body in *Aedes aegypti* shows homogeneous immunostaining in both lobes and in the peduncle. (E′–E‴) However, single optical sections through the vertical lobe, medial lobe, and the peduncle of *A. aegypti* reveal differential staining, similar to the condition in *T. castaneum*. Intense immunoreactivity is observed in the α, β, and β' subdivisions, whereas the γ lobe, the proximal part of the α lobe, and the medial division of the peduncle exhibit no immunoreactivity (arrowheads). All images show frontal aspects of the mushroom bodies, dorsal is towards the top and lateral to the left of each picture. blue: DAPI-labeled cell nuclei, green: synapsin-immunoreactivity, magenta: FMRFamide-like immunoreactivity. Scale bars: (A, D, E) 20 µm, (B, C) 50 µm.

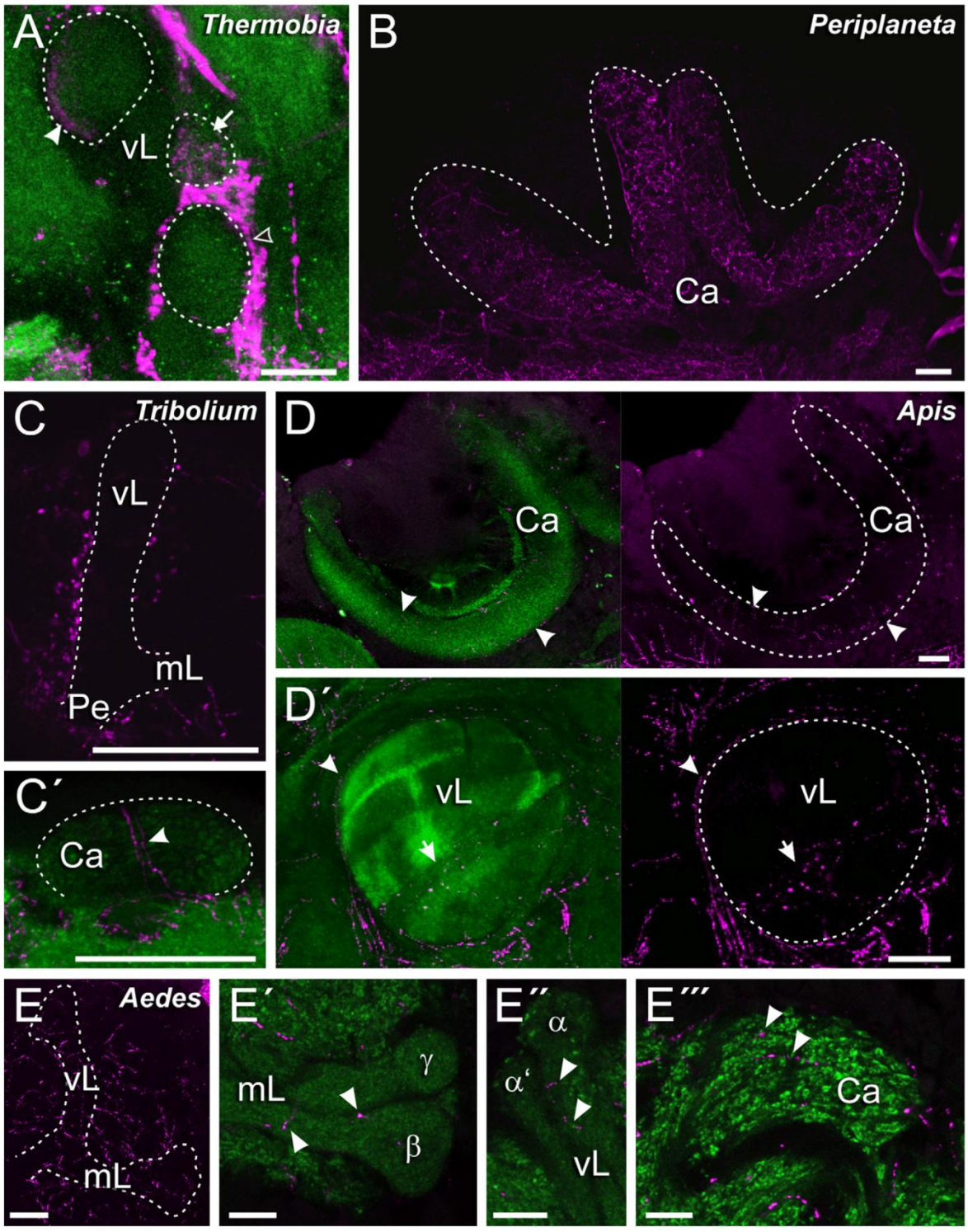
A
Thermobia
vL
B
Periplaneta
Ca
C
Tribolium
vL
mL
Pe
C´
Ca
D
Ca
Apis
Ca
D´
vL
vL
E
Aedes
vL
mL
E´
mL
γ
β
E″
α
α‘
vL
E‴
Ca

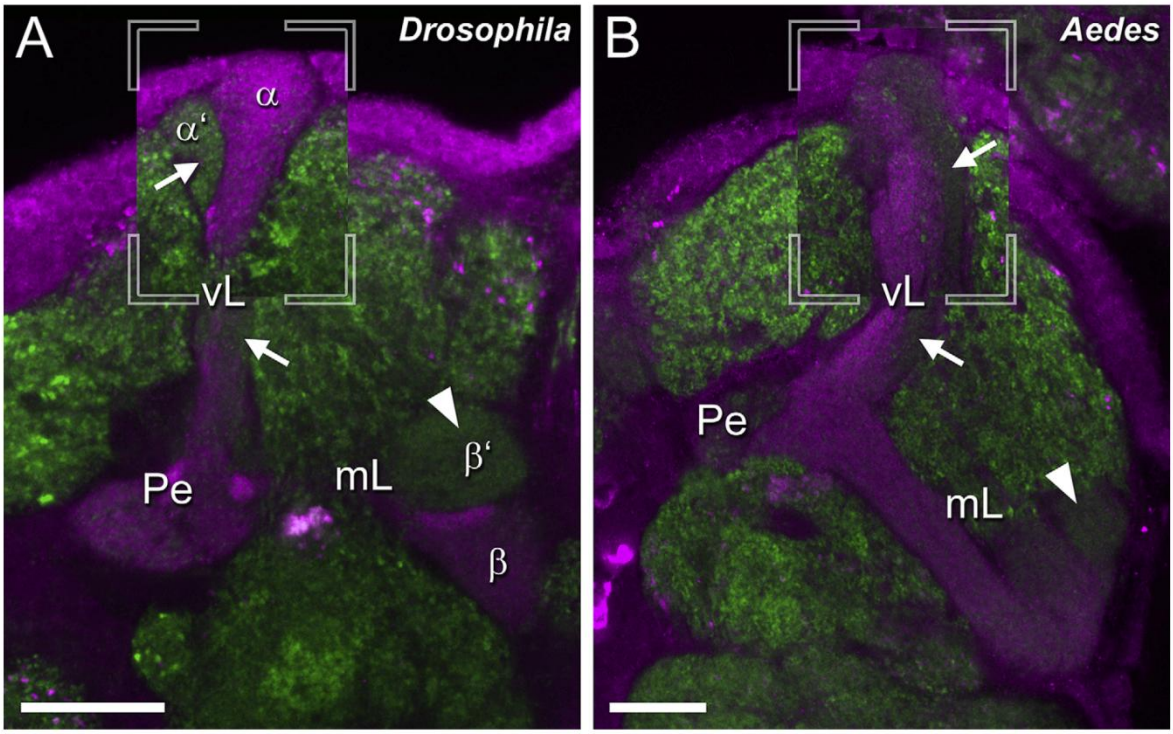

Fig. 8. sNPF-like immunoreactivity in the mushroom bodies of two dipteran insects. (A) A single optical section through the anterior part of the mushroom body in the brachyceran *Drosophila melanogaster* shows prominent staining in the peduncle (Pe), the vertical lobe (vL, insert superimposed from a different optical section), and the medial lobe (mL). Immunoreactivity resides in the α, β, and γ division; the α' division of vertical lobe (arrows) and the β' division of the medial lobe (arrowhead) are in fact immunonegative. (B) The mushroom bodies of the nematoceran *Aedes aegypti* shows a highly similar pattern of sNPF-like immunoreactivity. Staining is observed in the calyx (not shown), the peduncle and the lobes. In the peduncle, the vertical lobe (insert superimposed from a different optical section), and the medial lobe, particular divisions are devoid of immunostaining. The formation of the immunonegative divisions in the vertical lobe (arrow) and the medial lobe (arrowhead) closely matches the conditions observed in *D. melanogaster*. Both images show frontal views of the mushroom bodies, dorsal is towards the top and lateral to the left of the pictures. green: synapsin-immunoreactivity, magenta: sNPF-like immunoreactivity. Scale bars: 20 µm.

motif consisting of Arg-Leu/Pro-Arg-Phe/Trp-amide (Table 2). Outside Insecta, sequence mining has led to the prediction of short NPFs occurring in the mite *Tetranychus urticae* (Chelicerata; Christie et al., 2010) and the branchiopod *Daphnia pulex* (Crustacea; Gard et al., 2009). Insect sNPFs act on G-protein coupled receptors (GPCR) (Mertens et al., 2002; Feng et al., 2003; Chen and Pietrantonio, 2006) and have been shown to stimulate ovarian development (Schoofs et al., 2001), to be involved in adult diapause regulation (Huybrechts et al., 2004), to induce host seeking behavior in female mosquitoes (Brown et al., 1994), and to regulate feeding and growth (Lee et al., 2004).

The expression of sNPF in the central nervous system has been studied most comprehensively in the fruit fly. Immunohistological investigations and *in situ* hybridization experiments have revealed sNPF to be expressed in subpopulations of clock neurons (Johard et al., 2009), numerous other interneurons, olfactory receptor neurons and small sets of possibly neurosecretory cells innervating the *corpora cardiaca* and aorta (Nässel et al., 2008). However, the bulk of sNPF expressing neurons in the central nervous system are intrinsic mushroom body neurons. The majority of Kenyon cells show immunoreactivity towards specific sNPF-antisera and patterns of varying expression intensity are discernable within the mushroom body neuropil. While cell somata and dendritic arborizations in the calyx region exhibit comparatively weak and scattered immunoreactivity, strong immunolabeling can be observed in the peduncle and in the vertical and medial lobes (Johard et al., 2008). However, immunolabeling in these regions is restricted to the α-, β- and γ-divisions of the lobes – with a particularly strong signal in the distal parts –, to the heel, and to the outer perimeter of the peduncle. Probably indicating sNPF storage and release sites, this distribution pattern may correspond to regions where extrinsic neurons ramify within the mushroom bodies. In contrast, the α'- and β'-divisions of the lobes and the core of the peduncle are devoid of sNPF immunoreactivity.

Fig. 7. SIFamide-like immunoreactivity in insect mushroom bodies. (A) Immunostained fibers braid 'Trauben' of the vertical lobes (vL) in *Thermobia domestica* (black arrowhead). Moreover, individual 'Trauben' are also partially (white arrowhead) or even completely (arrow) innervated by immunoreactive fibers. (B) In the cockroach, immunopositive arborizations form a meshwork within the cup-shaped calyces (Ca). (C, C') Immunoreactive fibers and varicosities envelop parts of the vertical lobe in *Tribolium castaneum*. The vertical lobe itself is devoid of immunoreactivity, as are the medial lobe (mL) and the peduncle (Pe). The calyx is invaded by single immunostained fibers (arrowhead). (D, D') In the honeybee, the calyces are sparsely braided by immunostained fibers (arrowheads). Immunolabeled fiber processes also surround the vertical lobe (arrowheads) and immunopositive blebs are discernable in a distinct stratum of the lobe (arrow). (E–E''') In *Aedes aegypti*, scattered immunostaining (arrowheads) can be observed in the medial lobe, the vertical lobe, and the calycal neuropil. All images show frontal views of the mushroom bodies, dorsal is towards the top and lateral to the left of each picture. green: synapsin-immunoreactivity, magenta: SIFamide-like immunoreactivity. Scale bars: (A, E–E''') 20 µm, (B–D) 50 µm.

Our own immunohistochemical stainings employed one of the antisera originally used by Johard et al. (2008; for details see Materials and Methods section), directed against the drosophilid sNPF-3. sNPF-like staining in the fruit fly matches the detailed descriptions provided by Johard and colleagues (Johard et al., 2008; Nässel et al., 2008). Immunolabeling is observed in all parts of the mushroom body but is restricted to particular subdivisions of the lobes (Fig. 8A). A very similar staining pattern is evident in the mushroom body of *A. aegypti*, which also displays immunostaining in all subcompartments. Again, immunonegative subdivisions can be identified within the vertical and medial lobes (Fig. 8B), roughly corresponding to the layout of the α'- and β'-divisions in *Drosophila*. Similar to the conditions in *Drosophila*, the peduncle comprises an immunonegative segment and scattered immunostaining is dispersed throughout the calyx region. While the antiserum against sNPF-3 cannot be expected to produce specific immunostaining in non-dipteran insects, the corresponding staining patterns in the brachyceran and the nematoceran representative suggest mushroom body-associated sNPF expression to be highly conserved in Diptera.

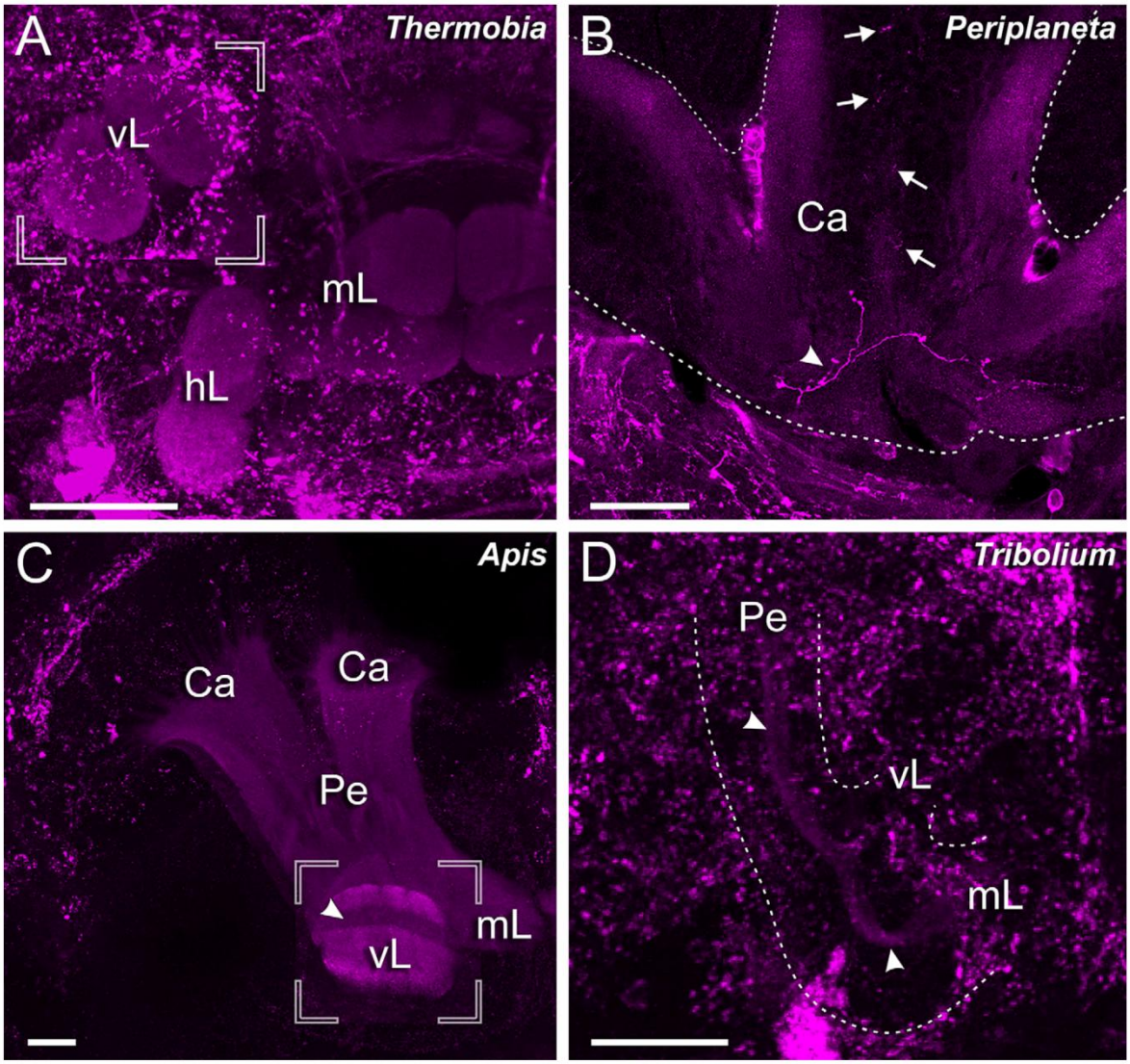

Fig. 9. Tachykinin-like immunoreactivity in insect mushroom bodies. Neuropil outlines in B and D are based on anti-synapsin immunostaining. (A) In *Thermobia domestica*, 'Trauben' of the horizontal (hl), medial (mL), and vertical lobes (vL, superimposed from a different projection plane) display homogeneous tachykinin-like immunostaining. (B) The calyces (Ca) of the cockroach *Periplaneta americana* are supplied with immunoreactive fibers (arrowhead) and exhibit scattered immunopositive varicosities (arrows). (C) Tachykinin-like immunostaining is prominent in the mushroom body of the honeybee, *Apis mellifera*. While all subcompartments of the neuropil exhibit immunoreactivity, strata of the vertical lobe (insert, superimposed from a different projection plane) show differences in their staining intensity (arrowhead). (D) In *Tribolium castaneum*, immunoreactive Kenyon cell processes form a core (arrowheads) that extends through the peduncle (Pe) and splits up to project into the vertical and medial lobe. All images show frontal views of the mushroom bodies, dorsal is towards the top and lateral to the left of each picture. Scale bars: (A–C) 50 µm,(D) 20 µm.

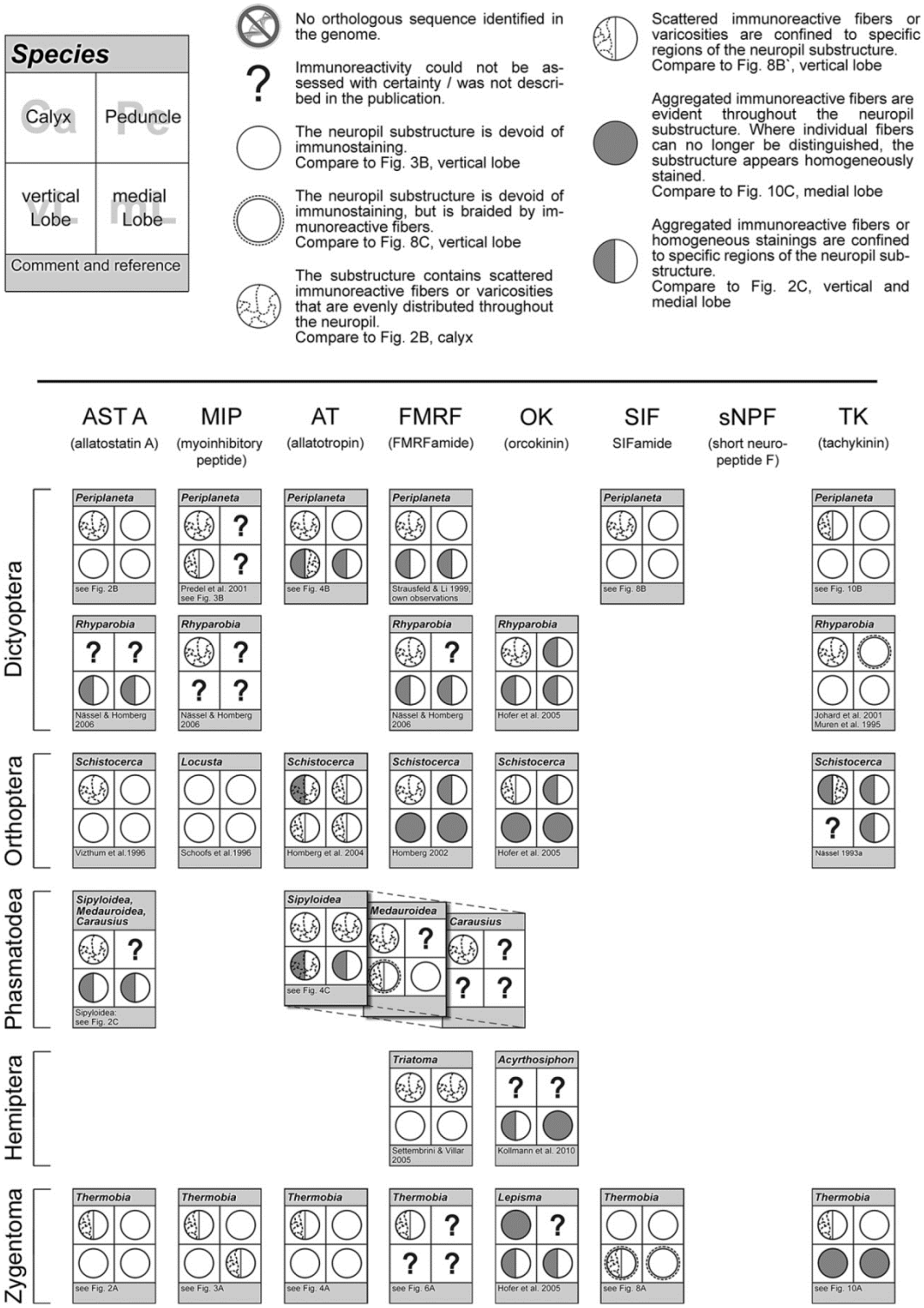

Fig. 10. Overview chart showing neuropeptide distribution in the mushroom bodies of an ametabolous zygentome species and various hemimetabolous insects (*Acyrthosiphon pisum, Baculum extradentatum, Carausius morosus, Lepisma saccharina, Locusta migratoria, Periplaneta americana, Rhyparobia (Leucophaea) maderae, Schistocerca gregaria, Sypiloidea sypilus, Thermobia domestica, Triatoma infestans*). Boxes for each respective species and neuropeptide display pictograms that provide basic information on the neuropeptide distribution in each of the four mushroom body subcompartments. Pictograms are explained in the legend above. Note that distribution patterns for some species have been extracted from the literature (references are included), while for other species, pictograms have been assigned based upon our own observations.

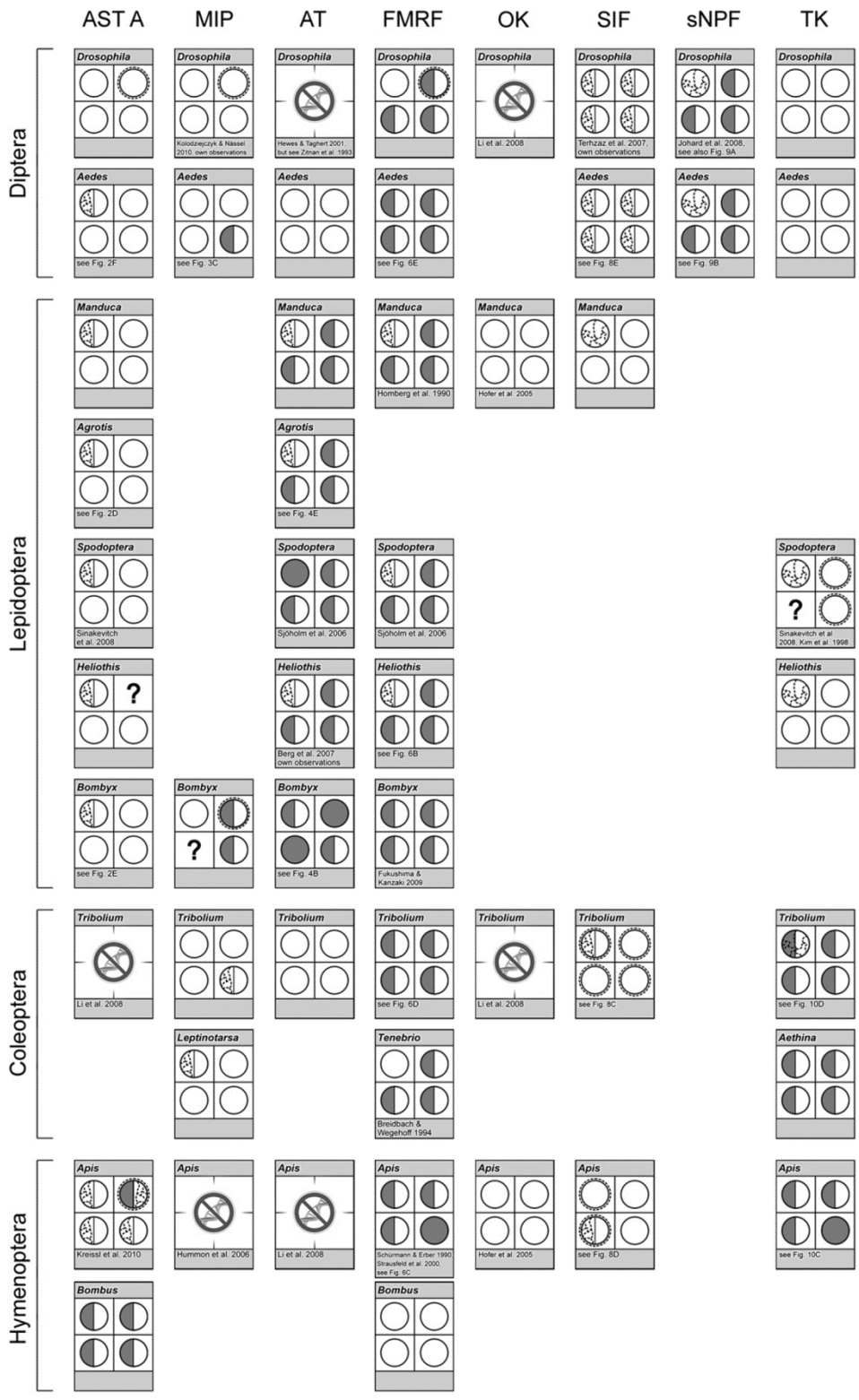
AST A
MIP
AT
FMRF
OK
SIF
sNPF
TK
Diptera
Lepidoptera
Coleoptera
Hymenoptera
Drosophila
Aedes
Manduca
Agrotis
Spodoptera
Heliothis
Bombyx
Tribolium
Leptinotarsa
Tenebrio
Aethina
Apis
Bombus
see Fig. 2F
see Fig. 3C
see Fig. 6E
see Fig. 8E
see Fig. 9B
see Fig. 2D
see Fig. 4E
see Fig. 6B
see Fig. 2E
see Fig. 4B
see Fig. 6D
see Fig. 8C
see Fig. 10D
see Fig. 8D
see Fig. 10C
Li et al. 2008
Hummon et al. 2006
Kreissl et al. 2010
Hewes & Taghert 2001, but see Zitnan et al. 1993
Kolodziejczyk & Nässel 2010, own observations
Terhzaz et al. 2007, own observations
Johard et al. 2008, see also Fig. 9A
Homberg et al. 1990
Hofer et al. 2005
Sjöholm et al. 2006
Berg et al. 2007 own observations
Fukushima & Kanzaki 2009
Breidbach & Wegehoff 1994
Schürmann & Erber 1990 Strausfeld et al. 2000, see Fig. 6C
Sinakevitch et al. 2008
Sinakevitch et al. 2008, Kim et al. 1998

3.8. Tachykinin-related peptides (TKRPs)

As their name suggests, invertebrate tachykinin-related peptides are thought to share a common ancestry with their vertebrate namesakes, making the tachykinins one of the oldest and most wide-spread neuropeptide families in the animal kingdom (Nässel, 1999; Severini et al., 2002). The first invertebrate tachykinins to be structurally analyzed were four peptide isoforms (Lom-TK I–IV) that were purified from *L. migratoria* (Schoofs et al., 1990a,b), each carrying the C-terminal FX_1GX_2R-amide motif that has since been recognized as the characteristic consensus sequence of invertebrate TKRPs. Up to now, TKRPs have been identified in a broad range of insect species, as well as in crustaceans, molluscs, echiurid worms and nematodes (Nässel, 1999; Severini et al., 2002; Van Loy et al., 2010). Similar to other neuropeptides, different TKRP isoforms in a particular species originate from cleavage and subsequent modification of large precursor proteins – in the American cockroach, for example, the TKRP-gene encodes a precursor that is processed into 13 distinct TKRPs (Predel et al., 2005), while in *Drosophila*, the processing of the precursor yields five TKRPs (Siviter et al., 2000).

TKRPs act on metabotropic receptors (termed DTKR und NKD in *Drosophila*; Van Loy et al., 2010) and have been shown to produce a variety of physiological effects *in vitro*, including contractions of gut, oviduct, and heart musculature, modulation of DUM neuron and motor neuron activity, and the release of adipokinetic hormone from the *corpora cardiaca* (reviewed in Nässel, 1999). Moreover, TKRPs were recently also demonstrated to affect behavior in the fruit fly. TKRP knockdown via RNA interference was shown to result in a reduction of odor perception sensitivity and an increase of locomotor activity, suggesting a modulatory function in the antennal lobes and the central complex (Winther et al., 2006). This notion was recently corroborated by knockdown experiments on TK receptors in olfactory sensory neurons (OSNs) that provided evidence for a signal modulation mediated by peptidergic interneurons of the antennal lobe connecting to OSNs (Ignell et al., 2009).

Tachykinin-like immunoreactivity in the brain of *L. migratoria* was described by Nässel (1993) who observed immunostaining in the posterior lobe of the calyx, the lateral portion of the peduncle and the ventral portion of the medial lobe, attributing it to extrinsic neurons arborizing in the different subcompartments of the mushroom bodies. A similar account for the cockroach *L. maderae* (now *R. maderae)* was published two years later (Muren et al., 1995), showing that in this species, tachykinin-like immunoreactivity is restricted to the calyces, with the peduncle and lobes exhibiting no immunostaining. A subsequent study that employed an antibody directed against a cockroach tachykinin (LemTRP-1) corroborated these results and revealed additional immunoreactivity in the neuropil surrounding the peduncle (Johard et al., 2001). In the lepidopteran *S. littoralis*, immunopositive fibers and varicosities are dispersed evenly throughout the calyx region (Sinakevitch et al., 2008). While this pattern again hints at an extrinsic innervation of the calycal neuropil, a small group of faintly immunopositive cells located laterally to the calyx has been interpreted as representing an immunoreactive subset of Kenyon cells in the moth (Sinakevitch et al., 2008).

Own investigations in the ametabolous representative *T. domestica* demonstrate immunostaining of homogeneous intensity in the 'Trauben' of all three lobes, possibly indicating the presence of tachykinin-like peptides in storage sites of intrinsic neurons (Fig. 9A). In *P. americana*, the tachykinin antiserum produces immunostaining in the calyx but not in other mushroom body subcompartments (Fig. 9B), corresponding to the observations of Muren et al. (1995) in *R. maderae*. Within the calycal neuropil, single immunoreactive fibers and scattered immunoreactive blebs are discernable. Immunoreactivity is prominent in the mushroom bodies of the honeybee, and homogeneous staining can be observed in most parts of the neuropil, especially in the median lobes, which exhibit uniform staining (Fig. 9C). The staining pattern suggests that in this species, tachykinin-like peptides are expressed by intrinsic mushroom body neurons – a finding that is in agreement with the results of an earlier study on the expression of the prepro-tachykinin gene in the brain of *A. mellifera* (Takeuchi et al., 2004). Using cDNA microarray and *in situ* hybridization techniques, these authors demonstrated that the expression of TKRPs is highly enriched in the mushroom bodies of *A. mellifera* (greater than seven-fold compared to other brain areas) and that the prepro-tachykinin gene is expressed in specific Kenyon cell subtypes (class I small-type and some large-type Kenyon cells). However, a differentiation between different Kenyon cell subtypes could not be reproduced in our experiments as cell somata exhibited no or only very faint immunoreactivity. In contrast, TKRP-like immunoreactivity in the flour beetle *T. castaneum* is strongly indicative of a selective expression of the neuropeptide in specific subsets of Kenyon cells (Fig. 9D). Immunostained Kenyon cell processes converge in a Y-shaped confluence in the calyx region, forming a core that extends through the peduncle and into the vertical and medial lobe. Studies on the development of the mushroom bodies in *T. castaneum* (Zhao et al., 2008) suggest that this pattern of immunoreactivity could correspond to a population of newborn Kenyon cells produced by two neuroblasts located on top of each calyx.

In summary, the TKRPs are involved in the mushroom body circuitry of all analyzed insect groups apart from Diptera, in which the neuropils are completely devoid of any tachykinin immunoreactivity (Figs. 10 and 11). TKRP-like immunostaining in intrinsic mushroom body neurons is observed in *T. domestica*, *S. gregaria*, *A. mellifera*, and the coleopterans *A. tumida* and *T. castaneum*. In most of these species, the calycal neuropil also receives immunopositive extrinsic fibers. In contrast, the two examined moth and cockroach species display TKRP-like immunoreactivity exclusively in extrinsic fibers projecting into the calyx region.

4. Conclusion

In higher animals (e.g. molluscs, annelids, arthropods, chordates), brains are typically organized in distinct neuropils that can be characterized by their spatial location and gross anatomy, their specific architecture, and often by a certain function. In animals of the same species or of closely related taxa, these neuroanatomical characters show a high degree of evolutionary conservation (Kutsch and Breidbach, 1994). Perhaps more surprisingly, neuropils sharing anatomical and/or functional commonalities can even be identified across vast phylogenetic distances. For example, the olfactory bulbs of vertebrates and the antennal lobes of insects display a similar neuroanatomical organization and a similar function, acting as primary processing centers for olfactory information (for a review see Hildebrand and Shepherd, 1997; Schachtner et al., 2005). Insect mushroom bodies, usually characterized as second order olfactory neuropils involved in higher integration processes and learning

Fig. 11. Overview chart showing neuropeptide distribution in the mushroom bodies of various holometabolous insects (*Aedes aegypti, Aethina tumida, Agrotis segetum, Apis mellifera, Bombus terrestris, Bombyx mori, Drosophila melanogaster, Heliothis virescens, Leptinotarsa decemlineata, Manduca sexta, Spodoptera littoralis, Tenebrio molitor, Tribolium castaneum*). For explanations, see Fig. 10.

(e.g. Menzel, 2001; Heisenberg, 2003, but see above), are frequently homologized with highly similar structures in the brains of other arthropods (Loesel and Heuer, 2010). Moreover, recent studies also support a far-reaching homology to comparable brain centers in annelid worms (Heuer and Loesel, 2008) and even point towards a common evolutionary origin of mushroom bodies and the vertebrate pallium (Tomer et al., 2010).

Similar to neuroarchitectural traits, the distribution of neuropeptides in the insect nervous system also seems to follow a conserved pattern (reviewed in Nässel, 2002; Nässel and Homberg, 2006; Nässel and Winther, 2010). This is not particularly surprising, because it is well accepted that only a combination of neuroarchitecture in concert with the activity of neuroactive substances and their receptors can shape the activity pattern of a given neuronal circuit. Major insights into such complex network properties come from work on the crustacean stomatogastric ganglion (e.g. Nusbaum et al., 2001; Marder and Bucher, 2007; Marder and Taylor, 2011). However, just as evolutionary adaptations and selective pressures shape the organization of particular neuropils such as the mushroom bodies (for a review see Strausfeld et al., 2009), the same forces can also be expected to transform expression patterns and functional implications of neuropeptides. The data presented in this work clearly support such a view.

Though the distribution of mushroom body-associated neuropeptides across the examined species shows a rather diverse picture, some evolutionary considerations can be inferred from a careful analysis of the available data. Immunohistological findings from the literature and from own experiments show that except for SIFamide (see below), each of the seven other neuropeptide families investigated is occasionally present in intrinsic mushroom body neurons in certain taxa (Figs. 10 and 11). Due to the small diameter of the axon-like Kenyon cell processes, neuropeptide immunostaining in the peduncle and lobes usually appears diffuse, whereas staining of Kenyon cell bodies and the calyx neuropil is typically very weak or even indiscernible (compare Supplementary Fig. 1) – an observation that is explained by cellular neuropeptide transport and processing mechanisms (Nässel and Homberg, 2006; Johard et al., 2008). A closer look at the peptide immunoreactivity of intrinsic mushroom body neurons reveals that certain taxa predominantly use different peptides. Orcokinins are present in intrinsic mushroom body neurons of all examined hemimetabolous representatives but are not utilized by Kenyon cells of holometabolous insects. Although the genome of the honeybee contains an orcokinin-encoding gene that is expressed in the brain (Hummon et al., 2006), the mushroom bodies show no immunoreactivity towards the antiserum (Hofer et al., 2005). The fact that orthologous genes are lacking in *Drosophila* and in *T. castaneum* (Li et al., 2008) supports the notion that orcokinins have experienced a loss of function in holometabolous insects. Further focusing on distribution patterns in holometabolous representatives (Fig. 11), AST-A-like immunoreactivity in intrinsic mushroom body neurons could only be observed in Hymenoptera, albeit in variable patterns. Allatotropin-like immunostaining of intrinsic mushroom body neurons is restricted to Lepidoptera; allatotropin-encoding genes are lacking in *Drosophila* and *A. mellifera* (Hewes and Taghert, 2001; Li et al., 2008) and the mushroom bodies of *A. aegypti* and *T. castaneum* exhibit no immunoreactivity. In the five investigated lepidopteran species, staining patterns are very similar, suggesting a conserved function of allatotropin in the mushroom body circuitry of this group. Considering that allatotropin-like immunoreactivity was also observed in Kenyon cells of dictyopteran, orthopteran and phasmatodean representatives (Fig. 10), it could be surmised that an ancestral mushroom body-related function has been strengthened in Lepidoptera but has been lost or superseded in other holometabolous taxa. However, in the most ancestral insect investigated, the zygentome *T. domestica*, the mushroom body neuropils were devoid of intrinsic allatotropin-like immunostaining. A comparison of tachykinin-like immunoreactivity in intrinsic mushroom body neurons reveals a certain degree of conservation in individual groups: Kenyon cells in Orthoptera, Hymenoptera, and Coleoptera exhibit immunostaining, whereas those in Dictyoptera, Diptera, and Lepidoptera are unlabeled (Figs. 10 and 11). The distribution of MIP-like immunoreactivity is inconclusive, as staining could only be observed in intrinsic neurons of *B. mori* and *A. aegypti*. Data for other lepidopteran species are missing, and in *Drosophila*, the mushroom bodies are devoid of immunostaining. sNPF-like immunoreactivity is highly congruent in the two dipteran representatives (Figs. 8 and 11), but further insights into the involvement of this peptide in the mushroom bodies of other insects are currently impeded by the lack of specific antisera for non-dipteran species. Probably due to an indiscriminative binding to different FaRPs (see above), the FMRFamide antiserum labeled Kenyon cells in nearly every species investigated – notable exceptions being *T. domestica*, *T. infestans* and *B. terrestris*. In summary, Kenyon cells in different groups of holometabolous insects seem to utilize only a limited range of neuropeptides. While sNPF appears to be the sole neuropeptide expressed in Kenyon cells of *Drosophila* (Johard et al., 2008), at least two different neuropeptides are present in Lepidoptera and three peptides have been found in *A. mellifera*. Hymenopteran mushroom bodies and those of the honeybee in particular, are among the most elaborate in insects (Strausfeld et al., 2009). They receive multimodal input (e.g. Gronenberg, 2001; Galizia and Rössler, 2010) and harbor high learning capacities (e.g. Menzel and Giurfa, 2001) that have often been associated with social behaviors. From this point of view, a higher variability of neuropeptides expressed by intrinsic mushroom body neurons in *A. mellifera* would seem to correlate well with the increased functional demands and the larger behavioral repertoire compared to other holometabolous species. However, among the hemimetabolous taxa examined, three different neuropeptides are present in the mushroom bodies of *R. maderae* and even four in those of *S. gregaria*, both of which are not exactly renowned for their learning prowess or sophisticated social behavior. Thus, it appears that increased cognitive and social abilities are not necessarily correlated with a specific evolution of neuropeptide families (Predel and Neupert, 2007).

While antisera directed against A-type allatostatins, myoinhibitory peptides, allatotropin, FMRFamide related peptides, orcokinin, short neuropeptide Fs, and tachykinins label intrinsic mushroom body neurons in certain taxa, SIFamide-like immunoreactivity is always clearly restricted to extrinsic neurons. At least in the holometabolous insects, SIFamide-like innervation very likely stems from four cell bodies located in the *pars intercerebralis* (Verleyen et al., 2004; Roller et al., 2008). These neurons show a wide field innervation of many brain areas and therefore seem to act as general modulators that do not necessarily affect the mushroom bodies specifically. Also, SIFamide-like innervation of the mushroom bodies shows a considerable degree of variation across the investigated taxa (Figs. 10 and 11), impeding attempts at an evolutionary interpretation. Apart from SIFamide, the source of the neuropeptidergic extrinsic innervation of the mushroom bodies is mostly unknown and there is certainly more effort needed to unravel the identity of these neurons. Thus, we can only compare whether there is extrinsic innervation of the mushroom bodies or not, but we are not able to tell whether this innervation stems from homologues neurons. In most of the investigated species, the mushroom bodies are supplied by extrinsic fibers carrying different neuropeptides (Figs. 10 and 11), suggesting that an external modulation by neuropeptides is a general feature of the mushroom body circuitry. Innervation of the calyx region and of other parts of

the mushroom body is not mutually exclusive, but an innervation of the calycal neuropil – the supposed main input region of the mushroom bodies – is most often observed, even if the rest of the neuropil receives no innervation.

The present account provides immunohistochemical data on the distribution of eight major neuropeptides in the mushroom bodies of 24 insect species belonging to nine different orders – including the four major holometabolous groups, four hemimetabolous groups and the apterygote Zygentoma. About half of the presented data stems from own investigations; the other half has been compiled from the available literature. A comparative analysis of the complete dataset draws a very versatile picture of mushroom body-associated neuropeptide expression, which seems to mirror the functional diversity of these higher brain centers. While the intrinsic mushroom body neurons contain different neuropeptides in different groups, the number of neuropeptide transmitters utilized by the Kenyon cells shows no apparent correlation to increased cognitive and social abilites of the animals. Allatotropin and orcokinin possibly represent ancient signaling molecules of the Kenyon cells, as evidenced by their wide-spread occurrence in the hemimetabolous taxa and their presence in the mushroom body-like neuropils of collembolans (Kollmann et al., 2011a), basal hexapods that form an outgroup to the insects. The lack of allatotropin in Kenyon cells of all holometabolous taxa but Lepidoptera might then be interpreted as a secondary loss, and its preservation in Lepidoptera as an indicator for an ancestral allatotropin-driven property of the mushroom body circuitry in this order. However, apart from a central effect on the circadian rhythm (Petri et al., 2002), little is known about the function of allatotropin in the insect central nervous system. Further insights into a 'peptidergic ground plan' of the mushroom body circuitry can possibly be derived from conserved extrinsic innervation patterns. However, in order to identify conserved patterns, homologies must be formulated. These homologies cannot solely rely on the expression of neuroactive substances but have to take the origin of immunopositive fibers and the location of the respective cell bodies into account. For example, in a study on the evolution of the antennal lobes in Tetraconata, extrinsic peptidergic innervation via centrifugal AST-A positive neurons has been proposed to be evolutionary conserved (Schachtner et al., 2005). The source of these AST-A positive fibers could, however, only be unraveled in *M. sexta* (Utz and Schachtner, 2005) and in *A. aegypti* (unpublished data, Ignell and Schachtner). In both cases, large, possibly homologous neurons located laterally in the anterior portion of the subesophageal ganglion are the source for the extrinsic innervation of the antennal lobe.

In summary, the presented data suggest that the evolutionary transformations of the peptidergic signaling system of the mushroom bodies mirror the broad range of functions that these neuropils have adopted in different insects (see Table 1). Thus, the quest to deduce an 'ancestral neuropeptide ground pattern' of the mushroom bodies seems to be closely linked to unravelling the ancestral function of these neuropils. However, differentiating between ancestral and derived traits/functions is always a daunting task, given that phylogenetically 'primitive' species are not exempt from selective pressures and had the same amount of time to evolve as their 'advanced' relatives. One way to approach such difficulties lies in a broad, yet considerate taxon sampling. Thus, while this paper ends with the usual call for more data, it hopefully also serves as a starting point for future investigations.

Acknowledgments

Part of the research in the J. Schachtner's laboratory is sponsored by the German Science Foundation (DFG) within the framework of the priority program 'Integrative analysis of olfaction' (SPP 1392, SCHA 678/13-2). Several former and present members of the lab are gratefully acknowledged for contributing original stainings to the dataset summarized in this article: Anna Boehm, Max Diesner, Sergius Frank, Wolf Huetteroth, Anna Reifenrath and Anna L. Rupenthal. Expert lab assistance was provided by Ljubinka Cigoja and Martina Kern. We also thank colleagues from different laboratories for supplying us with animal specimens and different neuropeptide antibodies (see Materials section). We further acknowledge John Wiley and Sons for allowing us to reproduce selected figures.

Appendix A. Supplementary data

Supplementary data related to this article can be found online at doi:10.1016/j.asd.2012.02.005.

References

Altstein, M., Nässel, D.R., 2010. Neuropeptide signaling in insects. In: Geary, T.G., Maule, A.G. (Eds.), Neuropeptide Systems as Targets for Parasite and Pest Control Landes Bioscience and Science, Austin, TX. Springer, pp. 155–165.

Baggerman, G., Boonen, K., Verleyen, P., De Loof, A., Schoofs, L., 2005. Peptidomic analysis of the larval *Drosophila melanogaster* central nervous system by two-dimensional capillary liquid chromatography quadrupole time-of-flight mass spectrometry. Journal of Mass Spectrometry 40, 250–260.

Bang, S., Hyun, S., Hong, S.-T., Kang, J., Jeong, K., Park, J.-J., Choe, J., Chung, J., 2011. Dopamine signalling in mushroom bodies regulates temperature-preference behaviour in Drosophila. PLoS Genetics 7, e1001346.

Barth, M., Heisenberg, M., 1997. Vision affects mushroom bodies and central complex in *Drosophila melanogaster*. Learning and Memory 4, 219–229.

Bell, R.A., Joachim, F.A., 1978. Techniques for rearing laboratory colonies of the tobacco hornworm, *Manduca sexta*, and pink ballworms. Annals of the Entomological Society of America 69, 365–373.

Bellés, X., Graham, L.A., Bendena, W.G., Ding, Q.I., Edwards, J.P., Weaver, R.J., Tobe, S.S., 1999. The molecular evolution of the allatostatin precursor in cockroaches. Peptides 20, 11–22.

Berg, B.G., Schachtner, J., Utz, S., Homberg, U., 2007. Distribution of neuropeptides in the primary olfactory center of the heliothine moth *Heliothis virescens*. Cell and Tissue Research 327, 385–398.

Berghammer, A., Bucher, G., Maderspacher, F., Klingler, M., 1999. A system to efficiently maintain embryonic lethal mutations in the flour beetle *Tribolium castaneum*. Development Genes and Evolution 209, 382–389.

Bhalerao, S., Sen, A., Stocker, R., Rodrigues, V., 2003. Olfactory neurons expressing identified receptor genes project to subsets of glomeruli within the antennal lobe of *Drosophila melanogaster*. Journal of Neurobiology 54, 577–592.

Blackburn, M.B., Wagner, R.M., Kochansky, J.P., Harrison, D.J., Thomas-Laemont, P., Raina, A.K., 1995. The identification of two myoinhibitory peptides, with sequence similiarities to the galanins, isolated from the ventral nerve cord of *Manduca sexta*. Regulatory Peptides 57, 213–219.

Blackburn, M.B., Jaffe, H., Kochansky, J., Raina, A.K., 2001. Identification of four additional myoinhibitory peptides (MIPs) from the ventral nerve cord of *Manduca sexta*. Archives of Insect Biochemistry and Physiology 48, 121–128.

Boerjan, B., Cardoen, D., Bogaerts, A., Landuyt, B., Schoofs, L., Verleyen, P., 2010. Mass spectrometric profiling of (neuro)-peptides in the worker honeybee, *Apis mellifera*. Neuropharmacology 58, 248–258.

Breidbach, O., Wegerhoff, R., 1994. FMRFamide-like immunoreactive neurons in the brain of the beetle, *Tenebrio molitor* L. (Coleoptera: Tenebrionidae): constancies and variations in development from the embryo to the adult. International Journal of Insect Morphology and Embryology 23, 383–404.

Brown, M., Klowden, M., Crim, J., Young, L., Shrouder, L., Lea, A., 1994. Endogenous regulation of mosquito host-seeking behavior by a neuropeptide. Journal of Insect Physiology 40, 399–406.

Bungart, D., Dircksen, H., Keller, R., 1994. Quantitative determination and distribution of the myotropic neuropeptide orcokinin in the nervous system of astacidean crustaceans. Peptides 15, 393–400.

Carlsson, M.A., Diesner, M., Schachtner, J., Nässel, D.R., 2010. Multiple neuropeptides in the *Drosophila* antennal lobe suggest complex modulatory circuits. Journal of Comparative Neurology 518, 3359–3380.

Cassenaer, S., Laurent, G., 2007. Hebbian STDP in mushroom bodies facilitates the synchronous flow of olfactory information in locusts. Nature 448, 709–713.

Cassenaer, S., Laurent, G., 2012. Conditional modulation of spike-timing-dependent plasticity for olfactory learning. Nature Advance Online Publication. doi:10.1038/nature10776.

Chen, M.-E., Pietrantonio, P.V., 2006. The short neuropeptide F-like receptor from the red imported fire ant, *Solenopsis invicta* Buren (Hymenoptera: Formicidae). Archives of Insect Biochemistry and Physiology 61, 195–208.

Christie, A.E., Sousa, G.L., Rus, S., Smith, C.M., Towle, D.W., Hartline, D.K., Dickinson, P.S., 2008. Identification of A-type allatostatins possessing-YXFGI/

Vamide carboxy-termini from the nervous system of the copepod crustacean *Calanus finmarchicus*. General and Comparative Endocrinology 155, 526–533.
Christie, A.E., Nolan, D.H., Ohno, P., Hartline, N., Lenz, P.H., 2010. Identification of chelicerate neuropeptides using bioinformatics of publicly accessible expressed sequence tags. General and Comparative Endocrinology 170, 144–155.
Clynen, E., Baggerman, G., Veelaert, D., Cerstiaens, A., Van der Horst, D., Harthoorn, L., Derua, R., Waelkens, E., De Loof, A., Schoofs, L., 2001. Peptidomics of the pars intercerebralis-corpus cardiacum complex of the migratory locust, *Locusta migratoria*. European Journal of Biochemistry/FEBS 268, 1929–1939.
Connolly, J.B., Roberts, I.J., Armstrong, J.D., Kaiser, K., Forte, M., Tully, T., O'Kane, C.J., 1996. Associative learning disrupted by impaired G_s signaling in *Drosophila* mushroom bodies. Science 274, 2104–2107.
Crittenden, J.R., Skoulakis, E.M.C., Han, K.-A., Kalderon, D., Davis, R.L., 1998. Tripartite mushroom body architecture revealed by antigenic markers. Learning and Memory 5, 38–51.
Davey, M., Duve, H., Thorpe, A., East, P., 1999. Characterisation of the helicostatin peptide precursor gene from *Helicoverpa armigera* (Lepidoptera: Noctuidae). Insect Biochemistry and Molecular Biology 29, 1119–1127.
Davis, N.T., Veenstra, J.A., Feyereisen, R., Hildebrand, J.G., 1997. Allatostatin-like-immunoreactive neurons of the tobacco hornworm, *Manduca sexta*, and isolation and identification of a new neuropeptide related to cockroach allatostatins. Journal of Comparative Neurology 385, 265–284.
Davis, N.T., Blackburn, M.B., Golubeva, E.G., Hildebrand, J.G., 2003. Localization of myoinhibitory peptide immunoreactivity in *Manduca sexta* and *Bombyx mori*, with indications that the peptide has a role in molting and ecdysis. Journal of Experimental Biology 206, 1449–1460.
Davis, R.L., 2004. Olfactory learning. Neuron 44, 31–48.
Davis, R.L., 2005. Olfactory memory formation in *Drosophila*: from molecular to systems neuroscience. Annual Review of Neuroscience 28, 275–302.
de Belle, J.S., Heisenberg, M., 1994. Associative odor learning in *Drosophila* abolished by chemical ablation of mushroom bodies. Science 263, 692–695.
de Jong-Brink, M., ter Maat, A., Tensen, C.P., 2001. NPY in invertebrates: molecular answers to altered functions during evolution. Peptides 22, 309–315.
Dircksen, H., Skiebe, P., Abel, B., Agricola, H., Buchner, K., Muren, J.E., Nässel, D.R., 1999. Structure, distribution, and biological activity of novel members of the allatostatin family in the crayfish *Orconectes limosus*. Peptides 20, 695–712.
Doeffinger, C., Hartenstein, V., Stollewerk, A., 2010. Compartmentalization of the precheliceral neuroectoderm in the spider *Cupiennius salei*: development of the arcuate body, optic ganglia, and mushroom body. Journal of Comparative Neurology 518, 2612–2632.
Donly, B.C., Ding, Q., Tobe, S.S., Bendena, W.G., 1993. Molecular cloning of the gene for the allatostatin family of neuropeptides from the cockroach *Diploptera punctata*. Proceedings of the National Academy of Sciences of the United States of America 90, 8807–8811.
Dubnau, J., Grady, L., Kitamoto, T., Tully, T., 2001. Disruption of neurotransmission in *Drosophila* mushroom body blocks retrieval but not acquisition of memory. Nature 411, 476–480.
Duve, H., Johnsen, A.H., East, P.D., Thorpe, A., 1994. Comparative aspects of the FMRFamides of blowflies: isolation of the peptides, genes, and functions. In: Davey, K.G., Peter, R.E., Tobe, S.S. (Eds.), Perspective in Comparative Endocrinology. National Research Council of Canada, Ottawa, pp. 91–96.
Duve, H., East, P., Thorpe, A., 1999. Regulation of lepidopteran foregut movement by allatostatins and allatotropin from the frontal ganglion. Journal of Comparative Neurology 413, 405–416.
Duve, H., Audsley, N., Weaver, R.J., Thorpe, A., 2000. Triple co-localisation of two types of allatostatin and an allatotropin in the frontal ganglion of the lepidopteran *Lacanobia oleracea* (Noctuidae): innervation and action on the foregut. Cell and Tissue Research 300, 153–163.
Duve, H., Johnsen, a H., Sewell, J.C., Scott, a G., Orchard, I., Rehfeld, J.F., Thorpe, A., 1992. Isolation, structure, and activity of -Phe-Met-Arg-Phe-NH2 neuropeptides (designated calliFMRFamides) from the blowfly *Calliphora vomitoria*. Proceedings of the National Academy of Sciences of the United States of America 89, 2326–2330.
Duve, H., Johnsen, a H., Scott, a G., Yu, C.G., Yagi, K.J., Tobe, S.S., Thorpe, A., 1993. Callatostatins: neuropeptides from the blowfly *Calliphora vomitoria* with sequence homology to cockroach allatostatins. Proceedings of the National Academy of Sciences of the United States of America 90, 2456–2460.
Ehmer, B., Gronenberg, W., 2002. Segregation of visual input to the mushroom bodies in the honeybee (*Apis mellifera*). Journal of Comparative Neurology 451, 362–373.
Elliott, K.L., Hehman, G.L., Stay, B., 2009. Isolation of the gene for the precursor of Phe-Gly-Leu-amide allatostatins in the termite *Reticulitermes flavipes*. Peptides 30, 855–860.
Elliott, K.L., Chan, K.K., Stay, B., 2010. Evidence for a Phe-Gly-Leu-amide-like allatostatin in the beetle *Tenebrio molitor*. Peptides 31, 402–407.
Erber, J., Masuhr, T., Menzel, R., 1980. Localization of short-term memory in the brain of the bee, *Apis mellifera*. Physiological Entomology 5, 343–358.
Espinoza, E., Carrigan, M., Thomas, S.G., Shaw, G., Edison, A.S., 2000. A statistical view of FMRFamide neuropeptide diversity. Molecular Neurobiology 21, 35–56.
Fahrbach, S.E., Dobrin, S., 2009. The how and why of structural plasticity in the honey bee brain. In: Dukas, R., Ratcliffe, J. (Eds.), Cognitive Ecology II. University of Chicago Press, pp. 37–48.
Fahrenbach, W.H., 1977. The brain of the horseshoe crab (*Limulus polyphemus*) II. Architecture of the corpora pedunculata. Tissue and Cell 9, 157–166.
Farris, S.M., Sinakevitch, I., 2003. Development and evolution of the insect mushroom bodies: towards the understanding of conserved developmental mechanisms in a higher brain center. Arthropod Structure and Development 32, 79–101.
Farris, S.M., Strausfeld, N.J., 2001. Development of laminar organization in the mushroom bodies of the cockroach: Kenyon cell proliferation, outgrowth, and maturation. Journal of Comparative Neurology 439, 331–351.
Farris, S.M., 2005a. Evolution of insect mushroom bodies: old clues, new insights. Arthropod Structure and Development 34, 211–234.
Farris, S.M., 2005b. Developmental organization of the mushroom bodies of *Thermobia domestica* (Zygentoma, Lepismatidae): insights into mushroom body evolution from a basal insect. Evolution and Development 7, 150–159.
Farris, S.M., 2008a. Structural, functional and developmental convergence of the insect mushroom bodies with higher brain centers of vertebrates. Brain, Behavior and Evolution 72, 1–15.
Farris, S.M., 2008b. Tritocerebral tract input to the insect mushroom bodies. Arthropod Structure and Development 37, 492–503.
Farris, S.M., 2008c. Evolutionary convergence of higher brain centers spanning the protostome–deuterostome boundary. Brain, Behavior and Evolution 72, 106–122.
Farris, S.M., 2011. Locusts provide clues to insect mushroom body function. Brain, Behavior and Evolution 77, 3–4.
Feng, G., Reale, V., Chatwin, H., Kennedy, K., Venard, R., Ericsson, C., Yu, K., Evans, P.D., Hall, L.M., 2003. Functional characterization of a neuropeptide F-like receptor from *Drosophila melanogaster*. European Journal of Neuroscience 18, 227–238.
Fiala, A., Müller, U., Menzel, R., 1999. Reversible downregulation of protein kinase A during olfactory learning using antisense technique impairs long-term memory formation in the honeybee, *Apis mellifera*. Journal of Neuroscience 19, 10125–10134.
Fiala, A., 2007. Olfaction and olfactory learning in *Drosophila*: recent progress. Current Opinion in Neurobiology 17, 720–726.
Flögel, J.H.L., 1876. Ueber den feineren Bau des Arthropodengehirns. Tageblatt der Versammlung Deutscher Naturforscher und Ärzte 49, 115–120.
Fukushima, R., Kanzaki, R., 2009. Modular subdivision of mushroom bodies by Kenyon cells in the silkmoth. Journal of Comparative Neurology 513, 315–330.
Fusé, M., Zhang, J.R., Partridge, E., Nachman, R.J., Orchard, I., Bendena, W.G., Tobe, S.S., 1999. Effects of an allatostatin and a myosuppressin on midgut carbohydrate enzyme activity in the cockroach *Diploptera punctata*. Peptides 20, 1285–1293.
Galizia, C.G., Rössler, W., 2010. Parallel olfactory systems in insects: anatomy and function. Annual Review of Entomology 55, 399–420.
Gard, A.L., Lenz, P.H., Shaw, J.R., Christie, A.E., 2009. Identification of putative peptide paracrines/hormones in the water flea *Daphnia pulex* (Crustacea; Branchiopoda; Cladocera) using transcriptomics and immunohistochemistry. General and Comparative Endocrinology 160, 271–287.
Gronenberg, W., Heeren, S., Hölldobler, B., 1996. Age-dependent and task-related morphological changes in the brain and the mushroom bodies of the ant *Camponotus floridanus*. Journal of Experimental Biology 199, 2011–2019.
Gronenberg, W., 1986. Physiological and anatomical properties of optical input-fibres to the mushroom body in the bee brain. Journal of Insect Physiology 32, 695–704.
Gronenberg, W., 2001. Subdivisions of hymenopteran mushroom body calyces by their afferent supply. Journal of Comparative Neurology 435, 474–489.
Grünewald, B., 1999. Physiological properties and response modulations of mushroom body feedback neurons during olfactory learning in the honeybee, *Apis mellifera*. Journal of Comparative Physiology A 185, 565–576.
Guo, F., Yi, W., Zhou, M., Guo, A., 2011. Go signaling in mushroom bodies regulates sleep in *Drosophila*. Sleep 34, 273–281.
Hammer, M., Menzel, R., 1998. Multiple sites of associative odor learning as revealed by local brain microinjections of octopamine in honeybees. Learning and Memory 5, 146–156.
Hammer, M., 1993. An identified neuron mediates the unconditioned stimulus in associative olfactory learning in honeybees. Nature 366, 59–63.
Hanström, B., 1928. Vergleichende Anatomie des Nervensystems der wirbellosen Tiere unter Berücksichtigung seiner Funktion. Springer, Berlin, 368 pp.
Hauser, F., Neupert, S., Williamson, M., Predel, R., Tanaka, Y., Grimmelikhuijzen, C.J.P., 2010. Genomics and peptidomics of neuropeptides and protein hormones present in the parasitic wasp *Nasonia vitripennis*. Journal of Proteome Research 9, 5296–5310.
Heisenberg, M., Borst, a, Wagner, S., Byers, D., 1985. *Drosophila* mushroom body mutants are deficient in olfactory learning. Journal of Neurogenetics 2, 1–30.
Heisenberg, M., 1998. What do the mushroom bodies do for the insect brain? An introduction. Learning and Memory 5, 1–10.
Heisenberg, M., 2003. Mushroom body memoir: from maps to models. Nature Reviews Neuroscience 4, 266–275.
Heuer, C.M., Loesel, R., 2008. Immunofluorescence analysis of the internal brain anatomy of *Nereis diversicolor* (Polychaeta, Annelida). Cell and Tissue Research 331, 713–724.
Heuer, C.M., Müller, C.H.G., Todt, C., Loesel, R., 2010. Comparative neuroanatomy suggests repeated reduction of neuroarchitectural complexity in Annelida. Frontiers in Zoology 7, 1–21.
Hewes, R.S., Taghert, P.H., 2001. Neuropeptides and neuropeptide receptors in the *Drosophila melanogaster* genome. Genome Research 11, 1126–1142.
Hildebrand, J.G., Shepherd, G.M., 1997. Mechanisms of olfactory discrimination: converging evidence for common principles across phyla. Annual Review of Neuroscience 20, 595–631.

Hinke, W., 1961. Das relative postembryonale Wachstum der Hirnteile von *Culex pipiens, Drosophila melanogaster* und *Drosophila*-Mutanten. Zeitschrift für Morphologie und Ökologie der Tiere 50, 81–118.
Hofer, S., Dircksen, H., Tollbäck, P., Homberg, U., 2005. Novel insect orcokinins: characterization and neuronal distribution in the brains of selected dicondylian insects. Journal of Comparative Neurology 490, 57–71.
Holmgren, N., 1916. Zur vergleichenden Anatomie des Gehirns von Polychaeten, Onychophoren, Xiphosuren, Arachniden, Crustaceen, Myriapoden und Insekten. Kungliga Svenska Vetenskaps Akademiens Handlingar 56, 1–303.
Homberg, U., Kingan, T.G., Hildebrand, J.G., 1990. Distribution of FMRFamide-like immunoreactivity in the brain and suboesophageal ganglion of the sphinx moth *Manduca sexta* and colocalization with SCPB-, BPP-, and GABA-like immunoreactivity. Cell and Tissue Research 259, 401–419.
Homberg, U., Brandl, C., Clynen, E., Schoofs, L., Veenstra, J.A., 2004. Mas-allatotropin/Lom-AG-myotropin I immunostaining in the brain of the locust, *Schistocerca gregaria*. Cell and Tissue Research 318, 439–457.
Homberg, U., 2002. Neurotransmitters and neuropeptides in the brain of the locust. Microscopy Research and Technique 56, 189–209.
Honegger, H., Schürmann, F., 1975. Cobalt sulphide staining of optic fibres in the brain of the cricket, *Gryllus campestris*. Cell and Tissue Research 225, 213–225.
Hong, S.-T., Bang, S., Hyun, S., Kang, J., Jeong, K., Paik, D., Chung, J., Kim, J., 2008. cAMP signalling in mushroom bodies modulates temperature preference behaviour in *Drosophila*. Nature 454, 771–775.
Huber, F., 1960. Untersuchen ueber die Funktion des Zentralnervensystems und insbesondere des Gehirnes bei der Fortbewegung und der Lauterzeugung der Grillen. Zeitschrift für Vergleichende Physiologie 44, 60–132.
Hummon, A.B., Richmond, T.A., Verleyen, P., Baggerman, G., Huybrechts, J., Ewing, M. a, Vierstraete, E., Rodriguez-Zas, S.L., Schoofs, L., Robinson, G.E., Sweedler, J.V., 2006. From the genome to the proteome: uncovering peptides in the *Apis* brain. Science 314, 647–649.
Huybrechts, J., Nusbaum, M., Bosch, L.V., Baggerman, G., De Loof, A., Schoofs, L., 2003. Neuropeptidomic analysis of the brain and thoracic ganglion from the Jonah crab, *Cancer borealis*. Biochemical and Biophysical Research Communications 308, 535–544.
Huybrechts, J., De Loof, A., Schoofs, L., 2004. Diapausing Colorado potato beetles are devoid of short neuropeptide FI and II. Biochemical and Biophysical Research Communications 317, 909–916.
Huybrechts, J., Bonhomme, J., Minoli, S., Prunier-Leterme, N., Dombrovsky, A., Abdel-Latief, M., Robichon, A., Veenstra, J.A., Tagu, D., 2010. Neuropeptide and neurohormone precursors in the pea aphid, Acyrthosiphon pisum. Insect Molecular Biology 19 (Suppl. 2), 87–95.
Ignell, R., Root, C.M., Birse, R.T., Wang, J.W., Nässel, D.R., Winther, A.M.E., 2009. Presynaptic peptidergic modulation of olfactory receptor neurons in *Drosophila*. Proceedings of the National Academy of Sciences of the United States of America 106, 13070–13075.
Ito, K., Suzuki, K., Estes, P., Ramaswami, M., Yamamoto, D., Strausfeld, N.J., 1998. The organization of extrinsic neurons and their implications in the functional roles of the mushroom bodies in *Drosophila melano- gaster* Meigen. Learning and Memory 5, 52–77.
Janssen, I., Schoofs, L., Spittaels, K., Neven, H., Vanden Broeck, J., Devreese, B., van Beeumen, J., Shabanowitz, J., Hunt, D.F., De Loof, A., 1996. Isolation of NEB-LFamide, a novel myotopic neuropeptide from the grey fleshfly. Molecular and Cellular Endocrinology 117, 157–165.
Johard, H.A.D., Muren, J.E., Nichols, R., Larhammar, D.S., Nassel, D.R., 2001. A putative tachykinin receptor in the cockroach brain: molecular cloning and analysis of expression by means of antisera to portions of the receptor protein. Brain Research 919, 94–105.
Johard, H.A.D., Enell, L.E., Gustafsson, E., Trifilieff, P., Veenstra, J.A., Nässel, D.R., 2008. Intrinsic neurons of drosophila mushroom bodies express short neuropeptide F: relations to extrinsic neurons expressing different neurotransmitters. Journal of Comparative Neurology 507, 1479–1496.
Johard, H.A.D., Yoishii, T., Dircksen, H., Cusumano, P., Rouyer, F., Helfrich-Förster, C., Nässel, D.R., 2009. Peptidergic clock neurons in *Drosophila*: ion transport peptide and short neuropeptide F in subsets of dorsal and ventral lateral neurons. Journal of Comparative Neurology 519, 59–73.
Joiner, W.J., Crocker, A., White, B.H., Sehgal, A., 2006. Sleep in *Drosophila* is regulated by adult mushroom bodies. Nature 441, 757–760.
Jortner, R.A., Farivar, S.S., Laurent, G., 2007. A simple connectivity scheme for sparse coding in an olfactory system. Journal of Neuroscience 27, 1659–1669.
Kataoka, H., Toschi, A., Li, J.P., Carney, R.L., Schooley, D.A., Kramer, S.J., 1989. Identification of an allatotropin from adult *Manduca sexta*. Science 243, 1481–1483.
Keenan, C.L., Coss, R., Koopowitz, H., 1981. Cytoarchitecture of primitive brains: golgi studies in flatworms. Journal of Comparative Neurology 195, 697–716.
Keene, A.C., Waddell, S., 2007. *Drosophila* olfactory memory: single genes to complex neural circuits. Nature Reviews: Neuroscience 8, 341–354.
Kim, Y.-J., Bartalska, K., Audsley, N., Yamanaka, N., Yapici, N., Lee, J.-Y., Kim, Y.-C., Markovic, M., Isaac, E., Tanaka, Y., Dickson, B.J., 2010. MIPs are ancestral ligands for the sex peptide receptor. Proceedings of the National Academy of Sciences of the United States of America 107, 6520–6525.
Kingan, T.G., Teplow, D.B., Phillips, J.M., Riehm, J.P., Rao, K.R., Hildebrand, J.G., Homberg, U., Kammer, A.E., Jardine, I., Griffin, P.R., 1990. A new peptide in the FMRFamide family isolated from the CNS of the hawkmoth, *Manduca sexta*. Peptides 11, 849–856.
Kingan, T., Shabanowitz, J., Hunt, D., Witten, J., 1996. Characterization of two myotrophic neuropeptides in the FMRFamide family from the segmental ganglia of the moth *Manduca sexta*: candidate neurohormones and neuromodulators. Journal of Experimental Biology 199, 1095–1104.
Klagges, B.R.E., Heimbeck, G., Godenschwege, T.A., Hofbauer, A., Pflugfelder, G.O., Reifegerste, R., Reisch, D., Schaupp, M., Buchner, S., Buchner, E., 1996. Invertebrate synapsins: a single gene codes for several isoforms in Drosophila. Journal of Neuroscience 16, 3154–3165.
Koladich, P.M., Cusson, M., Bendena, W.G., Tobe, S.S., McNeil, J.N., 2002. Cardioacceleratory effects of *Manduca sexta* allatotropin in the true armyworm moth, *Pseudaletia unipuncta*. Peptides 23, 645–651.
Kollmann, M., Huetteroth, W., Schachtner, J., 2011a. Brain organization in Collembola (springtails). Arthropod Structure and Development 40, 304–316.
Kollmann, M., Minoli, S., Bonhomme, J., Homberg, U., Schachtner, J., Tagu, D., Anton, S., 2011b. Revisiting the anatomy of the central nervous system of a hemimetabolous model insect species: the pea aphid *Acyrthosiphon pisum*. Cell and Tissue Research 343, 343–355.
Kolodziejczyk, A., Nässel, D.R., 2010. A novel wide-field neuron with branches in the lamina of the *Drosophila* visual system expresses myoinhibitory peptide and may be associated with the clock. Cell and Tissue Research 343, 357–369.
Kreissl, S., Strasser, C., Galizia, C.G., 2010. Allatostatin immunoreactivity in the honeybee brain. Journal of Comparative Neurology 518, 1391–1417.
Kutsch, W., Breidbach, O., 1994. Homologous structures in the nervous systems of Arthropoda. In: Evans, P.D. (Ed.), Advances in Insect Physiology 24. TJ Press Ltd, Padstow, Cornwall, pp. 1–113.
Lane, M.E., Kalderon, D., 1993. Genetic investigation of cAMP-dependent protein kinase function in Drosophila development. Genes and Development 7, 1229–1243.
Lange, A.B., Peeff, N.M., Orchard, I., 1994. Isolation, sequence, and bioactivity of FMRFamide-related peptides from the locust ventral nerve cord. Peptides 15, 1089–1094.
Lange, A.B., Bendena, W.G., Tobe, S.S., 1995. The effect of the thirteen Dip-allatostatins on myogenic and induced contractions of the cockroach (*Diploptera punctata*) hindgut. Journal of Insect Physiology 41, 581–588.
Lee, K.Y., Horodyski, F.M., Chamberlin, M.E., 1998. Inhibition of midgut ion transport by allatotropin (Mas-AT) and *Manduca* FLRFamides in the tobacco hornworm *Manduca sexta*. Journal of Experimental Biology 201, 3067–3074.
Lee, T., Lee, A., Luo, L., 1999. Development of the *Drosophila* mushroom bodies: sequential generation of three distinct types of neurons from a neuroblast. Development 126, 4065–4076.
Lee, K.-Y., Chamberlin, M.E., Horodyski, F.M., 2002. Biological activity of *Manduca sexta* allatotropin-like peptides, predicted products of tissue-specific and developmentally regulated alternatively spliced mRNAs. Peptides 23, 1933–1941.
Lee, K.-S., You, K.-H., Choo, J.-K., Han, Y.-M., Yu, K., 2004. *Drosophila* short neuropeptide F regulates food intake and body size. Journal of Biological Chemistry 279, 50781–50789.
Lenz, C., Williamson, M., Grimmelikhuijzen, C.J., 2000. Molecular cloning and genomic organization of an allatostatin preprohormone from *Drosophila melanogaster*. Biochemical and Biophysical Research Communications 273, 1126–1131.
Li, Y., Strausfeld, N.J., 1997. Morphology and sensory modality of mushroom body extrinsic neurons in the brain of the cockroach, *Periplaneta americana*. Journal of Comparative Neurology 387, 631–650.
Li, Y., Strausfeld, N.J., 1999. Multimodal efferent and recurrent neurons in the medial lobes of cockroach mushroom bodies. Journal of Comparative Neurology 409, 647–663.
Li, Y., Hernandez-Martinez, S., Noriega, F.G., 2004. Inhibition of juvenile hormone biosynthesis in mosquitoes: effect of allatostatic head factors, PISCF- and YXFGL-amide-allatostatins. Regulatory Peptides 118, 175–182.
Li, B., Predel, R., Neupert, S., Hauser, F., Tanaka, Y., Cazzamali, G., Williamson, M., Arakane, Y., Verleyen, P., Schoofs, L., Schachtner, J., Grimmelikhuijzen, C.J.P., Park, Y., 2008. Genomics, transcriptomics, and peptidomics of neuropeptides and protein hormones in the red flour beetle *Tribolium castaneum*. Genome Research 18, 113–122.
Liu, L., Wolf, R., Ernst, R., Heisenberg, M., 1999. Context generalization in *Drosophila* visual learning requires the mushroom bodies. Nature 400, 753–756.
Loesel, R., Heuer, C.M., 2010. The mushroom bodies – prominent brain centres of arthropods and annelids with enigmatic evolutionary origin. Acta Zoologica 91, 29–34.
Lorenz, M.W., Kellner, R., Hoffmann, K.H., 1995a. Identification of two allatostatins from the cricket, *Gryllus birnaculatus* de Geer (Ensifera, Gryllidae): additional members of a family of neuropeptides inhibiting juvenile hormone biosynthesis. Regulatory Peptides 57, 227–236.
Lorenz, M.W., Kellner, R., Hoffmann, K.H., 1995b. A family of neuropeptides that inhibit juvenile hormone biosynthesis in the cricket, *Gryllus bimaculatus*. Journal of Biological Chemistry 270, 21103–21108.
Lorenz, M.W., Kellner, R., Hoffmann, K.H., Gäde, G., 2000. Identification of multiple peptides homologous to cockroach and cricket allatostatins in the stick insect *Carausius morosus*. Insect Biochemistry and Molecular Biology 30, 711–718.
Mao, Z., Davis, R.L., 2009. Eight different types of dopaminergic neurons innervate the *Drosophila* mushroom body neuropil: anatomical and physiological heterogeneity. Frontiers in Neural Circuits 3, 5.
Marder, E., Bucher, D., 2007. Understanding circuit dynamics using the stomatogastric nervous system of lobsters and crabs. Annual Review of Physiology 69, 291–316.

Marder, E., Taylor, A.L., 2011. Multiple models to capture the variability in biological neurons and networks. Nature Neuroscience 14, 133–138.
Marder, E., Calabrese, R.L., Nusbaum, M.P., Trimmer, B., 1987. Distribution and partial characterization of FMRFamide-like peptides in the stomatogastric nervous systems of the rock crab, *Cancer borealis*, and the spiny lobster, *Panulirus interruptus*. Journal of Comparative Neurology 259, 150–163.
Martin, J., Ernst, R., Heisenberg, M., 1998. Mushroom bodies suppress locomotor activity in *Drosophila melanogaster*. Learning and Memory 5, 179–191.
Masek, P., Scott, K., 2010. Limited taste discrimination in *Drosophila*. Proceedings of the National Academy of Sciences of the United States of America 107, 14833–14838.
Matsumoto, S., Brown, M., Crim, J., Vigna, S., Lea, A., 1989. Isolation and primary structure of neuropeptides from the mosquito, *Aedes aegypti*, immunoreactive to FMRFamide antiserum. Insect Biochemistry 19, 277–283.
Maule, A.G., Shaw, C., Halton, D.W., Thim, L., Johnston, C.F., Fairweather, I., Buchanan, K.D., 1991. Neuropeptide F: a novel parasitic flatworm regulatory peptide from *Moniezia expansa* (Cestoda: Cyclophyllidea). Parasitology 102, 309–316.
Mcguire, S.E., Le, P.T., Davis, R.L., 2001. The role of *Drosophila* mushroom body signaling in olfactory memory. Science 10, 1126–1129.
McNeil, J.N., Tobe, S.S., 2001. Flights of fancy: possible roles of allatostatin and allatotropin in migration and reproductive success of *Pseudaletia unipuncta*. Peptides 22, 271–277.
Medina, L., Abellán, A., 2009. Development and evolution of the pallium. Seminars in Cell and Developmental Biology 20, 698–711.
Menzel, R., Giurfa, M., 2001. Cognitive architecture of a mini-brain: the honeybee. Trends in Cognitive Sciences 5, 62–71.
Menzel, R., Leboulle, G., Eisenhardt, D., 2006. Small brains, bright minds. Cell 124, 237–239.
Menzel, R., 2001. Searching for the memory trace in a mini-brain, the honeybee. Learning and Memory 8, 53–62.
Mertens, I., Meeusen, T., Huybrechts, R., De Loof, A., Schoofs, L., 2002. Characterization of the short neuropeptide F receptor from *Drosophila melanogaster*. Biochemical and Biophysical Research Communications 297, 1140–1148.
Meyering-Vos, M., 2003. Expression of allatostatins in the mediterranean field cricket, *Gryllus bimaculatus* de Geer (Ensifera, Gryllidae). Comparative Biochemistry and Physiology Part B: Biochemistry and Molecular Biology 136, 207–215.
Miao, Y., Waters, E.M., Witten, J.L., 1998. Developmental and regional-specific expression of FLRFamide peptides in the tobacco hornworm, *Manduca sexta*, suggests functions at ecdysis. Journal of Neurobiology 37, 469–485.
Mizunami, M., Weibrecht, J.M., Strausfeld, N.J., 1993. A new role for the insect mushroom bodies: place memory and motor control. In: Beer, R.D., Ritzmann, R., McKenna, T. (Eds.), Biological Neural Networks in Invertebrate Neuroethology and Robotics. Academic Press, Cambridge, MA, pp. 199–225.
Mizunami, M., Okada, R., Li, Y., Strausfeld, N.J., 1998a. Mushroom bodies of the cockroach: activity and identities of neurons recorded in freely moving animals. Journal of Comparative Neurology 402, 501–519.
Mizunami, M., Weibrecht, J.M., Strausfeld, N.J., 1998b. Mushroom bodies of the cockroach: their participation in place memory. Journal of Comparative Neurology 402, 520–537.
Muren, J.E., Lundquist, C.T., Nässel, D.R., 1995. Abundant distribution of locustatachykinin-like peptide in the nervous system and intestine of the cockroach *Leucophaea maderae*. Philosophical Transactions of the Royal Society B 348, 423–444.
Nambu, J.R., Murphy-Erdosh, C., Andrews, P.C., Feistner, G.J., Scheller, R.H., 1988. Isolation and characterization of a *Drosophila* neuropeptide gene. Neuron 1, 55–61.
Nässel, D.R., Homberg, U., 2006. Neuropeptides in interneurons of the insect brain. Cell and Tissue Research 326, 1–24.
Nässel, D.R., Winther, A.M.E., 2010. *Drosophila* neuropeptides in regulation of physiology and behavior. Progress in Neurobiology 92, 42–104.
Nässel, D.R., Enell, L.E., Santos, J.G., Wegener, C., Johard, H.A.D., 2008. A large population of diverse neurons in the *Drosophila* central nervous system expresses short neuropeptide F, suggesting multiple distributed peptide functions. BMC Neuroscience 9, 90.
Nässel, D.R., 1993. Insect myotropic peptides: differential distribution of locustatachykinin- and leucokinin-like immunoreactive neurons in the locust brain. Cell and Tissue Research 274, 27–40.
Nässel, D.R., 1999. Tachykinin-related peptides in invertebrates: a review. Peptides 20, 141–158.
Nässel, D.R., 2002. Neuropeptides in the nervous system of *Drosophila* and other insects: multiple roles as neuromodulators and neurohormones. Progress in Neurobiology 68, 1–84.
Neder, R., 1959. Allometrisches Wachstum von Hirnteilen bei drei verschieden grossen Schabenarten. Zoologische Jahrbücher. Abteilung für Anatomie und Ontogenie der Tiere 77, 411–464.
Nishino, H., Iwasaki, M., Yasuyama, K., Hongo, H., Watanabe, H., Mizunami, M., 2012. Visual and olfactory input segregation in the mushroom body calyces in a basal neopteran, the American cockroach. Arthropod Structure and Development 41, 3–16.
Nusbaum, M.P., Blitz, D.M., Swensen, A.M., Wood, D., Marder, E., 2001. The roles of co-transmission in neural network modulation. Trends in Neurosciences 24, 146–154.
Oeh, U., Lorenz, M.W., Dyker, H., Lösel, P., Hoffmann, K.H., 2000. Interaction between *Manduca sexta* allatotropin and manduca sexta allatostatin in the fall armyworm *Spodoptera frugiperda*. Insect Biochemistry and Molecular Biology 30, 719–727.
Oeh, U., 2003. Myotropic effect of helicokinins, tachykinin-related peptides and *Manduca sexta* allatotropin on the gut of *Heliothis virescens* (Lepidoptera: Noctuidae). Journal of Insect Physiology 49, 323–337.
Okada, R., Ikeda, J., 1999. Sensory responses and movement-related activities in extrinsic neurons of the cockroach mushroom bodies. Journal of Comparative Physiology A 185, 115–129.
Olsen, S.R., Bhandawat, V., Wilson, R.I., 2007. Excitatory interactions between olfactory processing channels in the *Drosophila* antennal lobe. Neuron 54, 89–103.
Ons, S., Sterkel, M., Diambra, L., Urlaub, H., Rivera-Pomar, R., 2010. Neuropeptide precursor gene discovery in the Chagas disease vector *Rhodnius prolixus*. Insect Molecular Biology 20, 29–44.
Orchard, I., Lange, A.B., Bendena, W.G., 2001. FMRFamide-related peptides: a multifunctional family of structurally related neuropeptides in insects. Advances in Insect Physiology 28, 267–329.
Ott, S.R., Rogers, S.M., 2010. Gregarious desert locusts have substantially larger brains with altered proportions compared with the solitarious phase. Proceedings of the Royal Society B 277, 3087–3096.
Otto, D., 1971. Untersuchungen zur zentralnervösen Kontrolle der Lauterzeugung von Grillen. Zeitschrift für Vergleichende Physiologie 74, 227–271.
Paemen, L., Tips, A., Schoofs, L., Proost, P., Van Damme, J., De Loof, A., 1991. Lom-AG-myotropin: a novel myotropic peptide from the male accessory glands of *Locusta migratoria*. Peptides 12, 7–10.
Paemen, L., Schoofs, L., Loof, A., 1992. Localization of Lom-AG-myotropin I-like substances in the male reproductive and nervous tissue of the locust, *Locusta migratoria*. Cell and Tissue Research 268, 91–97.
Park, C., Hwang, J.S., Kang, S.W., Lee, B.H., 2002. Molecular characterization of a cDNA from the silk moth *Bombyx mori* encoding *Manduca sexta* allatotropin peptide. Zoological Science 19, 287–292.
Pascual, N., Castresana, J., Valero, M.-L., Andreu, D., Bellés, X., 2004. Orcokinins in insects and other invertebrates. Insect Biochemistry and Molecular Biology 34, 1141–1146.
Paulk, A.C., Gronenberg, W., 2008. Higher order visual input to the mushroom bodies in the bee, *Bombus impatiens*. Arthropod Structure and Development 37, 443–458.
Peng, Y., Xi, W., Zhang, W., Zhang, K., Guo, A., 2007. Experience improves feature extraction in *Drosophila*. The Journal of Neuroscience 27, 5139–5145.
Perez-Orive, J., Mazor, O., Turner, G.C., Cassenaer, S., Wilson, R.I., Laurent, G., 2002. Oscillations and sparsening of odor representations in the mushroom body. Science 297, 359–365.
Petri, B., Homberg, U., Loesel, R., Stengl, M., 2002. Evidence for a role of GABA and Mas-allatotropin in photic entrainment of the circadian clock of the cockroach *Leucophaea maderae*. Journal of Experimental Biology 205, 1459–1469.
Pitman, J.L., McGill, J.J., Keegan, K.P., Allada, R., 2006. A dynamic role for the mushroom bodies in promoting sleep in *Drosophila*. Nature 441, 753–756.
Pratt, G.E., Farnsworth, D.E., Siegel, N.R., Fok, K.F., Feyereisen, R., 1989. Identification of an allatostatin from adult *Diploptera punctata*. Biochemical and Biophysical Research Communications 163, 1243–1247.
Predel, R., Neupert, S., 2007. Social behavior and the evolution of neuropeptide genes: lessons from the honeybee genome. BioEssays 29, 416–421.
Predel, R., Rapus, J., Eckert, M., 2001. Myoinhibitory neuropeptides in the american cockroach. Peptides 22, 199–208.
Predel, R., Neupert, S., Wicher, D., Gundel, M., Roth, S., Derst, C., 2004. Unique accumulation of neuropeptides in an insect: FMRFamide-related peptides in the cockroach, *Periplaneta americana*. European Journal of Neuroscience 20, 1499–1513.
Predel, R., Neupert, S., Roth, S., Derst, C., Nässel, D.R., 2005. Tachykinin-related peptide precursors in two cockroach species. FEBS Journal 272, 3365–3375.
Predel, R., Russell, W.K., Russell, D.H., Lopez, J., Esquivel, J., Nachman, R.J., 2008. Comparative peptidomics of four related hemipteran species: pyrokinins, myosuppressin, corazonin, adipokinetic hormone, sNPF, and periviscerokinins. Peptides 29, 162–167.
Predel, R., Neupert, S., Garczynski, S.F., Crim, J.W., Brown, M.R., Russell, W.K., Russell, D.H., Nachman, R.J., 2010. Neuropeptidomics of the mosquito *Aedes aegypti*. Journal of Proteome Research 1, 2006–2015.
Price, D., Greenberg, M., 1977. Structure of a molluscan cardioexcitatory neuropeptide. Science 197, 671.
Riehle, M.A., Garczynski, S.F., Crim, J.W., Hill, C. a, Brown, M.R., 2002. Neuropeptides and peptide hormones in *Anopheles gambiae*. Science 298, 172–175.
Roller, L., Yamanaka, N., Watanabe, K., Daubnerová, I., Žitňan, D., Kataoka, H., Tanaka, Y., 2008. The unique evolution of neuropeptide genes in the silkworm *Bombyx mori*. Insect Biochemistry and Molecular Biology 38, 1147–1157.
Rudwall, A.J., Sliwowska, J., Nässel, D.R., 2000. Allatotropin-like neuropeptide in the cockroach abdominal nervous system: myotropic actions, sexually dimorphic distribution and colocalization with serotonin. Journal of Comparative Neurology 428, 159–173.
Schachtner, J., Schmidt, M., Homberg, U., 2005. Organization and evolutionary trends of primary olfactory brain centers in Tetraconata (Crustacea + Hexapoda). Arthropod Structure and Development 34, 257–299.
Schildberger, K., 1984. Multimodal interneurons in the cricket brain: properties of identified extrinsic mushroom body cells. Journal of Comparative Physiology A 154, 71–79.
Schneider, L.E., Taghert, P.H., 1988. Isolation and characterization of a *Drosophila* gene that encodes multiple neuropeptides related to Phe-Met-Arg-Phe-NH2

(FMRFamide). Proceedings of the National Academy of Sciences of the United States of America 85, 1993–1997.
Schoofs, L., Clynen, E., Cerstiaens, a, Baggerman, G., Wei, Z., Vercammen, T., Nachman, R., De Loof, A., Tanaka, S., 2001. Newly discovered functions for some myotropic neuropeptides in locusts. Peptides 22, 219–227.
Schoofs, L., Holman, G.M., Hayes, T.K., Nachman, R.J., De Loof, A., 1990a. Locusta-tachykinins I and II, two novel insect neuropeptides with homology to peptides of the vertebrate tachykinin family. FEBS Letters 261, 340–397.
Schoofs, L., Holman, G.M., Hayes, T.K., Nachman, R.J., Kochansky, J.P., De Loof, A., 1990b. Locustatachykinins III and IV: two additional insect neuropeptides with homology to peptides of the vertebrate tachykinin family. Regulatory Peptides 31, 199–212.
Schoofs, L., Holman, G.M., Hayes, T.K., Nachman, R.J., De Loof, A., 1991. Isolation, identification and synthesis of locustamyoinhibiting peptide (LOM-MIP), a novel biologically active neuropeptide from *Locusta migratoria*. Regulatory Peptides 36, 111–119.
Schoofs, L., Veelaert, D., Vanden Broeck, J., De Loof, A., 1996. Immunocytochemical distribution of locustamyoinhibiting peptide (Lom-MIP) in the nervous system of *Locusta migratoria*. Regulatory Peptides 63, 171–179.
Schroll, C., Riemensperger, T., Bucher, D., Ehmer, J., Völler, T., Erbguth, K., Gerber, B., Hendel, T., Nagel, G., Buchner, E., Fiala, A., 2006. Light-induced activation of distinct modulatory neurons triggers appetitive or aversive learning in *Drosophila* larvae. Current Biology: CB 16, 1741–1747.
Schröter, U., Menzel, R., 2003. A new ascending sensory tract to the calyces of the honeybee mushroom body, the subesophageal-calycal tract. Journal of Comparative Neurology 465, 168–178.
Schürmann, F.W., Erber, J., 1990. FMRFamide-like immunoreactivity in the brain of the honeybee (*Apis mellifera*). A light- and electron microscopical study. Neuroscience 38, 797–807.
Schwaerzel, M., Monastirioti, M., Scholz, H., Friggi-Grelin, F., Birman, S., Heisenberg, M., 2003. Dopamine and octopamine differentiate between aversive and appetitive olfactory memories in *Drosophila*. The Journal of Neuroscience 23, 10495–10502.
Secher, T., Lenz, C., Cazzamali, G., Sørensen, G., Williamson, M., Hansen, G.N., Svane, P., Grimmelikhuijzen, C.J., 2001. Molecular cloning of a functional allatostatin gut/brain receptor and an allatostatin preprohormone from the silkworm *Bombyx mori*. Journal of Biological Chemistry 276, 47052–47060.
Settembrini, B.P., Villar, M.J., 2005. FMRFamide-like immunocytochemistry in the brain and subesophageal ganglion of *Triatoma infestans* (Insecta: Heteroptera). Coexpression with beta-pigment-dispersing hormone and small cardioactive peptide B. Cell and Tissue Research 321, 299–310.
Severini, C., Improta, G., Falconieri-Erspamer, G., Salvadori, S., Erspamer, V., 2002. The tachykinin peptide family. Pharmacological Reviews 54, 285–322.
Simões, P., Ott, S.R., Niven, J.E., 2011. Associative olfactory learning in the desert locust, *Schistocerca gregaria*. The Journal of Experimental Biology 214, 2495–2503.
Sinakevitch, I., Farris, S.M., Strausfeld, N.J., 2001. Taurine-, aspartate-, and glutamate-like immunoreactivity identifies chemically distinct subdivisions of kenyon cells in the cockroach mushroom body. Journal of Comparative Neurology 439, 352–367.
Sinakevitch, I., Sjöholm, M., Hansson, B.S., Strausfeld, N.J., 2008. Global and local modulatory supply to the mushroom bodies of the moth *Spodoptera littoralis*. Arthropod Structure and Development 37, 260–272.
Sinakevitch, I., Grau, Y., Strausfeld, N.J., Birman, S., 2010. Dynamics of glutamatergic signaling in the mushroom body of young adult *Drosophila*. Neural Development 5, 10.
Siviter, R.J., Coast, G.M., Winther, A.M., Nachman, R.J., Taylor, C. a, Shirras, A.D., Coates, D., Isaac, R.E., Nässel, D.R., 2000. Expression and functional characterization of a *Drosophila* neuropeptide precursor with homology to mammalian preprotachykinin A. Journal of Biological Chemistry 275, 23273–23280.
Sjöholm, M., Sinakevitch, I., Ignell, R., Strausfeld, N.J., Hansson, B.S., 2005. Organization of Kenyon cells in subdivisions of the mushroom bodies of a lepidopteran insect. The Journal of Comparative Neurology 491, 290–304.
Sjöholm, M., Sinakevitch, I., Strausfeld, N.J., Ignell, R., Hansson, B.S., 2006. Functional division of intrinsic neurons in the mushroom bodies of male *Spodoptera littoralis* revealed by antibodies against aspartate, taurine, FMRF-amide, Mas-allatotropin and DC0. Arthropod Structure and Development 35, 153–168.
Skiebe, P., Dreger, M., Meseke, M., Evers, J.F., Hucho, F., 2002. Identification of orcokinins in single neurons in the stomatogastric nervous system of the crayfish, *Cherax destructor*. Journal of Comparative Neurology 444, 245–259.
Sokoloff, A., 1966. The Genetics of Tribolium and Related Species. In: Advances in Genetics, Suppl. 1. Academic Press, New York.
Spittaels, K., Vankeerberghen, A., Schoofs, L., Proost, P., Van Damme, J., De Loof, A., 1996a. Isolation and characterization of *Locusta migratoria* accessory gland myotropin I (Lom-Ag-MT-I) from the brain of the colorado potato beetle, *Leptinotarsa decemlineata*. Archives of Insect Biochemistry and Physiology 31, 149–155.
Spittaels, K., Verhaert, P., Shaw, C., Johnston, R.N., Devreese, B., Van Beeumen, J., De Loof, A., 1996b. Insect neuropeptide F (NPF)-related peptides: isolation from colorado potato beetle (*Leptinotarsa decemlineata*) brain. Insect Biochemistry and Molecular Biology 26, 375–382.
Stangier, J., Hilbich, C., Burdzik, S., Keller, R., 1992. Orcokinin: a novel myotropic peptide from the nervous system of the crayfish, *Orconectes limosus*. Peptides 13, 859–864.
Stay, B., Tobe, S.S., 2007. The role of allatostatins in juvenile hormone synthesis in insects and crustaceans. Annual Review of Entomology 52, 277–299.
Strausfeld, N.J., Li, Y., 1999. Representation of the calyces in the medial and vertical lobes of cockroach mushroom bodies. Journal of Comparative Neurology 409, 626–646.
Strausfeld, N.J., Buschbeck, E.K., Gomez, R.S., 1995. The arthropod mushroom body: its functional roles, evolutionary enigmas and mistaken identities. In: Breidbach, O., Kutsch, W. (Eds.), The Nervous Systems of Invertebrates: An Evolutionary and Comparative Approach. Birkhäuser, Basel, pp. 349–381.
Strausfeld, N.J., Homberg, U., Kloppenberg, P., 2000. Parallel organization in honey bee mushroom bodies by peptidergic kenyon cells. Journal of Comparative Neurology 424, 179–195.
Strausfeld, N.J., Strausfeld, C.M., Stowe, S., Rowell, D., Loesel, R., 2006. The organization and evolutionary implications of neuropils and their neurons in the brain of the onychophoran *Euperipatoides rowelli*. Arthropod Structure and Development 35 (3), 169–196.
Strausfeld, N.J., Sinakevitch, I., Brown, S.M., Farris, S.M., 2009. Ground plan of the insect mushroom body: functional and evolutionary implications. Journal of Comparative Neurology 513, 265–291.
Strausfeld, N.J., 1998. Crustacean – insect relationships: the use of brain characters to derive phylogeny amongst segmented invertebrates. Brain, Behavior and Evolution 52, 186–206.
Strausfeld, N.J., 2002. Organization of the honey bee mushroom body: representation of the calyx within the vertical and gamma lobes. Journal of Comparative Neurology 450, 4–33.
Svidersky, V.L., Plotnikova, S.I., 2004. On structural-functional organization of dragonfly mushroom bodies and some general considerations about purpose of these formations. Journal of Evolutionary Biochemistry and Physiology 40, 608–624.
Taghert, H., Schneider, L.E., 1990. Interspecific comparison of a *Drosophila* gene encoding FMRFamide-related neuropeptides. Journal of Neuroscience 10, 1929–1942.
Takeuchi, H., Yasuda, A., Yasuda-Kamatani, Y., Sawata, M., Matsuo, Y., Kato, A., Tsujimoto, A., Nakajima, T., Kubo, T., 2004. Prepro-tachykinin gene expression in the brain of the honeybee *Apis mellifera*. Cell and Tissue Research 316, 281–293.
Tanaka, N.K., Tanimoto, H., Ito, K., 2008. Neuronal assemblies of the *Drosophila*. Journal of Comparative Neurology 508, 711–755.
Tang, S., Guo, A., 2001. Choice behavior of *Drosophila* facing contradictory visual cues. Science 294, 1543–1547.
Tomer, R., Denes, A.S., Tessmar-Raible, K., Arendt, D., 2010. Profiling by image registration reveals common origin of annelid mushroom bodies and vertebrate pallium. Cell 142, 800–809.
Truesdell, P.F., Koladich, P.M., Kataoka, H., Kojima, K., Suzuki, A., McNeil, J., Mizoguchi, A., Tobe, S.S., Bendena, W.G., 2000. Molecular characterization of a cDNA from the true armyworm *Pseudaletia unipuncta* encoding *Manduca sexta* allatotropin peptide. Insect Biochemistry and Molecular Biology 30, 691–702.
Turner, R.S., 1946. Observations on the central nervous system of *Leptoplana acticola*. Journal of Comparative Neurology 85, 53–65.
Unoki, S., Matsumoto, Y., Mizunami, M., 2005. Participation of octopaminergic reward system and dopaminergic punishment system in insect olfactory learning revealed by pharmacological study. European Journal of Neuroscience 22, 1409–1416.
Utz, S., Schachtner, J., 2005. Development of A-type allatostatin immunoreactivity in antennal lobe neurons of the sphinx moth *Manduca sexta*. Cell and Tissue Research 320, 149–162.
Utz, S., Huetteroth, W., Wegener, C., Predel, R., Schachtner, J., 2007. Direct peptide profiling of lateral cell groups of the antennal lobes of *Manduca sexta* reveals specific composition and changes in neuropeptide expression during development. Developmental Neurobiology 67, 764–777.
Van Loy, T., Vandersmissen, H.P., Poels, J., Van Hiel, M.B., Verlinden, H., Vanden Broeck, J., 2010. Tachykinin-related peptides and their receptors in invertebrates: a current view. Peptides 31, 520–524.
Vanden Broeck, J., 2001. Neuropeptides and their precursors in the fruitfly, *Drosophila melanogaster*. Peptides 22, 241–254.
Veelaert, D., Schoofs, L., Tobe, S.S., Yu, C.G., Vullings, H.G.B., Couillaud, F., Loof, A.D., 1995. Immunological evidence for an allatostatin-like neuropeptide in the central nervous system of *Schistocerca gregaria*, *Locusta migratoria* and *Neobellieria bullata*. Cell and Tissue Research 279, 601–611.
Veenstra, J.A., Costes, L., 1999. Isolation and identification of a peptide and its cDNA from the mosquito *Aedes aegypti* related to *Manduca sexta* allatotropin. Peptides 20, 1145–1151.
Veenstra, J.A., Hagedorn, H.H., 1993. Sensitive enzyme immunoassay for *Manduca* allatotropin and the existence of an allatotropin-immunoreactive peptide in *Periplaneta americana*. Archives of Insect Biochemistry and Physiology 23, 99–109.
Veenstra, J.A., Lambrou, G., 1995. Isolation of a novel RFamide peptide from the midgut of the American cockroach, *Periplaneta americana*. Biochemical and Biophysical Research Communications 213, 519–524.
Veenstra, J.A., Lehman, H.K., Davis, N.T., 1994. Short communication: Allatotropin is a cardioaccelatory peptide in *Manduca sexta*. Journal of Experimental Biology 188, 347–354.
Veenstra, J.A., Noriega, F.G., Graf, R., Feyereisen, R., 1997. Identification of three allatostatins and their cDNA from the mosquito *Aedes aegypti*. Peptides 18, 937–942.
Verleyen, P., Huybrechts, J., Baggerman, G., Lommel, A., van, De Loof, A., Schoofs, L., 2004. SIFamide is a highly conserved neuropeptide: a comparative study in different insects. Biochemical and Biophysical Research Communications 320, 334–341.

Verleyen, P., Huybrechts, J., Schoofs, L., 2009. SIFamide illustrates the rapid evolution in arthropod neuropeptide research. General and Comparative Endocrinology 162, 27–35.
Vitzthum, H., Homberg, U., Agricola, H., 1996. Distribution of Dip-Allatostatin I-like immunoreactivity in the brain of the locust *Schistocerca gregaria* with detailed analysis of immunostaining in the central complex. Journal of Comparative Neurology 369, 419–437.
Waddell, S., Armstrong, J.D., Kitamoto, T., Kaiser, K., Quinn, W.G., 2000. The amnesiac gene product is expressed in two neurons in the *Drosophila* brain that are critical for memory. Cell 103, 805–813.
Wadepuhl, M., 1983. Control of grasshopper singing behavior by the brain responses to electrical stimulation. Zeitschrift für Tierpsychologie 63, 173–200.
Walker, R.J., Papaioannou, S., Holden-Dye, L., 2009. A review of FMRFamide- and RFamide-like peptides in metazoa. Invertebrate Neuroscience: IN 9, 111–153.
Wasielewski, O., Skonieczna, M., Kodrík, D., 2009. Role of allatostatin-like factors from the brain of *Tenebrio molitor* females. Archives of Insect Biochemistry and Physiology 71, 223–235.
Weiss, M.J., 1981. Structural patterns in the corpora pedunculata of orthoptera: a reduced silver analysis. Journal of Comparative Neurology 203, 515–553.
Wessnitzer, J., Webb, B., 2006. Multimodal sensory integration in insects - towards insect brain control architectures. Bioinspiration and Biomimetics 1, 63–75.
Williamson, M., Lenz, C., Winther, A.M., Nässel, D.R., Grimmelikhuijzen, C.J., Winther, M.E., 2001. Molecular cloning, genomic organization, and expression of a B-type (cricket-type) allatostatin preprohormone from *Drosophila melanogaster*. Biochemical and Biophysical Research Communications 281, 544–550.
Winther, A.M.E., Acebes, A., Ferrús, A., 2006. Tachykinin-related peptides modulate odor perception and locomotor activity in *Drosophila*. Molecular and Cellular Neurosciences 31, 399–406.
Withers, G.S., Fahrbach, S.E., Robinson, G.E., 1993. Selective neuroanatomical plasticity and division of labour in the honeybee. Nature 364, 238–240.
Woodhead, A.P., Stay, B., Seidel, S.L., Khan, M.A., Tobe, S.S., 1989. Primary structure of four allatostatins: neuropeptide inhibitors of juvenile hormone synthesis. Proceedings of the National Academy of Sciences of the United States of America 86, 5997–6001.
Xi, W., Peng, Y., Guo, J., Ye, Y., Zhang, K., Yu, F., Guo, A., 2008. Mushroom bodies modulate salience-based selective fixation behavior in *Drosophila*. European Journal of Neuroscience 27, 1441–1451.
Yagi, K.J., Kwok, R., Chan, K.K., Setter, R.R., Myles, T.G., Tobe, S.S., Stay, B., 2005. Phe-Gly-Leu-amide allatostatin in the termite *Reticulitermes flavipes*: content in brain and corpus allatum and effect on juvenile hormone synthesis. Journal of Insect Physiology 51, 357–365.
Yasuda, A., Yasuda-Kamatani, Y., Nozaki, M., Nakajima, T., 2004. Identification of GYRKPPFNGSIFamide (crustacean-SIFamide) in the crayfish *Procambarus clarkii* by topological mass spectrometry analysis. General and Comparative Endocrinology 135, 391–400.
Yasuda-Kamatani, Y., Yasuda, A., 2000. Identification of orcokinin gene-related peptides in the brain of the crayfish *Procambarus clarkii* by the combination of MALDI-TOF and on-line capillary HPLC/Q-Tof mass spectrometries and molecular cloning. General and Comparative Endocrinology 118, 161–172.
Yew, J.Y., Wang, Y., Barteneva, N., Dikler, S., Kutz-Naber, K.K., Li, L., Kravitz, E.A., 2009. Analysis of neuropeptide expression and localization in adult *Drosophila melanogaster* central nervous system by affinity cell-capture mass spectrometry. Journal of Proteome Research 8, 1271–1284.
Zhang, K., Guo, J.Z., Peng, Y., Xi, W., Guo, A., 2007. Dopamine-mushroom body circuit regulates saliency-based decision-making in *Drosophila*. Science 316, 1901–1904.
Zhao, X., Coptis, V., Farris, S.M., 2008. Metamorphosis and adult development of the mushroom bodies of the red flour beetle, *Tribolium castaneum*. Developmental Neurobiology 68, 1487–1502.

Appendix A. Supplementary data

The following are the Supplementary data related to this article.

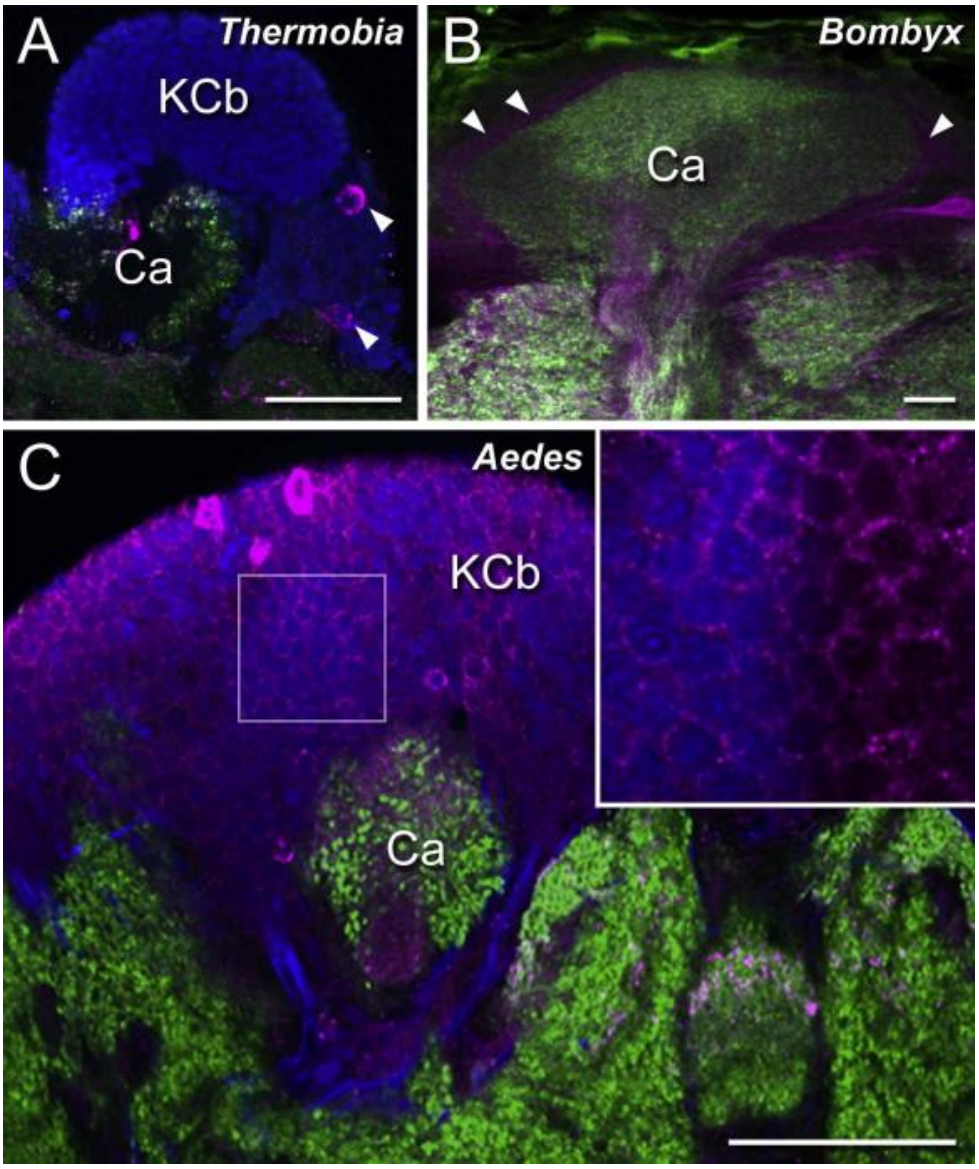

Supplementary Fig. 1.

Immunoreactivity of Kenyon cell bodies towards different neuropeptide antisera. (A) MIP-like immunoreactivity in the brain of the apterygote *Thermobia domestica*. Individual immunostained somata (arrowheads) are located medial to the clearly demarcated aggregation of Kenyon cell bodies (KCb) capping the calycal neuropil (Ca); immunoreactive Kenyon cell somata are not evident. (B) Allatotropin-like immunoreactivity in the calyx region of the silkmoth *Bombyx mori*. The antiserum produces pronounced staining in the peduncle and lobes of the mushroom body (compare Fig.4D), but immunolabeling of Kenyon cell somata is rather faint and can only be observed in a thin cortex of cell bodies (arrowheads). (C) sNPF-like immunoreactivity in the calyx region of the mosquito *Aedes aegypti*. The antiserum labels intrinsic mushroom body neurons, producing immuostaining in the Kenyon cell bodies, the peduncle, and the lobes (refer to Fig. 8). As Kenyon cell somata are almost completely occupied by the cell nuclei, immunostaining in this region is limited to a thin halo surrounding each nucleus, resulting in a reticulated staining pattern (insert). blue: DAPI-labeled cell nuclei, green: synapsin-immunoreactivity, magenta: MIP-like (A), allatotropin-like (B), or sNPF-like (C) immunoreactivity. Scale bars: 50 µm.

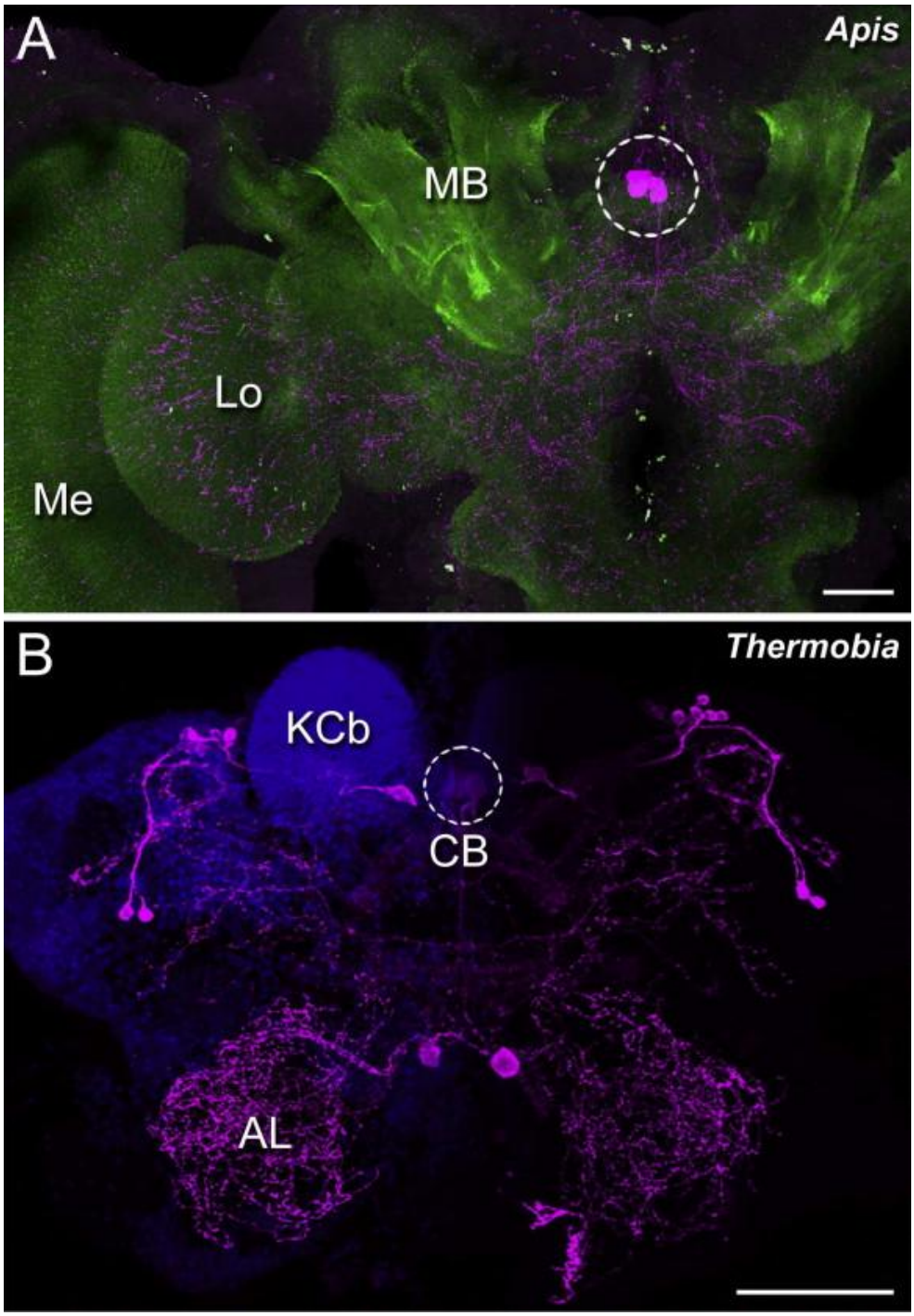

Supplementary Fig. 2.

(A) Maximum projection of SIFamide-like immunoreactivity (magenta) and anti-synapsin staining (green) in the brain of the honeybee, Apis mellifera. Four immunostained cell bodies located in the pars intercerebralis (dashed circle) provide ramifications that extend throughout the brain and supply most of the major neuropils, including the mushroom bodies (MB), the lobula (Lo) and the medulla (Me). (B) Maximum projection of SIFamide-like immunoreactivity (magenta) and cell nuclei labeling (blue, only left side) in the brain of the apterygote Thermobia domestica. Comparatively large immunopositive somata are located in the pars intercerebralis (dashed circle) and medial to the antennal lobes (AL). Smaller somata reside lateral to the tightly packed Kenyon cell bodies (KCb) and in the lateral protocerebrum. Immunostained fibers form arborizations throughout the brain, innervating major neuropils like the antennal lobes and the central body (CB). Scale bars: 100 µm.

Chapter 6:

Discovery of a Novel Insect Neuropeptide Signaling System Closely Related to the Insect Adipokinetic Hormone and Corazonin Hormonal System

Discovery of a Novel Insect Neuropeptide Signaling System Closely Related to the Insect Adipokinetic Hormone and Corazonin Hormonal Systems*[S]

Received for publication, July 16, 2009, and in revised form, December 4, 2009 Published, JBC Papers in Press, January 12, 2010, DOI 10.1074/jbc.M109.045369

Karina K. Hansen[‡1], Elisabeth Stafflinger[‡1], Martina Schneider[‡], Frank Hauser[‡], Giuseppe Cazzamali[‡], Michael Williamson[‡], Martin Kollmann[§], Joachim Schachtner[§], and Cornelis J. P. Grimmelikhuijzen[‡2]

From the [‡]Center for Functional and Comparative Insect Genomics, Department of Biology, University of Copenhagen, DK-2100 Copenhagen, Denmark and the [§]Department of Animal Physiology, University of Marburg, D-35032 Marburg, Germany

Neuropeptides and their G protein-coupled receptors (GPCRs) play a central role in the physiology of insects. One large family of insect neuropeptides are the adipokinetic hormones (AKHs), which mobilize lipids and carbohydrates from the insect fat body. Other peptides are the corazonins that are structurally related to the AKHs but represent a different neuropeptide signaling system. We have previously cloned an orphan GPCR from the malaria mosquito *Anopheles gambiae* that was structurally intermediate between the *A. gambiae* AKH and corazonin GPCRs. Using functional expression of the receptor in cells in cell culture, we have now identified the ligand for this orphan receptor as being pQVTFSRDWNAamide, a neuropeptide that is structurally intermediate between AKH and corazonin and that we therefore named ACP (AKH/corazonin-related peptide). ACP does not activate the *A. gambiae* AKH and corazonin receptors and, vice versa, AKH and corazonin do not activate the ACP receptor, showing that the ACP/receptor couple is an independent and so far unknown peptidergic signaling system. Because ACP is structurally intermediate between AKH and corazonin and the ACP receptor between the AKH and corazonin receptors, this is a prominent example of receptor/ligand co-evolution, probably originating from receptor and ligand gene duplications followed by mutations and evolutionary selection, thereby yielding three independent hormonal systems. The ACP signaling system occurs in the mosquitoes *A. gambiae*, *Aedes aegypti*, and *Culex pipiens* (Diptera), the silkworm *Bombyx mori* (Lepidoptera), the red flour beetle *Tribolium castaneum* (Coleoptera), the parasitic wasp *Nasonia vitripennis* (Hymenoptera), and the bug *Rhodnius prolixus* (Hemiptera). However, the ACP system is not present in 12 *Drosophila* species (Diptera), the honeybee *Apis mellifera* (Hymenoptera), the pea aphid *Acyrthosiphon pisum* (Hemiptera), the body louse *Pediculus humanus* (Phthiraptera), and the crustacean *Daphnia pulex*, indicating that it has been lost several times during arthropod evolution. In particular, this frequent loss of hormonal systems is unique for arthropods compared with vertebrates.

Adipokinetic hormone (AKH)[3] is an insect neuropeptide produced by the corpora cardiaca, a neuroendocrine organ closely associated with the insect brain (1). During high physical activities such as flight and intense locomotion, AKH is released into the circulation and transported to the fat body, where it binds to its G protein-coupled receptors (GPCRs) (2). Activation of these GPCRs stimulates the release of carbohydrates (trehalose) and lipids, which are needed to fuel the high physical activity of the insect (1). AKHs and their GPCRs, however, are also involved in hemolymph carbohydrate homeostasis by releasing trehalose under nonstress conditions, a process that in *Drosophila* larvae is counteracted by insulin-like peptides and the insulin receptor, which decrease hemolymph trehalose concentrations. Thus, AKH and insulin in insects act comparably to glucagon and insulin in mammals during blood sugar homeostasis (3).

The AKHs are a large family of small, structurally related peptides, all being 8–10 amino acid residues long (1). The structure of the AKH peptide produced by the malaria mosquito *Anopheles gambiae* (4) is shown in Fig. 1. AKHs occur in all insects investigated so far, with some insects producing more than one AKH (1, 5). AKH peptides also occur in crustaceans, where they are named red pigment-concentrating hormone, because of their function in color adaptation (1).

The insect corazonins are widespread in insects and are undecapeptides that are structurally related to the AKHs, which is illustrated for the *A. gambiae* corazonin in Fig. 1. The insect corazonin receptors have recently been identified (6, 7). They do not cross-react with AKHs and the AKH receptors do not cross-react with corazonins, showing that these are two independent hormonal systems (2, 6). Phylogenetic tree analyses show that not only the AKH and cora-

* This work was supported by the Danish Research Agency, Novo Nordisk Foundation, and Deutsche Forschungsgemeinschaft.

[S] The on-line version of this article (available at http://www.jbc.org) contains supplemental Figs. S1–S5 and Tables S1 and S2.

The nucleotide sequence(s) reported in this paper has been submitted to the GenBank™/EBI Data Bank with accession number(s) EU138885, EU138886, FJ158649, FJ532055, FJ554531, and GQ217536.

[1] Both authors contributed equally to this work.

[2] To whom correspondence should be addressed: E-mail: cgrimmelikhuijzen@bio.ku.dk.

[3] The abbreviations used are: AKH, adipokinetic hormone; Aa, *Aedes aegypti*; ACP, AKH/corazonin-related peptide; ACPR, ACP receptor; AKHR, AKH receptor; Ag, *Anopheles gambiae*; Am, *Apis mellifera*; Bm, *Bombyx mori*; CCAP, crustacean cardioactive peptide; CCAPR, CCAP receptor; CHO, Chinese hamster ovary; Cp, *Culex pipiens*; CRZR, corazonin receptor; Dm, *Drosophila melanogaster*; EGFP, enhanced green fluorescent protein; GPCR, G protein-coupled receptor; Nv, *Nasonia vitripennis*; qPCR, quantitative PCR; Tc, *Tribolium castaneum*; PBS, phosphate-buffered saline; RACE, rapid amplification of cDNA ends; Ag, *Anopheles gambiae*; Bm, *Bombyx mori*; On, *Ostrinia nubilalis*; Rp, *Rhodnius prolixus*.

Neuropeptide name	Amino acid sequence
AKH	pQLTF--TPAW--amide
ACP (AKH/corazonin-related peptide)	pQVTF--SRDWNAamide
Corazonin	pQ-TFQYSRGWTNamide

FIGURE 1. **Comparison between AKH, corazonin, and ACP (AKH/corazonin-related peptide) from the malaria mosquito *A. gambiae*.** Residues that are identical between all three peptides are highlighted in *red*. Amino acid residues that are identical between ACP and corazonin only are highlighted in *green*. A pair of conserved (not identical but very similar) residues between AKH and ACP is highlighted in *blue*.

zonin neuropeptides but also the AKH and corazonin receptors are closely related, suggesting co-evolution of receptors and ligands in a process, where the ancestor receptor and neuropeptide genes have duplicated. This is followed by mutations and evolutionary selection, leading to two independent hormonal systems each with its own physiological role (Fig. 2) (6–9).

The physiological roles of corazonin in insects are, so far, not well understood. The peptide increases heartbeat in cockroaches (10) and induces color change (darkening) associated with starvation, swarming, and migration in crowded locust populations (11), and in some insects, it is involved in the control of motor behavior associated with molting (12). These findings could perhaps mean that corazonin is also involved in the management of stress situations, suggesting that AKHs and corazonins have specialized in the control of different aspects of stress or high physical activities, which would fit well with the receptor/ligand co-evolution hypothesis mentioned above.

In an attempt to understand the function and evolution of AKH and corazonin receptors, we have annotated these and related GPCRs in insects with a sequenced genome (8, 9) and subsequently cloned and characterized many of them. In this process, we have also cloned an AKH and a corazonin receptor from the malaria mosquito *A. gambiae* and characterized them as receptors specifically activated by *A. gambiae* AKH and corazonin, respectively (13). In addition to these two receptors, however, a third *A. gambiae* receptor was annotated and cloned that was closely related to the AKH and corazonin receptors but could not be activated by AKH, corazonin, or any other peptide from our peptide library (13). In this paper, we identify the ligand for this orphan receptor as a peptide that is structurally intermediate between AKH and corazonin, and which we name AKH/corazonin-related peptide (ACP; see Fig. 1). Because the ACP receptor is also structurally intermediate between the AKH and corazonin receptors, this finding is a prominent example of receptor/ligand co-evolution (Fig. 2). Furthermore, we show that the novel ACP/receptor couple is widely occurring in insects, suggesting that it is an important insect signaling system.

EXPERIMENTAL PROCEDURES

Animals—*A. gambiae* (strain G-3) was kindly supplied by Dr. Robert E. Sinden, Imperial College, London, UK. *Bombyx mori* (hybrid strain of Lyon 200 BA and Lyon 300 AB) was a kind gift from Dr. Søren Wilken Rasmussen (Carlsberg Laboratory, Copenhagen, Denmark); *Tribolium castaneum* (strain GA-1) was a generous gift from Prof. Martin Klingler (University of Erlangen-Nürnberg, Germany). A transgenic *T. castaneum* strain, where the central nervous system is marked with fluorescent color,[4] was kindly supplied by Prof. Gregor Bucher (University of Göttingen, Germany) and Dr. Michalis Averof (Foundation for Research and Technology, Crete, Greece). *Nasonia vitripennis* was a kind gift from Prof. Jack Werren (University of Rochester). All insects have been cultured in our laboratory, using standardized conditions.

cDNA Cloning, PCR, and qPCR—For PCR, total RNA was isolated using TRIzol reagent (Invitrogen) or the NucleoSpin RNA II kit (Macherey-Nagel). cDNA was synthesized and amplified using the SMART RACE cDNA amplification kit (Clontech) or, for 5′RACE, the FirstChoice RLM-RACE kit (Ambion).

The cloning of the *A. gambiae* ACP receptor (Ag-ACPR-A) has been published previously (13). The coding sequence of *A. gambiae* ACPR-B was amplified using the sense primer 5′-CCGCTAGCGCCGCCATGTACCTGGCAGCCGGCTTA-3′ (the underlined nucleotides correspond to nucleotide positions 1–21 of supplemental Fig. S1) and the antisense primer 5′-CCGCTAGCCTAAATGAGATGTTTTTCAAGATACTC-3′ (the underlined nucleotides correspond to nucleotide positions 1399–1425 of supplemental Fig. S1).

The coding sequence of the *T. castaneum* ACP preprohormone was amplified using the sense primer 5′-GCTATATAAAGTTGCTAGTCCGCC-3′ and the antisense primer 5′-TTATCGTCGGCCACTGAAAAT-3′. The coding sequence of the *T. castaneum* ACP receptor was amplified using the sense primer 5′-CCGCTAGCCGCGCGATGCAAGCGGTTGGTAAAATG-3′ (the underlined nucleotides correspond to nucleotide positions 1–21 of supplemental Fig. S3) and the antisense primer 5′-CCGCTAGCCTATAAAACAGCAGAACTGTAATAATC-3′ (the underlined nucleotides correspond to nucleotide positions 1348–1374 of supplemental Fig. S3). 3′RACE of the *T. castaneum* ACP receptor was made with the sense primer 5′-GAAAGGGCTAGGAGCAGAACC-3′ (corresponding to the nucleotide positions 799–819 of supplemental Fig. S3) followed by nested sense primer 5′-GCAGAACCTTAAGGATGACCATC-3′ (corresponding to the nucleotide positions 812–834 of supplemental Fig. S3). 5′RACE of the *T. castaneum* ACP receptor was made with the antisense primer 5′-GCCAGTCAATCTCCAGCCAACCTCG-3′ (corresponding to the nucleotide positions 300–324 of supplemental Fig. S3) followed by the nested sense primer 5′-AATCAAATCAGCGATGGCAAGATGGCG-3′ (corresponding to nucleotide positions 250–277 of supplemental Fig. S3), using the FirstChoice RLM-RACE kit (Ambion).

All PCR products were cloned into pCR4-TOPO (Invitrogen) using the TOPO TA cloning kit (Invitrogen) and sequenced. The PCR product of the receptor coding sequence was subcloned into the pIRES2-EGFP expression vector (Clontech) using the Rapid DNA ligation kit (Roche Applied Science) and sequenced.

[4] M. Averof and G. Bucher, unpublished data.

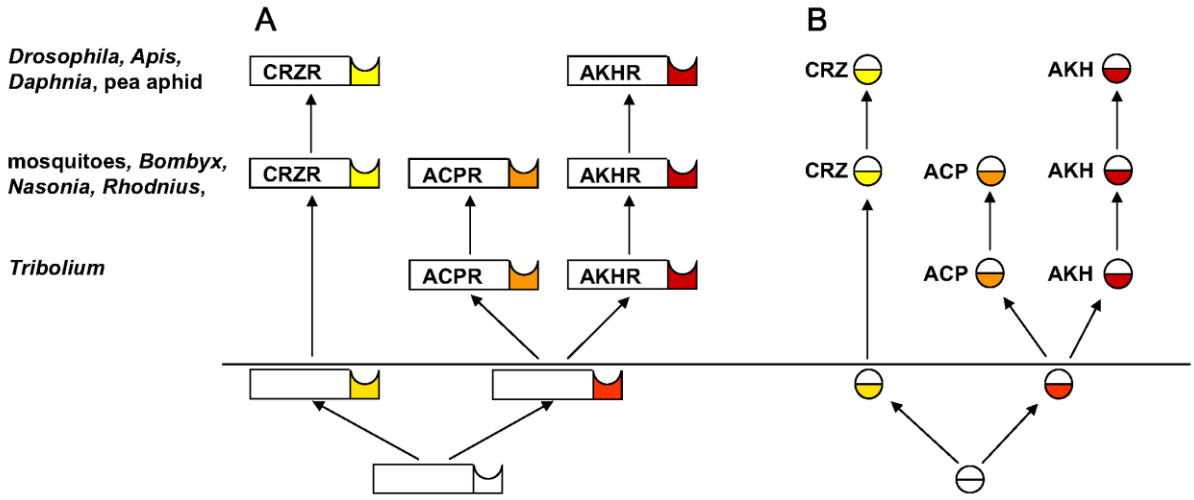

FIGURE 2. **Proposed scenario for the receptor/ligand co-evolution, leading to receptors specific for either AKH, ACP, or corazonin.** The receptors and ligands *below* the *horizontal line* are ancestral and therefore not identifiable. The *white areas* in the receptors indicate structural relationship. The same holds for the ligands. AKHs and their receptors are highlighted in *red*, corazonins and their receptors in *yellow*, and ACPs and their receptors are marked in *orange*. The ancestral receptors and ligands drawn immediately *below* the *horizontal line* have intermediate colors. *A*, an ancestral receptor (*bottom, white*) duplicates and, after mutations, these duplications give rise to two receptors that are the ancestors of the corazonin and AKH/ACP receptors. Subsequently, the AKH/ACP receptor gene duplicates again, giving rise (after mutations) to the AKH and ACP receptors. This scenario is supported by the branching pattern of Fig. 8. Note that in some present day insects, the corazonin or ACP receptor has been lost (see also Fig. 11), but there always is an AKH receptor (Fig. 8 and Table 1). *B*, similar scenario as in *A* for the ligands. It is unknown whether the ligands or receptors duplicated first. The steps given in *A* and *B* have time windows that overlap (= co-evolution between *A* and *B*).

qPCR was carried out on an MX3000 machine (Stratagene) using a Brilliant® SYBR® Green qPCR Master Mix from Stratagene. qPCR for the *T. castaneum* ACP preprohormone and *T. castaneum* ACP receptor was performed using the primers mentioned in supplemental Table S1. *T. castaneum* genes, coding for actin, rps3, rpl32, elf1, and tubulin, were used as reference genes (see supplemental Table S1 for primer sequences and accession numbers). All primer pairs have been tested for dimerization, efficiency (90–110%), and amplification of only one product. The most stable reference genes and gene normalization expression factors were determined by the software program geNORM (14). All experiments have been repeated at least three times. Water was used as nontemplate control.

Bioassays—Chinese hamster ovary (CHO) cells stably expressing the human G-protein G16 (CHO/G16) were grown as described previously (15) and transfected using FuGENE HD transfection reagent (Roche Applied Science). The bioluminescence assay was performed as described earlier (2). We tested our library of eight biogenic amines and 48 neuropeptides (see supplemental Table S2; all synthesized by GeneMed Synthesis, San Antonio, TX, or Bachem, Bubendorf, Switzerland). For peptide structures, see this study and Refs. 16, 17.

RNA Interference—Double-stranded RNAs were synthesized using the T7 MegaScript kit (Ambion); genes for *Trc*ACPR (1374 bp) and EGFP (358 bp), both flanked by T7 sites, were used as templates. To purify the double-stranded RNA, ethanol precipitation was carried out after DNase treatment, and the pellet was dissolved in 20 μl of H_2O. Concentration of the double-stranded RNA in this sample was determined using Nanodrop. Approximately 2-day-old female pupae were injected with 1 μg/μl double strand RNA (ACPR or EGFP) and subsequently transferred to flour, including 5% yeast, and kept at 32 °C until hatching. 14 days after injection, three groups of 15 or 25 injected virgin female adult beetles were mated with 15 wild type males. Eggs were counted after 3 days. 14 and 21 days after injection, RNA was isolated from three ACPR- or EGFP-injected beetles, and the level of ACPR mRNA was determined by qPCR using 5′-CACCGCCAGGAATTACAGAT-3′ as sense primer and 5′-GCGACCTGGGTTCAAAACTA-3′ as antisense primer.

Immunocytochemistry—Brains and ganglia of first instar *Tribolium* larvae were dissected in a drop of cold phosphate-buffered saline (0.1 M PBS, pH 7.4) using a transgenic line, where the central nervous system is labeled with fluorescent color[4] and fixed subsequently in 4% formaldehyde (Roth, Karlsruhe, Germany) in 0.1 M PBS for 1–2 h on ice. The brains were then rinsed three times for 10 min at room temperature in 0.1 M PBS followed by preincubation overnight at 4 °C in 5% normal goat serum (Jackson ImmunoResearch) in 0.1 M PBS containing 0.3% Triton X-100 (PBST). Brains were then incubated in a solution containing the polyclonal ACP (1:10,000) and the monoclonal synapsin antibody (1:200) in PBST containing 5% normal goat serum for 1 day at 4 °C. The monoclonal synapsin antibody was used to selectively label neuropilar areas in the brain (kindly provided by Dr. E. Buchner, Würzburg, Germany). The polyclonal ACP rabbit antibody was obtained commercially from GeneMed Synthesis. The brains were rinsed three times for 10 min with PBST before they were incubated with a secondary goat anti-rabbit antibody conjugated to Cy3 and a goat anti-mouse antibody coupled to Cy5 (both 1:300, Jackson ImmunoResearch) in PBST and 5% normal goat serum for 1 day at 4 °C. Afterward, the brains were rinsed with PBS three times for 10 min and sub-

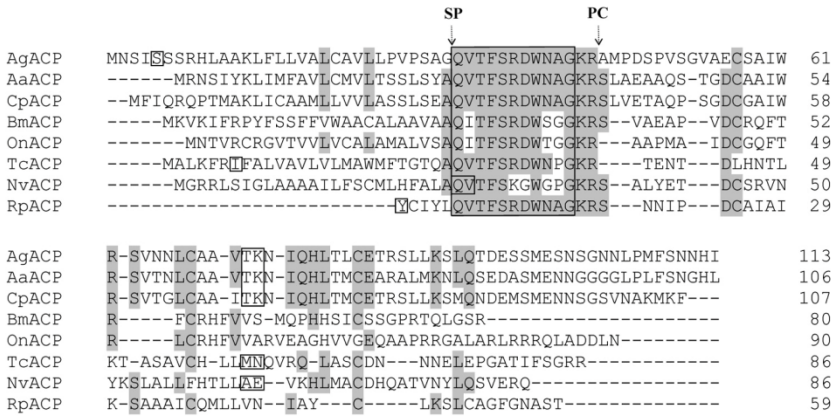

FIGURE 3. **Alignment of the ACP preprohormone from the mosquitoes *A. gambiae* (*Ag-ACP*), *A. aegypti* (*Aa-ACP*), *C. pipiens* (*Cp-ACP*), the silkworm *B. mori* (*Bm-ACP*), the European corn borer *O. nubilalis* (*On-ACP*), the red flour beetle *T. castaneum* (*Tc-ACP*), the parasitic wasp *N. vitripennis* (*Nv-ACP*), and the bloodsucking bud *R. prolixus* (*Rp-ACP*).** Amino acid residues that are common in at least four preprohormones are *highlighted*. The immature ACP sequences are framed by a *large box*. The *arrows* indicate the sites where signal peptidase (*SP*) removes the signal peptide or where prohormone convertase (*PC*) liberates immature ACPs from the prohormone. We could not find a complete signal peptide for *R. prolixus* ACP. The mature ACPs have the structures shown in Fig. 4. Intron positions are indicated by small one- or two-amino acid residue boxes, where the splice junction is located between the codons for these two amino acid residues. The preprohormone sequences have been annotated from the sequenced genomes from the above-mentioned insects, except for the *O. nubilalis* sequence (GenBank™ accession number GH989528), which has been derived from an EST library clone; in addition, we have cloned the *T. castaneum* sequence (GenBank™ accession number GQ217536).

Species	Amino acid sequence
A. gambiae	pQVTFSRDWNAamide
A. aegypti	pQVTFSRDWNAamide
C. pipiens	pQVTFSRDWNAamide
B. mori	pQITFSRDWSGamide
O. nubilalis	pQITFSRDWTGamide
T. castaneum	pQVTFSRDWNPamide
N. vitripennis	pQVTFSKGWGPamide
R. prolixus	pQVTFSRDWNAamide
L. migratoria	pQVTFSRDWSPamide

FIGURE 4. **Structures of mature ACPs deduced from eight insect preprohormone sequences (*cf.* Fig. 3).** *L. migratoria* ACP was isolated from extracts (20). Residues common to at least six ACPs are highlighted in *red*.

sequently mounted in 80% glycerol, 20% PBS. The whole mount preparations were scanned at 1024 × 1024 pixel resolution with a ×63 glycerol objective (Leica, Germany) using a Leica TCS SP5 confocal laser scanning microscope. Controls included preimmune antiserum (1:10,000) and ACP antiserum (1:10,000) preabsorbed with ACP (10^{-7} M), both of which did not give any staining.

Software—DNA sequence comparisons were done using Vector NTI (Invitrogen). Protein sequence alignments were carried out using ClustalW. The phylogenetic tree of Fig. 8 was generated by the Megalign program of the Lasergene software package (DNASTAR). The receptor proteins were aligned by the ClustalW method using the PAM series protein weight matrix and default multiple sequence alignment parameters. We searched the nucleotide collection (nr/nt) and the non-human and non-mouse ESTs data bases at NCBI using the TBLASTN program (blast.ncbi.nlm.nih.gov).

For the phylogenetic trees shown in supplemental Fig. S5, alignments were performed using ClustalW with the Blosum scoring matrix. Bootstrapping was performed using Phylip protdist to generate 100 replicates. The tree diagrams were drawn using Phylodendron. For the construction of the above-mentioned trees, we used the seven-transmembrane regions of cloned or annotated receptors with the following GenBank™ accession numbers: Nv-AKHR (XP_001599670); Tc-AKHR (DQ422965); Am-AKHR (AAX83121); Aa-AKHR (EAT36594); Ag-AKHR (AY298745); Bm-AKHR (AF403542); Dm-AKHR (AF077299); Aa-ACPR (EAT38429); Cp-ACPR (EDS28711); Ag-ACPR (AY553322 and EU138885, two splice variants); Tc-ACPR (EU138886); Nv-ACPR (XP_001605342); Bm-ACPR-1 (EU138887); Bm-ACPR-2 (BAG68428); Cp-CRZR (EDS44142 and EDS44143, we manually joined the split gene); Ag-CRZR (AY301275); Dm-CRZR (AF373862); Bm-CRZR (BAG68420); Am-CRZR (XP_392570); Bm-CCAPR-1 (BAG68429); Bm-CCAPR-2 (BAG68425); Tc-CCAPR-2 (ABN79652); Am-CCAPR (XP_001122652); Nv-CCAPR (XP_001602277); Ag-CCAPR-2 (XP_321101); Aa-CCAPR (EAT39546); Ag-CCAPR-1 (AAS77205); Cp-CCAPR (EDS26677); Dm-CCAPR (AY219842); Tc-CCAPR (ABN79651); Tc-inotocin receptor (ABX00684); Nv-inotocin receptor (XP_001600203); and Dm-FMRFamide receptor (AAL83921). For the other receptors in Fig. 8 or supplemental Fig. S5, there are no GenBank™ accession numbers available. Prediction of transmembrane helices of the receptor protein was done using the TMHMM server. The signal peptide was predicted by the SignalP server. EC_{50} values were calculated using Prism software.

RESULTS

Identification of the Insect ACPs and ACP Preprohormones—We have previously cloned the *A. gambiae* AKH and corazonin receptors and a third, closely related receptor that, however, remained an orphan (13). To find a candidate ligand for this orphan receptor, we screened the genomic data base from *A. gambiae* (18) with various insect AKH and corazonin sequences, using TBLASTN. This search yielded an *A. gambiae* gene (see also GenBank™ accession number XP_563757), coding for a preprohormone (Fig. 3) that could give rise to a peptide that was related to both AKH and corazonin (Fig. 1) and that we

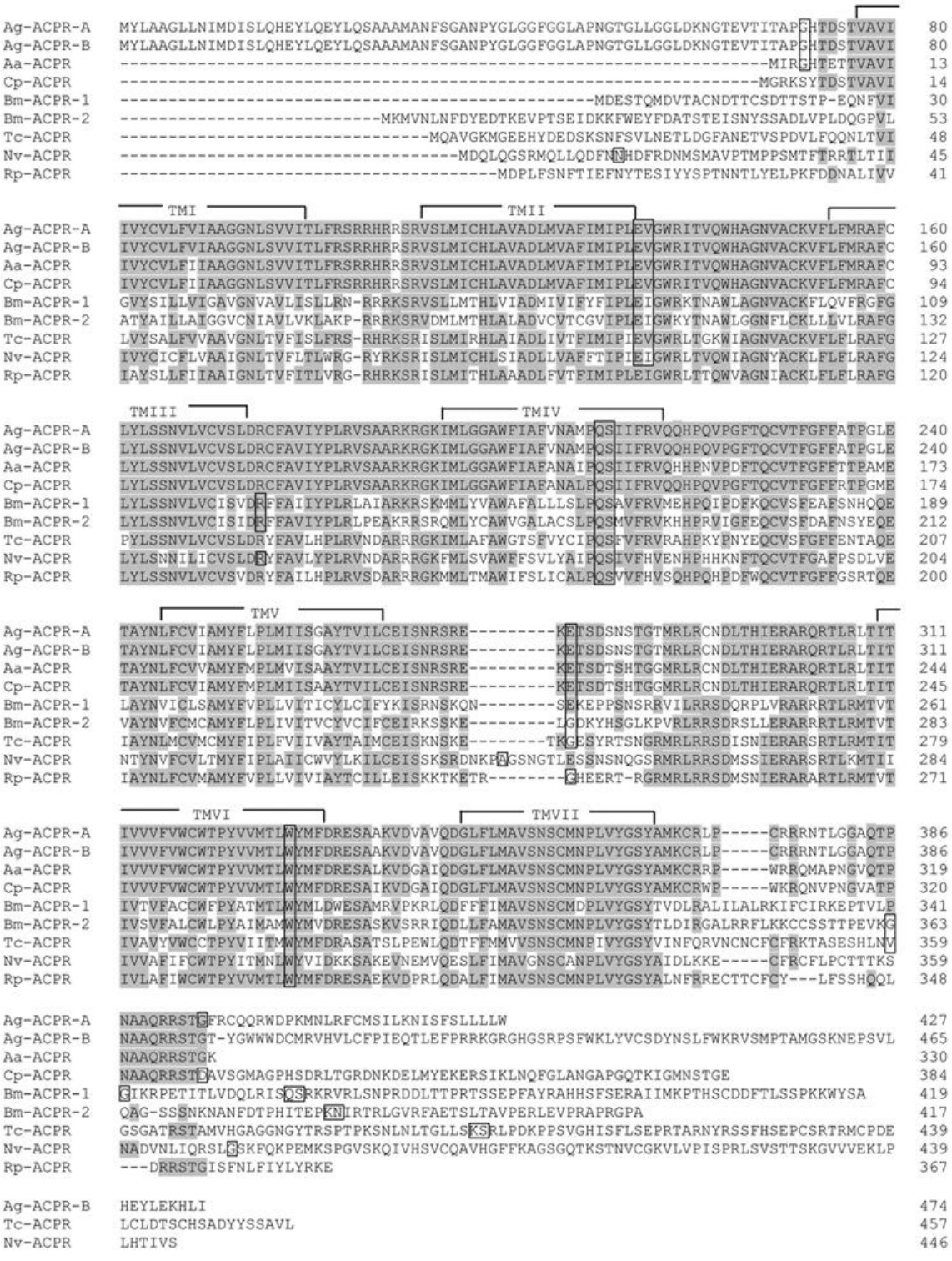
TMI
TMII
TMIII
TMIV
TMV
TMVI
TMVII

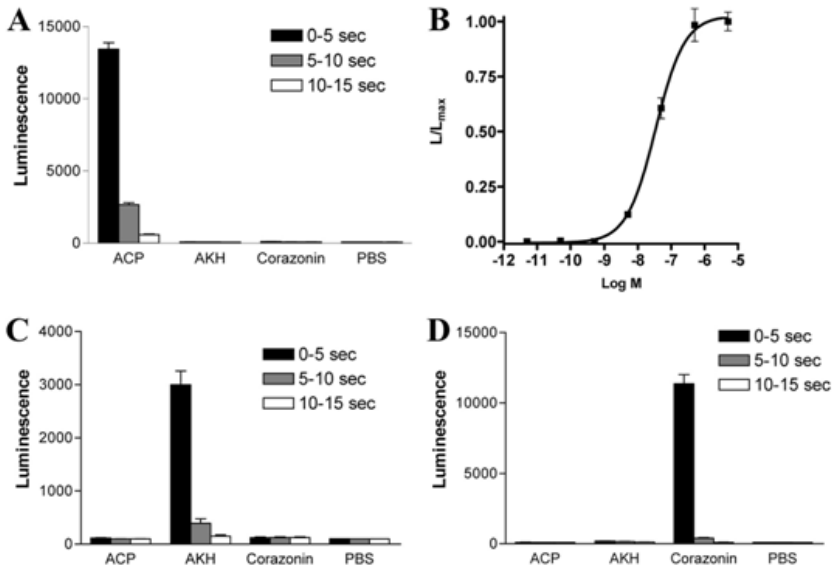

FIGURE 6. **Bioluminescence responses of CHO cells expressing *A. gambiae* neuropeptide receptors.** In all panels, the S.E. are given as *vertical bars*, which are sometimes smaller than the symbols used (*squares* or *lines*). In these cases only the symbols are given. The number of samples (*n*) to calculate S.E. are as follows: *A*, $n = 3$; *B–D*, $n = 4$. *A*, CHO/G-16 cells, expressing the *A. gambiae* ACP receptor variant-A, 0–5 s (*black*), 5–10 s (*gray*), and 10–15 s (*white*), after addition of 10^{-6} M *A. gambiae* ACP. Note that the bioluminescence response after addition of ACP is about 200 times over background (which is 70 bioluminescence units). Addition of *A. gambiae* AKH (5×10^{-6} M), corazonin (5×10^{-6} M) (for structures see Fig. 1), or PBS did not activate the receptor. Also, more than 40 other insect neuropeptides and biogenic amines (a list is given in supplemental Table S2) did not activate the receptor (tested up to 10^{-5} M). *B*, dose-response curve of the effect (during 0–15 s) of *A. gambiae* ACP in CHO/G-16 cells expressing the *A. gambiae* variant-A ACP receptor. The EC_{50} for ACP is 5×10^{-8} M. *C*, cells expressing the *A. gambiae* AKH receptor (13). This receptor is only activated by *A. gambiae* AKH, and not by ACP, corazonin, or PBS (same concentrations tested as in *A*). *D*, cells expressing the *A. gambiae* corazonin receptor (13). This receptor is only activated by *A. gambiae* corazonin and not by ACP, AKH, or PBS (same concentrations tested as in *A*).

named ACP (AKH/corazonin-related peptide). TBLASTN searches of other sequenced insect genomes showed that similar ACP preprohormone genes did occur in the yellow fever mosquito *Aedes aegypti* and in the West Nile virus transmitting mosquito *Culex pipiens* (Fig. 3). Mosquitoes belong to the insect order Diptera, but, surprisingly, other Diptera with a sequenced genome, such as the 12 different *Drosophila* species (19), did not have an ACP preprohormone gene. However, the silkworm *B. mori*, the European corn borer *Ostrinia nubilalis* (both belonging to the Lepidoptera), the red flour beetle *T. castaneum* (Coleoptera), the parasitic wasp *N. vitripennis* (Hymenoptera), and the bloodsucking bug *Rhodnius prolixus* (Hemiptera) did contain ACP preprohormone genes (Fig. 3), whereas we were unable to find such genes in the honeybee *Apis mellifera* (Hymenoptera), the pea aphid *Acyrthosiphon pisum* (Hemiptera), the body louse *Pediculus humanus* (Phthiraptera) and in the water flea *Daphnia pulex*, the only crustacean, whose genome has been sequenced.

Fig. 3 aligns all eight ACP preprohormones identified so far. In all cases, the ACP sequences are located directly after the signal peptide sequence and have dibasic (KR) processing sites at their C termini. The mature ACPs are shown in Fig. 4. It is striking that the first five to eight amino acid residues of these ACPs are nearly identical among all listed insects, whereas the last two residues are somewhat variable.

Two other research groups have found insect ACPs. The peptide was first identified in extracts from the locust *Locusta migratoria* by Siegert in 1999 (20) and in 2006 by Kaufmann and Brown (21) after screening of the *A. gambiae* genomic data base. Both peptides were described as AKH peptides with unknown functions (20, 21). Because the genome from *L. migratoria* has not been sequenced, we could not annotate its preprohormone gene (Fig. 3). Based on its striking similarities with both AKHs and corazonins, the ACPs are good candidates for being ligands for orphan GPCRs that are structurally related to both the AKH and corazonin receptors.

Cloning and Identification of Insect ACP Receptors—We recloned the orphan receptor from *A. gambiae* that we published previously (13). This work yielded two transcription variants; variant-A (*Ag-ACPR-A*, Fig. 5) was identical to the published orphan receptor transcript (13), and variant-B was an unpublished splicing variant with a different intracellular C terminus (supplemental Figs. S1 and S2).

Screening of all available insect and arthropod genomes and EST data bases with these *A. gambiae* orphan receptor sequences using TBLASTN yielded nearly identical sequences from the mosquitoes *A. aegypti*, and *C. pipiens* (one gene in each species) and closely related sequences from the silkworm *B. mori* (two genes), the beetle *T. castaneum* (one gene), the wasp *N. vitripennis* (one gene), and the bloodsucking bug *R. prolixus* (one gene) (Fig. 5). However, we did not find ACP receptor sequences in any of the 12 *Drosophila* species with a sequenced genome (19), in the honeybee *A. mellifera* (22), in the pea aphid *A. pisum*, in the body louse *P. humanus*, or in the water flea *D. pulex*.

FIGURE 5. **Alignment of nine insect ACP receptor sequences.** The receptors from *A. gambiae* (*Ag-ACPR-A* and *-B*; GenBank™ accession number EU138885) and *T. castaneum* (Tc-ACPR; GenBank™ accession number EU138886) have been cloned, expressed in CHO cells, and identified as ACP receptors (Figs. 6 and 7 and supplemental Figs. S1, S3, and S4). The other receptors have been retrieved from their genomic data bases using TBLASTN and subsequently undergone manual curation. Amino acid residues that are common to at least four receptors are highlighted. Transmembrane (*TM*) helices are indicated by TMI–TMVII. Introns are indicated by *boxes*.

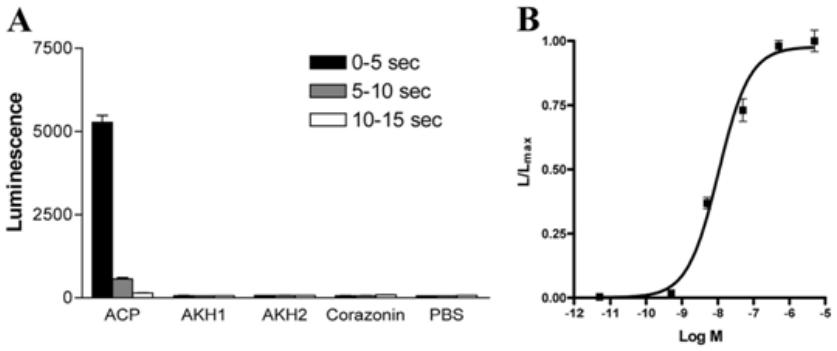

FIGURE 7. **Bioluminescence responses of cells expressing the *T. castaneum* ACP receptor.** The figure is presented in the same way as in Fig. 6. The number of samples (*n*) used to calculate S.E. are as follows: *A*, (ACP and PBS), $n = 4$; *A* (AKH-1 and -2, corazonin), $n = 3$; *B*, $n = 4$. *A*, *T. castaneum* ACP receptor is only activated by *T. castaneum* ACP but not by *T. castaneum* AKH1, AKH2, corazonin (for structures see Ref. 5), or PBS (same concentrations tested as in Fig. 6*A*). More than 40 other insect or invertebrate neuropeptides and 8 biogenic amines (supplemental Table S2) did also not activate the receptor (tested up to 10^{-5} M). *B*, EC_{50} for *T. castaneum* ACP is 1×10^{-8} M.

To check whether these annotated orphan receptors represent the GPCRs for insect ACPs, we also cloned, in addition to the *A. gambiae* sequences, the *T. castaneum* receptor sequence (supplemental Fig. S3). CHO cells were stably transfected with cDNA sequences coding for the two *A. gambiae* receptor variants, and the *T. castaneum* receptor and clonal cell lines were selected, expressing each receptor effectively. Addition of 10^{-6} M *A. gambiae* ACP to the CHO cells expressing the receptor variant-A (*Ag-ACPR-A*, Fig. 5) resulted in a strong receptor response, which we measured as bioluminescence and which was about 200 times over background (Fig. 6*A*). A dose-response curve showed that this response had an EC_{50} value of 5×10^{-8} M (Fig. 6*B*). The *A. gambiae* ACP receptor could not be activated by *A. gambiae* AKH or corazonin or by a library of more than 40 insect neuropeptides, showing that the receptor was specific for ACP (Fig. 6*A*). Similarly, the *A. gambiae* AKH receptor (13) was specific for AKH and did not react with ACP or corazonin (Fig. 6*C*), and the *A. gambiae* corazonin receptor (13) was specific for corazonin and did not react with ACP or AKH (Fig. 6*D*). The *A. gambiae* ACP receptor variant-B (*Ag-ACPR-B*, Fig. 5) had a much lower affinity for ACP and was, like the *A. gambiae* receptor, not cross-reacting with AKH or corazonin (supplemental Fig. S5). The ACP receptor from *T. castaneum* had the highest affinity for ACP with an EC_{50} value of 1×10^{-8} M for activation by *T. castaneum* ACP (Fig. 7). Also, this receptor was specific for ACP and did not cross-react with the two *T. castaneum* AKHs (5) or corazonin (Fig. 7*A*).

Phylogenetic tree analyses showed that all ACP receptors from holometabolous insects (Fig. 5) cluster closely and that they group between the insect AKH and corazonin receptors (Fig. 8). This strongly suggests that also the *A. aegypti*, *C. pipiens*, *B. mori*, and *N. vitripennis* receptors (Fig. 5) are ACP receptors.

In addition to the receptors, phylogenetic tree analyses of the ACP, AKH, and corazonin preprohormones show that also these proteins form separate clusters and that the ACP preprohormones group between the AKH and corazonin preprohormones (supplemental Fig. S5). Thus, the evolutionary patterns of the ACP, AKH, and corazonin preprohormones and ACP, AKH, and corazonin receptors look the same, supporting a scenario of receptor/ligand co-evolution as given in Fig. 2.

Expression of the ACP Receptor and Peptide Genes in Tribolium—We have used quantitative PCR (qPCR) to assess the expression of the ACP receptor and ACP preprohormone genes in adult *T. castaneum*. We found that in adult animals the receptor was mostly expressed in the head (presumably the brain), being 15 times higher than in the whole beetle and about 30 times higher than in the torso (thorax plus abdomen) (Fig. 9*A*). During development, the ACP receptor gene is prominently expressed shortly before and after hatching (20 times adult animals) (Fig. 9*B*). The ACP preprohormone gene had similar expression patterns (Fig. 9, *C* and *D*).

RNA Interference—To find a physiological role for the ACP hormonal system, we injected *T. castaneum* female pupae with double strand RNA for the ACP receptor. qPCR of treated beetles 14 and 21 days after injection showed a marked suppression of the targeted transcript (55–65% down-regulation compared with EGFP injected controls). However, we were unable to detect any differences in physical appearance, egg number, or mortality between the ACP receptor knockdown and control beetles.

Immunocytochemistry—We stained the first larval stage of *T. castaneum* with antibodies against *T. castaneum* ACP. These experiments showed three strongly stained neurons and one weakly stained neuron in each hemisphere of the larval brain (Fig. 10*A*). These neurons projected to the brain neuropil, the subesophageal ganglion, and the thoracic and abdominal ganglia (Fig. 10, *A* and *B*). Based on the varicose appearance of these projections, we suggest a neurosecretory role for ACP.

DISCUSSION

In this study, we describe ACP and its receptor, which constitute a novel signaling system in insects. The ACPs are structurally intermediate between the AKHs and corazonins (Fig. 1), and the same is true for the ACP preprohormones and the AKH and corazonin preprohormones (supplemental Fig. S5). Furthermore, the ACP receptors are structurally intermediate between the AKH and corazonin receptors (Fig. 8). Already for the AKH and corazonin signaling system, a co-evolution between ligands and receptors has been proposed (6, 7). The existence of a third signaling system intermediate between the AKH and corazonin systems is therefore an even more convincing example of receptor and ligand co-evolution, where an ancestral receptor and ligand gene duplicate several times followed by mutations and evolutionary selection, leading to three signaling systems (Fig. 2). The branching pattern of Fig. 8 suggests that the AKH and ACP receptors originated by duplication of an ancestral receptor that emerged after an earlier dupli-

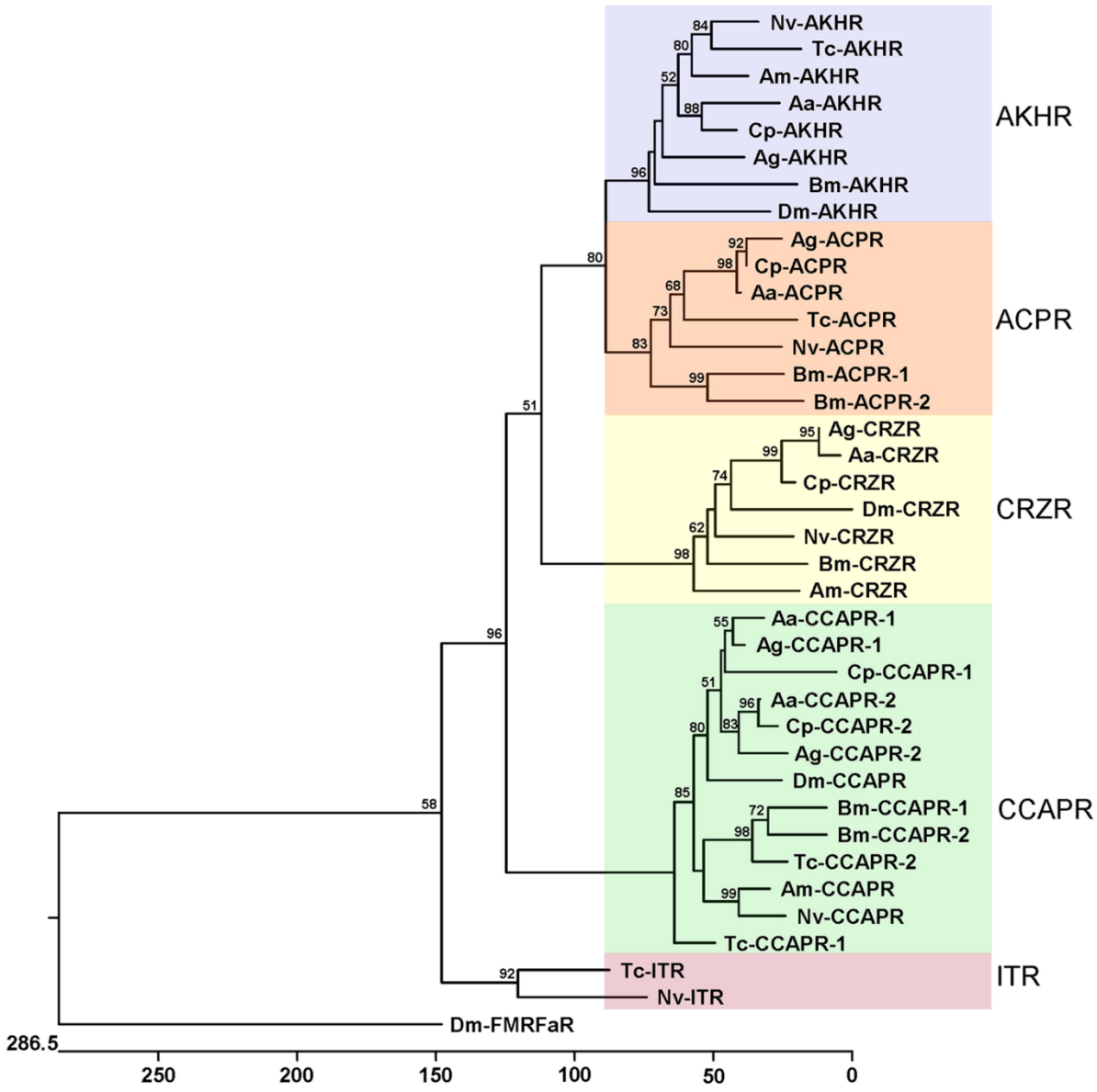

FIGURE 8. **Phylogenetic tree analysis of cloned or annotated neuropeptide receptors from holometabolous insects with a sequenced genome belonging to the cluster of AKH receptors (*AKHR*), ACP receptors (*ACPR*), corazonin receptors (*CRZR*), CCAP receptors (*CCAPR*), or inotocin receptors (*ITR*).** The length of each branch represents the evolutionary distance (measured as amino acid residue exchanges, see *abscissa*) between each receptor and the common ancestor of that receptor and its neighbor. Bootstrap values (only those above 50) are given where the branches split. The tree is rooted by the *Drosophila* FMRFamide receptor (*Dm-FMRFaR*). The GenBank™ accession numbers of the receptors used in this figure are given under "Experimental Procedures." Abbreviations are as follows: *Aa* (*A. aegypti*); *Ag* (*A. gambiae*); *Am* (*A. mellifera*), *Bm* (*B. mori*), *Cp* (*C. pipiens*), *Dm* (*Drosophila melanogaster*), *Nv* (*N. vitripennis*), and *Tc* (*T. castaneum*).

cation, leading to the development of the corazonin receptor (see also Fig. 2*A*). Whether this ancestral receptor is more AKH- or ACP-like is uncertain. In branchiopods (crustaceans such as *D. pulex*), which are believed to be the direct ancestor group of insects (23), AKH but not ACP receptors occur, which would suggest that the AKH system is more primordial. Lindemans *et al.* (24) provide a list of gonadotropin-releasing hormone-resembling peptides in lower invertebrates that also show some resemblance to AKHs. However, it is difficult to decide whether these peptides are more AKH- than ACP-like and which of the two peptides is the most ancient.

The ACP receptor cannot be activated by AKH and corazonin, and vice versa, the AKH receptor cannot be activated by ACP and corazonin and the corazonin receptor not by ACP and AKH (Figs. 6 and 7). These results show that the ACP, AKH, and corazonin systems, after they have evolved from their com-

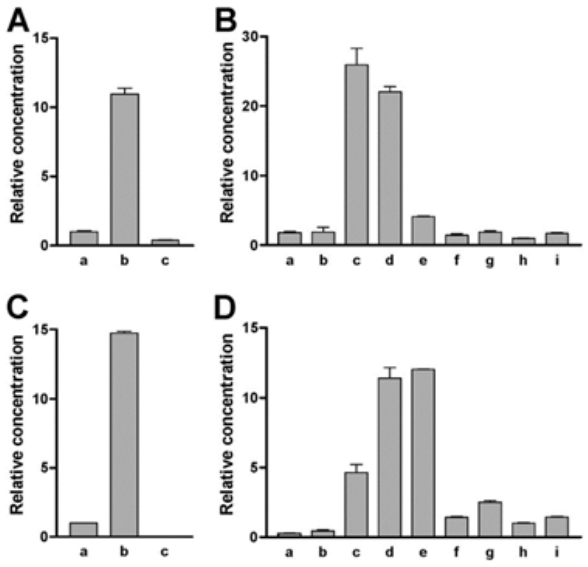

FIGURE 9. **qPCR of the ACP receptor and ACP preprohormone mRNAs in adult *T. castaneum* and in different developmental stages.** In each column at least 60 animals were pooled. The qPCR experiments were run as triplets; the *bars* (which sometimes are smaller than the lines) represent S.E. geNORM (14) has been used to calculate normalization factors of the most stable reference genes for each experiment, which are the genes coding for rps3 and rpl32 in *A* and *C* and rpl32, elf1, and actin in *B* and *D*. *A*, ACP receptor mRNA in adult mixed male and female animals as follows: *a*, whole bodies; *b*, heads; *c*, torsi (body minus head). The receptor mRNA concentrations given are relative to *a* (= 1); *b* is highly significantly different from *a* ($p = 0.0006$). *B*, ACP receptor mRNA in different developmental stages (the sexes were mixed except for adult animals) as follows: *a*, eggs 0–24 h after egg laying; *b*, eggs 24–48 h after egg laying; *c*, eggs 48–72 h after egg laying; *d*, larvae 96–120 h after egg laying (about 0–1 day after hatching); *e*, larvae 15–16 days after egg laying; *f*, larvae 20–21 days after egg laying; *g*, pupae (24–25 days after egg laying); *h*, adult female ; and *i*, adult male animals (27 days or more after egg laying). The receptor mRNA concentrations given are relative to *h* (= 1). The difference between *c* and *h* ($p = 0.0089$) and *d* and *h* ($p = 0.0002$) is highly significant. *C*, ACP preprohormone mRNA in the same tissues as given in *A*. The mRNA concentrations given are relative to *a* (= 1); *b* is highly significantly different from *a* ($p = 0.00005$). *D*, ACP preprohormone mRNA in the same developmental stages as given in *B*. The mRNA concentrations given are relative to *h* (= 1). The difference between *c* and *h* ($p = 0.0068$), *d* and *h* ($p = 0.0002$), *e* and *h* ($p = 0.0001$), and *g* and *h* ($p = 0.0051$) is highly significant.

mon ancestral neuropeptide/receptor signaling system (Fig. 2), are now three independent signaling systems that can co-exist without direct interference.

How far is the neuropeptide receptor/ligand co-evolution, as we have depicted it here for the ACP, AKH, and corazonin hormonal systems (Fig. 2), unique for insects or for animals in general? In vertebrates, there are also some clear examples of neuropeptide receptor/ligand co-evolution. All vertebrates, for example, have an oxytocin- and a vasopressin-like peptide. In mammals, there are one oxytocin and three vasopressin (V1a, V1b, and V2) receptors, and these GPCRs are structurally closely related (16). Also, the oxytocin and vasopressin peptides are structurally very similar, as are their preprohormones each of which contains a similar neurophysin part characterized by seven cystine bridges (16). Within its range of physiological concentrations, oxytocin does not activate the vasopressin receptors, and vice versa vasopressin does not activate the oxytocin receptor (25, 26), so they are, like the insect ACP, AKH, and corazonin systems, independent hormonal systems that can co-exist without direct interference. Interestingly, although oxytocin and vasopressin have different actions, they also have overlapping roles especially in the control of social and reproductive behaviors (27). This again would be in agreement with a common evolutionary origin of the two hormonal systems, where some aspects of the original function of the ancestral system would have been conserved in both the oxytocin and vasopressin systems. Other examples of receptor neuropeptide ligand co-evolution are the mammalian glycoprotein hormones and their receptors (28, 29) and the opioid/orphanin peptides and their receptors (30).

In insects or protostome invertebrates in general, examples of neuropeptide ligand/receptor co-evolution are quite scarce. Clear examples are first, the glycoprotein hormones and their receptors, simply because their evolutionary origins and diversification (by duplications) occurred long before the split of proto- and deuterostomia (8, 9, 29). The second example is the capa/pyrokinin system, where two structurally related preprohormones produce capa and pyrokinin neuropeptides that act on two or three structurally related receptors (7–9). The third example is our current findings of the co-evolution of the ACP, AKH, corazonin, and their receptor genes. There are no further obvious examples of neuropeptide ligand/receptor co-evolution in insects (8, 9), although additional examples might be discovered in the future, when more insect GPCRs are being deorphanized.

The ACP signaling system is widespread in insects. It occurs in Hemimetabola (insects with an incomplete metamorphosis, where the young insects, called nymphae, resemble the adult animals), such as *R. prolixus* and locusts (Fig. 4) (20), and it occurs in representatives from all four major orders of Holometabola (insects with a complete metamorphosis, from wormlike larvae to mainly flying adults) as follows: Diptera, Lepidoptera, Coleoptera, and Hymenoptera (Fig. 11). However, some dipterans, such as the 12 *Drosophila* species with a sequenced genome (19), hymenopterans, such as the honeybee *A. mellifera* (22), and some hemimetabolous insects, such as the pea aphid *A. pisum* and the body louse *P. humanus*, have lost the ACP/receptor system. This suggests that the ACP signaling system has been abandoned several times during insect evolution (see dead-end signs in Fig. 11) and confirms earlier observations that insects easily can duplicate or abandon hormonal systems (5, 8, 9, 16). We have seen this phenomenon, for example, for the corazonin hormonal system that is widespread, but does not occur in Coleoptera (9), and for the recently discovered inotocin system that does occur in Coleoptera but is absent in Diptera, Lepidoptera, and some Hymenoptera (16).

Fig. 8 illustrates in more detail how common neurohormone receptor gene duplications and losses are in holometabolous insects. This figure shows five receptor types, the AKH, ACP, corazonin, inotocin, and crustacean cardioactive peptide (CCAP) receptors (2, 6, 7, 16, 31). These five receptor types form a distinct branch in phylogenetic tree analyses of insect neuropeptide receptors (8, 9), suggesting that they have a common evolutionary origin. Although, as discussed above, the AKH, ACP, and corazonin peptides are structurally related, the inotocin and CCAP peptide sequences are quite different, both

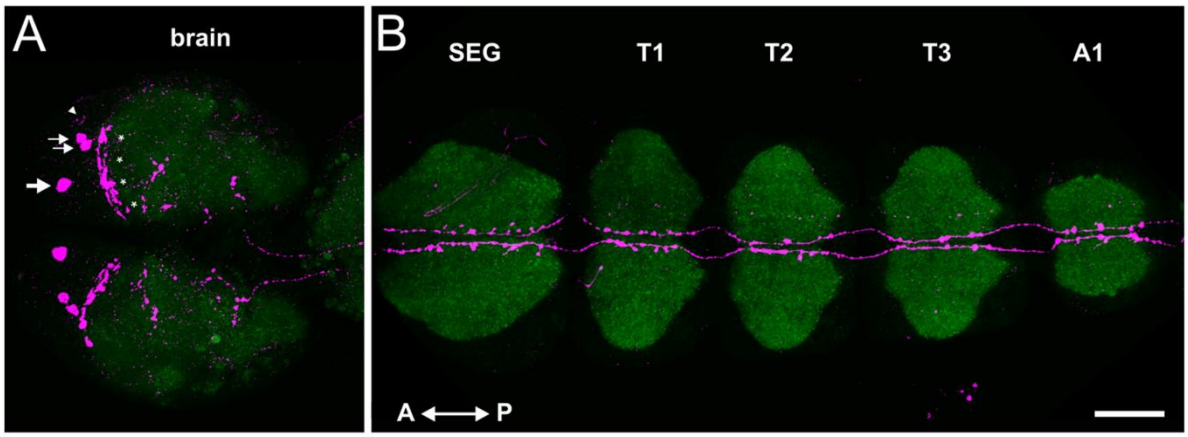

FIGURE 10. **ACP immunostaining of the central nervous system of first instar larvae of *T. castaneum*.** The images are maximum projections of 166 (*A*) and 156 (*B*) optical sections. *A*, in each hemisphere of the brain, we find one large cell body (*large arrow*), a pair of smaller cell bodies (*two small arrows*), and a peripheral weakly stained neuron (*arrowhead*, not visible on the *left side*). These neurons are lying anterior to the central brain neuropil (stained *green* by a synapsin antibody) and project strongly varicose processes to the anterior border of the central brain neuropil (indicated by *asterisks*). *B*, projections descend from the brain to the subesophageal ganglion (*SEG*) and thoracic (*T1–3*) and abdominal ganglia (only A1 is shown). These projections are strongly varicose, especially within the ganglia, suggesting an endocrine (or paracrine) function of ACP. *A*, anterior; *P*, posterior; the scale for both figures is 25 µm.

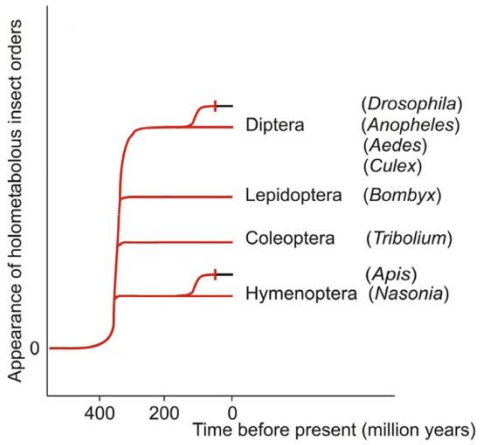

FIGURE 11. **Presence of the ACP/receptor couple in major orders of the Holometabola (highlighted in *red*).** This signaling system occurs in all four major orders but is absent in 12 *Drosophila* species (Diptera) and in the honeybee *A. mellifera* (Hymenoptera), showing that it has been abandoned at least two times during the evolution of holometabolous insects. The ACP/receptor couple is also present in some hemimetabolous insects (*R. prolixus*) but absent in others (*A. pisum* and *P. humanus*), suggesting that also in Hemimetabola this hormonal system has been abandoned several times.

TABLE 1

Number of deorphanized or annotated AKH receptors (AKHR), ACP receptors (ACPR), corazonin receptors (CRZR), CCAP receptors (CCAPR), and inotocin receptors (ITR) in various holometabolous insects with a sequenced genome

Note that for some receptors (indicated by asterisks) only a partial sequence could be identified. Also note that when a receptor is absent its neuropeptide ligand is also absent, meaning that a complete hormonal system is lacking.

	AKHR	ACPR	CRZR	CCAPR	ITR	Σ
D. melanogaster	1	0	1	1	0	3
A. aegypti	1	1	1*	2**	0	5
A. gambiae	1	1	1	2	0	5
C. pipiens	1*	1	1	2**	0	5
B. mori	1	2	1	2	0	6
T. castaneum	1	1	0	2	1	5
A. mellifera	1	0	1	1	0	3
N. vitripennis	1	1	1*	1	1	5

* Indicates a partial sequence.
** Indicates one of the two sequences is partial.

being small cyclic neuropeptides with no sequence homologies to the AKHs, ACPs, and corazonins (1, 16, 17). Some insects such as the 12 *Drosophila* species with a sequenced genome and the honeybee have only one AKH, one corazonin, and one CCAP receptor, whereas they have lost the ACP and inotocin systems (Fig. 8 and Table 1) (8, 9, 16). Other insects, such as the three mosquito species, the silkworm *B. mori*, and the parasitic wasp *N. vitripennis*, are rich in members of the receptor cluster; in addition to AKH, and corazonin, they have retained the ACP system (Fig. 11); moreover, the CCAP receptor gene has been duplicated in many of them (Fig. 8 and Table 1). Furthermore, the ACP receptor has been duplicated in *B. mori*, and the inotocin system has been retained in *T. castaneum* and *N. vitripennis*. Thus, *B. mori* has six members and many other insects have five members of this neuropeptide receptor cluster, whereas the different *Drosophila* species and the honeybee have only three (Fig. 8 and Table 1).

Receptor duplications are also common in vertebrates, because most vertebrate neuropeptides have two or more receptors, which are structurally related. However, receptor losses are extremely seldom in these animals, and we are aware of only one example, where three (out of originally seven) neuropeptide Y receptor subtypes have been lost in some teleost fishes (32). To our knowledge, there are no examples of losses of whole hormonal (receptor plus ligand) systems in vertebrates, such as we have seen for the ACP system in branches of the Hymenoptera and Diptera (Fig. 11). Thus, this phenomenon of neuropeptide/receptor losses is quite unique for insects.

How can we explain these hormonal system (receptor plus ligand) duplications and losses in insects (Table 1)? One could

imagine that a certain insect species needs a complete palette of a related group of neuropeptide hormonal systems (generated by gene duplications as exemplified in Fig. 8 and Table 1) to survive in its extreme habitat or complex ecological niche, whereas other insects are less exposed and would suffice with fewer receptors. Thus, neuropeptide hormonal system duplications and losses would reflect the life style of a certain insect and in how far a certain physiological process needs multiple control points or back-up systems (= multiple hormonal systems) or not (= basic package). Could these considerations help us to understand Table 1? Unfortunately, we are unable to give an overall explanation of Table 1, which is due, in our eyes, to our incomplete understanding of the actions of the five hormonal systems given in this table.

What is the function of the newly discovered ACP signaling system? We do not know this yet, but gene expression studies using qPCR show that both the receptor and the peptide genes are highly expressed shortly before and after hatching of *T. castaneum* larvae (Fig. 9). This suggests a role of the ACP system in early larval development or physiology. Peptide or receptor gene knockdown experiments in *T. castaneum*, where systemic RNA interference works very effectively (33), should be the method of choice to further unravel the function of the ACP system. So far, however, we have been unable to see a clear effect of ACP receptor down-regulation using RNA interference. This might be due to the presence of multiple hormonal back-up systems (discussed above) or to our inability to see small behavioral changes. Anatomical work in early larvae suggests that ACP is an endocrine or paracrine hormone released into the anterior part of the central neuropil of the brain (Fig. 10*A*) and thoracic and abdominal ganglia (Fig. 10*B*). This might point to a role of ACP as a neuromodulator, perhaps influencing motor behavior.

Finally, our study has clarified a confusion with respect to AKH neuropeptide nomenclature, because two of the peptides that we now know are ACPs (those from *L. migratoria* and *A. gambiae*, Fig. 1) have been described in the literature as AKHs (20, 21). These peptides, however, do not activate the AKH receptor and should not be named AKHs. The corazonins have never been regarded as AKHs and the same should hold for the ACPs.

Acknowledgment—We thank Christine Stubbendorff for typing the manuscript.

REFERENCES

1. Gäde, G., Hoffmann, K. H., and Spring, J. H. (1997) *Physiol. Rev.* **77,** 963–1032
2. Staubli, F., Jorgensen, T. J., Cazzamali, G., Williamson, M., Lenz, C., Sondergaard, L., Roepstorff, P., and Grimmelikhuijzen, C. J. (2002) *Proc. Natl. Acad. Sci. U.S.A.* **99,** 3446–3451
3. Kim, S. K., and Rulifson, E. J. (2004) *Nature* **431,** 316–320
4. Riehle, M. A., Garczynski, S. F., Crim, J. W., Hill, C. A., and Brown, M. R. (2002) *Science* **298,** 172–175
5. Li, B., Predel, R., Neupert, S., Hauser, F., Tanaka, Y., Cazzamali, G., Williamson, M., Arakane, Y., Verleyen, P., Schoofs, L., Schachtner, J., Grimmelikhuijzen, C. J., and Park, Y. (2008) *Genome Res.* **18,** 113–122
6. Cazzamali, G., Saxild, N., and Grimmelikhuijzen, C. J. (2002) *Biochem. Biophys. Res. Commun.* **298,** 31–36
7. Park, Y., Kim, Y. J., and Adams, M. E. (2002) *Proc. Natl. Acad. Sci. U.S.A.* **99,** 11423–11428
8. Hauser, F., Cazzamali, G., Williamson, M., Blenau, W., and Grimmelikhuijzen, C. J. (2006) *Prog. Neurobiol.* **80,** 1–19
9. Hauser, F., Cazzamali, G., Williamson, M., Park, Y., Li, B., Tanaka, Y., Predel, R., Neupert, S., Schachtner, J., Verleyen, P., and Grimmelikhuijzen, C. J. (2008) *Front. Neuroendocrinol.* **29,** 142–165
10. Veenstra, J. A. (1989) FEBS Lett. **250,** 231–234
11. Tawfik, A. I., Tanaka, S., De Loof, A., Schoofs, L., Baggerman, G., Waelkens, E., Derua, R., Milner, Y., Yerushalmi, Y., and Pener, M. P. (1999) *Proc. Natl. Acad. Sci. U.S.A.* **96,** 7083–7087
12. Zitnan, D., Kim, Y. J., Zitnanová, I., Roller, L., and Adams, M. E. (2007) *Gen. Comp. Endocrinol.* **153,** 88–96
13. Belmont, M., Cazzamali, G., Williamson, M., Hauser, F., and Grimmelikhuijzen, C. J. P. (2006) *Biochem. Biophys. Res. Commun.* **344,** 160–165
14. Vandesompele, J., De Preter, K., Pattyn, F., Poppe, B., Van Roy, N., De Paepe, A., and Speleman, F. (2002) *Genome Biol.* **3,** research0034.1–0034.11
15. Stables, J., Green, A., Marshall, F., Fraser, N., Knight, E., Sautel, M., Milligan, G., Lee, M., and Rees, S. (1997) *Anal. Biochem.* **252,** 115–126
16. Stafflinger, E., Hansen, K. K., Hauser, F., Schneider, M., Cazzamali, G., Williamson, M., and Grimmelikhuijzen, C. J. (2008) *Proc. Natl. Acad. Sci. U.S.A.* **105,** 3262–3267
17. Nässel, D. R. (2002) *Prog. Neurobiol.* **68,** 1–84
18. Holt, R. A., Subramanian, G. M., Halpern, A., Sutton, G. G., Charlab, R., Nusskern, D. R., Wincker, P., Clark, A. G., Ribeiro, J. M., Wides, R., Salzberg, S. L., Loftus, B., Yandell, M., Majoros, W. H., Rusch, D. B., Lai, Z., Kraft, C. L., Abril, J. F., Anthouard, V., Arensburger, P., Atkinson, P. W., Baden, H., de Berardinis, V., Baldwin, D., Benes, V., Biedler, J., Blass, C., Bolanos, R., Boscus, D., Barnstead, M., Cai, S., Center, A., Chaturverdi, K., Christophides, G. K., Chrystal, M. A., Clamp, M., Cravchik, A., Curwen, V., Dana, A., Delcher, A., Dew, I., Evans, C. A., Flanigan, M., Grundschober-Freimoser, A., Friedli, L., Gu, Z., Guan, P., Guigo, R., Hillenmeyer, M. E., Hladun, S. L., Hogan, J. R., Hong, Y. S., Hoover, J., Jaillon, O., Ke, Z., Kodira, C., Kokoza, E., Koutsos, A., Letunic, I., Levitsky, A., Liang, Y., Lin, J. J., Lobo, N. F., Lopez, J. R., Malek, J. A., McIntosh, T. C., Meister, S., Miller, J., Mobarry, C., Mongin, E., Murphy, S. D., O'Brochta, D. A., Pfannkoch, C., Qi, R., Regier, M. A., Remington, K., Shao, H., Sharakhova, M. V., Sitter, C. D., Shetty, J., Smith, T. J., Strong, R., Sun, J., Thomasova, D., Ton, L. Q., Topalis, P., Tu, Z., Unger, M. F., Walenz, B., Wang, A., Wang, J., Wang, M., Wang, X., Woodford, K. J., Wortman, J. R., Wu, M., Yao, A., Zdobnov, E. M., Zhang, H., Zhao, Q., Zhao, S., Zhu, S. C., Zhimulev, I., Coluzzi, M., della, Torre, A., Roth, C. W., Louis, C., Kalush, F., Mural, R. J., Myers, E. W., Adams, M. D., Smith, H. O., Broder, S., Gardner, M. J., Fraser, C. M., Birney, E., Bork, P., Brey, P. T., Venter, J. C., Weissenbach, J., Kafatos, F. C., Collins, F. H., and Hoffman, S. L. (2002) *Science* **298,** 129–149
19. Clark, A. G., Eisen, M. B., Smith, D. R., Bergman, C. M., Oliver, B., Markow, T. A., Kaufman, T. C., Kellis, M., Gelbart, W., Iyer, V. N., Pollard, D. A., Sackton, T. B., Larracuente, A. M., Singh, N. D., Abad, J. P., Abt, D. N., Adryan, B., Aguade, M., Akashi, H., Anderson, W. W., Aquadro, C. F., Ardell, D. H., Arguello, R., Artieri, C. G., Barbash, D. A., Barker, D., Barsanti, P., Batterham, P., Batzoglou, S., Begun, D., Bhutkar, A., Blanco, E., Bosak, S. A., Bradley, R. K., Brand, A. D., Brent, M. R., Brooks, A. N., Brown, R. H., Butlin, R. K., Caggese, C., Calvi, B. R., Bernardo, de Carvalho, A., Caspi, A., Castrezana, S., Celniker, S. E., Chang, J. L., Chapple, C., Chatterji, S., Chinwalla, A., Civetta, A., Clifton, S. W., Comeron, J. M., Costello, J. C., Coyne, J. A., Daub, J., David, R. G., Delcher, A. L., Delehaunty, K., Do, C. B., Ebling, H., Edwards, K., Eickbush, T., Evans, J. D., Filipski, A., Findeiss, S., Freyhult, E., Fulton, L., Fulton, R., Garcia, A. C., Gardiner, A., Garfield, D. A., Garvin, B. E., Gibson, G., Gilbert, D., Gnerre, S., Godfrey, J., Good, R., Gotea, V., Gravely, B., Greenberg, A. J., Griffiths-Jones, S., Gross, S., Guigo, R., Gustafson, E. A., Haerty, W., Hahn, M. W., Halligan, D. L., Halpern, A. L., Halter, G. M., Han, M. V., Heger, A., Hillier, L., Hinrichs, A. S., Holmes, I., Hoskins, R. A., Hubisz, M. J., Hultmark, D., Huntley, M. A., Jaffe, D. B., Jagadeeshan, S., Jeck, W. R., Johnson, J., Jones, C. D., Jordan, W. C., Karpen, G. H., Kataoka, E., Keightley, P. D., Kheradpour, P., Kirkness, E. F., Koerich, L. B., Kristiansen, K., Kudrna, D., Ku-

lathinal, R. J., Kumar, S., Kwok, R., Lander, E., Langley, C. H., Lapoint, R., Lazzaro, B. P., Lee, S. J., Levesque, L., Li, R., Lin, C. F., Lin, M. F., Lindblad-Toh, K., Llopart, A., Long, M., Low, L., Lozovsky, E., Lu, J., Luo, M., Machado, C. A., Makalowski, W., Marzo, M., Matsuda, M., Matzkin, L., McAllister, B., McBride, C. S., McKernan, B., McKernan, K., Mendez-Lago, M., Minx, P., Mollenhauer, M. U., Montooth, K., Mount, S. M., Mu, X., Myers, E., Negre, B., Newfeld, S., Nielsen, R., Noor, M. A., O'Grady, P., Pachter, L., Papaceit, M., Parisi, M. J., Parisi, M., Parts, L., Pedersen, J. S., Pesole, G., Phillippy, A. M., Ponting, C. P., Pop, M., Porcelli, D., Powell, J. R., Prohaska, S., Pruitt, K., Puig, M., Quesneville, H., Ram, K. R., Rand, D., Rasmussen, M. D., Reed, L. K., Reenan, R., Reily, A., Remington, K. A., Rieger, T. T., Ritchie, M. G., Robin, C., Rogers, Y. H., Rohde, C., Rozas, J., Rubenfield, M. J., Ruiz, A., Russo, S., Salzberg, S. L., Sanchez-Gracia, A., Saranga, D. J., Sato, H., Schaeffer, S. W., Schatz, M. C., Schlenke, T., Schwartz, R., Segarra, C., Singh, R. S., Sirot, L., Sirota, M., Sisneros, N. B., Smith, C. D., Smith, T. F., Spieth, J., Stage, D. E., Stark, A., Stephan, W., Strausberg, R. L., Strempel, S., Sturgill, D., Sutton, G., Sutton, G. G., Tao, W., Teichmann, S., Tobari, Y. N., Tomimura, Y., Tsolas, J. M., Valente, V. L., Venter, E., Venter, J. C., Vicario, S., Vieira, F. G., Vilella, A. J., Villasante, A., Walenz, B., Wang, J., Wasserman, M., Watts, T., Wilson, D., Wilson, R. K., Wing, R. A., Wolfner, M. F., Wong, A., Wong, G. K., Wu, C. I., Wu, G., Yamamoto, D., Yang, H. P., Yang, S. P., Yorke, J. A., Yoshida, K., Zdobnov, E., Zhang, P., Zhang, Y., Zimin, A. V., Baldwin, J., Abdouelleil, A., Abdulkadir, J., Abebe, A., Abera, B., Abreu, J., Acer, S. C., Aftuck, L., Alexander, A., An, P., Anderson, E., Anderson, S., Arachi, H., Azer, M., Bachantsang, P., Barry, A., Bayul, T., Berlin, A., Bessette, D., Bloom, T., Blye, J., Boguslavskiy, L., Bonnet, C., Boukhgalter, B., Bourzgui, I., Brown, A., Cahill, P., Channer, S., Cheshatsang, Y., Chuda, L., Citroen, M., Collymore, A., Cooke, P., Costello, M., D'Aco, K., Daza, R., De Haan, G., DeGray, S., DeMaso, C., Dhargay, N., Dooley, K., Dooley, E., Doricent, M., Dorje, P., Dorjee, K., Dupes, A., Elong, R., Falk, J., Farina, A., Faro, S., Ferguson, D., Fisher, S., Foley, C. D., Franke, A., Friedrich, D., Gadbois, L., Gearin, G., Gearin, C. R., Giannoukos, G., Goode, T., Graham, J., Grandbois, E., Grewal, S., Gyaltsen, K., Hafez, N., Hagos, B., Hall, J., Henson, C., Hollinger, A., Honan, T., Huard, M. D., Hughes, L., Hurhula, B., Husby, M. E., Kamat, A., Kanga, B., Kashin, S., Khazanovich, D., Kisner, P., Lance, K., Lara, M., Lee, W., Lennon, N., Letendre, F., LeVine, R., Lipovsky, A., Liu, X., Liu, J., Liu, S., Lokyitsang, T., Lokyitsang, Y., Lubonja, R., Lui, A., MacDonald, P., Magnisalis, V., Maru, K., Matthews, C., McCusker, W., McDonough, S., Mehta, T., Meldrim, J., Meneus, L., Mihai, O., Mihalev, A., Mihova, T., Mittelman, R., Mlenga, V., Montmayeur, A., Mulrain, L., Navidi, A., Naylor, J., Negash, T., Nguyen, T., Nguyen, N., Nicol, R., Norbu, C., Norbu, N., Novod, N., O'Neill, B., Osman, S., Markiewicz, E., Oyono, O. L., Patti, C., Phunkhang, P., Pierre, F., Priest, M., Raghuraman, S., Rege, F., Reyes, R., Rise, C., Rogov, P., Ross, K., Ryan, E., Settipalli, S., Shea, T., Sherpa, N., Shi, L., Shih, D., Sparrow, T., Spaulding, J., Stalker, J., Stange-Thomann, N., Stavropoulos, S., Stone, C., Strader, C., Tesfaye, S., Thomson, T., Thoulutsang, Y., Thoulutsang, D., Topham, K., Topping, I., Tsamla, T., Vassiliev, H., Vo, A., Wangchuk, T., Wangdi, T., Weiand, M., Wilkinson, J., Wilson, A., Yadav, S., Young, G., Yu, Q., Zembek, L., Zhong, D., Zimmer, A., Zwirko, Z., Jaffe, D. B., Alvarez, P., Brockman, W., Butler, J., Chin, C., Gnerre, S., Grabherr, M., Kleber, M., Mauceli, E., and MacCallum, I. (2007) *Nature* **450,** 203–218

20. Siegert, K. J. (1999) *FEBS Lett.* **447,** 237–240
21. Kaufmann, C., and Brown, M. R. (2006) *Insect Biochem. Mol. Biol.* **36,** 466–481
22. Weinstock, G. M. Robinson, G. E., Gibbs, R. A., Worley, K. C., Evans, J. D., Maleszka, R., Robertson, H. M., Weaver, D. B., Beye, M., Bork, P., Elsik, C. G., Hartfelder, K., *et al.* (2006) *Nature* **443,** 931–949
23. Glenner, H., Thomsen, P. F., Hebsgaard, M. B., Sørensen, M. V., and Willerslev, E. (2006) *Science* **314,** 1883–1884
24. Lindemans, M., Liu, F., Janssen, T., Husson, S. J., Mertens, I., Gäde, G., and Schoofs, L. (2009) *Proc. Natl. Acad. Sci. U.S.A.* **106,** 1642–1647
25. Birnbaumer, M., Seibold, A., Gilbert, S., Ishido, M., Barberis, C., Antaramian, A., Brabet, P., and Rosenthal, W. (1992) *Nature* **357,** 333–335
26. Kimura, T., Tanizawa, O., Mori, K., Brownstein, M. J., and Okayama, H. (1992) *Nature* **356,** 526–529
27. Donaldson, Z. R., and Young, L. J. (2008) *Science* **322,** 900–904
28. Park, J. I., Semyonov, J., Chang, C. L., and Hsu, S. Y. (2005) *Endocrine* **26,** 267–276
29. Van Loy, T., Vandersmissen, H. P., Van Hiel, M. B., Poels, J., Verlinden, H., Badisco, L., Vassart, G., and Vanden Broeck, J. (2008) *Gen. Comp. Endocrinol.* **155,** 14–21
30. Dreborg, S., Sundström, G., Larsson, T. A., and Larhammar, D. (2008) *Proc. Natl. Acad. Sci. U.S.A.* **105,** 15487–15492
31. Cazzamali, G., Hauser, F., Kobberup, S., Williamson, M., and Grimmelikhuijzen, C. J. (2003) *Biochem. Biophys. Res. Commun.* **303,** 146–152
32. Salaneck, E., Larsson, T. A., Larson, E. T., and Larhammar, D. (2008) *Gene* **409,** 61–71
33. Tomoyasu, Y., Miller, S. C., Tomita, S., Schoppmeier, M., Grossmann, D., and Bucher, G. (2008) *Genome Biol.* **9,** R10

SUPPLEMENTAL DATA

FIGURE S1

cDNA and deduced amino acid sequence of the ACP receptor from *Anopheles gambiae* variant-B. Nucleotides are numbered from 5' – to 3' –end. Amino acid residues are numbered from the first start (ATG) codon in the open reading frame. The stop codon is indicated by an asterisk in the amino acid sequence. Exon-intron boundaries are highlighted in grey. The seven transmembrane regions are boxed and labelled TMI-VII. In-frame stop codons in the 5'UTR are underlined. The putative polyadenylation signal in the 3'-noncoding region is underlined twice. Putative glycosylation sites in the extracellular N-terminus are indicated by triangles.

FIGURE S2

Schematic representation of the alternative splicing of the *A. gambiae* ACP receptor gene. This alternative splicing gives rise to two receptor mRNA variants, lacking (A) or containing (B) exon 7 (highlighted in yellow). The shorter (A) variant yields Ag-ACPR-A; the larger (B) Ag-ACPR-B. The red bars represent transmembrane regions of the receptor.

FIGURE S3

cDNA and deduced amino acid sequence of the ACP receptor from *Tribolium castaneum*. The sequences are presented in the same way as Fig. S1.

FIGURE S4

Bioluminescence responses of non-transfected CHO/G-16 cells (A) and CHO/G-16 cells, expressing the *A. gambiae* receptor variant-B (B), after addition of $5x10^{-6}$ M *A. gambiae* ACP. The figure is presented in the same way as in Fig. 6. (C) Dose-response curve of the effect of *A. gambiae* ACP on CHO/G-16 cells expressing the *A. gambiae* variant-B receptor. The EC_{50} *A. gambiae* is about $1x10^{-7}$ M. The number of samples (n) to calculate SEM are: A, n = 4; B, n = 6; C, n = 4.

FIGURE S5

Phylogenetic tree analyses of various insect ACP, AKH, and corazonin preprohormones (A) and ACP, AKH, and corazonin receptors (B). The sequences used in A are taken from Fig. 3; those in B from Fig. 8.

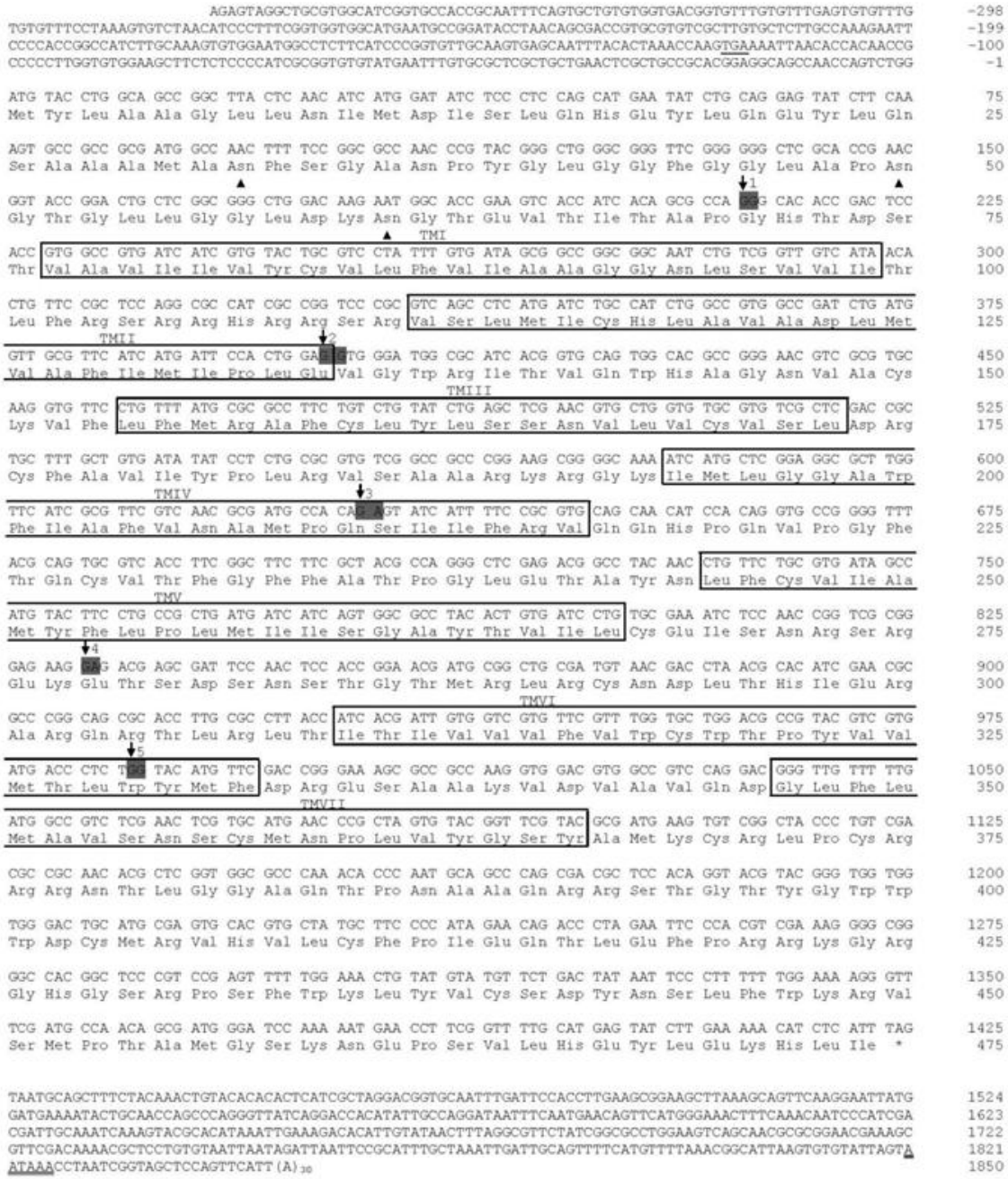
AGAGTAGGCTGCGTGGCATCGGTGCCACCGCAATTTCAGTGCTGTGTGGTGACGGTGTTTGTGTTTGAGTGTGTTTG -298
TGTGTTTCCTAAAGTGTCTAACATCCCTTTCGGTGGTGGCATGAATGCCGGATACCTAACAGCGACCGTGCGTGTCGCTTGTGCTCTTGCCAAAGAATT -199
CCCCACCGGCCATCTTGCAAAGTGTGGAATGGCCTCTTCATCCCGGTGTTGCAAGTGAGCAATTTACACTAAACCAAGTGAAAATTAACACCACAACCG -100
CCCCCTTGGTGTGGAAGCTTCTCTCCCCATCGCGGTGTGTATGAATTTGTGCGCTCGCTGCTGAACTCGCTGCCGCACGGAGGCAGCCAACCAGTCTGG -1
ATG TAC CTG GCA GCC GGC TTA CTC AAC ATC ATG GAT ATC TCC CTC CAG CAT GAA TAT CTG CAG GAG TAT CTT CAA 75
Met Tyr Leu Ala Ala Gly Leu Leu Asn Ile Met Asp Ile Ser Leu Gln His Glu Tyr Leu Gln Glu Tyr Leu Gln 25
AGT GCC GCC GCG ATG GCC AAC TTT TCC GGC GCC AAC CCG TAC GGG CTG GGC GGG TTC GGG GGG CTC GCA CCG AAC 150
Ser Ala Ala Ala Met Ala Asn Phe Ser Gly Ala Asn Pro Tyr Gly Leu Gly Gly Phe Gly Gly Leu Ala Pro Asn 50
1
GGT ACC GGA CTG CTC GGC GGG CTG GAC AAG AAT GGC ACC GAA GTC ACC ATC ACA GCG CCA CCG CAC ACC GAC TCC 225
Gly Thr Gly Leu Leu Gly Gly Leu Asp Lys Asn Gly Thr Glu Val Thr Ile Thr Ala Pro Gly His Thr Asp Ser 75
TMI
ACC GTG GCC GTG ATC ATC GTG TAC TGC GTC CTA TTT GTG ATA GCG GCC GGC GGC AAT CTG TCG GTT GTC ATA ACA 300
Thr Val Ala Val Ile Ile Val Tyr Cys Val Leu Phe Val Ile Ala Ala Gly Gly Asn Leu Ser Val Val Ile Thr 100
CTG TTC CGC TCC AGG CGC CAT CGC CGG TCC CGC GTC AGC CTC ATG ATC TGC CAT CTG GCC GTG GCC GAT CTG ATG 375
Leu Phe Arg Ser Arg Arg His Arg Arg Ser Arg Val Ser Leu Met Ile Cys His Leu Ala Val Ala Asp Leu Met 125
TMII
2
GTT GCG TTC ATC ATG ATT CCA CTG GAG GTG GGA TGG CGC ATC ACG GTG CAG TGG CAC GCC GGG AAC GTC GCG TGC 450
Val Ala Phe Ile Met Ile Pro Leu Glu Val Gly Trp Arg Ile Thr Val Gln Trp His Ala Gly Asn Val Ala Cys 150
TMIII
AAG GTG TTC CTG TTT ATG CGC GCC TTC TGT CTG TAT CTG AGC TCG AAC GTG CTG GTG TGC GTG TCG CTC GAC CGC 525
Lys Val Phe Leu Phe Met Arg Ala Phe Cys Leu Tyr Leu Ser Ser Asn Val Leu Val Cys Val Ser Leu Asp Arg 175
TGC TTT GCT GTG ATA TAT CCT CTG CGC GTG TCG GCC GCC CGG AAG CGG GGC AAA ATC ATG CTC GGA GGC GCT TGG 600
Cys Phe Ala Val Ile Tyr Pro Leu Arg Val Ser Ala Ala Arg Lys Arg Gly Lys Ile Met Leu Gly Gly Ala Trp 200
TMIV
3
TTC ATC GCG TTC GTC AAC GCG ATG CCA CAG AGT ATC ATT TTC CGC GTG CAG CAA CAT CCA CAG GTG CCG GGG TTT 675
Phe Ile Ala Phe Val Asn Ala Met Pro Gln Ser Ile Ile Phe Arg Val Gln Gln His Pro Gln Val Pro Gly Phe 225
ACG CAG TGC GTC ACC TTC GGC TTC TTC GCT ACG CCA GGG CTC GAG ACG GCC TAC AAC CTG TTC TGC GTG ATA GCC 750
Thr Gln Cys Val Thr Phe Gly Phe Phe Ala Thr Pro Gly Leu Glu Thr Ala Tyr Asn Leu Phe Cys Val Ile Ala 250
TMV
ATG TAC TTC CTG CCG CTG ATG ATC ATC AGT GGC GCC TAC ACT GTG ATC CTG TGC GAA ATC TCC AAC CGG TCG CGG 825
Met Tyr Phe Leu Pro Leu Met Ile Ile Ser Gly Ala Tyr Thr Val Ile Leu Cys Glu Ile Ser Asn Arg Ser Arg 275
4
GAG AAG GAG ACG AGC GAT TCC AAC TCC ACC GGA ACG ATG CGG CTG CGA TGT AAC GAC CTA ACG CAC ATC GAA CGC 900
Glu Lys Glu Thr Ser Asp Ser Asn Ser Thr Gly Thr Met Arg Leu Arg Cys Asn Asp Leu Thr His Ile Glu Arg 300
TMVI
GCC CGG CAG CGC ACC TTG CGC CTT ACC ATC ACG ATT GTG GTC GTG TTC GTT TGG TGC TGG ACG CCG TAC GTC GTG 975
Ala Arg Gln Arg Thr Leu Arg Leu Thr Ile Thr Ile Val Val Val Phe Val Trp Cys Trp Thr Pro Tyr Val Val 325
5
ATG ACC CTC TGG TAC ATG TTC GAC CGG GAA AGC GCC GCC AAG GTG GAC GTG GCC GTC CAG GAC GGG TTG TTT TTG 1050
Met Thr Leu Trp Tyr Met Phe Asp Arg Glu Ser Ala Ala Lys Val Asp Val Ala Val Gln Asp Gly Leu Phe Leu 350
TMVII
ATG GCC GTC TCG AAC TCG TGC ATG AAC CCG CTA GTG TAC GGT TCG TAC GCG ATG AAG TGT CGG CTA CCC TGT CGA 1125
Met Ala Val Ser Asn Ser Cys Met Asn Pro Leu Val Tyr Gly Ser Tyr Ala Met Lys Cys Arg Leu Pro Cys Arg 375
CGC CGC AAC ACG CTC GGT GGC GCC CAA ACA CCC AAT GCA GCC CAG CGA CGC TCC ACA GGT ACG TAC GGG TGG TGG 1200
Arg Arg Asn Thr Leu Gly Gly Ala Gln Thr Pro Asn Ala Ala Gln Arg Arg Ser Thr Gly Thr Tyr Gly Trp Trp 400
TGG GAC TGC ATG CGA GTG CAC GTG CTA TGC TTC CCC ATA GAA CAG ACC CTA GAA TTC CCA CGT CGA AAG GGG CGG 1275
Trp Asp Cys Met Arg Val His Val Leu Cys Phe Pro Ile Glu Gln Thr Leu Glu Phe Pro Arg Arg Lys Gly Arg 425
GGC CAC GGC TCC CGT CCG AGT TTT TGG AAA CTG TAT GTA TGT TCT GAC TAT AAT TCC CTT TTT TGG AAA AGG GTT 1350
Gly His Gly Ser Arg Pro Ser Phe Trp Lys Leu Tyr Val Cys Ser Asp Tyr Asn Ser Leu Phe Trp Lys Arg Val 450
TCG ATG CCA ACA GCG ATG GGA TCC AAA AAT GAA CCT TCG GTT TTG CAT GAG TAT CTT GAA AAA CAT CTC ATT TAG 1425
Ser Met Pro Thr Ala Met Gly Ser Lys Asn Glu Pro Ser Val Leu His Glu Tyr Leu Glu Lys His Leu Ile * 475
TAATGCAGCTTTCTACAAACTGTACACACACTCATCGCTAGGACGGTGCAATTTGATTCCACCTTGAAGCGGAAGCTTAAAGCAGTTCAAGGAATTATG 1524
GATGAAAATACTGCAACCAGCCCAGGGTTATCAGGACCACATATTGCCAGGATAATTTCAATGAACAGTTCATGGGAAACTTTCAAACAATCCCATCGA 1623
CGATTGCAAATCAAAGTACGCACATAAATTGAAAGACACATTGTATAACTTTAGGCGTTCTATCGGCGCCTGGAAGTCAGCAACGCGCGGAACGAAAGC 1722
GTTCGACAAAACGCTCCTGTGTAATTAATAGATTAATTCCGCATTTGCTAAATTGATTGCAGTTTTCATGTTTTAAACGGCATTAAGTGTGTATTAGTA 1821
ATAAACCTAATCGGTAGCTCCAGTTCATT(A)30 1850

Fig. S1

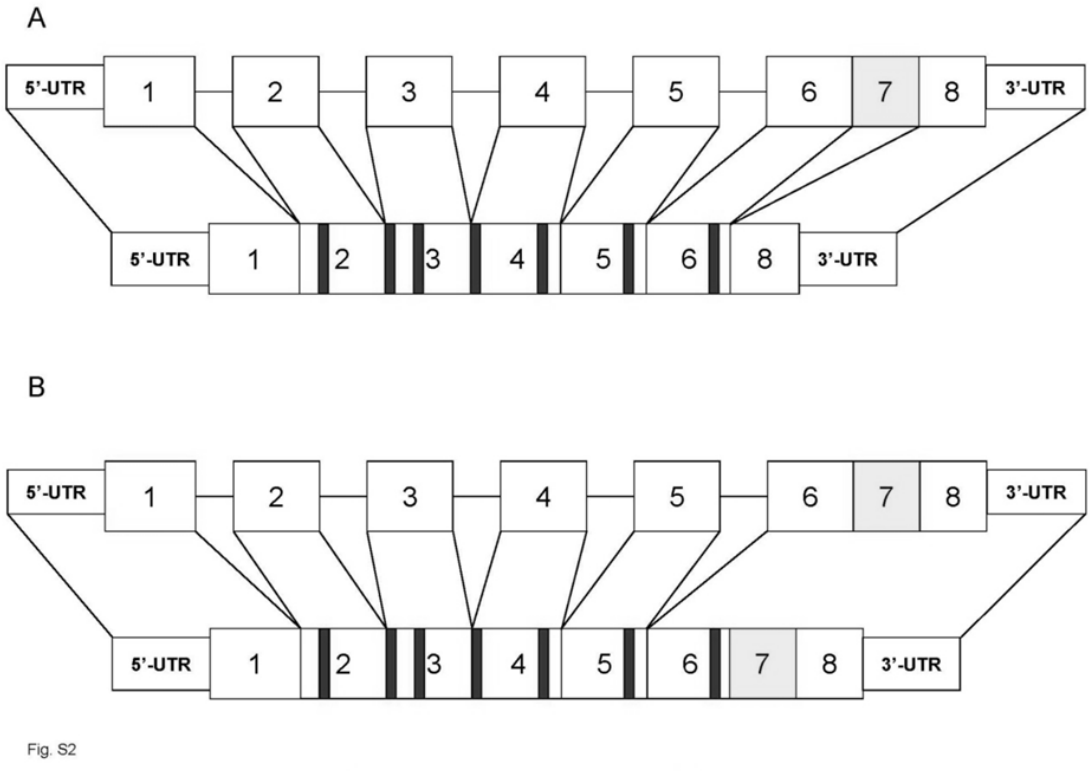
A
5'-UTR
1
2
3
4
5
6
7
8
3'-UTR
5'-UTR
1
2
3
4
5
6
8
3'-UTR
B
5'-UTR
1
2
3
4
5
6
7
8
3'-UTR
5'-UTR
1
2
3
4
5
6
7
8
3'-UTR

Fig. S2

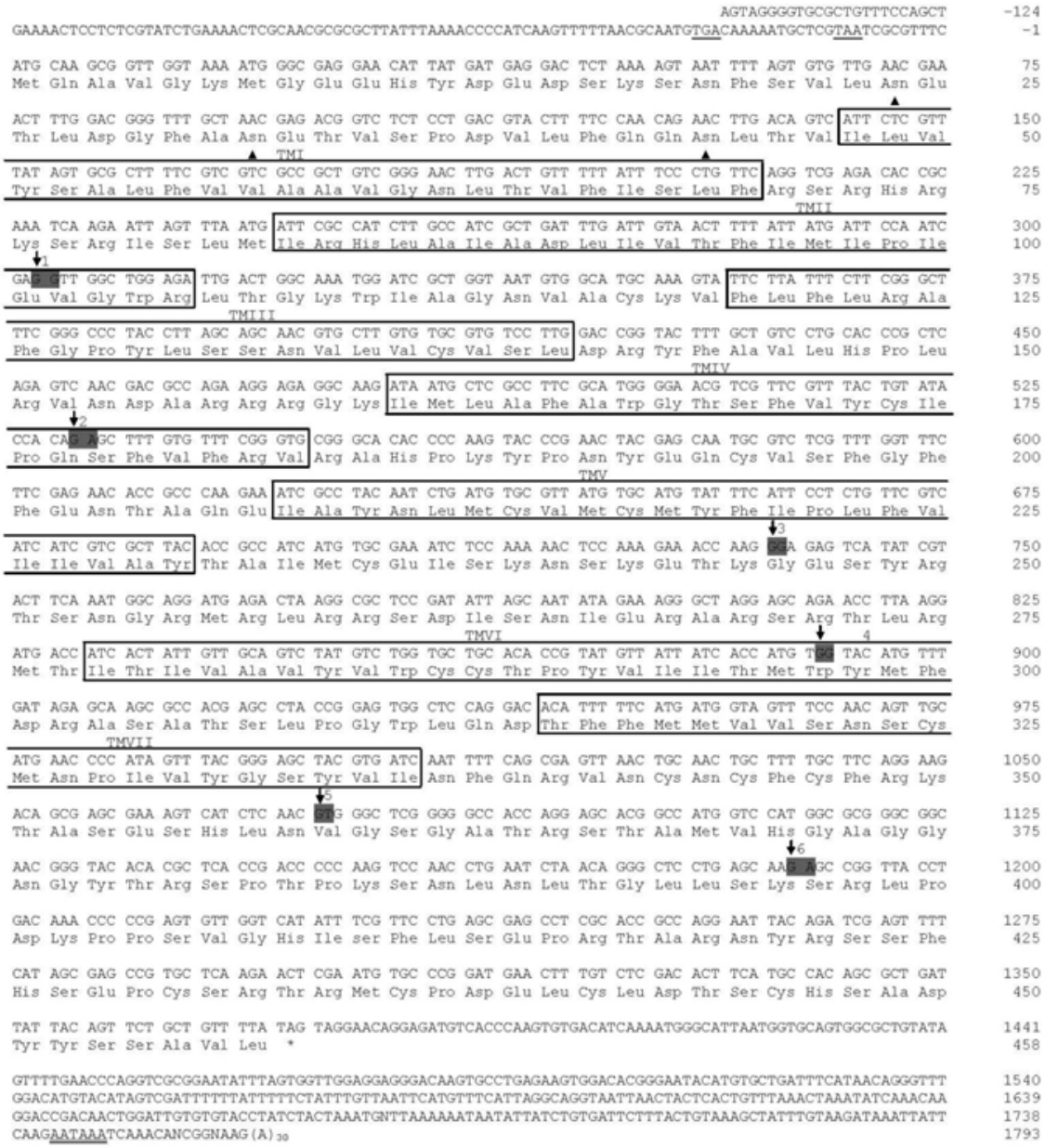
AGTAGGGGTGCGCTGTTTCCAGCT -124
GAAAACTCCTCTCGTATCTGAAAACTCGCAACGCGCGCTTATTTAAAACCCCATCAAGTTTTTAACGCAATGTGACAAAAATGCTCGTAATCGCGTTTC -1
ATG CAA GCG GTT GGT AAA ATG GGC GAG GAA CAT TAT GAT GAG GAC TCT AAA AGT AAT TTT AGT GTG TTG AAC GAA 75
Met Gln Ala Val Gly Lys Met Gly Glu Glu His Tyr Asp Glu Asp Ser Lys Ser Asn Phe Ser Val Leu Asn Glu 25
ACT TTG GAC GGG TTT GCT AAC GAG ACG GTC TCT CCT GAC GTA CTT TTC CAA CAG AAC TTG ACA GTC ATT CTC GTT 150
Thr Leu Asp Gly Phe Ala Asn Glu Thr Val Ser Pro Asp Val Leu Phe Gln Gln Asn Leu Thr Val Ile Leu Val 50
TMI
TAT AGT GCG CTT TTC GTC GTC GCC GCT GTC GGG AAC TTG ACT GTT TTT ATT TCC CTG TTC AGG TCG AGA CAC CGC 225
Tyr Ser Ala Leu Phe Val Val Ala Ala Val Gly Asn Leu Thr Val Phe Ile Ser Leu Phe Arg Ser Arg His Arg 75
TMII
AAA TCA AGA ATT AGT TTA ATG ATT CGC CAT CTT GCC ATC GCT GAT TTG ATT GTA ACT TTT ATT ATG ATT CCA ATC 300
Lys Ser Arg Ile Ser Leu Met Ile Arg His Leu Ala Ile Ala Asp Leu Ile Val Thr Phe Ile Met Ile Pro Ile 100
1
GAG GTT GGC TGG AGA TTG ACT GGC AAA TGG ATC GCT GGT AAT GTG GCA TGC AAA GTA TTC TTA TTT CTT CGG GCT 375
Glu Val Gly Trp Arg Leu Thr Gly Lys Trp Ile Ala Gly Asn Val Ala Cys Lys Val Phe Leu Phe Leu Arg Ala 125
TMIII
TTC GGG CCC TAC CTT AGC AGC AAC GTG CTT GTG TGC GTG TCC TTG GAC CGG TAC TTT GCT GTC CTG CAC CCG CTC 450
Phe Gly Pro Tyr Leu Ser Ser Asn Val Leu Val Cys Val Ser Leu Asp Arg Tyr Phe Ala Val Leu His Pro Leu 150
TMIV
AGA GTC AAC GAC GCC AGA AGG AGA GGC AAG ATA ATG CTC GCC TTC GCA TGG GGA ACG TCG TTC GTT TAC TGT ATA 525
Arg Val Asn Asp Ala Arg Arg Arg Gly Lys Ile Met Leu Ala Phe Ala Trp Gly Thr Ser Phe Val Tyr Cys Ile 175
2
CCA CAG AGC TTT GTG TTT CGG GTG CGG GCA CAC CCC AAG TAC CCG AAC TAC GAG CAA TGC GTC TCG TTT GGT TTC 600
Pro Gln Ser Phe Val Phe Arg Val Arg Ala His Pro Lys Tyr Pro Asn Tyr Glu Gln Cys Val Ser Phe Gly Phe 200
TMV
TTC GAG AAC ACC GCC CAA GAA ATC GCC TAC AAT CTG ATG TGC GTT ATG TGC ATG TAT TTC ATT CCT CTG TTC GTC 675
Phe Glu Asn Thr Ala Gln Glu Ile Ala Tyr Asn Leu Met Cys Val Met Cys Met Tyr Phe Ile Pro Leu Phe Val 225
3
ATC ATC GTC GCT TAC ACC GCC ATC ATG TGC GAA ATC TCC AAA AAC TCC AAA GAA ACC AAG AGA GAG TCA TAT CGT 750
Ile Ile Val Ala Tyr Thr Ala Ile Met Cys Glu Ile Ser Lys Asn Ser Lys Glu Thr Lys Gly Glu Ser Tyr Arg 250
ACT TCA AAT GGC AGG ATG AGA CTA AGG CGC TCC GAT ATT AGC AAT ATA GAA AGG GCT AGG AGC AGA ACC TTA AGG 825
Thr Ser Asn Gly Arg Met Arg Leu Arg Arg Ser Asp Ile Ser Asn Ile Glu Arg Ala Arg Ser Arg Thr Leu Arg 275
TMVI
4
ATG ACC ATC ACT ATT GTT GCA GTC TAT GTC TGG TGC TGC ACA CCG TAT GTT ATT ATC ACC ATG TGG TAC ATG TTT 900
Met Thr Ile Thr Ile Val Ala Val Tyr Val Trp Cys Cys Thr Pro Tyr Val Ile Ile Thr Met Trp Tyr Met Phe 300
GAT AGA GCA AGC GCC ACG AGC CTA CCG GAG TGG CTC CAG GAC ACA TTT TTC ATG ATG GTA GTT TCC AAC AGT TGC 975
Asp Arg Ala Ser Ala Thr Ser Leu Pro Gly Trp Leu Gln Asp Thr Phe Phe Met Met Val Val Ser Asn Ser Cys 325
TMVII
ATG AAC CCC ATA GTT TAC GGG AGC TAC GTG ATC AAT TTT CAG CGA GTT AAC TGC AAC TGC TTT TGC TTC AGG AAG 1050
Met Asn Pro Ile Val Tyr Gly Ser Tyr Val Ile Asn Phe Gln Arg Val Asn Cys Asn Cys Phe Cys Phe Arg Lys 350
5
ACA GCG AGC GAA AGT CAT CTC AAC GTG GGC TCG GGG GCC ACC AGG AGC ACG GCC ATG GTC CAT GGC GCG GGC GGC 1125
Thr Ala Ser Glu Ser His Leu Asn Val Gly Ser Gly Ala Thr Arg Ser Thr Ala Met Val His Gly Ala Gly Gly 375
6
AAC GGG TAC ACA CGC TCA CCG ACC CCC AAG TCC AAC CTG AAT CTA ACA GGG CTC CTG AGC AAG AGC CGG TTA CCT 1200
Asn Gly Tyr Thr Arg Ser Pro Thr Pro Lys Ser Asn Leu Asn Leu Thr Gly Leu Leu Ser Lys Ser Arg Leu Pro 400
GAC AAA CCC CCG AGT GTT GGT CAT ATT TCG TTC CTG AGC GAG CCT CGC ACC GCC AGG AAT TAC AGA TCG AGT TTT 1275
Asp Lys Pro Pro Ser Val Gly His Ile ser Phe Leu Ser Glu Pro Arg Thr Ala Arg Asn Tyr Arg Ser Ser Phe 425
CAT AGC GAG CCG TGC TCA AGA ACT CGA ATG TGC CCG GAT GAA CTT TGT CTC GAC ACT TCA TGC CAC AGC GCT GAT 1350
His Ser Glu Pro Cys Ser Arg Thr Arg Met Cys Pro Asp Glu Leu Cys Leu Asp Thr Ser Cys His Ser Ala Asp 450
TAT TAC AGT TCT GCT GTT TTA TAG TAGGAACAGGAGATGTCACCCAAGTGTGACATCAAAATGGGCATTAATGGTGCAGTGGCGCTGTATA 1441
Tyr Tyr Ser Ser Ala Val Leu * 458
GTTTTGAACCCAGGTCGCGGAATATTTAGTGGTTGGAGGAGGGACAAGTGCCTGAGAAGTGGACACGGGAATACATGTGCTGATTTCATAACAGGGTTT 1540
GGACATGTACATAGTCGATTTTTTATTTTTCTATTTGTTAATTCATGTTTCATTAGGCAGGTAATTAACTACTCACTGTTTAAACTAAATATCAAACAA 1639
GGACCGACAACTGGATTGTGTGTACCTATCTACTAAATGNTTAAAAAATAATATTATCTGTGATTCTTTACTGTAAAGCTATTTGTAAGATAAATTATT 1738
CAAGAATAAATCAAACANCGGNAAG(A)30 1793

Fig. S3

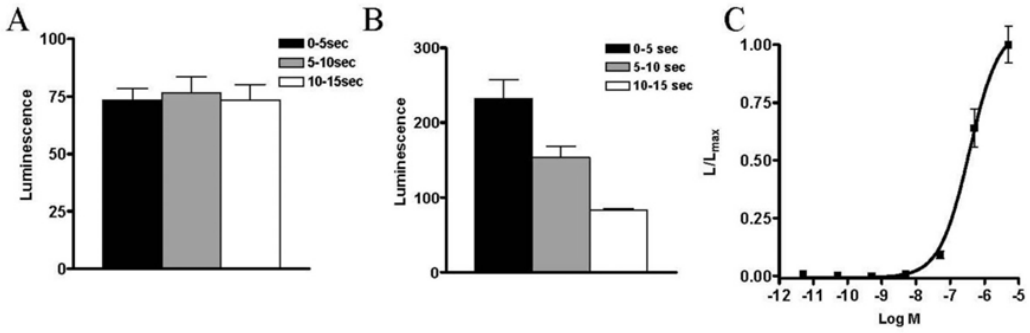
A
100
75
50
25
0
Luminescence
0-5sec
5-10sec
10-15sec
B
300
200
100
0
Luminescence
0-5 sec
5-10 sec
10-15 sec
C
1.00
0.75
0.50
0.25
0.00
L/Lmax
-12 -11 -10 -9 -8 -7 -6 -5
Log M

Fig. S4


Tc-AKH1
Tc-AKH2
Dm-AKH
Am-AKH
Ag-AKH
Aa-AKH
Bm-AKH1
Bm-AKH2
Bm-ACP
Nv-ACP
Tc-ACP
Ag-ACP
Cp-ACP
Aa-ACP
Ag-CRZ
Aa-CRZ
Nv-CRZ
Bm-CRZ
Dm-CRZ
Am-CRZ

Fig. S5A

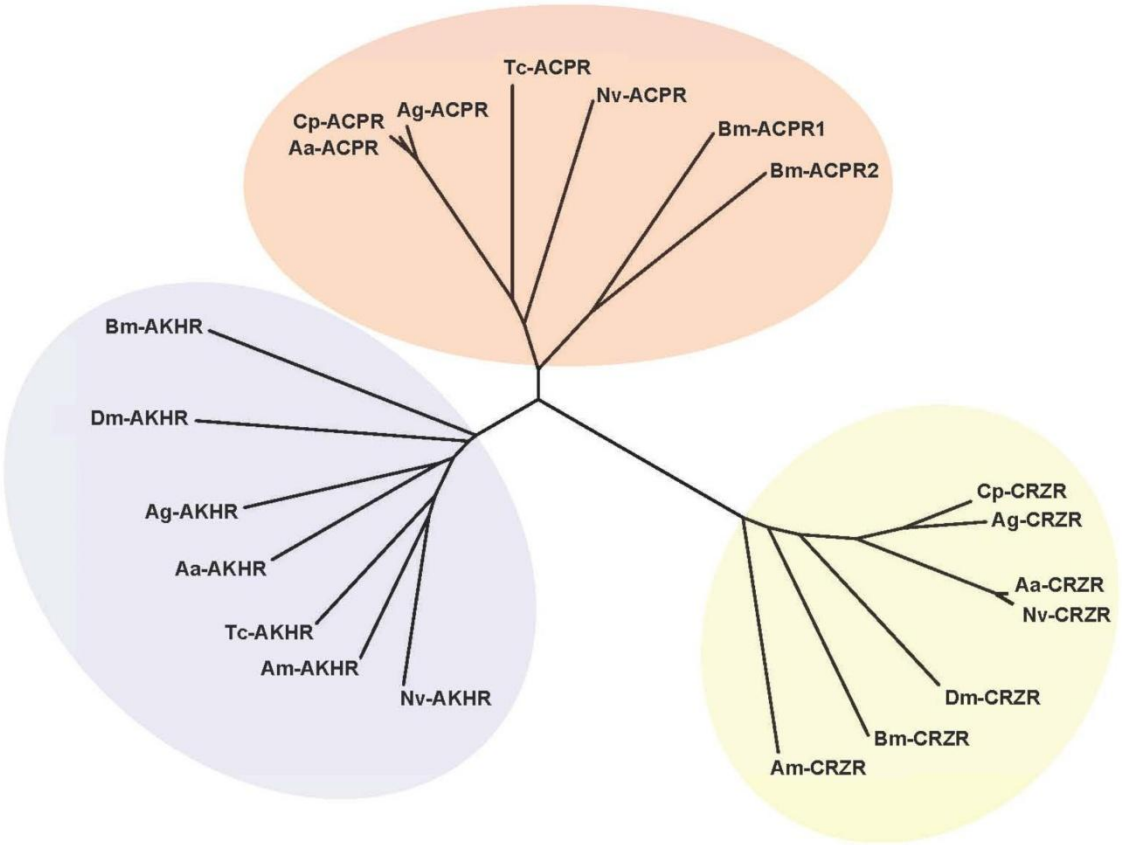
Tc-ACPR
Nv-ACPR
Cp-ACPR
Ag-ACPR
Aa-ACPR
Bm-ACPR1
Bm-ACPR2
Bm-AKHR
Dm-AKHR
Ag-AKHR
Aa-AKHR
Tc-AKHR
Am-AKHR
Nv-AKHR
Cp-CRZR
Ag-CRZR
Aa-CRZR
Nv-CRZR
Dm-CRZR
Bm-CRZR
Am-CRZR

Fig. S5B

Table S1. Primers used for qPCR

Gene	Sense Primer Sequence	Antisense Primer Sequence	GenBank accession no.
ACP preprohormone	5'-ACTTGTGGCGGTGCTAGTTC-3'	5'-TCGGACTTGGTTCATAAGCAG-3'	GQ217536
ACP receptor	5'-GTGGCTCCAGGACACATTTT-3'	5'-TTGTCAGGTAACCGGCTCTT-3'	EU138886
Ribosomal protein S3	5'- TGTGGCGCTAAAGGGTGT-3'	5'- TTGTCAGGCAGAGGCTTTTT-3'	XM_965494
Ribosomal protein L32	5'-GGCACCAGTCTGACCGTTAT-3'	5'-ATCAACAACACTTCCAGTTCCTT-3'	XM_964471
Elongation factor 1-α	5'- CGTCTTCCGCTCCAGGAC-3'	5'- CTTCACGGACACGTTCTTCA-3'	XM_961260
Tubulin alpha 6	5'- CGAGGATGTCGCCTGTGA-3'	5'- CCCAAAAGCCGGTTTAAGTT-3'	XM_968998
Actin	5'-CTTCGAGACAGTTAATGTCAGAATTG-3'	5'- AAAACCATCTTCTTGCCAATG-3'	XM_962504

Table S2: Peptides and biogenic amines tested in our bioassay

Peptides

Drosophila melanogaster	AKH	pQLTFSPDWamide
	allatostatin-A4	TTRPQPFNFGLamide
	allatostatin-B1	AWQSLQSSWamide
	allatostatin-B2	AWKSMNVAWamide
	allatostatin-B5	DQWQKLHGGWamide
	allatostatin-C	pQVRYRQCYFNPISCF
	capa-1	GANMGLYAFPRVamide
	capa-2	ASGLVAFPRVamide
	capa-3	TGPSASSGLWFGPRLamide
	CCAP	PFCNAFTGCamide
	corazonin	pQTFQSRGWTNamide
	ecdysis triggering hormone-1	DDSSPGFFLKITKNVPRLamide
	ecdysis triggering hormone-2	GENFAIKNLKTIPRIamide
	hug-γ	pQLQSNGEPAYRVRTPRLamide
	PNamide	NVGTLARDFQLPIPNamide
	TY-amide	YIGSLARAGGLMTYamide
	myosuppressin	TDVDHVFLRFamide
	neuropeptide F	SNSRPPRKNDVNTMADAYKFLQDLD TYYGDRARVRFamide
	pigment dispersing hormone	NSELINSLLSLPKNMNDAamide
	proctolin	RYLPT
	pyrokinin-2	SVPFKPRLamide
	short neuropeptide F1	AQRSPSLRLRFamide
	SIFamide	AYRKPPFNGSIFamide
	sulfakinin-0	NQKTMSFGamide
	sulfakinin-2	GGDDQFDDYGHMRFamide
	tachykinin-3	APTGFTGMRamide
Anopheles gambiae	ACP	pQVTFSRDWNAamide
	AKH	pQLTFTPAWamide
	capa-1	GPTVGLFAFPRVamide
	capa-2	pQGLVPFPRVamide
Tribolium castaneum	ACP	pQVTFSRDWNPamide
	AKH-1	pQLNSTDSWamide
	AKH-2	pQLNFTPNW--amide
	inotocin	CLITNCPRGamide
Leucophea madeira	leucokinin-3	DQGFNSWGamide
	leucomyosuppressin	pQDVDHVFLRFamide
	leucopyrokinin	ETSFTPRLamide
Manduca sexta	allatotropin	GFKNVEMMTARGFamide
	AKH	pQLTFTSSWG-amide

Locusta migratoria	hypertrehalosaemic peptide	pQVTFSRDWSPamide
Periplaneta americana	perisulfakinin	EQFDDYGHMRFamide
Lymnea stagnalis	conopressin G	CFIRNCPKGamide
Conus geographicus	conopressin S	CIIRNCPRGamide
Arapaima gigas	isotocin	CYISNCPIGamide
Homo sapiens	oxytocin	CYIQNCPLGamide
	vasopressin	CYFQNCPRGamide
Rana esculenta	vasotocin	CYIQNCPRGamide

Biogenic amines

adrenaline
dopamine
histamine
melatonin,
noradrenaline
serotonin
octopamine
tyramine

Chapter 7:

Novel antennal lobe substructures revealed in the small hive beetle *Aethina tumida*

Cell Tissue Res (2016) 363:679–692
DOI 10.1007/s00441-015-2282-9

REGULAR ARTICLE

Novel antennal lobe substructures revealed in the small hive beetle *Aethina tumida*

Martin Kollmann[1] · Anna Lena Rupenthal[1] · Peter Neumann[2] · Wolf Huetteroth[1,3] · Joachim Schachtner[1]

Received: 14 February 2015 / Accepted: 17 August 2015 / Published online: 24 October 2015

Abstract The small hive beetle, *Aethina tumida*, is an emerging pest of social bee colonies. *A. tumida* shows a specialized life style for which olfaction seems to play a crucial role. To better understand the olfactory system of the beetle, we used immunohistochemistry and 3-D reconstruction to analyze brain structures, especially the paired antennal lobes (AL), which represent the first integration centers for odor information in the insect brain. The basic neuroarchitecture of the *A. tumida* brain compares well to the typical beetle and insect brain. In comparison to other insects, the AL are relatively large in relationship to other brain areas, suggesting that olfaction is of major importance for the beetle. The AL of both sexes contain about 70 olfactory glomeruli with no obvious size differences of the glomeruli between sexes. Similar to all other insects including beetles, immunostaining with an antiserum against serotonin revealed a large cell that projects from one AL to the contralateral AL to densely innervate all glomeruli. Immunostaining with an antiserum against tachykinin-related peptides (TKRP) revealed hitherto unknown structures in the AL. Small TKRP-immunoreactive spherical substructures are in both sexes evenly distributed within all glomeruli. The source for these immunoreactive islets is very likely a group of about 80 local AL interneurons. We offer two hypotheses on the function of such structures.

Keywords Olfactory system · Neuropeptide · Serotonin · Insect · 3D reconstruction

Electronic supplementary material The online version of this article (doi:10.1007/s00441-015-2282-9) contains supplementary material, which is available to authorized users.

✉ Joachim Schachtner
joachim.schachtner@biologie.uni-marburg.de

[1] Department of Biology, Animal Physiology, Philipps-University Marburg, Karl-von-Frisch-Str. 8, 35032 Marburg, Germany

[2] Institute of Bee Health, Vetsuisse Faculty, University of Bern, Bern, Switzerland

[3] Present address: Department of Biology, Neurobiology, University of Konstanz, 78457 Konstanz, Germany

Introduction

The small hive beetle *Aethina tumida* (Murray 1867, Coleoptera: Nitidulidae) is a parasite and scavenger of colonies of social bees (honeybees: *Apis mellifera*: cf. Neumann and Elzen 2004; bumblebees: *Bombus impatiens*: Spiewok and Neumann 2006; stingless bees: *Trigona carbonaria*: cf. Greco et al. 2010 and *Austroplebeia australis*: cf. Halcroft et al. 2011). Both larvae and adults of the *A. tumida* feed on pollen, honey and bee brood, leading to fermentation of the honey and devastation of the combs, often resulting in the full structural collapse of the entire nest (Lundie 1940; Schmolke 1974; Neumann and Elzen 2004). In its native range in sub-Saharan Africa, *A. tumida* is a rather harmless parasite, mostly affecting weak and stressed colonies (Lundie 1940; Hepburn and Radloff 1998; Neumann and Elzen 2004; Neumann and Ellis 2008). However, *A. tumida* has become an invasive species. It was introduced into the USA (1996), Egypt (2000), Australia (2001) and into Europe twice (2004 and 2014; see Neumann and Ellis 2008; Mutinelli et al. 2014) and now has well-established new populations in North America and Australia (Neumann and Elzen 2004; Neumann and Ellis 2008). In these areas, *A. tumida* can be considered a significant pest of managed honeybees (Neumann and Elzen 2004) and possibly of wild bees (Neumann 2015).

To control this emerging pest, Neumann and Elzen (2004) speculated about the possibility of a *A. tumida* pheromone that

could be used for trapping systems. Indeed, male-produced aggregation pheromones of other species in the family Nitidulidae are known from *Carpophilus obsoletus* and are used for pest control (Petroski et al. 1994). Today, a great variety of insect pheromones (especially for Lepidoptera and Coleoptera) are known and used for trapping systems (www.pherobase.com). Although pheromone communication has not yet been demonstrated in the small hive beetle, it has been shown that *A. tumida* is highly attracted to volatiles emitted by adult honey bees (*A. mellifera*), bumble bees (*Bombus impatiens*), stored pollen, wax, brood, and honey (Suazo et al. 2003; Graham et al. 2011; de Guzman et al. 2011). Furthermore, *A. tumida* prefer to fly before or after dusk (Schmolke 1974) suggesting that visual cues are less important than olfactory cues when it comes to locating beehives for mating. Altogether, understanding the olfactory system of *A. tumida* might be instrumental in controlling this pest.

In insects, olfactory information is detected by olfactory sensory neurons (OSNs) housed in olfactory sensilla on the antenna and the maxillary palps (reviewed in Hansson and Stensmyr 2011). They pass the information on to the neuronal network in the antennal lobes (AL), the first integration centers for odor information in the insect brain. Typically, AL are substructured in spheroidal compartments, the olfactory glomeruli. Typically, OSNs that express the same specific odorant receptor converge onto the same glomerulus (Vosshall et al. 2000). The glomerulus number ranges between about 40 in Diptera up to several hundred in Hymenoptera (Schachtner et al. 2005; Mysore et al. 2009; Kuebler et al. 2010). In various orders of neopteran insects, including Coleoptera, Dictyoptera, Diptera, Hymenoptera and Lepidoptera, sexual dimorphic glomeruli have been described (Kondoh et al. 2003; Kleineidam et al. 2005; Schachtner et al. 2005; Hu et al. 2011). Such glomerular dimorphism may have been evolved independently where it was needed, e.g., for long-distance pheromone detection or for the detection of specific odors like host plant volatiles or trail pheromone (Hansson and Stensmyr 2011). In the AL, olfactory information is processed by local interneurons (LN) and relayed to projection neurons (PN) that connect to other brain areas including the mushroom bodies (MB) or the lateral horn (LH). Additionally, the AL receives innervation from a few unique centrifugal neurons (CN) that provide efferent input from other brain areas (reviewed in Schachtner et al. 2005).

Antennal lobes across insect species contain a wide range of neuromediators including excitatory and inhibitory transmitters like acetylcholine and GABA (e.g., Bicker 1999; Homberg 2002; Schachtner et al. 2005; Berg et al. 2009; Fusca et al. 2015). In addition, AL neurons contain neuromediators like biogenic amines, gaseous signaling molecules like NO and a large variety of neuropeptides, suggesting important involvement for proper olfactory behavior (e.g., Schachtner et al. 2005; Berg et al. 2007; Utz et al. 2008; Carlsson et al. 2010; Binzer et al. 2014; Siju et al. 2014; Fusca et al. 2015). For example, in moths and flies, serotonin (5HT) is able to modulate the sensitivity of odors and sex pheromones (Linn and Roelofs 1986; Gatellier et al. 2004; Hill et al. 2003; Kloppenburg and Hildebrand 1995; Dacks et al. 2009). Another example are the tachykinin-related neuropeptides (TKRP), controlling olfactory sensitivity and locomotor activity in the fruit fly *Drosophila melanogaster* (Ignell et al. 2009; Winther et al. 2006; Winther and Ignell 2010).

Typically, neuromediators are distributed across all glomeruli of the AL (Schachtner et al. 2005; Carlsson et al. 2010; Binzer et al. 2014; Neupert et al. 2012; Siju et al. 2014). However, there are exceptions in which only one or several glomeruli receive innervations by neurons that express specific neuromediators like serotonin in the ant (*Camponotus laevigatus*; Dacks et al. 2006), short neuropeptide F (sNPF) in the mosquito (*Aedes aegypti*; Siju et al. 2014) and in the fly (*Drosophila melanogaster*; Carlsson et al. 2010), or serotonin and several neuropeptides in collembolans (Kollmann et al. 2011a).

The life cycle of *A. tumida* involves long-distance dispersal to new food sources (Neumann et al. 2012), preferentially after dusk (cf. Neumann and Elzen 2004). Therefore, olfaction seems to play a pivotal role for the adult beetles (reviewed in Neumann and Elzen 2004). Given that olfaction is that important for the behavior of the animal, the anatomy of the brain, especially of the central olfactory pathway, might very likely reflect this importance. We hypothesize that brain neuropils involved in processing of olfactory information should be enlarged in relationship to other brain areas. We also hypothesize that a sequential invasion of bee colonies, as was postulated by Elzen et al. (2000), with males first and females following could be reflected by specialized glomeruli, e.g., sexual dimorphic glomeruli as described for several other insect species. In addition, we are looking for any specialization in the central olfactory pathway that could reflect the special life style of *A. tumida*.

Materials and Methods

Experimental animals

Adult *Aethina tumida* were collected from naturally infested colonies of the African honeybee subspecies *Apis mellifera scutellata* at the experimental farm of the Department of Zoology and Entomology, University of Pretoria, South Africa. After collection, the beetles were immediately sexed following a routine procedure (Neumann et al. 2013). According to European legislation, import of live *A. tumida* to Germany is illegal (Commission Decisions EC No 2003/881 and Commission Regulation (EC) N° 1398/2003). Therefore, the

beetles were decapitated in Pretoria and the heads were fixed for 12 h at 4 °C in 4 % FA (formaldehyde FA; Roth, Karlsruhe, Germany) in PBS (phosphate-buffered saline, 0.01 M, pH 7.4). They were rinsed for 15 min in PBS and afterwards stored in PBS in glass vials in a customized cooling device and then sent by express delivery to the Philipps University of Marburg (Marburg, Germany).

Immunohistochemistry

Primary antibodies In the current study, we used antibodies against the synaptic vesicle protein synapsin, the biogenic amine serotonin and an antiserum recognizing tachykinin-related peptides (summarized in Table 1).

The monoclonal antibody from mouse against a fusion protein consisting of a glutathione-S-transferase and the first amino acids of the presynaptic vesicle protein synapsin I coded by its 5′-end (SYNORF1; 3C11, #151101) was used to selectively label neuropilar areas. It was used in combination with one additional primary antibody raised in rabbit. The synapsin antibody was kindly provided by Dr. Erich Buchner (University of Würzburg, Germany). This antibody was first described by Klagges et al. (1996) and has been used in many insect studies to label neuropilar areas (e.g., Utz et al. 2008; Heuer et al. 2012; Binzer et al. 2014). The antibody was used at a dilution of 1:100.

The polyclonal antiserum against serotonin (5HT) was raised in rabbit against paraformaldehyde-coupled conjugates of BSA (bovine serum albumin) and 5HT (DiaSorin, Dietzenbach, Germany). Its specificity for the insect nervous system has been shown in several studies (e.g., Dacks et al. 2006). It was used at a dilution of 1:5000.

The polyclonal TKRP antiserum was kindly provided by Dr. H. Agricola (University of Jena, Germany). It was raised in rabbits against locustatachykinin-2 (Lom-TK II, APLSGFYGVRamide) glutaraldehyde-conjugated to bovine thyroglobulin (Veenstra et al. 1995). The antiserum is also known to detect tachykinin-related peptides (TKRPs; consensus sequence FXGXRamide) in other insects (e.g., Vitzthum and Homberg 1998; Heuer et al. 2012; Binzer et al. 2014). In beetles, specificity for the anti-TKRP antiserum has so far been confirmed in *Tribolium castaneum* by preabsorption of the antiserum with synthetic Lom-TK II (Binzer et al. 2014). In the current study, we used the anti-TKRP antiserum to reveal morphological structures of the brain of *A. tumida*. It was used at a dilution of 1:2000.

Secondary antibodies Goat anti-mouse antibodies conjugated to Cy5 (GAM-Cy5) and goat anti-rabbit antibodies conjugated to Cy3 (GAR-Cy3) were used as secondary antibodies (each 1:300; Jackson ImmunoResearch, Westgrove, PA, USA).

Whole mount double immunostainings Brains of *A. tumida* were dissected out of the head capsule, fixed overnight at 4 °C in 4 % FA in PBS, followed by rinsing (4×10 min) with PBS at RT (room temperature). Afterwards, brains were preincubated for 2 days in PBT (PBS containing 0.3 % Triton-X 100; Sigma Aldrich, Steinheim, Germany) with 5 % NGS (normal goat serum; Jackson ImmunoResearch). The primary antibody anti-synapsin (1:100) was used in combination with the anti Lom-TK II (1:5000) or anti 5HT antiserum (1:2000) diluted in PBT with 1 % NGS. Brains were incubated for 2 days at 4 °C. After rinsing (4×10 min) with PBT at RT, brains were incubated in secondary antibodies (GAM-Cy5 and GAR-Cy3; 1:300) in PBT with 1 % NGS at 4 °C for 2 days in the dark. After rinsing (6×10 min) with PBT at RT and washing in distilled H_2O for 10 min, brains were dehydrated in an ascending alcohol series (30, 50, 70, 90, 95 %, 2×100 % ethanol, 5 min each). Followed by clearing the tissue in methyl salicylate (10 min; Merck, Darmstadt, Germany) the brains were finally mounted in resin (Permount; Fisher Scientific, Pittsburgh, PA, USA). During the immunostaining procedure, all washing and incubation steps were performed on a laboratory orbital shaker (MS 3 digital; IKA, Staufen, Gemany).

Data processing

Fluorescence was analyzed with a confocal laser scanning microscope (Leica TCS SP5 Microsystems; Leica, Wetzlar, Germany), with the object lenses ×20 oil objective (HCX PL APO lambda blue ×20/ NA=0.70 Imm UV, working distance: 260 µm; Leica), ×40 oil objective (HCX PL APO lambda blue ×40/ NA=1.25 Oil UV, working distance: 100 µm; Leica), and ×63 glycerol objective (HCX PL APO ×63/ NA=1.30 Glyc 21 °C CS working distance: 260 µm; Leica). We scanned with a resolution of 1024×1024 or 512×512 pixels, a line average of 2, speed of 200 Hz, a digital zoom of 1–2,

Table 1 List of antibodies used, including dilution, source, donor and reference for each antibody

Name, anti-	Shortcut	Dilution	Source	Donor	Reference
D. melanogaster Synapsin I	α-Synapsin	1:100	Mouse	Dr. Buchner	Klagges et al. 1996
Serotonin	α-5HT	1:2000	Rabbit	DiaSorin	–
Locusta migratoria Tachykinin II	α-Lom-TK II	1:5000	Rabbit	Dr. Agricola	Veenstra et al. 1995

and z-steps varying from 0.5 to 1.0 μm for detailed scans and from 3.0 to 5.0 μm for overview scans.

Image segmentation, reconstruction and visualization

Brain structures were 3-D reconstructed using AMIRA 5.2 (Visage Imaging, Berlin, Germany). Segmentation and reconstruction were performed according to Kurylas et al. (2008) and El Jundi et al. (2009). In short, data of the CLSM image stacks were opened in the segmentation editor of AMIRA. From all three spatial directions (lateral to lateral, anterior to posterior and dorsal to ventral) of the respective structure, 3–12 layers (depending on the size of the structure) were labeled and finally wrapped to obtain a voxel-based 3-D model. By using the tool "SurfaceGen", we transferred the voxel-based 3-D model into a polygonal surface model. Standard color codes were used for the reconstructed neuropils (Brandt et al. 2005). For further global processing (i.e., contrast and brightness optimization) and final figure arrangements, snapshots were taken in AMIRA and subsequently processed in Corel Draw 13 (Corel, Ottawa, ON, Canada). Diagrams generated with Excel XP (Microsoft, Redmond, WA, USA) were imported and revised in Corel Draw 13 without any further modification. For statistical analyses, we used a two-tailed *t* test in Origin 6.0 (OriginLab, Northampton, MA, USA) and Excel XP.

Results

General organization of the brain

A 3-D reconstruction of the brain of *Aethina tumida* was created based on confocal sections of an adult female stained with anti-synapsin antibody (Fig. 1) (movie of a rotating 3-D reconstruction and a camera path through the synapsin staining of a brain can be found in the digital supplements, ESM 1 and 2; 3-D reconstructions of single male and female AL can be found in ESM 3). The brain contains all typical neuropils known from most insects including neuropils of the optic lobes, the antennal lobes, mushroom body and neuropils of the central complex (e.g., *Drosophila melanogaster*, Rein et al. 2002; honeybee *Apis mellifera*, Brandt et al. 2005; desert locust *Schistocerca gregaria*, Kurylas et al. 2008; sphinx moth *Manduca sexta*, el Jundi et al. 2009; red flour beetle *Tribolium castaneum*, Dreyer et al. 2010). We reconstructed all neuropils that were clearly identifiable and separable (8 paired and 3 unpaired neuropils).

In the optical lobes, we reconstructed the paired medulla (Me), lobula (Lo), lobula plate (LoP) and accessory medulla (aMe). The central complex is located in the center of the protocerebrum. Its reconstruction includes the unpaired upper and lower unit of the central body (CBU, CBL), the paired Noduli (No) and the dorso-posteriorly located unpaired protocerebral bridge (PB).

The paired mushrooms bodies are placed lateral to both sides of the central complex. We reconstructed calyx (Ca) and pedunculus (Pe) separately. The Pe contains the vertical lobe (vL) and medial lobe (mL). The Pe and the lobes are separated into an inner core region, which is densely stained with synapsin antibody (Fig. 1; non-transparent-shaped part of the MB) and a less densely anti-synapsin stained exterior region (Fig. 1; transparent-shaped part of the MB).

Organization of the antennal lobe

In total, we analyzed 12 ALs of 7 males and 9 ALs of 5 females. Characteristically for insects (Schachtner et al. 2005), in *A. tumida* the AL are organized in small, spherical substructures, the olfactory glomeruli, which are arranged around a central coarse neuropil. The small hive beetle possesses 72.0±3.9 glomeruli per AL in males (n=12 ALs) and 71.1±3.4 glomeruli per AL in females (n=9 ALs) (p=0.588).

The average size of one glomerulus is 10.7±1.8 μm^3 in males (n=12 ALs / n=864 glomeruli) and 10.1±1.8 μm^3 in females (n=9 ALs / n=640 glomeruli). For approximation of the AL size, the volumes of all glomeruli within the AL were summed; extraglomerular space and central coarse neuropil were not included. Mean volume of male AL is 730.0± 120.5 μm^3 (n=12 ALs), compared to 719.2±114.9 μm^3 in females (n=9 ALs). Taken together, male and female ALs of *A. tumida* were statistically indifferent in regard of glomeruli number (p=0.588), overall glomeruli size (p=0.875), or on the level of the AL volume (p=0.997).

It is known from several insect species that conspicuously larger glomeruli appear in one of the sexes, typically at the entrance site of the antennal nerve (Schachtner et al. 2005; Hu et al. 2011). To verify whether this might also be true for the small hive beetle, we grouped the different-sized glomeruli of males (n=12 ALs; n=864 glomeruli) and females (n=9 ALs; n=640 glomeruli) according to their volume (0–999 μm^3= group 0; 1000–1999 μm^3=group 1; …35,000–35,999 μm^3= group 35), followed by analyzing the relative abundance of these different size groups (Fig. 2) (data of glomeruli from all ALs of one sex were pooled). No conspicuous sexual dimorphism could be seen. Middle-sized glomeruli with a volume between 4000 μm^3 and 11,999 μm^3 seemed to be the most common ones, while small glomeruli (between 1000 and 2999 μm^3) and large glomeruli (between 17,000 and 20, 999 μm^3) were less abundant. In addition, a varying number of a few larger glomeruli (between 21,000 and 35,999 μm^3) occur in both sexes. Analysis of the position of the three largest glomeruli per AL revealed that they are not clustered and that they distribute randomly within the anterior half of the AL, with no particular correlation to the site where the antennal nerve enters the AL.

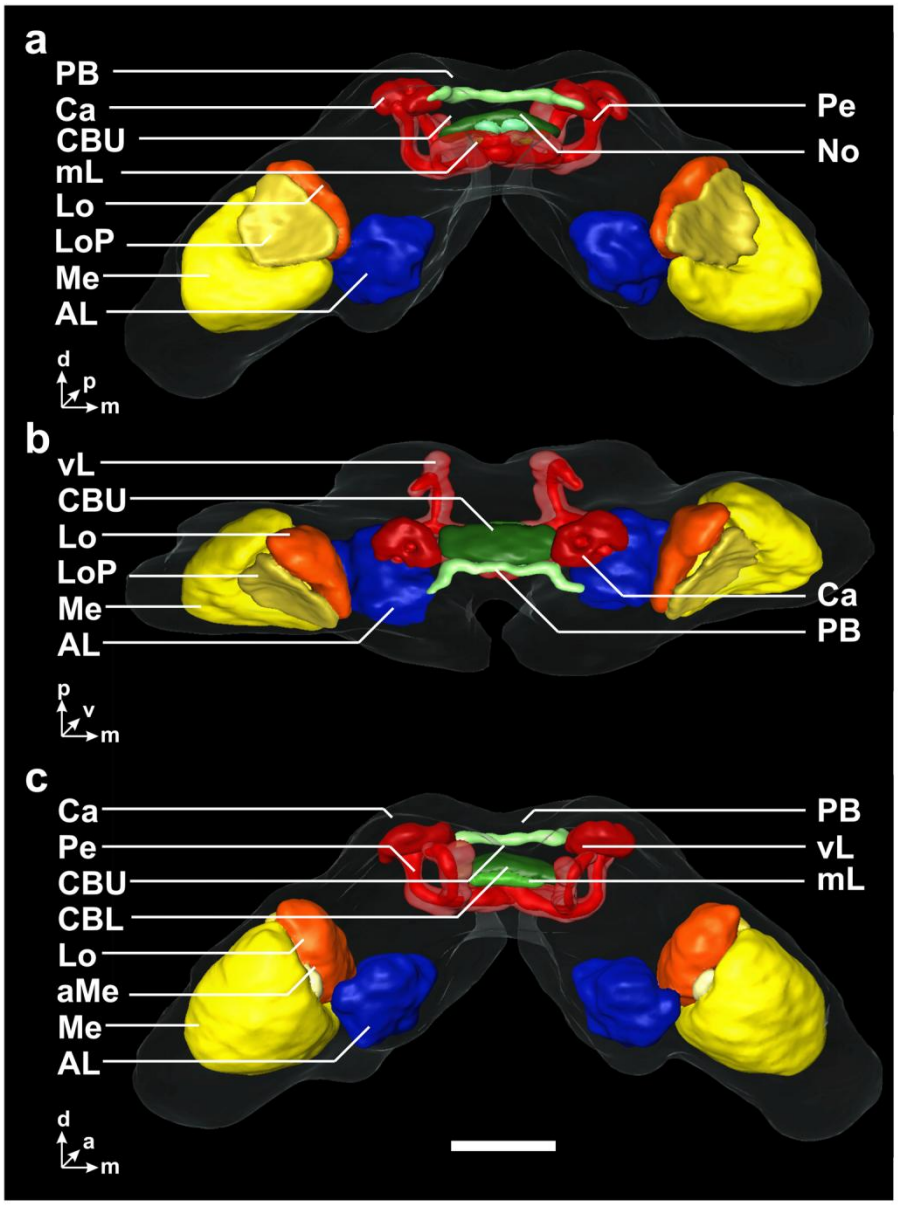

Fig. 1 3-D reconstruction of the female brain of *Aethina tumida* in **a** anterior, **b** dorsal, and **c** posterior view. The neuropils were reconstructed with the AMIRA tools SurfaceGen and SurfaceView. The color code of the labeled neuropils is consistent with Brandt et al. (2005). *AL* antennal lobe, *Ca* Calyx, *CBL* lower unit of the central body, *CBU* upper unit of the central body, *aMe* accessory medulla, *Lo* lobula, *LoP* lobula plate, *Me* medulla, *No* noduli, *PB* protocerebral bridge and *Pe* pedunculus with lobes. *Orientation bars*: *a* = anterior, *d* = dorsal, *m* = median, *p* = posterior, *v* = ventral. *Scale bar* 100 µm

In summary, we found no evidence for any sexual dimorphism in the AL on the level of AL size, glomerulus number and individual or overall glomerulus size.

Tachykinin-related peptides in the antennal lobes

Immunostaining with the anti TKRP antiserum in *A. tumida* revealed small, spherical substructures within all glomeruli (Fig. 3; see also ESM 4). In the anti-synapsin staining, these internal substructures are only slightly more strongly labeled in comparison to the surrounding neuropil of the glomerulus (Fig. 5b, c). Each AL contains about 230 of these substructures (males: 245.7±14.3, n=3 ALs; females: 224.6±19.1, n=5 ALs). We did not find a sexual dimorphism (p=0.154). All observed glomeruli contain between one and ten substructures, which are never attached to the outer rim of a glomerulus but usually distributed evenly across the glomerular volume (Fig. 3; ESM 4). In both sexes, the number of substructures in a glomerulus correlates with the volume of the glomerulus (males: n=3 ALs, n=224 glomeruli, R^2=0.99; females: n=5 ALs, n=350 glomeruli, R^2=0.95 (Fig. 4).

The staining of TKRP-ir glomerular substructures most likely originates from a set of about 80±18 (n=6 ALs) neurons

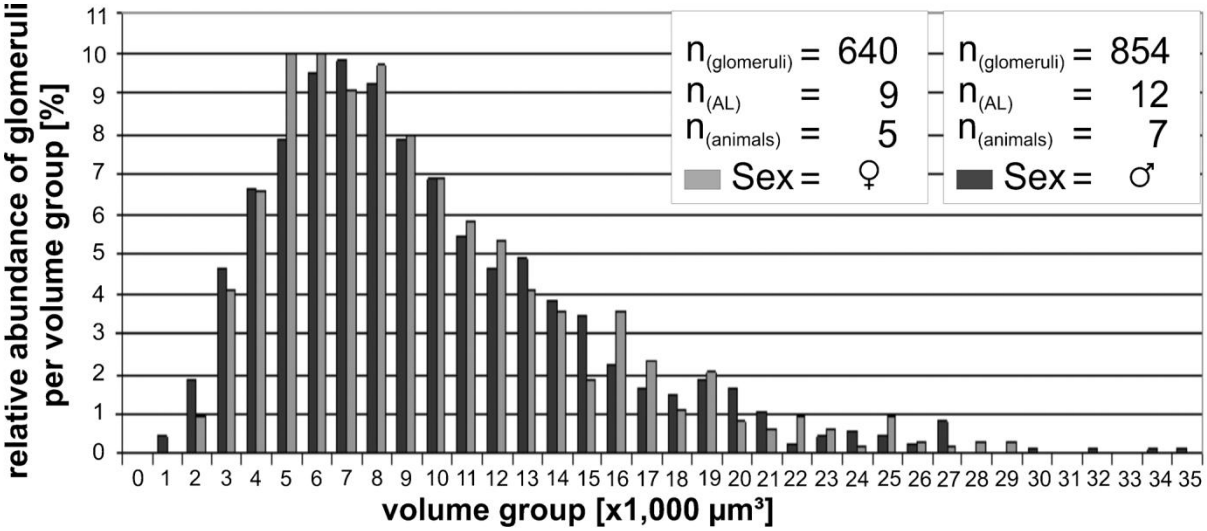

Fig. 2 Relative abundance of different sized glomeruli of both sexes of *Aethina tumida*. The *x*-axis represents the different glomerular volumes, shown as volume groups (0–999 µm³=group 0; 1000–1999 µm³=group 1; …35,000–35,999 µm³=group 35). The *y*-axis represents the relative abundance in percent of the different size groups

located laterally in the AL (Fig. 3d–f, arrowheads), presumably exclusively local interneurons, which project their processes into the AL (Fig. 3d–f, arrows; see also electronic supplementary material, ESM 5). As the antennal nerve shows no immunoreactivity to the TKRP antibody, we exclude that the staining of TKRP-ir glomerular substructures originates from OSNs. We also did not find any TKRP-ir fibers leaving the AL or entering the AL from other brain regions, excluding that the TKRP-ir glomerular substructures originate from projection neurons (PN) or centrifugal neurons (CN).

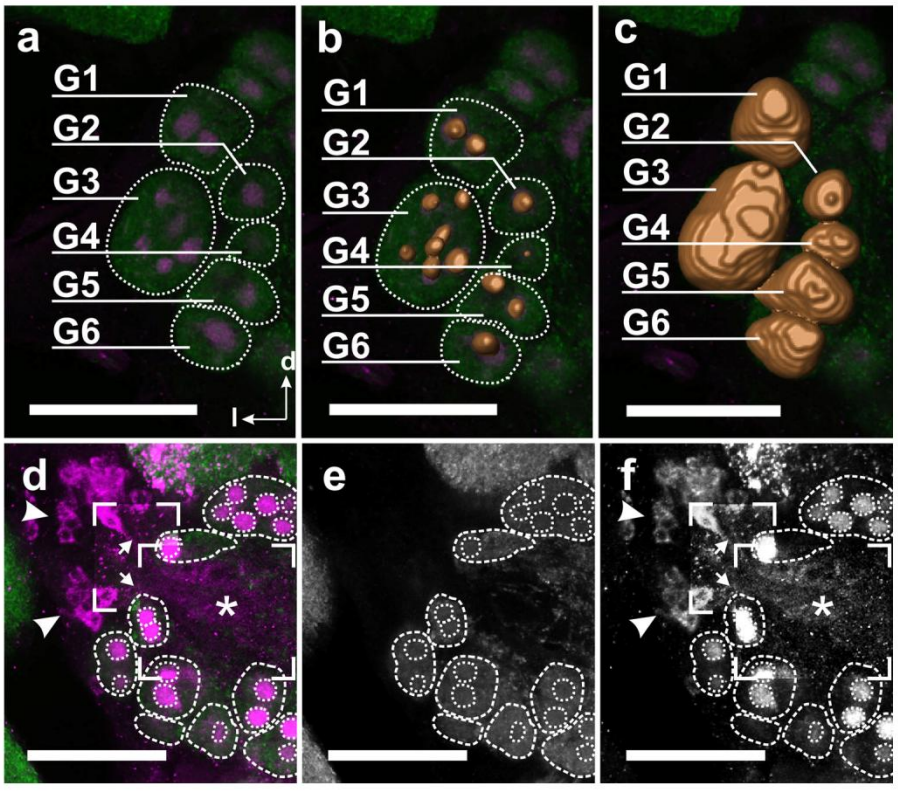

Fig. 3 The antennal lobe (AL) of *Aethina tumida* stained with an antibody against synapsin (*green*) and Lom TKII (*magenta*). **a** Single optical section of an AL. Several individual glomeruli (*G1–G6, dotted lines*), containing TKRP-ir glomerular substructures. **b**, **c** 3-D reconstructions of glomerular substructures (**b**) and of the glomeruli (**c**) of the set of glomeruli outlined in (**a**). **d**–**f** Staining with antibodies against synapsin (**e**) and TKRP (**f**) and overlay of both (**d**; synapsin in *green*, TKRP in *magenta*) showing TKRP-ir local AL interneurons (*arrowheads*) and their axons (*arrows*) projecting into the core area of the AL (*asterisk*), from where they give rise to TKRP-ir substructures. *Boxed areas* in (**d**) and (**f**) are enhanced in brightness and contrast to better visualize fibers of the local AL interneurons. *Orientation bars* in (**a**) valid for all subfigures: **l**=lateral, **d**=dorsal. *Scale bars* 50 µm

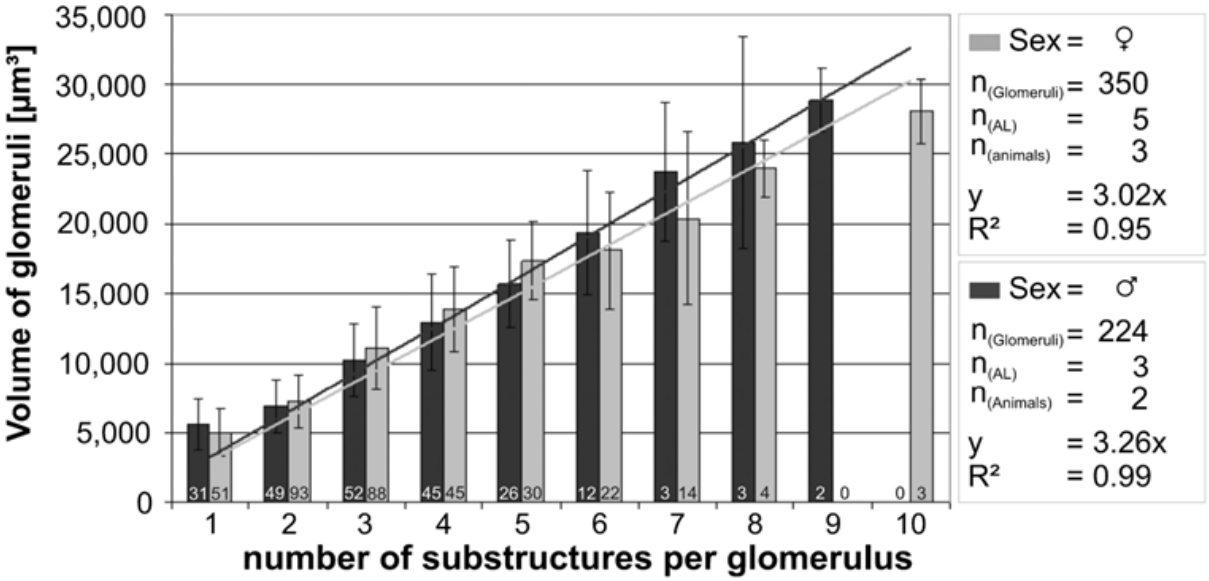

Fig. 4 Abundance of glomerular substructures (*x*-axis) in relation to glomerulus size (*y*-axis). *Numbers at the base of the bars* represent sample number (number of glomeruli). The diagram shows a linear relationship between glomerulus size and number of glomerular substructures, with a coefficient of determination of 0.95 for male and 0.99 for female animals

Serotonin in the antennal lobes

All glomeruli of one AL are innervated by axons branching from one, brightly stained main fiber, entering the AL at its medio-ventral side (Fig. 5a, unfilled arrowheads). The origin of this 5HT-ir main fiber is most likely a single cell body, dorso-lateral to the AL at the contralateral side (as demonstrated in Fig. 5a; arrow). The primary neurite runs through the AL without obvious branching and exits the AL at its dorsal side (Fig. 5a, filled arrowheads). From here, the fiber runs dorsally and crosses to the contralateral hemisphere of the superior protocerebrum where a divergent branch forms putative dendritic arborizations. The main fiber continues ventrally, to enter the contralateral AL (Fig. 5a, unfilled arrowheads). The TKRP-ir glomerular substructures are not innervated by the 5HT-ir branches although some are touched just at their surface (Fig. 5b–d).

Discussion

General organization of the *A. tumida* brain

The overall anatomy of the brain of *A. tumida* (Fig. 1) compares well to other beetle brains regarding major neuropils including the optical lobes (OL), antennal lobes (AL), mushroom bodies (MB) and central body complex (CBX) (e.g., Van Haeften 1993; Breidbach and Wegerhoff 1994; Larsson et al. 2004; Dreyer et al. 2010; Hu et al. 2011).

The OL of *A. tumida* contain the paired medulla (Me), lobula (Lo), lobula plate (LoP) and accessory medulla (aMe). The LoP has so far only been found in Ephemeroptera, Trichoptera, Coleoptera, Lepidoptera, Diptera (Strausfeld 2005) and Heteroptera (Settembrini and Villar 2005). The AL consists of about 70 glomeruli, which seems to be a typical number for beetles; there are about 70 glomeruli in the red flour beetle *Tribolium castaneum* (Dreyer et al. 2010), about 60 glomeruli in the scarab beetle *Holotrichia diomphalia* (Hu et al. 2011), and about 70 glomeruli in the cockchafer *Melolontha hippocastani* (third instar; Weissteiner et al. 2012). The AL will be discussed in more detail below. The paired MB contains the calyx (Ca) and the pedunculus (Pe), which is divided in the vertical and medial lobe (vL and mL). The Pe, vL and mL can be separated in a densely synapsin-stained core region and a less densely stained exterior region. This separation is in accordance with observations in the red flour beetle (Zhao et al. 2008; Binzer et al. 2014) and the African scarabid beetle *Pachnoda marginata* (Larsson et al. 2004). The medial part of the right mL is overlapping the medial part of the left mL, as has been observed in other beetles like *T. castaneum* (Dreyer et al. 2010) or the blind cave beetle *Neaphaenops tellkampfii* (Ghaffar et al. 1984). The unpaired central complex (CBX) can be separated into the protocerebral bridge (PB) and the central body (CB), which consists in the upper and lower unit (CBU and CBL), as well as the paired noduli (NO). This organization of the CBX is paralleled in other beetles like *T. castaneum* (Dreyer et al. 2010) or the mealworm beetle *Tenebrio molitor* (Breidbach and Wegerhoff 1994), as well as in many other insects (Homberg 2008).

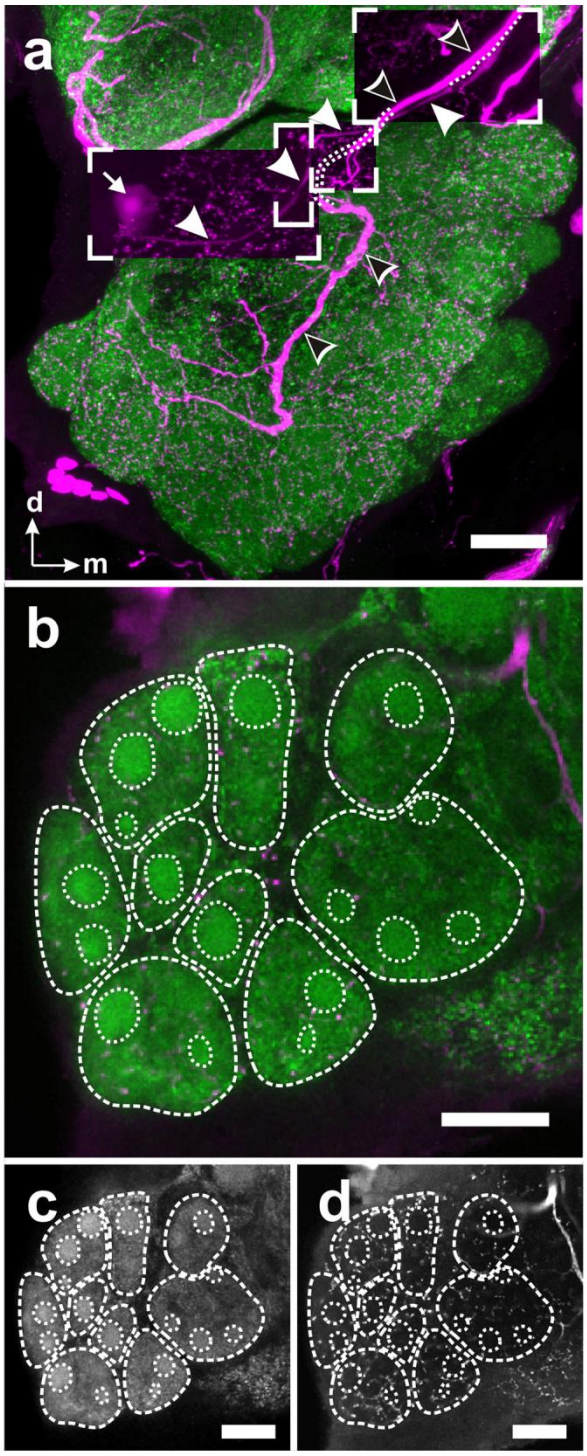

Fig. 5 Antennal lobe (AL) of *Aethina tumida* stained with anti-synapsin (*green*) and anti-serotonin (*magenta*) antibodies. **a** The maximum projection shows the branching of a single serotonin immunoreactive (5HT-ir) fiber, entering the AL at the dorsal site (*unfilled arrowheads*). Dorso-lateral to the AL, a single 5HT-ir cell body can be observed (*arrow*) projecting dorsal (*filled arrowheads*) without any branching or varicosities out of the AL. **b**–**d** Single optical section of an AL. The glomerular substructures in the AL glomeruli are distinctly brighter stained with the synapsin antibody than the surrounding area of the glomeruli (**b**, **c** *dotted lines*). 5HT-ir fibers clearly stay outside the glomerular substructures (**d**). *Orientation bars*: *m*=median, *d*= dorsal. *Scale bars* 20 μm

Comparison with relative brain neuropil volumes of other insects reveals that the AL of *A. tumida* are comparably large, only surpassed by *T. castaneum* and the Madeira cockroach *Rhyparobia maderae* (Table 2). The AL of *A. tumida* take up about a fifth of the compared relative neuropil volumes, resembling the ratio found in *T. castaneum*, while the relative AL volume of *R. maderae* is even larger. *T. castaneum* is considered as an insect relying dominantly on olfactory cues (Dreyer et al. 2010), as are cockroaches (*Periplaneta americana*, Sakura and Mizunami 2001). In summary, this result supports the hypothesis that, for *A. tumida*, similar as stated for *T. castaneum*, olfactory cues are of major importance for their specialized behavior.

The relative volumes of the MB are remarkably smaller in *A. tumida* (11.5 %) compared to *T. castaneum* but still larger than in the majority of compared insects (Table 2). MBs are higher integrative centers of the insect brain that are best known for their involvement in olfactory learning (e.g., McGuire et al. 2001; Menzel 2001; Heisenberg 2003; Davis 2004). However, insect MB are not solely higher centers of the olfactory pathway but are involved in the integration and processing of a broad range of sensory modalities including processing of visual, gustatory and mechanosensory information as well as contributions to sleep regulation, place memory and temperature preference (reviewed in Heuer et al. 2012). Farris and Roberts (2005) demonstrated that generalist plant-feeding scarab beetles (Scarabaeidae) have larger MB, while specialist dung-feeding scarab beetles have smaller MB. Interestingly, this difference in MB volume is independent of size and glomerulus number of the AL, the primary input olfactory neuropil of the MB. This observation may offer a possible explanation for the difference in MB volume between feeding specialist *A. tumida* and feeding generalist *T. castaneum*, which evolved as saprophytic insects and naturally occur under the bark of trees, in rotten wood and infrequently in the nests of some Hymenoptera (Sokoloff 1977; Grimm 2001; Arnaud et al. 2005).

In *A. tumida*, the OLs are with about two-thirds of the relative neuropil volume, larger than the OLs of *Tribolium*. In insects, larger OLs typically correlate with larger complex eyes (e.g., Ghaffar et al. 1984; Gronenberg and Liebig 1999; Ehmer and Gronenberg 2004; Beutel et al. 2005; Kuebler et al. 2010). *Tribolium* has relative small compound eyes (80–83 ommatidia per eye; Friedrich et al. 1996) compared to other insect species including *A. tumida*.

Table 2 Comparison of relative neuropil volume of *Aethina tumida* with eight different insect species including sex and sample number (*Drosophila melanogaster*, Rein et al. 2002; *Apis mellifera*, Brandt et al. 2005; *Schistocerca gregaria*, Kurylas et al. 2008; *Rhyparobia maderae*, Wei et al. 2010; *Manduca sexta*, el Jundi et al. 2009; *Godyris zavaleta*, Montgomery and Ott 2014; *Heliothis virescens*, Kvello et al. 2009, *Tribolium castaneum*, Dreyer et al. 2010; and *Aethina tumida*, this work). With exception of the lobula plate, only neuropils with complements in all examined animals were compared (medulla, lobula complex, and lobula plate; antennal lobes, mushroom calyces and pedunculi and the upper and lower unit of the central body)

Order	Diptera	Hymenoptera	Orthoptera	Blattodea	Lepidoptera				Coleoptera		
Species	*D.melanogaster*	*A. mellifera*	*S. gregaria*	*R.maderae*	*M. sexta*		*G.zavaleta*	*H.Virescens*	*T. castaneum*		*A.tumida*
Sex	♀	Forager	♂	♂	♀	♂	♂/♀	♀	♀	♂	♀
N	28	20	10	20	12	12	8/8	10	20	20	1
AL (%)	9.5	8.5	9.7	35.6	12.8	15.0	8.7	15.7	22.4	24.5	21.6
MB (%)	7.5	32.7	16.0	37.2	6.9	6.8	6.1	13.6	21.9	23.8	11.5
OL (%)	79.6	57.9	72.6	23.0	79.4	77.3	84.4	64.5	50.1	45.1	62.1
CB (%)	3.4	0.9	1.7	4.2	0.9	0.9	0.8	6.1	5.6	6.6	4.8

The role of the central body is probably best described as a central coordinator in sensory and motor integration (for reviews, see Strauss 2002; Wessnitzer and Webb 2006; Homberg 2008). With 4.8 %, the relative volume of the central body of *A. tumida* is smaller than the same structure in *Tribolium* and *Heliothis virescens* but still larger than in the fly, honey bee, locust, cockroach or two Lepidoptera species. This suggests for the two beetles a more prominent function of the central complex than in most other insects. In this context, it would be interesting to have more comparable central complex volumes of other Coleoptera with different lifestyles, e.g., water beetles or non-flying beetles.

Olfactory driven behavior and sexual dimorphism

Males of the related beetle *Carpophilus obsoletus* release an aggregation pheromone that attracts both sexes (Petroski et al. 1994), leading to the hypothesis that a similar pheromone could guide *A. tumida* into host beehives that have already been parasitized (Elzen et al. 2000; Neumann and Elzen 2004). However, a sequential arrival of male and female *A. tumida* could not be observed (Spiewok and Neumann 2012). This does not rule out sex-specific differences in olfaction; females seem to be more responsive to beehive volatiles than males (Suazo et al. 2003) and this might be reflected in a sexual dimorphism of the olfactory system of *A. tumida*.

Sexual dimorphism has been described in various insect species on different levels of the olfactory pathway ranging from the periphery to the central nervous system including the antenna (e.g., beetles: Kaissling 1971; Ågren 1985; Allsopp 1990; Renou et al. 1998; Diptera: Clements 1999; Ruther et al. 2000; Stocker 2001; Hymenoptera: Streinzer et al. 2013; moths: Schneider 1992; Rospars and Hildebrand 2000; Huetteroth and Schachtner 2005), the specificity, number and/or distribution of olfactory receptors (e.g., moths: Miura et al. 2009; Nakagawa et al. 2005; or Diptera: Bohbot et al. 2007), the morphology and number of glomeruli in the AL (Kondoh et al. 2003; Schachtner et al. 2005; Hu et al. 2011; Kelber et al. 2010; Streinzer et al. 2013) and higher order brain structures (e.g., *Drosophila*: Cachero et al. 2010). Detailed analyses of the antennae of *A. tumida* are missing. So far, there is no evidence that demonstrates a sexual dimorphism at the level of the antenna of the small hive beetle and information on the distribution of olfactory receptors for beetles is rare. For *T. castaneum*, transcription analyses of female and male antenna show no sexual dimorphism in the expression of odorant receptors (Dippel et al., in preparation); data for the small hive beetle are so far lacking.

Differently sized sexual dimorphic glomeruli have been observed in a wide range of insects, including beetles, cockroaches, bees, ants, moths, flies, and mosquitoes (Schachtner et al. 2005; Vosshall and Stocker 2007; Hu et al. 2011). Typically, these are one up to five glomeruli of a so-called "macroglomerular complex" in males to detect sex pheromones or in ants to detect trail pheromones, or "female sex-specific glomeruli" to detect host plants for oviposition. Such glomeruli are normally positioned at the entrance area of the antennal nerve into the AL (Hansson 1997; Anton and Homberg 1999; Rospars and Hildebrand 2000; Schachtner et al. 2005; Kleineidam et al. 2005). Hu et al. (2011) demonstrated such a sexual dimorphism for the first time in a beetle, identifying a single macroglomerulus in the AL of the Korean black chafer (*Holotrichia diomphalia*). The current study addresses the AL morphology of *A. tumida* in detail but neither male macroglomeruli nor female sex-specific glomeruli could be found.

A difference in number of glomeruli between sexes is common among insects. Yellow fever mosquito females have one additional glomerulus (Ignell et al. 2005) and *Pieris brassicae* female butterflies have three glomeruli more than their male counterparts (Rospars 1983). In hymenopterans, female

honeybee workers possess about 160 glomeruli compared to about 106 glomeruli in males (Arnold et al. 1985; Flanagan and Mercer 1989; Brockmann and Brückner 2001). In beetles, varying glomerulus numbers between sexes have so far not been described. In *A. tumida*, we found with about 70 glomeruli in both sexes no sexual dimorphism. In summary, the absence of a sexual dimorphism in the AL of *A. tumida* does not favor the work of Spiewok and Neumann (2012) or of Neumann and Elzen (2004) and can on this level of analysis not add to a better understanding of why female *A. tumida* respond more strongly to beehive volatiles than males (Suazo et al. 2003). A detailed analysis of the *A. tumida* antenna including distribution of olfactory sensillae and the identification and distribution of olfactory receptors would be necessary. Such insights could be helpful to create/optimize olfactory beetle traps. In addition, analysis of higher brain centers in the olfactory pathway including mushroom body and lateral horn might provide additional insights.

Serotonin-ir neuron in the AL

The observed innervation of all glomeruli of one AL by only one 5HT-ir cell body is common among insects (Dacks et al. 2006), as well as for ancestral hexapods, as observed in collembolans (Kollmann et al. 2011a). The described anatomy of the 5HT-ir neuron has been described for Coleoptera before and can also be found in Lepidoptera, Trichoptera, non-Schizophoran Diptera and Neuroptera (Dacks et al. 2006), and is very likely also true for aphids (Kollmann et al. 2011b). A side branch of the 5HT-ir neuron into the ipsilateral lateral protocerebrum as observed in many insects (including Coleoptera; Dacks et al. 2006) could not be found in *A. tumida*.

Glomerular substructures

Immunostaining with an antiserum recognizing tachykinin-related peptides (TKRPs) resulted in the discovery of small, spherical substructures, which are evenly distributed among all glomeruli, with no obvious difference between both sexes. These substructures seem to originate from a cluster of cell bodies, presumably local interneurons, lateral in the AL. Immunostaining with the same antiserum in two other beetles, *Tenebrio molitor* (Wegerhoff et al. 1996) and *T. castaneum* (Binzer et al. 2014), resulted in a cluster of local interneurons located in a similar position lateral in the AL. They provide the glomeruli with a dense meshwork of projections but did not give rise to spheroidal structures as described here. Similar to *A. tumida*, the antiserum did not reveal fibers in the antennal nerve or fibers belonging to either projection or centrifugal neurons (Wegerhoff et al. 1996; Binzer et al. 2014). Similarly, in all other insects where TKRP stainings were performed, the antisera labeled only local interneurons in the AL and no other neuron types (Schachtner et al. 2005; Carlsson et al. 2010; Neupert et al. 2012; Binzer et al. 2014; Siju et al. 2014). In summary and in contrast to all other insects examined before, the TKRP positive local neurons provide each glomerulus with particular islet-like projections.

In ALs of insects, all or only a subpopulation of glomeruli can be the target of individual neurons or of populations of neurons and a variety of innervation patterns of olfactory glomeruli by AL neurons (LNs, PNs) or CNs has so far been described either by filling of single neurons or by immunostaining (summarized in Fig. 6; reviewed in Schachtner et al. 2005; Seki and Kanzaki 2008; Husch et al. 2009; Carlsson et al. 2010; Chou et al. 2010; Seki et al. 2010; Neupert et al. 2012; Binzer et al. 2014; Siju et al. 2014). Comparing the different patterns of glomerulus supply via central neurons (CNs, LNs, PNs), innervation can occur (a) only at the surface, (b) scattered throughout the whole glomerulus, (c) or only through parts of the glomerulus, (d) up to massive dense innervation of the whole, or (e) a distinct area of a glomerulus, or (f) as described in this study, through islet-like projections, which are evenly distributed throughout the glomerulus (Fig. 6). From our analysis, we cannot distinguish, whether an individual islet structure is supplied via a single axon or by more axons and whether islets of a single glomerulus are innervated by several or only by one neuron as suggested in Fig. 6f.

The role of LNs in the AL network is to shape the olfactory representation within and between the olfactory glomeruli to eventually form the output profile of the PNs via complex inhibitory and excitatory interactions (Stopfer et al. 1997; Sachse and Galizia 2002; Wilson and Laurent 2005; Olsen et al. 2007, 2010; Root et al. 2007; Shang et al. 2007; Silbering and Galizia 2007; Olsen and Wilson 2008; Okada et al. 2009; Tanaka et al. 2009; Chou et al. 2010; Seki et al. 2010; Wilson 2013; Nagel et al. 2015). It is interesting that the small hive beetle developed, at least for a subpopulation of LNs, a morphologically different pattern of glomerulus innervation compared to other insects. With the available data, we can only speculate on the function of the islet-like innervation.

We offer two hypotheses. Our first hypothesis argues that the islet-like innervation is another effective way to provide the glomerular network with information carried by neuromediators, e.g., neuropeptides. Such neuromediators can act as paracrine neurohormones, affecting a broad area surrounding the release site, also known as "volume transmission", in contrast to "wiring" (Agnati et al. 1995; Nässel 2002). Considering the facts that the islet number is linearly correlated to glomerulus volume (Fig. 4) and that they are evenly distributed in each glomerulus, the islet contents could affect the glomerulus network over prolonged periods of time or in an otherwise temporally unique fashion. Our second hypothesis interprets the islets as a specific adaptation of the beetles to their lifestyle to cope with the complex chemical communication in a beehive with an olfactory system of a beetle. The TKRP immunostaining unmasks a group of LNs,

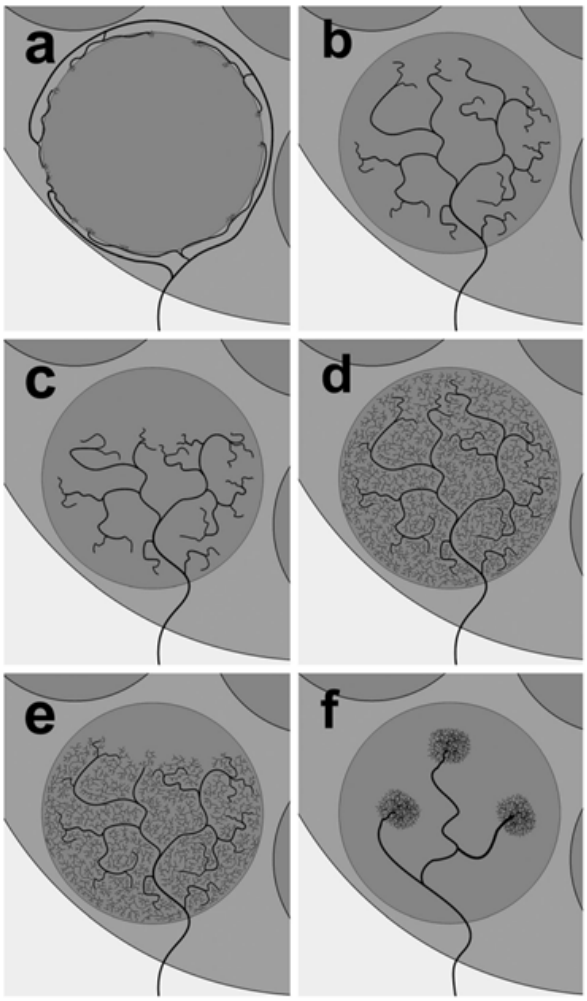

Fig. 6 Schematic drawing of the principal innervation pattern of glomeruli. **a** Glomeruli are just sparsely innervated at the surface. **b** The innervation is scattered through the whole glomerulus. **c** The innervation is just scattered through a distinct area of the glomerulus. **d** The whole glomerulus is densely innervated by fine branches, which appears in immunohistological stainings as a bright, uniform staining. **e** A distinct area of the glomerulus is densely innervated by fine branches. **f** Branching appears just in several, small, distinct areas of the glomerulus (glomerular substructures), which are evenly distributed throughout the glomerulus

which are part of such a particular network. It is known that chemical communication mainly based on pheromones is very important for bees (Slessor et al. 2005; Trhlin and Rajchard 2011). To manage this olfactory task, worker bees have about 64,000 OSNs (Esslen and Kaissling 1976), a large number of glomeruli (152–166 per AL in workers; Arnold et al. 1985) and about 170 ORs (Robertson and Wanner 2006). For a parasitic insect living in a beehive survival and breeding success may highly depend on the ability to understand at least parts of the chemical communication of its host. As the repertoire of the beetle is restricted to about 70 glomeruli per AL, the islets could be part of a system that allows the beetle to compensate for this disadvantage by expanding the glomerular coding space. The genome sequence of another beetle, *T. castaneum*, revealed a much higher number of functional ORs than olfactory glomeruli and it is still enigmatic what role these surplus ORs could play. The islets could be innervated by OSNs carrying different ORs than the OSNs that principally innervate the glomerulus. Following this line, the islets would functionally stand as specific "glomeruli" within the ordinary glomeruli and thus exaggerate the potential of the olfactory system of the beetle to cope with a more complex odor environment. The synapsin immunostaining is slightly stronger than in the surrounding parts of the glomeruli, suggesting a higher synaptic density within the islets. This argues for specialized zones with high synaptic communication between the involved neurons. If these islet-like zones are targeted by specialized OSNs and/or LNs, PNs remain to be shown in the future by backfills from the antenna and a thorough analysis of intrinsic end extrinsic antennal lobe neurons.

Summary

Analyzing the brain of *A. tumida* by means of immunohistochemistry and 3-D reconstruction revealed a basic brain neuroarchitecture comparable to other beetle and insect brains. In relationship to other brain areas and in comparison to other insects, the AL are relatively large, suggesting that olfaction is of major importance for the beetle. The AL of both sexes house about 70 glomeruli with no obvious size differences of the glomeruli between males and females. In accordance to what is typically found in other insects, staining with a 5HT antiserum revealed a large cell that projects from one AL to the contralateral AL to densely innervate all glomeruli. Immunostaining with an antiserum recognizing TKRPs revealed small spherical substructures, which are in both sexes evenly distributed among all olfactory glomeruli. The source for the TKRP-ir structures is very likely a group of about 80 local AL interneurons. The number of substructures ranges between one and ten and correlates linearly with the volume of the glomeruli. In total, one AL contains about 230 of these islets. For this unusual finding, we offer two hypotheses. First, these evenly distributed substructures could act as massive releasing sites to deliver the neuromediator throughout the particular glomerulus. Second, the islets act as specialized subcompartments that expand the functional coding space of the beetle's olfactory system.

Acknowledgments We thank Dr. Agricola for kindly providing the *Locusta migratoria* Tachykinin II antibody, as well as Dr. Buchner for the supply of the *Drosophila melanogaster* Synapsin I antibody. We thank the Department of Zoology and Entomology of the University of Pretoria (Pretoria/Tshwane South Africa) for providing kind local support and laboratory facilities. We also want to thank Martina Kern for expert technical assistance.

References

Agnati Z, Zoli M, Strömberg I, Fuxe K (1995) Intercellular communication in the brain: wiring versus volume transmission. Neuroscience 69:711–726

Âgren L (1985) Architecture of a lamellicorn flagellum (*Phyllopertha horticola*, Scarabeidae, Coleoptera, Insecta). J Morphol 186:85–94

Allsopp PG (1990) Sexual dimorphism in the adult antennae of *Antitrogus parvulus* Britton and *Lepidiota negatoria* Blackburn (Coleoptera: Scarabaeidae: Melolonthinae). J Aust Entomol Soc 29:261–266

Anton S, Homberg U (1999) Antennal lobe structure. In: Hansson BS (ed) Insect olfaction. Springer, Berlin, pp 97–124

Arnaud L, Brostaux Y, Lallemand S, Haubruge E (2005) Reproductive strategies of *Tribolium* flour beetles. J Insect Sci 5:33

Arnold G, Masson C, Budharugsa S (1985) Comparative study of the antennal lobes and their afferent pathway in the worker bee and the drone *Apis mellifera*. Cell Tissue Res 242:593–605

Berg BG, Schachtner J, Utz S, Homberg U (2007) Distribution of neuropeptides in the primary olfactory centre of the heliothine moth *Heliothis virescens*. Cell Tissue Res 327:385–398

Berg BG, Schachtner J, Homberg U (2009) Distribution of GABA and neuropeptides in the antennal lobe of the heliothine moth *Heliothis virescens*. Cell Tissue Res 335:593–605

Beutel RG, Pohl H, Hünefeld F (2005) Strepsipteran brains and effects of miniaturization (Insecta). Arthropod Struct Dev 34:301–313

Bicker G (1999) Histochemistry of classical neurotransmitters in antennal lobes and mushroom bodies of the honeybee. Microsc Res Tech 45: 174–183

Binzer M, Heuer CM, Kollmann M et al (2014) Neuropeptidome of *Tribolium castaneum* antennal lobes and mushroom bodies. J Comp Neurol 522:337–357

Bohbot J, Pitts RJ, Kwon HW, Rützler M, Robertson HM, Zwiebel LJ (2007) Molecular characterization of the *Aedes aegypti* odorant receptor gene family. Insect Mol Biol 16:525–537

Brandt R, Rohlfing T, Rybak J, Krofczik S, Maye A, Westerhoff M, Hege HC, Menzel R (2005) Threedimensional average-shape atlas of the honeybee brain and its applications. J Comp Neurol 492:1–19

Breidbach O, Wegerhoff R (1994) FMRFamide-like immunoreactive neurons in the brain of the beetle, Tenebrio molitor L. (coleoptera – tenebrionidae): constancies and variations in development from the embryo to the adult. Int J Insect Morphol Embryol 4:383–404

Brockmann A, Brückner D (2001) Structural differences in the drone olfactory system of two phylogenetically distant Apis species, *A. florea* and *A. mellifera*. Naturwissenschaften 88:78–81

Cachero S, Ostrovsky AD, Yu JY, Dickson BJ, Jefferis GSXE (2010) Sexual dimorphism in the fly brain. Curr Biol 20:1589–1601

Carlsson MA, Diesner M, Schachtner J, Nässel D (2010) Multiple neuropeptides in the Drosophila antennal lobe suggest complex modulatory circuits. J Comp Neurol 518:3359–3380

Chou YH, Spletter ML, Yaksi E, Leong JC, Wilson RI, Luo L (2010) Diversity and wiring variability of olfactory local interneurons in the *Drosophila* antennal lobe. Nat Neurosci 13:439–449

Clements AN (1999) The biology of mosquitoes: sensory reception and behaviour. CABI, Wallingford

Dacks AM, Christensen TA, Hildebrand JG (2006) Phylogeny of a serotonin-immunoreactive neuron in the primary olfactory center of the insect brain. J Comp Neurol 498:727–746

Dacks AM, Green DS, Root CM, Nighorn AJ, Wang JW (2009) Serotonin modulates olfactory processing in the antennal lobe of *Drosophila*. J Neurogenet 23:366–377

Davis RL (2004) Olfactory learning. Neuron 44:31–48

De Guzman LI, Frake AM, Rinderer TE, Arbogast RT (2011) Effect of height and color on the efficiency of pole traps for *Aethina tumida* (Coleoptera: Nitidulidae). J Econ Entomol 104:26–31

Dreyer D, Vitt H, Dippel S, Goetz B, el Jundi B, Kollmann M, Huetteroth W, Schachtner J (2010) 3D standard brain of the red flour beetle *Tribolium castaneum*: a tool to study metamorphic development and adult plasticity. Front Syst Neurosci 4:3

Ehmer B, Gronenberg W (2004) Mushroom body volumes and visual interneurons in ants: comparison between sexes and castes. J Comp Neurol 469:198–213

el Jundi B, Huetteroth W, Kurylas AE, Schachtner J (2009) Anisometric brain dimorphism revisited: implementation of a volumetric 3D standard brain in *Manduca sexta*. J Comp Neurol 517:210–225

Elzen PJ, Baxter JR, Westervelt D, Randall C, Wilson WT (2000) A scientific note on observations of the small hive beetle, *Aethina tumida* Murray (Coleoptera Nitidulidae) in Florida, USA. Apidologie 31:593–594

Esslen J, Kaissling KE (1976) Zahl und Verteilung antennaler Sensillen bei der Honigbiene (*Apis mellifera* L.). Zoomorphologie 83:227–251

Farris SM, Roberts NS (2005) Coevolution of generalist feeding ecologies and gyrencephalic mushroom bodies in insects. Proc Natl Acad Sci U S A 102:17394–17399

Flanagan D, Mercer AR (1989) An atlas and 3-D reconstruction of the antennal lobes in the worker honey bee, *Apis mellifera* L. (Hymenoptera: Apidae). Int J Insect Morphol Embryol 18:145–159

Friedrich M, Rambold I, Melzer RR (1996) The early stages of ommatidial development in the flour beetle *Tribolium castaneum* (Coleoptera; Tenebrionidae). Dev Genes Evol 206:136–146

Fusca D, Schachtner J, Kloppenburg P (2015) Colocalization of allatotropin and tachykinin-related peptides with classical transmitters in physiologically distinct subtypes of olfactory local interneurons in the cockroach (*Periplaneta americana*). J Comp Neurol 523: 1569–1586

Gatellier L, Nagao T, Kanzaki R (2004) Serotonin modifies the sensitivity of the male silkmoth to pheromone. J Exp Biol 207:2487–2496

Ghaffar H, Larsen JR, Booth GM, Perkes R (1984) General morphology of the brain of the blind cave beetle, *Neaphaenops tellkampfii* Erichson (Coleoptera - Carabidae). Int J Insect Morphol Embryol 13:357–371

Graham JR, Ellis JD, Carroll MJ, Teal PEA (2011) *Aethina tumida* (Coleoptera: Nitidulidae) attraction to volatiles produced by *Apis mellifera* (Hymenoptera: Apidae) and Bombus impatiens (Hymenoptera: Apidae) colonies. Apidologie 3:326–336

Greco MK, Hoffmann D, Dollin A, Duncan M, Spooner-Hart R, Neumann P (2010) The alternative Pharaoh approach: stingless bees mummify beetle parasites alive. Naturwissenschaften 97:319–323

Grimm R (2001) Faunistik und Taxonomie einiger Arten der Gattung *Tribolium* Macleay, 1825, mit Beschreibung von drei neuen Arten aus Afrika. (Coleoptera, Tenebrionidae). Entomofauna 22:393–404

Gronenberg W, Liebig J (1999) Smaller brains and optic lobes in reproductive workers of the ant Harpegnathos. Naturwissenschaften 86: 343–345

Halcroft M, Spooner-Hart R, Neumann P (2011) Behavioural defence strategies of the stingless bee, *Austroplebeia australis*, against the small hive beetle, *Aethina tumida*. Insect Soc 58:245–253

Hansson BS (1997) Antennal lobe projection patterns of pheromone-specific olfactory receptor neurons in moths. In: Cardé RT, Minks AK (eds) Insect pheromone research. Springer, New York, pp 164–183

Hansson BS, Stensmyr MC (2011) Evolution of insect olfaction. Neuron 72:698–711

Heisenberg M (2003) Mushroom body memoir: from maps to models. Nat Rev Neurosci 4:266–275

Hepburn HR, Radloff SE (1998) Honeybees of Africa. Springer, Berlin

Heuer CM, Kollmann M, Binzer M, Schachtner J (2012) Neuropeptides in insect mushroom bodies. Arthropod Struct Dev 41:199–226

Hill ES, Okada K, Kanzaki R (2003) Visualization of modulatory effects of serotonin in the silkmoth antennal lobe. J Exp Biol 206:345–352

Homberg U (2002) Neurotransmitters and neuropeptides in the brain of the locust. Microsc Res Tech 56:189–209

Homberg (2008) Evolution of the central complex in the arthropod brain with respect to the visual system. Arthropod Struct Dev 37(5):347–362

Hu JH, Wang ZY, Sun F (2011) Anatomical organization of antennal-lobe glomeruli in males and females of the scarab beetle *Holotrichia diomphalia* (Coleoptera: Melolonthidae). Arthropod Struct Dev 40:420–428

Huetteroth W, Schachtner J (2005) Standard three-dimensional glomeruli of the *Manduca sexta* antennal lobe: a tool to study both developmental and adult neuronal plasticity. Cell Tissue Res 319:513–524

Husch A, Paehler M, Fusca D, Paeger L, Kloppenburg P (2009) Distinct electrophysiological properties in subtypes of nonspiking olfactory local interneurons correlate with their cell type-specific Ca2+ current profiles. J Neurophysiol 29:11582.11592

Ignell R, Dekker T, Ghaninia M, Hansson BS (2005) Neuronal architecture of the mosquito deutocerebrum. J Comp Neurol 493:207–240

Ignell R, Root CM, Birse RT, Wang JW, Nässel DR, Winther ÅM (2009) Presynaptic peptidergic modulation of olfactory receptor neurons in *Drosophila*. Proc Natl Acad Sci U S A 106:13070–13075

Kaissling KE (1971) Insect olfaction. In: Handbook of sensory physiology, vol 4. Springer, Berlin, pp 351–431

Kelber C, Rössler W, Kleineidam CJ (2010) Phenotypic plasticity in number of glomeruli and sensory innervation of the antennal lobe in leaf-cutting ant workers (*A. vollenweideri*). Dev Neurobiol 70: 222–234

Klagges BRE, Heimbeck G, Godenschwege TA, Hofbauer A, Pflugfelder GO, Reifegerste R, Reisch D, Schaupp M, Buchner S, Buchner E (1996) Invertebrate synapsins: a single gene codes for several isoforms in Drosophila. J Neurosci 16:3154–3165

Kleineidam CJ, Obermayer M, Halbich W, Rössler W (2005) A macroglomerulus in the antennal lobe of leaf-cutting ant workers and its possible functional significance. Chem Senses 30:383–392

Kloppenburg P, Hildebrand JG (1995) Neuromodulation by 5-hydroxytryptamine in the antennal lobe of the sphinx moth *Manduca sexta*. J Exp Biol 198:603–611

Kollmann M, Minoli S, Bonhomme J, Homberg U, Schachtner J, Tagu D, Anton S (2011a) Revisiting the anatomy of the central nervous system of a hemimetabolous model insect species: the pea aphid *Acyrthosiphon pisum*. Cell Tissue Res 343:343–355

Kollmann M, Huetteroth W, Schachtner J (2011b) Brain organization in Collembola (springtails). Arthropod Struct Dev 40:304–316

Kondoh Y, Kaneshiro KY, Kimura K, Yamamoto D (2003) Evolution of sexual dimorphism in the olfactory brain of Hawaiian Drosophila. Proc R Soc Lond B 270:1005–1013

Kuebler LS, Kelber C, Kleineidam CJ (2010) Distinct antennal lobe phenotypes in the leaf-cutting ant (*Atta vollenweideri*). J Comp Neurol 518:352–365

Kurylas AE, Rohlfing T, Krofczik S, Jenett A, Homberg U (2008) Standardized atlas of the brain of the desert locust, *Schistocerca gregaria*. Cell Tissue Res 333:125–145

Kvello P, Løfaldli BB, Rybak J, Menzel R, Mustaparta H (2009) Digital, three-dimensional average shaped atlas of the *Heliothis virescens* brain with integrated gustatory and olfactory neurons. Front Syst Neurosci 3:14. doi:10.3389/neuro.06.014.2009

Larsson MC, Hansson BS, Strausfeld NJ (2004) A simple mushroom body in an African scarabid beetle. J Comp Neurol 478:219–232

Linn CE, Roelofs WL (1986) Modulatory effects of octopamine and serotonin on male sensitivity and periodicity of response to sex pheromone in the cabbage looper moth, *Trichoplusia ni*. Arch Insect Biochem Physiol 3:161–171

Lundie AE (1940) The small hive beetle, *Aethina tumida*. Bulletin no 220, South African Department of Agriculture and Forestry, Pretoria

McGuire SE, Le PT, Davis RL (2001) The role of *Drosophila* mushroom body signaling in olfactory memory. Science 10:1126–1129

Menzel R (2001) Searching for the memory trace in a mini-brain, the honeybee. Learn Mem 8:53–62

Miura N, Nakagawa T, Tatsuki S, Touhara K, Ishikawa Y (2009) A male-specific odorant receptor conserved through the evolution of sex pheromones in *Ostrinia* moth species. Int J Biol Sci 5:319–330

Montgomery SH, Ott SR (2014) Brain composition in *Godyris zavaleta*, a diurnal butterfly, reflects an increased reliance on olfactory information. J Comp Neurol 523:869–891

Mutinelli F, Montarsi F, Federico G, Granato A, Ponti AM, Grandinetti G et al (2014) Detection of *Aethina tumida* Murray (Coleoptera: Nitidulidae.) in Italy: outbreaks and early reaction measures. J Apic Res 53:569–575

Mysore K, Subramanian KA, Sarasij RC, Suresh A, Shyamala BV, VijayRaghavan K, Rodrigues V (2009) Caste and sex specific olfactory glomerular organization and brain architecture in two sympatric ant species, *Camponotus sericeus* and *Camponotus compressus* (Fabricius, 1798). Arthropod Struct Dev 38:485–497

Nagel KI, Hong EJ, Wilson RI (2015) Synaptic and circuit mechanisms promoting broadband transmission of olfactory stimulus dynamics. Nat Neurosci 18:56–65

Nakagawa T, Sakurai T, Nishioka T, Touhara K (2005) Insect sex-pheromone signals mediated by specific combinations of olfactory receptors. Science 307:1638–1642

Nässel DR (2002) Neuropeptides in the nervous system of Drosophila and other insects: multiple roles as neuromodulators and neurohormones. Prog Neurobiol 68:1–84

Neumann P (2015) Small hive beetle in Italy: what can we expect in the future? In: Carreck NL (ed) The small hive beetle in Europe. International Bee Research Association, Groombridge

Neumann P, Ellis JD (2008) The small hive beetle (*Aethinatumida* Murray, Coleoptera: Nitidulidae): distribution, biology and control of an invasive species. J Apic Res 47:181–183

Neumann P, Elzen PJ (2004) The biology of the small hive beetle (*Aethina tumida* Murray, Coleoptera: Nitidulidae): Gaps in our knowledge of an invasive species. Apidologie 35:229–247

Neumann P, Hoffmann D, Duncan M, Spooner-Hart R, Pettis JS (2012) Long-range dispersal of small hive beetles. J Agic Res 51:214–215

Neumann P, Evans J, Pettis JS, Pirk CWW, Schäfer MO, Tanner G, Ellis JD (2013) Standard methods for small hive beetle research. In: Dietemann V, Ellis JD, Neumann P (Eds) The COLOSS BEEBOOK, Volume II: standard methods for *Apis mellifera* pest and pathogen research. J Apic Res 52: 1–32

Neupert S, Fusca D, Schachtner J, Kloppenburg P, Predel R (2012) Towards a single-cell-based analysis of neuropeptide expression in *Periplaneta americana* antennal lobe neurons. J Comp Neurol 520: 694–716

Okada R, Awasaki T, Ito K (2009) Gamma-aminobutyric acid (GABA)-mediated neural connections in the *Drosophila* antennal lobe. J Comp Neurol 514:74–91

Olsen SR, Wilson RI (2008) Lateral presynaptic inhibition mediates gain control in an olfactory circuit. Nature 452:956–960

Olsen SR, Bhandawat V, Wilson RI (2007) Excitatory interactions between olfactory processing channels in the Drosophila antennal lobe. Neuron 54:89–103

Olsen SR, Bhandawat V, Wilson RI (2010) Divisive normalization in olfactory population codes. Neuron 66:287–299

Petroski RJ, Bartelt RJ, Vetter RS (1994) Male-produced aggregation pheromone of *Carpophilusobsoletus* (Coleoptera, Nitidulidae). J Chem Ecol 20:1483–1493

Rein K, Zöckler M, Mader MT, Grübel C, Heisenberg M (2002) The *Drosophila* standard brain. Curr Biol 12:227–231

Renou M, Tauban D, Morin J-P (1998) Structure and function of antennal poreplate sensilla of *Oryctes rhinoceros* (L.) (Coleoptera : Dynastinae). Int J Insect Morphol Embryol 27:227–233

Robertson HM, Wanner KW (2006) The chemoreceptor superfamily in the honey bee, Apis mellifera: expansion of the odorant, but not gustatory, receptor family. Genome Res 16:1395–1403

Root CM, Semmelhack JL, Wong AM, Flores J, Wang JW (2007) Propagation of olfactory information in *Drosophila*. Proc Natl Acad Sci U S A 104:11826–11831

Rospars JP (1983) Invariance and sex-specific variations of the glomerular organization in the antennal lobes of a moth, *Mamestra brassicae*, and a butterfly, *Pieris brassicae*. J Comp Neurol 220: 80–96

Rospars JP, Hildebrand JG (2000) Sexually dimorphic and isomorphic glomeruli in the antennal lobes of the sphinx moth *Manduca sexta*. Chem Senses 25:119–129

Ruther J, Reinecke A, Thiemann K, Tolasch T, Francke W, Hilker M (2000) Mate finding in the forest cockchafer, *Melolontha hippocastani*, mediated by volatiles from plants and females. Physiol Entomol 25:172–179

Sachse S, Galizia CG (2002) Role of inhibition for temporal and spatial odor representation in olfactory output neurons: a calcium imaging study. J Neurophysiol 87:1106–1117

Sakura M, Mizunami M (2001) Olfactory learning and memory in the cockroach *Periplaneta americana*. Zool Sci 18:21–28

Schachtner J, Schmidt M, Homberg U (2005) Organization and evolutionary trends of primary olfactory brain centers in Tetraconata (Crustacea and Hexapoda). Arthropod Struct Dev 34:257–299

Schmolke MD (1974) A study of *Aethina tumida*: the small Hive Beetle, Project Report. University of Rhodesia, Harare

Schneider D (1992) 100 years of pheromone research: an essay on Lepidoptera. Naturwissenschaften 79:241–250

Seki Y, Kanzaki R (2008) Comprehensive morphological identification and GABA immunocytochemistry of antennal lobe local interneurons in *Bombyx mori*. J Comp Neurol 506:93–107

Seki Y, Rybak J, Wicher D, Sachse S, Hansson BS (2010) Physiological and morphological characterization of local interneurons in the *Drosophila* antennal lobe. J Neurophysiol 104:1007–1019

Settembrini BP, Villar MJ (2005) FMRFamide-like immunocyrochemistry in the brain and subesophageal ganglion of *Triatoma infestans* (Insecta: Heteroptera). Coexpression with ß-pigment-dispersing hormone and small cardioactive peptide. Cell Tissue Res 321:299–310

Shang Y, Claridge-Chang A, Sjulson L, Pypaert M, Miesenböck G (2007) Excitatory local circuits and their implications for olfactory processing in the fly antennal lobe. Cell 128:601–612

Siju KP, Schachtner J, Reifenrath A, Scheiblich H, Neupert S, Predel R, Hansson B, Ignell R (2014) Neuropeptides in the antennal lobe of the yellow fever mosquito, *Aedes aegypti*. J Neurophysiol 522:592–608

Silbering AF, Galizia CG (2007) Processing of odor mixtures in the *Drosophila* antennal lobe reveals both global inhibition and glomerulus-specific interactions. J Neurosci 27:11966–11977

Slessor KN, Winston ML, Le Conte Y (2005) Pheromone communication in the honeybee (*Apis mellifera* L.). J Chem Ecol 31:2731–2745

Sokoloff A (1977) The biology of tribolium with special emphasis on genetic aspects. Oxford University Press, London

Spiewok S, Neumann P (2006) Infestation of commercial bumblebee (*Bombus impatiens*) field colonies by small hive beetles (*Aethina tumida*). Ecol Entomol 31:623–628

Spiewok S, Neumann P (2012) Sex ratio and dispersal of small hive beetles. J Agric Res 51:216–217

Stocker RF (2001) *Drosophila* as a focus in olfactory research: mapping of olfactory sensilla by fine structure, odor specificity, odorant receptor expression, and central connectivity. Microsc Res Tech 55:284–296

Stopfer M, Bhagavan S, Smith BH, Laurent G (1997) Impaired odour discrimination on desynchronization of odour-encoding neural assemblies. Nature 390:70–74

Strausfeld NJ (2005) The evolution of crustacean and insect optic lobes and the origins of chiasmata. Arthropod Struct Dev 34:235–256

Strauss R (2002) The central complex and the genetic dissection of locomotor behaviour. Curr Opin Neurobiol 12:633–638

Streinzer M, Kelber C, Pfabigan S, Kleineidam CJ, Spaethe J (2013) Sexual dimorphism in the olfactory system of a solitary and a eusocial bee species. J Comp Neurol 521:42–55

Suazo A, Torto B, Teal PEA, Tumlinson JH (2003) Response of the small hive beetle (*Aethinatumida*) to honey bee (*Apis mellifera*) and beehive-produced volatiles. Apidologie 34:525–533

Tanaka NK, Ito K, Stopfer M (2009) Odor-evoked neural oscillations in *Drosophila* are mediated by widely branching interneurons. J Neurosci 29:8595–8603

Trhlin M, Rajchard J (2011) Chemical communication in the honeybee (*Apis mellifera* L.): a review. Vet Med 56:265–273

Utz S, Huetteroth W, Vömel M, Schachtner J (2008) Mas-allatotropin in the developing antennal lobe of the sphinx moth *Manduca sexta*: distribution, time course, developmental regulation and colocalization with other neuropeptides. Dev Neurobiol 68:123–142

Van Haeften T (1993) Location and function of serotonin in the central and peripheral nervous system of the Colorado potato beetle. PhD thesis, University of Wageningen, The Netherlands. (ISBN 1993 90 5485 141 4)

Veenstra JA, Lau GW, Agricola HJ, Petzel DH (1995) Immunohistochemical localization of regulatory peptides in the midgut of the female mosquito *Aedes aegypti*. Histochem. Cell Biol 104:337–347

Vitzthum H, Homberg U (1998) Immunocytochemical demonstration of locustatachykinin-related peptides in the central complex of the locust brain. J Comp Neurol 390:455–469

Vosshall LB, Stocker RF (2007) Molecular architecture of smell and taste in *Drosophila*. Annu Rev Neurosci 30:505–533

Vosshall LB, Wong AM, Axel R (2000) An olfactory sensory map in the fly brain. Cell 102:147–159

Wegerhoff R, Breidbach O, Lobemeier M (1996) Development of locustatachykinin immunopositive neurons in the central complex of the beetle *Tenebrio molitor*. J Comp Neurol 375:157–166

Wei H, el Jundi B, Homberg U, Stengl M (2010) Implementation of pigment-dispersing factor- immunoreactive neurons in a standardized atlas of the brain of the cockroach *Leucophaea maderae*. J Comp Neurol 518:4113–4133

Weissteiner S, Huetteroth W, Kollmann M, Weißbecker B, Romani R, Schachtner J, Schütz S (2012) Cockchafer larvae smell host root scents in soil. PLoS ONE 7(10)

Wessnitzer J, Webb B (2006) Multimodal sensory integration in insects – towards insect brain control architectures. Bioinspir Biomim 1:63–75

Wilson RI (2013) Early olfactory processing in *Drosophila*: mechanisms and principles. Annu Rev Neurosci 36:217–241

Wilson RI, Laurent G (2005) Role of GABAergic inhibition in shaping odor-evoked spatiotemporal patterns in the *Drosophila* antennal lobe. J Neurosci 25:9069–9079

Winther ÅME, Ignell R (2010) Local peptidergic signaling in the antennal lobe shapes olfactory behavior. Fly 4:167–171

Winther ÅME, Acebes A, Ferrús A (2006) Tachykinin-related peptides modulate odor perception and locomotor activity in *Drosophila*. Mol Cell Neurosci 31:399–406

Zhao X, Coptis V, Farri SM (2008) Metamorphosis and adult development of the mushroom bodies of the red flour beetle, *Tribolium castaneum*. Dev Neurobiol 68:1487–1502

Supplementary material

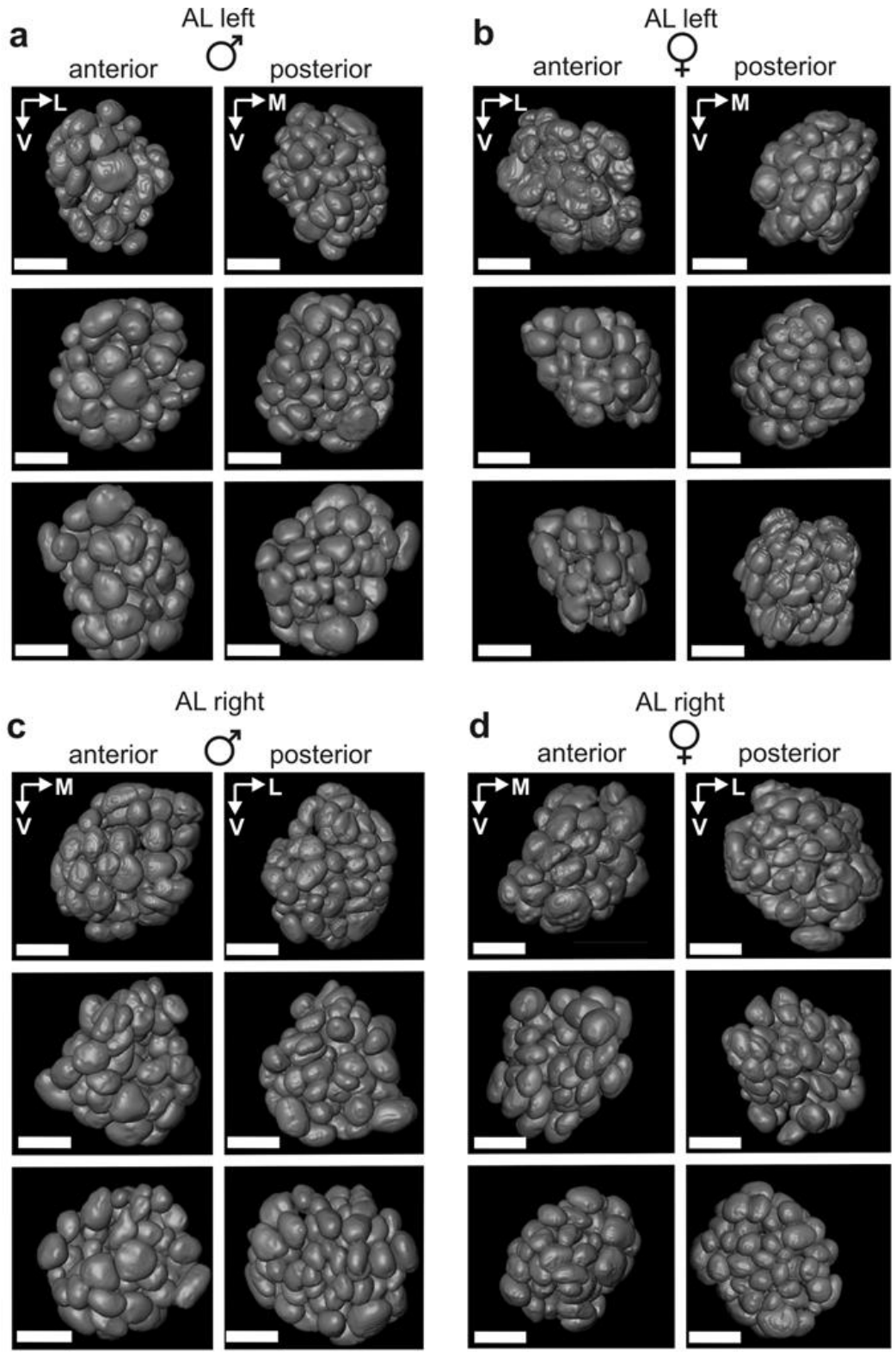

Fig. 7

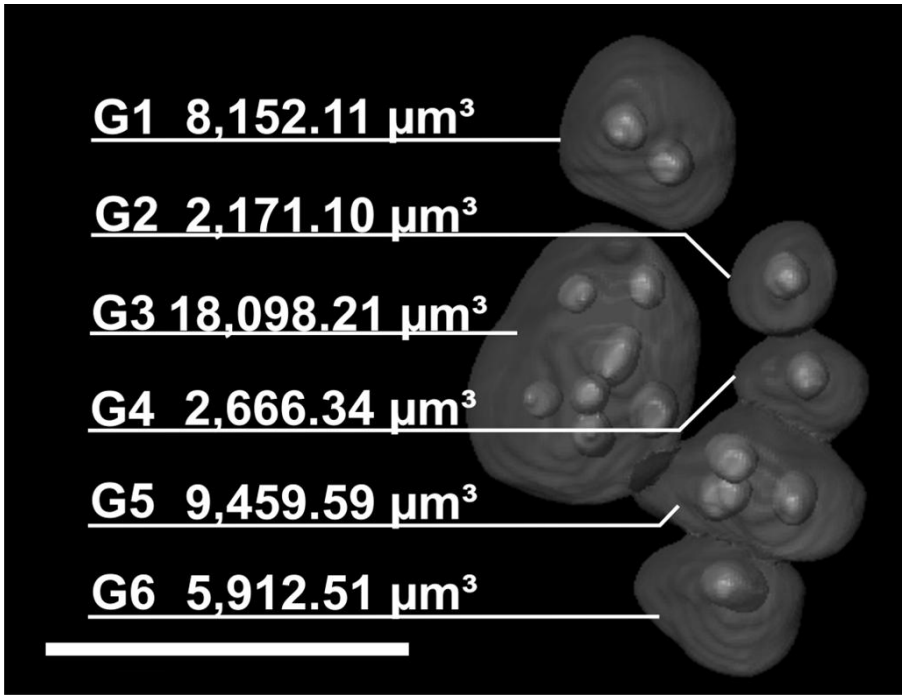
G1 8,152.11 µm³
G2 2,171.10 µm³
G3 18,098.21 µm³
G4 2,666.34 µm³
G5 9,459.59 µm³
G6 5,912.51 µm³

Fig. 8

Chapter 8:

Variations on a theme:
antennal lobe architecture across Coleoptera

Variations on a theme:

antennal lobe architecture across Coleoptera

Martin Kollmann[1], Rovenna Schmidt[1,2] , Carsten M. Heuer[1,3], Joachim Schachtner[1]

[1]: Department of Biology - Animal Physiology, Philipps-University Marburg, Karl-von-Frisch-Str. 8, D-35032 Marburg, Germany

[2]: Institute of Veterinary Anatomy, Histology and Embryology, Justus-Liebig University Giessen, Frankfurter Strasse 98, D-35392, Germany

[3]: Fraunhofer-Institut für Naturwissenschaftlich-Technische Trendanalysen INT, Appelsgarten 2, D-53879 Euskirchen, Germany

Abbreviations

AL	antennal lobe
AN	antennal nerve
CA	calyx
CN	Centrifugal neuron
DAPI	4',6-diamidinophenyindole
LN	Local interneuron
MB	mushroom body
OR	olfactory receptor
OSN	olfactory sensory neurons
PBS	phosphate buffered saline
PN	Projection neuron
TKRP	Tachykinin-related peptides
TKRP-ir	TKRP immunoreactive

Abstract

Beetles comprise about 400,000 described species, nearly one third of all known animal species. The enormous success of the order Coleoptera is reflected by a rich diversity of lifestyles, behaviors, morphological, and physiological adaptions. All these evolutionary adaptions that have been driven by a variety of parameters over the last about 300 million years, make the Coleoptera an ideal field to study the evolution of the brain on the interface between the basic bauplan of the insect brain and the adaptions that occurred. In the current study we concentrated on the paired antennal lobes (AL), the part of the brain that is typically responsible for the first processing of olfactory information collected from olfactory sensilla on antenna and mouthparts. We analyzed 63 beetle species from 22 different families and thus provide a hitherto unreached comparison of principal neuroarchitecture of the AL. On the examined anatomical level, we found a broad diversity including AL containing a wide range of glomeruli numbers reaching from 50 to 150 glomeruli and several species with numerous small glomeruli, resembling the microglomerular design described in acridid grasshoppers and diving beetles, and substructures within the glomeruli that have to date only been described for the small hive beetle, *Aethina tumida*. A first comparison of the various anatomical features of the AL with available descriptions of lifestyle and behaviors did so far not reveal useful correlations. In summary, the current study provides a solid basis for further studies to unravel mechanisms that are basic to evolutionary adaptions of the insect olfactory system.

Introduction

Beetles first appeared in the early Permian (around 270 - 300 million years ago) [1-3]. Their evolutionary success appears to have been sparked by an initial burst of speciation and consolidated through high diversification and low extinction rates throughout history [4]. This has been attributed to their effective adaptation to geological and climatic changes [5] and a coleopteran co-evolution with mammals [6] and angiosperms [7].

Today, Coleoptera is the most species-rich metazoan order. With about 400,000 described species, beetles represent approximately 30% of all known animal species [2,8-10]. Based on this enormous species richness, Coleoptera display a vast diversity of lifestyles and behaviors, inhabiting all biomes but the marine environment and comprising, inter alia, nocturnal and diurnal species, mutualistic and parasitic symbionts, generalists and specialists, carnivorous, herbivorous, detritivorous and coprophagous taxa [11].

This huge diversity is mirrored by numerous physiological and morphological adaptations. We here seek to explore whether the diversity is also reflected by neuroanatomical adaptions in the central nervous system. Beetles provide an excellent opportunity to explore the extent of such adaptions within a single insect order. Since olfaction plays a prominent role in the life history of insects (finding food, hosts, mates etc.; [12- 17], we focused our investigation on the primary olfactory neuropil, the paired antennal lobes (AL).

In insects, olfactory information is detected by olfactory sensory neurons (OSN) housed in olfactory sensilla on the antennae and the labial and/or maxillary palps of the mouthparts [18-20]. Via the antennal nerve (AN), olfactory input from the antenna is passed on to the AL, the first

integration center for olfactory information. Typically, the AL comprises spherical subcompartments, the olfactory glomeruli [20,21] and also typically, all OSN expressing the same type of olfactory receptor (OR) converge onto the same glomerulus [22]. The number of glomeruli can vary among different species, ranging from about 40 to sometimes several hundred [21,23,24]. Within the AL, the olfactory information is processed by a complex network of neurons, including OSN, local interneurons (LN), projections neurons (PN), and centrifugal neurons (CN) [21]. The olfactory representation within the AL is shaped by the neuronal network and by a variety of neuroactive substances, most notably the inhibitory transmitter gamma amino-butyric acid (GABA), the excitatory transmitter acetylcholine [25-31] but also biogenic amines, neuropeptides like e.g. Tachykinin-related peptides (TKRP), and gaseous signaling molecules [21,32-34]. The PN forward the processed olfactory information via antennal lobe tracts (ALT) to higher brain centers (in particular the mushroom bodies [MB] and the lateral horn [LH] [21,35]).

Despite their diversity and species richness, as well as their preeminent ecological and economic importance [2,8], a comprehensive and comparative analysis of the coleopteran olfactory system has not been conducted to date. Detailed information on the AL of Coleoptera is scarce [21] - only the AL of the scarab beetle *Holotrichia diomphalia* [36], of the red flour beetle *Tribolium castaneum* [33,37,38], and of the small hive beetle *Aethina tumida* [39] have been investigated in greater detail. Exhibiting 60-90 spherical glomeruli, the AL in these species conform to the basic bauplan of a typical insect AL [21]. However, for some beetle species, atypical AL anatomies have been reported. The AL of Dytiscinae (diving beetles) have been described as non-glomerular [40- 42] and AL seem to be missing altogether in aquatic Gyrinidae (whirligig beetles) – possibly representing a loss-of-function and indicating anosmia in these animals [42,43]. However, a recent study found numerous small glomeruli within Dytiscinae [44]. Recent investigations in *A. tumida*, using antibodies against TKRP, a neuropeptide known to modulate olfactory sensitivity and locomotor activity in the fruit fly *Drosophila melanogaster* [45- 47], revealed hitherto undescribed substructures within the olfactory glomeruli [39].

In the current study, we investigated the AL of 63 beetle species from 22 different families, thus providing the most exhaustive dataset on AL neuroarchitecture within an insect order to date. Glomeruli numbers were obtained for 32 of the examined beetle species, reaching from 50 to 150 glomeruli (with 80 to 120 glomeruli in the majority of animals) and revealing much more diversity than would be expected from existing studies [33,36-39]. The observed neuroanatomical diversity of coleopteran AL organization also includes several species with numerous small glomeruli (comparable to the situation in acridid grasshoppers and diving beetles) and AL substructures recently described for the small hive beetle, *Aethina tumida* [39].

Results

General architecture and number of glomeruli within the coleopteran antennal lobes

We obtained numbers of olfactory glomeruli in 32 coleopteran species (Fig. 1). With regard to their general neuroanatomical makeup, the AL could be categorized into two groups: 1) AL containing 50 – 150 more or less spherical or oval shaped glomeruli of a regular size, typically arranged around a central coarse neuropil, comparable to the conditions found in the majority of insects (e.g. in Diptera, Hymenoptera, or Lepidoptera, [21]). In the majority of the examined beetles, the number of glomeruli per AL ranges from 80 to 120 glomeruli. 2) AL comprising approximately 400 – 1,000 small glomeruli, comparable to the microglomeruli of locusts and other Acrididae [21,48]. Interestingly, within Coleoptera, such microglomeruli are only observed within two families that are not closely related to each other (Coccinellidae and Dytiscidae; see below). In general, the number of glomeruli does not vary much within families, with the exception of Dytiscidae (one species with about 1,000 and one with about 400 - 500 glomeruli).

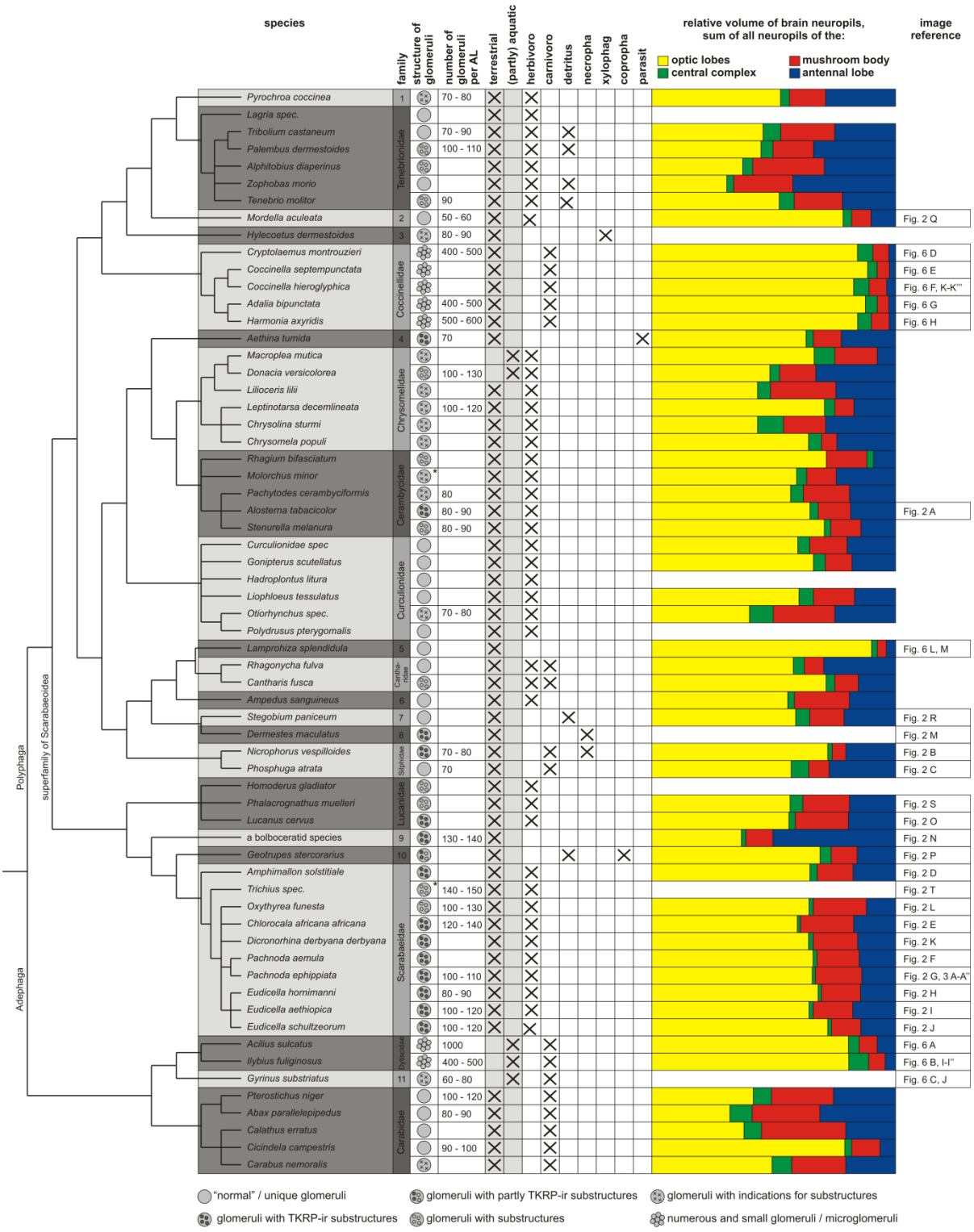

Fig. 1: Phylogenetic tree of the investigated Coleopteran species, providing information on the design of their antennal lobes, their lifestyles (information on habitat and major nutrition) and their relative neuropil volumes. Families in which only a single species was examined are: 1 = Pyrochroidae; 2 = Mordellidae; 3 = Lymexylidae; 4 = Nitidulidae; 5 = Lampyridae; 6 = Elateridae; 7 = Ptinidae; 8 = Dermestidae; 9 = Bolboceratidae; 10 = Geotrupidae; 11 = Gyrinidae. Icons to the right of the family names show whether AL substructures could be observed and whether these are -immunoreactive to tachykinin-related peptide (TKRP) or if a microglomerular organization could be observed (see legend at the bottom; *: no immunostainings against TKRP are available). Data on lifestyle of the animals extracted from: [49- 53].

TKRP-ir substructures in antennal lobe glomeruli

Among the 63 investigated beetle species, the olfactory glomeruli of almost 25 % exhibited TKRP-immunoreactive (TKRP-ir) substructures similar to those described in *A. tumida* [39]. In addition to the Nitidulid *A. tumida*, TKRP-ir glomerular substructures were observed in representatives of six different families (Cerambycidae, Dermestidae, Silphidae, Lucanidae, Bolboceratidae, and Scarabaeidae). However, careful in-group comparisons in four families revealed that TKRP-ir substructures cannot per se be regarded as characteristic of a respective family.

For example, within Cerambycidae (longhorn beetles), only *A. tabacicolor* exhibits TKRP-ir substructures (Fig. 2 A). In the Cerambycidae *P. cerambyciformis*, *S. melanura*, and *R. bifasciatum* TKRP-ir fibers/areas can be observed in various regions of the brain (primarily in the protocerebrum) but in the AL, marked TKRP-ir stainings were absent. In the Silphidae (burying beetles), *N. vespilloides* and *P. atrata* were investigated. While the former possesses well defined TKRP-ir substructures within its glomeruli (Fig. 2 B), the AL of *P. atrata* exhibit a homogeneous TKRP-ir staining pattern that does not indicate such structuring (Fig. 2 C). The family in which we identified the most species exhibiting TKRP-ir substructures are the Scarabaeidae. Within this family, seven of the investigated animals display well-defined TKRP-ir substructures within their glomeruli (*A. solstitiale* [Fig. 2 D], *C. africana africana* [Fig. 2 E], *P. aemula* [Fig. 2 F], *P. ephippiata* [Fig. 2 G], *E. hornimanni* [Fig. 2 H], *E. aethiopica* [Fig. 2 I], and *E. schultzeorum* [Fig. 2 J]), while one species (*D. derbyana derbyana* [Fig. 2 K]) exhibits only weakly demarcated TKRP-ir substructures. One species (*O. funesta* [Fig. 2 L]) possess a granular TKRP-ir staining pattern within its glomeruli, while the stainings against synapsin reveals a substructured organization in some glomeruli (Fig. 2 L, arrowhead).

Furthermore, well-defined TKRP-ir substructures were observed in *D. maculatus* (Fig. 2 M) and in a bolboceratid species (Fig. 2 N), while in comparison, *L. cervus* (Fig. 2 O arrowheads) exhibited only weakly demarcated TKRP-ir substructures. In *G. stercorarius*, many of the glomeruli show weakly labeled TKRP-ir substructures (Fig. 2 P arrowheads), while some of the glomeruli are homogeneously labeled (Fig. 2 P arrow).

In all other species, inspection of TKRP-immunoreactivity of AL revealed a homogeneous (like for *Tenebrio molitor* [Fig. 2 Q]) or evenly granular staining of the glomeruli (like in *S. paniceum* [Fig. 2 R] or *O. funesta* [Fig. 2 L]), or no glomerular TKRP-immunoreactivity at all (like in *P. muelleri* [Fig. 2 S]).

As already described for *O. funesta* (Fig. 2 L), in some of the examined species, the substructures are clearly labeled in stainings against synapsin and/or axonal actin (phalloidin), indicating dense synaptic networks. These species include a bolboceratid species (Fig. 2 N arrowheads), *P. aemula* (Fig. 2 F arrowhead), *P. ephippiata* (Fig. 2 G arrowhead), *O. funesta* (Fig. 2 L arrowheads), *P. muelleri* (Fig. 2 S arrowhead) and *Trichius spec.* (Fig. 2 T arrowheads), while some species showed indications for such substructures (like in digital supplement Fig. S1).

Comparable TKRP-ir substructures are unknown from other insects. TKRP-ir stainings in the AL of other insects have usually been described as homogeneous or uniform, like in *D. melanogaster* [32], *Spodoptera litura* [54], *Aedes aegypti* [34], *Periplaneta americana* [55], or *Leucophaea maderae* [56]. This also applies to insects with atypical glomeruli (like the many small microglomeruli in Acrididae [21,48]). For example, in the acridid *Schistocerca gregaria* TKRP-ir labeled fibers could only be observed within the interglomerular space [57].

Innervation of the TKRP-ir substructures

What types of neurons contribute to the formation of the glomerular substructures in Coleoptera? In *A. tumida*, Kollmann et al. [39] could identify about 80 TKRP-ir LN entering the AL and the substructures of the glomeruli, but did not observe TKRP-ir in the antennal nerve (AN). Similarly, in this work, all animals with TKRP-ir substructures show TKRP-ir LN entering the AL but a lack of TKRP-ir in the AN.

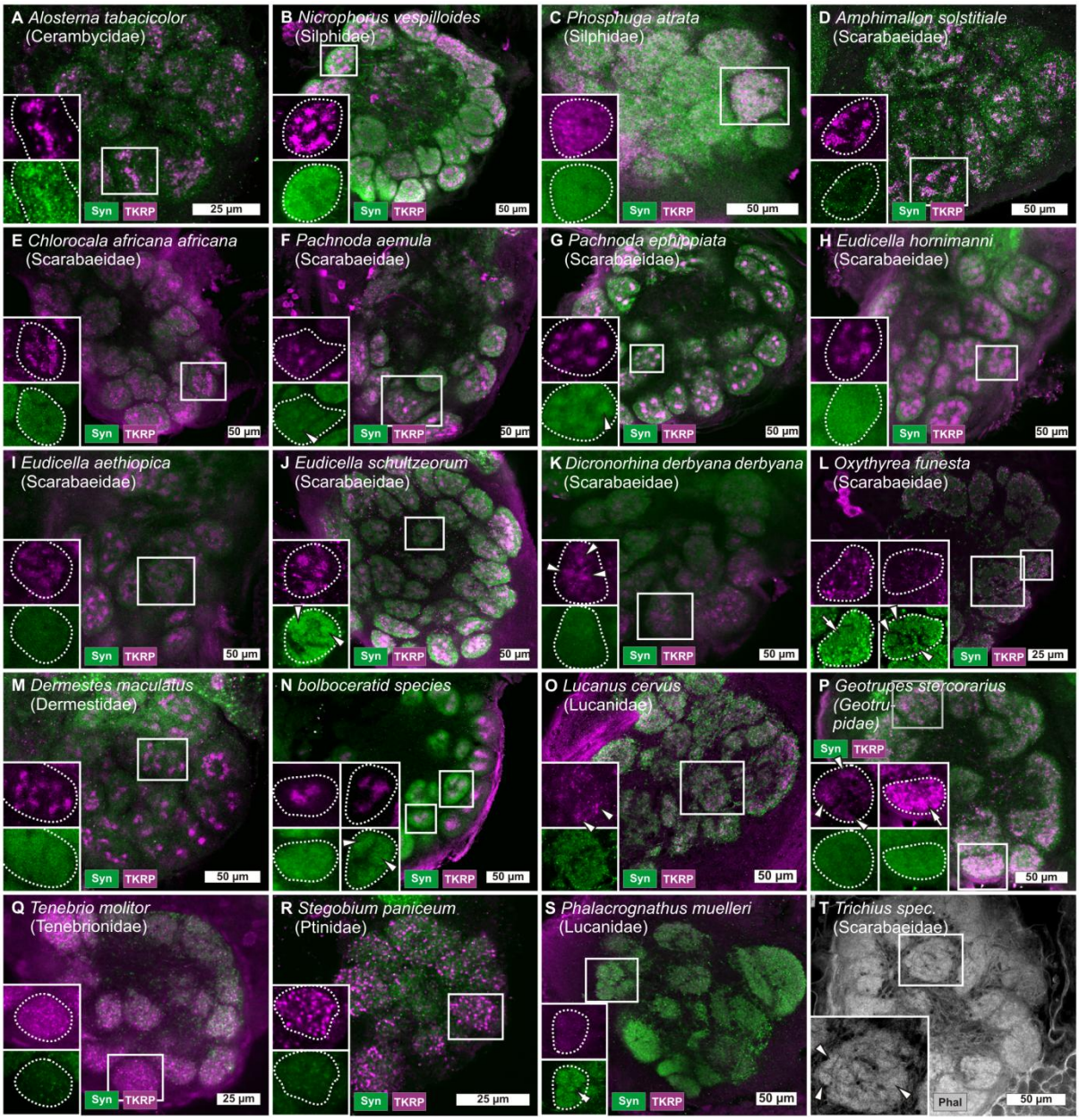

Fig. 2: Coleopteran antennal lobes (AL) labeled with various markers (immunostainings against synapsin [Syn, green] and Tachykinin-related peptide [TKRP, magenta] as well as phalloidin labeling [Phal, grey]). Boxes in the lower left corner show details of single glomeruli, marked in the overview images. Arrowheads show glomerular substructures (F, G, J - L, N - P, S, and T), arrows show homogenously stained glomeruli (L, P).

To further elucidate whether only LN contribute to the formation of the glomerular substructures, or whether there is also a contribution of OSN, we performed antennal backfills in a large scarabeid species, *P. ephippiata* and combined it with immunostainings against TKRP.

The backfill stainings clearly leave out the spherical TKRP-ir substructures (Fig. 3 A), showing that OSN do not contribute to the innervation of the substructures. The TKRP immunostaining is mainly restricted to the substructures but several TKRP-ir varicosities occur in the remainder of the glomeruli (Fig. 3 A arrowheads).

Discussion

Like the vertebrate central nervous systems, insect nervous systems are typically organized according to a basic bauplan. The bauplan of the central olfactory pathway of insects consists of the paired AL, the first integration center for olfactory

information and higher integration areas, including the MB and the LH [21,35]. The AL typically contain olfactory glomeruli that are usually interpreted as functional subunits for odor discrimination [58,59]. The principal glomerular organization can also be found in first order olfactory integration centers of other animal groups, including vertebrates [60,61], crustaceans [21], and mollusks [62,63].

The architecture of insect AL has been studied in several species, ranging from basal species like e.g. silverfish to derived species like e.g. Drosophila [reviewed e.g. in 21], but also in sister groups like e.g. Archaeognatha [64] or Collembola [65]. However, a systematic investigation including a higher number of specimen (particularly of one order) has so far not been undertaken. Our study on 63 beetle species from 22 different families is the first study that allows a direct comparison within this largest insect group.

Number of olfactory glomeruli covers a large range in Coleoptera

A comparison of glomeruli numbers in 32 of the examined beetle species revealed a hitherto undescribed variation. Glomeruli numbers ranged from 50 -150 in beetle species with regular glomeruli to about 1,000 microglomeruli in the examined ladybugs and diving beetles. Schachtner at al. [21] speculated that the AL of ancestral insects may have consisted of about 40 olfactory glomeruli. Deviations from this basic bauplan range from a complete (secondary) loss of glomeruli, as argued by some authors for aquatic beetles and dragonflies [41-43], to thousands of so called microglomeruli, to be found in e.g. acridid grasshoppers [21,48] but also in some diving beetle species [44]. However, in most insects, the variation of the basic theme is mainly reflected by a varying number of “typical” or regular glomeruli ranging from about 40, like in drosophilids, up to several hundred in some ant species [23]. On the basis of available data, Schachtner et al. [21] speculated in their review that the number of regular glomeruli (excluding orthopteran microglomeruli) in a given insect order might be well conserved and might exhibit only small

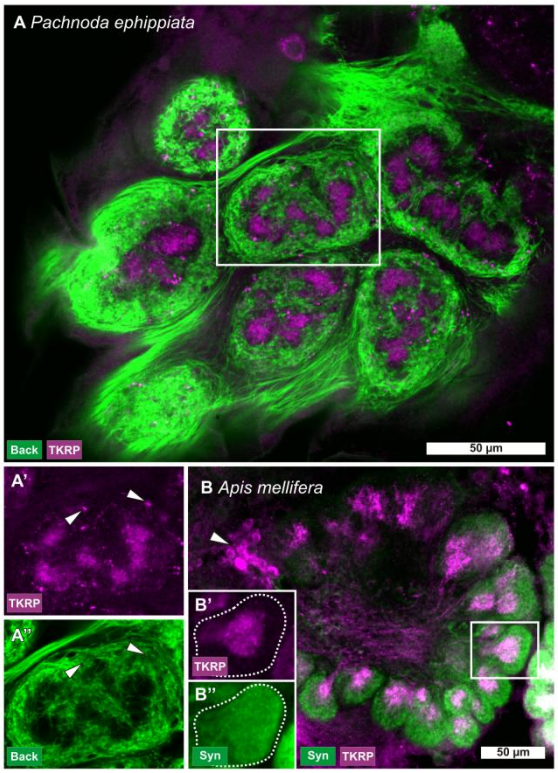

Fig. 3: Antennal lobes (AL) of *Pachnoda ephippiata* (Scarabaeidae) (A, A', and A'') and of *Apis mellifera* (B, B', and B''). Antennal backfills in *P. ephippiata* (A, A', A'') demonstrate that olfactory sensory neurons (OSN) of the antenna (green) do not innervate the glomerular substructures, while the tachykinin related peptide immunoreactive (TKRP-ir) local neurons (LN) (magenta) innervate mostly exclusive the glomerular substructures, save for several varicosities outside the substructures (A', A'' arrowheads). A' and A'' represent the labeling shown in the inset in A separated in the single channels. In *A. mellifera* (B, B', and B'') TKRP immunoreactivity in the glomerular core areas seems to stem primarily from LN (magenta; arrowhead), while the whole glomeruli labeled with the anti synapsin (Syn, green). B' and B'' represent the two separated labels shown in the inset in B.

variations reflecting specific ecological or ethological needs of the respective species. Meanwhile, this idea has only been corroborated by findings in ant species that possess up to several hundred glomeruli [23]. The findings of the current study question the general statement that insect orders have a conserved number of regular glomeruli [21]. However, the observed variation within the number of glomeruli in the Coleoptera possibly results from their huge diversity and their many adaptations. Conversely, at the family level, the number of glomeruli seems well conserved (Fig. 1).

Microglomeruli in particular Coleoptera families

Atypical AL and glomeruli occur in various insects. For instance, the AL of the Odonata *Libellula depressa consist of* small, spherical knots [66], while previously the Odonata AL (like the AL of Ephemeroptera) had been described as a- or nonglomerular [21,66]. In Hemiptera, AL have also been described as aglomerular (*Trioza apicalis* [67]) or as diminutive with only 13 glomeruli-like structures (*Scaphoideus titanus* [68]). Also the AL of the Phthiraptera *Columbicola columbae* shows no clearly defined glomeruli or any other compartments [69]. Conversely, as mentioned earlier, in the Acrididae (like *Schistocerca gregaria* and *Chorthippus albomarginatus*), the AL comprises thousands of small microglomeruli [21,48].

AL with a microglomerular organization have already been observed in some beetle species. The AL of diving beetles (Dytiscidae) have earlier been reported to show a nonglomerular organization or even to be totally absent in some representatives [40-42]. However, a recent in-depth study in ten representatives from this group found small and very numerous glomeruli in the AL, similar to the microglomeruli of Acrididae [44]. This is in accordance with our own data from *A. sulcatus* with about 1,000 glomeruli per AL and *I. fuliginosus* with about 400 - 500 glomeruli per AL (Fig. 6 A and B).

Moreover, the current study revealed AL with numerous small glomeruli, comparable to those observed in the diving beetles or Acrididae, in terrestrial Coccinellidae (ladybugs). Difficult to characterize in synapsin or phalloidin stainings, backfills and antibody stainings against TKRP helped to identify numerous small glomeruli (Fig. 6 E-G arrowheads) and to differentiate the AL from a structure which we identified as the lobus glomerulatus (LG) (Fig. 6 G), a deutocerebral structure typically found in hemimetabolous insects but recently also reported to occur in beetles [38]. In all five investigated Coccinellidae, the AL is remarkably small (Fig. 1) and consists of numerous minute glomeruli (approximately 400 - 600 glomeruli per AL).

Glomerular substructures in the Coleoptera

A recent study described a novel type of TKRP-ir substructures in the olfactory glomeruli of the small hive beetle *A. tumida* [39] that were evenly distributed across all glomeruli and innervated by TKRP-ir LN. The authors speculated that such a specialized organization may reflect a need to better handle the complex olfactory coding in a beehive in which these animals live as parasites. The current study shows that such an arrangement is by no means unique to *A. tumida*, as a similar organization of comparable TKRP-ir substructures was observed in 15 of the examined beetles. In addition, even more of the beetles showed substructures that were only revealed in synapsin and/or phalloidin labelings, but not evident solely based on TKRP immunostainings. These substructures are widely distributed across the phylogenetic tree but may be conserved within certain families.

Phylogenetic distribution of substructured glomeruli in the Coleoptera

Substructures in olfactory glomeruli (TKRP-ir and non-TKRP-ir) occur in evolutionary distant families (Fig. 1). In the 22 investigated families, TKRP-ir substructures occur in species of seven families. Taking glomerular substructures that only showed in synapsin/phalloidin labelings into account as well, we found such structures in a total of 10 beetle families. Species displaying clearly demarcated glomerular substructures all belong to the polyphageous coleoptera. Of the examined 15 species that belong to the superfamily of the Scarabaeoidea (comprising the four families Lucanidae, Bolboceratidae, Geotrupidae, and Scarabaeidae), ten species showed TKRP-ir substructures in all glomeruli, one shows TKRP-ir substructures in several glomeruli, and the remaining four species showed substructures visualized only in the synapsin/phalloidin labeling. We conclude that glomerular substructures are a conserved feature of the Scarabaeoidea. In the other examined polyphagous Coleoptera, the situation is less clear, either because only a single species of the respective family was studied or because we found species with and without clear substructures in the same family. For example, in

the Tenebrionidae, half of the six examined species showed synapsin-ir substructures or substructures labeled with phalloidin. A similar situation occurred in Cerambycidae with three of the five examined species displaying such substructures.

In the silphids, we found one species (*N. vespilloides*), which is showing TKRP-ir substructures, while the other species (*P. atrata*) exhibits unstructured glomeruli. For Nitidulidae and Dermestidae, only one species was investigated, each showing the typical TKRP-ir glomerular substructuring. All examined adephageous beetles lacked clear glomerular substructures. In summary, the spotty distribution of glomerular substructures across the different groups suggests that it is not a conserved feature in Coleoptera but may have evolved independently in several beetle taxa.

Innervation of the TKRP-ir substructures

To examine whether OSN may in addition to the LN contribute to the glomerular substructures, we exemplarily performed antennal backfills in a large scarabeid species, *P. ephippiata,* and combined it with immunostainings against TKRP. The results clearly underline the findings in *A. tumida* that OSN do not contribute to the innervation of the substructures (Fig. 3 A) [39]. Based on these data, we propose that such glomerular substructures in beetles are generally organized according to this scheme. Further studies have to reveal whether other AL neuron types like PN and CN may also in addition contribute to the substructures. However, paired serotonin-immunoreactive (5HT-ir) CN that typically innervate all olfactory glomeruli have been shown in many insect species and seem to be a basic feature of insect AL [21,70]. In *A.tumida*, projections of the 5HT-ir CN innervate all glomeruli but spare the substructures [39].

How could glomerular substructures evolve from the basic non structured pattern?

Typically, insect OSN expressing the same specific odorant receptor (OR) converge on the same glomerulus, with one OSN typically expressing only one specific OR [71-73]. In insects, an innervation of particular areas of a glomerulus by OSN is known from several species including *D. melanogaster* and some lepidopteran species, but it is especially well investigated in *A. mellifera* [21,29,74-81]. There, the bulk of the glomeruli can be separated into two compartments: the outer cortex (also called cortex rind, cortex layer, cortical cap, cap, or peripheral area) and the inner core (sometimes termed base or basal area). OSN axons seem to project exclusively into the cortex (with exception of seven glomeruli within *A. mellifera*, which are innervated by the T4 tract [81-83]). Additionally, two types of LN have been observed, exclusively targeting the core region of a glomerulus, the other projecting into the core and the cortex. With regards to PN, uniglomerular PN have branches in the core and cortex, multiglomerular PN branch only in the cortex area [29,74,81]. Own data in *A. mellifera* showed TKRP-ir LN innervating the core area (Fig. 3 B - B'), comparable to immunostainings against the neuropeptide allatostatin [83]. However, multiple cores per glomerulus, like the multiple substructures in beetles haven't been observed in *A. mellifera* (Fig. 3 B).

Assuming that a glomerulus with two compartments, as observed in *A. mellifera, D. melanogaster,* and some Lepidoptera [29,74,81] reflects the basic architecture of a glomerulus of the holometabolous insects, multiple cores represent a derived situation. Glomeruli with multiple cores or substructures could be envisioned to have resulted from an incomplete fusion of such basic glomeruli, where the original core areas remained separated (Fig. 4 A). Alternatively, multiple glomerular substructures in a single glomerulus might have arisen through a differentiation of a single core into multiple cores (respectively substructures) (Fig. 4 B).

In the “fusion scenario” outlined above (Fig. 4 A), one would expect the fused glomerulus to inherit the innervation of its progenitors, i.e. to be innervated by OSN carrying different specific OR, either homogenously (Fig. 4 C left hand) or in separated regions (Fig. 4 C right hand). Alternatively, the “differentiation scenario” (Fig. 4 B), would suggest that the differentiated glomerulus should still be innervated by OSN expressing just one specific OR (Fig. 4 D). Future

experiments utilizing transgenic lines and fluorescence *in situ* hybridization to label specific OR, or antibodies against specific OR (capable of staining axonal projections) could help to answer this question by visualizing OSN innervation patterns of individual glomeruli.

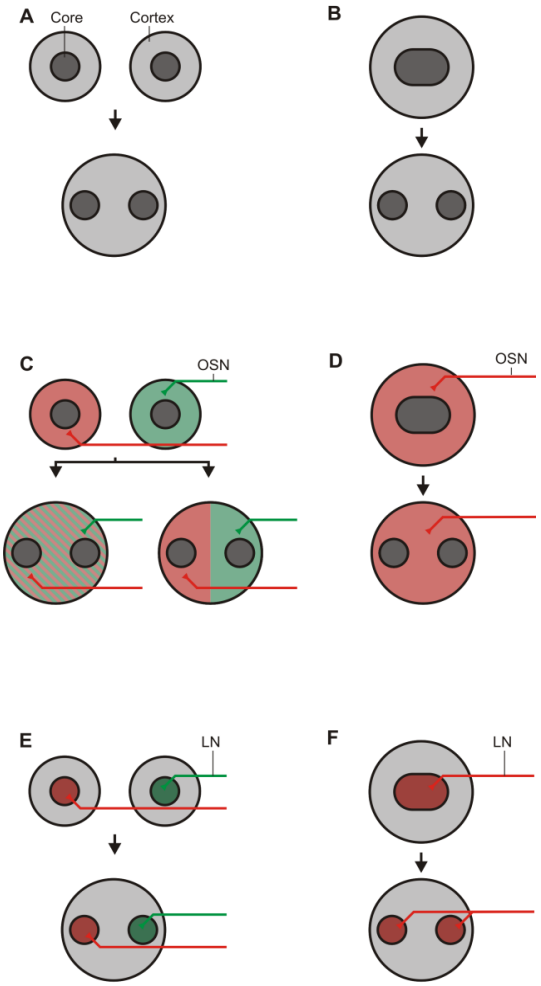

Fig. 4: *Considerations to the evolutionary origin the glomerular substructures. In principal, substructures could originate from the fusion of two (or more) glomeruli, each consisting of one cortex and one core, resulting in a glomerulus with one cortex and two cores / substructures (A). Substructures could also originate from a glomerulus with one cortex and one core and a subsequent division of the single core in multiple cores / substructures (B). C to F showing the possible principal innervation pattern as consequences of the two models (A and B) for olfactory sensory neurons (OSN) (C and D) for local interneurons (LN) (E and F) (see text).*

In addition, selective labeling of single uniglomerular LN by dye filling with glass micropipettes would give insight whether the single substructures of one glomerulus are innervated via the same or different LN and would therefore help to understand how the multi cored glomeruli may have evolved. If a dye filled uniglomerular LN projects only in one core of a glomerulus with multiple cores (Fig. 4 E), it is very likely, that this glomerulus originated from the fusion of single glomeruli. On the other hand, if a labeled uniglomerular LN projects into all cores of a glomerulus (Fig. 4 F), this would support the idea, that the multiple substructures of a glomerulus result from a single glomerulus whose core has differentiated into multiple cores (respectively substructures).

Multiple substructures in olfactory glomeruli outside Coleoptera

Up to now, glomeruli with clearly separated multiple substructures outside the beetles have only been observed in the Gryllidae *Gryllus bimaculatus*. Ignell et al. [48] and Yoritsune and Aonuma [84] described "microglomerular substructures", "microglomerular cluster", or only "microglomeruli" (not to be confused with the microglomeruli from Acrididae) within the "regular" glomeruli. Own stainings with phalloidin, and anti-synapsin and anti-TKRP antisera in the Gryllidae *Gryllus assimilis* and *Acheta domesticus* revealed also microglomerular substructures (Fig. 5 A and B arrowheads), showing that the observation in *G. bimaculatus* is not an isolated case. Both species lack anti-TKRP immunoreactivity within the entire AL including the glomerular substructures. However, in contrast to our finding in the beetles, the glomerular substructures of *G. bimaculatus* are innervated by OSN [20,48]. To explain the microglomeruli within the AL of *G. bimaculatus*, Ignell et al. [48] argued, that glomeruli with restricted terminal arborizations of OSN within one glomerulus can be found in many insect AL (Diptera [85-87], Blattodea [88,89], Hymenoptera [90-93], Lepidoptera [74]). They hypothesized that such "multicompartmented uniquely identifiable glomeruli" could be fragmented into individual microglomeruli, potentially by a dichotomy of OSN axons before they enter a glomerulus. The microglomerular substructures observed in *G. bimaculatus* could thus be regarded as an evolutionary intermediate between "regular AL with normal glomeruli" (known from most insects [21]) and microglomerular antennal lobes found in the Acrididae" [48].

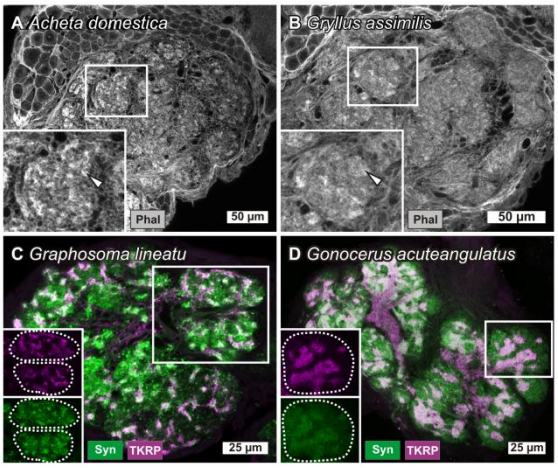

Fig. 5: Glomerular substructures of hemimetabolous insects: the two Gryllidae *Acheta domestica* (A) and *Gryllus assimilis* (B) and the two Hemiptera *Graphosoma lineatum* (C) and *Gonocerus acuteangulatus*. Boxes in the upper left of each image show a magnified view, respectively the two separated channels of the inset within the image. In *A. domestica* (A) and *G. assimilis* (B) staining with phalloidin (Phal) revealed glomerular substructures (arrowheads), resembling the situation in *Gryllus bimaculatus* [48,84]. Staining with an antibody against tachykinin related peptide (TKRP) (magenta) and synapsin (Syn) (green) revealed irregular shaped and interconnected TKRP immunoreactive substructuring within the glomeruli of two Hemiptera species: *G. lineatum* (about 205 glomeruli) (C) and *G. acuteangulatus* (about 185 glomeruli) (D).

TKRP-immunostainings revealed glomerular substructures in the approximately 200 glomeruli (per AL) of the two Hemipteran species *Graphosoma lineatum* (Pentatomidae) and *Gonocerus acuteangulatus* (Coreidae) (Fig. 5 C and D). In contrast to the glomerular substructures observed in the Coleoptera, the TKRP-ir substructures of the two hemipteran species are of an irregular shape and are interconnected with each other (Fig. 5 C and D). Unlike in Gryllidae but similar to the TKRP-ir substructures of Coleoptera the TKRP-ir substructures of the Hemiptera are innervated by TKRP-ir LN, while the AN lacks any TKRP immunoreactivity. Whether the substructures of the two hemipteran species are innervated by OSN, as described for *G. bimaculatus* [48,84] or whether they lack innervations by OSN as observed in the Coleoptera remains unknown.

Correlation of glomeruli architecture to brain architecture and lifestyle

On a gross ecological and ethological level (primarily terrestrial or aquatic habitat, nutrition; [49-53] substructured glomeruli in different Coleoptera could not be correlated with a specific lifestyle (Fig. 1). There is also no correlation to the relative volumes of the four major brain neuropils (antennal lobes, optic lobes, central complex and mushroom bodies) (Fig. 1) or to total / absolute volumes of the AL.

Lifestyle (major nutrition) and the architecture of the AL (size of AL or the number of its glomeruli) have also been found to be uncorrelated within Scarabaeidae [94]. However, Farris and Roberts [94] noted that differences in the feeding habits of Scarabaeidae (generalists vs. specialists) are reflected in the architecture of the MB. This might indicate that (at least in Coleoptera) lifestyle / preference of nutrition is rather reflected in the morphology of higher olfactory integration centers (the MB), a structure that is important for olfactory discrimination, learning, and memory storage and retrieval [59, 95-97], than in the morphology of the primary olfactory integration center (the AL).

Numerous small glomeruli, comparable to the microglomeruli of Acrididae [21,48] could be identified in two coleopteran families, namely ladybugs and diving beetles. Despite obvious differences in habitat (terrestrial vs aquatic), both groups are primarily predatory and possess well-developed optic lobes with a huge relative volume (Fig. 1). A comparable microglomerular pattern can also be observed within the strongly visual orientating, predatory odonate *Libellula depressa* [66]. Interestingly, in all three taxa, the CA show remarkable reductions or is even lacking (see below). Though not predatory, the locust *Schistocerca gregaria,* which also displays large optical neuropils, possesses AL comprised of many microglomeruli [98]. While the correlation of numerous microglomeruli and large optical neuropils thus does not seem to imply predatory behavior per se, it points towards a possible and hitherto unstudied linkage between these two brain centers in distantly related insect taxa.

Olfaction with atypical AL

Besides regular-shaped AL glomeruli, as known from many insects like *D. melanogaster*, *A. mellifera*, and many moth species [21], several authors described insect AL with deviating glomerular design, including AL with numerous small glomeruli (microglomeruli), AL with small and spherical knots, non-glomerular AL or AL comprising poorly demarcated and hardly distinguishable glomeruli (e.g. described as "AL with glomerular-like structures") [21,48,66-69]. In some cases, it has been hypothesized that such poorly developed AL and/or the absence of clearly defined glomeruli might be an indicator of a poorly developed sense of smell or even anosmia. Odonata, for instance, have repeatedly been speculated to be (almost) anosmic [21,40-42,99]. However, recent studies were able to confirm that the *antenna of the* odonate *L. depressa possess about* 120 OSN in 40 sensilla [100] and that the odonate *Ischnura elegans* clearly responds to odors (in behavioral and electrophysiological assays [101]). Similarly, in *C. columbae* (a louse species exhibiting a non-glomurular AL), olfactory sensilla [102] and an odor response could be observed [103]. Aquatic beetles, often discussed to be anosmic [40-42], have also been demonstrated

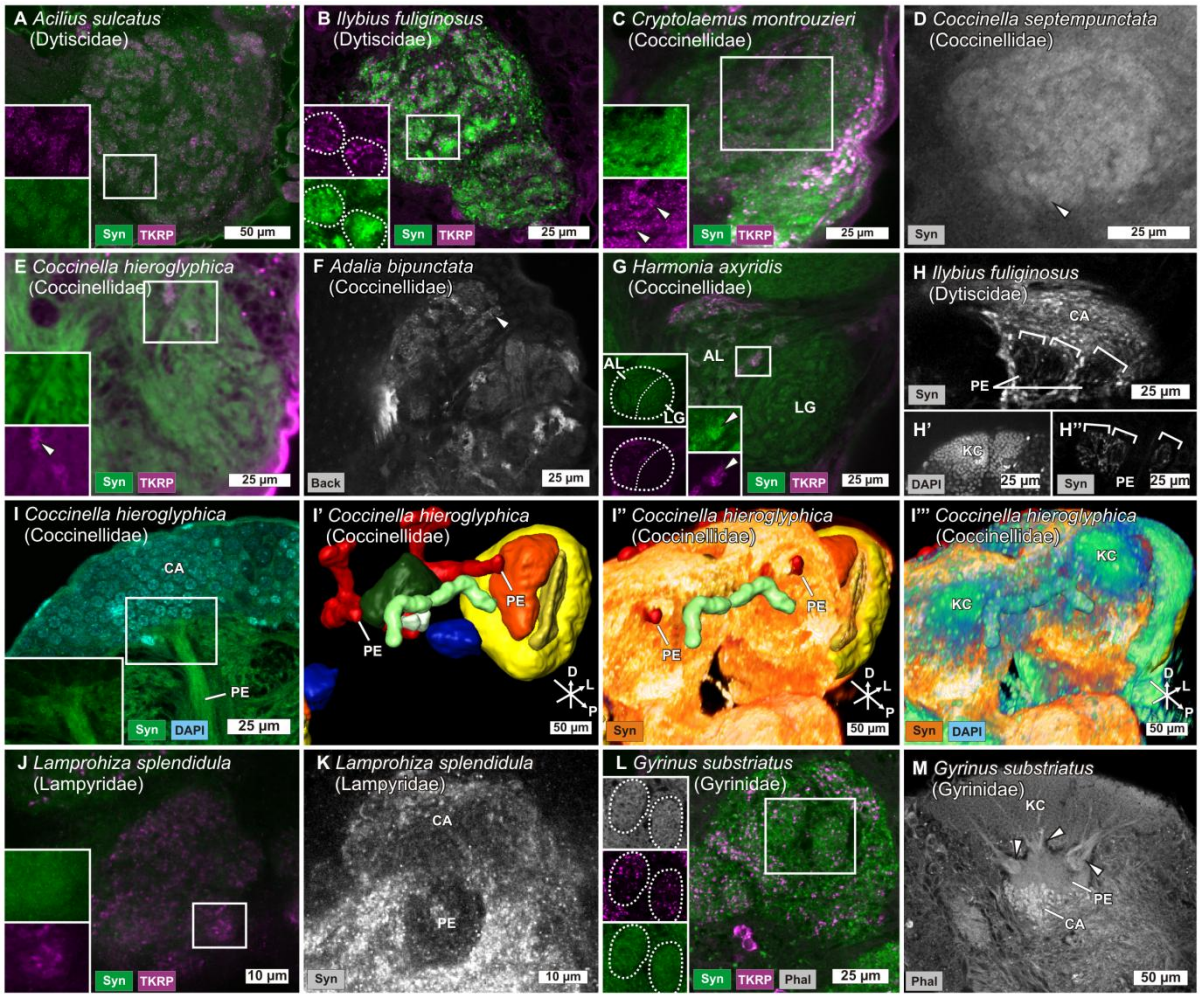

Fig. 6: Antennal lobes (AL) (A-G, J, L) and mushroom bodies (MB) (H-I'', K, M) of different Coleoptera stained with antibodies against synapsin (Syn) and against tachykinin related peptides (TKRP) or labeled with DAPI or phalloidin (Phal). Boxes in the upper left show details of single glomeruli (A-C, E, G, J, L) or part of the MB (I) marked in the overview images, or they show the superstition between the AL and the lobus glomerulatus (LG) in the ladybug *Harmonia axyridis* (G). Arrowheads showing single glomeruli (C-G). Notice the trichotomy of the mushroom bodies peduncle (PE) (square brackets in H and H'' and arrowheads in M) of the aquatic beetles *Ilybius fuliginosus* and *Gyrinus substriatus*. The Calyx (CA) is absent in the ladybug *Coccinella hieroglyphica* as seen in the staining with Phal (I) and in the 3D-reconstruction and 3D-projektion (volume rendering) of Syn and DAPI (I'-I'''). In both cases, no Ca is visible between PE and Kenyon cells (KC). Orientation bars in I' to I''': D = dorsal, P = posterior, L = lateral.

to respond to kairomone cues to avoid predators [104], to pheromones to find mating partners [105], or to other olfactory stimuli [106]. The notion that a well-defined AL with a distinctive glomerular organization is not per se a mandatory prerequisite for olfaction is also underscored by our observations of microglomeruli within five ladybug species, which clearly possess antenna bearing olfactory sensilla [107-110] and which have repeatedly been demonstrated to respond to olfactory stimuli [111-117]. This is also in line with similar observations described for *S. gregaria* [118-120].

Insects with poorly developed AL / glomeruli typically also exhibit poorly developed or even lacking mushroom body (MB) calyces (CA), as has been reported e.g. in Dytiscidae [42,44, own observations, Fig. 6 H, H', H''], Odonata [41,42,66], and Hemiptera [41,67,68,121]. The five ladybug species investigated in this work also show small AL with diffusely demarcated microglomeruli (Fig. 6 C-G) and also completely lack a CA, while the peduncle (PE) and the Kenyon cells (KC) are still clearly identifiable (Fig. 6 I-I'''). The co-occurrence of small / lacking AL or poorly defined olfactory glomeruli and small / lacking CA seems to be a repeating pattern within insect neuroanatomy.

The firefly *L. splendidula*, which spends up to 3 years as a nymph that feeds on snails, before it transforms into the reproducing adult that lives for just about one week and does not feed [51,122], has only small AL associated with equally small CA (Fig. 1, 6 J, K). AL and glomeruli in *L. splendidula* are unidentifiable based on stainings with a synapsin antibody or with phalloidin, but become barely visible in stainings with a TKRP antibody (Fig. 6 J). However, due to the elusive nature of the glomerular boundaries, a reliable counting of the glomeruli is not possible. The small AL and CA possibly reflect a reduced need for olfaction in the adult animal, which does not feed during its short life span (it even lacks developed mouthparts) and finds its mating partner primarily by visual cues [123,124]. *Similar observations are known from the* heteropteran *Diceroprocta semicincta*, which lives up to 17 years underground as feeding nymph before emerging as non-feeding, reproducing adult. In this short time period, the animals mainly focus on finding mating partners, using auditory stridulation cues rather than olfactory cues, which is reflected in a reduction of AL and CA [42,125].

Feeding habits have been speculated to be another reason for reduced or underdeveloped AL (glomeruli). In Hemiptera, *S. titanus* is (at least in Europe) considered to be a feeding specialist that is monophagous on grapevine, while its relative *Hyalesthes obsoletus* is characterized as a generalist that feeds on different wild host plants. Notably, specialist *S. titanus* has approximately 150 times less OSNs than *H. obsoletus* and about 10 times less and more poorly defined glomeruli than *H. obsoletus* [68], with both species lacking CA.

A contrary example, however, is provided by the whirligig beetle *Dineutus sublineatus,* which lacks AL but has a clearly identifiable CA [43]. Previously, lacking AL in aquatic beetles have been interpreted as a secondary loss. This statement is based on the fact that for land living animals, which re-adapt to an aquatic habitat, olfactory perception under water is very difficult, in consequence leading to a loss-of-function and (almost) anosmic animals [40-43]. The well-developed CA in *D. sublineatus* had been explained by the strong involvement of the CA in visual data processing. However, our data clearly show AL glomeruli (Fig. 6 L) and a CA (Fig. 6 M) within the whirligig beetle *G. substriatus*, questioning the general statement that whirligig beetle (like all other aquatic insects) lacks antennal lobes [43].

Finally, it must be emphasized that small, less developed, or lacking AL (and in most cases the correlating small or lacking CA) are most likely not an intrinsic feature of a given taxon (homology), but convergent adaptations to a similar (or even particular) lifestyle and specific ecological and ethological requirements.

Summary

In this work we focused on the diversity of the antennal lobes, the first integrations centers for olfactory information within the Coleoptera. We investigated the AL of 63 different coleopteran species of 22 families. Beside coleopteran AL, containing typically 80 to 120 glomeruli per AL and with regular shaped glomeruli, as known from

most insects like *D. melanogaster*, we found AL with A) substructures within their glomeruli, often correlated with TKRP immunoreactivity and B) remarkable small but numerous glomeruli within coleopteran AL, similar to the microglomeruli of the Acrididae.

26 of the investigated coleopteran species (stemming from 16 families) show explicit substructures within their AL glomeruli. In 15 of the investigated species (stemming from 7 families), AL substructures are TKRP-ir originating from a cluster of LN lateral from the AL. Antennal nerve backfills, exemplarily performed in one beetle species revealed, that the glomerular TKRP-ir substructures are avoid of OSN innervation. Together with the finding that also the antennal nerves of all other examined beetle species are devoid of TKRP-ir fibers, we conclude that the glomerular substructures in beetles are typically not innervated by OSN but by LN. These features make the glomerular substructures to a particular trait only found in several beetle species as it has until today not been described in insects outside the coleoptera. From the distribution of this trait between the different beetle families, we speculate that this trait has evolved independently several times. We offer two hypotheses on the origin of the glomerular substructures. They might either originate from the fusion of single glomeruli or result from a compartmentalization within particular glomeruli.

In five ladybug species and two diving beetle species we found many noticeable small glomeruli, resembling the microglomeruli of the Acrididae. In ladybugs we found in average about 500 of this small glomeruli and in the two diving beetle species in average about 750 small glomeruli per AL. These glomeruli are ill defined and only visualized by antennal backfills or staining with TKRP antibody. Insects with such ill-defined glomeruli or a-glomerular AL often have reduced or lacking CA. This is also true for the MB of the ladybug (total lack of CA) and diving beetle species (reduced CA). The finding of OSN innervated microglomeruli in the two distant beetle families support the hypothesis that microglomeruli are a derived trait that evolved several times within the insects.

Materials and Methods

Animals

Three coccinellid species (*Adalia bipunctata*, *Cryptolaemus montrouzieri*, and *Coccinella septempunctata*) were purchased from "SAUTTER & STEPPER GmbH" (Ammerbuch, Germany). Three Tenebrionide species (*Alphitobius diaperinus*, *Zophobas morio*, and *Tenebrio molitor*) were obtained from "b.t.b.e. Insektenzucht GmbH" (Schnürpflingen, Germany). Two scarabaeid species, *Eudicella schultzeorum* and *Pachnoda aemula,* were acquired at a reptiles' fair in Frankfurt, six other species (*Chlorocala africana africana*, *Dicronorhina derbyana derbyana*, *Eudicella hornimanni*, and *Eudicella aethiopica*) were a generous gift from Jutta Renda from "Käferzucht" (Sinsheim-Hilsbach, Germany), and the Scarabaeidae *Pachnoda ephippiata* were a kind gift from Florian Schlusche (University of Konstanz, Germany). The Lucanidae *Phalacrognathus muelleri* and *Homoderus gladiator* were provided from a private rearing by Stefan Dippel (Momberg, Germany). Bolboceratidae specimens were a generous gift from Reinhard Predel and Susanne Neupert (University of Cologne, Germany) and were originally collected at Aha Hills, Namibia. Specimens of *Nicrophorus vespilloides* were a generous gift of Sandra Steiger (University of Ulm, Germany). *Dermestes maculatus* was kindly provided by Christian von Hoermann (University of Ulm, Germany). *Stegobium paniceum* and *Palembus dermestoide* were a generous gift from Mathias Schott (University of Gießen, Germany). The chrysomelid *Macroplea mutica* was a gift from Gregor Kölsch (University of Hamburg, Germany). The chrysomelid *Leptinotarsa decemlineata* and the curculionid *Gonipterus scutellatus* were kindly provided by Stefan Schütz (University of Göttingen, Germany). The following animals were collected in the vicinity of the Philipps University of Marburg (Germany), endangered animals we collected and dissected under permission from the conservation agency Marburg (Untere Naturschutzbehörde Marburg; 67 22 04 - zim from 2013.06.19, 2014.07.15, and 2014.08.07): *Pyrochroa coccinea, Lagria spec*., *Coccinella hieroglyphica*, *Harmonia axyridis*, *Donacia versicolorea, Chrysolina sturmi, Lilioceris lilii, Rhagium bifasciatum, Molorchus minor, Pachytodes cerambyciformis, Alosterna*

tabacicolor, Stenurella melanura, Curculionidae spec, Hadroplontus litura, Liophloeus tessulatus, Otiorhynchus spec., Polydrusus pterygomalis, Lamprohiza splendidula, Rhagonycha fulva, Cantharis fusca, Ampedus sanguinus, Phosphuga atrata, Lucanus cervus, Amphimallon solstitiale, Oxythyrea funesta, Acilius sulcatus, Gyrinus substriatus, Pterostichus niger, Abax parallelepipedus, Calathus erratus, Coccinella hieroglyphica, Cicindela campestris, Hylecoetus dermestoides, Geotrupes stercorarius, Carabus nemoralis. Data from the Nitidulidae *Aethina tumida* are obtained from Kollmann et al. [39]. Data for the Tenebrionid *T. castaneum* are obtained from Dreyer et al. [37], Binzer et al. [33], and Dippel et al. [38].

The foragers of *Apis mellifera* were kindly provided by the Bieneninstitut Kirchhain (Germany). Two Gryllidae (*Gryllus assimilis* and *Acheta domestica*) have been obtained from b.t.b.e. Insektenzucht GmbH. The two Heteroptera (*Gonocerus acuteangulatus* and *Graphosoma lineatum*) were collected close to the Philipps University of Marburg. Age and sex of the animals are not taken into account in the current study.

Phylogenetic relationships of the investigated animals

For Coleopteran gross phylogeny, we referred to Hunt et al. [8], who inferred phylogenetic relationships within the order based on sequence analyses of 18S rRNA, mitochondrial 16S rRNA and *cox1*.

For higher resolution of individual branches, we drew on the coccinellid phylogeny published by [126], the carabid phylogenies put forward by [127,128], the chryosmelid phylogeny provided by [129], and the phylogenetic trees for the superfamily Scarabaeoidea detailed in [130-132].

Primary antisera

Similar to other insect studies [e.g. 33,133,134], a monoclonal primary antibody from mouse against a fusion protein consisting of a glutathione-S-transferase and the first amino acids of the presynaptic vesicle protein synapsin I coded by its 5'-end (SYNORF1; 3C11, #151101) was used to selectively label neuropil areas. The synapsin antibody was kindly provided by Dr. Erich Buchner (University of Würzburg, Germany) and was first described by Klagges et al. [135]. The antibody was used at a dilution of 1:100. The specificity of this antibody in the beetle *T. castaneum* has been demonstrated by Utz et al. [133].

The polyclonal antiserum against tachykinin-related peptide (TKRP) is against the *Locusta migratoria* tachykinin II (Lom-TK II, APLSGFYGVRamide) and was raised in rabbit. It was kindly provided by Dr. H. Agricola (K1-50820091) (University of Jena, Germany) and first described by Veenstra et al. [136]. In beetles, specificity of the antibody was confirmed for *T. castaneum* [33]. It was used at a dilution of 1:2,000.

Secondary antibodies

Goat anti-mouse antibodies conjugated to Cy5 (GAM-Cy5) and goat anti-rabbit antibodies conjugated to Cy3 or Cy5 (GAR-Cy3 / GAR-Cy5) were used as secondary antibodies (each 1:300; Jackson ImmunoResearch, Westgrove, PA, USA).

Further markers

Alexa Fluor 488-coupled phalloidin (Molecular Probes, Eugene, OR, USA) was used to visualize axonal f-actin and thus to reveal whole brain anatomy. It was used at a dilution of 1:200.

DAPI (4',6-diamidinophenyindole; Sigma Aldrich, Steinheim, Germany) was used as a nuclear marker to identify neuronal somata. It was used at a dilution of 1:20,000.

Neurobiotin (Vector Laboratories, Burlingame, UK) was used for the antennal backfills in a 4% solution, diluted in 1 M KCl. It was visualized with Cy3 conjugated streptavidin (1/200; Dianova, Hamburg, Germany).

Double immunostainings of whole mount preparations

Brains were dissected under PBS (phosphate buffered saline; 0.01 M; pH 7.4) and were fixed overnight at 4 °C in 4% PFA (paraformaldehyde; Roth, Karlsruhe, Germany) in PBS. In some cases, brains were transferred in PBS and were stored for several days at 4°C. Subsequently brains were washed 2 - 3 x 10 - 15 min (depending on the size of the brain), treated with collagenase-dispase (1 mg/ml in PBS; Sigma Aldrich) for 30 - 90 sec and washed 3 - 4 x 10 - 15 min. Afterwards brains were preincubated for 1 to 3 days in PBT (PBS added with 0.3% Triton-X 100, Sigma Aldrich) with 5% NGS (normal goat serum; Jackson Immuno Research) at 4 °C. As primary antibodies we used anti-synapsin (1:100) in combination with anti-TKRP (1:20,000), diluted in PBT with 1% NGS. Brains were incubated for 2 - 5 days at 4 °C. After rinsing (4 - 6 x 10 - 15 min) with PBT, brains were incubated in secondary antibodies (GAM-Cy5 and GAR-Cy3; 1:300; Jackson ImmunoResearch) and Alexa Fluor 488 Phalloidin (0.5%) and DAPI (1:20,000) in PBT with 1% NGS at 4 °C for 2 - 5 days in the dark. After rinsing (4 - 6 x 10 - 15 min) with PBT, brains were dehydrated in an ascending alcohol series (30%, 50%, 70%, 90%, 95%, 2 x 100% ethanol, 3 - 7 min each) at room temperature. The tissue was then cleared to transparency in methyl salicylate (Merck, Darmstadt, Germany). Brains were finally mounted in resin (Permount, Fisher Scientific, Pittsburgh, PA, USA), using 2 - 10 layers of reinforcing rings as spacers (Zweckform, Oberlaindern, Germany) to prevent tissue compression.

Backfills of the antenna

Cold-anesthetized animals were mounted with their backs on microscope slides, using dental wax (S-U-wax wire, 2.0 mm, hard; Schuler Dental, Ulm, Germany) and a soldering iron at low temperature (100 °C; Solder-Unit ST 081; Star Tec Products, Bremen, Germany). The head was carefully waxed to the thorax and the base of the antenna was fixed with modeling clay (Das große Dino-Knet-Set; moses. Verlag GmbH, Kempen, Germany) and by using a soldering iron. The distal lamellate segments of the antenna were cut off. Glass micropipettes were drawn (Model P-97, Sutter Instrument, Novato, USA) from borosilicate glass (inner diameter, 0.75 mm; outer diameter, 1.5 mm; Hilgenberg, Malsfeld, Germany) and broken to a tip diameter matching the diameter of the antenna. Micropipettes were filled with 4% neurobiotin (Vector Laboratories, Burlingame, UK) solved in 1 M KCl and fitted onto the antenna stump. After 4 hours at RT micropipettes were removed, brains were dissected, fixed, digested with collagenase, and washed as described above. Brains were stained with an antibody against TKRP (1:20,000) and the marker Alexa Fluor 488 Phalloidin (0.5%) and DAPI (1:20,000) in PBT with 1% NGS for 3 (*H. axyridis*) or 5 (*P. ephippiata*) days at 4°C. Neurobiotin was visualized with Cy3-conjugated streptavidin (1:200) and Lom-TK II was visualized with GAR-Cy5 (1:300) in PBT with 1% NGS for 2 (*H. axyridis*) or 4 (*P. ephippiata*) days at 4°C. Brains were embedded as described above.

Data processing

Fluorescence was analyzed with a confocal laser scanning microscope (Leica TCS SP5, Bensheim, Germany). The following object lenses were used: 10x oil objective (HC PL APO CS 10x/0.40 IMM, working distance: 360 µm; Leica), 20x oil objective (HCX PL APO lambda blue 20x/0.70 Imm UV, working distance: 260 µm; Leica); 40x oil objective (HCX PL APO lambda blue 40x/1.25 Oil UV, working distance: 100 µm; Leica) und 63x glycerol objective (HCX PL APO 63x/1.30 Glyc 21°C CS working distance: 0.26 mm; Leica). Specimens were scanned with a resolution of 1024 x 1024 pixels, a line average of 2-3, speed of 200 Hz, a digital zoom of 1-3 and z-steps varying from 0.5 to 5 µm.

Image segmentation, reconstruction, and visualization

Confocal image stacks were analyzed with AMIRA 5.2 - 5.6 (FEI, Hillsboro, OR, USA). For segmentation and reconstruction, we referred to Kurylas et al. [98]. In short, image stacks were edited in the "Segmentation Editor" of AMIRA. After labelling several sections in all three spatial directions (anterior to posterior, left to right and dorsal to ventral) of the neuropils / glomeruli,

labeled segments were wrapped to gain a voxel-based 3-D model, which was then transformed (via "SurfaceGen") into a polygonal surface model. A standard color code from Brandt et al. [137]. was used. Volume data was obtained using the function "MaterialStatistics", volume date for neuropils from *T. castaneum* and *Aethina tumida* were obtained from Dreyer et al. [37] and Kollmann et al. [39]. For image generation and final figure arrangements, snapshots were taken in AMIRA and subsequently processed by using global image adjustments (for example contrast and brightness optimization) in Corel Draw 13 (Corel Corporation, Ottawa, Ontario, CA).

Determination of the number of glomeruli

To obtain the number of glomeruli for selected species, individual glomeruli within the AL were reconstructed as described above. Due to the large amount of different species, only one AL per species was further investigated. Reconstructions were obtained from the most pronounced and well-defined labeling for each species (labeling with phalloidin, with an antibody against TKRP / synapsin, and/or backfills with neurobiotin). To accelerate the analysis to a reasonable time expense, we reconstructed the glomeruli that were clearly distinguishable and calculated the total number from the average volume of the glomeruli and the volume of the respective AL. The careful calculation included in addition the extraglomerular space and the core area in the center of the AL. From the 63 investigated species, we determined the glomeruli number of 30 species. 5 of the 30 species possess numerous, small glomeruli, similar to the microglomeruli of Acrididae [21, 48]. In case of microglomeruli we reconstructed 25 glomeruli before extrapolation of the total number of glomeruli. In the remaining 25 species, we reconstructed about 90% (11 species), 70 to 80% (6 species) or 30 to 70% (8 species) of the glomeruli before extrapolation. Data for from *T. castaneum* and *Aethina tumida* were obtained from Dreyer et al. [37], Kollmann et al. [39] and Dippel et al. [38].

Acknowledgements

We thank Dr. Agricola (University of Jena, Germany) for kindly providing the *Locusta migratoria* Tachykinin II antibodyand Dr. Buchner (University of Würzburg, Germany) for the supply of the *Drosophila melanogaster* Synapsin I antibody. We thank the various persons who supplied us with the different beetle species (as listed in the Materials and Methods) and that helped to collect beetles, in particular Joss von Hadeln, Dr. Keram Pfeiffer, Dr. Sabine Dietrich, and Dr. Kathrin Schuster (all University of Marburg, Germany). We furthermore tank Dr. Martin Brändle (University of Marburg, Germany) for helping in identification of certain species. We also want to thank Martina Kern for expert technical assistance and Carolin Knoll and Constanze Wendlandt for assistance in dissection of some beetle species.

References

1. Crowson RA. The biology of the Coleoptera. London: Academic Press; 1981.

2. Grimaldi D, Engel MS. Evolution of the insects. Cambridge: Cambridge University Press; 2005.

3. Kukalova-Peck J, Beutel RG. Is the Carboniferous† *Adiphlebia lacoana* really the "oldest beetle"? Critical reassessment and description of a new Permian beetle family. European Journal of Entomology. 2012;109(4):633-645.

4. Smith DM, Marcot JD. The fossil record and macroevolutionary history of the beetles. Proceedings of the Royal Society of London B: Biological Sciences. 2015;282:20150060.

5. Erwin TL. The taxon pulse: a general pattern of lineage radiation and extinction among carabid beetles. In: Ball GE, editors. Taxonomy, Phylogeny and

Zoogeography of Beetles and Ants. Dordrecht: W Junk; 1985. pp. 437–472

6. Davis ALV, Scholtz CH, Philips TK. Historical biogeography of scarabaeine dung beetles. Journal of Biogeography. 2002;29(9):1217-1256.

7. Farrell BD. "Inordinate Fondness" Explained: Why Are There So Many Beetles?. Science. 1998;281(5376):555-559.

8. Hunt T, Bergsten J, Levkanicova Z, Papadopoulou A, John OS, Wild R et al. A comprehensive phylogeny of beetles reveals the evolutionary origins of a superradiation. Science. 2007;318(5858):1913-1916.

9. Hauser F, Cazzamali G, Williamson M, Park Y, Li B, Tanaka Y et al. A genome-wide inventory of neurohormone GPCRs in the red flour beetle *Tribolium castaneum*. Frontiers in Neuroendocrinology. 2008;29(1):142-165.

10. Chapman AD. Number of Living Species in Australia and the World. Report for the Australian Biological Resources Study, Canberra, Australia. September; 2009.

11. Foottit RG, Adler PH. Insect biodiversity: science and society. Chichester: John Wiley & Sons; 2009

12. Visser JH. Host Odor Perception in Phytophagous Insects. Annual Review of Entomology. 1986;31(1):121–144.

13. Tegoni M. Campanacci V. Cambillau C. Structural aspects of sexual attraction and chemical communication in insects. Trends in Biochemical Sciences. 2004;29(5):257–264.

14. Dahanukar A, Hallem EA, Carlson JR. Insect chemoreception. Current Opinion in Neurobiology. 2005;15(4):423-430.

15. Whiteman NK, Pierce NE. Delicious poison: genetics of *Drosophila* host plant preference. Trends in Ecology and Evolution. 2008;23(9):473–478.

16. de Bruyne M, Smart R, Zammit E, Warr CG. Functional and molecular evolution of olfactory neurons and receptors for aliphatic esters across the *Drosophila* genus. Journal of Comparative Physiology A. 2010;196(2):97-109.

17. Leal WS. Odorant Reception in Insects: Roles of Receptors, Binding Proteins, and Degrading Enzymes. Annual Review of Entomology. 2013;58:373–391.

18. Steinbrecht RA. Structure and function of insect olfactory sensilla. In: Bock GR, Cardew G, editors. Ciba Foundation Symposium 200-Olfaction in Mosquito-Host Interactions. Chichester: John Wiley & Sons; 1996. pp. 158-183.

19. de Bruyne M, Warr CG. Molecular and cellular organization of insect chemosensory neurons. Bioessays. 2006;28(1):23-34.

20. Hansson BS, Stensmyr M. Evolution of Insect Olfaction. Neuron. 2011;72(5):698-711.

21. Schachtner J, Schmidt M, Homberg U. Organization and evolutionary trends of primary olfactory brain centers in Tetraconata (Crustacea+Hexapoda). Arthropod Structure and Development. 2005;34(3):257–299.

22. Vosshall LB. Olfaction in drosophila. Current opinion in neurobiology. 2000;10(4):498-503.

23. Mysore K, Subramanian KA, Sarasij RC, Suresh A, Shyamala BV, VijayRaghavan K, et al. Caste and sex specific olfactory glomerular organization and brain architecture in two sympatric ant species, *Camponotus sericeus* and *Camponotus compressus* (Fabricius, 1798). Arthropod Structure and Development. 2009;38(6):485-497

24. Kuebler LS, Kelber C, Kleineidam CJ. Distinct antennal lobe phenotypes in the leaf-cutting ant (*Atta vollenweideri*). Journal of Comparative Neurology. 2010;518(3):352-365.

25. Stopfer M, Bhagavan S, Smith BH, Laurent G. Impaired odour discrimination on desynchronization of odour-encoding neural assemblies. Nature. 1997;390(6655):70–74.

26. Sachse S, Galizia CG. Role of Inhibition for Temporal and Spatial Odor Representation in Olfactory Output Neurons: A Calcium Imaging Study. Journal of Neurophysiology. 2002;87(2):1106–1117.

27. Shang Y, Claridge-Chang A, Sjulson L, Pypaert M, Miesenböck G. Excitatory Local Circuits and Their Implications for Olfactory Processing in the Fly Antennal Lobe. Cell. 2007;128(3):601–612.

28. Silbering AF, Galizia CG. Processing of Odor Mixtures in the *Drosophila* Antennal Lobe Reveals both Global Inhibition and Glomerulus-Specific Interactions. The Journal of Neuroscience. 2007;27(44):11966–11977.

29. Okada R, Awasaki T, Ito K. Gamma-aminobutyric acid (GABA)-mediated neural connections in the *Drosophila* antennal lobe. Journal of Comparative Neurology. 2009;514(1):74–91.

30. Olsen SR, Bhandawat V, Wilson RI. Divisive normalization in olfactory population codes. Neuron. 2010;66(2):287–299.

31. Nagel KI, Hong EJ, Wilson RI. Synaptic and circuit mechanisms promoting broadband transmission of olfactory stimulus dynamics. Nature Neuroscience. 2015;18(1):56–65.

32. Carlsson M, Diesner M, Schachtner J, Nässel D. Multiple neuropeptides in the *Drosophila* antennal lobe suggest complex modulatory circuits. The Journal of Comparative Neurology. 2010;518(16):3359-3380.

33. Binzer M, Heuer CM, Kollmann M, Kahnt J, Hauser F, Grimmelikhuijzen C et al. Neuropeptidome of *Tribolium castaneum* antennal lobes and mushroom bodies. Journal of Comparative Neurology. 2013;522(2):337-357.

34. Siju KP, Reifenrath A, Scheiblich H, Neupert S, Predel R, Hansson, et al. Neuropeptides in the antennal lobe of the yellow fever mosquito, *Aedes aegypti*. Journal of Comparative Neurology. 2014;522(3):592–608.

35. Galizia CG, Rössler W. Parallel Olfactory Systems in Insects: Anatomy and Function. Annual Review of Entomology. 2010;55(1):399-420.

36. Hu J-H, Wang Z-Y, Sun F. Anatomical organization of antennal-lobe glomeruli in males and females of the scarab beetle *Holotrichia diomphalia* (Coleoptera: Melolonthidae). Arthropod Structure and Development. 2011;40(5):420-428.

37. Dreyer D, Vitt H, Dippel S, Goetz B, El Jundi B, Kollmann M, et al. 3D Standard Brain of the Red Flour Beetle *Tribolium castaneum*: A Tool to Study Metamorphic Development and Adult Plasticity. Frontiers in Systems Neuroscience. 2010;4:3-3.

38. Dippel S, Kollmann M, Oberhofer G, Montino A, Knoll C, Krala M, et al. Morphological and Transcriptomic Analysis of a Beetle Chemosensory System Reveals a Gnathal Olfactory Center. eLife. *submitted*.

39. Kollmann M, Rupenthal AL, Neumann P, Huetteroth W, Schachtner J. Novel antennal lobe substructures revealed in the small hive beetle *Aethina tumida*. Cell and tissue research. 2016;363(3):679-692.

40. Strausfeld NJ. Crustacean–insect relationships: the use of brain characters to derive phylogeny amongst segmented

invertebrates. Brain, Behavior and Evolution. 1998;52(4-5):186–206.

41. Strausfeld NJ, Hansen L, Li Y, Gomez RS, Ito K. Evolution, discovery, and interpretations of arthropod mushroom bodies. Learning and Memory. 1998;5(1):11–37.

42. Strausfeld NJ, Sinakevitch I, Brown SM, Farris SM. Ground plan of the insect mushroom body: functional and evolutionary implications. Journal of Comparative Neurology. 2009;513(3):265–291.

43. Lin C, Strausfeld NJ. Visual Inputs to the Mushroom Body Calyces of the Whirligig Beetle, Dineutus sublineatus: Modality Switching in an Insect. Journal of Comparative Neurology. 2013;520(12):2562–2574.

44. Panov A.A. Not All Dytiscidae Have Poorly Developed Mushroom Bodies: The Enigma of Cybister lateralimarginalis. Entomological Review. 2013;94(5):654–663.

45. Ignell R, Root CM, Birse RT, Wang JW, Nassel DR, Winther ÅME. Presynaptic peptidergic modulation of olfactory receptor neurons in *Drosophila*. Proceedings of the National Academy of Sciences. 2009;106(31):13070-13075.

46. Winther ÅME, Acebes A, Ferrús A. Tachykinin-related peptides modulate odor perception and locomotor activity in *Drosophila*. Molecular and Cellular Neurosciences. 2006;31(3):399-406.

47. Winther ÅME, Ignell R. Local peptidergic signaling in the antennal lobe shapes olfactory behavior. Fly. 2010;4(2):167–171.

48. Ignell R, Anton S, Hansson BS. The Antennal Lobe of Orthoptera – Anatomy and Evolution. Brain, Behavior and Evolution. 2001;57(1):1-17.

49. Bense U. Longhorn beetles: illustrated key to the Cerambycidae an Vesperidae of Europe. Margraf Verlag: Weikersheim; 1995.

50. Zahradník J. Käfer Mittel- und Nordwesteuropas. Ein Bestimmungsbuch für Biologen und Naturfreunde. Hamburg: Parey; 1985.

51. Horn H, Kögel F. Käfer: Unsere häufigsten und schönsten Arten entdecken, bestimmen, beobachten. München: BLV Verlagsgesellschaft GmbH; 2000.

52. Gerstmeier R. Käfer: Extra: Haus- und Vorratsschädlinge, 2nd edition. Stuttgart: Kosmos; 2003.

53. Zahradník J. Illustriertes Lexikon der Käfer. Eggolsheim: Dörffler; 2010.

54. Kim MY, Lee BH, Kwon D, Kang H, Nässel DR. Distribution of tachykinin-related neuropeptide in the developing central nervous system of the moth *Spodoptera litur* a. Cell and Tissue Research. 1998;294(2):351-365.

55. Fusca D, Schachtner J, Kloppenburg P. Colocalization of allatotropin and tachykinin-related peptides with classical transmitters in physiologically distinct subtypes of olfactory local interneurons in the cockroach (*Periplaneta americana*). Journal of Comparative Neurology. 2015;523(10):1569-1586.

56. Nässel DR. Functional roles of neuropeptides in the insect central nervous system. Naturwissenschaften. 2000;87(10):439–449.

57. Ignell R. Monoamines and neuropeptides in antennal lobe interneurons of the desert locust, *Schistocerca gregaria* : an immunocytochemical study. Cell and Tissue Research. 2001;306(1):143-156.

58. Wilson RI. Early olfactory processing in *Drosophila*: mechanisms and principles.

Annual Review of Neuroscience. 2013;36:217-241.

59. Galizia CG. Olfactory coding in the insect brain: data and conjectures. European Journal of Neuroscience. 2014;39(11):1784-1795.

60. Hildebrand JG, Shepherd GM. MECHANISMS OF OLFACTORY DISCRIMINATION: Converging Evidence for Common Principles Across Phyla. Annual Review Neuroscience. 1997;20(1):595-631.

61. Ache B, Young J. Olfaction: Diverse Species, Conserved Principles. Neuron. 2005;48(3):417-430.

62. Chase R, Tolloczko B. Synaptic glomeruli in the olfactory system of a snail, *Achatina fulica*. Cell Tissue Res. 1986;246(3):567-573.

63. Wertz A, Rössler W, Obermayer M, Bickmeyer U. Functional neuroanatomy of the rhinophore of *Aplysia punctata*. Frontiers in Zoology. 2006;3(6):1-11

64. Mißbach C, Harzsch S, Hansson BS. New insights into an ancient insect nose: the olfactory pathway of *Lepismachilis y-signata* (Archaeognatha: Machilidae). Arthropod Structure and Development. 2011;40(4):317-333.

65. Kollmann M, Huetteroth W, Schachtner J. Brain organization in Collembola (springtails). Arthropod structure & development. 2011;40(4):304-316.

66. Rebora M, Dell'Otto A, Rybak J, Piersanti S, Gaino E, Hansson BS. The antennal lobe of *Libellula depressa* (Odonata, Libellulidae). Zoology. 2013;116(4):205–214.

67. Kristoffersen L. Hansson BS, Anderbrant O, Larsson MC. Aglomerular hemipteran antennal lobes – basic neuroanatomy of a small nose. Chemical Senses. 2008;33(9):771–778.

68. Stacconi MVR, Hansson BS, Rybak J, Romani R. Comparative Neuroanatomy of the Antennal Lobes of 2 Homopteran Species. Chemical Senses. 2014;39(4):283-294.

69. Crespo JG, Vickers NJ. Antennal lobe organization in the slender pigeon louse, *Columbicola columbae* (Phthiraptera: Ischnocera). Arthropod Structure and Development. 2012;41(3):227-230.

70. Dacks AM, Christensen TA, Hildebrand JG. Phylogeny of a serotonin-immunoreactive neuron in the primary olfactory center of the insect brain. The Journal of Comparative Neurology. 2006;498(6):727-746.

71. Stocker RF. *Drosophila* as a focus in olfactory research: mapping of olfactory sensilla by fine structure, odor specificity, odorant receptor expression, and central connectivity. Microscopy Research and Technique. 2001;55(5):284–296.

72. Keller A, Vosshall LB. Decoding olfaction in Drosophila. Current Opinion in Neurobiology. 2003;13(1):103-110.

73. Vosshall LB, Stocker RF. Molecular architecture of smell and taste in *Drosophila*. Annual Review of Neuroscience. 2007;30:505–533.

74. Koontz MA, Schneider D. Sexual dimorphism in neuronal projections from the antennae of silk moths (*Bombyx mori, Antherea polyphemus*) and the gypsy moth (*Lymantria dispar*). Cell and Tissue Research. 1987;249(1):39–50.

75. Homberg U, Christensen TA, Hildebrand JG. Structure and function of the deutocerebrum in insects. Annual Review of Entomology. 1989;34(1):477-501.

76. Fonta C, Sun XJ, Masson C. Morphology and spatial distribution of bee antennal lobe interneurones responsive to odours. Chemical Senses. 1993;18(2):101-119.

77. Anton S, Homberg U. Antennal lobe structure. In Insect olfaction. Springer Berlin: Heidelberg; 1999.

78. Galizia CG, McIlwrath SL, Menzel R. A digital three-dimensional atlas of the honeybee antennal lobe based on optical sections acquired by confocal microscopy. Cell and Tissue Research. 1999;295(3):383-394.

79. Hummel T, Zipursky SL. Afferent Induction of Olfactory Glomeruli Requires N-Cadherin. Neuron. 2004;42(1):77-88.

80. Tanaka NK, Endo K, Ito K. Organization of antennal lobe-associated neurons in adult *Drosophila melanogaster* brain. Journal of Comparative Neurology. 2012;520(18):4067–4130.

81. Sinakevitch IT, Smith AN, Locatelli F, Huerta R, Bazhenov M, Smith BH. *Apis mellifera* octopamine receptor 1 (AmOA1) expression in antennal lobe networks of the honey bee *(Apis mellifera*) and fruit fly (*Drosophila melanogaster*). Frontiers in Systems Neuroscience. 2013;7(10):70.

82. Kirschner S, Kleineidam CJ, Zube C, Rybak J, Grünewald B, Rössler W. Dual olfactory pathway in the honeybee, *Apis mellifera*. The Journal of Comparative Neurology. 2006;499(6):933-952.

83. Kreissl S, Strasser C, Galizia CG. Allatostatin immunoreactivity in the honeybee brain. Journal of Comparative Neurology. 2010;518(9):1391-1417.

84. Yoritsune A, Aonuma H. The anatomical pathways for antennal sensory information in the central nervous system of the cricket, *Gryllus bimaculatus*. Invertebrate Neuroscience. 2012;12(2):103-117.

85. Stocker RF, Lienhard MC, Borst A, Fischbach KF. Neuronal architecture of the antennal lobe in *Drosophila melanogaster*. Cell and Tissue Research. 1990;262(1):9-34.

86. Stocker RF. The organization of the chemosensory system in *Drosophila melanogaster*: a review. Cell and Tissue Research. 1994;275(1):3-26.

87. Shanbhag SR, Singh K, Singh RN. Fine structure and primary sensory projections of sensilla located in the sacculus of the antennae of *Drosophila melanogaster*. Cell and Tissue Research. 1995;282(2):237–249.

88. Ernst KD, Boeckh J. A neuroanatomical study on the organization of the central antennal pathways in insects. III. Neuroanatomical characterization of physiologically defined response types of deutocerebral neurons in *Periplaneta americana.* Cell and Tissue Research. 1983;229(1)1-22.

89. Nishikawa M, Yokohari F, Ishibashi T. Central projections of the antennal cold receptor neurons and hygroreceptor neurons of the cockroach *Periplaneta americana*. Journal of Comparative Neurology. 1995;361(1):165–176.

90. Pareto A. Die zentrale Verteilung der Fühlerafferenz bei Arbeiterinnen der Honigbiene, *Apis mellifera* L. Zeitschrift für Zellforschung. 1972;131(1):109–146.

91. Mobbs PG. The brain of the honeybee *Apis mellifera*. I. The connections and spatial organization of the mushroom bodies. Philosophical Transactions of the Royal Society B. 1982;298(1091):309–354.

92. Arnold G, Masson C, Budharugsa S. Comparative study of the antennal lobes and their afferent pathway in the worker bee and the drone (*Apis mellifera*). Cell and Tissue Research. 1985;242(3): 593-605.

93. Brockmann A, Brückner D. Projection pattern of poreplate sensory neurones in honey bee worker, *Apis mellifera* L. (Hymenoptera: Apidae). International Journal of Insect Morphology and Embryology. 1995;24(4):405-411.

94. Farris SM, Roberts NS. Coevolution of generalist feeding ecologies and gyrencephalic mushroom bodies in insects. Proceedings of the National Academy of Sciences of USA. 2005;102(48):17394-17399.

95. Menzel R. Searching for the memory trace in a mini-brain, the honeybee. Learning and Memory. 2001;8(2):53-62.

96. Heisenberg M. Mushroom body memoir: from maps to models. Nature Reviews Neuroscience. 2003;4(4):266-275.

97. Davis RL. Olfactory Learning. Neuron. 2004;44(1):31-48.

98. Kurylas AE, Rohlfing T, Krofczik S, Jenett A, Homberg U. Standardized atlas of the brain of the desert locust, *Schistocerca gregaria*. Cell and Tissue Research. 2008;333(1):125–145.

99. Hanström B. Inkretorische Organe, Sinnesorgane, und Nervensystemen des Kopfes einiger niederer Insektenordnungen. Stockholm: Amyvist & Wiksells; 1940. 18:1–265.

100. Rebora M, Piersanti S, Gaino E. The antennal sensilla of the adult of *Libellula depressa* (Odonata: Libellulidae). Arthropod structure and development. 2008;37(6):504-510.

101. Piersanti S, Frati F, Conti E, Gaino E, Rebora M, Salerno G. First evidence of the use of olfaction in Odonata behaviour. Journal of Insect Physiology. 2014;62:26–31.

102. Smith VS. Avian louse phylogeny (Phthiraptera: Ischnocera): a cladistic study based on morphology. Zoological Journal of the Linnean Society. 2001;132(1):81–144.

103. Rakshpal R. On the behavior of pigeon louse, *Columbicola columbae* Linn. (Mallophaga). Parasitology. 1959;49(1-2):232–241.

104. Åbjörnsson K, Wagner B, Axelsson A, Bjerselius R, Olsén K. Responses of *Acilius sulcatus* (Coleoptera: Dytiscidae) to chemical cues from perch (Perca fluviatilis). Oecologia. 1997;111(2):166-171.

105. Herbst C, Baier B, Tolasch T, Steidle JLM. Demonstration of sex pheromones in the predaceous diving beetle *Rhantus suturalis* (MacLeay 1825) (Dytiscidae). Chemoecology. 2011;21(1):19-23.

106. Hodgson ES. A Study of Chemoreception in Aqueous and Gas Phases. The Biological Bulletin. 1953;105(1):115.

107. Jourdan H, Barbier R, Bernard J, Ferran A. Antennal sensilla and sexual dimorphism of the adult ladybird beetle *Semiadalia undecimnotata* Schn. (Coleoptera: Coccinellidae). International Journal of Insect Morphology and Embryology. 1995;24(3):307-322.

108. Hatfield LD, Frazier JL, Coons LB. Antennal sensilla of the pecan weevil, *Curculio caryae* (Horn) (Coleoptera:Curculionidae). International Journal of Insect Morphology and Embryology. 1976;5(4-5):279-287.

109. Smith CM, Frazier JL, Coons LB, Knight WE. Antennal sensilla of the clover head weevil *Hypera meles* (F.) (Coleoptera: Curculionidae). International Journal of Insect Morphology and Embryology. 1976;5(6):349-55.

110. Fischer DC, Kogan M. Chemoreceptors of adult Mexican bean beetles: External morphology and role in food preference. Entomologia Experimentalis et Applicata. 1986;40(1):3-12.

111. Iperti G. Perspectives d'utilisation rationnelle des coccinelles aphidiphages dans la protection des cultures. 90 ème Congrès des Soc. Savantes, Nice. 1965;2:544-555.

112. Gencer NS, Kumral NA, Sivritepe HO, Seidi M, Susurluk H, Senturk B. Olfactory

response of the ladybird beetle *Stethorus gilvifrons* to two preys and herbivore-induced plant volatiles. Phytoparasitica. 2009;37(3):217-224.

113. Gencer NS, Kumral NA, Sivritepe HO, Seidi M, Susurluk H, Senturk B. Olfactory response of the ladybird beetle *Stethorus gilvifrons* to two preys and herbivore-induced plant volatiles. Phytoparasitica, 2009;37(3):217-224.

114. Al Abassi S, Birkett M, Pettersson J, Pickett J, Woodcock C. Ladybird beetle odour identified and found to be responsible for attraction between adults. Cellular and Molecular Life Sciences (CMLS). 1998;54(8):876-879.

115. Al Abassi S, Birkett MA, Pettersson J, Pickett JA, Wadhams LJ, Woodcock CM. Response of the Seven-spot Ladybird to an Aphid Alarm Pheromone and an Alarm Pheromone Inhibitor is Mediated by Paired Olfactory Cells. Journal of Chemical Ecology. 2000;26(7):1765-1771.

116. Schaller M, Nentwig W. Olfactory orientation of the seven-spot ladybird beetle, *Coccinella septempunctata* (Coleoptera: Coccinellidae): attraction of adults to plants and conspecific females. European Journal of Entomology. 2000;97(2):155-159.

117. Sarkar A, Mukherjee A, Barik A. Olfactory responses of *Epilachna dodecastigma* (Coleoptera: Coccinellidae) to long-chain fatty acids from Momordica charantia leaves. Arthropod-Plant Interactions. 2013;7(3):339-348.

118. Hansson BS, Grosmaitre X, Anton S, Njagi PGN. Physiological responses and central nervous projections of antennal olfactory receptor neurons in the adult desert locust, *Schistocerca gregaria* (Orthoptera: Acrididae). Journal of Comparative Physiology A. 1996;179(2) 157-167.

119. Ochieng SA, Hallberg E, Hansson BS. Fine structure and distribution of antennal sensilla of the desert locust, *Schistocerca gregaria* (Orthoptera: Acrididae). Cell and tissue research. 1998;291(3):525-536.

120. Hansson BS. Responses of olfactory receptor neurones to behaviourally important odours in gregarious and solitarious desert locust, *Schistocerca gregaria*. Physiological Entomology. 1999;24(1):28-36.

121. Kollmann M, Minoli S, Bonhomme J, Homberg U, Schachtner J, Tagu D, et al. Revisiting the anatomy of the central nervous system of a hemimetabolous model insect species: the pea aphid *Acyrthosiphon pisum*. Cell and tissue research. 2011;343(2):343-355.

122. Schwalb H. Beiträge zur Biologie der einheimischen Lampyriden *Lampyris noctiluca* Geoffr. und *Phausis splendidula* Lec. und experimentelle Analyse ihres Beutefang- und Sexualverhaltens. Zoologische Jahrbücher: Abteilung für Systematik, Geographie und Biologie der Tiere. 1961;88:399–550.

123. Iwasaki M, Itoh T, Yokohari F, Tominaga Y. Identification of Antennal Hygroreceptive Sensillum and Other Sensilla of the Firefly, *Luciola cruciata*. Zoological Science. 1995;12(6):725-732.

124. Lau TFS, Ohba N, Arikawa K, Meyer-Rochow VB. Sexual dimorphism in the compound eye of *Rhagophthalmus ohbai* (Coleoptera: Rhagophthalmidae): II. Physiology and function of the eye of the male. Journal of Asia-Pacific Entomology. 2007;10(1):27-31.

125. Marshall DC. Periodical cicada life-cycle variations, the historical emergence record, and the geographic stability of brood distributions. Annals of the Entomological Society of America. 1002;94(3):386–399.

126. Magro A, Lecompte E, Magné F, Hemptinne J-L, Crouau-Roy B. Phylogeny of ladybirds (Coleoptera: Coccinellidae):

are the subfamilies monophyletic? Molecular Phylogenetics and Evolution. 2010;54(3):833–848.

127. Maddison D, Baker MD, Ober KA. Phylogeny of carabid beetles as inferred from 18S ribosomal DNA (Coleoptera: Carabidae). Systematic Entomology. 1999;24(2):103–138.

128. Raupach MJ, Astrin JJ, Hannig K, Peters MK, Stoeckle MY, Wägele JW. Molecular species identification of Central European ground beetles (Coleoptera: Carabidae) using nuclear rDNA expansion segments and DNA barcodes. Frontiers in Zoology. 2010;7(26):1-15.

129. Gómez-Zurita J, Hunt T, Vogler AP. Multilocus ribosomal RNA phylogeny of the leaf beetles (Chrysomelidae). Cladistics. 2008;24(1):34-50.

130. Browne J, Scholtz CH. A phylogeny of the families of Scarabaeoidea (Coleoptera). Systematic Entomology. 1999;24(1):51-84.

131. Browne J, Scholtz CH. Evolution of the scarab hindwing articulation and wing base: a contribution toward the phylogeny of the Scarabaeidae (Scarabaeoidea: Coleoptera). Systematic Entomology. 1998;23(4):307-326.

132. Ahrens D, Schwarzer J, Vogler A. The evolution of scarab beetles tracks the sequential rise of angiosperms and mammals. Proceedings of the Royal Society B: Biological Sciences. 2014;281(1791):20141470-20141470.

133. Utz S, Huetteroth W, Vömel M, Schachtner J. Mas-allatotropin in the developing antennal lobe of the sphinx moth *Manduca sexta*: Distribution, time course, developmental regulation and colocalization with other neuropeptides. Developmental Neurobiology. 2008;68(1):123-142.

134. Heuer CM, Kollmann M, Binzer M, Schachtner J. Neuropeptides in insect mushroom bodies. Arthropod Structure and Development. 2012;41(3):199-226.

135. Klagges BR, Heimbeck G, Godenschwege TA, Hofbauer A, Pflugfelder GO, Reifegerste R, et al. Invertebrate synapsins: a single gene codes for several isoforms in *Drosophila*. Journal of Neuroscience. 1996; 16(10):3154–3165.

136. Veenstra JA, Lau GW, Agricola HJ, Petzel DH. Immunohistochemical localization of regulatory peptides in the midgut of the female mosquito *Aedes aegypti*. Histochemistry and Cell Biology. 1995;104(5):337-347.

137. Brandt R, Rohlfing T, Rybak J, Krofczik S, Maye A, Westerhoff M et al. Three-dimensional average-shape atlas of the honeybee brain and its applications. The Journal of Comparative Neurology. 2005;492(1):1-19.

Digital supplements

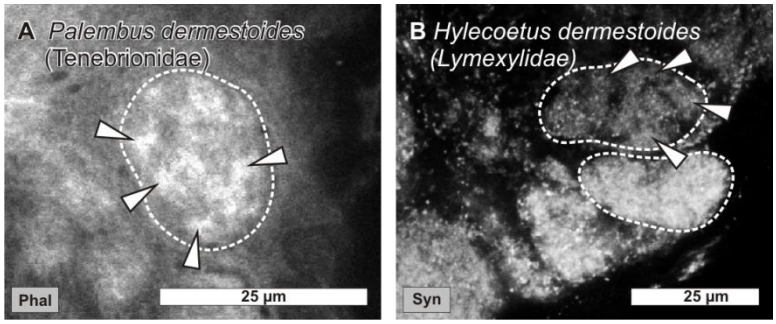

Digital supplement Fig. S1: AL glomeruli of two beetle species from two families as examples for inhomogeneous staining that we interpret as indications for glomerular substructures (arrowheads) stained with phalloidin (Phal) and synapsin (Syn).

Additional digital supplements

The following four figures are not included in the submitted manuscript, they are only part of this theses.

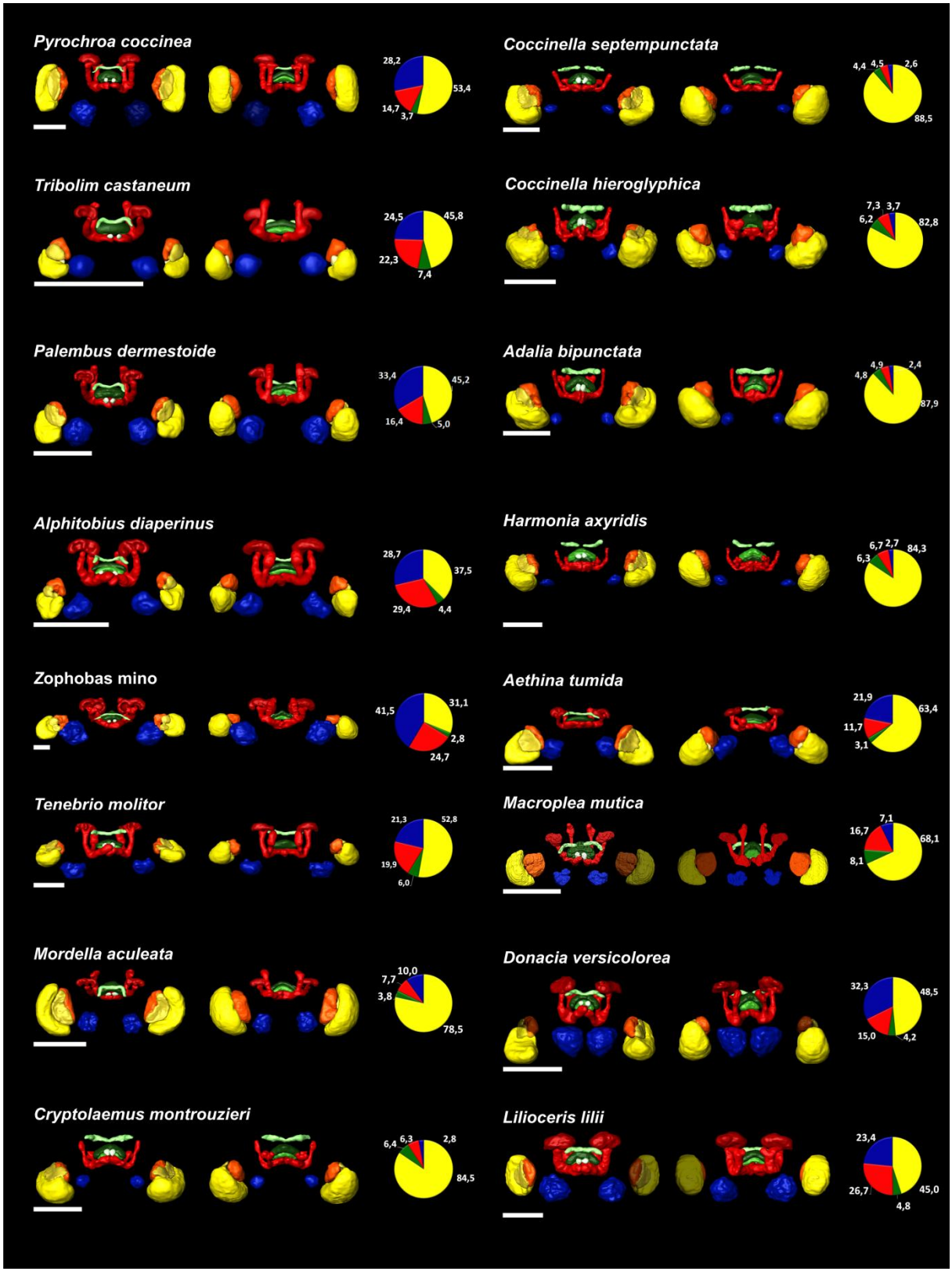

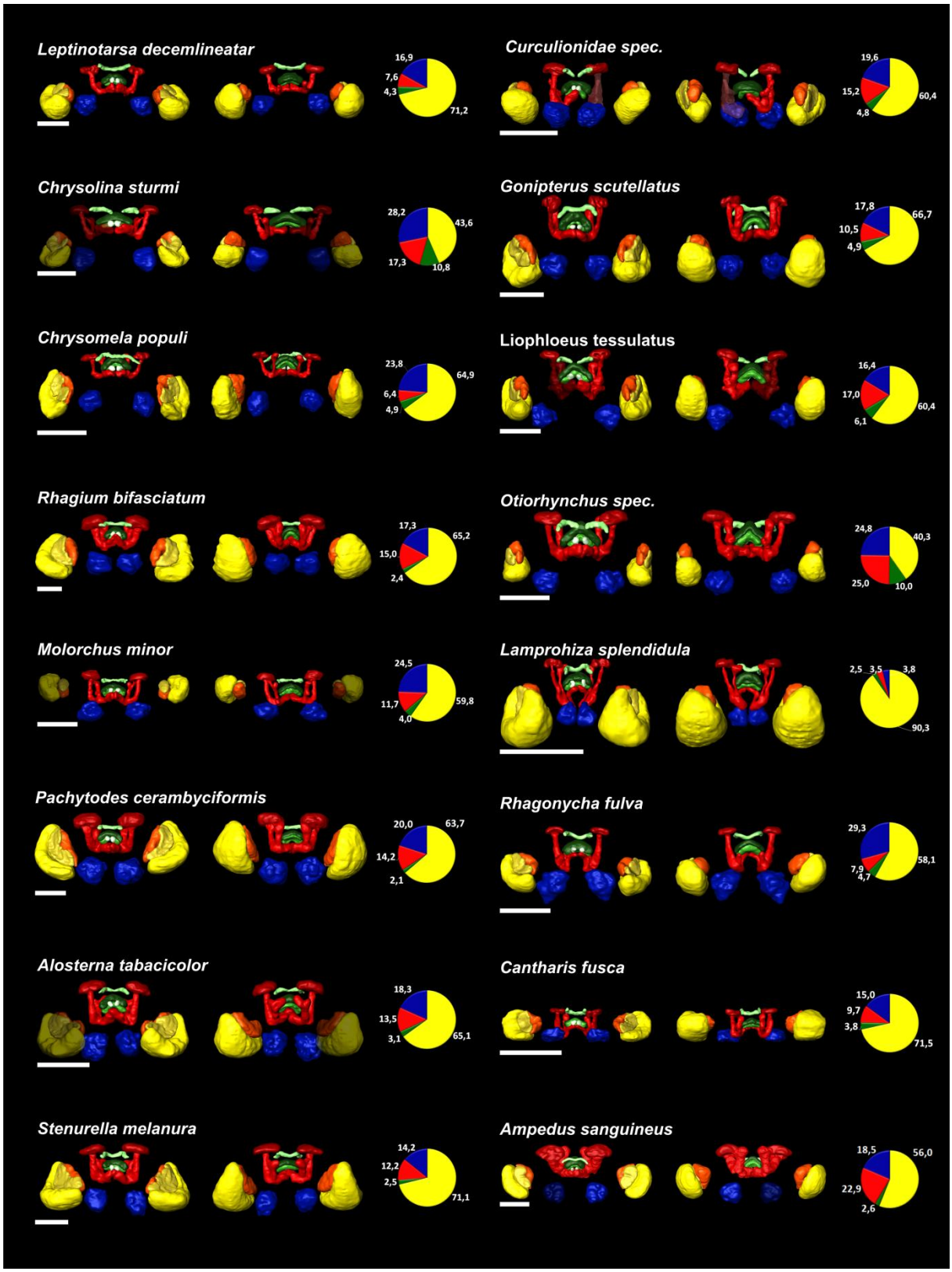
Leptinotarsa decemlineatar
16,9
7,6
4,3
71,2
Curculionidae spec.
19,6
15,2
4,8
60,4
Chrysolina sturmi
28,2
43,6
17,3
10,8
Gonipterus scutellatus
17,8
66,7
10,5
4,9
Chrysomela populi
23,8
64,9
6,4
4,9
Liophloeus tessulatus
16,4
17,0
6,1
60,4
Rhagium bifasciatum
17,3
65,2
15,0
2,4
Otiorhynchus spec.
24,8
40,3
25,0
10,0
Molorchus minor
24,5
11,7
4,0
59,8
Lamprohiza splendidula
2,5
3,5
3,8
90,3
Pachytodes cerambyciformis
20,0
63,7
14,2
2,1
Rhagonycha fulva
29,3
7,9
4,7
58,1
Alosterna tabacicolor
18,3
13,5
3,1
65,1
Cantharis fusca
15,0
9,7
3,8
71,5
Stenurella melanura
14,2
12,2
2,5
71,1
Ampedus sanguineus
18,5
56,0
22,9
2,6

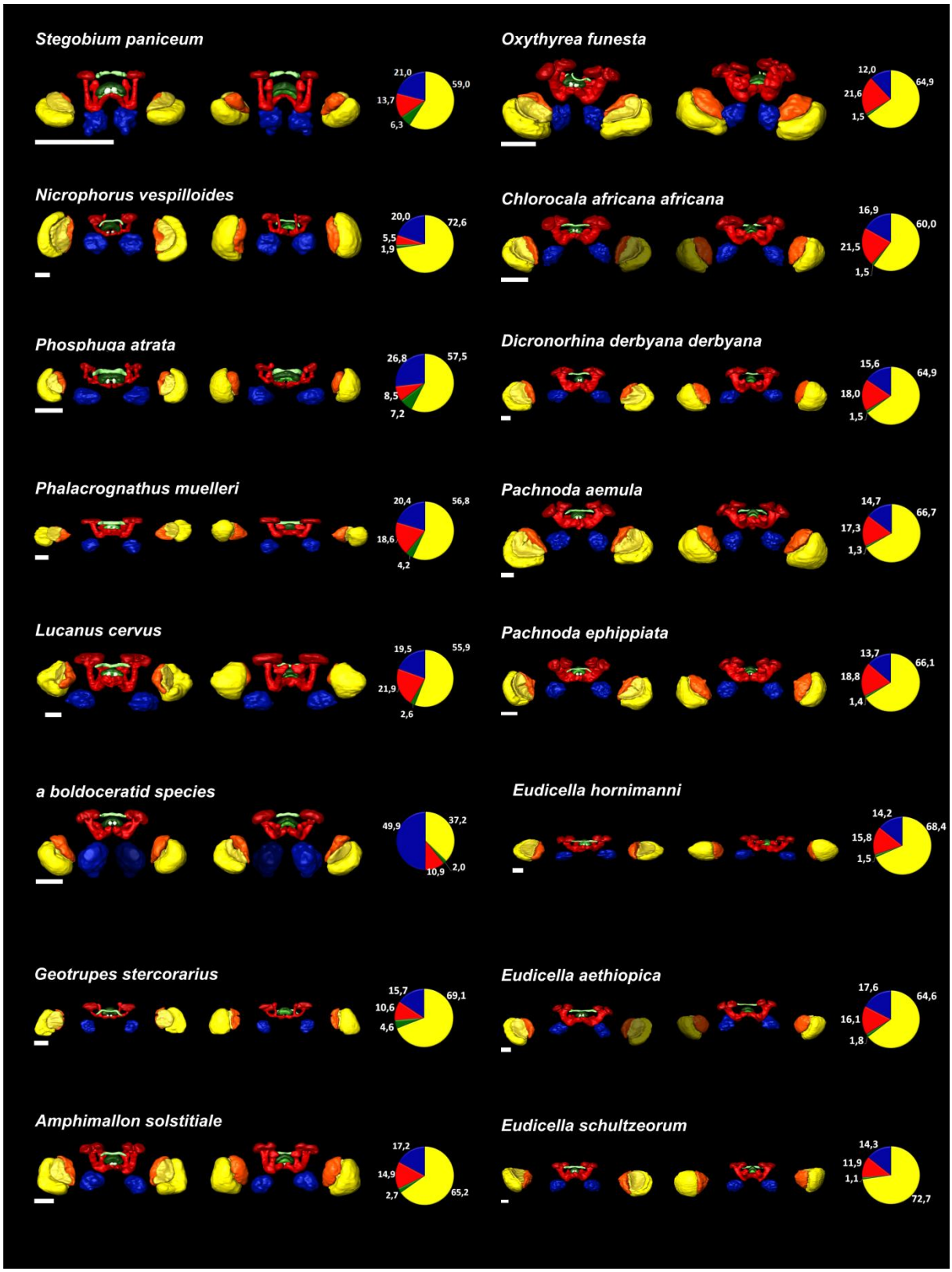
Stegobium paniceum
21,0
59,0
13,7
6,3
Oxythyrea funesta
12,0
64,9
21,6
1,5
Nicrophorus vespilloides
20,0
72,6
5,5
1,9
Chlorocala africana africana
16,9
60,0
21,5
1,5
Phosphuga atrata
26,8
57,5
8,5
7,2
Dicronorhina derbyana derbyana
15,6
64,9
18,0
1,5
Phalacrognathus muelleri
20,4
56,8
18,6
4,2
Pachnoda aemula
14,7
66,7
17,3
1,3
Lucanus cervus
19,5
55,9
21,9
2,6
Pachnoda ephippiata
13,7
66,1
18,8
1,4
a boldoceratid species
49,9
37,2
10,9
2,0
Eudicella hornimanni
14,2
68,4
15,8
1,5
Geotrupes stercorarius
15,7
69,1
10,6
4,6
Eudicella aethiopica
17,6
64,6
16,1
1,8
Amphimallon solstitiale
17,2
14,9
2,7
65,2
Eudicella schultzeorum
14,3
11,9
1,1
72,7

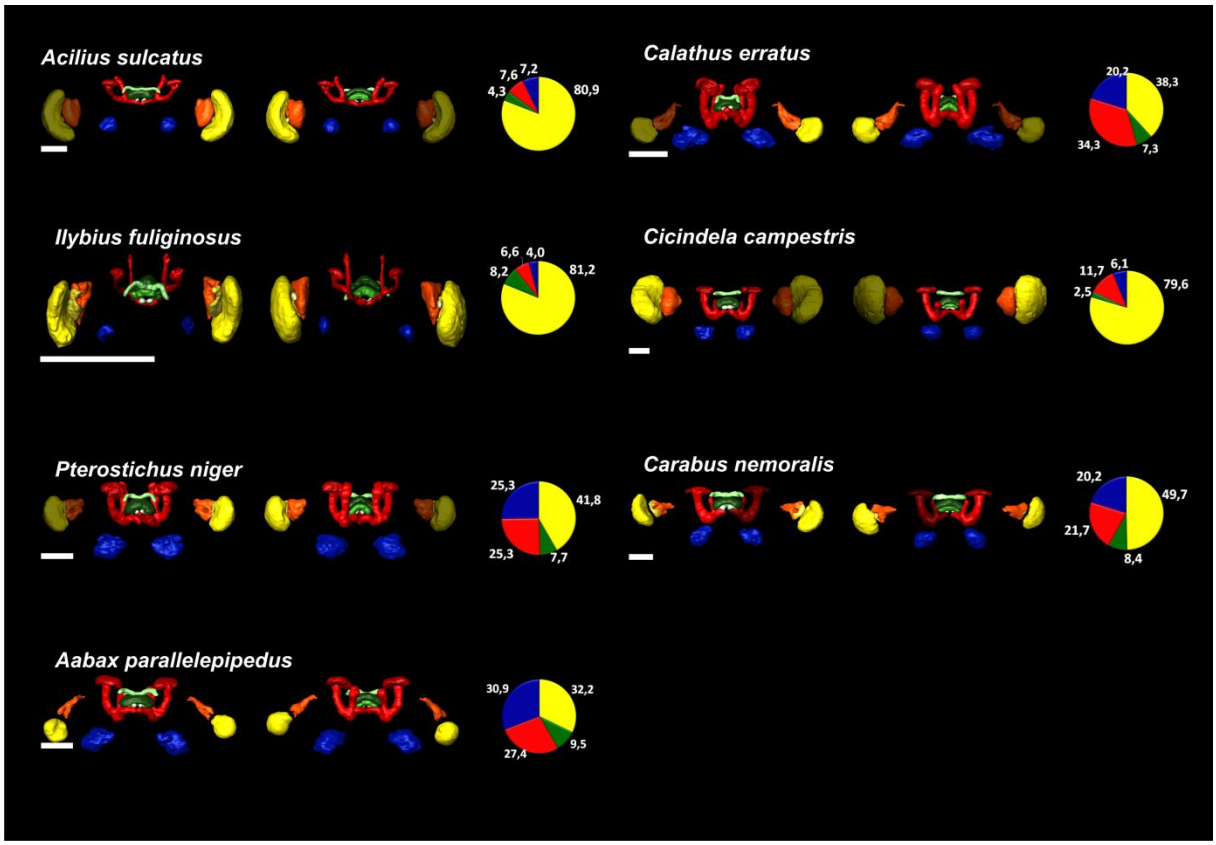

Fig. Additional supplement 1-4. 3D reconstructions of 55 different Copeoptera brains (anterior [left] and posterior [right] view). The neuropils were reconstructed with the AMIRA tools SurfaceGen and SurfaceView. In some cases, neuropils had been damaged durig preperation, so that the reconstruction of the neuropile was not possible. These neuropils are displayd as trasparent mirror images of the respectiv neuropils of the other brain hemisphere. The color code of the labeled neuropils is consistent with Brandt et al. (2005). Pie charts represent the relative volume of the four main neuropil groops (antennal lobes: blue, optic lobes: yellow, central complex; green, and mushroom bodies: red; numerical values in percent). The order of the species is acording to the order in Fig. 1 in the manuscripte. Reconstruction from *Aethina tumida* are obtained from Kollmann et al. (2016), reconstruction for *Tribolium castaneum* are obtained from Dreyer et al. (2010). Scalebar: 200 µm each.

Brandt R, Rohlfing T, Rybak J, Krofczik S, Maye A, Westerhoff M, et al. Threedimensional average-shape atlas of the honeybee brain and its applications. Journal of Comparative Neurology. 2005;492(1):1-19.

Dreyer D, Vitt H, Dippel S, Goetz B, El Jundi B, Kollmann M, et al. 3D Standard Brain of the Red Flour Beetle *Tribolium castaneum*: A Tool to Study Metamorphic Development and Adult Plasticity. Frontiers in Systems Neuroscience. 2010;4:3.

Kollmann M, Rupenthal AL, Neumann P, Huetteroth W, Schachtner J. Novel antennal lobe substructures revealed in the small hive beetle *Aethina tumida*. Cell and tissue research. 2016;363(3):679-692.

Final summary, discussion, and outlook

In this thesis I investigated the brains - particularly the olfactory system - of the Coleoptera, the largest order in the animal kingdom. Therefore the brain of one species - the red four beetle *Tribolium castaneum* - had been investigated in high detail. Brains of larval and adult *T. castaneum* had been 3D reconstructed and its olfactory pathway had been examined closely. We analyzed the distribution of its neuropeptides within its primary and higher olfactory integration centers and analyzed one peptide family in detail. Additionally, we investigated the neuroarchitecture of the antennal lobe (AL) - the primary olfactory integration center of insects - of 62 further coleopteran species and we examined the distribution of eight neuropeptide families within the mushroom body (MB) - a higher olfactory integration center of insects - in 24 insect species.

The brain of *T. castaneum* and its olfactory pathway

The brain of the first instar larva of *T. castaneum* is comparable to the larval brains of many Holometabola and similar to the larval brain of the closely related *Tenebrio molitor* (Koniszewski et al., 2016). It displays a central body (CB) consisting only of an upper unit, while in comparison to several other insects (e.g. *T. molitor*, Wegerhoff and Breidbach, 1992) the protocerebral bridge is already well developed. The MB is divided in the calyx and pedunculus including its lobes. The optic lobes (OL) consist only of the anlagen, and the AL is consisting of glomeruli, as described for the larval brains of numerous species. The larval AL contains about 40-50 glomeruli. The adult brain presents the same principal organization as known from countless insects, showing all four major neuropils (AL, OL, MB, and CB-complex) and its subcompartments (Dreyer et al., 2010). Also the lobula plate (LoP) of the OL has been identified, so far only documented reliably for Ephemeroptera, Trichoptera, Coleoptera, Lepidoptera, and Diptera (Strausfeld, 2005). They have very large AL (compared to the brain), indicating a high relevance of olfaction for this species.

At first glance, the olfactory pathway of *T. castaneum* is pretty similar to that of most other insects (Schachtner et al., 2005). The antenna and the mouthparts are equipped with a broad set of different chemoreceptive sensilla whose sensory neurons express several various receptor types. The AL is composed of many (about 70 - 90) spherical glomeruli and we found projections from the AL to two higher brain areas of the olfactory pathway, namely the MB and the lateral horn (LH) (Dippel et al., submitted). However, we found four features in the olfactory pathway of the adult *T. castaneum*, never described for other Coleoptera, respectively other insects before.

1) From several insects (especially Diptera) it is known, that the mouthparts are the main gustatory organs and the antenna are more important for olfaction (Dahanukar et al., 2001; Bohbot et al., 2007; Vermehren-Schmaedick et al., 2011). However, in *T. castaneum* antennae and mouthparts express similar numbers and levels of gustatory receptors (GR) and the mouthparts express a relatively high number and level of olfactory receptors (OR) (Dippel et al., submitted). This may reflect the beetles' ground-dwelling behavior and indicates, that the animal is also gathering a lot of gustatory information with its antenna.

2) In *T. castaneum* the olfactory information, gathered by the mouthparts, is projected via forwarding neurons terminating in an unpaired, medial located, glomerular organized structure (containing about 30 - 40 glomeruli), we called "gnathal olfactory center" (GOC) and which is labeled in the transgenic line, partially labeling the cells expressing the general olfactory co-receptor Orco (odorant receptor co-receptor) (Dippel et al., submitted). This has never been observed in insects before.

3) Neurons forwarding chemoreceptive information from the mouthparts also terminate within a structure near the AL, a structure we identified as lobus glomerulatus (LG) (Dippel et al., submitted). A neuropil previously described only in hemimetabolous insects and was considered lacking in Holometabola (Ernst et al., 1977; Ignell et al., 2000; Schachtner et al., 2005; Hofer et al., 2005; Farris, 2008).

4) In insects the processed information from the AL is usually forwarded to the MB and LH via a varying number of antennal lobe tracts (ALT) (usually between 1 and 3, depending on the insect order) (Schachtner et al., 2005; Galizia and Rössler, 2010). For Coleoptera it had been assumed, that they possess 1 or 2 of this ALT, but we could demonstrate for the first time, that beetles (at least *T. castaneum*) have 3 ALT (Dippel et al., submitted), typical for most Holometabola (Galizia and Rössler, 2010).

While point 1) could be explained by the adaptation to the ground-dwelling lifestyle of the animal and point 3) and 4) are observations known from other insects, point 2) is a unique observation for insects. It is interesting, that the mouthparts of *T. castaneum* express 49 OR, from which 28 are significantly enriched (compared to the body) and that the GOC consists of 30 - 40 glomeruli. This constellation resembles the central dogma of insect olfaction known from the AL (Jefferis 2005; Vosshall and Stocker 2007; Kaupp 2010). Indicating, that all olfactory sensory neurons (OSN) of the mouthparts, expressing the same OR, projecting into the same of the 30 - 40 glomeruli of the GOC. Also interesting is, that 27 of the 49 OR expressed in the mouthparts, are exclusively expressed in the mouthparts. Showing that the mouthparts percept and process (partly) different olfactory information than the antenna (Dippel et al., submitted).

However, without further detailed analyses of this structure, its full contribution to the entire olfactory pathway remains unknown. Electrophysiological analyses or calcium imaging in combination with olfactory and / or gustatory stimuli might give more insight into its function and dye injection into the GOC would reveal connections to higher brain areas (e.g. into the MB and / or LH). While backfills of single sensilla of the mouthparts and / or transgenic lines labeling single OR (expressed at the mouthparts), respectively antibody against this OR (capable of staining the axons) might support the theory of the central dogma for the GOC.

Altogether, our findings strongly indicate, that during evolution different taxa developed different strategies to adapt to their ecological niches. This also shows that it is somehow critical to only rely on data of one - or a small group of - model organism and that it is often beneficial to analyze different organisms.

Neuropeptides within the olfactory pathway of insects

We investigated the neuropeptides present in the AL and MB of adult *T. castaneum* by using mass spectrometry. By additionally using antibodies against eight different neuropeptide families, we were able to visualize the distribution of these neuropeptide families within the brain in detail (Binzer et al., 2014).

Mass spectrometry showed that different neuronal tissues have their respective tissue-specific, reproducible fingerprints. Such fingerprints are an important base for further analyses of endo- and exogenous influences (like age, starvation, isolation, mating, or other conditions) on the distribution / concentration of certain neuropeptides. Mass spectrometry will be a vital tool, allowing us to observe such potential changes in the peptide concentration very fast and for a huge number of individuals. This will lead to a better understanding of the modulatory effects and functions of neuropeptides in *T. castaneum* and other insects.

By analyzing immunohistological stainings of the MB of 24 different insect species against eight neuropeptide families, we demonstrated, that the distribution of a neuropeptide familie seems to be conserved within some insect orders, but it differs in most cases, especially between different orders. This vast variation of the distribution of neuropeptides within the MB might reflect its

broad range of function, observed in different insects (Heuer et al., 2012).

To better understand how this neuropeptide family distributions are conserved within an order, it would be interesting to investigate this distributions in detail in different families of a single order, containing animals with similar and with different lifestyles, and animals with close and far phylogenetic relation. Therefore the immunohistological stainings against the neuropeptide tachykinin related peptide (TKRP) within 63 different coleopteran species (Kollmann et al., submitted) is a valuable set of data to answer this question of conserved neuropeptide family distribution in MB and other neuropils within insects.

We additionally investigated the neuropeptide family ACP (adipokinetic hormone /corazonin-related peptide) and its receptor within *T. castaneum* in detail and compared them with the structurally similar adipokinetic hormone (AKH) and corazonins (CRZ) and their receptors. AKH and CRZ are both known to be related to physiological activity and metabolic stress (Gade et al., 1997; Staubli et al., 2002; Veenstra, 1989; Tawfik et al., 1999; Zitnan et al., 2007). The function of ACP is yet not fully understood, it seems to have no impact onto the growth, reproduction and mortality of adult animals, but it is highly expressed in late embryos and early larvae, suggesting a function in early larval development or physiology (Hansen et al., 2010).

Despite the structural similarity of the three neuropeptides and their respective receptors, AKH doesn't activates the CRZ receptor and CRZ doesn't activates the AKH receptor, in addition ACP neither activates the AKH receptor nor CRZ receptor (Staubli et al., 2002; Cazzamali et al., 2002; Belmont et al., 2006). Furthermore, the ACP receptor cannot be activated by AKH or by CRZ (Hansen et al., 2010).

Structural similarities of these three neuropeptide families and their receptors and their appearance in the phylogenetic tree of Insecta (respectively Tetraconata) leads to the conclusion, that they result from gene duplication from a single precursor (Hansen et al., 2010).

The AL of Coleoptera and the architecture of their glomeruli

By performing immunohistological stainings with an antibody against the neuropeptide TKRP and against the synaptic vesicle protein synapsin, respectively against the F-actin marker phalloidin we investigated the AL of 63 different coleopteran species. Apart from the round and spherical glomeruli, as known from most insects like Diptera, Hymenoptera, or Lepidoptera (Schachtner et al., 2005), seven of the investigated Coleoptera show AL consisted of many, small glomeruli like the microglomeruli of Acrididae (Ignell et al., 2001; Schachtner et al., 2005). In additional 26 species, the glomeruli exhibit substructures within their glomeruli, in 15 of these species, this substructures are TKRP-ir. Further 12 species showed some kind of indications for (non TKRP-ir) substructures. The number of glomeruli per AL range from 50 to 150 and 400 to 1,000 for AL with microglomeruli. Microglomeruli as well as substructured glomeruli can be observed in different families (not closely related to each other), therefore we speculate that this traits have evolved independently several times (Kollmann et al., submitted).

A microglomerular organization of an coleopteran AL has been reported for diving beetles by some authors (e.g. Hanström, 1940; Panov, 2013), while other authors described the AL of diving beetles as aglomerular (e.g. Strausfeld et al., 1998; Strausfeld et al., 2009). However, our own observations clearly show the existence of microglomeruli within the AL in the two examined diving beetles. Additionally, our data also show microglomerular organized AL in the five investigated lady bug species, which AL had never been described before (Kollmann et al., submitted).

The glomeruli substructures of Coleoptera are subcompartments within the glomerulus. Each glomerulus contains several of these substructures which are typically distributed evenly within the glomerulus. In *Aethina tumida* we could demonstrate, that the number of substructures per glomerulus correlates linear with the volume of the glomerulus (Kollmann et al., 2016). The substructures are identifiable by stainings against TKRP (which labels only the substructures of the

glomerulus), or by their intense labeling with the synapsin antibody, respectively with phalloidin.

Antennal backfills in one species showed, that the substructures are avoid of OSN innervations. In species with TKRP-ir substructures, the antennal nerve never presents a TKRP immunoreactivity, while the TKRP-ir substructures were always innervated by TKRP-ir local interneurons (LN).

Substructured glomeruli had also been observed in insects like *Apis mellifera*, *Drosophila melanogaster* and some lepidopteran species (e.g. Koontz and Schneider, 1987; Sinakevitch et al., 2013), but there only a single substructure per glomerulus (avoided by OSN and innervated by LN) can be found. In *Gryllus bimaculatus*, there are multiple substructures per glomerulus, but they are innervated by OSN (Ignell et al., 2001). Showing that the findings in Coleoptera are unique for insects.

The substructured glomeruli might either originate from the fusion of single glomeruli (each with a single substructure per glomerulus as known from *A. mellifera*, *D. melanogaster* and some lepidopteran species; e.g. Koontz and Schneider, 1987; Sinakevitch et al., 2013) or they result from a compartmentalization within such a glomerulus.

Resume

In this thesis, the brain architecture and especially the olfactory system of Coleoptera had been investigated for the first time in high detail. We revealed new insights of the olfactory (respectively chemoreceptive) pathway of these animals, which are the largest insect order and the most successful animals on earth. The findings will help to establish *T. castaneum* as the first coleopteran model organism for insect neuroscience and in particular for insect olfaction.

References

Belmont M., Cazzamali G., Williamson M., Hauser F., Grimmelikhuijzen C.J.P. (2006) Identification of four evolutionarily related G protein-coupled receptors from the malaria mosquito *Anopheles gambiae*. Biochemical and Biophysical Research Communications. 344:160–165.

Binzer M., Heuer C.M., Kollmann M., Kahnt J., Hauser F., Grimmelikhuijzen C.J., Schachtner J. (2014) Neuropeptidome of *Tribolium castaneum* antennal lobes and mushroom bodies. Journal of Comparative Neurology. 522:337–357.

Bohbot J., Pitts R.J., Kwon H-W., Rützler M., Robertson H.M., Zwiebel L.J. (2007) Molecular characterization of the Aedes aegypti odorant receptor gene family. Insect Molecular Biology. 16:525–537.

Cazzamali G., Hauser F., Kobberup S., Williamson M., Grimmelikhuijzen C.J.P. (2003) Molecular identification of a *Drosophila* G protein-coupled receptor specific for crustacean cardioactive peptide. Biochemical and Biophysical Research Communications. 303:146–152.

Dahanukar A., Foster K., van der Goes van Naters W.M., Carlson J.R. (2001) A Gr receptor is required for response to the sugar trehalose in taste neurons of *Drosophila*. Nature Neuroscience 4:1182–1186.

Dippel S., Kollmann M., Oberhofer G., Montino A., Knoll C., Krala M., Rexer K-H., Frank S., Kumpf R., Schachtner .J, Wimmer E.A. (submittet in eLife, 12.05.2016) Morphological and Transcriptomic Analysis of a Beetle Chemosensory System Reveals a Gnathal Olfactory Center. Re-Sumbitted in eLife.

Dreyer D., Vitt H., Dippel S., Goetz B., El Jundi B., Kollmann M., Huetteroth W., Schachtner J. (2010) 3D Standard Brain of the Red Flour Beetle *Tribolium castaneum*: A Tool to Study Metamorphic Development and Adult Plasticity. Frontiers in Systems Neuroscience. 4,3.

Ernst D.K.D., Boeckh J., Boeckh V. (1977) A neuroanatomical study on the organization of the central antennal pathways in insects. Cell and Tissue Research. 176:285–308.

Farris S.M. (2008) Tritocerebral tract input to the insect mushroom bodies. Arthropod Structure and Development. 37:492–503.

Gade G., Hoffmann K.H., Spring J.H. (1997) Hormonal regulation in insects: facts, gaps, and

future directions. Physiological Reviews. 77:963–1032.

Galizia C.G., Rössler W. (2010) Parallel Olfactory Systems in Insects: Anatomy and Function. Annual Review of Entomology. 55:399–420.

Hansen K.K., Stafflinger E., Schneider M., Hauser F., Cazzamali G., Williamson M., Kollmann M., Schachtner J., Grimmelikhuijzen C.J. (2010) Discovery of a novel insect neuropeptide signaling system, closely related to the insect adipokinetic hormone and corazonin hormonal systems. The Journal of Biological Chemistry. 285:10736-10747.

Hanström B. (1940) Inkretorische Organe, Sinnesorgane, und Nervensystemen des Kopfes einiger niederer Insektenordnungen. Kungl/Svenska Vetenskapsakademiens Handlingar. 18:8.

Heuer C.M., Kollmann M., Binzer M., Schachtner J. (2012). Neuropeptides in insect mushroom bodies. Arthropod Structure and Development. 41:199-226.

Hofer S., Dircksen H., Tollbäck P., Homberg U. (2005) Novel insect orcokinins: Characterization and neuronal distribution in the brains of selected dicondylian insects. Journal of Comparative Neurology. 490:57–71.

Ignell R., Anton S., Hansson S.B. (2001) The Antennal Lobe of Orthoptera – Anatomy and Evolution. Brain, Behavior and Evolutio. 57:1–17.

Ignell R., Anton S., Hansson S.B. (2001) The Antennal Lobe of Orthoptera – Anatomy and Evolution. Brain, Behavior and Evolution. 57:1–17.

Jefferis G.S.X.E. (2005) Insect Olfaction: A Map of Smell in the Brain. Current Biolegy. 15:R668–R670

Kaupp U.B. (2010) Olfactory signalling in vertebrates and insects: differences and commonalities. Nature Reviews Neuroscience. 11:188-200.

Kollmann M., Rupenthal A.L., Neumann P., Huetteroth W., Schachtner J. (2016). Novel antennal lobe substructures revealed in the small hive beetle *Aethina tumida*. Cell and tissue research. 363:679-692.

Kollmann M., Schmidt R., Heuer C.M., Schachtner J. (sumbitted in Plos Biology, 2016.05.19) Variations on a theme: antennal lobe architecture across Coleoptera. Sumbitted in PLOS Biology.

Koniszewski N.D.B., Kollmann M., Bigham M., Farnworth M., He B., Büscher M., Hütteroth W., Binzer M., Schachtner J., Bucher G. (2016). The insect central complex as model for heterochronic brain development—background, concepts, and tools. Development genes and evolution. 226:209-219.

Koontz M.A., Schneider D. (1987) Sexual dimorphism in neuronal projections from the antennae of silk moths (*Bombyx mori, Antherea polyphemus*) and the gypsy moth (*Lymantria dispar*). Cell and Tissue Research. 249:39–50.

Panov A.A. (2013) Not All Dytiscidae Have Poorly Developed Mushroom Bodies: The Enigma of Cybister lateralimarginalis. Entomological Review. 94:654–663.

Schachtner J., Schmidt M., Homberg U. (2005) Organization and evolutionary trends of primary olfactory brain centers in Tetraconata (Crustacea+Hexapoda). Arthropod Structure and Development. 34:257–299.

Sinakevitch I.T., Smith A.N., Locatelli F., Huerta R., Bazhenov M., Smith B.H. (2013) *Apis mellifera* octopamine receptor 1 (AmOA1) expression in antennal lobe networks of the honey bee *(Apis mellifera*) and fruit fly (*Drosophila melanogaster*). Frontiers in Systems Neuroscience. 7:70.

Sinakevitch I.T., Smith A.N., Locatelli F., Huerta R., Bazhenov M., Smith B.H. (2013) *Apis mellifera* octopamine receptor 1 (AmOA1) expression in antennal lobe networks of the honey bee *(Apis mellifera*) and fruit fly (*Drosophila melanogaster*). Frontiers in Systems Neuroscience. 7:70.

Staubli F., Jorgensen T.J., Cazzamali G., Williamson M., Lenz C., Sondergaard L., Roepstorff P., Grimmelikhuijzen C.J.P. (2002) Molecular identification of the insect adipokinetic hormone receptors. Proceedings of the National Academy of Sciences of USA. 99:3446-3451.

Strausfeld N.J. (2005). The evolution of crustacean and insect optic lobes and the origins of chiasmata.

Arthropod Structure and Development. 34:235-25610.

Strausfeld N.J., Hansen L., Li Y., Gomez R.S., Ito K. (1998) Evolution, discovery, and interpretations of arthropod mushroom bodies. Learning and Memory. 5:11–37.

Strausfeld N.J., Sinakevitch I., Brown S.M., Farris S.M. (2009) Ground plan of the insect mushroom body: functional and evolutionary implications. Journal of Comparative Neurology. 513:265–291.

Tawfik A.I., Tanaka S., De Loof A., Schoofs L., Baggerman G., Waelkens E., Derua R., Milner Y., Yerushalm, Y., Pener M.P. (1999) Identification of the gregarization-associated dark-pigmentotropin in locusts through an albino mutant. Proceedings of the National Academy of Sciences of USA. 96:7083–7087.

Veenstra J.A. (1989) Isolation and structure of corazonin, a cardioactive peptide from the American cockroach. FEBS Lett. 250:231–234.

Vermehren-Schmaedick A., Scudder C., Timmermans W., Morton D.B. (2011) *Drosophila* gustatory preference behaviors require the atypical soluble guanylyl cyclases. Journal of Comparative Physiology A. 197:717–727.

Vosshall L.B., Stocker R.F. (2007) Molecular architecture of smell and taste in *Drosophila*. Annual Review of Neuroscience. 30:505–533.

Wegerhoff R., Breidbach O. (1992) Structure and development of the larval central complex in a holometabolous insect, the beetle *Tenebrio molitor*. Cell and Tissue Research. 268:341-358.

Zitnan D., Kim Y.J., Zitnanova´ I., Roller L., Adams M.E. (2007) Complex steroid–peptide–receptor cascade controls insect ecdysis. General and Comparative Endocrinology. 153:88–9

Zusammenfassung auf Deutsch

Ziel der Doktorarbeit

Insekten sind die erfolgreichsten Tiere auf der Erde und sie haben einen großen Einfluss auf alle terrestrischen Ökosysteme. Sie haben ebenfalls einen großen Einfluss auf die Menschheit, sei es durch Bestäubung von Agrarpflanzen, Zerstörung von Ernten durch Fraßschäden oder durch Übertragung von Krankheiten auf Menschen und Nutztiere.

Die meisten Insekten nutzen ihr Geruchssystem zur Bewältigung wichtiger Aufgaben wie z. B. dem Finden von Nahrung oder Geschlechtspartnern. Obwohl Käfer zu der diversesten und größten Insektenordnung gehören, wurde bei Käfern dieses wichtige Geruchsystem noch nie im Detail untersucht.

Um das Geruchssystem der Käfer zu erforschen, wurde 1) ein Organismus – der Rotbraune Reismehlkäfer *Tribolim castaneum* – im Detail untersucht und 2) bestimmte neuronale Merkmale des Geruchssystems von zahlreichen Käfern und Insekten untersucht und miteinander verglichen, um dadurch ein breiteres Bild des Geruchssystems der Käfer zu erhalten.

1: Vom Gehirn von *T. castaneum* wurden sowohl von Larven als auch von adulten Tieren 3D-Rekonstruktionen angefertigt. Das Geruchssystem des adulten Tieres wurde umfangreich untersucht. Dies beinhaltete unter anderem A) die Morphologie der Antennen und deren chemorezeptiver Sensillen sowie die Neuroarchitektur der Gehirnareale, welche an der Verarbeitung der Geruchsinformationen beteiligt sind, als auch B) molekulare Daten über das Geruchssystem wie z. B. der Identifikation und Verteilung von olfaktorischen und gustatorischen Rezeptoren. Zusätzlich untersuchten wir die Verteilung von Neuropeptiden im primären olfaktorischen Integrationszentrum – dem Antennallobus (AL) – und einem höheren olfaktorischen Intergrationszentrum – dem Pilzkörper (engl. mushroom body: MB).

2: Der zweite Fokus dieser Doktorarbeit lag auf der Untersuchung bestimmter Merkmale des Geruchssystems in unterschiedlichen Arten. Hierzu wurde A) die Verteilung von acht Neuropeptidfamilien in den MB von insgesamt 24 unterschiedlichen Insektenarten untersucht und miteinander verglichen. Weiterhin wurde B) der AL von insgesamt 63 verschiedenen Käferarten erforscht und miteinander verglichen. Hierbei fiel auf, dass bei vielen der untersuchten Arten die olfaktorischen Glomeruli ungewöhnliche Substrukturierungen aufwiesen, wie sie so noch nie in Insekten oder anderen Tieren beobachtet wurden. In einem weiteren Projekt wurde die Verteilung dieser Substrukturierungen in einer Art genauer untersucht und beobachtet, dass die Zahl der Substrukturierungen linear mit der Größe der Glomeruli korreliert.

Diese Doktorarbeit hat erstmalig detailliert das Geruchssystem von Käfern erforscht und dabei mehrere Charakteristika entdeckt, die so noch nie bei Insekten, bzw. Käfern, beobachtet wurden. Diese Arbeit ist ein fundamentaler Schritt zur Etablierung von *T. castaneum* als ersten Käfer-Modellorganismus in der Neurobiologie, speziell für die Erforschung der Olfaktorik.

Einleitung

Insekten sind die artenreichste und diverseste Klasse im Tierreich. Von den ca. 1,4 Millionen beschriebenen Tierarten weltweit sind ungefähr 1 Millionen Arten Insekten, was ungefähr 70 % aller bekannten Tierarten ausmacht (Chapman, 2009). Sie sind von unverzichtbarer Bedeutung für die Ökologie des Planeten und die Ökonomie der Menschen.

Insekten bilden die Grundlage vieler Nahrungsnetze, sind essenziell für die Bestäubung und Verbreitung unzähliger Pflanzen und wichtig für die Aufarbeitung des Erdreichs (Carpenter,

1928; Majer, 1987; Shurin et al., 2005). Auf die menschliche Gesellschaft haben Insekten zusätzliche Auswirkungen, sowohl positive als auch negative. Insekten stellen einerseits viele bedeutende Güter, wie z.B. Honig, Wachs oder Seide her, sie bestäuben angebaute Lebensmittel, verbessern die Nutzbarkeit von landwirtschaftlich genutzten Böden und leisten (biologische) Schädlingsbekämpfung (Foottit und Adler, 2009). Auf der anderen Seite sind sie für die Verbreitung zahlreicher Krankheiten bei Menschen (http://www.who.int/mediacentre/factsheets/fs387/en/ Zuletzt abgerufen: 23.10.2015) und Nutztieren (Hungerford, 1990) verantwortlich und stellen eine der größten Bedrohungen für die Agrarindustrie dar (Altieri und Nicholls, 2004).

Der Geruchssinn

Die überragende Mehrheit der Insekten nutzt ihren Geruchssinn um sich – speziell über weite Distanzen – zu orientieren. Der Geruchssinn hat für viele Vorgänge im Leben eines Insekts eine nicht wegzudenkende Bedeutung, z. B. um Nahrung, Geschlechtspartner, optimale Eiablageplätze, Unterschlupf oder Ansammlungen von Artgenossen zu finden oder um Prädatoren auszuweichen (Borden, 1985; Visser, 1986; Scrimgeour et al., 1994; Abjörnsson et al., 1997; Tegoni et al., 2004; Dahanuka et al., 2005; Whiteman und Pierce, 2008; De Bruyne et al., 2010; Herbst et al., 2011; Leal, 2013). Bei geringerer Distanz wird er für die intraspezifische Kommunikation sowie zur Evaluation der Qualität von Nahrung, Geschlechtspartnern und Eiablageplätzen genutzt (Laska et al., 1999; Johansson und Jones, 2007; Liu et al., 2008; Whiteman und Pierce, 2008; Yang et al., 2008; Dicke, 2009; Weiss et al., 2011; Stensmyr et al., 2012; Sun et al., 2012; Linz et al., 2013; Paczkowski et al., 2014;

Die Geruchsbahn der Insekten

Der Ausgangspunkt der Geruchsbahn der Insekten sind die olfaktorischen Sensillen auf den Antennen und teilweise auf den Mundwerkzeugen (von Frisch, 1921; Schneider und Kaissling, 1957; Stocker, 2001; Misof et al., 2007; Rebora et al., 2008; Dippel et al., 2015). Olfaktorische Sensillen sind Ausstülpungen der Antennenkutikula und weisen Porenstrukturen auf ihrer Oberfläche auf. Diese Poren münden in den inneren Hohlraum der Sensillen, welche mit hydrophiler Sensillen-Lymphe gefüllt sind und die Dendriten der olfaktorischen Sensorneuronen (OSN) beinhalten, auf deren Oberfläche die olfaktorischen Rezeptoren (OR) liegen (Starausfeld und Lee, 1990; Steinbrech, 1997; Shanbhag et al., 1999).

Damit die in der Luft befindlichen und meist hydrophoben Duftmoleküle die hydrophile Sensillenlymphe überwinden können, um mit den OR zu interagieren, sind Geruchsbindungsproteine (engl. olfactory binding protein: OBP) vonnöten, ihre exakte Funktion ist bisher nicht vollständig verstanden (Laughlin et al., 2008; Hansson und Stensmyr, 2011; Leal, 2013). Vermutlich arbeiten sie als eine Art "Shuttle-System", welches die Duftstoffe an der inneren Mündung der Poren der Sensillen aufnimmt und durch den hydrophoben Raum zur Oberfläche der OSN transportiert. Um eine andauernde Erregung der OR zu vermeiden, befinden sich in der Lymphe Duftstoff-Zersetzungs-Enzyme (engl. odorant-degrading enzymes: ODE), welche die Duftstoffe in der Lymphe abbauen.

Die OR lassen sich in zwei verschiedene Typen von Rezeptoren unterteilen, welche normalerweise zusammen als Dimere auftreten. Der erste Typ umfasst eine Vielzahl von unterschiedlichen, spezifischen, ligandenbindenden OR (häufig als ORx bezeichnet). Der zweite Typ ist ein genereller Rezeptor, wovon es in einer Insektenart üblicherweise nur eine einzelne Version gibt (meist als Duftstoff-Rezeptor-Ko-Rezeptor [engl. odorant receptor co-receptor: Orco] bezeichnet). Der genaue Weg der molekularen Signaltransduktion ist nicht vollständig verstanden (Sato et al., 2008; Smart et al., 2008; Wicher et al., 2008; Ha und Smith, 2009; Martin und Alcorta, 2011; Getahun et al., 2013; Nolte et al., 2013; Stengl und Funk, 2013; Missbach et al., 2014).

Die Signale der OSN gelangen über den Antennalnerv in den Antennallobus (AL), dem ersten Geruchsverarbeitungszentrum im Insektengehirn. Üblicherweise besteht der AL aus ca. 40 bis 80 (teilweise wesentlich mehr) kleinen,

kugeligen Untereinheiten, den Glomeruli (Ignell et al., 2005, Schachtner et al., 2005, Ghaninia et al., 2007; Mysore et al., 2009; Dreyer et al., 2010). Typischerweise verschalten alle OSN, die den gleichen spezifischen OR exprimieren, in denselben Glomerulus. Die Glomeruli selbst entstehen durch die Verschaltung von vier verschiedenen Neuronentypen, den OSN, den lokalen Interneuronen (LN), den Projektionsneuronen (PN) und den Zentrifugalneuronen (engl. centrifugal neurons: CN). Durch eine komplizierte Verschaltung dieser Neuronen untereinander und ein komplexes Set an aktivierenden, hemmenden und modulierenden Neuromediatoren wird das eingehende Signal verarbeitet und über die PN an höhere Hirnareale weitergeleitet (Müller, 1997; Bicker, 1999a,b; Homberg und Müller, 1999; Hansson und Anton, 2000; Homberg, 2002; Nässel, 2002; Carlsson et al., 2010; Neupert et al., 2012; Binzer et al., 2014; Siju et al., 2014, Fusca et al., 2015).

Die PN leiten die verarbeitete Geruchsinformation über die Antennallobus -Trakte (ALT) zu den Pilzkörpern (engl. mushroom bodies: MB) und zum Lateralen Horn (LH). Dies sind höhere, integrative Zentren die eine Vielzahl von Aufgaben erfüllen, von denen hier das Geruchslernen, Geruchserkennen und Geruchsbewerten sowie das Auslösen von bestimmten geruchsassoziierten Verhaltensweisen besonders erwähnenswert sind (de Belle und Heisenberg, 1994; Connolly et al., 1996; Heimbeck et al., 2001; Mcguire et al., 2001; Menzel, 2001; Heisenberg, 2003; Wang et al., 2003; Davis, 2004; Jefferis et al., 2007; Yamagata et al., 2007; Heuer et al., 2012; Strutz et al., 2014).

Die Bedeutung der Käfer

Käfer sind mit Abstand die artenreichste und diverseste Ordnung innerhalb der Insekten und des gesamten Tierreiches. Von den knapp über 1,4 Millionen beschriebenen Tierarten gehören ungefähr 400.000 Arten zur Ordnung der Coleoptera. Beinahe 30 % aller beschriebenen Tierarten sind somit Käfer (Grimaldi und Engel, 2005; Hunt et al., 2007; Hauser et al., 2008). Sie zählen zu den größten agrar- und forstwirtschaftlichen Schädlingen (Perlak et al., 1993; Cox, 1999; Nowak et al., 2001; Myers und Hosking, 2002; Simberloff, 2003; Altieri und Nicholls, 2004; Muirhead et al., 2006; Müller et al., 2008; Foottit und Adler, 2009; Safranyik et al., 2010; Fera, 2012; Stadelmann et al., 2013; Seidl et al., 2014) und trotz ihres immensen ökologischen und ökonomischen Einflusses (Grimaldi und Engel, 2005; Hunt et al., 2007) gibt es unter der Vielzahl von Insekten-Modellorganismen in der Neurobiologie (und speziell in der Olfaktorik) keine Käferart.

***Tribolium castaneum* als Modellorganismus**

Der Rotbraune Reismehlkäfer *T. castaneum* (Herbst, 1797) (Bonneton, 2008) gehört zur weitverbreiteten Familie der Tenebrionidae, in denen die Gattung *Tribolium* einige der bedeutendsten Schädlinge für gelagerte Nahrung beinhaltet (Nakakita, 1982; Angelini und Jockusch, 2008; Angelini et al., 2009).

T. castaneum ist bereits seit einiger Zeit ein Modellorganismus innerhalb der Entwicklungsbiologie (Brown et al., 2009). Es ist die zweite Insektenart, deren Genom vollständig entschlüsselt wurde (Wang et al., 2007; Richards et al., 2008; Kim et al., 2010), weswegen eine Vielzahl an genetischen Methoden an diesem Tier angewendet werden können (Bucher et al., 2002; Tomoyasu und Denell, 2004; Trauner et al., 2009; Schinko et al., 2010; Schinko et al., 2012). Darüber hinaus ist *T. castaneum* sehr einfach zu kultivieren mit geringen Ansprüchen an Nahrung und Platz, einer kurzen Generationszeit und einer hohen Reproduktionsrate. Ferner ist diese Art sehr langlebig, wodurch man an ihr Langzeiteffekte / Langzeitauswirkungen gut untersuchen kann (Bucher, 2009). All diese Gründe machen *T. castaneum* zu einem ausgezeichneten Insekten-Modellorganismus für die Ordnung der Käfer.

Kapitel 1: Das 3D-Standardgehirn des Rotbraunen Reismehlkäfers *Tribolium castaneum*: Ein Werkzeug zur Untersuchung der Entwicklung während der Metamorphose und der Adultplastizität

Originaltitel: 3D Standard Brain of the Red Flour Beetle Tribolium Castaneum: A Tool to Study Metamorphic Development and Adult Plasticity

Für ein besseres Verständnis und als Grundlage für weitere Forschungen an dem Gehirn von *T. castaneum* wurden für beide Geschlechter Standardgehirne erstellt. Hierfür wurden individuelle Gehirne von jeweils 20 frisch adult gehäuteten (A0) weiblichen und männlichen Tieren mit Hilfe der Software AMIRA 3D-rekonstruiert. Dafür war eine immunhistochemische Färbung mit einem Antikörper gegen Synapsin erforderlich. Synapsin ist ein cytoplasmatisches Membranprotein der synaptischen Vesikel, welches für die Verankerung am Cytoskelett sowie für die Verschmelzung mit der Synapsenmembran und damit die Ausschüttung der Neurotransmitter wichtig ist. Der Antikörper gegen Synapsin färbt somit ubiquitär das gesamte Nervensystem (Klagges et al., 1996).

Die 3D-Rekonstruktion basiert auf dem "virtuellen Insektengehirn"-Protokoll (engl. virtual insect brain: VIB) und beinhaltet acht paarige und drei unpaarige Neuropile. Von den optischen Loben (OL) sind die Medulla, Lobula Platte, Lobula und die akzessorische Medulla rekonstruiert. Vom Pilzkörper (engl. mushroom body: MB) sind der Calyx und der Pedunkulus inklusive seiner beiden Loben rekonstruiert. Vom Zentralkomplex (engl. central body complex: CBX) sind die Neuropile der oberen und unteren Einheit des Zentralkörpers, sowie dessen Noduli, als auch die Protocerebralbrücke rekonstruiert. Von den Antennalloben (AL) ist die Gesamtheit aller Glomeruli und der zentrale Bereich des ALs (welcher die sich aufteilenden Nerven des Antennalnervs beinhaltet) rekonstruiert. Die Rekonstruktionen der einzelnen Neuropile beinhalten zusätzlich Volumeninformationen, die einen Größenvergleich der einzelnen Gehirnareale zwischen den Geschlechtern ermöglichen. Jedoch konnte in dem untersuchten Altersstadium (A0) in keinem der rekonstruierten neuronalen Strukturen ein Sexualdimorphismus festgestellt werden.

Zusätzlich wurden von den ca. 70 Glomeruli, die in den AL beider Geschlechter gefunden wurden, acht individuelle Glomeruli charakterisiert und in den AL von je zehn männlichen und weiblichen Tieren 3D-rekonstruiert und volumetrisch vermessen. Die Charakterisierung der acht Glomeruli geschah basierend auf ihrer Position, Form und Lage innerhalb des AL. Diese acht Glomeruli konnten zuverlässig in über 75 % aller untersuchten AL identifiziert werden. Die Volumendaten zeigen, dass in diesem Altersstadium in den untersuchten Glomeruli kein volumenbasierter Sexualdimorphismus vorliegt. Ferner konnte kein Hinweis auf einen makroglomerulären Komplex bzw. sexspezifische Glomeruli gefunden werden. Allerdings ist darauf hinzuweisen, dass in dieser Arbeit die Gehirne von frisch adult gehäuteten Tieren, die noch nicht sexuell ausgereift sind, untersucht wurden. Es ist durchaus möglich, dass sexuell ausgereifte Tiere, einen nachweisbaren volumetrischen Sexualdimorphismus im AL aufweisen. Ferner ist nicht auszuschließen, dass ein Sexualdimorphismus auf anderen Ebenen als dem Neuropilvolumen vorhanden sein könnte (z.B. synaptische Verschalungen oder Neurotransmitter).

Der Vergleich der relativen Volumendaten der Neuropile zwischen unterschiedlichen Insektenarten – von denen ein Standardgehirn vorhanden ist (*Drosophila melanogaster,* Rein et al., 2002; *Apis mellifera*, Brandt et al., 2005; *Schistocerca gregaria,* Kurylas et al., 2008; und *Manduca sexta*, el Jundi et al., 2009) – zeigt, dass *T. castaneum* zum Teil stärkere Abweichungen zu den anderen Arten aufweist. Jedoch ist eine Vergleichbarkeit mit den Volumendaten der anderen Spezies suboptimal, da 1) die Daten meist nur von einem Geschlecht vorhanden sind, 2) Daten nur von einem Altersstadium vorhanden sind oder das Alter nicht bekannt ist oder 3)

potentielle individuelle Erfahrungen der Tiere nicht bekannt sind. Insbesondere ist auffällig, dass von den untersuchten Arten die OL von *T. castaneum* das geringste relative Volumen aufweisen, was vermutlich auf die kleinen Komplexaugen zurückzuführen ist, die aus nur 80 bis 83 Ommatidien pro Auge bestehen (Friedrich et al., 1996). Auf der anderen Seite hat *T. castaneum* von den untersuchten Tieren das größte relative AL-Volumen. Dies lässt vermuten, dass der Geruchssinn für die Käfer von relativ hoher Bedeutung ist, was auch bedingt mit den Beobachtungen bezüglich der Lebensweise der Tiere in Einklang steht. Die relative Größe der AL spiegelt sich auch in dem hohen relativen Volumenwerten der MB wieder, welche besonders dafür bekannt sind, dass sie die höheren Integrationzentren für Gerüche sind (Menzel, 2001; Heisenberg, 2003). Diesbezüglich ist es auch möglich, dass die recht hohe Lebenserwartung von *T. castaneum* (Bucher, 2009) für das große relative Volumen der MB sorgt, wie dies auch von dem Schmetterling *Heliconius charitonius* bekannt ist (Sivinsky, 1989). Die genaue Funktion des CBX ist noch nicht genau bekannt, aber am besten beschrieben ist seine Funktion als sensorisches und motorisches Integrationszentrum (Strauss, 2002; Wessnitzer und Webb, 2006; Homberg, 2008). Erstaunlicherweise zeigt *T. castaneum* von den zu vergleichenden Insekten das größte relative Volumen des Zentralkörpers, was eine höhere komplexe Funktion vermuten lässt. Diesbezüglich wäre es interessant, die relativen Volumendaten anderer Käfer zum Vergleich zu haben, speziell von Tieren, welche andere Lebensweisen aufzeigen (speziell von im Wasser lebenden oder nicht flugfähigen Käfern).

Diese Arbeit liefert ein Standardgehirn für männliche und weibliche Tiere der Art *T. castaneum* und ist damit ein wichtiges Werkzeug zur Erforschung von Adultplastizität und Gehirnentwicklung der Insekten und ein wichtiger Grundstock für weitere Arbeiten, welche sich mit dem Gehirn dieser Art beschäftigen.

Kapitel 2: Der Zentralkomplex der Insekten als Modell für Heterochronie in der Gehirnevolution - Hintergrund, Konzepte und Werkzeuge

Originaltitel: The insect central complex as model for heterochronic brain development - background, concepts, and tools

Obwohl das Gehirn der Insekten meist aus demselben Set von Neuropilen besteht (Schachtner et al., 2005; Strausfeld, 2005; Homberg, 2008; Strausfeld et al., 2009), weist deren Zusammensetzung, Anordnung und Entwicklung innerhalb der Insekten große Variationen auf, was vermutlich auf evolutionäre Anpassungen zurückzuführen ist. Die zellulären und genetischen Mechanismen der Entwicklung der Insektengehirne wurden bisweilen hauptsächlich an *Drosophila melanogaster* untersucht. Welche Prozesse hier aber für die Diversität innerhalb der Insekten verantwortlich sind, ist weitestgehend unbekannt.

In *D. melanogaster* entsteht das gesamte Nervensystem aus unterschiedlichen neuronalen Zelllinien, welche sich aus dem Neuroblasten (den neuronalen Stammzellen) entwickeln und welche sich in Nerven- oder Gliazellen differenzieren können (Skeath und Thor, 2003; Urbach und Technau, 2004; Brody und Odenwald, 2005; Technau et al., 2006; Egger et al., 2008; Hartenstein et al., 2008). Hierbei sind viele Aspekte innerhalb der Klasse der Insekten konserviert (Stollewerk und Simpson, 2005; Wheeler et al. 2005; Biffar und Stollewerk, 2014), jedoch ist wenig über die Homologien der einzelnen Zelllinien zwischen den vielen Insektenhaften bekannt.

Um diese Homologien besser verstehen zu können, wäre es notwendig, einzelne Zellen über ihre Entwicklung hinweg zu untersuchen. Hierbei sollten solche Zellen nicht nur die gleiche Lage/Morphologie aufweisen, sondern auch vergleichbare aktive Transkriptionsfaktoren und Neuromediatoren aufweisen. Für den Inter-Spezies-Vergleich sollte man diesbezüglich nicht mehr von Zelllinien reden, sondern von "homologen Zellen, welche von konservierten Transkriptionsfaktoren reguliert werden".

Auszuwählende Modelorganismen zur Untersuchung der Evolution und Entwicklung der Insektengehirne sollten optimaler Weise Unterschiede in Größe und Architektur ihrer Neuropile aufweisen und gut zugänglich für genetische Modifikationen sein. Diesbezüglich würden die Mittelmeergrille (*Gryllus bimaculatus*), die Fruchtfliege (*D. melanogaster*) und der Rotbraune Reismehlkäfer (*Tribolium castaneum*) geeignete Modelorganismen darstellen.

Der Zentralkomplex (engl. central compex: CX) ist ein Neuropil, welches gut geeignet ist, um die Evolution und Entwicklung der Insektengehirne zu untersuchen. Hervorzuheben ist hier die unterschiedliche Morphologie des CX in einigen Arten (Homberg, 2008) sowie die in vielen Arten beschriebene Heterochronie (unterschiedliche Zeitpunkte der Differenzierung des CX während seiner Entwicklung in unterschiedlichen Insektenarten) (Panov, 1959; Wegerhoff und Breidbach, 1992; Loesel at al., 2002; Boyan und Reichert, 2011; Boyan und Williams, 2011; Ito et al., 2014, Pfeiffer und Homberg, 2014).

Um *T. castaneum* als einen Modelorganismus für die Erforschung der Evolution und Entwicklung des CX zu etablieren, wurde in dieser Arbeit der CX des ersten Larvenstadions (L1) charakterisiert. Durch histochemische Färbungen mit Antikörpern gegen fünf unterschiedliche Neuromediatoren sowie mit Färbungen gegen Synapsen und Färbungen mit Phalloidin, konnte der larvale CX genau beschrieben und mit den korrespondierenden Färbungen adulter Tiere verglichen werden. Basierend auf den histochemischen Färbungen erfolgte eine 3D-Rekonstruktion des L1 Gehirnes.

Mit dem Modellorganismus *T. castaneum* verfügt man über diverse transgene Linien, welche hilfreich sind, um die Evolution und Entwicklung der Insektengehirne zu erforschen. Hierzu zählen die Linie G11410 (Posnien et al., 2011; Binzer et al., 2013), welche die Pilzkörper markiert, die Linie Neuron-Red, welche Neuronen markiert (Posnien et al., 2011), die Linie *Tc-asense*, welche ein Neuroblasten-Marker ist, und die Linie 6XP3, welche Glia markiert. Die letzten beiden Linien wurden in dieser Arbeit mittels immunhistochemischen Färbungen gegen DC0 (labelt selektiv den Pilzkörper; Farris und Strausfeld, 2003) und gegen Repo (labelt selektiv Gliazellen; Halter et al., 1995) verifiziert.

T. castaneum stellt mit seinen zahlreichen Möglichkeiten der genetischen Manipulation, hilfreichen transgenen Linien und seiner heterochronen Einordnung seines CX zwischen *D. melanogaster* und *G. bimaculatus* einen idealen Modellorganismus zur Erforschung der Entwicklung und Evolution des Insektengehirnes und speziell des CX da.

Kapitel 3: Morphologische und transcriptomische Analysen des chemosensitiven Systems eines Käfers zeigen ein olfaktorisches Zentrum im Unterschlundganglion

Originaltitel: Morphological and Transcriptomic Analysis of a Beetle Chemosensory System Reveals a Gnathal Olfactory Center

Die Geruchswahrnehmung der Insekten beginnt auf der Antenne (teilweise auch Mundwerkzeugen). Dort befinden sich in den olfaktorischen Sensillen die olfaktorischen Sensor-Neurone (OSN), welche die olfaktorischen Rezeptoren (OR) exprimieren. Typischerweise treten die OR als Heterodimere auf, bestehend aus einem generellen OR (engl. odorant receptor co-receptor: Orco) in Kombination mit einem spezifischen oder speziellen OR (teilweise als ORx bezeichnet). Der Kontakt vom Duftstoff und OR wird hierbei vermutlich durch Geruchsbindungsproteine (engl. olfactory binding protein: OBP) vermittelt. Die Geruchsinformationen der Antennen werden dann mittels Antennalnerv (AN) zum Antennallobus (AL) – dem primären Geruchsverarbeitungszentrum im Gehirn – weitergeleitet. Der AL besteht aus sphärischen Untereinheiten (den Glomeruli), welche durch einen komplexen Schaltplan verschiedener Neuronentypen untereinander kommunizieren. Auf diese Weise verarbeitet der AL die eingebenden Signale der Antenne und leiten sie weiter zum Pilzkörper (engl. mushroom bodies: MB) und zum Lateralen Horn (LH) (Schachtner et

al., 2005; Laughlin et al., 2008; Vosshall und Hansson, 2011). Dieses Geruchssystem wurde in dieser Arbeit im Käfer *Tribolium castaneum* detailliert untersucht.

Mittels transgener Linien, *Fluoreszenz-in-situ-Hybridisierung* (FISH) und Immunhistochemie gegen Orco konnte gezeigt werden, dass auf den letzten drei Segmenten jeder Antenne insgesamt ca. 725 OSN vorzufinden sind, während auf den restlichen Antennensegmenten keine OSN nachgewiesen werden konnten.

Durch transgene Linien und durch elektronenmikroskopische und immunhistochemische Untersuchungen konnten vier unterschiedliche Typen an Mechanorezeptoren sowie drei Typen an chemorezeptiven Sensillen charakterisiert werden. Diese weisen je nach Typ ein charakteristisches Verteilungsmuster auf den letzten drei Antennensegmenten auf. Insgesamt wurden ca. 150 chemorezeptive Sensillen pro Antenne nachgewiesen.

Basierend auf immunhistochemischen Färbungen gegen das Neuropeptid Tachykinin und gegen das Vesikelprotein Synapsin, konnten je AL ca. 90 Glomeruli identifiziert werden.

Backfills der Antenne markierten den gesamten (ipsilateralen) AL bis auf einen einzelnen Glomerulus, welcher exklusiv durch Backfills der Mundwerkzeuge markiert wird. Die Backfills der Antenne projizieren zusätzlich in das ipsilaterale antennale und motorsensorische Zentrum (engl. antennal mechanosensory and motor center: AMMC) sowie in das Unterschlundganglion (engl. gnathal ganglion: GNG). Backfills der Mundwerkzeuge projizieren im AL ausschließlich in einen (den oben erwähnten) Glomerulus, in den Lobus Glomerulatus (LG), in das primäre gustatorische Zentrum (engl. primary gustatory center: PGC) und in eine unpaarige, glomerulär organisierte Struktur (ca. 30 bis 40 Glomeruli) in GNG, welche wir als olfaktorisches Zentrum des GNG (engl. gnathal olfactory center: GOC) benannten. Diese Region ist auch in der transgenen *Orco*-Gal4/*UAS*-DsRed Linie markiert, welche partiell die OSN labeln. Dies unterstützt die Hypothese, dass das GOC an der Geruchsverarbeitung beteiligt ist.

Ausgehend vom AL konnten wird 3 AL-Trakte (ALT) identifizieren, die zum LH und CA projizieren. Basierend auf histochemischen Färbungen mit den Kernmarker DAPI konnten die Zahl der Kenyon Zellen (engl. Kenyon cells = KC) – welche den MB bilden – auf ca. 2.800 pro MB bestimmt werden.

Durch Gen-Annotation konnte die Menge der exprimierten Gene bestimmt werden, welche an der Chemorezeption von *T. castaneum* beteiligt sind. Diese beinhaltet unter anderem die Gene für ionotropische (Glutamat ähnliche) Rezeptoren (IR), gustatorische Rezeptoren (GR), OR, OBP und Duftstoff-Zersetzungs-Enzyme (engl. odorant-degrading enzymes: ODE). Dies geschah für unterrichtliche Gewebegruppen (Antennen, Kopf ohne Antennen aber mit Mundwerkzeugen, Mundwerkzeuge, Beine und Körper) und beide Geschlechter der Tiere, was einen Vergleich der jeweiligen Expressionslevel ermöglicht.

Im gesamten Geruchssystem von *T. castaneum* (sowohl bei den Daten bezüglich der Morphologie von Antenne und Gehirn als auch bezüglich der Genexpression) konnte kein Sexualdimorphismus festgestellt werden.

Einer der auffälligsten Befunde ist, dass auf den Antennen von *T. castaneum* auffällig viele unterschiedliche GR gefunden worden. Diese GR werden in annähernd derselben Konzentration exprimiert wie auf den Mundwerkzeugen. Zusätzlich weisen auch die Mundwerkzeuge relativ viele OR auf. Von vielen Insekten (vor allem von Dipteren) ist dies anders bekannt. Dort findet man eher eine striktere organotrope Trennung zwischen olfaktorischem und gustatorischem System (Antenne und Mundwerkzeuge) (Dahanukar et al., 2001; Bohbot et al., 2007; Vermehren-Schmaedick et al., 2011). Die weniger strikte Trennung bei *T. castaneum* könnte daher stammen, dass die Lebensweise von *T. castaneum*, sein Verhalten und die Habitate die es bewohnt, dazu führen, dass die Antennen der Tiere häufiger mit potentieller Nahrung in Berührung kommen, als dies beispielsweise bei Dipteren der Fall ist.

Ein weiterer Befund ist die Charakterisierung des GOC, eine Struktur, welche in dieser Form – und der vermuteten geruchsverarbeitenden Funktion – noch nie bei Insekten beschrieben wurde. Ferner ist die Identifikation von drei ALT (statt wie bisher

angenommen nur maximal zwei ALT) ein neuer Befund, der so noch nie bei Käfern entdeckt wurde (Galizia und Rössler, 2010).

Ein zusätzliches Novum ist die Charakterisierung des LG in *T. castaneum*, einem Neuropil, von dem es bisher hieß, dass es ausschließlich in hemimetabolen Insekten zu finden sei (Ernst et al., 1977; Ignell et al., 2000; Schachtner et al., 2005; Hofer et al., 2005; Farris, 2008).

Diese Befunde zeigen, dass bezüglich des Geruchssystems der Insekten, *T. castaneum* ein spannender, ergänzender Modellorganismus zu den bisher etablierten Insekten ist, da er neue und interessante Einblicke in dieses Forschungsfeld bringt.

Kapitel 4: Das Neuropeptidom des Antennallobus und Pilzkörpers von *Tribolium castaneum*

Originaltitel: The neuropeptidome of *Tribolium castaneum* antennal lobes and mushroom bodies

Neuropeptide sind die größte und diverseste Gruppe an Signalmolekülen im Nervensystem von Insekten, was sich zum Teil auch durch ihren komplexeren biologischen Syntheseweg erklären lässt (Nässel, 2002; Predel et al., 2004; Altstein und Nässel, 2010).

Das Genom von *Tribolium castaneum* hat 41 identifizierte Peptid-Präkursor-Gene (Richards et al., 2008), welche voraussichtlich für ca. 80 Neuropeptide codieren (Li et al., 2008). Von diesen 41 Präkursor-Genen kodieren 22 für Neuropeptide, welche innerhalb der Insekten hoch konserviert sind (Hauser et al., 2010).

Über die genauen Funktionen der Neuropeptide im Insektennervensystem ist noch nicht viel bekannt, wobei erste Erkenntnisse bei *Drosophila melanogaster* gewonnen werden konnten (z.B. Renn et al., 1999; Winther et al., 2006; Terhzaz et al., 2007; Chen und Ganetzky, 2012; Hergarden et al., 2012). Jedoch ist *D. melanogaster* ein evolutionär abgewandelter Vertreter der Diptera (Meusemann et al., 2010; Wiegmann et al., 2011), was den phylogenetisch basaleren *T. castaneum* – welcher wie *D. melanogaster* gut zugänglich für diverse genetische Manipulationen ist (Bucher et al., 2002; Brown et al., 2003; Tomoyasu und Denell, 2004; Peel, 2009; Trauner et al., 2009) – neben *D. melanogaster* zu einem guten Modellorganismus macht, der geeignet ist, die Funktion der Neuropeptide zu erforschen.

T. castaneum ist ein Organismus, für dessen Überleben das Geruchssystem eine essentielle Bedeutung hat (hohe Zahl an Geruchsrezeptoren, Gehirn mit vergrößerten Zentren für Geruchsverarbeitung) (Cox und Collins, 2002; Engsontia et al., 2008; Dreyer et al., 2010). Diesbezüglich liegen in dieser Arbeit die primären und höheren Integrationszentren für Geruchsverarbeitung im Vordergrund (Antenallobus [AL] und Pilzkörper [engl. mushroom body: MB]), welche massenspektrometrisch (mittels "Direct Peptide Profiling") und immunhistochemisch untersucht wurden. Für das "Direct Peptide Profiling" wird der MB vor der Analyse in seine Substrukturen (Calyx: Ca, Pedunculus: Pe, medial Lobus: mL und vertikal Lobus: vL) zerlegt.

Bei der massenspektrometrischen Analyse zeigten die jeweiligen untersuchten Gewebetypen (AL und Substrukturen des MB) ein sehr gut reproduzierbares Muster. Der charakteristische massenspektrometrische "Fingerabdruck" des AL und des MB unterscheidet sich in vielerlei Hinsicht voneinander. Die "Fingerabdrücke" der einzelnen Substrukturen des MB hingegen sind untereinander relativ ähnlich, der "Fingerabdruck" des lateralen Protocerebrums unterscheidet sich jedoch sowohl stark von dem des AL als auch von dem der MB Substrukturen.

Mittels massenspektrometrischer Analysen konnten in den AL der Männchen (n = 20) 28 putative Neuropeptide nachgewiesen werden, die zu elf Neuropeptidfamilien gehören. Ungefähr die Hälfte der 28 im AL gefundenen Neuropeptide konnte in 100 % der Proben nachgewiesen werden (Detektionshäufigkeit = 100 %). Ca. 2/3 der 28 im AL gefundenen Neuropeptide haben eine Detektionshäufigkeit von mehr als 75 %.

Hingegen konnten durch die massenspektrometrische Untersuchung der vier

MB Substrukturen (n = 20 Ca; 20 Pe; 20 mL; 20 vL) insgesamt 37 unterschiedliche putative Neuropeptide nachgewiesen werden, die zu 16 Neuropeptidfamilien gehören. Auffällig ist, dass es im Vergleich zum AL im MB wesentlich mehr Neuropeptide gibt, die in nur wenigen Samples nachgewiesen werden können. Während im AL ca. 2/3 der nachgewiesenen Neuropeptide eine Detektionshäufigkeit von mindestens 75 % haben, so haben im Ca nur ca. 1/12 aller im MB nachgewiesenen Neuropeptide eine Detektionshäufigkeit von mehr als 75 %. Im Pe sind es ca. 1/7, im mL ca. 1/6 und im vL ca. 1/5 der im MB nachgewiesenen Neuropeptide, welche eine Detektionshäufigkeit von mindestens 75 % haben. Ferner gibt es im MB nur wenige Neuropeptide, die in allen vier Substrukturen mit einer hohen Detektionshäufigkeit auftauchen. Lediglich eine Form des "kurzen Neuropeptides F" (engl. short neuropeptide F: sNPF) konnte in allen vier MB Substrukturen mit einer Detektionshäufigkeit von 100 % nachgewiesen werden und nur zwei weitere Neuropeptide haben in allen vier MB Substrukturen eine Detektionshäufigkeit von mindestens 75 %. Darüber hinaus konnte nur ein Neuropeptid gefunden werden (Allatotropin: AT), welches zwar in den AL nachgewiesen werden konnte, jedoch nicht im MB.

Weiterhin wurden immunhistochemische Färbungen der AL und MB mit acht unterschiedlichen Neuropeptidantikörpern angefertigt, um die massenspektrometrischen Daten zu verifizieren und deren Lokalisation im Gewebe darzustellen. Die Detektionshäufigkeit der Neuropeptide in den AL und MB korreliert mit der Intensität/Verteilung der immunhistochemischen Färbemuster in diesen Neuropilen. So hat das Neuropeptid Periviscerokinin 2 (PVK 2) im AL eine Detektionshäufigkeit von 55 % und bei den immunhistochemischen Färbungen gegen dieses Neuropeptid zeigt der AL auch nur in vereinzelten Regionen ein schwaches Färbemuster. Hingegen haben die Neuropeptide SIF-Amid, Myhoinhibitorisches Peptid (MIP) und Tachykinin (TK) eine hohe Detektionshäufigkeit und können immunhistochemisch in hoher Intensität im ganzen AL nachgewiesen werden. Dieses Prinzip lässt sich auch mit den Neuropeptiden in den Substrukturen des MB beobachten.

Die Daten der vorliegenden Studie bilden eine wichtige Grundlage für das Verständnis und zur Erforschung der modulierenden Eigenschaften von Neuropeptiden, speziell in den olfaktorischen Neuropilen von Insekten. Ferner kann die zeitsparende Technik, welche in dieser Arbeit für *T. castaneum* etabliert wurde, genutzt werden, um die Adultplastizität von Neuropeptiden zu erforschen.

Kapitel 5: Neuropeptide in den Pilzkörpern von Insekten

Originaltitel: Neuropeptides in insect mushroom bodies

Die Pilzkörper (engl. mushroom body: MB) der Insekten sind paarige Neuropile und weisen eine charakteristische Form auf (Heisenberg, 1998). Die MB bestehen aus der Fasermasse der sogenannten Kenyon Zellen (engl. Kenyon cells: KC), welche die intrinsischen Neuronen der MB sind. Die KC befinden sich bei den meisten Arten in beiden Hemisphären des Gehirns im n-anterioren Bereich und ihre Zahl ist stark artabhängig und variiert zwischen ca. 2.500 in *Drosophila melanogaster* (Hinke, 1961) und ca. 175.000 in *Periplaneta americana* (Neder, 1959). Die Dendriten der KC bilden meist den kappen- oder becherförmigen Calyx (Ca), der normalerweise direkt n-posterior der KC liegt. Die Axone der KC bündeln sich und verlaufen als säulenförmige Struktur nach n-posterior und bilden den Pedunculus (Pe), welcher sich normalerweise auf der Höhe des Zentralkomplexes in zwei Loben aufteilt. Der mediale Lobus (mL) verläuft meist direkt n-posterior des Zentralkomplexes hin zur Sagittalebene des Gehirns, der vertikale Lobus (vL) verläuft meist nach n-anterior/n-dorsal bis an die Abgrenzung des Gehirns (Heisenberg, 1998; Strausfeld et al., 2009).

Die MB sind höhere Integrationszentren für eine Vielzahl unterschiedlichster, sensorischer Eingänge und erfüllen somit zahlreiche Funktionen. Am besten bekannt und am meisten erforscht sind die MB in ihrer Rolle des erlernen von Gerüchen und der damit verbundenen Gedächtnisspeicherung

und -abrufung (Mcguire et al., 2001; Menzel, 2001; Heisenberg, 2003; Davis, 2004). Morphologisch spiegelt sich dies in den prominenten Trakten wieder, welche die Antennalloben (erstes olfaktorisches Intergrationszentrum) und die MB verbinden. Dies wurde besonders in *D. melanogaster* (Heisenberg et al., 1985; de Belle und Heisenberg, 1994; Connolly et al., 1996; Dubnau et al., 2001) und in der Honigbiene *Apis mellifera* (Erber et al., 1980; Hammer, 1993; Hammer und Menzel, 1998; Fiala et al., 1999) aber auch in zahlreichen anderen Insektenarten beobachtet (Farris, 2005).

Das exakte neuronale Netzwerk, welchem die oben genannten Funktionen zugrunde liegen, ist bisher noch nicht vollständig verstanden. Es wird vermutet, dass jeder spezifische Duft ein individuelles Set an KC aktiviert (Perez-Orive et al., 2002; Jortner et al., 2007), was wiederum ein individuelles Output-Signal erzeugt, welches sich dann in einem entsprechenden Verhalten wiederspiegelt (Schwaerzel et al., 2003; Unoki et al., 2005; Schroll et al., 2006). In diesem neuronalen Netzwerk spielen eine Vielzahl an Neurotransmittern eine essentielle Rolle. Die größte und diverseste Gruppe an Neurotransmittern (nicht nur innerhalb der MB sondern innerhalb des ganzen Insektennervensystems) sind die Neuropeptide (Altstein und Nässel, 2010).

In dieser Arbeit betrachten wir die immunhistochemischen Färbemuster in den MB von acht verschiedenen Neuropeptid Antikörpern in neun verschiedenen Insektenordnungen (insgesamt werden Daten von 24 verschiedenen Arten gezeigt). Der Übersicht halber wurden die Daten (neben einer ausführlicheren Beschreibung) in eine grafische Matrix eingetragen, welche für die jeweiligen Arten und Neuropeptide die Färbemuster innerhalb des Ca, des Pe und der beiden Loben (vL und mL) zeigen. Zum Erstellen der Matrix wurden 36 Datensätze aus Veröffentlichungen genutzt, wobei im Falle von acht dieser Datensätze eigens angefertigte Präparate herangezogen wurden, um diese Daten zu unterstützen. Weitere 48 Datensätze basieren ausschließlich auf eigens angefertigten Präparaten.

Innerhalb der Insekten ist die neuronale Architektur normalerweise stark konserviert, sodass die generelle Form und Lage der einzelnen Neuropile stets leicht wiederzuerkennen ist (Kutsch und Breidbach, 1994). In vielen der bisher beobachteten Fälle trifft dieser hohe Grad der Konservierung auch auf die Verteilung der Neuropeptide (und deren Rezeptoren) zu. Dies bedeutet, dass die immunhistochemischen Färbemuster von Neuropeptid Antikörpern in unterschiedlichen Insektenarten starke Gemeinsamkeiten aufweisen (Nässel, 2002; Nässel und Homberg, 2006; Nässel und Winther, 2010). Wie jedoch auch Evolution und Selektion einen Einfluss auf die Form der MB innerhalb der unterschiedlichen Insektenarten/Insektenordnungen haben (Strausfeld et al., 2009), so kann dies auch einen Einfluss auf die Verteilung der Neuropeptide (und deren Rezeptoren) innerhalb des MB haben.

Die Immunfärbungen zeigen, dass die Neuropeptide in den meisten Fällen immer im MB nachgewiesen werden können (wenn auch teilweise nur vereinzelte Färbemuster in vereinzelten Regionen), jedoch findet man beim Vergleich zwischen den unterschiedlichen Insektenarten meistens große Unterschiede im Detail. Dies bezieht sich zum einen auf die An-, bzw. Abwesenheit von etwaigen Färbungen in den Substrukturen des MB (Ca, Pe, vL und mL), zum anderen auf unterschiedliche Färbemuster (z.B. intensive Färbung der ganzen Substruktur oder nur vereinzelte Fasern) in den jeweiligen Substrukturen des MB. Nur bei wenigen Neuropeptiden findet man konservierte Muster innerhalb einer Insektenordnung (wie z.B. das Neuropeptid AST A in Lepidopteren und in den Phasmatodea oder die Peptide SIF-Amide und sNPF in Dipteren oder auch FMRFamid in Blattodeen), was für diese Peptide in diesen Arten auf eine konservierte Funktion hinweisen könnte. Hier ist es jedoch schwer über Homologien zu sprechen, zumindest wenn die Innervation nicht intrinsisch ist und damit nicht von den KC abstammt. Denn um eine Homologie der extrinsischen Färbungen zu postulieren wäre eine Identifikation der jeweiligen korrespondierenden Zellkörper erforderlich, was in den meisten Literaturquellen und Präparaten nicht möglich war.

In einigen Fällen kann man bei den jeweiligen Neuropeptiden innerhalb einer Insektenordnung größere Gemeinsamkeiten bei den immunhistochemischen Färbemustern finden (wie z.B. FMRMamid in Dipteren, Lepidopteren oder Phasmiden). Häufig sind aber selbst innerhalb einer Ordnung die Färbemuster sehr unterschiedlich (z.B. TK und AST A in Blattodeen, MIP und AST A in Dipteren, oder MIP in Coleoptera). Bei all den untersuchten Arten gab es nie ein Neuropeptid, dessen Antikörperfärbung bei allen Ordnungen ein absolut einheitliches Färbemuster zeigte.

Die häufige Variabilität der immunhistochemischen Färbemuster eines Neuropeptid-Antikörpers innerhalb der MB einer Ordnung – oder auch zwischen den Ordnungen – könnte die hohe Bandbreite der Funktionen der MB widerspiegeln (siehe Tabelle 1 in Kapitel 5 [Englischer Teil der Dissertation]), sodass im Laufe der Evolution Selektionsprozesse nicht nur einen Einfluss auf die Morphologie der MB hatten, sondern auch auf dessen Neuropeptide. Um weiterhin Aussagen treffen zu können, wäre es hilfreich, mehr Daten zu sammeln, sodass man für die jeweiligen Ordnungen und Peptide mehrere Datensätze zum Vergleich hat, um besser Gemeinsamkeiten oder Unterschiede zu erkennen.

Kapitel 6: Die Entdeckung eines neuen Insekten Neuropeptid-Signal-Systems, nahe verwandt zu dem Signal-System der Hormone Adipokin und Corazonin

Originaltitel: Discovery of a Novel Insect Neuropeptide Signaling System Closely Related to the Insect Adipokinetic Hormone and Corazonin Hormonal Systems

Neuropeptide und deren Rezeptoren spielen eine wichtige Rolle im Nervensystem von Insekten. Zwei Neuropeptid-Systeme (Neuropeptid und Rezeptor), die sich strukturell stark ähneln, sind die des Adipokinetischen Hormons (AKH) und des Corazonins (CRZ). Ein weiterer Neuropeptid-Rezeptor, welcher 2006 im Malaria-Moskito *Anopheles gambiae* identifiziert wurde (Belmont et al., 2006), dessen Ligand aber bisher unbekannt war, liegt strukturell zwischen dem AKH- und CRZ-Rezeptor. Aufgrund dieser strukturellen Ähnlichkeit wurde der Rezeptor "AKH/Corazonin-verwandtes Peptid-Repeptor" (engl.: AKH/corazonin-related peptide-receptor: ACP; bzw. ACP-Rezeptor) genannt.

Trotz der hohen strukturellen Ähnlichkeit aktiviert weder AKH noch CRZ die Rezeptoren der jeweiligen anderen Neuropeptid-Systeme oder den ACP-Rezeptor (Staubli et al., 2002; Cazzamali et al., 2002; Belmont et al., 2006). Dies ist ein gutes Beispiel für Rezeptor/Liganden Koevolution (Cazzamali et al., 2002; Park et al., 2002; Hauser et al., 2006; Hauser et al., 2008) und es ist zu vermuten, dass alle drei Rezeptoren und ihre Liganden durch Genduplikation entstanden sind. Diese Idee der Koevolution spiegelt sich auch in den Funktionen der Neuropeptid-Systeme von AKH und CRZ wieder, welche vermutlich zum größten Teil mit physiologischer Aktivität und metabolischem Stress in Verbindung stehen (Gade et al., 1997; Staubli et al., 2002; Veenstra, 1989; Tawfik et al., 1999; Zitnan et al., 2007). Die Funktionen des ACP-Neuropeptid-Systems ist bisweilen unbekannt.

Um die Funktion und Evolution dieser Neuropeptid-Systeme besser zu verstehen, wurden deren Rezeptoren annotiert, geklont und beschrieben. Das Neuropeptid-System des ACP wird in dieser Arbeit erstmalig beschrieben.

Durchsuchungen von Gendatenbanken identifizierten ein Gen für ein Peptid, welches als Ligand für den in *A. gambiae* gefundenen ACP-Rezeptor (Belmont et al., 2006) infrage kommt und dementsprechend als ACP bezeichnet wurde. So wie auch die AKH-, CRZ- und ASP-Rezeptoren untereinander große strukturelle Ähnlichkeiten aufweisen, so tun dies auch deren aktivierende Peptide. Ein vergleichbares ACP-Peptid konnten auch in sieben weiteren Insektenarten identifiziert werden (den Moskitos *Aedes aegypti* und *Culex pipiens*, den Schmetterlingen *Bombyx mori* und *Ostrinia nubilalis*, dem Käfer *Tribolium castaneum*, der Wespe *Nasonia vitripennis* und der Wanze *Rhodnius prolixus*). Jedoch gibt es auch Insekten, in denen kein ACP-Peptid nachgewiesen werden

konnte (Honigbiene *Apis mellifera*, Erbsenblattlaus *Acyrthosiphon pisum*, Laus *Pediculus humanus* und 12 verschiedenen *Drosopila* Spezies), auch im Wasserfloh *Daphnia pulex* konnte es nicht identifiziert werden. Dies lässt vermuten, dass das ACP Neuropeptid-System während der Evoluten der Insekten an unterschiedlichen Stellen verloren gegangen ist. Solche punktuellen Verluste von Neuropeptid-Systemen wurden bei Insekten bereits mehrfach beobachtet (Li et al., 2008; Hauser et al., 2006 und 2008; Stafflinger et al., 2008).

Auch die ACP-Rezeptoren weisen große Übereinstimmungen bei vielen der untersuchten Spezies auf (*A. aegypti, C. pipiens, B. mori, T. castaneum, N. vitripennis und R.prolixus*). Bei den Arten, bei denen das APC-Peptid nicht nachgewiesen werden konnte, konnte ebenfalls kein Rezeptor identifiziert werden (*Apis mellifera, A. pisum, P. humanus*, 12 *Drosopila* Spezies und *D. pulex*).

Die ACP-Rezeptoren von *A. gambiae* und *T. castaneum* wurden kloniert und jeweils in chinesischen Hamster-Ovarien (engl.: Chinese hamster ovaries: CHO) exprimiert. Diese CHO zeigten bei Zugabe von ACP eine charakteristische Dosis-Antwort-Kurve, jedoch nicht bei Zugabe von AKH oder CRZ oder 40 anderen getesteten Insekten Neuropeptiden. CHO in denen *A. gambiae* AKH-, bzw. CRZ-Rezeptor exprimiert wird, zeigen keine Kreuzreaktion mit CRZ, bzw. AKH oder mit ACP, was die Spezifität dieses Rezeptors demonstriert.

Der phylogenetische Vergleich der untersuchten Holometabola zeigt, dass im Stammbaum sowohl die Rezeptoren als auch die Peptide von AKH, CRZ und ACP Cluster bilden und jeweils die Cluster von ACP zwischen denen von AKH und CRZ liegen, was die Theorie der Koevolution unterstützt. Es ist zu vermuten, dass das Neuropeptid-Systeme von AKH und ACP von einem gemeinsamen, einzelnen Vorläufersystem abstammt. Da in *D. pulex* (einem Krebs, welche vermutlich die direkten Vorfahren der Insekten sind [Glenner et al., 2006]) kein ACP wohl aber AKH-Rezeptoren nachgewiesen werden konnten, ist zu vermuten, dass das ACP-Neuropeptid-System aus dem AKH-Neuropeptid-Systeme hervorgegangen ist.

Mittels quantitativer PCR bei *T. castaneum* konnte gezeigt werden, dass sowohl die mRNA des ACP-Rezeptors als auch das Peptid im adulten Tier im Kopf (vermutlich im Gehirn) bis zu 30 mal stärker exprimiert wird als im restlichen Körper (Abdomen und Thorax). Die stärkste Expression konnte jedoch in späten Embryonen und der frühen Larve gefunden werden (kurz vor und nach Schlupf). Immunhistochemische Färbungen dieses frühen Larvenstadiums zeigen vier ACP-immunreaktive Zellen pro Hemisphäre, dessen Fortsätze in das Gehirn, Thorakal- und Abdominalganglion projizieren.

Die genaue Funktion des Peptides ist nicht bekannt. RNA-Interferenz gegen den ACP-Rezeptor in weiblichen Puppen von *T. castaneum* zeigte keinen messbaren Effekt auf den Habitus, die Reproduktion oder Mortalität. Da jedoch Peptid und Rezeptor in späten Embryonen/frühen Larven besonders stark exprimiert wird, ist eine Funktion in der Entwicklung der frühen Larvenentwicklung oder deren Physiologie anzunehmen.

Kapitel 7: Eine neu entdeckte Antennallobus-Struktur im kleinen Beutenkäfer *Aethina tumida*

Originaltitel: Novel antennal lobe substructures revealed in the small hive beetle *Aethina tumida*

Der kleine Beutenkäfer *Aethina tumida* ist ein aus Afrika stammender Parasit, welcher Völker diverser Bienenarten befällt (Neumann und Elzen, 2004; Spiewok und Neumann, 2006; Greco et al., 2010; Halcroft et al.; 2011), sich mittlerweile in anderen Ländern über den Globus verbreitet (Neumann und Elzen, 2004; Neumann und Ellis, 2008; Mutinelli et al., 2014) und dort eine ernstzunehmende Bedrohung für die Wildbestände und Imkerei darstellt (Lundie, 1940; Schmolke, 1974; Neumann und Elzen, 2004). Bisher konnte in dieser Käferart kein Aggregationspheromon identifiziert werden, wie es von anderen Mitgliedern dieser Familie bekannt ist, jedoch werden die Käfer von Gerüchen der Bienen, beziehungsweise Gerüchen aus deren Kolonien, angelockt (Suazo et al., 2003; Graham et

al., 2011; de Guzman et al., 2011), während das visuelle System der Tiere vermutlich nicht von großer Bewandtnis dafür ist. Dies lässt vermuten, dass der Geruchssinn dieser Parasiten ein Schlüssel zu ihrer Bekämpfung sein könnte, weswegen der Schwerpunkt dieser Veröffentlichung auf der Untersuchung des Antennallobus (AL) von *A. tumida* liegt.

Zur Untersuchung des Nervensystems von *A. tumida* wurden für immunhistochemische (IHC) Färbungen Antikörper gegen die beiden Neuromediatoren Serotonin (5HT) und Tachykinin (TK) sowie gegen das ubiquitär Vesikelprotein Synapsin – welches das Nervensystem ubiquitär markiert (Klagges et al., 1996) – verwendet. Von den Neuromediatoren ist bekannt, dass sie bei unterschiedlichsten Insektenarten stets im AL vorzufinden sind, wo sie voraussichtlich steuernd/modulierend in die Geruchsverarbeitung eingreifen (Linn und Roelofs, 1986; Kloppenburg und Hildebrand, 1995; Hill et al., 2003; Gatellier et al., 2004; Winther et al., 2006; Dacks et al., 2009, Ignell et al., 2009; Winther und Ignell, 2010).

Die 3D-Rekonstruktion des Gehirns zeigt eine insektentypische Neuroanatomie wie sie auch bei vielen anderen Käfern vorzufinden ist (Van Haeften, 1993; Breidbach und Wegerhoff, 1994; Larsson et al., 2004; Dreyer et al., 2010; Hu et al., 2011). Folgende Neuropile konnten identifiziert und rekonstruiert werden: Von den optischen Loben konnten die Medulla, die Lobula und die Lobula Platte rekonstruiert werden. Von dem Zentralkomplex wurden die obere und untere Einheit des Zentralkörpers sowie dessen Noduli, als auch die Protocerebralbrücke, rekonstruiert. Vom Pilzkörper konnte der Calyx sowie der Pedunkulus mit seinen beiden Loben rekonstruiert werden. Von den Antennalloben (AL) wurden alle Glomeruli und der innere Bereich des AL (welcher den sich aufteilenden Antennalnerv beinhaltet) rekonstruiert.

Bei den Männchen beinhaltet der AL 72,0 ± 3,9 Glomeruli, bei den Weibchen 71,1 ± 3,4 Glomeruli. Sowohl in der Zahl der Glomeruli, als auch in der Größe der AL, bzw. der Glomeruli konnte kein signifikanter Unterschied zwischen den Geschlechtern festgestellt werden. Des Weiteren konnten keine Hinweise auf die Existenz eines makroglomerulären Komplexes bzw. sexspezifischer Glomeruli gefunden werden.

Die Immunfärbungen mit dem TK Antikörper zeigten TK-immunreaktive (TK-ir) Substrukturen innerhalb der Glomeruli auf. Die Zahl dieser TK-ir Substrukturen pro Glomerulus ist linear zur Größe der Glomeruli, sie sind gleichmäßig im Glomerulus verteilt und befinden sich niemals direkt an der Außenbegrenzung der Glomeruli. Die Verteilung weist keinen Sexualdimorphismus auf. Die TK-immunreaktivität stammt offensichtlich von lokalen Interneuronen (LN).

Bei den IHC Färbungen mit dem Antikörper gegen 5TH konnte ein feines Netzwerk an 5HT-immunreaktive (5HT-ir) Nerven entdeckt werden, welches sich in allen Glomeruli der AL ausbreitet, jedoch werden keine der TK-ir Substrukturen der Glomeruli innerviert. Die Innervation dieses 5HT-ir Netzwerkes eines AL stammt von nur einer einzelnen Zelle, die jeweils lateral des kontralateralen AL liegt und ohne ersichtliche Verzweigungen zum gegenüberliegenden AL projiziert, wie auch bei anderen Insekten beschrieben (Dacks et al., 2009).

Im Vergleich zu acht anderen Insektenarten, von denen Volumendaten der Gehirne verfügbar sind, ist besonders erwähnenswert, dass *A. tumida* auffällig große AL ausweist, was die Hypothese stützt, dass der Geruchssinn für das Verhalten dieser Tiere von besonderer Bedeutung ist. Die MB hingegen weisen ein eher geringeres relatives Volumen auf. Da die MB in erster Linie dafür bekannt sind, höhere Integrationszentren für Gerüche zu sein (Heuer et al., 2012), korreliert dies auf den ersten Blick nicht mit der relativ großen AL. Jedoch konnte bei Käfern gezeigt werden (Farris und Roberts, 2005), dass Tiere, die in ihrer Nahrungssuche spezialisiert sind (wie dies auch bei *A. tumida* der Fall ist), kleinere MB haben als Nahrungsgeneralisten (unabhängig von der relativen Größe ihrer AL).

Die sphärischen TK-ir Substrukturen, wie sie in *A. tumida* gezeigt wurden, sind für Insekten ungewöhnlich und wurden so noch nie beschrieben. Herkömmlich gibt es für LN fünf verschiedene Innervationsmuster der Glomeruli: 1) nur vereinzelte Fasern auf der Oberfläche des Glomerulus, 2) einzelne Fasern innerhalb des

ganzen Glomerulus oder 3) oder nur in Teilen des Glomerulus, 4) ein dichtes Fasergeflecht von LN im ganzen Glomerulus oder 5) nur in Teilen des Glomerulus (Schachtner et al., 2005; Seki und Kanzaki, 2008; Husch et al., 2009; Carlsson et al., 2010; Chou et al., 2010; Seki et al., 2010; Neupert et al., 2012; Binzer et al., 2014; Siju et al., 2014). Für die Funktion der TK-ir Substrukturen des AL werden hier zwei Hypothesen vorgestellt. 1) Da diese sphärischen Substrukturen einheitlich im ganzen Glomerulus verteilt sind und ihre Zahl linear mit der Größe der Glomeruli korreliert, könnten sie als massive Neuromodulator-Ausschüttungszonen dienen, welche den Glomerulus schnell und einheitlich mit Neuromediatoren (die lokal als Neurohormone wirken könnten) versorgen. 2) Die einzelnen Substrukturen könnten funktionell wie einzelne, unabhängige Glomeruli arbeiten, wodurch eventuell die "Leistungsfähigkeit" des AL verbessert werden könnte. Da dieser Käfer mit seinen ca. 70 Glomeruli ein Parasit in Kolonien von Bienen ist, welche typischerweise weitaus mehr Glomeruli haben (152 bis 166 pro AL in Arbeiterinnen der Honigbiene; Arnold et al., 1985) und sehr stark mittels Pheromonen kommunizieren (Slessor et al., 2005; Trhlin und Rajchard, 2011), wäre es für das Überleben und Fortpflanzen des Käfers von Vorteil, mittels eines "leistungsstärkeren" AL (zu einem Teil) die Kommunikation im Bienenstock zu verstehen.

Ohne weitere Studien, wie z.B. Backfills der Antennen und/oder einer exakteren Untersuchung einzelner AL-Neuronen, ist es schwer die beiden Hypothesen zu überprüfen.

Kapitel 8: Variationen über ein Thema: Antennallobus Architektur der Coleoptera

Originaltitel: Variations on a theme: antennal lobe architecture across Coleoptera

Trotz der großen Artenvielfalt und Diversität sowie des ökonomischen und ökologischen Einflusses der Coleoptera (Crowson, 1981; Grimaldi und Engel, 2005; Hunt et al., 2007; Hauser et al., 2008; Chapman, 2009; Foottit und Adler, 2009; Kukalová-Peck und Beutel, 2012) wurde das olfaktorische System dieser Tiere nicht ausführlich untersucht. Detaillierte anatomische Daten über den Antennallobus (AL) – das primäre olfaktorische Integrationszentrum – von adulten Käfern gibt es nur vom Blatthornkäfer *Holotrichia diomphalia* (Hu et al. 2011), Rotbraunen Reismehlkäfer *Tribolium castaneum* (Dreyer et al., 2008; Dippel et al., in Revision [Siehe Kapitel 3]) und vom Kleinen Beutenkäfer *Aethina tumida* (Kollmann et al., 2015).

In der vorliegenden Arbeit beschreiben wir die Neuroanatomie der AL der Käfer, basierend auf histochemischen Färbungen an insgesamt 63 unterschiedlichen Käferarten. Hierfür verwendeten wir zwei Antikörper, wovon einer gegen das Neuropeptid Tachykinin (engl. Tachykinin Related Peptides: TKRP) und der andere gegen das Vesikelprotein Synapsin gerichtet ist. Ferner wurden zwei Gewebemarker verwendet, wovon der eine f-Aktin (Pahalloidin) und der andere Zellkerne (DAPI) markiert.

Auf den ersten Blick ähnelt die Anatomie der meisten Käfer AL derer der meisten anderen Insekten, wie dies z.B. auch für *Drosophila melanogaster* beschrieben ist (Schachtner et al., 2005). Bei den Käfern schwankt die Zahl der Glomeruli pro AL zwischen 50 und 150; allerdings liegt der repräsentative Wert beim größten Teil der Käfer zwischen 80 und 120 Glomeruli. Bei den Coccinellidae (Marienkäfern) und den Dytiscidae (Schwimmkäfern) besteht der AL allerdings aus zahlreichen kleineren sphärischen Strukturen, ähnlich den Mikroglomeruli von Acrididae (Feldheuschrecken) (Ignell et al., 2001, Schachtner et al., 2005). Hier liegt die Zahl der Glomeruli pro AL für Marienkäfer bei ungefähr 400 bis 600 und für Schwimmkäfer bei ca. 400 bis 1.000.

In 15 der 63 untersuchten Arten konnten in den Glomeruli Tachykinin immunreaktive (TKRP-ir), sphärische Substrukturen gefunden werden, wie sie schon für *A. tumida* beschrieben wurden (Kollmann et al., 2015). Dort korreliert die Größe der Glomeruli linear mit der Anzahl der TKRP-ir-Untereinheiten. Basierend auf den Färbungen mit Phallodidin bzw. mit dem Synapsin Antikörper wurden in zahlreichen weiteren Arten Substrukturen in den AL identifiziert.

Die Arten, welche diese TKRP-ir-Substrukturen aufwiesen, stammen aus 7 Familien, die über den ganzen Stammbaum der Käfer verteilt sind. Auch innerhalb dieser Familien ist dieses Phänomen scheinbar nicht vollständig konserviert.

Ferner konnte bei Arten, deren Glomeruli Substrukturen aufweisen (egal ob TKRP-ir oder nicht) keine Korrelation zu deren Ernährungsart sowie deren Habitat (terrestrisch oder strakt assoziiert zu aquatischen Lebensräumen) gefunden werden. Auch die relativen Volumenwerte der jeweiligen Neuropile, bzw. das absolute Volumen der AL, scheinen in keinerlei Korrelation zu den TKRP-ir-Substrukturen zu stehen. Lediglich bei den Marien- und Schwimmkäfern – welche eine mikroglomeruläre Organisation der AL aufweisen – konnte eine Korrelation gefunden werden. Eine ähnliche Strukturierung der AL findet man auch bei Libellen (Rebora et al., 20013), welche ebenso wie Marien- und Schwimmkäfern Räuber sind und sich offensichtlich stark auf ihr visuelles System verlassen. Ferner weisen alle drei Gruppen (Marienkäfer, Schwimmkäfern und Libellen) stark reduzierte oder gar fehlende Calyces auf. Jedoch konnte für jede dieser Gruppen gezeigt werden, dass die Tiere einen funktionierenden Geruchssinn aufweisen (Iperti, 1965; Hodgson, 1953; Abjörnsson et al., 1997; Al Abassi et al., 2000; Herbst et al., 2011; Sarkar et al., 2013; Piersanti et al., 2014).

Bei allen 15 Käferarten mit TKRP-ir-Substrukturen konnte gezeigt werden, dass die Immunreaktivität dieser Untereinheiten nicht von TKRP-ir-Rezeptorneuronen der Antenne stammen, sondern dass stets TKRP-ir-lokale Interneuronen (LN) in die AL innervieren und für die TKRP-ir-Färbung der Substrukturen verantwortlich sind. Bei der Art *Pachnoda ephippiata* wurden Antennen-Backfills zusammen mit immunhistochemischen Färbungen gegen Synapsin und TKRP durchgeführt. Hier konnte bestätigt werden, dass die TKRP-ir-Substrukturen nicht von der Antenne (also den olfaktorischen Sensor-Neuronen [OSN]) her innerviert werden, da die Backfills ausschließlich die Teile der Glomeruli labeln, die nicht zu den TKRP-ir-Substrukturen gehören. Hingegen projizieren die TKRP-ir LN fast ausschließlich in die TKRP-ir-Substrukturen. Diese Organisation von Neuronen ist in vergleichbarer Form von einigen Insekten (z.B. Bienen, Fliegen und Motten) bekannt, wo sich der Glomerulus in einen einzelnen inneren Kern – den Core – und einen einzelnen darumliegenden Cortex aufteilt. Auch bei diesen Arten wird lediglich der Cortex von den OSN innerviert (Koontz and Schneider, 1987, Homberg et al., 1989; Anton und Homberg, 1999; Galizia et al., 1999; Okada et al., 2009; Tanaka et al., 2012; Sinakevitch et al., 2013). Bei den AL von Bienen sind nur die Kerne der Glomeruli TKRP-ir.

Bezüglich der Entstehungen dieser Substrukturen ist es vorstellbar, dass bei den Käfern die vielen TKRP-ir-Untereinheiten in einem Glomerulus das Resultat einer Verschmelzung mehrerer Glomeruli sind, welche ursprünglich jeweils aus einem Kern und einem Cortex bestanden. Alternativ wäre es vorstellbar, dass die LN beim Einwachsen in den Glomerulus in verschiedenen Teilabschnitten eines Glomerulus terminieren und dort jeweils zur Bildung individueller Cores führen, die von einem Cortex umgeben sind.

Backfills einzelner Antennen-Sensillen und/oder transgene Linien, welche einen spezifischen Geruchsrezeptor der Antenne labeln, (bzw. Antikörper gegen solche Rezeptoren) könnten helfen, das genaue Schaltbild der Neuronen der TKRP-ir Untereinheiten besser zu verstehen.

Finale Zusammenfassung, Diskussion und Ausblick

In dieser Doktorarbeit wurde das Gehirn – speziell das Geruchssystem – von Käfern im Detail untersucht. Hierfür wurde eine Spezies – der Rotbraune Reismehlkäfer *Tribolium castaneum* – ausführlich analysiert. Dies beinhaltete unter anderem dessen Neuroanatomie, Verteilung von chemorezeptiven Rezeptorneuronen auf Antennen und Mundwerkzeugen und die Verteilung von Neuropeptiden im AL und MB. Zusätzlich wurde der AL von weiteren 62 Käferarten und die Verteilung von acht Neuropeptidfamilien im MB von 24 Insektenarten untersucht.

Das Gehirn von *T. castaneum* und sein olfaktorisches System

Sowohl das Gehirn der adulten, als auch der larvalen Tiere (erstes Larvenstadium), weisen große Übereinstimmungen mit den jeweiligen Entwicklungsstadien anderer Insektenarten auf. Die vier Hauptneuropilgruppen sind stets zu erkennen (CBX, MB, OL und AL), wobei bei den Larven die OL nur als Anlagen vorliegen (Dreyer et al., 2010; Koniszewski et al., 2016). Die OL der adulten Tiere verfügen über eine LoP, welche bisher nur bei wenigen Insektenordnungen nachgewiesen werden konnte (Strausfeld, 2005).

Interessant sind vor allem vier Charakteristika im Gehirn der adulten Tiere, welche teilweise so noch nie bei holometabolen Insekten bzw. generell bei Insekten beobachtet wurden (Dippel et al., eingereicht).

1) Von mehreren Insektenarten ist bekannt, dass die Mundwerkzeuge primär gustatorische und die Antennen primär olfaktorische Funktionen erfüllen (Dahanukar et al., 2001; Bohbot et al., 2007; Vermehren-Schmaedick et al., 2011). Bei *T. castaneum* ist eine solche scharfe Abgrenzung jedoch nicht zu ziehen, da auf den Antennen vergleichbar viele GR exprimiert werden – fast in derselben Konzentration wie auf den Mundwerkzeugen. Zusätzlich weisen die Mundwerkzeuge viele OR auf. Dies könnte darauf zurückzuführen sein, dass *T. castaneum* eine Lebensweise führt, durch die die Antennen der Tiere häufiger mit potentieller Nahrung in Berührung kommen.

2) Im GNG konnten wir eine unpaare, glomerulär organisierte (30-40 Glomeruli) Struktur (GOC) identifizieren, welche sowohl von der partiell Orco labelnden Linie markiert wird, als auch von Backfills der Mundwerkzeuge. Diese Befunde implementieren sehr stark eine olfaktorische Funktion dieser Struktur, welche noch in keinem Insekt beschrieben wurde.

3) Wir konnten in *T. castaneum* einen LG identifizieren, von dem es bisher hieß, dass er nicht in holometabolen Insekten zu finden ist (Ernst et al., 1977; Ignell et al., 2000; Schachtner et al., 2005; Hofer et al., 2005; Farris, 2008).

4) Wir konnten erstmalig bei Käfern zeigen, dass sie über drei, statt wie bisher angenommen nur über ein oder zwei ALT verfügen. (Galizia und Rössler, 2010).

Punkt 1) lässt sich wie erörtert vermutlich über den Lebensstil der Käfer erklären und 3) und 4) sind Beobachtungen, die zumindest aus anderen Insektenarten bekannt sind. Jedoch ist Punkt 2) ein Novum. Interessant ist hierbei, dass auf den Mundwerkzeugen 49 unterschiedliche OR exprimiert werden, wovon 28 signifikant hoch exprimiert werden (im Vergleich von Expressionsleveln der Mundwerkzeuge relativ zu denen des Körpers) und dass die Zahl der glomerulären Strukturen im GOC zwischen 30 und 40 liegt (Dippel et al., eingereicht). Diese Relation (von OR zu glomerulären Strukturen) erinnert an das zentrale Dogma der Insekten-Olfaktorik, welches besagt, dass (typischerweise) ein OSN nur einen Typ spezifischer OR exprimiert und, dass alle OSN mit dem gleichen spezifischen OR auf denselben Glomerulus des AL verschalten. Bezüglich dieses Dogmas hat die Zahl der exprimierten speziellen OR gleich der Zahl der Glomeruli zu sein (Jefferis 2005; Vosshall und Stocker 2007; Kaupp 2010). Ob jedoch alle Neuronen der Mundwerkzeuge, die den gleichen spezifischen OR exprimieren, auch in dieselbe glomeruläre Struktur des GOC projizieren, ist unbekannt. Dies ließe sich über Backfills einzelner Sensillen der Mundwerkzeuge, über transgene Linien (die OR labeln, welche auf den Mundwerkzeugen exprimiert werden) oder über Antikörper gegen solche OR testen. Funktionelles Kalzium-Imaging mit gleichzeitiger olfaktorischer und/oder gustatorischer Stimulierung der Mundwerkzeuge könnte Aufschluss über die Funktion des GOC geben. Farbstoffinjektion in das GOC würde zeigen ob, bzw. mit welchen höheren geruchsverarbeiteten Gehirnrealen (z.B. MB oder LH) diese Struktur in Verbindung steht.

Unsere Beobachtungen weisen darauf hin, dass unterschiedliche Arten im Laufe ihrer Evolution unterschiedliche Strategien und Modifikationen ihrer olfaktorischen neuronalen Netzwerke entwickelt haben, um sich ihrer Umwelt anzupassen. Dies betont die Notwendigkeit unterschiedliche Spezies zu untersuchen, statt sich in der Forschung vorwiegend auf einen oder wenige Modellorganismen zu stützen.

Neuropeptide in den geruchsverarbeitenden Gehirnzentren

Wir untersuchten das Peptidom des AL und MB von *T. castaneum* mittels Massenspektrometrie und visualisierten die Verteilung der Neuropeptidfamilien in besagten Regionen mittels Immunhistochemie. Die massenspektrometrischen Untersuchungen ergaben gewebespezifische "Fingerabdrücke". Diese Technik kann zukünftig verwendet werden, um schnell und effektiv endo- und exogene Einflüsse auf die Expression von Neuropeptiden im Nervensystem von Insekten zu untersuchen (Binzer et al., 2013).

Eine Untersuchung der Neuropeptidverteilung in den MB von 24 unterschiedlichen Insektenarten hat ergeben, dass deren Verteilungsmuster zwar innerhalb einer Ordnung teilweise konserviert sein kann, jedoch findet man in den meisten Fällen größere Abweichungen zwischen Arten innerhalb einer Ordnung und insbesondere zwischen den Ordnungen (Heuer et al., 2012). Die großen Variationen im Verteilungsmuster der Neuropeptide könnte mit der großen Bandbreite der Funktionen des MB innerhalb der Insekten in Verbindung stehen (Heuer et al., 2012). Um einen detaillierteren Einblick und dadurch ein besseres Verständnis über die Konservierung von Neuropeptiden in den MB (und anderen Neuropilen) der Insekten zu erlangen, wäre es erstrebenswert, die Verteilung eines einzelnen Neuropeptides in vielen Arten einer einzelnen Insektenordnung zu betrachten. Die Färbungen gegen TKRP in 63 Käferarten (Kollmann et al., eingereicht) wären zur Beantwortung dieser Frage ein hilfreicher Datensatz.

Zusätzlich untersuchten wir die Neuropeptidfamilie ACP und deren Rezeptor in *T. castaneum* im Detail und verglichen es mit dem strukturell ähnlichen Neuropeptidfamilien AKH und CRZ. AKH und CRZ sind beide für die Bewältigung von metabolischem Stress von Bedeutung (Gade et al., 1997; Staubli et al., 2002; Veenstra, 1989; Tawfik et al., 1999; Zitnan et al., 2007). Die Funktion von ACP ist noch nicht genau bekannt, es hat in adulten Tieren keinen Einfluss auf Wachstum, Reproduktion und die Mortalitätsrate, jedoch werden das Peptid und der Rezeptor in späten Embryonen und frühen Larven stark exprimiert, was vermuten lässt, dass ACP für die frühe larvale Entwicklung und/oder Physiologie von Bedeutung ist (Hansen et al., 2010).

Trotz der großen strukturellen Ähnlichkeit der drei Neuropeptide, bzw. deren Rezeptoren, kann der AKH-Rezeptor weder von CRZ oder ACP aktiviert werden, noch kann der CRZ-Rezeptor von AKH oder ACP aktiviert werden (Staubli et al., 2002; Cazzamali et al., 2002; Belmont et al., 2006). Ferner kann der ACP-Rezeptor nicht von AKH oder CRZ aktiviert werden (Hansen et al., 2010).

Basierend auf den großen strukturellen Ähnlichkeiten der Peptide, bzw. der Rezeptoren und ihrer starken phylogenetischen Verwandtschaft zueinander (auch in anderen Taxa), ist davon auszugehen, dass die drei Neuropeptide, bzw. deren Rezeptoren, durch Genduplikation aus einem gemeinsamen Vorläufer entstanden sind (Hansen et al., 2010).

Der AL der Käfer und die Architektur ihrer Glomeruli

Bei den detaillierten Untersuchungen der Architektur der AL von 63 Käferarten fanden wir neben den AL mit runden, sphärischen Glomeruli – wie sie bei den meisten Insekten beschrieben werden (Schachtner et al., 2005) – in sieben Spezies eine Vielzahl sehr kleiner Glomeruli, vergleichbar mit den Mikroglomeruli der Acrididae (Ignell et al., 2001; Schachtner et al., 2005). In 26 weiteren Arten wiesen die Glomeruli eine Substruktur auf, in 15 dieser Arten waren diese Substrukturen TKRP-ir. In zusätzlichen 12 Arten gab es schwache Anhaltspunkte zur Existenz von (nicht TRKR-ir) Substrukturen. Die Zahl der Glomeruli pro AL liegt zwischen 50 und 150, bzw. zwischen 400 und 1.000 Mikroglomeruli. Sowohl Mikroglomeruli als auch Substrukturen konnten in unterschiedlichen Familien verteilt im ganzen Stammbaum der Käfer gefunden werden, was vermuten lässt, dass es sich dabei jeweils um unabhängige Entwicklungen handelt (Kollmann et al., eingereicht).

Einige Autoren beschrieben bereits Mikroglomeruli in den AL von Schwimmkäfern (Hanström, 1940; Panov, 2013), andere Autoren beschrieben dessen AL jedoch als aglomerulär (e.g. Strausfeld et al., 1998; Strausfeld et al., 2009). Eigene Befunde der zwei untersuchten Schwimmkäferarten zeigen einen eindeutig mikroglomerulär organisierten AL. Ebenfalls die fünf untersuchten Marienkäfer Arten zeigen einen mikroglomerulären AL (Kollmann et al., eingereicht).

In den meisten Fällen lässt sich erkennen, dass diese Substrukturen gleichmäßig im AL verteilt liegen und von detaillierteren Untersuchungen von *A. tumida* ist sowohl bekannt, dass die Zahl der Substrukturen linear mit der Größe der Glomeruli korreliert als auch, dass es offensichtlich keinen Sexualdimorphismus gibt (Kollmann et al., 2016). Backfills in *P. ephippiata* zeigten, dass diese Substrukturen nicht von OSN innerviert werden. wohingegen TKRP-ir LN fast ausschließlich die TKRP-ir-Substrukturen innervieren (Kollmann et al., eingereicht).

Substrukturierte Glomeruli konnten bereits in vereinzelten Insektenarten beobachtet werden (*A. mellifera*, *D. melanogaster* und vereinzelten Lepidoptera-Arten) (Koontz and Schneider, 1987; Sinakevitch et al., 2013). In diesen Arten kann jeder Glomerulus in zwei Regionen aufgeteilt werden: In einen einzelnen Kern und in eine einzelne Rinde (nur letztere wird von OSN innerviert). In *G. bimaculatus* wurden multiple Substrukturen pro Glomerulus beobachtet, jedoch sind hier die Substrukturen von OSN innerviert (Ignell et al., 2001). Die Substrukturen von *A. mellifera*, *D. melanogaster*, vereinzelten Lepidoptera-Arten und *G. bimaculatus* unterschieden sich in ihrer Organisation erheblich von denen der Coleoptera, wodurch die Substrukturen der Käfer als einzigartig innerhalb der Insekten zu bezeichnen sind.

Wir postulieren zwei Hypothesen, woher diese Substrukturen der Käfer stammen könnten. Entweder sind sie das Resultat einer Verschmelzung von mehreren Glomeruli, welche sich in zwei Regionen aufteilen lassen (wie z.B. bei *A. mellifera*), oder das Resultat einer Kompartimentierung solcher Glomeruli. Transgene Linien, welche einzelne OR labeln, oder Antikörper gegen einzelne OR könnten dabei helfen, die detaillierte Architektur und eventuell die Entstehung dieser Substrukturen der Käfer zu verstehen (Kollmann et al., eingereicht).

Resümee

In dieser Doktorarbeit wurde die Neuroarchitektur des Gehirns – speziell das Geruchssystem – von Käfern erstmalig detailliert untersucht. Dadurch entstanden neue Erkenntnisse über das Geruchsystem (bzw. das chemorezeptive System) der Käfer, der größten und diversesten Ordnung im Reich der Tiere. Diese Erkenntnisse sind äußerst hilfreich bei der Etablierung von *T. castaneum* als ersten Käfer-Modellorganismus in der Neurobiologie, speziell für die Erforschung der Olfaktorik.

Literatur

Abjörnsson K., Wagner B.M.A., Axelson A., Bjerselius R., Olsén K.H. (1997) Responses of *Acilius sulcatus* (Coleoptera: Dytiscidae) to Chemical Cues from Perch (Perca fluviatilis). Oecologia 111: 166–171.

Al Abassi S., Birkett M.A., Pettersson J., Pickett JA., Wadhams LJ., Woodcock CM. (2000) Response of the Seven-spot Ladybird to an Aphid Alarm Pheromone and an Alarm Pheromone Inhibitor is Mediated by Paired Olfactory Cells. Journal of Chemical Ecology 26:1765-1771.

Altieri M.A., Nicholls C.I. (2004) Biodiversity and Pest Management in Agroecosystems, 2nd edn. Haworth Press Inc., Binghamton.

Altstein M., Nässel D.R. (2010) Neuropeptide signaling in insects. Advances in Experimental Medicine and Biology. 692:155–165.

Altstein M., Nässel D.R. (2010) Neuropeptide signaling in insects. Advances in Experimental Medicine and Biology. 692:155–165.

Angelini D.R., Jockusch E.L. (2008) Relationships among pest flour beetles of the genus *Tribolium*

(Tenebrionidae) inferred from multiple molecular markers. Molecular Phylogenetics and Evolution. 46:127–141.

Angelini D.R., Kikuchi M., Jockusch E.L. (2009) Genetic patterning in the adult capitate antenna of the beetle Tribolium castaneum. Developmental Biology. 327: 240–251.

Anton S., Homberg U. (1999) Antennal lobe structure. In Insect olfaction. Springer Berlin Heidelberg.

Arnold G., Masson C., Budharugsa S. (1985) Comparative study of the antennal lobes and their afferent pathway in the worker bee and the drone *Apis mellifera*. Cell and Tissue Research. 242:593–605.

Belmont M., Cazzamali G., Williamson M., Hauser F., Grimmelikhuijzen C.J.P. (2006) Identification of four evolutionarily related G protein-coupled receptors from the malaria mosquito *Anopheles gambiae*. Biochemical and Biophysical Research Communications. 344:160–165.

Bicker G. (1999a) Biogenic amines in the brain of the honeybee: cellular distribution, development, and behavioral functions. Microscopy Research and Technique. 44:166–178.

Bicker G. (1999b) Histochemistry of classical neurotransmitters in antennal lobes and mushroom bodies of the honeybee. Microscopy Research and Technique. 45:174–183.

Biffar L., Stollewerk A. (2014) Conservation and evolutionary modifications of neuroblast expression patterns in insects. Developmental Biology. 388:103–116.

Binzer M., Heuer C.M., Kollmann M., Kahn J., Hauser F., Grimmelikhuijzen C.J.P., Schachtner J. (2014) Neuropeptidome of *Tribolium castaneum* antennal lobes and mushroom bodies. Journal of Comparative Neurology. 522:337–357.

Bohbot J., Pitts R.J., Kwon H-W., Rützler M., Robertson H.M., Zwiebel L.J. (2007) Molecular characterization of the Aedes aegypti odorant receptor gene family. Insect Molecular Biology. 16:525–537.

Bonneton F. (2008). The beetle by the name of Tribolium: typology and etymology of *Tribolium castaneum* Herbst, 1797. Insect Biochemistry and Molecular Biology. 38:377–37910.

Borden J.H. (1985) Aggregation pheromones. In: KerkutGA, ed. Comprehensive insect physiology, biochemistry and pharmacology. Vol. 9: Behavior. Oxford, UK: Pergamon Press, 257–285.

Boyan G., Williams L. (2011) Embryonic development of the insect central complex: insights from lineages in the grasshopper and Drosophila. Arthropod Structure and Development: 40:334–348.

Boyan G.S., Reichert H. (2011) Mechanisms for complexity in the brain: generating the insect central complex. Trends in Neurosciences. 34:247–257.

Brandt R., Rohlfing T., Rybak J., Krofczik S., Maye A., Westerhoff M., Hege H. C., Menzel R. (2005) Three-dimensional average-shape atlas of the honeybee brain and its applications. Journal of Comparative Neurology. 492:1–1910.

Breidbach O., Wegerhoff R. (1994) FMRFamide-like immunoreactive neurons in the brain of the beetle, *Tenebrio molitor* L. (coleoptera – tenebrionidae): constancies and variations in development from the embryo to the adult. International Journal of Insect Morphology and Embryology. 4:383-404.

Brody T., Odenwald W.F. (2005) Regulation of temporal identities during *Drosophila* neuroblast lineage development. Current Opinion in Cell Biology. 17:672–675

Brown S. J., Shippy T. D., Miller S., Bolognesi R., Beeman R. W., Lorenzen M. D., Bucher G., Wimmer E. A., Klingler M. (2009) The red flour beetle, *Tribolium castaneum* (Coleoptera): a model for studies of development and pest biology. Cold Spring Harbor Protocols. pdb.emo126. doi: 10.1101/pdb.emo126.

Brown S.J., Denell R.E., Beeman R.W. (2003) Beetling around the genome. Genetics Research. 82:155–161.

Bucher G. (2009) The beetle book. Available online at http://wwwuser.gwdg.de/~gbucher1/tribolium-

castaneum-beetle-book1.pdf [Zuletzt abgerufen: 15.09. 2015].

Bucher G., Scholten J., Klingler M. (2002) Parental RNAi in Tribolium (Coleoptera). Current Biology. 12:85–86.

Carlsson M.A., Diesner M., Schachtner J., Nässel D. (2010) Multiple neuropeptides in the *Drosophila* antennal lobe suggest complex modulatory circuits. Journal of Comparative Neurology. 518:3359-3380.

Carpenter G.H. (1928) The Biology of Insects. Sidgwick and Jackson, London.

Cazzamali G., Saxild N., Grimmelikhuijzen C.J.P (2002) Molecular cloning and functional expression of a *Drosophila* corazonin receptor. Biochemical and Biophysical Research Communications. 298:31–36.

Chapman A.D. (2009) Numbers of living species in Australia and the world. Toowoomba, Australia: 2nd edition. Australian Biodiversity Information Services. Available online at http://155.187.2.69/biodiversity/abrs/publications/other/species-numbers/2009/pubs/nlsaw-2nd-complete.pdf [Zuletzt abgerufen: 19.10.2015].

Chen X., Ganetzky B. (2012) A neuropeptide signaling pathway regulates synaptic growth in Drosophila. The Journal of Cell Biology. 196:529–543.

Chou Y.H., Spletter M.L., Yaksi E., Leong J.C., Wilson R.I., Luo L. (2010) Diversity and wiring variability of olfactory local interneurons in the *Drosophila* antennal lobe. Nature Neuroscience. 13:439–449.

Connolly J.B., Roberts I.J., Armstrong J.D., Kaiser K., Forte M., Tully T., O'Kane C.J. (1996). Associative learning disrupted by impaired G_s signaling in *Drosophila* mushroom bodies. Science. 274:2104-2107.

Cox G.W. (1999). Alien Species in North America and Hawaii: Impacts on Natural Ecosystems. Island Press, Washington.

Cox P.D., Collins L.E. (2002) Factors affecting the behaviour of beetle pests in stored grain, with particular reference to the development of lures. Journal of Stored Products Research. 38:95–115.

Crowson RA. (1981), The Biology of Coleoptera, Academic Press, London.

Dacks A.M., Christensen T.A., Hildebrand J.G. (2006) Phylogeny of a serotonin-immunoreactive neuron in the primary olfactory center of the insect brain. Journal of Comparative Neurology. 498:727–746.

Dahanukar A., Foster K., van der Goes van Naters W.M., Carlson J.R. (2001) A Gr receptor is required for response to the sugar trehalose in taste neurons of *Drosophila*. Nature Neuroscience 4:1182–1186.

Dahanukar A., Hallem E.A., Carlson J.R. (2005) Insect chemoreception. Current Opinion in Neurobiology. 15:423–430.

Davis R.L. (2004) Olfactory learning. Neuron. 44:31-48.

de Belle J.S., Heisenberg M. (1994) Associative odor learning in *Drosophila* abolished by chemical ablation of mushroom bodies. Science. 263:692-695.

De Bruyne M., Smart R., Zammit E., Warr C.G. (2010) Functional and molecular evolution of olfactory neurons and receptors for aliphatic esters across the *Drosophila* genus. Journal of Comparative Physiology A. 196:97–109.

De Guzman L.I., Frake A.M., Rinderer T.E., Arbogast R.T. (2011) Effect Of Height and Color on the Efficiency of Pole Traps for *Aethina tumida* (Coleoptera: Nitidulidae). Journal of Economic Entomology. 104:26-31.

Dicke M. (2009) Behavioural and community ecology of plants that cry for help. Plant, Cell and Environment.32:654–665.

Dippel S., Kollmann M., Oberhofer G., Montino A., Knoll C., Krala M., Rexer K-H., Frank S., Kumpf R., Schachtner .J, Wimmer E.A. (eingereicht in eLife, 12.05.2016) Morphological and Transcriptomic Analysis of a Beetle Chemosensory System Reveals a Gnathal Olfactory Center. Re-Sumbitted in eLife.

Dreyer D., Vitt H., Dippel S., Goetz B., El Jundi B., Kollmann M., Huetteroth W., Schachtner J. (2010) 3D Standard Brain of the Red Flour Beetle Tribolium Castaneum: A Tool to Study Metamorphic Development and Adult Plasticity. Frontiers in Systems Neuroscience. 4:3.

Dubnau J., Grady L., Kitamoto T., Tully T. (2001) Disruption of neurotransmission in Drosophila mushroom body blocks retrieval but not acquisition of memory. Nature. 411:476-480.

Egger B., Chell J.M., Brand A.H. (2008) Insights into neural stem cell biology from flies. Philosophical Transactions of the Royal Society B. 363:39–56.

el Jundi B., Huetteroth W., Kurylas A. E., Schachtner J. (2009) Anisometric brain dimorphism revisited: implementation of a volumetric 3D standard brain in *Manduca sexta*. Journal of Comparative Neurology. 517:210–225.

Engsontia P., Sanderson A.P., Cobb M., Walden K.K.O., Robertson H.M., Brown S. (2008) The red flour beetle's large nose: an expanded odorant receptor gene family in *Tribolium castaneum*. Insect Biochemistry and Molecular Biology. 38:387–397.

Erber J., Masuhr T., Menzel R. (1980) Localization of short-term memory in the brain of the bee, *Apis mellifera*. Physiological Entomology. 5:343-358.

Ernst D.K.D., Boeckh J., Boeckh V. (1977) A neuroanatomical study on the organization of the central antennal pathways in insects. Cell and Tissue Research. 176:285–308.

Farris S.M. (2005) Evolution of insect mushroom bodies: old clues, new insights. Arthropod Structure and Development. 34:211-234.

Farris S.M. (2008) Tritocerebral tract input to the insect mushroom bodies. Arthropod Structure and Development. 37:492–503

Farris S.M., Roberts N.S. (2005) Coevolution of generalist feeding ecologies and gyrencephalic mushroom bodies in insects. Proceedings of the National Academy of Sciences of the United States of America. 102:17394–17399.

Farris S.M., Strausfeld N.J. (2003) A unique mushroom body substructure common to both basal cockroaches and to termites. Journal of Comparative Neurology. 456: 305–320

Fera (2012) Exploring the economic consequences of Epitrix spp. establishing across main crop potato production in England and options to reduce the likelihood of their introduction. Available online at http://s3.amazonaws.com/zanran_storage/ewda.csl.gov.uk/ContentPages/2522759539.pdf [Zuletzt abgerufen: 28.08.2015].

Fiala A., Müller U., Menzel R. (1999) Reversible downregulation of protein kinase A during olfactory learning using antisense technique impairs long-term memory formation in the honeybee, *Apis mellifera*. Journal of Neuroscience. 19:10125-10134.

Fonta C., Sun XJ., Masson C. (1993) Morphology and spatial-distribution of bee antennallobe interneurons responsive to odors. Chemical Senses. 18:101–119.

Foottit R.G., Adler P.H. (2009). Insect biodiversity: science and society. Oxford (UK): Wiley-Blackwell.

Friedrich M., Rambold I., Melzer R.R. (1996) The early stages of ommatidial development in the flour beetle *Tribolium castaneum* (Coleoptera; Tenebrionidae). Development Genes and Evolution. 206:136-146.

Fusca D., Schachtner J., Kloppenburg P. (2015) Colocalization of allatotropin and tachykinin-related peptides with classical transmitters in physiologically distinct subtypes of olfactory local interneurons in the cockroach (*Periplaneta americana*). Journal of Comparative Neurology. 523:1569-1586.

Gade G., Hoffmann K.H., Spring J.H. (1997) Hormonal regulation in insects: facts, gaps, and future directions. Physiological Reviews. 77:963–1032.

Galizia C.G., McIlwrath S.L., Menzel R. (1999) A digital three-dimensional,atlas of the honeybee antennal lobe based on optical sections acquired, by confocal microscopy. Cell and Tissue Research. 295:383–394.

Galizia C.G., Rössler W. (2010) Parallel Olfactory Systems in Insects: Anatomy and Function. Annual Review of Entomology. 55:399–420.

Gatellier L., Nagao T., Kanzaki R. (2004) Serotonin modifies the sensitivity of the male silkmoth to pheromone. Journal of Experimental Biology. 207:2487–2496.

Getahun M.N., Olsson S.B., Lavista-Llanos S. Hansson, B.S. & Wicher, D. (2013) Insect Odorant Response Sensitivity Is Tuned by Metabotropically Autoregulated Olfactory Receptors. PLoS ONE 8:e58889. doi: 10.1371/journal.pone.0058889

Ghaninia M., Hansson BS., Ignell R. (2007) The antennal lobe of the African malaria mosquito, *Anopheles gambiae* – innervation and three-dimensional reconstruction. Arthropod Structure and Development, 36:23–39.

Glenner H., Thomsen P.F., Hebsgaard M.B., Sørensen M.V., Willerslev E. (2006) The Origin of Insects. Science. 314:1883–1884.

Graham J.R., Ellis J.D., Carroll M.J., Teal P.E.A. (2011) *Aethina tumida* (Coleoptera: Nitidulidae) attraction to volatiles produced by *Apis mellifera* (Hymenoptera: Apidae) and *Bombus impatiens* (Hymenoptera: pidae) colonies. Apidologie. 3:326–336.

Greco M.K., Hoffmann D., Dollin A., Duncan M., Spooner-Hart R., Neumann P. (2010) The alternative Pharaoh approach: stingless bees mummify beetle parasites alive. Naturwissenschaften. 97:319-323.

Grimaldi D., Engel M.S. (2005) Evolution of the Insects. Cambridge University Press, Cambridge.

Ha T.S., Smith D.P. (2009) Odorant and pheromone receptors in insects. Frontiers in cellulare neuroscience. doi: 10.3389/neuro.03.010.2009.

Halcroft M., Spooner-Hart R., Neumann P. (2011) Behavioural defence strategies of the stingless bee, Austroplebeia australis, against the small hive beetle, Aethina tumida. Insectes Sociaux. 58: 245-253.

Halter D.A., Urban J., Rickert C., Ner S.S., Ito K., Travers A.A., Technau G.M. (1995). The homeobox gene repo is required for the differentiation and maintenance of glia function in the embryonic nervous system of *Drosophila melanogaster*. Development. 121:317-332.

Hammer M. (1993) An identified neuron mediates the unconditioned stimulus in associative olfactory learning in honeybees. Nature. 366:59-63.

Hammer M., Menzel R. (1998). Multiple sites of associative odor learning as revealed by local brain microinjections of octopamine in honeybees. Learning and Memory. 5:146-156.

Hansen K.K., Stafflinger E., Schneider M., Hauser F., Cazzamali G., Williamson M., Kollmann M., Schachtner J., Grimmelikhuijzen C.J. (2010) Discovery of a novel insect neuropeptide signaling system, closely related to the insect adipokinetic hormone and corazonin hormonal systems. The Journal of Biological Chemistry. 285:10736-10747.

Hansson B.S., Anton S. (2000) Function and morphology of the antennal lobe: new developments. Annual Review of Entomology. 45: 203–231.

Hansson B.S., Stensmyr M.C. (2011) Evolution of Insect Olfaction. Neuron. 72: 698-711.

Hanström B. (1940) Inkretorische Organe, Sinnesorgane, und Nervensystemen des Kopfes einiger niederer Insektenordnungen. Kungl/Svenska Vetenskapsakademiens Handlingar. 18:8.

Hartenstein V., Spindler S., Pereanu W., Fung S. (2008) The development of the *Drosophila* larval brain. Advances in Experimental Medicine and Biology. 628:1–31.

Hauser F., Cazzamali G., Williamson M. Park Y., Li B., Tanaka Y., Predel R., Neupert S., Schachtner J., Verleyen P., Grimmelikhuijzen C.J.P. (2008) A genome-wide inventory of neurohormone GPCRs in the red flour beetle *Tribolium castaneum*. Frontiers in Neuroendocrinology. 29:142–165.

Hauser F., Cazzamali G., Williamson M., Blenau W. and Grimmelikhuijzen C.J.P. (2006) A review of neurohormone GPCRs present in the fruitfly *Drosophila melanogaster* and the honey bee *Apis mellifera*. Progress in Neurobiology. 80:1–19.

Hauser F., Cazzamali G., Williamson M., Park Y., Li B., Tanaka Y., Predel R., Neupert S., Schachtner J., Verleyen P., Grimmelikhuijzen C. (2008). A genome-wide inventory of neurohormone GPCRs in the red flour beetle *Tribolium castaneum*. Frontiers in Neuroendocrinology. 29:142–165.

Hauser F., Neupert S., Williamson M., Predel R., Tanaka Y., Grimmelikhuijzen C.J.P. (2010) Genomics and peptidomics of neuropeptides and protein hormones present in the parasitic wasp Nasonia vitripennis. Journal of Proteome Research. 9:5296–5310.

Heimbeck G., Bugnon V., Gendre N., Keller A., Stocker R.F. (2001) A central neural circuit for experience-independent olfactory and courtship behavior in *Drosophila melanogaster*. Proceedings of the National Academy of Sciences of USA. 98:15336-15341.

Heisenberg M. (1998) What do the mushroom bodies do for the insect brain? An introduction. Learning and Memory. 5:1-10.

Heisenberg M. (2003) Mushroom body memoir: from maps to models. Nature Reviews Neuroscience. 4:266-75.

Heisenberg M., Borst A, Wagner S., Byers D. (1985) *Drosophila* mushroom body mutants are deficient in olfactory learning. Journal of Neurogenetics. 2:1-30.

Hendel T., Nagel G., Buchner E., Fiala A. (2006) Light-induced activation of distinct modulatory neurons triggers appetitive or aversive learning in *Drosophila* larvae. Current Biology: 16:1741-1747.

Herbst C., Baier B., Tolasch T., Steidle J.L.M. (2011) Demonstration of Sex Pheromones in the Predaceous Diving Beetle, *Rhantus suturalis* (MacLeay, 1825) (Dytiscidae). Chemoecology. 21:19–23.

Hergarden A.C., Tayler T.D., Anderson D.J. (2012) Allatostatin-A neurons inhibit feeding behavior in adult Drosophila. Proceedings of the National Academy of Sciences of the United States of America. 109:3967–3972.

Heuer C.M., Kollmann M., Binzer M., Schachtner J. (2012). Neuropeptides in insect mushroom bodies. Arthropod Structure and Development. 41:199–226.

Hill E.S., Okada K., Kanzaki R. (2003) Visualization of modulatory effects of serotonin in the silkmoth ntennal lobe. The Journal of Experimental Biology. 206:345–352.

Hinke W. (1961) Das relative postembryonale Wachstum der Hirnteile von *Culex pipiens*, *Drosophila melanogaster* und *Drosophila*-Mutanten. Zeitschrift für Morphologie und Ökologie der Tiere. 50:81-118.

Hodgson E.S. (1953) A Study of Chemoreception in Aqueous and Gas Phases. The Biological Bulletin. 105:115–127.

Hofer S., Dircksen H., Tollbäck P., Homberg U. (2005) Novel insect orcokinins: Characterization and neuronal distribution in the brains of selected dicondylian insects. Journal of Comparative Neurology. 490:57–71.

Homberg U. (2002) Neurotransmitters and neuropeptides in the brain of the locust. Microscopy Research and Technique. 56:189–209.

Homberg U. (2008) Evolution of the central complex in the arthropod brain with respect to the visual system. Arthropod Structure and Development. 37:347–362.

Homberg U., Christensen T.A., Hildebrand J.G. (1989) Structure and function of the deutocerebrum in insects. Annual Review of Entomolog. 34:477-501.

Homberg U., Müller U. (1999) Neuroactive substances in the antennal lobe. In: Hansson B.S. (Ed.), Insect Olfaction. Springer Berlin, Heidelberg.

Hu J.H., Wang Z.Y., Sun F. (2011) Anatomical organization of antennal-lobe glomeruli in males and females of the scarab beetle *Holotrichia diomphalia* (Coleoptera: Melolonthidae). Arthropod Structure and Development. 40:420–428.

Hummel T., Zipursky SL. (2004) Afferent induction of olfactory glomeruli requires N-cadherin. Neuron. 42:77–88.

Hungerford T.G. (1990) Diseases of Livestock. McGraw-Hill, Sydney.

Hunt T., Bergsten J., Levkanicova Z., Papadopoulou A., John OS., Wild R., Hammond P.M., Ahrens D., Balke M., Caterino M.S., Gómez-Zurita J., Ribera I., Barraclough T.G., Bocakova M., Bocak L., Vogler, A.P. (2007) A comprehensive phylogeny of beetles reveals the evolutionary origins of a superradiation. Science 318:1913–1916.

Husch A., Paehler M., Fusca D., Paeger L., Kloppenburg P. (2009) Distinct electrophysiological properties in subtypes of nonspiking olfactory local interneurons correlate with their cell type-specific Ca^{2+} current profiles. Journal of Neurophysiology. 29:11582-11592.

i5K Konsortium (2013) The i5K Initiative: advancing arthropod genomics for knowledge, human health, agriculture, and the environment. Journal of Heredity. 104:595-600.

Ignell R., Anton S., Hansson B.S. (2000) The maxillary palp sensory pathway of Orthoptera. Arthropod Structure and Development. 29:295–305.

Ignell R., Anton S., Hansson S.B. (2001) The Antennal Lobe of Orthoptera – Anatomy and Evolution. Brain, Behavior and Evolution. 57:1–17.

Ignell R., Dekker T., Ghaninia M., Hansson BS. (2005) Neuronal architecture of the mosquito deutocerebrum. Journal of Comparative Neurology. 493: 207–240.

Ignell R., Root C.M., Birse R.T., Wang J.W., Nässel D.R., Winther Å.M. (2009) Presynaptic peptidergic modulation of olfactory receptor neurons in *Drosophila*. Proceedings of the National Academy of Sciences of the United States of America. 106:13070–13075.

Iperti G. (1965) Perspective d'utilisation rationnelle des coccinelles aphidiphages dans la protection des cultures. 90e Congrès national des sociétés savantes. Nice 2:544-555.

Ito K., Shinomiya K., Ito M., Armstrong J.D., Boyan G., Hartenstein V., Harzsch S., Heisenberg M., Homberg U., Jenett A., Keshishian H., Restifo L.L., Rossler W., Simpson J.H., Strausfeld N.J., Strauss R., Vosshall L.B. (2014) A systematic nomenclature for the insect brain. Neuron. 81:755–765.

Jefferis G.S.X.E. (2005) Insect Olfaction: A Map of Smell in the Brain. Current Biolegy. 15:668–670.

Jefferis G.S.X.E., Potter C.J., Chan A.M., Marin E.C., Marin E.C., Rohlfing T., Maurer Jr C.R., Luo L. (2007) Comprehensive maps of Drosophila higher olfactory centers: spatially segregated fruit and pheromone representation. Cell. 128:1187–1203.

Johansson B.G., Jones T.M. (2007) The role of chemical communication in mate choice. Biological Reviews. 82:265–289.

Jortner R.A., Farivar S.S., Laurent G. (2007) A simple connectivity scheme for sparse coding in an olfactory system. Journal of Neuroscience. 27:1659-1669.

Kaupp U.B. (2010) Olfactory signalling in vertebrates and insects: differences and commonalities. Nature Reviews Neuroscience. 11:188-200.

Kim H.S., Murphy T., Xia J., Caragea D., Park Y., Beeman R.W., Lorenzen M.D., Butcher S., Manak J.R., Brown S.J. (2010) BeetleBase in 2010: revisions to provide comprehensive genomic information for Tribolium castaneum. Nucleic Acids Research. 38:D437–442.

Klagges B.R., Heimbeck G., Godenschwege T.A., Hofbauer A., Pflugfelder G.O., Reifegerste R., Reisch D., Schaupp M., Buchner S., Buchner E. (1996) Invertebrate synapsins: a single gene codes for several isoforms in *Drosophila*. The Journal of Neuroscience. 16:3154-165.

Kloppenburg P., Hildebrand J.G. (1995) Neuromodulation by 5-hydroxytryptamine in the antennal lobe of the sphinx moth *Manduca sexta*. Journal of Experimental Biology. 198:603–611.

Kollmann M., Rupenthal A.L., Neumann P., Huetteroth W., Schachtner J. (2016). Novel antennal lobe substructures revealed in the small hive beetle *Aethina tumida*. Cell and tissue research. 363:679-692.

Kollmann M., Schmidt R., Heuer C.M., Schachtner J. (eingereicht in Plos Biology, 2016.05.19) Variations

on a theme: antennal lobe architecture across Coleoptera. Sumbitted in PLOS Biology.

Koniszewski N.D.B., Kollmann M., Bigham M., Farnworth M., He B., Büscher M., Hütteroth W., Binzer M., Schachtner J., Bucher G. (2016). The insect central complex as model for heterochronic brain development—background, concepts, and tools. Development genes and evolution. 226:209-219.

Koontz M.A., Schneider D. (1987) Sexual dimorphism in neuronal projections from the antennae of silk moths (*Bombyx mori, Antherea polyphemus*) and the gypsy moth (*Lymantria dispar*). Cell and Tissue Research. 249:39–50.

Kukalova-Peck J., Beutel R.G. (2012) Is the Carboniferous† *Adiphlebia lacoana* really the "oldest beetle"? Critical reassessment and description of a new Permian beetle family. European Journal of Entomology. 109:633-645.

Kurylas A. E., Rohlfing T., Krofczik S., Jenett A., Homberg U. (2008) Standardized atlas of the brain of the desert locust, *Schistocerca gregaria*. Cell and Tissue Research. 333:125–14510.

Kutsch W., Breidbach O. (1994). Homologous structures in the nervous systems of Arthropoda. In: Evans P.D. (Ed.), Advances in Insect Physiology 24. TJ Press Ltd, Padstow.

Larsson M.C., Hansson B.S., Strausfeld N.J. (2004) A simple mushroom body in an African scarabid beetle. Journal of Comparative Neurology. 478:219–232.

Laska M., Galizia C.G., Giurfa M., Menzel R. (1999) Olfactory discrimination ability and odor structure-activity relationships in honeybees. Chemical Senses. 24:429–438.

Laughlin J.D., Ha T.S., Jones D.N., Smith D.P. (2008) Activation of pheromone-sensitive neurons is mediated by conformational activation of pheromone-binding protein. Cell. 133:1255–1265.

Leal W.S. (2013) Odorant Reception in Insects: Roles of Receptors, Binding Proteins, andegrading Enzymes. Annual Review of Entomology. 58:373–391.

Li B., Predel R., Neupert S., Hauser F., Tanaka Y., Cazzamali G., Williamson M., Arakane Y., Verleyen P., Schoofs L., Schachtner J., Grimmelikhuijzen C.J.P., Park Y. (2008) Genomics, transcriptomics, and peptidomics of neuropeptides and protein hormones in the red flour beetle *Tribolium castaneum*. Genome Research. 18:113–122.

Linn C.E., Roelofs W.L. (1986) Modulatory effects of octopamine and serotonin on male sensitivity and periodicity of response to sex pheromone in the cabbage looper moth, *Trichoplusia ni*. Archives of Insect Biochemistry and Physiology. 3:161–171.

Linz J., Baschwitz A., Strutz A., Dweck H.K.M., Sachse S., Hansson B.S., Stensmyr, M.C. (2013) Host plant-driven sensory specialization in Drosophila erecta. Proceedings of the Royal Society B: Biological Sciences. 280:20130626. doi:10.1098/rspb.2013.0626

Liu M., Yu H., Li G. (2008) Oviposition deterrents from eggs of the cotton bollworm, *Helicoverpa armigera* (Lepidoptera: Noctuidae): chemical identification and analysis by electroantennogram. Journal of Insect Physiology. 54:656–662.

Loesel R., Nässel D.R., Strausfeld N.J. (2002) Common design in a unique midline neuropil in the brains of arthropods. Arthropod Structure and Development. 31:77–91.

Lundie A.E. (1940) The small hive beetle, *Aethina tumida*. South African Department of Agriculture and Forestry. 220:30.

Majer J.D. (1987) The conservation and study of invertebrates in remnants of native vegetation. In: Saunders D.A., Arnold G.W., Burbridge A.A., Hopkins A.J.M. (Ed). Nature Conservation: The Role of Remnants of Native Vegetation. Surrey Beatty and Sons, Sydney.

Martin F, Alcorta E (2011) Regulation of olfactory transduction in the orco channel. Front Cell Neurosci. 5:21. doi: 10.3389/fncel.2011.00021

Mcguire S.E., Le P.T., Davis R.L. (2001) The role of *Drosophila* mushroom body signaling in olfactory memory. Science. 10:1126-1129.

Menzel R. (2001) Searching for the memory trace in a mini-brain, the honeybee. Learning and Memory. 8:53-62.

Meusemann K., Reumont B.M. von, Simon S., Roeding F., Strauss S., Kück P., Ebersberger I., Walzl M., Pass G., Breuers S., Achter V., Haeseler A. von, Burmester T., Hadrys H., Wägele J.W., Misof B. (2010) A phylogenomic approach to resolve the arthropod tree of life. Molecular Biology and Evolution. 27:2451–2464.

Misof B., Niehuis O., Bischoff I., Rickert A., Erpenbeck D., Staniczek A. (2007) Towards an 18S phylogeny of hexapods: accounting for group-specific character covariance in optimized mixed nucleotide/doublet models. Zoology. 110:409–429.

Missbach C., Dweck HK., Vogel H., Vilcinskas A., Stensmyr M.C., Hansson B.S., Grosse-Wilde E. (2014) Evolution of insect olfactory receptors. eLife. doi: 10.7554/eLife.02115

Muirhead J.R., Leung B., Overdijk C., Kelly D.W., Nandakumar K., Marchant K.R., MacIsaac H.J. (2006) Modelling local and long-distance dispersal of invasive emerald ash borer *Agrilus planipennis* (Coleoptera) in North America. Diversity and Distributions. 12:71–79.

Müller J., Bussler H., Gossner M., Rettelbach T., Duelli P. (2008) The European spruce bark beetle *Ips typographus* in a national park: from pest to keystone species. Biodiversity and Conservation. 17:979–3001.

Müller U. (1997) The nitric oxide system in insects. Progress in Neurobiology. 51:363–381.

Mutinelli F., Montarsi F., Federico G., Granato A., Ponti A.M., Grandinetti G., Ferrè N., Franco S., Duquesne V., Rivière M-P., Thiéry R., Henrikx P., Ribière-Chabert M., Chauzat M-P. (2014) Detection of *Aethina tumida* Murray (Coleoptera: Nitidulidae.) in Italy: outbreaks and early reaction measures. Journal of Apicultural Research. 53: 569-575.

Myers J.H., Hosking G. (2002) Eradication. In: Hallman G.J., Schwalbe C.P. (Ed). Invasive Arthropods in Agriculture: Problems and Solutions. Oxford and IBH Publishing, New Delhi.

Mysore K., Subramanian K.A., Sarasij R.C., Suresh A., Shyamala B.V., VijayRaghavan K., Rodrigues V. (2009) Caste and sex specific olfactory glomerular organization and brain architecture in two sympatric ant species, *Camponotus sericeus* and *Camponotus compressus* (Fabricius, 1798). Arthropod Structure and Development. 38:485–497.

Nakakita H. (1982) Effect of larval density on pupation of *Tribolium freemani* Hinton (Coleoptera: Tenebrionidae). Applied Entomology and Zoology. 17:269–276.

Nässel D.R. (1999) Tachykinin-related peptides in invertebrates: a review. Peptides. 20:141-158.

Nässel D.R. (2002) Neuropeptides in the nervous system of *Drosophila* and other insects: multiple roles as neuromodulators and neurohormones. Progress in Neurobiology. 68:1–84.

Nässel D.R., Homberg U. (2006). Neuropeptides in interneurons of the insect brain. Cell and Tissue Research. 326:1-24.

Nässel D.R., Winther A.M.E. (2010) *Drosophila* neuropeptides in regulation of physiology and behavior. Progress in Neurobiology. 92:42-104.

Neder R. (1959) Allometrisches Wachstum von Hirnteilen bei drei verschieden grossen Schabenarten. Zoologische Jahrbücher. Abteilung für Anatomie und Ontogenie der Tiere. 77:411-464.

Neumann P., Ellis J.D. (2008) The small hive beetle (*Aethina tumida* Murray, Coleoptera: Nitidulidae): distribution, biology and control of an invasive species. Journal of Apicultural Research. 47:181–183.

Neumann P., Elzen P.J. (2004) The biology of the small hive beetle (*Aethina tumida* Murray, Coleoptera: Nitidulidae): Gaps in our knowledge of an invasive species. Apidologie. 35:229–247.

Neupert S., Fusca D., Schachtner J., Kloppenburg P., Predel R. (2012) Towards a Single-cell-based analysis of neuropeptide expression in *Periplaneta americana* antennal lobe neurons. Journal of Comparative Neurology. 520:694-716.

Neupert S., Fusca D., Schachtner J., Kloppenburg P., Predel R. (2012) Towards a single-cell-based analysis of neuropeptide expression in *Periplaneta americana* antennal lobe neurons. Journal of Comparative Neurology. 520:694–716.

Nolte, A., Funk, N.W., Mukunda, L., Gawalek, P., Werckenthin, A., Hansson, B.S., Wicher D., Stengl, M. (2013) In situ Tip-Recordings Found No Evidence for an Orco-Based Ionotropic Mechanism of Pheromone-Transduction in *Manduca sexta*. PLoS ONE. 8:e62648. doi: 10.1371/journal.pone.0062648

Nowak D.J., Pasek J.E., Sequeira R.A., Crane D.E., Mastro V.C. (2001) Potential effect of *Anoplophora glabripennis* (Coleoptera: Cerambycidae) on urban trees in the United States. Journal of Economic Entomology. 94: 116–122.

Okada R., Awasaki T., Ito K. (2009) Gamma-aminobutyric acid (GABA)-mediated neural connections in the *Drosophila* antennal lobe. Journal of Comparative Neurology. 514:74–91.

Paczkowski S., Paczkowska M., Dippel S., Flematti G., Schütz S. (2014) Volatile Combustion Products of Wood Attract *Acanthocnemus nigricans* (Coleoptera: Acanthocnemidae). Journal of Insect Behavior. 27:228–238.

Panov A.A. (1959) Structure of the insect brain at successive stages of postembryonic development. II. the central body. Entomological Review. 38:276–283.

Panov A.A. (2013) Not All Dytiscidae Have Poorly Developed Mushroom Bodies: The Enigma of Cybister lateralimarginalis. Entomological Review. 94:654–663.

Park Y., Kim YJ., Adams M.E. (2002) Identification of G protein-coupled receptors for *Drosophila* PRXamide peptides, CCAP, corazonin, and AKH supports a theory of ligand-receptor coevolution. Proceedings of the National Academy of Sciences of the United States of America. 99:11423–11428.

Peel A.D. (2009) Forward genetics in *Tribolium castaneum*: opening new avenues of research in arthropod biology. Journal of Biology. 8:106.

Perez-Orive J., Mazor O., Turner G.C., Cassenaer S., Wilson R.I., Laurent G. (2002) Oscillations and sparsening of odor representations in the mushroom body. Science. 297:359-365.

Perlak F.J., Stone T.B., Muskopf Y.M., Petersen L.J., Parker G.B., McPherson S.A., Wyman J., Love S., Reed G., Biever D., Fischhoff D.A. (1993) Genetically improved potatoes: protection from damage by Colorado potato beetles. Plant Molecular Biology. 22:313–321.

Pfeiffer K., Homberg U. (2014) Organization and functional roles of the central complex in the insect brain. Annual Review of Entomology. 59:165–184.

Piersanti S., Frati F., Conti E., Gaino E., Rebora M., Salerno G. (2014) First evidence of the use of olfaction in Odonata behaviour. Journal of Insect Physiology. 62:26–31

Posnien N., Koniszewski N.D.B., Hein H.J., Bucher G. (2011) Candidate Gene Screen in the Red Flour Beetle *Tribolium* Reveals Six3 as Ancient Regulator of Anterior Median Head and Central Complex Development. PLOS Genet. 7, e1002418.

Predel R., Neupert S., Wicher D., Gundel M., Roth S., Derst C. (2004) Unique accumulation of neuropeptides in an insect: FMRFamide-related peptides in the cockroach, *Periplaneta americana*. European Journal of Neuroscience. 20:1499–1513.

Rebora M., Piersanti S., Gaino E. (2008) The antennal sensilla of the adult of *Libellula depressa* (Odonata: Libellulidae). Arthropod Structure and Development. 37:504–510.

Rein K., Zöckler M., Mader M. T., Grübel C., Heisenberg M. (2002) The *Drosophila* standard brain. Current Biology. 12:227–231.

Renn S.C., Park J.H., Rosbash M., Hall J.C., Taghert P.H. (1999) A pdf neuropeptide gene mutation and ablation of PDF neurons each cause severe abnormalities of behavioral circadian rhythms in *Drosophila*. Cell. 99:791–802.

Richards et al.; The Tribolium Genome Sequencing Consortium (2008) The genome of the model beetle and pest *Tribolium castaneum*. Nature 452: 949–955.

Richter S., Loesel R., Purschke G., Schmidt-Rhaesa A., Scholtz G., Stach T., Vogt L., Wanninger A., Brenneis G., Döring C., Faller S., Fritsch M., Grobe P., Heuer C.M., Kaul S., Møller O.S., Müller C.H., Rieger V., Rothe B.H., Stegner M.E.J., Harzsch S. (2010) Invertebrate neurophylogeny: suggested terms and definitions for a neuroanatomical glossary. Frontiers in Zoology. 7:29.

Safranyik L., Carroll A.L., Regniere J., Langor D.W., Riel W.G., Shore T.L., Peter B., Cooke B.J., Nealis V.G., Taylor S.W. (2010) Potential for range expansion of mountain pine beetle into the boreal forest of North America. The Canadian Entomologist. 142:415–442.

Sarkar A., Mukherjee A., Barik A. (2013) Olfactory responses of *Epilachna dodecastigma* (Coleoptera: Coccinellidae) to long-chain fatty acids from Momordica charantia leaves. Arthropod-Plant Interactions. 7:339-348.

Sato K., Pellegrino M., Nakagawa T.,Nakagawa T., Vosshall LB., Touhara K. (2008) Insect olfactory receptors are heteromeric ligand-gated ion channels. Nature. 452:1002–1006.

Schachtner J., Schmidt M., Homberg U. (2005) Organization and evolutionary trends of primary olfactory brain centers in Tetraconata (Crustacea+Hexapoda). Arthropod Structure and Development. 34:257–299.

Schinko J.B., Hillebrand K., Bucher G. (2012) Heat shock-mediated misexpression of genes in the beetle *Tribolium castaneum*. Development Genes and Evolution. 222:287–298.

Schinko J.B., Weber M., Viktorinova I., Kiupakis A., Averof M., Klingler M., Wimmer E.A., Bucher G. (2010) Functionality of the GAL4/UAS system in *Tribolium* requires the use of endogenous core promoters. BMC Developmental Biology. 10:53.

Schmolke M.D. (1974) A study of *Aethina tumida*: the small Hive Beetle. Project Report, University of Rhodesia. pp 178

Schneider D., Kaissling KE. (1957) Der Bau der Antenne des Seidenspinners *Bombyx mori* L. II. Sensillen, cuticulare Bildungen und innerer Bau. Zoologische Jahrbücher / Abteilung für Anatomie und Ontogenie der Tiere. 76:224–250.

Schroll, C., Riemensperger, T., Bucher, D., Ehmer, J., Völler, T., Erbguth, K., Gerber, B., Hendel T., Nagel G., Buchner E., Fiala A. (2006) Light-induced activation of distinct modulatory neurons triggers appetitive or aversive learning in *Drosophila* larvae. Current Biology.16:1741-1747.

Schwaerzel M., Monastirioti M., Scholz H., Friggi-Grelin F., Birman S., Heisenberg M. (2003) Dopamine and octopamine differentiate between aversive and appetitive olfactory memories in *Drosophila*. The Journal of Neuroscience. 23:10495-10502.

Scrimgeour G.J., Culp J.M., Cash K.J. (1994) Antipredator responses of mayfly larvae to conspecific and predator stimuli. Journal of the North American Benthological Society. 13: 299-309.

Seidl R., Schelhaas M.J., Rammer W., Verkerk P.J. (2014) Increasing forest disturbances in Europe and their impact on carbon storage. Nature Climate Change. 4:806–810.

Seki Y., Kanzaki R. (2008) Comprehensive morphological identification and GABA immunocytochemistry of antennal lobe local interneurons in *Bombyx mori*. Journal of Comparative Neurology. 506:93–107.

Shanbhag S.R., Müller B., Steinbrecht R.A. (1999) Atlas of olfactory organs of *Drosophila melanogaste*r: 1. Types, external organization, innervation and distribution of olfactory sensilla. International Journal of Insect Morphology and Embryology. 28:377–397.

Shurin J.B., Gruner D.S., Hillebrand H. (2005) All wet or dried up? Real differences between aquatic and terrestrial food webs. Proceedings of the Royal Society. B. Biological Sciences. 273: 1–9.

Siju K.P., Schachtner J., Reifenrath A., Scheiblich H., Neupert S., Predel R., Hansson B., Ignell R. (2014) Neuropeptides in the antennal lobe of the yellow fever mosquito, *Aedes aegypti*. Journal of Neurophysiology. 522:592–608.

Simberloff (2003). Introduced insects. In: Resh V.H., Card'e R.T. (Ed). Encyclopedia of Insects. Academic Press, Amsterdam.

Sinakevitch I.T., Smith A.N., Locatelli F., Huerta R., Bazhenov M., Smith B.H. (2013) *Apis mellifera* octopamine receptor 1 (AmOA1) expression in antennal lobe networks of the honey bee *(Apis mellifera*) and fruit fly (*Drosophila melanogaster*). Frontiers in Systems Neuroscience. 7:70.

Sivinsky J. (1989) Mushroom body development in nymphalid butterflies: a correlate of learning? Journal of Insect Behavior. 2:277–283.

Skeath J.B., Thor S. (2003) Genetic control of Drosophila nerve cord development. Current Opinion in Neurobiology. 13:8–15.

Slessor K.N., Winston M.L., Le Conte Y. (2005) Pheromone communication in the honeybee (*Apis mellifera* L.). Journal of Chemical Ecology. 31:2731–2745.

Smart R., Kiely A., Beale M., Vargas E., Carraher C., Kralicek A.V., Christie D.L., Chen C., Newcomb R.D., Warr C.G. (2008) *Drosophila* odorant receptors are novel seven transmembrane domain proteins that can signal independently of heterotrimeric G proteins. Insect Biochemistry and Molecular Biology. 38:770–780.

Spiewok S., Neumann P. (2006) Infestation of commercial bumblebee (*Bombus impatiens*) field colonies by small hive beetles (*Aethina tumida*). Ecological Entomology. 31: 623-628.

Stadelmann G., Bugmann H., Meier F., Wermelinger B., Bigler C. (2013) Effects of salvage logging and sanitation felling on bark beetle (*Ips typographus* L.) infestations. Forest Ecology and Management. 305:273-281.

Stafflinger E., Hansen K.K., Hauser F., Schneider M., Cazzamali G., Williamson M., Grimmelikhuijzen C.J.P. (2008) Cloning and identification of an oxytocin/vasopressin-like receptor and its ligand from insects. Proceedings of the National Academy of Sciences of the United States of America. 105:3262–3267.

Starausfeld N.J., Lee J.K. (1989) Structure, distribution and number of surface sensilla and their receptor cells on the olfactory appendage of the male moth *Manduca sexta*. Journal of Neurocytology. 19:519-538.

Staubli F., Jorgensen T.J., Cazzamali G., Williamson M., Lenz C., Sondergaard L., Roepstorff P., Grimmelikhuijzen C.J.P. (2002) Molecular identification of the insect adipokinetic hormone receptors. Proceedings of the National Academy of Sciences of the United States of America. 99:3446–3451.

Steinbrech R.A. (1997) Pore structures in insect olfactory sensilla: A review of data and concepts. International Journal of Insect Morphology and Embryology. 26:229–245.

Stengl M., Funk N.W. (2013) The role of the coreceptor Orco in insect olfactory transduction. Journal of Comparative Physiology A. 199:897–909.

Stensmyr M.C., Dweck H.K.M., Farhan A., Ibba I., Strutz A., Mukunda L., Linz J., Grabe V., Steck K., Lavista-Llanos S., Wicher D., Sachse S., Knaden M., Becher P.G., Seki Y., Hansson B.S. (2012) A Conserved Dedicated Olfactory Circuit for Detecting Harmful Microbes in *Drosophila*. Cell. 151:1345-1357.

Stocker R.F. (2001) *Drosophila* as a focus in olfactory research: mapping of olfactory sensilla by fine structure, odor specificity, odorant receptor expression, and central connectivity. Microscopy Research and Technique. 55:284–296.

Stollewerk A., Simpson P. (2005) Evolution of early development of the nervous system: a comparison between arthropods. Bioessays. 27:874–883.

Strausfeld N.J. (2005) The evolution of crustacean and insect optic lobes and the origin of chiasmata. Arthropod Structure and Development. 34:235-56.

Strausfeld N.J., Hansen L., Li Y., Gomez R.S., Ito K. (1998) Evolution, discovery, and interpretations of arthropod mushroom bodies. Learning and Memory. 5:11–37.

Strausfeld N.J., Sinakevitch I., Brown S.M., Farris S.M. (2009) Ground plan of the insect mushroom body: functional and evolutionary implications. Journal of Comparative Neurology. 513:265-291.

Strausfeld N.J., Sinakevitch I., Brown S.M., Farris S.M. (2009) Ground plan of the insect mushroom body: functional and evolutionary implications. Journal of Comparative Neurology. 513:265–291.

Strauss R. (2002). The central complex and the genetic dissection of locomotor behaviour. Current Opinion in Neurobiology. 12:633–638.

Strutz A., Soelter J., Baschwitz A., Farhan A., Grabe V., Rybak J., Knaden M., Schmuker M., Hansson B.S., Sachse S. (2014) Decoding odor quality and intensity in the *Drosophila* brain. eLife 3:e04147. doi: 10.7554/eLife.04147.

Suazo A., Torto B., Teal P.E.A., Tumlinson J.H. (2003) Response of the small hive beetle (*Aethina tumida*) to honey bee (*Apis mellifera*) and beehive-produced volatiles. Apidologie. 34:525–533.

Sun Y-L., Huang L-Q., Pelosi P., Wang C-Z. (2012) Expression in Antennae and Reproductive Organs Suggests a Dual Role of an Odorant-Binding Protein in Two Sibling Helicoverpa Species. PLoS ONE. 7: e30040. doi:10.1371/journal.pone.0030040

Tanaka N.K., Endo K., Ito K. (2012). Organization of antennal lobe-associated neurons in adult *Drosophila melanogaster* brain. Journal of Comparative Neurology. 520:4067–4130.

Tawfik A.I., Tanaka S., De Loof A., Schoofs L., Baggerman G., Waelkens E., Derua R., Milner Y., Yerushalm, Y., Pener M.P. (1999) Proceedings of the National Academy of Sciences of the United States of America. 96:7083–7087.

Technau G.M., Berger C., Urbach R. (2006) Generation of cell diversity and segmental pattern in the embryonic central nervous system of *Drosophila*. Developmental Dynamics. 235:861–869.

Tegoni M., Campanacci V., Cambillau C. (2004) Structural aspects of sexual attraction and chemical communication in insects. Trends in Biochemical Sciences. 29:257–264.

Terhzaz S., Rosay P., Goodwin S.F., Veenstra J.A. (2007) The neuropeptide SIFamide modulates sexual behavior in *Drosophila*. Biochemical and Biophysical Research Communications. 352:305–310.

Tomoyasu Y., Denell R.E. (2004). Larval RNAi in Tribolium (Coleoptera) for analyzing adult development. Development Genes and Evolution. 214:575–578.

Trauner J., Schinko J., Lorenzen M.D., Shippy T.D., Wimmer E.A., Beeman R.W., Klingler M., Bucher G., Brown S.J. (2009) Large-scale insertional mutagenesis of a coleopteran stored grain pest, the red flour beetle *Tribolium castaneum*, identifies embryonic lethal mutations and enhancer traps. BMC Biology 7:73.

Trhlin M., Rajchard J. (2011) Chemical communication in the honeybee (Apis mellifera L.): a review. Veterinarni Medicina. 56:265–273.

Unoki S., Matsumoto Y., Mizunami M. (2005) Participation of octopaminergic reward system and dopaminergic punishment system in insect olfactory learning revealed by pharmacological study. European Journal of Neuroscience. 22:1409-1416.

Urbach R., Technau G.M. (2004) Neuroblast formation and patterning during early brain development in *Drosophila*. Bioessays. 26:739–751.

Van Haeften T. (1993) Location and function of serotonin in the central and peripheral nervous system of the Colorado potato beetle. PhD Thesis. University of Wageningen, The Netherlands. (ISBN 1993 90 5485 141 4)

Veenstra J.A. (1989) Isolation and structure of corazonin, a cardioactive peptide from the American cockroach. FEBS Letters. 250:231–234.

Vermehren-Schmaedick A., Scudder C., Timmermans W., Morton D.B. (2011) *Drosophila* gustatory preference behaviors require the atypical soluble guanylyl cyclases. Journal of Comparative Physiology A. 197:717–727.

Visser J.H. (1986) Host Odor Perception in Phytophagous Insects. Annual Review of Entomology.31:121–144.

von Frisch, K. (1921) Über den Sitz des Geruchssinnes bei Insekten. Zoologische Jahrbücher / Abteilung für allgemeine Zoologie und Physiologie der Tiere. 38:1-368.

Vosshall L.B., Stocker R.F. (2007) Molecular architecture of smell and taste in *Drosophila*. Annual Review of Neuroscience. 30:505–533.

Wang L., Wang S., Li Y., Paradesi MS., Brown SJ. (2007) Beetle Base: the model organism database for Tribolium castaneum. Nucleic Acids Research: Oxford Journals. 35:0476–0479.

Wang, Y., Chiang, A.S., Xia, S., Kitamoto, T., Tully, T., Zhong, Y. (2003) Blockade of Neurotransmission in *Drosophila* Mushroom Bodies Impairs Odor Attraction, but Not Repulsion. Current Biology. 13:1900-1904.

Wegerhoff R., Breidbach O. (1992) Structure and development of the larval central complex in a holometabolous insect, the beetle *Tenebrio molitor*. Cell and Tissue Research. 268:341–358.

Weiss L.A., Dahanukar A., Kwon J.Y., Banerjee D., Carlson J.R. (2011) The Molecular and Cellular Basis of Bitter Taste in *Drosophila*. Neuron. 69:258–272.

Wessnitzer J., Webb B. (2006) Multimodal sensory integration in insects – towards insect brain control architectures. Bioinspiration and Biomimetics. 1:63–75.

Wheeler S.R., Carrico M.L., Wilson B A., Skeath J.B. (2005) The *Tribolium* columnar genes reveal conservation and plasticity in neural precursor patterning along the embryonic dorsal-ventral axis. Developmental Biology. 279**:**491–500.

Whiteman N.K., Pierce N.E. (2008) Delicious poison: genetics of *Drosophila* host plant preference. Trends in Ecology and Evolution. 23:473–478.

Wicher D., Schäfer R., Bauernfeind R., Stensmyr M.C., Heller R. Heinemann S.H., Hansson B.S. (2008) Drosophila odorant receptors are both ligand-gated and cyclic-nucleotide-activated cation channels. Nature. 452:1007–1011.

Wiegmann B.M., Trautwein M.D., Winkler I.S., Barr N.B., Kim J.W., Lambkin C., Bertone M.A., Cassel B.K., Bayless K.M., Heimberg A.M., Wheeler B.M., Peterson K.J., Pape T., Sinclair B.J., Skevington J.H., Blagoderov V., Caravas J., Kutty S.N., Schmidt-Ott U., Kampmeier G.E., Thompson F.C., Grimaldi D.A., Beckenbach A.T., Courtney G.W., Friedrich M., Meier R., Yeates D.K. (2011) Episodic radiations in the fly tree of life. Proceedings of the National Academy of Sciences of the United States of America. 208:5690–5695.

Winther Å.M.E., Ignell R. (2010) Local peptidergic signaling in the antennal lobe shapes olfactory behavior. Fly. 4:167–171.

Winther, Å.M.E., Acebes A., Ferrús A. (2006) Tachykinin-related peptides modulate odor perception and locomotor activity in *Drosophila*. Molecular and Cellular Neurosciences. 31:399-406.

Yamagata N., Nishino H., Mizunami M. (2007) Neural pathways for the processing of alarm pheromone in the ant brain. Journal of Comparative Neurology. 505:424–442.

Yang C.H., Belawat P., Hafen E., Jan L.Y., Jan Y.N. (2008) *Drosophila* egg-laying site selection as a system to study simple decision-making processes. Science. 319:1679–1683.

Zitnan D., Kim Y.J., Zitnanova´ I., Roller L., Adams M.E. (2007) Identification of the gregarization-associated dark-pigmentotropin in locusts through an albino mutant. General and Comparative Endocrinology. 153:88–96.

Zitnan D., Kim Y.J., Zitnanova´ I., Roller L., Adams M.E. (2007) Complex steroid–peptide–receptor cascade controls insect ecdysis. General and Comparative Endocrinology. 153:88–96.

Scientific curriculum vitae

Martin Kollmann

[redacted]

Enclosure:

- Curriculum Vitae
- Publications
- Conference Contributions

Personal data

Date of birth:	[redacted]	Place of birth:	Witten / Ruhr (Germany)
Marital status:	unmarried		

Academic education

08.09 - current	Philipps University of Marburg	
	Doctoral studies program:	Biology
	Intended degree:	**Doctor rerum naturalium**
	Title of the doctoral thesis:	"The beetle brain in comparison to other insects with a focus on the olfactory pathway" In the working group Prof. Dr. Schachtner Animal physiology / Neurobiology & Ethology
04.03 - 04.08	Philipps University of Marburg	
	Diploma program:	Biology
	Degree:	**Diploma (grade: 1,2)**
	Examination subjects:	- Animal physiology - Zoology - Ecology
	Title of the diploma thesis:	"Anatomical and immunohistological analysis of the collembola brain“ In the working group Prof. Dr. Schachtner Animal physiology / Neurobiology & Ethology
04.02 - 04.03	University of Kassel	
	Diploma program:	Physics

Basic military service at the German air force

09.01 -	Recruit training:	4te Luftwaffenausbildungsregiment 1, Budel, **Netherlands**
04.02	Unit:	1th FlaRakGrp 38, Bad Arolsen - **Orderly room (organisational tasks)**

Professional education

08.00 -	Elisabeth-Knipping-Schule (vocational high school), Kassel	
06.01	Degree	**Chemical-technical assistant (CTA) (grade: 1,4)**

School education

08.97 -	Elisabeth-Knipping-Schule (vocational high school), Kassel	
06.00	Degree:	**High school graduation / Abitur (grade: 1,5)**
	Intensive course:	- Chemistry - Physics

Career experience / Qualifications

08.09 - current **Research assistant / PhD student** at the Philipps University of Marburg / Department of Animal physiology / Neurobiology & Ethology:
- Research and collection of scientific data
- Organizing and supporting of projects for bachelor's and master's theses
- Organizing and supporting of numerous courses and lectures
- Presentation of data at scientific meetings via poster and oral presentation
- Writing publications for scientific journals
- Supervision of the CLSM for the whole department of biology

01.12 - 08.12 **Planning and organization of a meeting / PhD workshop** in Marburg: "NeuroDoWo 2012" (http://www.neurodowo2012.de; ca. 50 participants).
Point of responsibility: Planning of the event location; participant support; moderation; editing, designing and proofreading of the programme book

07.08 - 07.09 **Service contract** with the Philipps University of Marburg / cooperation with the **US Air Force**:
Planning, establishment and care of a breeding facility for solitary locusts (*Schistocerca gregaria*)

04.08 - 11.08 **Research assistant** at the INRA (Institut National de Recherche Agronomique), **Versailles, France**:
Research on the neuroanatomy of aphid brains via immunohistochemistry

03.06 - 07.06 Certificate for **laboratory animal science** at the Philipps University of Marburg:
40-hours hours course corresponding to the FELASA (federation of european laboratory animal science association)

06.01 - 09.01 **Working student** at MERCK KGaA, Darmstadt:
Operating in a laboratory for **quality assurance**

03.00 - 04.00 **Practical training** in the chemical company KEMPER SYSTEM GmbH & Co. KG; Vellmar in Kassel:
Operating in a laboratory for **quality assurance and development**

Additional skills

languages: - English (*fluent*)
EDV
- MS **Office**: Word, Excel, PowerPoint (*good knowledge*)
- **AMIRA** (3D Analysis Software for Life Sciences) (*good knowledge*)
- **Blender** (3D Software) (*basic knowledge*)
- graphic programs: - **CorelDRAW** (*extended knowledge*)
  - **Adobe Photoshop** (*basic knowledge*)

Personal activities and interests

- Artistically model assembling
- Fitness

Marburg, 22.06.2016

Publications

Kollmann M, Schmidt R, Heuer CM, Schachtner J
Variations on a theme: antennal lobe architecture across Coleoptera
Sumbitted in PLOS Biology

Dippel S*, **Kollmann M*,** Oberhofer G, Montino A, Knoll C, Krala M, Rexer K-H, Frank S, Kumpf R, Schachtner J, Wimmer EA [*Equal contribution]
Morphological and Transcriptomic Analysis of a Beetle Chemosensory System Reveals a Gnathal Olfactory Center
Re-Sumbitted in eLife

Koniszewski NDB*, **Kollmann M***, Bigham M, Farnworth M, He B, Büscher M, Hütteroth W, Binzer M, SchachtnerJ, Bucher G (2016) [*Equal contribution]
The insect central complex as model for heterochronic brain development—background, concepts, and tools
Dev Genes Evol. 1-11. DOI: 10.1007/s00427-016-0542-7

Kollmann M, Rupenthal A, Neumann P, Huetteroth H, Schachtner J (2015)
Novel antennal lobe substructures revealed in the small hive beetle *Aethina tumida Cell* Tissue Res. DOI 10.1007/s00441-015-2282-9

Lidke AK, Bannister S, Löwer AM, Apel DM, **Kollmann M**, Ackermann CF, García-Alonso J, Raible F**, Rebscher N.** (2014)
17β-Estradiol induces supernumerary primordial germ cells in embryos of the polychaete *Platynereis dumerilii*.
Gen Comp Endocrinol. 196:52-61. DOI:10.1016/j.ygcen.2013.11.017

Binzer J, Heuer CM, **Kollmann M**, Kahnt J, Hauser F, Grimmelikhuijzen CJP, Schachtner J (2014)
The neuropeptidome of *Tribolium castaneum* antennal lobes and mushroom bodies
J Comp Neurol. 522.2:337-357. DOI: 10.1002/cne.23399

Heuer CM*, **Kollmann M***, Binzer M, Schachtner J (2012) [*Equal contribution]
Neuropeptides in insect mushroom bodies
Arthropod Struct Dev 41 (3): 199-226. DOI: 10.1016/j.asd.2012.02.005

Weissteiner S, Hütteroth W, **Kollmann M**, Weißbecker B, Romani R, Schachtner J, Schütz S (2012)
Cockhafer larvae smell host root scents in soil
PLoS One 7(10):e45827. DOI: 10.1371/journal.pone.0045827

Kollmann M, Minoli S, Bonhomme J, Homberg U, Schachtner J, Tagu D, Anton S (2011)
Revisiting the anatomy of the central nervous system of a hemimetabolus model insect species: the pea aphid *Acyrthosiphon pisum*
Cell Tissue Res. 343(2): 343-55. DOI: 10.1007/s00441-010-1099-9

Kollmann M, Huetteroth W, Schachtner J (2011)
Brain organization in Collembola(springtails
Arthropod Struct Dev. 40(4):304-16. DOI: 10.1016/j.asd.2011.02.003

Hansen KK, Stafflinger E, Schneider M, Hauser F, Cazzamali G, Williamson M, **Kollmann M**, Schachtner J, Grimmelikhuijzen CJ (2010)
Discovery of a novel insect neuropeptide signaling system, closely related to the insect adipokinetic hormone and corazonin hormonal systems
J Biol Chem. 285(14):10736-47. DOI: 10.1074/jbc.M109.045369

Bruns S, Müllner T, **Kollmann M**, Schachtner J, Höltzel A, Tallarek U (2010)
Confocal laser scanning microscopy method for quantitative characterization of silica monolith morphology
Anal Chem. 82(15):6567-75. DOI: 10.1021/ac100909t

Dreyer D, Vitt H, Dippel S, Goetz B, El Jundi B, **Kollmann M**, Huetteroth W, Schachtner J (2010)
3D Standard Brain of the Red Flour Beetle *Tribolium Castaneum*: A Tool to Study Metamorphic Development and Adult Plasticity
Front Syst Neurosci. 04:03. DOI: 10.3389/neuro.06.003.2010

Conference contributions - Talks

Kollmann M, Dippel S, Binzer M, Christ P, Frank S, Crombach S, Kahnt J, Schütz S, Wimmer EA, Schachtner J (2014)
The olfactory pathway of *T. castaneum* and its peptidergic plasticity
107. Jahrestagung der Deutschen Zoologischen Gesellschaft, 3rd ANN Meeting, Göttingen. OP-SSI-09

Kollmann M, Nothvogel R, Baumrucker M, Heuer C, Schachtner J (2014)
The Diversity of Beetle Brains
107. Jahrestagung der Deutschen Zoologischen Gesellschaft, Göttingen. OP-NB-01

Kollmann M, Rovenna N, Baumrucker M, Carsten H, Joachim S (2014)
The diversity of beetle brains
Neuro DoWo 2014, Berlin. Vortrag, Abstract Seite p48

Kollmann M, Rovenna N, Carsten H, Joachim S (2013)
Show me your brain and I tell you who you are - The diversity of beetle brains
Neuro DoWo 2013, Göttingen. Vortrag, Abstract Seite p36

Kollmann M, Dippel S, Frank S, Crombach S, Schütz S, Wimmer EA, Schachtner J (2013)
Wie riechen Käfer? Das olfaktorische System des rotbraunen Reismehlkäfers *Tribolium castaneum*
Tag der Wissenschaft 2013 / Graduiertenzentrum Lebens- und Naturwissenschaften Marburg

Kollmann M, Dippel S, Frank S, Crombach S, Schütz S, Wimmer EA, Schachtner J (2012)
The different stages of the olfactory pathway of the red flour beetle *Tribolium castaneum*
105. Jahrestagung der Deutschen Zoologischen Gesellschaft, Konstanz T NB #101, p157

Kollmann M, Dippel S, Frank S, Schuetz S, Wimmer EA, Schachtner J (2012)
The anatomy of olfaction in *Tribolium*
Euro Evo Devo (EED) Meeting, Lissabon. Program No. 222, p87

Kollmann M, Dippel S, Frank S, Schachtner J, Schütz S, Wimmer EA (2011)
The olfactory pathway of the red flour beetle *Tribolium castaneum*
Neuro DoWo 2011, Bonn. Vortrag, Abstract Seite 32.

Kollmann M, Dippel S, Christ P, Frank S, Schachtner J, Schütz S, Wimmer EA (2010)
Post-metamorphic plasticity of the olfactory system of the red flour beetle *Tribolium castaneum*
Neuro DoWo 2010, Bielefeld. Vortrag, Abstract Seite 47.

Kollmann M, Huetteroth W, Schachtner J (2009)
Studies on a collembolan brain: Neuroanatomy and Immunocytochemistry
102. Jahrestagung der Deutschen Zoologischen Gesellschaft, Regensburg O NB.8

Kollmann M, Huetteroth W, Schachtner J (2009)
Studies on a collembolan brain: Neuroanatomy and Immunocytochemistry
Evolution of the Arthropod Nervous System, Max-Planck-Institut, Jena

Kollmann M, Dreyer D, Vitt H, Goetz B, Redelfs S, Schumacher D, Schachtner J (2009)
3D Standard brain of the red flour beetle *Tibolium castaneum*: A tool to study adult brain development and plasticity - The brain of Tribolium castaneum and its' plasticity
Regionales Tribolium meeting, Köln

Kollmann M, Huetteroth W, Schachtner J (2008)
Studies on a collembolan brain: Neuroanatomy and Immunocytochemistry
Neuro DoWo 2009, Saarbrücken. Vortrag, Abstract Seite 23.

Conference contributions - Posters

Trebels B, Götz B, **Kollmann M**, Schachtner J (2014)
Proliferation and plasticity in adult *Tribolium castaneum*
107. Jahrestagung der Deutschen Zoologischen Gesellschaft, Göttingen. PP-NB-17

Trebels B, **Kollmann M**, Goetz B, Schachtner J (2013)
Neurogenesis in the adult beetle brain
106. Jahrestagung der Deutschen Zoologischen Gesellschaft, München. PP-NB-52

Wendlandt C, **Kollmann M**, Dippel S, Schütz S, Wimmer EA, Schachtner J (2013)
Testing olfactory behaviour of *Tribolium castaneum* during the postmetamorphic period in a two-choice olfactometer
106. Jahrestagung der Deutschen Zoologischen Gesellschaft, München. PP-BB-27

Crombach SF, Christ P, **Kollmann M**, Binzer M, Schachtner J (2013)
Identification of GABA/GAD and TKRP-immunoreactive neurons in the olfactory system of *Tribolium csataneum*
106. Jahrestagung der Deutschen Zoologischen Gesellschaft, München. PP-NB-38

Kollmann M, Dippel S, Frank S, Crombach S, Schütz S, Wimmer EA, Schachtner J (2013)
The olfactory pathway of the red flour beetle *Tribolium castaneum*
Tenth Göttingen Meeting der Deutschen Neurowissenschaftlichen Gesellschaft, Göttingen. Proceedings: T19-9D, p867

Christ P, **Kollmann M**, Schachtner J (2013)
Activity dependent plasticity in the olfactory system of adult *Tribolium castaneum*
Tenth Göttingen Meeting der Deutschen Neurowissenschaftlichen Gesellschaft, Göttingen. Proceedings: T19-7D, p865

Christ P, **Kollmann M**, Schachtner J (2012)
Activity dependent plasticity in the olfactory system of adult *Tribolium castaneum*
105. Jahrestagung der Deutschen Zoologischen Gesellschaft, Konstanz P NB #139, p164

Crombach SF, **Kollmann M**, Schachtner J (2012)
Identification of putative GABAergic neurons in the brain and the olfactory system of the red flour beetle Tribolium castaneum
105. Jahrestagung der Deutschen Zoologischen Gesellschaft, Konstanz P NB #140, p165

Heuer CM, **Kollmann M**, Binzer M, Schachtner J (2012)
On a neuropeptidergic ground pattern in insect mushroom bodies
Euro Evo Devo (EED) Meeting, Lissabon. Program No. 228, p179

Christ P, **Kollmann M**, Schachtner J (2012)
Activity dependent plasticity in the olfactory system of adult *Tribolium castaneum*
Euro Evo Devo (EED) Meeting, Lissabon. Program No. 241, p159

Schachtner J, **Kollmann M**, Dippel S, Christ P, Frank S, Binzer M, Heuer C, Schuetz S, Wimmer EA (2012)
The olfactory system of the red flour beetle, *Tribolium castaneum*: Architecture and Postmetamorphic plasticity
Euro Evo Devo (EED) Meeting, Lissabon. Program No. 337, p124

Dippel S, **Kollmann M**, Metzger AC, Schuetz S, Schachtner J, Wimmer EA (2012)
Olfaction in the red flour Beetle *Tribolium castaneum*
XVI ISOT, Stockholm, Sweden. Program #100, p57

Kollmann M, Dippel S, Frank S,Binzer M, Heuer CM, Schütz S, Wimmer EA, Schachtner J (2011)
From the antenna to the mushroom body: The olfactory pathway of the red flour beetle *Tribolium castaneum*
104. Jahrestagung der Deutschen Zoologischen Gesellschaft, Saarbrücken P NB.22, p133

Diesner M, Christ P, **Kollmann M**, Götz B, Schachtner J (2011)
Cell proliferation in the brain of the red flour beetle *Tribolium castaneum*
104. Jahrestagung der Deutschen Zoologischen Gesellschaft, Saarbrücken P NB.21, p132

Binzer M, **Kollmann M**, Heuer CM, Schachtner J (2011)
Neuropeptides of the insect mushroom body
Ninth Göttingen Meeting der Deutschen Neurowissenschaftlichen Gesellschaft, Göttingen. T19-14B, p166.

Christ P, **Kollmann M**, Redelfs S, Schachtner J (2011)
Postmetamorphic plasticity of numbers of peptidergic neurons in the antennal lobe of *Tribolium castaneum* (Coleoptera)
Ninth Göttingen Meeting der Deutschen Neurowissenschaftlichen Gesellschaft, Göttingen. T19-28B, p167.

Dippel S, **Kollmann M**, Schachtner J, Schütz S, Wimmer EA (2011)
Biological function of odorant binding proteins in *Tribolium castaneum*.
Ninth Göttingen Meeting der Deutschen Neurowissenschaftlichen Gesellschaft, Göttingen. T19-5A, p163.

Christ P, **Kollmann M**, Redelfs S, Schachtner J (2010)
Postmetamorphic plasticity in the antennal lobe of *Tribolium castaneum*
103. Jahrestagung der Deutschen Zoologischen Gesellschaft, Hamburg P NB.11, p182

Frank S, **Kollmann M**, Goetz B, Dippel S, Huetteroth W, Schachtner J (2010)
Postmetamorphic plasticity of the *Tribolium castaneum* brain.
103. Jahrestagung der Deutschen Zoologischen Gesellschaft, Hamburg P NB.12, p182

Kollmann M, Huetteroth W, Schachtner J (2009)
Studies on a collembolan brain: Neuroanatomy and Immunocytochemistry
8th Göttingen Meeting der Deutschen Neurowissenschaftlichen Gesellschaft, Göttingen, Göttingen T4-1A

Kollmann M, Huetteroth W, Schachtner J (2008)
Neuroanatomy and immunocytochemistry of the collembolan brain
101. Jahrestagung der Deutschen Zoologischen Gesellschaft, Jena P MO.14, p157

Kollmann M, Huetteroth W, Schachtner J (2007)
Studies on a collembolan brain: 3D reconstruction and neurochemistry
100. Jahrestagung der Deutschen Zoologischen Gesellschaft, Köln N47, p124